



Yi Qin

MICRO-MANUFACTURING ENGINEERING AND TECHNOLOGY

William Andrew is an imprint of Elsevier
The Boulevard, Langford Lane, Kidlington, Oxford OX5 1GB, UK
30 Corporate Drive, Suite 400, Burlington, MA 01803, USA

First edition 2010

Copyright © 2010. Yi Qin. Published by Elsevier Inc. All rights reserved

The right of Yi Qin to be identified as the author of this work has been asserted in accordance with the Copyright, Designs and Patents Act 1988. All effort has been made by author to obtain permissions for figures and tables re-produced in this book.

No part of this publication may be reproduced, stored in a retrieval system or transmitted in any form or by any means electronic, mechanical, photocopying, recording or otherwise without the prior written permission of the publisher

Permissions may be sought directly from Elsevier's Science & Technology Rights Department in Oxford, UK: phone (+44) (0) 1865 843830; fax (+44) (0) 1865 853333; email: permissions@elsevier.com. Alternatively you can submit your request online by visiting the Elsevier website at <http://elsevier.com/locate/permissions>, and selecting *Obtaining permission to use Elsevier material*

Notice

No responsibility is assumed by the publisher for any injury and/or damage to persons or property as a matter of products liability, negligence or otherwise, or from any use or operation of any methods, products, instructions or ideas contained in the material herein. Because of rapid advances in the medical sciences, in particular, independent verification of diagnoses and drug dosages should be made

British Library Cataloguing in Publication Data

A catalogue record for this book is available from the British Library

Library of Congress Cataloging-in-Publication Data

A catalog record for this book is available from the Library of Congress

ISBN-13: 978-0-81-551545-6

For information on all William Andrew publications visit our website at books.elsevier.com

Printed and bound in the UK

10 11 12 13 14 10 9 8 7 6 5 4 3 2 1

PREFACE

Increased demand for MEMs and other micro-products has led to rapid development of technologies for micro-manufacturing individual parts and systems, including the development of new manufacturing processes, tools and machinery. This book is a collection of micro-manufacturing knowledge acquired by leading experts over the past decade that will not only inform on the subject of micro-manufacturing technologies and their industrial uses, but also will likely inspire new interest in a field which is attracting huge investments.

Unlike other books, some which are largely focused on the micro-manufacturing processes only, this book also covers manufacturing chains and manufacturing system issues, such as handling, testing, robotics and automation.

Manufacturing practitioners often have difficulty choosing the optimum technology for a particular product. Therefore, this book also focuses on practical technology, suitable tools, equipment and utilization. Readers with a basic understanding of or experience in mechanical, manufacturing, material, or product engineering will feel very comfortable with this material.

Areas of miniature- and micro-product manufacturing that are covered in this book include: micro-machining, micro-forming, micro-replication, lithography, thin film technology, surface engineering, laser-processing, micro-/nano-fibers, micro-tooling, micro-joining/assembly, as well as micro-handling, micro-robotics, inspection, testing and diagnosis, and manufacturing execution

systems. Micro-mechanics analysis and sustainability of micro-manufacturing technologies are also included. Each chapter was written either by a group of leading educator(s) or by experienced, notable engineer(s) or researcher(s), in a field related to micro-manufacturing. Most contributors were selected from leading partners of the recent/current EU-funded projects, including the MASMICRO project, which was one of the largest micro/nano-manufacturing projects funded through the EU fp6.

On behalf of all the authors, I would like to express my special gratitude to Professor Frank Travis for his precious comments on all draft chapters and careful checking of the final manuscripts. I would also like to thank Mr Quanren Zeng for re-preparing some illustrations/drawings for some chapters and Dr Pascal Meyer for providing the artwork for the book cover. Finally, thanks are expressed to all authors for their hard work in preparing the book chapters. Without their support, this book would not be possible.

**Professor Yi Qin (BEng, MEng, PhD, CEng,
MIMechE, FHeA, FIoN)**

*Department of Design, Manufacture
and Engineering Management
The University of Strathclyde
Glasgow G1 1XJ, United Kingdom*

*Tel: 0044 141 548 3130
Fax: 0044 141 552 7986
Email: qin.yi@strath.ac.uk*

CONTRIBUTORS

Mogens Arentoft

Dr Mogens Arentoft, leader of the Process and Micro-Technology Group at IPU, Denmark, has been working in cold forging, numerical and physical simulation and micro-forming areas for more than 15 years. He has coordinated and participated in several EU-funded projects. Since 2001, Dr Arentoft has been chairman of the Danish Cold Forging Group and member of the International Cold Forging Group, the Danish Metallurgical Association, ESAFORM and Danish Sheet Metal Forming Group. He has published over 50 international journal and conference papers.

Giuliano Bissacco

Dr Giuliano Bissacco, Assistant Professor of Manufacturing Engineering at the University of Padova, was Research Assistant (2001–2004) and Assistant Professor (2005–2007) at DTU, Denmark. Giuliano's research activities include design and manufacture of micro-mechanical components in metals, polymers and ceramics; development and optimization of micro-manufacturing processes for production of micro-components characterized with complex 3D geometry; development of innovative process chains for manufacture of micro-components, tooling processes and machine tools.

Email: giuliano.bissacco@unipd.it

Andrew Brockett

Mr Andrew Brockett, educated at the University of Strathclyde, gained a Masters in Product Design Engineering. During and after his study in Strathclyde, he worked for three years as a Research Assistant for the EU MASMICRO project, responsible for machine and tool design for micro-sheet-forming. Andrew is now a Project Engineer working in the energy industry.

Email: andrewbrockett@hotmail.co.uk

viii

Kai Cheng

Professor Kai Cheng, Chair Professor in Manufacturing Systems, Head of the AMEE (Advanced Manufacturing and Enterprise Engineering Department) at Brunel University, managed a series of the funded projects and published over 160 technical papers, five books and six book chapters. Kai is a fellow of the IET and IMechE, the European editor of *IJAMT* and a member of the editorial board of *IJMTM*. His current research interests include micro-manufacturing, design of precision machines, digital manufacturing and enterprise technologies.

Email: kai.cheng@brunel.ac.uk

Ioannis S. Chronakis

Dr Ioannis S. Chronakis, Associate Professor and Research Project Manager at Swerea IVF, Sweden, takes a lead in the research for the development and applications of micro-/nano-structured materials and their processing technologies. He received his PhD in physical chemistry at Cranfield University, worked respectively in Lund University (Sweden) and INRA (France), published over 50 research papers and book chapters and holds three patents in micro-nanotechnology.

Email: ioannis.chronakis@swerea.se

Arnaud De Grave

Dr Arnaud De Grave, MSc in Manufacturing Engineering, PhD in Industrial Engineering, works as an Associate Professor at the Department of Mechanical Engineering, DTU, Denmark. His research interests are design and manufacture of micro-products (mainly metal, polymer and ceramic based, with dimensions under the millimeter range), including complex and innovative process chains for replication of components at the micro scale. He also has activities in lifecycle assessment of micro-technologies and is interested in generic design methodology.

Email: adg@ipl.dtu.dk

Rasmus Solmer Eriksen

Mr Rasmus Eriksen is a trained technician and worked with industrial production machines for several years. He received an MSc in 2005 in Electrical Engineering at DTU, Denmark, and then worked for one year at IPU as engineer consultant in the division of technology development. In 2006 Rasmus joined the group of Micro-/Nano-Manufacturing at DTU where he is working towards his PhD. His research is focused on tool design for bulk forming of micro-components and was part of the research team designing a fully functional prototype machine for micro-bulk forming with the MASMICRO project.

Email: rser@mek.dtu.dk

Bertrand Fillon

Dr Bertrand Fillon is the CTO of CEA/LITEN for new energy technologies, organic, electronic and nano-materials, France, and the scientific president of the French Polymer Cluster 'Plastipolis'. He has been the initiator of the polymer platform involving the different CEA research teams and Swiss laboratories CSEM. Between 1990 and 2003, he worked with Pechiney Packaging as a coordinator of their Global Packaging R&D activities and the leader of the Pechiney polymer expert group.

Email: bertrand.fillon@cea.fr

Gonzalo G. Fuentes

Dr Gonzalo G. Fuentes got his PhD in Material Science and Thin Films from the University Autonoma of Madrid, and researched in heteronanotubes and macro-molecular systems in Germany. Since 2003 he has been responsible for the international projects at the Center of Advanced Surface Engineering (with AIN), Spain. He participated in five EU funded research projects and coordinated several national and regional projects. He has published 45 scientific articles in peer reviewed journals.

Email: gfuentes@ain.es

Asta Gegeckaite

Dr Asta Gegeckaite is a Project Manager at Novo Nordisk. She has professional experience in

handling and assembly of micro-products, including testing, development and automation of assembly processes. She obtained a PhD within the program of Construction, Production, Civil Engineering and Transport and has a Master of Science Diploma in Materials Science (Polymeric Materials), a Civil Engineering Diploma within Qualification of Work Safety (similar to EHS) and a Bachelor of Science in Industrial Engineering.

Email: agek@novonordisk.com

Arnold Gillner

Dr Arnold Gillner studied Physics at the University of Darmstadt and obtained his PhD in Mechanical Engineering at the RWTH Aachen in 1994. Since 1985 he has worked as a scientist at the Fraunhofer-Institut for Laser Technology (ILT). Starting in 1992 he developed the Department for Micro-Technology at the ILT, which has since become a leading department. Together with more than 20 scientists he is developing industrial laser processes for micro-joining and packaging, micro- and nano-structuring, polymer applications and life science applications.

Email: arnold.gillner@ilt.fraunhofer.de

Hans Nørgaard Hansen

Dr Hans Nørgaard Hansen, Professor of Micro-Manufacturing, Technical University of Denmark, is heading the research group on Micro-/Nano-Manufacturing as well as the Manufacturing Engineering Section of the department. His research is focused on industrial production of products and components in metals, polymers and ceramics with critical dimensions in the micrometer range (product and material development, development of processes, process chains and production systems for micro-mechanical systems).

Email: hnha@mek.dtu.dk

Colin Harrison

Dr Colin Harrison, Senior Research Fellow, graduated in Engineering Science from the University of Aberdeen in 1984 having won the F.J. McGrigor prize for engineering; he then worked in the oil industry, before joining the University of Dundee working on discrete event simulation and computer

integrated manufacture with NCR. He then set up a successful consultancy before joining the University of Strathclyde studying for an MSc which led to a PhD, specializing in mechatronics and manufacturing automation. He then worked on the control and mechatronics aspects of the machine development for the EU MASMICRO project.

Email: c.harrison@strath.ac.uk

Christoph Hartl

Dr Christoph Hartl has been a Professor at the Cologne University of Applied Sciences since 2002. He worked as a General Manager responsible for the Hydroforming R&D Center of a German press manufacturer. He is also the Managing Director of the Institute of Production Technology and Production Organization GmbH and President of the Society for Technical and Scientific Education e.V. in Cologne. His current research is focused on micro-hydroforming technology, laser processing and process simulation.

Email: christoph.hartl@fh-koeln.de

Jens Holtkamp

Mr Jens Holtkamp studied Mechanical Engineering at the Aachen University of Technology (RWTH). Since 2004 he has been a research engineer at the Fraunhofer Institute for Laser Technology (ILT), Aachen, with the Department of Micro-Technology. He is a member of the group 'Micro Structuring' and his main field of the research is laser assisted forming processes.

Email: jens.holtkamp@ilt.fraunhofer.de

Pietro Larizza

Dr Pietro Larizza is in charge of the Research & Development Division of Masmec Srl, Italy, carrying out industrial research devoted to the Robotics, Automation, Measurement and Advanced Production Technologies. He is named as an Expert of the MIUR for the disciplines of electronics, electronics measurement and automatic controls. He has published various technical papers and holds several industrial patents on identification techniques and processing of medical images.

Email: piero.larizza@masmec.com

Malte Langmack

Mr Malte Langmack studied Mechanical Engineering with focus on Micro and Precision Engineering at the Technical University Berlin, Germany. Since 2007 he has been working as a research engineer in the field of micro-electrical discharge machining at the Centre of Micro Production Technology of the Fraunhofer IPK.

Email: Malte.Langmack-projekt@ipk.fraunhofer.de

Jainguo Lin

Professor Jianguo Lin, Head of Mechanics of Materials Division, Imperial College London, leads the research in material processing design and optimization via process modeling, and has published over 150 research papers over the last 20 years. He is a member of the editorial boards of five international journals, has an excellent track record in attracting research funding from EU, EPSRC, DTI and industries, and has organized a number of international conferences. Currently, he also heads a research group of 15 researchers working on various material-forming processes.

Email: jianguo.lin@imperial.ac.uk

Rafa López

Dr Rafael Lopez Tarazón has a degree in Telecommunications Engineering (Communications Branch). He worked in the R&D Department of Althea Productos Industriales, Spain, in 2000. In 2001 he was contracted by IBM as a System Engineer for wide-area networks in Madrid and Barcelona. He was a founding member of Robotnik Automation SLL in 2002 and since then has been the company's R&D manager.

Email: rlopez@robotnik.es

Yanling Ma

Dr Yanling Ma obtained her PhD and then worked as a Post-Doctoral Research Fellow at the University of Strathclyde. Her expertise is in tool/machine development for metal forming and micro-forming. She contributed to the machine and tool design for the micro-stamping machine system developed at Strathclyde. Before she joined the University of Strathclyde she worked

in the industry for 10 years. She is currently a Senior Project Engineer and Project Manager with Rutherford Appleton Laboratory, Science and Technology Facilities Council of the UK.

Email: yanling.ma@stfc.ac.uk

Matthias Meier

Mr Matthias Meier is a Project Manager and Researcher at the Ultraclean Technology and Micromanufacturing Department of the Fraunhofer Institute for Manufacturing Engineering and Automation (Fraunhofer IPA) in Stuttgart, Germany. His main area of research is in the Production-IT environment. Mr Meier holds an MSc in Information Technologies and a Dipl.-Ing. in Electrical Engineering from the University of Stuttgart, Germany.

Email: matthias.meier@ipa.fraunhofer.de

Pascal Meyer

Dr Pascal Meyer got his PhD in 1996 from the University of Franche-Comté (neutron dosimetry with a solid state nuclear track detector: the CR-39). After two years as an Assistant Professor at Franche-Comté, he has worked since 1998 as a Post-Doctoral Researcher at the Institute of Microstructure Technology of the Forschungszentrum Karlsruhe. His interests include the commercialization of microproducts, particularly those made with the LIGA process and their production (repeatability, quality, reliability, customer satisfaction, etc.).

Email: Pascal.Meyer@kit.edu

Johann Michler

Dr Johann Michler got his PhD at the Swiss Federal Institute of Technology Lausanne (EPFL) in the field of thin film mechanics. He has been working at EMPA since 2000 and is currently heading the Laboratory for Mechanics of Materials and Nanostructures of EMPA. He has published over 100 scientific publications and is co-founder of two companies on scientific instrumentation.

Email: Johann.Michler@empa.ch

Alexander Olowinsky

Dr Alexander Olowinsky studied Mechanical Engineering at the Aachen University of Technology

(RWTH), and joined the Fraunhofer Institute for Laser Technology in 1996 as a Project Engineer in the Department of Microtechnology. He received his doctoral degree in 2002 in the field of laser beam micro-forming. Since 2001 he has headed the group 'Micro-Joining Technology' with the activities in laser-based micro-joining processes such as welding, soldering, bonding and polymer welding.

Email: alexander.olowinsky@ilt.fraunhofer.de

Stig Irving Olsen

Dr Stig Irving Olsen obtained a Master of Science (Biology) from the University of Copenhagen and a PhD from the Technical University of Denmark. He is an Associate Professor in Sustainable Production, Department of Management Engineering, DTU. For more than 20 years he has been working on environmental research. Particular emphasis has been on the comparative aspects of LCA and RA in, for example, substitution and application of LCA for sustainable production in industry. Lately, use of LCA for technology assessment, especially nanotechnology, has been one of his major research areas.

Email: siol@man.dtu.dk

Fredrik Östlund

Mr Fredrik Östlund has an MSc in Engineering Physics from Uppsala University, Sweden, and has been working in the field of compression tests of semiconductor micro-pillars at the Laboratory for Mechanics and Materials at the Swiss Federal Laboratories for Materials Testing and Research (Empa) during last several years.

Email: Fredrik.Oestlund@empa.ch

Laetitia Philippe

Dr Laetitia Philippe got her PhD and completed her post-doctoral research in the field of local electrochemical processes and influences of mechanical deformations on electroformed nano-material properties. She is currently the group leader in Nanostructuration by Electrochemical Methods, in EMPA, Switzerland. Her research deals with the fabrication of metallic, semiconductor and composite nanostructures (wires and

dots), their nano-manipulation and mechanical characterizations.

Email: Laetitia.Philippe@empa.ch

Yi Qin

Prof Yi Qin is Director of Facilities and Deputy Director of Research, and Leader of the Research Group in Precision Engineering and Micro-Manufacturing at the University of Strathclyde. His research interests include micro/nano-manufacturing, micro-forming, precision forming, manufacturing system and numerical simulation. Yi has managed a series of funded RTD projects, including overall management of the EU FP6 Masmicro Project as the Project Coordinator. He has published over 120 technical papers, and acted as a reviewer for many leading journals and conferences, including a member of the editorial board of *IJMTM*. Yi has also given keynote speeches and invited presentations at more than 20 international conferences and workshops.

Email: qin.yi@strath.ac.uk

Akhtar Razali

Mr Akhtar Razali is currently doing his PhD in Micro-Manufacturing Technology at the University of Strathclyde, UK. He has been involved in a couple of research projects in micro-manufacturing. His research is focused on the development of handling methods and devices for micro-manufacturing applications. He worked as a lecturer in one of the local public universities in Malaysia before pursuing his PhD at Strathclyde. The subject he taught there concerned mechanical and electrical systems.

Email: akhtar.akhtar@strath.ac.uk

Markus Röhner

Mr Markus Röhner studied Mechanical Engineering at the Technical University Dresden and then worked as a Scientific Engineer and Deputy Leader of the group Micro-Production Technology, Institute for Machine Tools and Factory Management (IWF), Technical University Berlin (2005–2008). Since October 2008 Markus has been working as a Research Engineer at the

Fraunhofer Institute IPK where he is responsible for technology and strategic consultancy with various industrial partners.

Email: Markus.Roehner@ipk.fraunhofer.de

Karolina A. Rzepiejewska-Malyska

Miss Karolina A. Rzepiejewska-Malyska got her MSc in Engineering at the Warsaw University of Technology in the field of Micromechanics. Since 2006 she has been studying for her PhD focusing on the mechanical and tribological behaviors in the micro- and nano-scale of thin multilayered ceramic films for MEMS applications, in EMPA, Switzerland.

Email: Karolina.Rzepiejewska@empa.ch

Volker Saile

Volker Saile is a full professor in the faculty of mechanical engineering at Universität Karlsruhe in Germany and serves also as Director of the Institute for Microstructure Technology (IMT). IMT is a joint institute of Forschungszentrum Karlsruhe GmbH (now Karlsruhe Institute of Technology), a German national laboratory and the university in Karlsruhe. Dr. Saile received his Ph.D. in physics from Ludwig-Maximilians-Universität in München in 1976. Dr. Saile's research has focussed on microsystems technology including nano- and microfabrication of components and applications of such components or of entire systems in optics, fluidics, and analytics. He is particularly interested in applications of synchrotron radiation in X-ray lithography and in X-ray optical devices and systems.

Email: Volker.Saile@kit.edu

Felix Schmitt

Mr Felix Schmitt studied Mechanical Engineering at the Aachen University of Technology (RWTH) and finished his study with a major in micro-production technology there. Since 2005, he has been working as a Research Engineer at the Fraunhofer Institute for Laser Technology (ILT), Aachen, with the Department of Micro-Technology. He is part of the group 'Micro-Joining Technology'. His main field of the research is laser-beam micro-welding and soldering.

Email: felix.schmitt@ilt.fraunhofer.de

Joachim Schulz

Dr Joachim Schulz received his PhD in solid state physics. He started his research as a post-doctoral researcher at the Institute of Microstructure Technology of the Forschungszentrum Karlsruhe in 1991, where he led a group in LIGA sensor technology and the technology department for several years. After concentrating on implementing an automated production line for LIGA products (FELIG) he founded the company Microworks in 2007, which focuses on the production of high-precision parts using X-ray LIGA technology.
Email: Joachim.Schulz@kit.edu

Patrick Schwaller

Dr Patrick Schwaller got his PhD at the University of Zurich in the field of angle-resolved photoelectron spectroscopy. Since 2001 he has been working at EMPA (Switzerland) in the field of micro- and nano-mechanics with a focus on instrumented indentation techniques. In addition, he is also a lecturer at the Bern University of Applied Science.
Email: Patrick.Schwaller@empa.ch

Antonio J. Sánchez

Dr Antonio J. Sánchez got his PhD in Computer Science at the Polytechnic University of Valencia, Spain, in 2001. He is an Associate Professor at the same university. His teaching activities are in the areas of artificial vision and robotics. His research interests include intelligent robot programming and active vision. He has published various technical papers in these fields. Dr Sanchez has been a member of AERFAI since 1999 and a CEA-IFAC member since 2000.
Email: asanchez@isa.upv.es

David Stifter

Dr David Stifter studied solid state and semiconductor physics at JKU, Austria, and worked at Profactor GmbH and then at UAR GmbH where he focused on optical coherence tomography (OCT) for metrology and non-destructive material characterization. He is now with JKU as a Senior Scientist working on full-field coherent imaging methods and advanced non-linear optical

techniques for the characterization of surfaces and thin films. He is a reviewer for several international scientific journals and author/co-author of more than 70 peer-reviewed articles.
Email: david.stifter@jku.at

Xizhi Sun

Dr Xizhi Sun received her BSc and MSc degrees in Mechanical Engineering from Harbin Institute of Technology, China, in 2001 and 2003, respectively. She obtained her PhD in Precision and Micro-Machining in 2009 at Brunel University. Her current research interests include modeling and simulation of micro-manufacturing processes and design of precision machine tools, including reconfigurable machine tools for micro-manufacturing. She has published more than 10 technical papers in these fields.
Email: xizhi.sun@brunel.ac.uk

Peter T. Tang

Dr Peter T. Tang holds an MSc in Chemical Engineering and a PhD in Electrochemical Engineering and Microtechnology. He has worked for more than 15 years on electroplating and electrochemistry, and is a project leader of several national and EU research projects as well as contracted industrial projects. Peter has recently worked on pulse plating of nickel, copper, silver, zinc and various alloys, mainly within the field of micro-technology. He is the author of more than 65 scientific papers and holds seven patents in the field of electrochemistry, electroforming, pulse plating and selective metallization.
Email: tt@ipu.dk

Guido Tosello

Dr Guido Tosello got his PhD in Manufacturing Engineering at DTU, Denmark, with a focus on Polymer Micro-/Nano-Replication. He is currently an Assistant Professor of the university, and is responsible for several EU and national funded projects, especially in polymer technology and injection molding. He has authored and co-authored more than 60 technical publications/reports, and also acted as a reviewer for several

conferences on micro-/nano-manufacturing and precision engineering.

Email: guto@mek.dtu.dk

Eckart Uhlmann

Professor Eckart Uhlmann worked as a Scientific Engineer and Chief Engineer in IWF (1986–1994), and assumed various management responsibilities at Hermes Schleifmittel GmbH & Co., Hamburg (1994–1997), including responsibility as the vice president of the company (1995). Professor Uhlmann became the Director of the Fraunhofer Institute IPK and Director of the Chair of Machine Tools and Manufacturing Technology at the IWF of the TU Berlin in the Production Technology Center Berlin (1997).

Email: Eckart.Uhlmann@ipk.fraunhofer.de

Matthias Worgull

Dr Matthias Worgull currently works at the Institute for Microstructure Technology at

Forschungszentrum Karlsruhe (Karlsruhe Institute of Technology), Germany. His degree from the University of Karlsruhe was in Mechanical Engineering. He has been the leader of the Nanoreplication Group at the Institute since 2005 and the leader of the replication division since 2008.

Email: matthias.worgull@imt.fzk.de

Jie Zhao

Ms Jie Zhao obtained her first degree in Mechatronics Engineering at Xi'an Shiyou University, China, in 2005, and an MSc in Mechatronics and Automation Engineering at the University of Strathclyde, in 2006. In 2007 she started research in micro-manufacturing as a Research Assistant. Her work has been a mixture of mechatronics, machine/tool development, experimentation for micro-manufacturing, requirement engineering, as well as project management. Currently, she is working towards a PhD in Micro-Manufacturing.

Email: j.zhao@strath.ac.uk

Overview of Micro-Manufacturing

Yi Qin

INTRODUCTION

Manufacturing, as a general term referring to industry, is to make products that have been designed for certain applications. The meaning of ‘manufacture’ has, however, changed, especially during the last 20 years, in terms of what is being made, how it is made, how manufacturing is organized, etc. Manufacturing has been influenced not only by the increased demands on producing routine products and creating new products but also by social, economic and even political changes. The desire for a better quality of life, good health and high working efficiency has been one of major drives in the innovation of many products, such as new models of computers, cars, mobile phones, CD players, MP3 players, wide flat-screen displays, medical instruments/implants, etc. Dramatic changes in global, economic development during the last 15 years have significantly influenced how manufacturing is organized and implemented, e.g. new concepts concerning supply chains, new patterns for collaborations, etc., to such an extent that in a lot of cases, how to organize manufacturing becomes even more important than how the products are to be manufactured. How to achieve a balance between quality and cost is another major issue, since many industries are fighting for survival. Nevertheless, some general issues still apply to all sectors concerned, e.g. issues on how to quickly deploy new technologies and management

methods to improve manufacturing capability, efficiency and quality, no matter whether they belong to traditional, developed countries/regions or developing countries/regions. For the developed countries to compete with low-cost production, the manufacturing industry will need more innovations and changes of the focus. Reducing the cost by significantly improving efficiency and supply chains, maintaining technological advantages by continuously developing leading technologies/capabilities, and delivering higher quality and innovative products are being pursued. For the developing countries, low-cost manufacturing may only be a short-term solution and not the ultimate goal, as this will have limited impact/effect in the long term. From these considerations, as a contribution to competitive manufacturing, this book provides a useful reference for the manufacture of emerging miniature/micro-products, especially for improving mass-manufacturing capabilities and their applications for the manufacture of these products.

There are ever increasing demands on miniaturized/micro products/systems and components, e.g. MEMS (micro-electric-mechanical systems) and micro-systems, micro-reactors, fuel cells, micro-mechanical devices, micro-medical components, etc., which are now popularly used in vehicles, aircraft, telecommunication and IT facilities, home appliances, medical devices and implants. Manufacture of these products has received great

attention during recent years. At the same time, as nanotechnology becomes more and more mature and influential, more nanotechnology-based products have emerged, such as nano-devices for sensors, communication and medical treatment, nano-materials and coating/functionalized surfaces for enhanced performances, etc. To make these products in a volume production scale, effectively linking macro- and nano-world manufacturing is essential. Micro-manufacturing is the bridge between macro-manufacturing and nano-manufacturing.

Micro-manufacturing concerns manufacturing methods, technologies, equipment, organizational strategies and systems for the manufacture of products and/or features that have at least two dimensions that are within sub-millimeter ranges. Micro-manufacturing engineering is a general term which concerns a series of relevant activities within the chain of manufacturing micro-products/features, including design, analysis, materials, processes, tools, machinery, operational management methods and systems, etc. There is a huge diversity in micro-products, the main types being micro-electronics products, micro-optical electronics systems (MOES), micro-electronics mechanical systems (MEMS) and micro-optical electronics mechanical systems (MOEMS), depending on the combinations of product functionalities and/or working principles. Correspondingly, there are different methods and strategies which could be used to manufacture these products. Micro-manufacturing, in a wider context, should cover all these aspects relating to manufacturing these products/features. The definition of micro-manufacturing, or its gravity/focus, often varies from different sources.

There is an enormous amount of literature on the manufacture of MEMS and micro-systems. The technologies relating to design and fabrication of these micro-systems are sometimes referred to either as micro-system technology (MST) or MEMS techniques. In order to differentiate from other manufacturing techniques, micro-manufacturing techniques are often categorized respectively as MEMS manufacturing and non-MEMS manufacturing. MEMS

manufacturing involves, largely, techniques such as photolithography, chemical etching, plating, LIGA, laser ablation, etc. while non-MEMS manufacturing often involves techniques such as EDM, micro-mechanical cutting, laser cutting/patterning/drilling, micro-embossing, micro-injection molding, micro-extrusion, micro-stamping, etc. Regarding the materials used, micro-manufacturing is also sometimes categorized as silicon-based manufacturing and non-silicone material manufacturing. The purpose of differentiating these is sometimes to emphasize the importance of the latter as an urgent need for development, since silicon-based manufacturing is often seen as a 'mature' business.

For people who are involved in MEMS-based manufacturing, micro-manufacturing may be not a new term, as they may feel that manufacturing various MEMS has been undertaken by industry for many years, which has also been performed at volume-production scales. For people who are newly engaged in non-MEMS-based manufacturing, micro-manufacturing is somehow seen as a recently emerging field of significant challenges. This is not only because manufacturing will have to deal with much wider ranges of materials, which cannot be handled by traditional MEMS-based manufacturing techniques alone, but also because scaling down the processes, tools and machinery from conventional ones such as mechanical/thermal cutting/forming to meet the needs of achieving much smaller dimensions and sophisticated features is new and extremely challenging. In this sense, the emerging micro-manufacturing techniques often refer to non-silicon-based and even non-MEMS-based manufacturing. A new definition of micro-manufacturing, therefore, may be the 'manufacture of micro-products/features with scaled-down conventional technologies/processes'. These include processes such as micro-machining (mechanical, thermal, electric-chemical, electric discharge methods), micro-forming/replication, micro-additive (rapid methods, electro-forming, injection molding, etc.) and joining. Another focus of micro-manufacturing is the manufacture of products/components with miniature

machines/systems, rather than conventional, large-scale machines/systems.

This book is focused on the description of non-silicon-based manufacturing, especially non-MEMS manufacturing techniques and systems, although there are several chapters dealing with the techniques for both MEMS and non-MEMS manufacturing. This chapter is intended as an introduction to micro-manufacturing.

MICRO-PRODUCTS AND DESIGN CONSIDERATIONS FOR MANUFACTURING

Typical micro-products include MEMS and micro-systems for automotive and aerospace use such as pressure sensors, thermal sensors, temperature sensors, gas sensors, rate sensors, sound sensors, injection nozzles, etc., and the components include those for electrostatic, magnetic, pneumatic and thermal actuators, motors, valves and gears [1]. The products also include sensors for mass flow, micro-heat exchangers, micro-chemical reactors, tools/molds for forming/replication, etc., and the components include those for miniaturized electronics products such as mobile phones, MP3 players, CD players, iPods, etc. In the medical sector, the micro-fabricated parts span a wide range for implantable applications in various clinical areas. There are 94 active and 67 commercial 'end items' out of a total of 142, according to the literature [2]. Typical examples are sensors for cardiovascular, micro-machined ceramic packages, implantable devices, coatings on micro-polymers or metal parts, etc. It is fair to say that micro-products and components are almost everywhere in our lives.

Table 1-1 presents some examples of the products/parts which can be made with micro-fabrication techniques, particularly with mechanical and/or thermal micro-manufacturing processes.

Design of products for micro-manufacturing needs to address production issues fully, compared with the prototype products based on micro-technologies. High volume production of micro-components should be a target for design for micro-manufacturing. When these products

are designed, not only will functional requirements need to be considered but also micro-manufacturing related factors will have to be taken into account. This is because, as briefly described above, manufacturing these products renders more significant challenges, compared to the manufacture of macro-products. The following are some typical issues to be addressed at the design stage:

- **Overall dimensions of the parts/products:** overall dimensions of a part/product, like diameters, widths, lengths and thicknesses, are very much constrained by the overall capabilities of the processes and manufacturing facility (machines, handling devices, tools, etc.). Both maximum and minimum dimensions are the parameters to be checked with reference to the manufacturing system's capabilities. Complexity around dimensional scale issues is a dominant factor in micro-/nano-manufacturing. The question often asked may be how small rather than how large a part can be handled.
- **Part/component local features:** design of local features, such as hole/pocket radii and aspect ratios, widths/depths of channels or aspect ratios, wall thickness, area reductions, density of the local features, will be largely constrained by the processing capability in micro-/nano-manufacturing, especially those relying on the use of tools such as replicating processes. There is also the factor of relevant grain size effects of the material to be used. Local features will not only determine the tool geometry, but also affect stiffness/rigidity of the part/product structures, and hence affect the manipulation of the part/product. Manufacture of local features spread over a large area also renders challenges to many micro-manufacturing processes and equipment, even nano-manufacturing.
- **Shape capability:** shape capability considers the capability/limitation of a manufacturing process in dealing with the shapes to be produced. For example, a lot of processes are only able to deal with 2D/2.5D shapes while 3D shapes may need much more significant efforts such as new processes and expensive equipment. Rotational symmetry is probably favorite for micro-

TABLE 1-1

Components/ Parts	Sample Geometry/ Features	Possible Enabling Techniques	Typical Part Materials	Processing Accuracy	Typical Products/ Applications
Surface 2.5D functionalized structures	Local features in hundred nanometers to 10s of microns	Hot embossing/coining/ imprinting, ink-jetting, plating, direct writing, laser ablation, etc.	Polymers, glass, aluminum, copper, brass, steel, etc.	Several microns to nanometers	Micro-optical, fluidic devices, force transmit. surfaces, dies/ molds, etc.
Lead frames	Various geometry, local features as small as ten microns, thicknesses vary, such as between 0.3 and 0.01 mm	Micro-stamping, with/ without laser assistance, laser cutting, photo- chemical etching, etc.	Copper and alloys, nickel steel, etc.	Several microns or to 10% of the sheet thickness	Electronics products
Micro-pins	Diameters in 0.2–1 mm ranges, wall thickness in 50 to 200 microns possible, and tolerances <5 microns	Forward, and/or combined with backward extrusion, micro-shape rolling, micro-machining/EDM.	Various types of metals	Several microns to sub-microns	Various applications as IC carrier, micro- device assembly, electric contacts, etc.
Electro-thermal- mechanical actuator	2.5D/3D structural parts, various sectional geometries	Chemical etching and micro-stamping, laser cutting, efab.	SMA and other metal materials	Several microns	Micro-actuating devices
Micro-cups	Micro-cups, less than 1 mm in diameter, various thicknesses	Micro-deep drawing, micro-stamping, micro-spinning, micro-machining.	Molybdenum, copper, aluminum, steel	Several microns	Electron guns, pressure sensors, UV sensors, etc.
Micro-gears	Diameters of 1 mm or less, local features in 10s of microns	Micro-forging, micro-extrusion, micro-stamping, LIGA, micro-casting, PCE, micro-EDM, efab., etc.	Metals, polymers	Several microns to sub-microns	Micro-mechanical devices, watches
Shafts for micro- mechanical drivers	Less than 1 mm in diameters	Micro-extrusion, micro- machining/EDM.	Steels and alloys	Several microns to sub-microns	Micro-driving- devices, e.g. micro-spindles
Micro-screws, micro-cans	Diameters in 0.1–0.5 mm ranges	Micro-forging, extrusion, shape rolling, micro- machining.	Various metals	Several microns to sub-microns	Micro-devices, housing and assembly, etc.
Micro-gear shafts	Local features in 30–50 microns	Extruded with local heating, micro-radial extrusion, micro- machining, EDM.	Metals	Several microns to sub-microns	Micro-mechanical driving devices, watches

Components/ Parts	Sample Geometry/ Features	Possible Enabling Techniques	Typical Part Materials	Processing Accuracy	Typical Products/ Applications
Casing/housing of micro-devices	Thin sheets, from 0.1 to 0.01 mm	Micro-stamping, dipping, drawing, hydro- forming.	Stainless steel, aluminum, copper, etc.	Several microns	Micro- mechanical, electronics, medical, optical, chemical devices, etc.
Micro-tubular components	Outer diameters less than 1 mm, wall thickness larger than 20 microns	Micro-hydro-tube- forming, micro-rolling, micro-bending, laser machining, etc.	Metals	Several microns	Micro-shafts, micro-heat exchangers, micro-medical devices/implants
Micro-molds, dies and punches	Die-bore or inner pockets in less than 1 mm; punch diameter from 0.05 to 1 mm	Micro-EDM, laser- cutting, micro- machining, electro- forming, sintering, etc.	Tool steels, glass, powder, etc.	Several microns to sub-microns	Forming/ replicating processes, e.g. injection molding, embossing, extrusion, etc.

extrusion, for example, considering the effects of grains and grain sizes on the process. Any asymmetry may create difficulty in controlling the quality in micro-shaping. Excessive material accumulation, large reductions in area and sudden changes of the sections should also be avoided in forming/shaping. Others include the design of the draft for the workpiece for micro-forging, permitted drawing ratios and profiles of the drawn products in micro-sheet forming, etc. Conventional rules on shape capability of manufacturing may not be applicable to micro-manufacturing largely due to the sizes to be considered and limitation of the tool shapes that could be produced.

- **Tolerance and surface quality capability:** design of a macro-product would expect the designer to consult handbooks/standards before specifying a grade of tolerance and surface quality requirements. Design for micro-manufacturing may not be as straightforward as the design of a macro-product. Standards on manufacturing tolerances for design for micro-manufacturing, especially for non-MEMS-based manufacturing, have not been established

fully, while most of the data is 'in-house' determined/used. The designer may have to consult with the manufacturing engineers who are responsible for their own manufacturing capability.

- **Material capability:** selection of a material for micro-manufacturing will be constrained largely by availability of the material for volume production, due to the limited number of the suppliers currently operating in this field; however, the trend is improving, such as with nano-material suppliers, the number of which has increased significantly recently. New study/qualification of material properties may be needed if the material suppliers are not able to provide the material data relevant to micro-manufacturing, such as size effects and material property descriptions. The properties will have to be qualified for design uses, with consideration of size effects, and these have to be available with the inclusion of mechanical, thermal, electrical and magnetic properties, as appropriate, and others including biocompatibility, chemical compatibility, hydrophile and hydrophobe properties, etc. Grain sizes of the

material to be selected must also be known for most of the micro-manufacturing processes. Ultimately, the designer has to know which processes are most suitable for the materials selected, or materials suitable for available processes, etc.

- **Part/component material properties after processing:** involvement of large plastic deformations, damages, possible significant local temperature rise and thermal stresses during mechanical and thermal processes may, very likely, result in alteration of the material properties after processing. The micro-part/component material properties will play significant roles in determining part/component performance under working conditions than that for macro-components, such as those used in micro-sensors and medical implants. Part/component design is, therefore, constrained by the applicability of certain micro-manufacturing processes, e.g. chemical and high temperature processes, due to considerations of possibly adverse effects on the material properties.
- **Characteristics of volume production:** the design should also address significant characteristics of volume production in micro-manufacturing. Prototyping in a lab scale is significantly different from manufacturing the products in a production-scale. Achievable/targeted production yield, which is prescribed largely by the capability of the processes, machinery, tools and auxiliary equipment, will have an influence on the selection of the materials for manufacturing and design of the part/component and its features. Among those factors, handling the parts/components and interactions with tools are particular concerns that should be taken into account at the design stage.
- **Manufacturing cost:** Manufacturing cost is a major issue to be addressed. This is largely because micro-manufacturing often involves high investment in facilities and human resources and low product quantity requirements from each customer. Many factors prescribe the manufacturing cost, and a balance,

however, will have to be maintained between the feasible reduction of the cost for core processes and the cost involving the use of auxiliary processes. Some sophisticated geometry and tight tolerances may not be achievable solely with a single process, and using a process chain which may involve various processes is often inevitable. The designer has to be aware of how the design specifications will impact on planning for the manufacturing chains. He/she has to realize that the cost for tooling for some micro-manufacturing processes may be very high. A comparison among available manufacturing processes/chains and even involving supply chains may be needed, even at the design stage.

- **Synthesis factors:** design synthesis may be conducted by considering all factors discussed above. The results can be a basis for design optimization. Strong dependences of the component/part design on the manufacturing processes in micro-manufacturing suggest that design iterations and interactions with manufacturing personnel are often inevitable and necessary.

The design of micro-products is still a challenging task due to lack of sufficient standards, design/manufacturing rules and understanding of the manufacturing processes themselves. There is also a lack of effective software to support the design activities. Incorporating size effects into conventional design and analysis software and/or developing domain-specific design and analysis tools (software) will help to improve the situation. Modeling for different length scales such as micro-mechanics modeling, molecular dynamics modeling and multi-scale modeling, and integration of these into commercial software, are urgent needs for design for micro-manufacturing. Some of these will be mentioned in several chapters of this book.

MATERIAL FACTORS

Material properties have much more significant impact on the design/planning for micro-manufacturing, compared to that in

macro-manufacturing, which, for example, is reflected in the following aspects:

- Size effects on mechanical, thermal, electrical and magnetic properties, biocompatibility and chemical compatibility, hydrophile and hydrophobe properties, etc. need to be understood, and some of these may be significantly different, compared to the material behaviors in the macro-scale.
- As a consequence of the above, mechanisms of material conversion processes (separation, deformation, joining/deposition chemically and physically) will be different or affected, as well as interactions between the materials and processing tools (for tool-based processes).
- As a consequence of the above, selection of the means for enabling material conversion processes will be affected, the considerations including effectiveness and efficiency and effects on the material properties of the processing methods (mechanical, chemical, thermal, electric-chemical methods, etc.).
- Grain and grain boundaries, which may have less impact on the material conversion processes in macro-manufacturing, will have a more significant impact on the material conversion mechanisms as the dimensional scale decreases and the sizes of the grains become more relevant, such as influence on the interfacial friction and dislocation of grains and damages. This is particularly relevant in mechanical material conversion processes.
- Emphasis on the importance of the material-related issues in micro-manufacturing is also due to lack of sufficient, effective means for qualifying some material properties in the micro-scale, and hence insufficiently understanding these.

In design and planning for micro-manufacturing, special attention should be given to the micro-structures of materials such as grain sizes, grain boundaries, precipitations and intermetallics as second phase particles and their size and distribution in multi-crystalline structures, against the sizes of micro-products/features (less than 1 mm in dimension). Developing new materials and increasing volume of the materials available for

particular micro-manufacturing processes are needed: otherwise, micro-manufacturing will be constrained significantly by the limited number of the materials which could be processed in the micro-scale with the required quality and efficiency. A typical example is that the type of the materials usable in micro-replication/forming processes is quite limited by material flowability, strength, hardening and surface adhesive behaviors. For a volume production, fine grains and high plastic flowability of the material either at room temperature or at elevated temperature are preferred.

The following are some examples of the materials used in micro-manufacturing: materials with finer grain sizes; alloying of elements with high purity grades; modification of surface roughness, e.g. laser defined micro-structured surfaces; materials with defined strain hardening; materials originated from galvanic processes; single crystal material with mono-crystalline structure; materials by thin wire processing, e.g. bond wires for microelectronics; materials by thin foil precision cold rolling; materials with special coatings; materials with total or selective plating of strips; materials for thin film coating; materials for roll cladding strips; etc.

CONSIDERATIONS ON MANUFACTURING METHODS

Compared to the manufacture of macro-products, manufacturing methods and strategies in micro-manufacturing may be different. Manufacturing macro-products may be carried out by manufacturing individual components/parts by removing and/or deforming and/or adding materials, and then assembling them. These can be carried out either at a single industrial site or at different sites. Manufacturing micro-products may be carried out with patterning, deposition and layering methods within a single machine/manufacturing platform, e.g. integrating components/parts fabrication with assembly/packaging is often used in MEMS and micro-systems manufacturing. Micro-manufacturing largely uses non-traditional manufacturing methods or scaling down or

modifying the traditional methods, as appropriate, to fully address issues related to manufacturing in the micro-world. Further, manufacturing chains may also be different, compared to traditional manufacturing. These may be due to:

- **Material property:** conventional manufacturing methods may not be able to cope with special material properties, e.g. either too hard or too weak for a process, sticking onto micro-tools, not compatible to the mask materials, or original material properties cannot be altered during manufacturing, e.g. affected by mechanical work-induced heat or direct heating processes, etc.
- **Structural strength and stiffness:** components/parts may be too fragile to sustain any mechanical forces needed for processing materials, or too difficult to handle during processing and/or assembly/packaging.
- **Shape and size – length scale factors:** all factors associated with small dimensional scale manufacturing apply, e.g. inability of tool fabrication for mechanical cutting and plastic forming may force the consideration of non-mechanical approaches. Normal geometric shapes such as holes, slots, pockets, threads, etc. may not be a problem in macro-scale manufacturing, but these may be extremely difficult to achieve if the dimensions decrease to sub-millimeters. Alternative manufacturing methods to conventional ones such as patterning, deposition and layer manufacturing methods may have to be considered.
- **Difficulties for clamping/releasing:** due to the sizes and structuring strength/stiffness issues, it may be difficult to clamp/release the components/parts to be made by mechanical manufacturing methods such as mechanical cutting and forming. Alternative methods such as laser ablation, electro-forming and chemical etching may be considered.
- **Residual stress and surface integrity:** existence of the residual stresses and weakened surface integrity, induced by plastic deformations, cyclic loadings, thermal gradients, etc., may not be acceptable for some critical components/parts for micro-products, e.g. those for

medical implants and high grade sensors. Selection of processes may have to consider such issues and process chains may have to be optimized to address these issues.

Fundamentals of the roles that the reduced length scales could play in various processing mechanisms need to be understood, e.g. roles of the surface at different length scales and in different manufacturing processes with respect to surface fabrication and micro-/nano-manipulation, surface metrology, etc. [3–4]. These play a significant role in selecting manufacturing methods and in optimizing the manufacturing chains.

MANUFACTURING METHODS AND PROCESSES

Both conventional and non-conventional methods have been used to manufacture micro-products. There have also been emerging methods such as hybrid manufacturing. According to the type of energy to be deployed, manufacturing may be classified as mechanical, chemical, electro-chemical, electrical and laser processes. The working principles include mechanical forces, thermal, ablation, dissolution, solidification, recombination, polymerization/lamination and sintering [5]. According to the way in which the components/products are to be made, general manufacturing processes can also be classified into subtractive, additive, forming, joining and hybrid processes. The classification is equally applicable to micro-manufacturing. Typical manufacturing methods for producing components/products are as shown in Table 1-2.

Some typical micro-manufacturing methods/processes are detailed in this book. The following texts give an overview of some key methods and processes, as well as the current state of the development.

Mechanical Machining

Mechanical machining is a technology that has been widely investigated in the field of precision engineering. Micro-machining may be seen as an ultra-precision material removal process which is

TABLE 1-2 Typical Methods/Processes of Micro-Manufacturing (edited based on a table presented in [5])

Subtractive processes	Micro-mechanical cutting (milling, turning, grinding, polishing, etc.); micro-EDM; micro-ECM; laser beam machining; electro beam machining; photo-chemical machining; etc.
Additive processes	Surface coating (CVD, PVD); direct writing (ink-jet, laser-guided); micro-casting; micro-injection molding; sintering; photo-electro-forming; chemical deposition; polymer deposition; stereolithography; etc.
Deforming processes	Micro-forming (stamping, extrusion, forging, bending, deep drawing, incremental forming, superplastic forming, hydro-forming, etc.); hot-embossing; micro-/nano-imprinting; etc.
Joining processes	Micro-mechanical-assembly; laser-welding; resistance, laser, vacuum soldering; bonding; gluing; etc.
Hybrid processes	Micro-laser-ECM; LIGA and LIGA combined with laser-machining; micro-EDM and laser assembly; shape deposition and laser machining; efab.; laser-assisted micro-forming; micro-assembly injection molding; combined micro-machining and casting; etc.

able to achieve micro-form accuracy and several nanometer finishes [6]. From precision machining to micro-machining, some challenging issues are met such as predictability, producibility and productivity in micro-scale manufacturing [7]. It may be difficult to achieve complex 3D, intricate micro-features/components with mechanical micro-machining, although it is still a powerful technology in developing micro-components for various systems such as those operating on electronic, mechanical, fluidic, optical and radiative signals [8], e.g. the systems for micro-instrumentation, inertial sensing, biomedical devices, wireless communication, high density data storage, etc. as well as producing dies and molds for other manufacturing processes such as micro-forming and injection molding [6–8].

Due to the working principle of removing chips by mechanical forces, significant efforts have been devoted to the improvement of the precision of machine tools and development of error-compensation methods to ensure the required precision of the machine-tool-workpiece system. Main issues addressed include understanding of chip formation mechanisms and micro-machining mechanics, machine tool design with ‘optimal’ dynamics stiffness, optimal cutter geometry/materials and motion control, in-process inspection with high resolution metrology, etc. [6–7]. The trend for bench-top machine tool designs has now shifted from large-scale, ultra-high precision designs to miniature structures and low cost system designs. Ultra-high precision and high speed spindle design

is another topic attracting many researchers and industries. Diamond cutting tools, tools with nano-crystalline diamond coating [9], etc. are also important in micro-machining.

Micro-EDM

Electro-physical and chemical micro-machining processes play important roles in micro-manufacturing due to their special material removal mechanisms [10]. Electrical-discharge-machining (EDM) is especially suitable for manufacturing micro-components/tools due to its thermal material removal mechanism, which allows almost process force-free machining independently of the mechanical properties of the processed material. High precision EDM can process functional materials like hardened steel, cemented carbide and electrically conductive ceramics with sub-micron precision [11]. Its applications have extended far beyond dies/molds fabrication such as micro-gears, micro-fluidic devices, medical implants, etc. The processes include micro-wire electrical discharge machining, micro die sinking, micro-electrical discharge drilling, micro-electrical discharge contouring and micro-electrical discharge dressing.

Compared to conventional EDM, micro-EDM places more emphasis on the following:

- Precision of the machine, e.g. high precision control of the motion of the electrodes;
- Qualification of the wear of the electrodes, damage on the wire, and compensation for the wear/damage;

- Careful control of the frequency of discharge, level of the energy input, e.g. current and voltage;
- Better understanding of material properties, thermal conduction of the workpiece, melting and recasting processes, and their effect on the surface finish/integrity;
- Careful considerations of the set-up of gaps, component forms to be produced, flash of the debris, etc.

Besides the miniaturization of the tool electrodes, compared to conventional EDM, the minimum discharge energy of $0.1 \mu\text{J}$ is obtainable, which causes only very small material removal at one single discharge. This results in an extremely small gap width ranging from 1.5 to $5 \mu\text{m}$ [11]. To achieve a reasonable material removal rate, spark generators which are able to produce extremely high impulse frequencies have to be used, e.g. capable of impulse frequencies of up to 10 MHz .

Micro-electrochemical Machining (MECM)

ECM is another popular choice for making micro-parts, due to less effort needed for handling during the ECM, easy control of the process, relative simplicity in machine design/set-up (CNC possible) and the capability to process various materials, including high strength materials. Other attractive characteristics include burr-free surfaces, no thermal damage, no distortion of the part and no tool wear. The issues needing to be addressed in micro-manufacturing applications include controlling material removal, machining accuracy, power supply, design and development of micro-tools, roles of inter-electrode gap and electrolyte, etc. [12–13]. High surface roughness, relatively poor fatigue properties, difficulty to make sharp corners, etc. are some negative aspects to be taken into account when considering this process for manufacturing. For micro-machining, masks may be used (one side or two sides possible) for making finer geometry. For precision manufacturing, a pulsed power of relatively short duration (about 1 ms) may be used, which may enable

shorter inter-electrode gaps ($<50 \mu\text{m}$) to be utilized. These small gaps with good process control could yield accuracies of the order of $\pm 1 \mu\text{m}$ on $50 \mu\text{m}$ and surface roughness of $R_a 0.03 \mu\text{m}$.

Micro-forming

Micro-products may be produced with forming configurations, i.e. micro-forming. Metal forming offers some attractive characteristics that are superior to those of other processes, e.g. machining and chemical etching, considering such features as higher production rates, better material integrity, less waste, lower manufacturing costs, etc. Various forming/forging configurations are possible such as forging, extrusion, stamping, bending, hydro-expansion, superplastic forming, etc. Micro-forming may be achievable by effective scaling down of the process configurations, tools and even machines [14–17]. Some challenges do arise when the sizes/features reduce to tens or hundreds of microns, or the precision requirements for macro-/miniature parts reduce to less than a few microns. Major issues to be addressed include understanding of material deformation mechanisms and material/tool interfacial conditions, materials property characterization, process modeling and analysis, qualification of forming limits, process design optimization, etc., with emphasis on the related size effects. The following observations have been established based on a series of studies and RTD efforts:

- Conventional metal-forming process configurations such as forging, extrusion, stamping, coining, deep drawing, etc., may be equally used for the forming of miniature/micro-parts; process capabilities are likely to be constrained further due to additional material and interfacial and tooling considerations in micro-forming.
- The types of materials which could be formable at the micro-level are prescribed more significantly than for forming at the macro-level by the micro-structures and grain-boundary properties of the materials. The forming limits for these materials are, therefore, somewhat different, compared to those for the forming of macro-parts.

- Size effects may exist in material property and tool/material interfacial property characterization, depending largely on the micro-structures of the materials, which lead to the requirement of the definition of these parameters with reference to the actual materials and interfaces to be used.
- Machines, forming tools and handling devices are critical in the industrial applications of micro-forming technology.

Some traditional forming machine designs may be scaled down for micro-forming needs, as long as the machines are able to cooperate with the use of micro-tools of acceptable quality and efficiency. However, more particular considerations will have to be incorporated into machine design to meet engineering applications requirements, e.g. greater precision, handling of micro-parts/materials with higher rates and positional precision, etc. [18–20]. Several chapters of this book deal with the machine development for micro-forming, the results taken from an EU-funded project – MASMICRO [16–17]. Applications of the micro-forming technology also rely largely on the development of micro- and even nano-machining technologies. The latter is key to the fabrication of micro-tools and the preparation of micro-materials.

Laser Technology

Laser technology is qualified as an efficient micro-technology because of its high lateral resolution by minimized focusability down to a few microns, low heat input and high flexibility. One major advantage is its capability of processing various, non-silicon materials that are increasingly needed for manufacturing micro-products. Some examples for laser applications are micro-cutting, micro-drilling, micro-welding, soldering, selective bonding, micro-structuring and laser assisted forming [21]. Femtosecond laser micro-machining is a new approach emerging in the MEMS area, and some promising results have been shown in micro-machining and micro-system applications, including industrial material processing, biomedicine, photonics and semiconductors

[22]. The ultra-fast or ultra-short laser means that the laser pulse has a duration that is somewhat less than about 10 picoseconds – usually some fraction of a picosecond (femtosecond) (a picosecond = 1×10^{-12} second) [23]. It utilizes the ultra-short laser pulse properties to achieve an unprecedented degree of control in sculpting the desired micro-structures internal to the materials without collateral damage to the surroundings. It has been proven that micro-structuring with femtosecond laser pulses is an excellent tool for free design micro-fabrication of almost all kinds of materials [24]. With the filament, spatial scanning and other methods, many types of optical microstructures (including 3D) such as optical memory, waveguides, gratings, couplers and photonic crystals were produced successfully inside a wide variety of transparent materials of solid state and also liquid state [24].

Heating has been widely used for assisting in forming processes, largely due to the improvement of the material followability and reduced strength at elevated temperature. Therefore, the forming processes can be easier and forming loading can be reduced. The influence on the forming tools is a mixture of the reduction of the forming pressures and superimposition of thermal loads from the heating. Introducing heating helps to process materials with higher strength and/or to extend forming ability including component/part forms and dimensions and aspect ratios. Heating with laser is especially effective for the forming of sheet metals or thin sections from bulk materials [25]. By selectively applying the laser beam to the focused area(s), the laser can be used in processes such as bending, deep drawing, stamping, can extrusion, tube forming, etc. [21]. Transparent tools made of sapphire permit the guidance of the laser radiation directly onto the workpiece within the closed tool set during the process. This means that no separated preheating step is needed and extended processing time is avoided.

Replication Techniques

Replication techniques like LIGA, micro-injection molding, micro-casting and micro-embossing

are seen as solutions to low cost, mass production of micro-components/features, reel-to-reel UV embossing being a good example for mass production. Materials that can be processed with replicating techniques include metals, glass, polymers, etc. Especially, embossing, molding and casting are very effective for fabricating microstructures for optical elements/devices [26], which can produce high resolutions possibly in the nanometer ranges with some processes, and allow the fabrication of large areas and complex micro-structures. Processes for gratings, holograms and diffractive foils are well established. Efforts are continually being made to extend the process capability such as increasing the aspect ratios of the micro-structures, producing these in larger areas (such as replicating micro-structures with optical functions with dimensions between 200 nm and 50 μm on areas of up to half a square meter), combining embossing with other processes such as lithography, dry etching and thin-film coating, etc. Micro-powder injection molding (μPIM) is a potential low cost mass fabrication process for manufacturing micro-structures and micro-components [27]. It could be used for processing many different materials (e.g. ceramics and metals) for very complex geometries. For making small geometries, silicon mold inserts may be used, taking advantage of deep reactive ion etching. The processing parameters need to be carefully set in order to produce the required quality and small features. LIGA, an alternative micro-fabrication process combining deep X-ray lithography, plating-through-mask and molding, enables the highly precise manufacture of high aspect ratio micro-structures with large structural height ranging from hundreds to thousands of micrometers thickness which are difficult to be achieved with other manufacturing techniques. Significant progress in MEMS manufacturing is largely due to the introduction of the LIGA process. The polymer LIGA process is especially suitable for mass production. There is a chapter in this book specially describing this process.

Deposition Methods

The methods are seen as effective ones for fabricating multi-material devices with no need to increase the process chain. Possible methods for micro-manufacturing include laser-assisted chemical vapor deposition (LCVD), laser guided direct write (LGDW) and flow-guided direct write (FGDW), shape deposition modeling (SDM), localized electrochemical deposition, etc. [28]. For example, a similarity between the silicon-based MEMS methods and shape deposition manufacturing (SDM) is that 'both integrate additive and subtractive processes and use part and sacrificial materials to obtain functional structures' [29], while the latter is able to deal with more types of the materials.

A micro-rapid prototyping system based on a deposition technique may include micro-deposition, ultrasonic-based micro-powder feeding, dry powders cladding/sintering, laser micro-machining (a laser beam with a wavelength of 355 nm, for example) [29]. Fabrication of meso- and micro-structured devices by direct-write deposition and laser processing of dry fine powders is also possible [30], which is also seen to be an effective way to fabricate 3D structures with heterogeneous material compositions. The direct-write deposition system is able to produce a '100 μm minimum attainable feature size for device footprints ranging from sub-millimeter to a few centimeters' on a movable substrate. The prototype devices produced included micro-battery, interdigitated capacitor, fractal antenna, Swiss-roll micro-combustor, and functionally graded polymeric bioimplants. By combining an electric-chemical method and an etching method, a new manufacturing technique, so-called Efab manufacturing (a system developed by MEMGen, USA), has been developed [31]. The method adds layers from 2 to 20 microns thickness and is able to create 3D metallic features with support of the sacrificial material that is etched away late.

SDM combining micro-casting with other intermediate processing operations (CNC machining and shot peening) was also attempted to create

metallic parts [32]. The better product quality could be achieved with proper control of inter-layer metallurgical bonding (through substrate remelting) and the cooling rates of both the substrate and the deposited material. Another good example of fabricating complex metallic micro-structures is to use lithography and etching techniques to make sacrificial silicon molds. The multiple silicon layers are stacked and the metallic glass is then forced into the cavities under heat and pressure in an open air environment. Such an approach could be a solution for low cost manufacturing [33].

The inkjet technology offers a prospect for reliable and low cost manufacture of flat panel displays (FPD). Compared to other conventional processes, an inkjet printing method for color filters (C/F) in LCD or RGB patterning in OLED offers potential for the mass production of the enlarged display panels with low costs [34].

Assembly/Packaging

Basic processes for micro-assembly and packaging include mechanical placement/insertion/pressing, micro-welding; resistance/laser/vacuum soldering, micro-casting/molding, bonding; gluing, etc. Interconnection and packaging solutions (e.g. 3D molding of interconnect devices) are the key technologies for connecting micro-systems to the macro-world. Molded interconnect devices (MID) technologies include insert molding, one shot molding and two shot molding. Assembly/packaging gains more importance with the growth of complexity and miniaturization of the products and systems. Although significant progress has been made in the manufacture of individual micro-components/parts, as well as MEMS, there is still a significant amount of manual work involved in assembly/packaging of micro-products and systems. Assembly of individual technical components to hybrid micro-systems is often a bottleneck to large-scale production [35], which is evident especially in the areas of heterogeneous assembly, online inspection and quality control. Integration of micro- and nano-devices through

assembly is still a new area of challenge. A method for achieving electrical and mechanical interconnects for use in heterogeneous integration was combining metal reflow and a self-aligned, 3D micro-assembly [36], which allows for the batch processing of a large number of heterogeneous devices into one system without sacrificing performance. Micro-assembly injection molding gives another option for joining plastics and some inlay part such as fiber reinforced needle and other elements [37]. The use of lasers for welding has exhibited tremendous growth over the last decade for improving efficiency and reducing costs in a broad range of industries for the manufacture of both macro- and micro-components [21,38]. Efforts are continually being made for the better understanding of processes and for controlling key parameters for better quality and efficiency. Online inspection on joint quality is an important issue for industry. For some micro-device assemblies, there was almost no efficient online inspection system available for industry to use, and therefore quality control was extremely difficult. Another key issue for both MEMS- and non-MEMS-based manufacturing is the need for effective and efficient gripping techniques/systems and corresponding manipulation strategies/means for micro-assembly [39].

PROCESS CHAINS AND HYBRID PROCESSES

Manufacture of a component/product often cannot be completed with a single process: it may involve a process chain. Better quality and efficiency of the manufacture could be achieved with a properly defined process chain. This also applies to micro-manufacturing which often needs several processes to complete a component. A typical example is combination of plating/coating, chemical etching and stamping to make 3D micro-sheet components. If micro-tooling is considered, the process chain is extended even longer. Various process chains are possible in order to meet various design and manufacturing specifications. For example: combining lithographic tooling and

injection molding techniques could enable mass production of micro-components with various materials such as polymers, metals and ceramics [40]; and an LIGA process could be improved by fabricating micro-molds with direct femtosecond laser micro-machining [41] – an approach that may lead to practical, cost-effective 3D MEMS with various materials. Ultra-precision manufacturing of self-assembled micro-systems (UPSAMS) is another example of this kind of development, which combines ultra-precision micro-machining such as milling, turning, drilling, and grinding with sacrificial/structural multilayer manufacturing processes to produce self-assembled, 3D micro-systems and associated meso-scale interfaces from a variety of materials for MEMS applications [42]. With this process, a new class of micro-systems could be developed that is highly three dimensional, precisely machined, and automatically assembled. Rapid fabrication of micro-components may also be effected with a combination of UV-laser assisted prototyping, laser micro-machining of the mold inserts and replication via photo-molding [43] which deals with materials such as polymers and composites. Another example is equipment development and applications of the pulsed laser for micro-machining of large-area polymer substrates with micro-structures which involve rapid prototyping, bow-tie scanning, synchronized image scanning (mask projection technique), etc. The applications include flat panel displays, solar panels, super-long inkjet printer nozzles, micro-lenses, diffusing structures fabrication, etc. [44].

Ideally, a process chain for micro-manufacturing should be short in order to achieve high efficiency, reduce manufacturing errors, and eliminate unnecessary handling/transport/packaging of micro-components among different processes. Hybrid manufacturing processes may take advantage of the merits of individual micro-manufacturing methods/processes while some of the inherited disadvantages may be reduced or eliminated, e.g. shortening the process chains. For example, micro-EDM and laser assembly may be combined to fabricate 3D metal

microstructures [45]. The system may use a micro-EDM process to fabricate micro-parts and laser welding to assemble these micro-parts. By such a combination, increased numbers of the patterns, higher aspect ratios and higher joint strength of the microstructures could be achieved. Another merit is reduction or elimination of the number of post-assembly operations which may involve various efforts in handling and high precision positioning. A new technology based on laser transmission welding, combined with a photolithographic mask technique, enables assembly of plastic micro-fluidic devices, MOEMS and micro-arrays which require high positioning and welding accuracy in the micrometer range [46]. The system created consists of a diode laser with a mask and an automated alignment function to generate micro-welding seams with freely definable geometries. A fully automated mask alignment system with a resolution of less than or equal $2\ \mu\text{m}$ and a precise, non-contact energy input allows a fast welding of micro-structured plastic parts with high reproducibility and excellent welding quality, as reported [46]. Combining the ECM and EDM, i.e. so-called hybrid ECM/EDM, is another example of improving the material processing efficiency. In EDM, sparks are needed (dielectrics), while these are unwanted for ECM (electrolyte, short circuit). The sparks would be encouraged for combined ECM/EDM with appropriate control. The applications include drilling of small holes in hard alloys, wire-machining removal of metallurgical samples, manufacture of dies and molds, etc. Other hybrid processes include laser-ECM and ELID processes.

MANUFACTURING SYSTEMS/ EQUIPMENT

Traditionally, some micro-manufacturing processes (non-MEMS manufacturing) were often effected with large-scale equipment, such as that for micro-mechanical machining, micro-EDM and micro-metal forming. To perform micro-manufacturing tasks with such equipment,

significant efforts were made to improve the precision of the machine structures, to compensate for mechanical and thermal errors, as well as to increase the functionality, resolution and reliability of the monitoring systems. The cost paid to achieve these has been very high, while the resulting equipment is too expensive, which actually limits their applications.

Miniature Manufacturing Systems and Bench-top Machines

During the last 15 years bench-top/desktop machines or miniature manufacturing systems have been gradually developed and introduced to industry. The development of such machines/systems has attracted a lot of interest from research organizations and industries. A main consideration is that conventional facilities for manufacturing miniature/micro-products are not compatible, in sizes, to the products to be made in miniature/micro-manufacturing. Therefore, it is necessary to reduce the scale of the equipment which could, in turn, reduce the energy consumption and material requirements, reduce pollution, create a more user-friendly production environment, reduce equipment cost, etc. At the same time, as the scales of the machinery and auxiliary equipment are reduced, the mass of the mechanical parts is reduced dramatically and, as a result, the speed of the manufacturing tools could be increased, which could result in increase in production rates. Another advantageous feature often mentioned is that the force/energy loop and the control loops are significantly shorter for small machinery; therefore, the precision of the machinery could be increased comprehensively. Micro-factories are typical examples of such facilities.

During the last 15 years several demonstration micro-factories (also called miniature manufacturing systems) have been developed [47], notably in Japan, but now also worldwide: a review was provided in the literature [16]. These systems and machines indicate a trend of developing the equipment for micro- and nano-manufacturing. The development of a

micro-factory itself renders significant challenges to the development of manufacturing facilities, e.g. stringent requirements on machine elements and assembly, as well as monitoring and inspection. In turn, the development of miniature machines or micro-machines also promoted the development of a micro-factory, which has resulted in various new micro-factory concepts. To date, many miniature machines/desktop machines have come to market, such as desktop milling machines, EDM machines, injection molding machines, laser-processing equipment, miniature-forming presses, multi-process equipment, etc. Compared to the traditional micro-machine concepts, currently commercially available desktop machines are relatively larger but closer to industrial application requirements. These may be seen as bridging the gaps between the micro-machines and conventional, large-scale machines.

Led by the Institute of Product Development (IPU) of Denmark, a miniature press and flexible tool system was developed for the forming of micro-bulk products [18]. The press is driven by a linear servo motor and is capable of fast and accurate motion. The tool system enables eight different bulk-forming processes to be carried out by changing only small portions of the tool elements. Precision of the tool system is crucial due to narrow tolerances on the dimensions of the micro-components to be formed, which requires the manufacture of die cavities within the sub-millimeter range in diameter and within a few microns in geometrical accuracy.

A linear motor-driven micro-sheet-forming machine system (bench-top machine) was developed at the University of Strathclyde, UK [19], in collaboration with Pascoe Engineering of Scotland, Tekniker of Spain and other EU partners. The machine is capable of a series of micro-sheet-forming processes for forming thin sheet-metal parts with thicknesses below 100 microns. The machine has a capability of up to 800–1000 strokes per minute, a force capacity of 5 kN, and machine precision of 2–5 microns, with modular and flexible set-up. The machine is equipped with a newly designed, linear-stage driven, high

speed feeder which enables feeding accuracy (thin strips) of less than 5 microns. With properly designed pilot pins deployed in micro-sheet forming, higher positioning accuracy could be achieved. Another novel development was to transport the parts directly out of the tooling system with a novel part-carrying system. The machine is also equipped with a force-displacement monitoring system which reads the data directly from the tooling.

The Institute of Production (IFP) of the University of Applied Science Cologne, Germany, leads the development of the first generation hydroforming machine for the forming of miniature/micro-tubular components [20]. Hydroforming processes were employed successfully in industry for mass production predominantly relating to lightweight automotive components. The mass production of such components at present is, however, limited largely to parts with cross-sections of above about 20 mm in width. There was a lack of experience in the hydroforming of tubular, miniature/micro-parts. A machine system has been developed for forming miniature tubes down to 0.8 mm with thicknesses down to 20 microns. The applications of the system will significantly extend micro-manufacturing capabilities, especially the manufacture of hollow sectioned parts, such as those used in micro-housing, fluidic devices, light-weight structures in micro-mechanical devices, etc., which have not been achieved before.

A bench-top, multiple-axis machine tool capable of machining intricate 3D geometries in components with nano-scale tolerances was developed [48–49], led by Brunel University and Ultra-Precision Motion Ltd of the UK. The associated new series developments include an air bearing slideway and a rotary table with improved damping capacity (patented) and an ultra-high-speed air bearing spindle (Loadpoint Ltd/Ultra-Precision Motion Ltd of the UK), a piezo-driven fast tool servo system and piezoelectric actuation unit for vibration assisted machining (CEDRAT Technologies SA of France), new micro-diamond tools (Contour Fine Tooling Ltd of the UK), a robotic arm unit for

micro-components/tools handling and management (Carinthian Tech Research AG of Austria), and a tool and spindle condition monitoring system (University of Patras of Greece).

Multiple-process Equipment

Multiple-process equipment is an ideal solution to implement various process chains within an integrated platform, which could significantly reduce the number of component handlings. Another resulting benefit is reduction of the possible accumulation of manufacturing errors. The majority of the equipment/devices developed in micro-factory or miniature manufacturing systems cannot be classified as multiple-process equipment/devices since these are stand-alone machines which deal with a particular process.

The idea of multiple process equipment has received a very positive response in Asia, typical developments in this region including the multifunctional micro-machining equipment developed in a Chinese university which is able to perform several micro-machining processes on the same machine tool [50] – micro-electro discharge machining (EDM), micro-electrochemical machining (ECM), micro-ultrasonic machining (USM) as well as a combination of these. Using micro-EDM, micro-rods with a diameter of less than 5 μm were ground on a block electrode, and micro-holes and 3D microstructures were obtained. Shaped holes were machined with a combination of micro-EDM and micro-USM. Another similar multifunctional micro-machining system was developed in Ibaraki University of Japan, which is capable of micro-milling, turning, grinding, buffing, polishing, EDM, ECM, laser machining and combinations of these [51]. The applications included the fabrication of micro-lens molds. A recent development undertaken in National Taiwan University was a multi-function high precision table-top CNC machine [52]. With this machine, the machining processes such as micro-high speed milling and micro-EDM (die-sinking and wire EDM) can be performed on the same machine without need of unloading, reloading and readjusting the workpiece

for the subsequent operations. The system was also equipped with an in-process workpiece/features geometrical measurement system. Micro-electrodes as small as 8 μm in diameter and diameter/slenderness ratios as high as 100 could be achieved. Similar development is also seen in Singapore [53] – a multi-process miniature machine tool which includes processes such as micro-EDM, micro-ECM, micro-turning, drilling, and milling, as well as electrolytic in-process dressing (ELID), grinding and single point diamond tool cutting. A micro-factory as a whole may be seen as a platform that integrates several processes through several micro-machines on the same platform [47].

Another interesting development which targeted low cost equipment was a five-axis milling machine for machining micro-parts [54]. The machine presented was mainly composed of commercially available micro-stages, an air spindle and PC-based control board. The machine was used for machining micro-walls, micro-columns and micro-blades. Although this development does not involve multiple processes, it explores an interesting concept that targets low cost equipment which may be exploited for the development of multiple-process equipment.

Supporting Technologies/Devices/Systems for Micro-manufacturing

Considering handling at the micro-scale, factors such as gravity cannot be considered as a main force applied to the parts to be handled. Unwanted surface forces such as van der Waals, electrostatic and surface tension forces are dominant at such a scale [55]. The pick-and-place issue has to be addressed fully, due to the existence of adhesive forces. In micro-handling the possible joint backlash and structural vibration due to link flexibility may have to be controlled at the level of several microns during automated positioning. Higher care on manipulation and cleanliness are required also. The problems associated with micro-handling may be well understood, but a key challenge is still handling to match the high production rates to be deployed with some

miniature/micro-manufacturing machines such as micro-stamping machines. This is far more difficult to achieve, compared to that in a slow assembly/packaging process.

Sensor systems play an important role in many fields of manufacturing. Their applications in micro-manufacturing such as that in equipment and that for online inspection require high levels of accuracy/resolution of the sensors. Data processing near the sensors, extracting more information from the directly sensed information by signal analysis, system miniaturization, multi-sensor uses, etc. are the new demands [56]. Single-function transducers may now not be sufficient to meet the needs, and the system-based sensors as system components are being introduced: systems containing sensors, actuators and electronics are being developed.

Micro-manufacturing technologies are still being developed, and quality assurance plays an even more important role in order to 'efficiently support the transition of micro production processes from non-robust to stable processes' [57]. Quality assurance faces particular challenges at the production level – some common quality methods for macro-length scale manufacturing may be difficult or even impossible to be applied/implemented. The need for the development of the technologies and systems for dimensional metrology at different length scales and integrating them is evident. As critical dimensions are scaled down and geometrical complexity of the objects increases, the available technologies and systems may not be able to meet current and development needs. 'New measuring principles and instrumentation, tolerancing rules and procedures as well as traceability and calibration, etc. will have to be developed' [58]. There are no micro-specific tolerance guidelines for general tolerances and these currently largely rely on experience, which is, normally, not statistically established in a factory site and/or has not been approached in a systematic way [59]. 3D measurement technology that would enable fast, accurate measurement of solid shapes in sub-micron and even nanometer regions is essential for micro-manufacturing tasks, e.g. triangulation and optical interferometry may be used in the 3D

measurement of the dynamic behavior of the MEMS devices [60]. Concerning surface inspection methods and the performance of non-contact profilers, there is no single system which is able to offer all the features that a general purpose user would like simultaneously [61]. Providing all possible means available and integrating them into a flexible system to allow users to deal with different inspection requirements may be a solution to meet the manufacturing needs.

DEVELOPMENT AND UTILIZATION STRATEGIES OF MICRO-MANUFACTURING TECHNOLOGIES

A series of methods and technologies has been developed in the micro-manufacturing field and the trend will continue. These methods and technologies are, mostly, materials and products oriented. This is particularly the case for manufacturing since many particular considerations need to be taken into account in the manufacture of micro-products, as discussed in previous sections. As far as a method and technology developer is concerned, it is particularly important to understand how the end-users assess the methods and technologies developed, and how a decision is made on the selection and utilization of the manufacturing methods and technologies, even when the product manufacturing requirements are known. Since significant knowledge gaps still exist, especially for those emerging micro-manufacturing technologies, plus significant lack of standards and manufacturing/production guidelines, selecting an appropriate technology/process for the manufacture of a particular micro-product may not be a straightforward task.

A methodology for the evaluation of the emerging technologies, particularly MEMS technologies, was proposed [62] which involves a 'triple-gateway' analysis, in terms of considering commercially or socially worthwhile features of the technologies:

1. A market gateway analysis on new uses, user skepticism about 'improved' performance characteristics, requirements for behavior

adjustment by the user, competitive technologies, unpredictable technological development and legal barriers.

2. A systems-management gateway analysis on the organizational structures of the company and business.
3. Across the technology/gateway threshold concerning four elements of technology uncertainty: innovativeness of technology, number of constituent technologies, manufacturing difficulties, and institutional changes required to introduce the new technology [62].

In some cases, to have a clear view on the issues such as competitiveness of the technologies and unpredictability of the technological development is not easy to achieve, while the issues relating to possible manufacturing difficulties and institutional change needs are particularly important to an industry. Similarly, lifecycle assessment (LCA) methods may be introduced to the assessment of emerging technologies such as micro-/nanomanufacturing technologies, e.g. assessment on the impact on the environment (eco efficiency improvement) which may consider materials, production, uses and disposal, possibly taking future changes into account [63]. Other methods for assessing micro-manufacturing methods and technologies are also possible, each of which may be focused on a particular issue such as scientific and technological issues, collaborative issues, etc.

Assessment of the emerging technologies to be utilized with a view to fully understanding the implication and impact on the business is very important. Experience should be learnt from previous cases in the MEMS field which saw that some enterprises were struggling to survive or disappeared from the business. A business built on immature prototype designs and products with low volumes always takes a risk. Micro-/nanomanufacturing, at the moment, may still be an expensive business which is characterized by high investment in resources (facilities, knowledge and skills) and often by low volume production and lack of a complete business chain locally. Decision making on the development or utilization of the technologies should take these factors into account, together with other technological issues,

such as dealing with multi-materials, small geometries, increased and complex functionalities of products, etc.

In particular, the following aspects should be looked at strategically in relation to the strategies of the development and utilization of micro-manufacturing methods and technologies.

Manufacturing and Supply Chains

Development of micro-manufacturing technologies largely depends on the demands and enthusiasm from industry. The industry's decision is influenced significantly by the perspectives of new business to be brought or improvement which could be made to the existing business. Besides the efforts in developing individual manufacturing technologies, completing manufacturing chains and providing industry with flexibility to optimize the manufacturing chains are also very important. This is not because significant numbers of micro-parts/components often cannot be produced/completed with single technology alone but also because an optimized manufacturing chain may result in better quality and efficiency. Since no single technology could claim to be dominant, a possible solution to the industrial applications of micro-manufacturing is to provide various technologies and means for the industry to be able to effectively and efficiently form the required process chain(s), with lower cost. Completing supply chains for micro-manufacturing-based business is another important issue to be addressed. Forming effective micro-manufacturing business chains is often affected by the lack of the required material and high quality tool supply, as well as auxiliary facilities such as that for inspection and testing, although demands on micro-parts/components is highly evident. Without complete and efficient and manageable supply chains, a sustainable micro-manufacturing industry cannot be established. Strategic efforts should be made to complete manageable micro-manufacturing supply chains regionally and/or globally.

Advanced methods and systems for supply chain management for the semiconductor

industry, and the micro-electronics manufacturing industry in general, are mature and have been applied to the industry widely. These have not been developed exclusively for addressing the emerging micro-manufacturing industry. One of the main challenges also results from the fact that significant numbers of enterprises in micro-manufacturing are small and only of a short time in business, etc. Development in material and production planning with good knowledge of cost implications is insufficient for emerging micro-manufacturing, including lack of the advanced MRP systems exclusively for micro-manufacturing. The lack of standards exclusively for micro-products, materials, manufacturing methods and technologies also makes management of the supply chains more difficult. Good strategies are needed for marketing and financing, considering the nature of micro-manufacturing for a new business. Attention should also be paid to recycling and reusing micro-manufactured products and materials.

Integration with Other Manufacturing Activities/Sectors

A good solution for fostering a micro-manufacturing industry may be to become associated with some other business or to give support to micro-manufacturing at an early stage of the development. There are two considerations. First, micro-manufacturing cannot be an isolated activity and it should be an efficient means for linking macro- and nano-manufacturing. There will only be limited impact from nano-manufacturing if it is not effectively integrated with micro-manufacturing. It is the same for micro-manufacturing – effectively building micro-systems or integrating results from micro-technologies and science, into the macro-systems, will be a key measure to the success of micro-manufacturing. Second, development of new micro-manufacturing business needs strong backing from successful businesses in macro-manufacturing, technologically and financially. Currently, significant numbers of business and research activities in micro-manufacturing are actually transformed from

macro-manufacturing, which has helped the development of micro-manufacturing tremendously. More attention should, however, be paid to the issues associated with the micro-world for which some methods and technologies cannot be simply ‘scaled down’ from the macro-world.

The micro-/nano-manufacturing industry may be still small, compared to other industries like transport, space, health, etc. However, it should really play roles in driving other industries to a new level. These may be reflected in the following aspects:

- Traditional industry needs breakthrough/transformation/improvement, considering significant competition and demands on the new products and higher quality. Achieving these cannot rely on organizational measures alone, but also requires, significantly, technological measures. Research and technological development in micro-/nano-manufacturing is one of most promising areas that could deliver the required solutions.
- Research in developing new micro-/nano-materials will meet many material challenging issues faced in traditional material and manufacturing industry – an area in which, currently, significant competitions exist.
- Manufacturing-process concepts evolved in micro-/nano-manufacturing research will significantly change/update traditional manufacturing concepts in terms of effectiveness and efficiency, these being due to the need for better understanding and control of the manufacturing processes as well as to the new way in which the products are manufactured in micro-/nano-manufacturing. No matter which length scale is to be dealt with, the process development in micro-/nano-manufacturing is of general significance to all length scale manufacturing.
- To be able to meet much more stringent requirements in tool fabrication for micro-/nano-manufacturing the process will deliver new knowledge and enabling techniques for the whole tool industry, which will better equip the traditional tool industry for meeting

new challenges and competition. Typical examples include tool dimensional precision and surface quality, tool material performance, etc.

- New manufacturing machine and system concepts, such as bench-top, miniature, micro-machines and systems, will have a significant impact on all manufacturing sectors in design, fabrication and use of the machines, in relation to performance, impact on users and environment, energy-saving, etc.
- Micro-/nano-technology products designed and/or prototyped in other sectors may have to be brought to market in order to have real impact/economical gains – micro-/nano-manufacturing is a sector that can make it happen.

Technological Performance/Maturity Level

Compared to macro-manufacturing, one of the difficulties in assessing the technological performance/competitiveness of a micro-manufacturing process and the equipment lies in the significant number of existing uncertainties. Capabilities on material, geometry, tolerance, production rate, ease to link with other processes and equipment, etc., are often difficult to be defined in general terms, as these are often affected by many factors as described respectively in several sections of this chapter. The strong material, dimensions and environment dependence in micro-manufacturing, including the skills of the workers, make comparison of different processes and equipment very difficult to achieve. Nevertheless, the following aspects should be examined in terms of assessing the technological performance and maturity level of a micro-manufacturing process and equipment:

- Geometry associated performance: achievable overall dimensions, feature geometry, tolerances, surface finish, possibility for length scale integration manufacturing, etc.;
- Material associated performance: type of materials processable, material property requirements/constraints (e.g. micro-structures and surface integrity), post-processing requirements, etc.;

- Production associated performance: yield, reliability, scalability, online/in-process monitoring/inspection ability, ease for integration into process chains, dependence on skills/environment, impact on the environment, etc.;
- Cost factors: all costing items including that for auxiliary processes and equipment (e.g. that for handling, assembly/packaging, cleaning, etc.).

Other Issues

Besides a series of activities such as economic analysis, decision analysis, technological forecasting, information monitoring, risk assessment, market analysis, externalities/impact analysis, etc., education and training are important for the micro-manufacturing industry. These are needed due largely to micro-manufacturing being generally a knowledge-intensive business.

REFERENCES

- [1] M. Gad-el-Hak, Micropumps, microturbines, and flow physics in microdevices, *Proceedings of SPIE – The International Society for Optical Engineering* 5055 (2003) 242–257.
- [2] R.A.M. Receveur, F.W. Lindemans, N.F. De Rooij, Microsystem technologies for implantable applications, *J. of Micromechanics and Microengineering* 17 (5) (May 2007) R50–R80.
- [3] R.E. Williams, S. Melkote, W. Sun, Y. Huang, B. Kinsey, D.G. Yao, Recent advances in micro/meso-scale manufacturing processes, *American Society of Mechanical Engineers, Manufacturing Engineering Division, MED* 16–2 (2005) 863–884.
- [4] L. De Chiffre, H. Kunzmann, G.N. Peggs, D.A. Lucca, Surfaces in precision engineering, microengineering and nanotechnology, *CIRP Annals – Manufacturing Technology* 52 (2) (2003) 561–577.
- [5] L. Alting, F. Kimura, H.N. Hansen, G. Bissacco, Micro engineering, *CIRP Annals – Manufacturing Technology* 52 (2) (2003) 635–657.
- [6] S.Y. Liang, Mechanical machining and metrology at micro/nano scale, *Proc. of SPIE – The International Society for Optical Engineering*, 6280 I, Third International Symposium on Precision Mechanical Measurements (2006) 628002.
- [7] X. Luo, K. Cheng, D. Webb, F. Wardle, Design of ultraprecision machine tools with applications to manufacture of miniature tools and micro components, *J. of Materials Processing Technology* 167 (2–3) (Aug, 2005) 515–528.
- [8] K. Najafi, Micromachined micro systems: miniaturization beyond microelectronics, *IEEE Symposium on VLSI Circuits, Digest of Technical Papers, Honolulu, HI, USA* (June 2000) 6–13.
- [9] G.M. Robinson, M.J. Jackson, A review of micro and nanomachining from a materials perspective, *J. of Materials Processing Technology* 167 (2–3) (Aug, 30, 2005) 316–337.
- [10] K.P. Rajurkar, G. Levy, A. Malshe, M.M. Sundaram, J. McGeough, X. Hu, R. Resnick, A. DeSilva, Micro and nano machining by electro-physical and chemical processes, *CIRP Annals – Manufacturing Technology* 55 (2) (2006) 643–666.
- [11] E. Uhlmann, P. Sascha and K. Schauer, Micro milling of sintered tungsten–copper composite materials, *J. of Materials Processing Technology* 167 (2–3) 402–407.
- [12] B. Bhattacharyya, J. Munda, M. Malapati, Advancement in electrochemical micro-machining, *Int. J. of Machine Tools and Manufacture* 44 (15) (Dec. 2004) 1577–1589.
- [13] J.A. MacGeough, M.C. Leu, K.P. Rajurkar, A.K.M. De Silva, Q. Liu, Electroforming process and application to micro/macro manufacturing, *CIRP Annals – Manufacturing Technology* 50 (2) (2001) 499–514.
- [14] M. Geiger, M. Kleiner, R. Eckstein, N. Tiesler, U. Engel, Micro-forming, *Annals of the CIRP* 50 (2) (2001) 445–462.
- [15] U. Engel, S. Geibdorfer, Microforming technology – on the way to industrial application? *Proc. of the 1st Int. Conf. on Micro-manufacturing, Urbana-Champaign, USA* (Sept. 2006) 21–30.
- [16] Y. Qin, Micro-forming and miniature manufacturing systems – development needs and perspectives, *Keynote Paper (plenary address) of the 11th Int. Conf. of Metal Forming, Sept. 2006, Journal of Materials Processing Technology* 177 (1–3) (2006) 8–18.
- [17] Y. Qin, Development of an integrated manufacturing facility for mass-manufacture of miniature/micro-products, *Keynote Paper, Proc. of the 1st Int. Conf. on Micro-Manufacturing, Urbana-Champaign, USA* (Sept. 2006) 35–40.
- [18] M. Arentoft, N. Paldan, Production equipment for manufacturing of micro metal components, *Proc. of the 9th International ESAFORM Conference on Material Forming, April, Glasgow* (2006) 579–582.
- [19] Y. Qin et al., Development of a new machine system for the forming of micro-sheet-products, *Int. J. of Material Forming, Springer Paris, ISSN 1960-6214, DOI: 10.1007/s12289-008-0098-9* (April 2008) 1–4.
- [20] C. Hartl, J. Lungershausen, J. Eguia, G. Uriarte, F. Lopez Garcia, Micro hydroforming process and machine system for miniature/micro products, *Proc. of Int. Conf. 7th euspen, Bremen 2* (2007) 69–72.

- [21] A. Gillner, J. Holtkamp et al., Laser applications in microtechnology, *J. of Materials Processing Technology* 167 (2–3) 494–498.
- [22] M. Xia and Y. Tu, An investigation of femtosecond laser micromachining, *Proc. of 2005 International Conference on MEMS, NANO and Smart Systems* 296–300.
- [23] P. Bado, W. Clark and Ali Said, *Micromachining Handbook* (2001), Clark-MXR, Inc. Ultrafast Laser Machining Division, 7300 West Huron River Dr. Ann Arbor, MI 48130.
- [24] Y. Li, J. Tian, Q. Sun, Micro-fabrication by femtosecond laser pulses, *Proc. of SPIE – The International Society for Optical Engineering* 6149 (2006) 61490X.
- [25] X. Peng, Y. Qin, R. Balendra, A numerical investigation to the strategies of the localised heating for micro-part stamping, *Int. J. of Mechanical Sciences* 49 (3) (2007) 379–391.
- [26] C.K. Malek, V. Saile, Applications of LIGA technology to precision manufacturing of high-aspect-ratio micro-components and -systems: a review, *Microelectronics Journal* 35 (2) (February 2004) 131–143.
- [27] N.H. Loh, S.B. Tor, B.Y. Tay, Y. Murakoshi, R. Maeda, Micro powder injection molding of metal microstructures, *Materials Science Forum* 426–432 (5) (2003) 4289–4294.
- [28] V. Kadekar, W. Fang, F. Liou, Deposition technologies for micromanufacturing: a review, *ASME Transactions, J. of Manufacturing Science and Engineering* 126 (Nov. 2004) 787–795.
- [29] X.C. Li, H. Choi, Y. Yang, Micro rapid prototyping system for micro components, *Thin Solid Films* 420–421 (Dec. 2, 2002) 515–523.
- [30] P. Kumar, S. Das, Fabrication of meso- and micro-structured devices by direct-write deposition and laser processing of dry fine powders, *ASME International Mechanical Engineering Congress and Exposition* (2004) 519–524.
- [31] P. Dvorak, Manufacturing macro and micro designs, *Machine Design* (Oct. 10, 2003) 76–78.
- [32] C.H. Amon, et al., Shape deposition manufacturing with microcasting: processing, thermal and mechanical issues, *J. of Manufacturing Science and Engineering, Transactions of the ASME* 120 (3) (Aug. 1998) 656–665.
- [33] J.A. Bardt, et al., Precision molding of complex metallic micro-structures, *Proc. of the 1st Int. Conf. on Micro-manufacturing, Champaign, IL, USA* (Sept. 2007) 274–279.
- [34] B.H. Ryu, Y.M. Choi, Application of inkjet technology in flat panel display, *Proc. of Int. Meeting on Information Display 2* (2006) 913–918.
- [35] K. Najafi, Micropackaging technologies for integrated microsystems: applications to MEMS and MOEMS, *Proc. of SPIE – The International Society for Optical Engineering* 4982 (2003) ix–xxvii.
- [36] T. Huang, et al., 3-D, self-aligned, micro-assembled, electrical interconnects for heterogeneous integration, *Proc. of SPIE – The International Society for Optical Engineering* 4981 (2003) 189–201.
- [37] W. Michaeli, D. Opfermann, Micro assembly injection moulding, *Microsystem Technologies* 12 (7) (June 2006) 616–619.
- [38] R.P. Martukanitz, A critical review of laser beam welding, *Proceedings of SPIE – The International Society for Optical Engineering*, 5706, *Critical Review: Industrial Lasers and Applications* (2005) 11–24.
- [39] J. Cecil, D. Vasquez, D. Powell, A review of gripping and manipulation techniques for micro-assembly applications, *Int. J. of Production Research* 43 (4) (Feb. 15, 2005) 819–828.
- [40] D.F. Heaney, Mass production of micro-components utilising lithographic tooling and injection molding technologies, *Proc. of the 1st Int. Conf. on Micro-manufacturing, Champaign, IL, USA* (Sept. 2007) 280–283.
- [41] J.A. Palmer, et al., Advancing three-dimensional MEMS by complimentary laser micro manufacturing, *Proc. of SPIE - The International Society for Optical Engineering* 6109 (2006) 61090A.
- [42] A. Sharon, et al., Manufacturing of 3D microstructures using novel UPSAMS process (ultra precision manufacturing of self-assembled micro systems, *Proc. of the IEEE Micro Electro Mechanical Systems (MEMS)*(2003) 542–545.
- [43] W. Pfleging, Rapid fabrication of microcomponents – UV-laser assisted prototyping, laser micro-machining of mold inserts and replication via photomolding, *Microsystem Technologies* 9 (1–2) (2003) 67–74.
- [44] H.J. Booth, Recent applications of pulsed lasers in advanced materials processing, *Thin Solid Films* 453–454 (2003) 450–457.
- [45] C.L. Kuo, J.D. Huang, H.Y. Liang, Fabrication of 3D metal microstructures using a hybrid process of micro-EDM and laser assembly, *Int. J. of Advanced Manufacturing Technology* 21 (10–11) (2003) 796–800.
- [46] J.W. Chen, J. Zybko, J. Clements, Diode laser bonding of planar MEMS, MOEMS, and microfluidic devices, *Materials Research Society Symposium Proceedings*, 872, *Micro- and Nanosystems – Materials and Devices* (2005) 309–314.
- [47] Y. Okazaki, N. Mishima, K. Ashida, Microfactory – concept, history and development, *ASME Transactions, J. of Manufacturing Science and Engineering* 126 (Nov. 2004) 837–844.
- [48] D. Huo and K. Cheng, Design of a 5-axis ultraprecision micro milling machine – UltraMill: Part 1 Holistic design approach, design considerations, and specifications, in the special issue in the *Int. J. of Advanced Manufacturing Technology*, to be published in 2009.

- [49] D. Huo and K. Cheng, Design of a 5-axis ultraprecision micro milling machine – UltraMill: Part 2 Integrated dynamic modelling, design optimization and analysis, in the special issue in the *Int. J. of Advanced Manufacturing Technology*, in press.
- [50] B.X. Jia et al., Research on multifunctional micro machining equipment, *Materials Science Forum*, 471-472, *Advances in Materials Manufacturing Science and Technology* (2004) 37–42.
- [51] L. Zhou, et al., Development of a multifunctional micro-machining system and its applications, *Key Engineering Materials* 238–239 (2003) 3–8.
- [52] Y.S. Liao, S.T. Chen, C.S. Lin, A multi-function high precision tabletop CNC machine for making micro-parts developed in National Taiwan University, *Proc. of the 1st ICOMM* (Sept. 2006) 48–52.
- [53] M. Rahman, H.S. Lima, K.S. Neo, A. Senthil Kumara, Y.S. Wong, X.P. Li, Tool-based nanofinishing and micromachining, *J. of Materials Processing Technology* 185 (1–3) (2007) 2–16.
- [54] Y.B. Bang, K.M. Lee, S. Oh, 5-axis micro milling machine for machining micro parts, *Int. J. of Advanced Manufacturing Technology* 25 (9–10) (May 2005) 888–894.
- [55] A.J. Sanchez-Salmeron, R. Lopez-Tarazon, R. Guzman-Diana, C. Ricolfe-Viala, Recent development in micro-handling systems for micro-manufacturing, *J. of Materials Processing Technology* 167 (2–3) (Aug. 30, 2005) 499–507.
- [56] P.R. Hauptmann, Selected examples of intelligent (micro) sensor systems: state-of-the-art and tendencies, *Measurement Science and Technology* 17 (3) (Mar. 1, 2006) 459–466.
- [57] J. Fleischer, G. Lanza, M. Schlipf, I. Behrens, Quality assurance in micro production, *Microsystem Technologies* 12 (7) (June 2006) 707–712.
- [58] H.N. Hansen, K. Carneiro, H. Haitjema, L. De Chiffre, Dimensional micro and nano metrology, *CIRP Annals – Manufacturing Technology* 55 (2) (2006) 721–743.
- [59] A. Albers, N. Burkardt, J. Marz, J. Oerding, M. Ohmer, Concept of a micro gear tolerance management: what really happened!, *VDI Berichte 1904 I* (2005) 959–981.
- [60] H. Tsukahara, Three-dimensional measurement technologies for advanced manufacturing, *Fujitsu Scientific and Technical J* 43 (1) (January 2007) 76–86.
- [61] R. Artigas, F. Laguarda, C. Cadevall, Dual-technology optical sensor head for 3D surface shape measurements on the micro and nano-scales, *Proc. of SPIE – The International Society for Optical Engineering*, 5457, *Optical Metrology in Production Engineering* (2004) 168–174.
- [62] B. Benson, A.P. Sage, G. Cook, Emerging technology-evaluation methodology. With application to micro-electromechanical systems, *IEEE Transactions on Engineering Management* 40 (2) (May 1993) 114–123.
- [63] S.I. Olsen, M.S. Jorgensen, Environmental assessment of micro/nano production in a life cycle perspective, *Materials Research Society Symposium Proceedings* 895 (2006) 159–166.

Micro-/Nano-Machining through Mechanical Cutting

Xizhi Sun and Kai Cheng

INTRODUCTION

The emergence of miniature and micro-products and components is increasingly demanding the production of parts with dimensions in the range of a few tens of nanometers to a few millimeters. Micro-/nano-cutting is one of the key technologies to enable the realization of micro-products, while a great many micro-manufacturing processes have been developed.

In this chapter, micro-/nano-cutting is defined as the fabrication of miniature and micro-components using geometrically defined cutter edges. Typical micro-/nano-cutting operations include micro-milling, micro-turning, micro-drilling and micro-grinding.

Similarly to the conventional cutting operation, in micro-/nano-cutting the surface of the workpiece is mechanically removed using tools, but the depth of cut is normally at the level of a micrometer or less. As the unit removal size decreases, issues of tool cutting-edge geometry, grain size and orientation, etc., considered to have little or no influence at larger scales, become dominant factors with strong influences on the resulting machining accuracy, surface integrity and quality of the machined component [1]. In this chapter, therefore, emphasis is placed on the issues that prevail in micro-/nano-cutting, which is essentially different from the conventional cutting process. Furthermore, the chapter focuses on the precision machines for micro-/nano-cutting

and the application of the process in various fields.

FUNDAMENTALS OF THE MICRO-/NANO-CUTTING PROCESS

While the mechanisms of conventional cutting are well established, micro-/nano-cutting mechanics and the associated intricate issues are less well understood. The depths of cut involved are several orders of magnitude smaller than those of conventional cutting, so that it is necessary to examine closely the micro-/nano-cutting process. Unlike conventional machining, where shear and friction dominate, micro-/nano-cutting may involve significant sliding along the flank face of the tool due to the elastic recovery of the workpiece material. The effects of plowing may also become important due to the large effective negative rake angle resulting from the tool edge radius. In addition, the sub-surface plastic deformation and the partition of thermal energies may also be quite different from those of traditional cutting [2]. This section discusses the fundamentals of the micro-/nano-cutting process.

Specific Energy and Cutting Force

Specific energy and cutting force are important physical parameters for understanding cutting

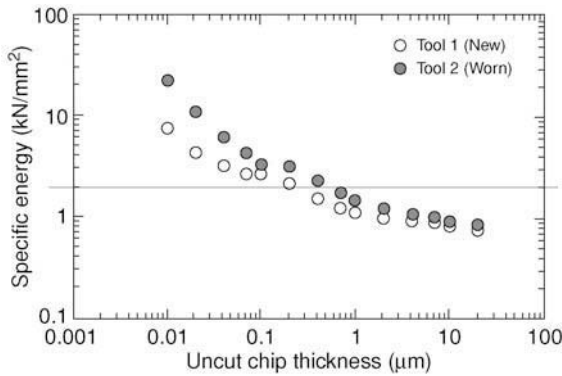


FIGURE 2-1 Specific energy versus uncut chip thickness for new and worn diamond tools.

phenomena, as they clearly reflect the chip removal process. As shown in Fig. 2-1 [3], the specific energy generally increases with the decreasing depth of cut, within the range from 10 nm to 20 μm . This is because the effective rake angle will increase as the depth of cut decreases, and the larger the rake angle the greater the specific energy. This phenomenon is often called the ‘size effect’.

Micro-/nano-cutting is also characterized by the high ratio of the normal to the tangential components of the cutting force, as shown in Fig. 2-2 [3], that is, the resultant cutting force becomes closer to the thrust direction when the depth of cut becomes smaller. Since the depth of cut is very small in micro-/nano-cutting, the workpiece is mainly processed by the cutting edge and compression will thus become dominant in the deformation of the workpiece material, which will result in larger friction force at the tool/chip interface and consequently in a greater cutting ratio. This indicates a transition

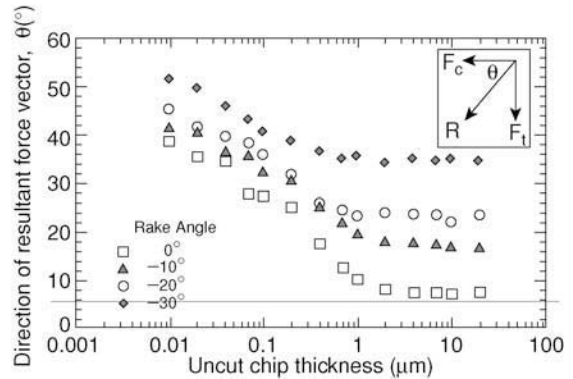


FIGURE 2-2 Resultant force vector versus uncut chip thickness at various rake angles.

from the shearing-dominated process in conventional cutting to a plowing-dominated process in micro-/nano-cutting.

Minimum Chip Thickness and Chip Formation

The definition of minimum chip thickness is the minimum undeformed chip thickness below which no chip can be formed stably.

Figure 2-3 shows the chip formation with respect to the chip thickness [4]. In Fig. 2-3(a), where the uncut chip thickness, h , is smaller than the minimum chip thickness, h_c , only elastic deformation results and no workpiece material will be removed by the cutter. When the uncut chip thickness approaches the minimum chip thickness, as shown in Fig. 2-3(b), chips will be formed due to the shearing of the workpiece. However, since elastic deformation still exists, the removed depth is generally smaller than the desired depth. If the uncut chip thickness is larger

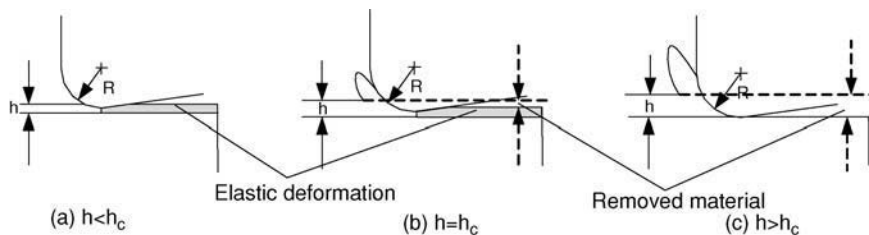


FIGURE 2-3 Schematic diagram of the effect of the minimum chip thickness.

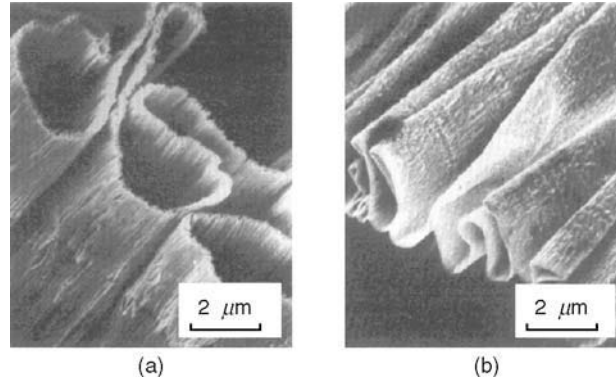


FIGURE 2-4 SEM micrographs of chips generated from nanometric cutting; (a) thickness of chip 1 nm; (b) thickness of chip 30 nm.

than the minimum chip thickness, as shown in Fig. 2-3(c), elastic deformation is significantly reduced and results in the removal of the entire depth of cut as a chip.

Due to this minimum chip thickness effect, the micro-/nano-cutting process is affected by two mechanisms: chip removal ($h > h_c$) and plowing/rubbing ($h < h_c$). From a practical point of view, the minimum chip thickness is a measure of the extreme machining accuracy attainable because the generated surface roughness is mainly attributed to the plowing/rubbing process when the uncut chip thickness is less than the minimum chip thickness. The extent of plowing/rubbing and the nature of the micro-deformation during plowing/rubbing contribute significantly to increased cutting forces, burr formation, and increased surface roughness. Therefore, knowledge of the minimum chip thickness is essential in the selection of appropriate machining conditions [5]. Ikawa et al. [6] obtained an undeformed thickness on the order of a nanometer, as shown in Fig. 2-4, by a well-defined diamond tool with an edge radius of around 10 nm.

The minimum chip thickness depends on the cutting edge radius, workpiece material and the micro-cutting of steel, finding that the minimum chip thickness is 20% and 30% of the cutting edge radius for the pearlite and ferrite, respectively. However, Shimada et al. [8] observed that the minimum chip thickness can be around 5% of the cutting edge radius for the cutting of copper

and aluminum, through molecular dynamics simulation.

Ductile Mode Cutting

The machining of brittle materials such as germanium, silicon, and optical glasses at a large depth of cut in conventional cutting has a tendency to generate a rough surface and sub-surface cracking. As a result, the machining of brittle materials is normally achieved using conventional processing techniques such as polishing. However, intricate features, the surface finish quality of the workpiece produced, and a greater material removal rate of processing demand an effective means for the fabrication of brittle materials.

There is a transition in the material removal mechanism of brittle materials, from brittle to ductile, when the depth of cut decreases [9]. Based on this feature, cutting in a ductile mode below the critical depth of cut has been attempted with the aim of obtaining a good surface finish and an uncracked surface. Since the chip thickness in micro-cutting can be of the order of the critical depth of cut, micro-cutting can serve as a novel means of fabricating unique features with brittle materials that are not achievable by polishing or other techniques [1].

The results of many researches indicate that the tool geometry and the cutting conditions are two major factors affecting the value of the critical depth of cut. It was found that the critical depth

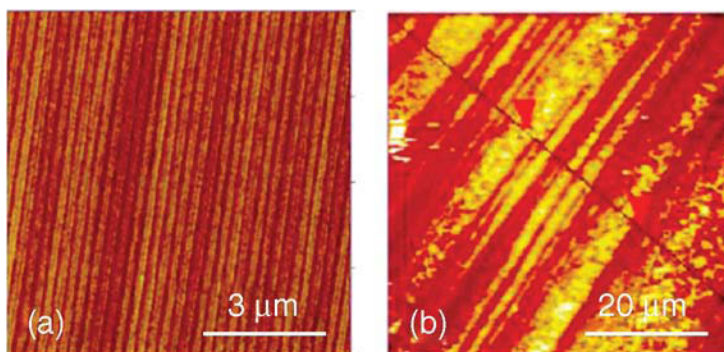


FIGURE 2-5 Silicon surfaces machined at a cutting speed of 90 m/min and a depth of cut of 1 μm : (a) feed rate of 0.4 mm/min (ductile-mode cutting); and (b) feed rate of 1 mm/min (brittle-mode cutting).

of cut increases with the increase of the cutting velocity and the negative rake angle [10,11]. However, it is difficult to achieve ductile-mode cutting with a greater feed rate, as shown in Fig. 2-5 [12].

Effect of Workpiece-material Micro-structure

The crystalline grain size of most workpiece materials is of the same order as the depth of cut in micro-cutting, so that chip formation normally takes place by the breaking up of the individual grains of a polycrystalline material. Most polycrystalline materials are thus treated as a collection of grains with random orientation and anisotropic properties [1]. The crystalline graphic-orientation affects the chip formation, the surface generation, and the variation of the cutting forces [13]. There is a distinct difference between micro-cutting and conventional cutting, where the material can be treated as isotropic and homogeneous. To et al. [14] obtained the effects of the crystallographic orientation and the depth of cut on the surface roughness by conducting the diamond turning of single-crystal aluminum rods, as illustrated in Fig. 2-6.

MODELING THE MICRO-/NANO-CUTTING PROCESS

In the past, extensive cutting tests were performed to understand cutting mechanics and optimize various cutting process variables. However, it is

difficult to investigate the micro-/nano-cutting process solely by the experimental approach due to the substantial cost of micro-tooling, the required careful preparation of samples, and the considerable amount of testing involved on machine tools, which is both time consuming and expensive. Furthermore, the in-process observation and accurate measurement of results are also very challenging.

The micro-/nano-cutting process is very complex because of the size effect, elastic/plastic deformation and fracture with high strain rates, and varying material properties during the process. Analytical modeling is thus considered extremely difficult at the current level of

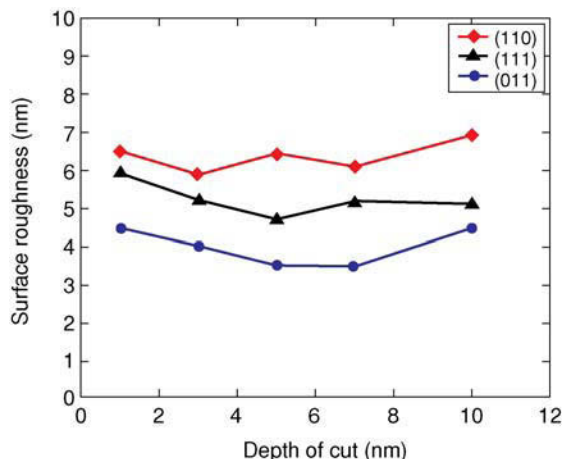


FIGURE 2-6 The effects of the crystallographic orientation and the depth of cut on the surface roughness.

understanding of material behavior. Most analytical-modeling efforts are based on kinematics from empirical observation combined with classical cutting models at the macro level. The applicability and accuracy of these models are subject to many limitations [1].

Although analytical models involve many assumptions, the numerical modeling of micro-/nano-cutting provides a powerful tool to assist scientific understanding of the process. Using numerical models, the effects of various cutting conditions can be obtained easily and effectively while undertaking less expensive experiments. Finite element (FE) modeling and molecular dynamics (MD) modeling are two popular numerical modeling and simulation techniques for micro-/nano-cutting. More recently, multi-scale modeling methods based on combining FEM and MD have emerged to overcome the disadvantages of each method and to enable the simulation of the cutting process more realistically.

In the following sub-sections, details of these key modeling methods of micro-/nano-cutting are discussed, with examples presented from published research work.

FE Modeling

The FE method is based on the principle of continuum mechanics, in which materials are defined as continuous structures and the effects of micro-constituents such as crystal structure, grain size,

and inter-atomic distances are ignored. In an FE model, only the value of the variables of nodes can be obtained exactly: between the nodes, the values of the variables are determined by interpolation [15]. Hence, the number of nodes and the distances between the nodes are selected based on the required calculation accuracy.

The application of FE simulation to the cutting process provides an effective means to understand the mechanics and characteristics of the cutting process. A typical FE cutting model is shown in Fig. 2-7 [15], where the workpiece is fixed and the tool is in motion. During cutting simulation, the interaction of nodes between the interface of the workpiece and the tool is transferred to other nodes of the workpiece. The interactions between nodes can be described by three kinds of finite-element formulation: Lagrangian formulation, which requires a remeshing algorithm or a chip-separation criterion to form the chip; Eulerian formulation, which needs a prior assumption of a chip shape; and arbitrary Lagrangian Eulerian formulation. For the description of large plastic deformation and large strain rate of a material during the cutting process, the well-known Johnson-Cock formulation is often used.

The application of the FE method in cutting has been attracting a lot of research interest since the 1970s. Although micro-cutting could be significantly different from conventional cutting, the governing principles, e.g. plasticity and tool/chip tribology, should remain but be heavily subject to

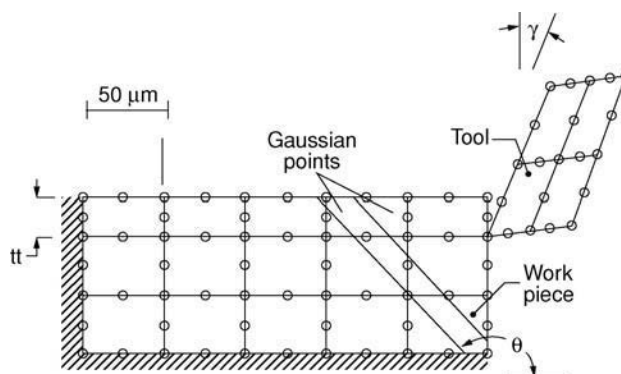


FIGURE 2-7 An illustration of an FEM cutting model.

the size effect [16]. According to these principles, various aspects in the micro-cutting process have been investigated using the FE method, including:

1. Material removal and chip formation;
2. Effects of tooling geometry and process parameters;
3. Effects of material micro-structure;
4. Residual stress in micro-cutting.

MD Modeling

Molecular dynamics (MD) simulation is a well-established methodology for detailed microscopic modeling at the molecular scale. It is based upon a model of the molecules of the matter or system concerned, according to their atomic structure. Potential functions are used to describe the molecular interactions, and the interatomic forces can be derived from the differentiation of the potential function. The motions of individual atoms are usually assumed to be governed by Newton's second law. The numerical solutions to the motion equations give the trajectories of the atoms, which can be used to determine the macroscopic static and dynamic characteristics of the system.

In the late 1980s, a research group in Lawrence Livermore National Laboratory (LLNL) started the MD simulation of the diamond turning of single-crystal copper [17]. Since then, MD has been successfully applied to a variety of phenomena in micro-/nano-cutting.

A typical nanometric cutting MD model is shown in Fig. 2-8 [6], which can be used to study the cutting zone and cutting parameters in micro-/nano-cutting.

The topics investigated by MD simulation are as follows:

1. The effect of crystal orientation on surface roughness;
2. Chip formation and the machined surface generation;
3. Minimum undeformed chip thickness in nanometric cutting;
4. Cutting forces and cutting temperature;
5. Side flow and pile up phenomena in the cutting process;
6. Surface integrity.

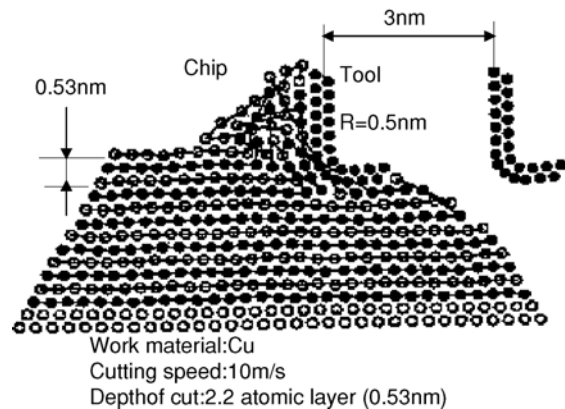


FIGURE 2-8 MD simulation model of the nanometric cutting of single-crystal copper.

Although MD simulation has become a useful tool in analyzing the nanometric machining process, further research and development are expected in the following areas:

1. Improvement of the model dimensions and computational speed;
2. Establishing more accurate potential functions for workpieces and cutting tools;
3. Developing a material model including defects, such as vacancies, dislocations, grain boundaries;
4. Tool wear simulation.

Multi-scale Modeling

Molecular dynamics (MD) simulation and the finite-element (FE) method have been successfully applied in the simulation of the machining process. However, the two methods have their own respective limitations. For example, MD simulation can only cover the phenomena occurring at nanometric scale because of the physical dimension, the computational cost and the scale, while the FE method is suited to model meso- and macro-scale machining and to simulate macro-parameters such as the temperature in the cutting zone, the stress/strain distribution and cutting forces, etc. A natural approach to the simulation of multi-scale processes is to combine an MD simulation for the critical regions within the

system with an FE method for continuum coverage of the remainder of the system. The hybrid approach provides an atomistic description near the interface and a continuum description deep into the substrate, increasing the accessible dimensional scales, and greatly reducing the computational cost while increasing the modeling accuracy and capacity.

Several multi-scale simulation methods have been developed such as the FEAT method, the quasi-continuum (QC) method, the MAAD method, and the CGMD method. A remarkably successful approach is the QC method proposed by Tadmor et al. in 1996 [18]. QC is a way of simulating the macro-scale non-linear deformation of crystalline solids using MD. An integrated MD-FE approach has been proposed by the authors for the multi-scale simulation of the micro-/nano-cutting process with diamond tools based on the QC method [19].

Figure 2-9 is a schematic diagram of the model used for the multi-scale simulation of nanometric cutting of single-crystal copper [19]. It can be seen that the mesh density becomes greater when proceeding upwards. At the top the interface meshes disappear, and there are atoms instead of mesh, entirely. The size of the work material is $0.2 \times 0.1 \mu\text{m}$, taking into account the transition from nanometer to micrometer. The number of atoms to be computed at the 50th step time is no more than 20,000, which is much less compared to 1.25×10^7 atoms included in the model for MD simulation. This model is an embodiment

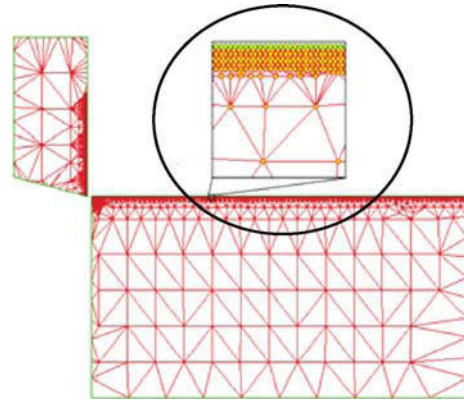


FIGURE 2-9 Multi-scale model for nanometric cutting of single-crystal copper.

of the concept of multi-scale simulation for micro-machining.

Figure 2-10 shows the simulation plots at the first time step and the 50th time step, and the corresponding atoms' velocity contour line.

PRECISION MACHINES FOR MICRO-/NANO-CUTTING

Ultra-precision Machine Tools

Ultra-precision machine tools play an important role in the implementation of micro-/nano-cutting, while they directly determine machining accuracy, productivity, producibility and repeatability. There have been great market demands for ultra-precision machine tools which are capable of

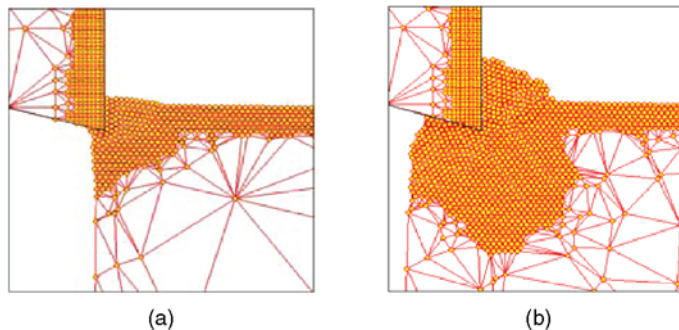


FIGURE 2-10 Instantaneous diagram of copper's cutting simulation by the multi-scale method: (a) at the first time step; (b) at the 50th time step.

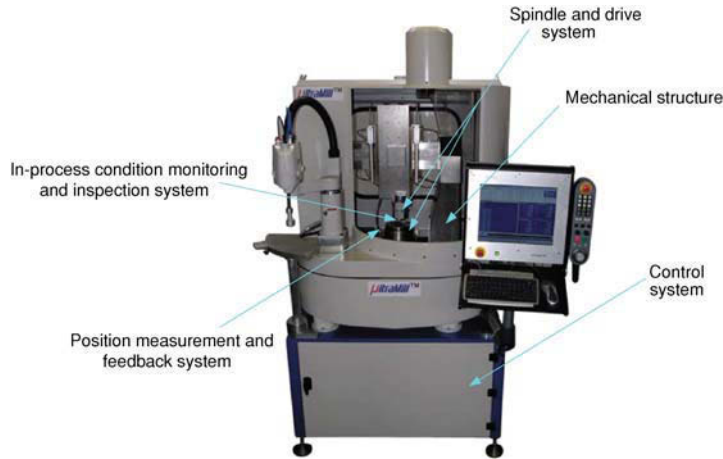


FIGURE 2-11 Schematic figure of a five-axis micro-milling machine [20].

machining increasingly more complex-structured components and products (e.g. axially asymmetric surfaces and freeform surfaces) with greater accuracy and finer surface finish, and coping with any newly emerging materials for high throughput and cost-effective manufacturing. These demands and requirements have led to the significant development of a new generation of machine tools.

Figure 2-11 illustrates a five-axis ultra-precision micro-milling machine, developed at Brunel University. A typical ultra-precision machine tool has five major sub-systems, including a mechanical structure, a spindle and drive system, a control system, a position-measurement and feedback system, and an in-process condition-monitoring and inspection system. These sub-systems critically determine the performance of the overall machine tool system.

Mechanical Structure. The mechanical structure provides a framework and mechanical support for all the machine components. It encompasses important components such as the machine base, column, worktable, slide, spindle cases and carriages. The major factors for machine design and selection include [21]:

1. Structural configuration;
2. Stiffness and damping;
3. Structural connectivity and interface;
4. Structure dynamics and associated performance.

A robust design of mechanical structure should aim to achieve high structural-loop stiffness, good damping properties, a symmetrical and closed-loop structural configuration, minimization of heat deformation, long-term stability and isolation of environmental effects.

Material is also a key factor in determining the final machine performance. While cast iron and granite have been widely used for fabricating machine bases and slideways, polymer concrete has become popular for ultra-precision machine tools where light weight with high damping capacity and rigidity is required. Structural materials with a low thermal expansion coefficient and high dimensional stability have also found application, including super-invar, synthetic granite, ceramics and Zerodur.

Spindle and Drive System. The spindle is a key component of a precision machine and it has significant impact on machined components in terms of form/dimensional accuracy and surface quality. Two types of spindles are most commonly used in precision machine tools, i.e. aerostatic bearing spindles and oil hydrostatic bearing spindles. They are capable of high rotational speed with high motion accuracy. Aerostatic bearing spindles usually have lower stiffness than oil hydrostatic bearing spindles, but they have lower thermal deformation than the latter. Aerostatic bearing spindles are widely used in machine tools

with medium and small loading capacity, whereas oil hydrostatic bearing spindles are more suitable for large and heavily loaded machine tools.

More recently, the groove technique has been used in the design of bearings. A grooved hybrid air bearing combines aerostatic and aerodynamic design principles to optimize ultra-high speed performance.

Several drive mechanisms can be used for ultra-precision machine tools, including piezoelectric actuators, linear-motor direct drives and friction drives. Piezoelectric actuators usually have a short stroke with high motion accuracy and wide response bandwidth. They have been employed in fine tool positioning so as to achieve high precision control of the cutting tool (e.g. a diamond-cutting tool).

Linear-motor direct drives (AC or DC) usually have a long stroke and they do not need conversion mechanisms such as lead screws, and racks and pinions. They offer better stiffness, acceleration, speed, motion smoothness, repeatability and accuracy, etc. [21], although their applications in the machine-tools industry are still relatively new.

Friction drives also have a long stroke and usually consist of a driving wheel, a flat or round bar and a supporting back-up roller. They offer low friction force, smooth motion, and good repeatability and reproducibility due to elastic deformation induced by the preload.

Control System. Following the invention of Computer Numerical Control (CNC) in the early 1970s, many companies started to develop their control systems for machine tools. The control system typically includes motors, amplifiers, switches and the controller. High speed multi-axis CNC controllers play an essential role in efficient and precision control of servo drives, error compensation (thermal and geometrical errors), optimized tool setting and direct entry of the equation of shapes [22]. Advanced PC-based control systems have achieved nanometer or even sub-nanometer levels of control resolution for ultra-precision and micro-manufacturing purposes, such systems also being used commonly in the majority of commercially available ultra-precision machines.

Position Measurement and Feedback System. Ultra-precision machine tools necessarily require an ultra-precision position measurement and feedback system. Laser encoders (laser-interferometer based) are particularly suitable because interferometers have an intrinsically high resolution. Interferometers also have the ability to eliminate Abbe errors. They have a typical resolution of 20 nm (digital), and sub-nanometer resolution can also be achieved with an analog system via external interpolation. The installation may be made simpler by means of fiber-optics laser launch and integrated interferometer optics. Some laser holographic-linear scales have a resolution of better than 10 nm.

Another alternative technique is to use ultra-high resolution optical encoders. They can provide resolution close to that of laser encoders, but in a more industrially feasible and simple manner. There is a trend of more optical encoders being adopted on industrially used precision and ultra-precision machines.

In-process Condition Monitoring and Inspection System. Intelligent and smart machine tools are an important development for ultra-precision applications. To meet these requirements, some sensors are generally required to monitor the operation of the machine tool and to combine multi-functionality, reliability, sensitivity and compactness. Monitoring the machining status during ultra-precision machining is usually difficult because of the associated very small energy emissions and cutting forces compared with the conventional machining processes. Thermal effects have been known to be the largest source of dimensional errors. It is therefore important to implement online temperature monitoring. Condition monitoring may be also applied to other parameters or variables, e.g. cutting force, chatter and vibration. It is desirable to use multiple sensors to realize the smart and intelligent machine tool. Furthermore, tool wear, tool breakage and its engaging process demand a great deal of attention in micro-/nano-machining because of the high precision and fragile micro-tools involved.

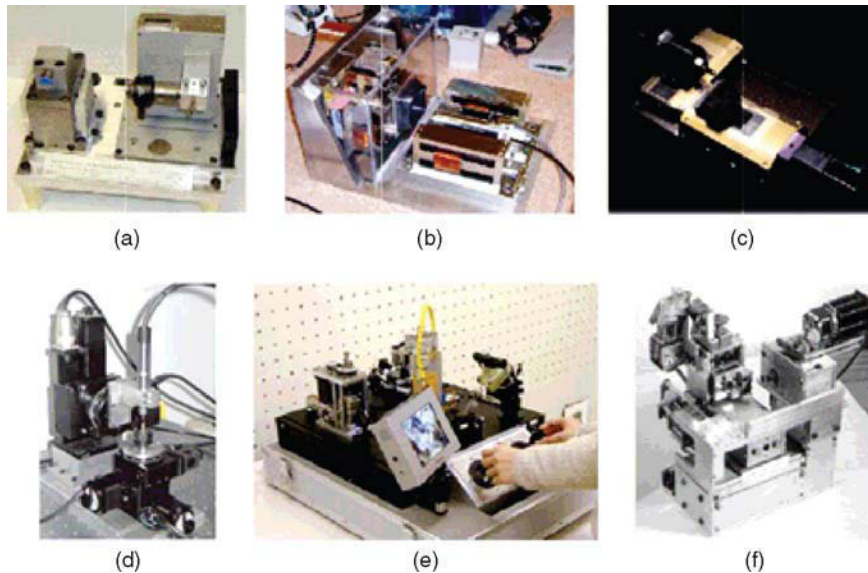


FIGURE 2-12 Typical micro- and meso-machines [4].

Micro- and Meso-machines

Traditional ultra-precision machines are currently the major means for undertaking micro-/nano-cutting because of their feasible performance and availability. However, these machines are generally very expensive, working in a tight temperature control environment, and they are energy and resources inefficient. To match the micro-manufacturing of miniature and micro-components, the concept of micro- and meso-machine tools has been proposed by some researchers, as shown in Fig. 2-12 [4].

Micro- and meso-machines and their integration for the micro-manufacturing system/micro-factory are suitable for the fabrication of micro-products at low cost, requiring the occupation of less space, and being of low energy consumption and greater mobility, etc. Compared to a conventional ultra-precision machine, a micro- or meso-machine has the five essential characteristics of decreased heat deformation, less material consumption, smaller vibration amplitudes, smaller footprint and thus smaller space occupation, and less energy consumption [23].

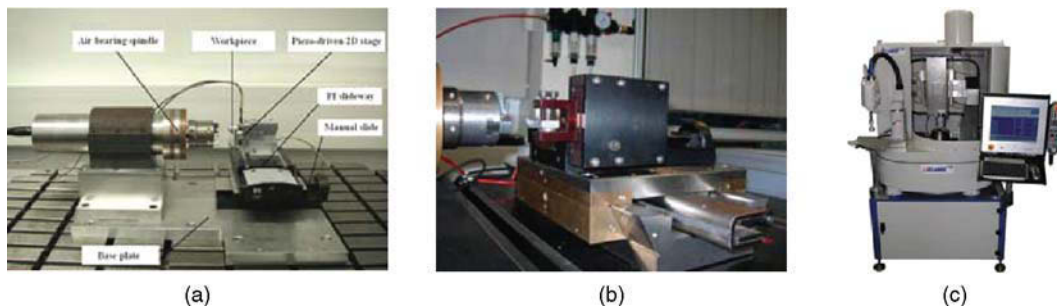


FIGURE 2-13 Micro- and meso-machines developed at Brunel University: (a) a desktop micro-milling/turning test rig; (b) a three-axis bench-top diamond-turning machine; and (c) a five-axis bench-top micro-milling machine.



FIGURE 2-14 Mirror surface achieved on the three-axis diamond-turning machine.

At Brunel University, three meso-machines have been developed for machining micro-components and -products. Figure 2-13(a) shows a desktop micro-milling/turning test rig which has a two-dimensional piezo-driven stage for vibration-assisted cutting. Figure 2-13(b) shows a three-axis bench-top diamond-turning machine, a mirror surface, as illustrated in Fig. 2-14, being achievable on this machine. Figure 2-13(c) is a five-axis bench-top micro-milling machine which is still under development with the specifications as follows:

1. Overall size: 1140 × 910 × 1865 mm.
2. Working XYZ: 150 × 150 × 100 mm.
3. Slides and rotary table: direct drive and air bearings with squeeze film dampers to achieve

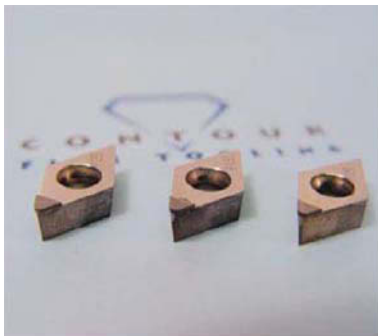
a nanometric level of positioning and machining accuracy.

4. Spindle speed: 250k rpm to cope with small diameter of tools and micro-features.
5. Mechanical handling and visual inspection integrated into the machine design.
6. Machining accuracy: <100 nm.
7. Surface roughness: <10 nm.
8. Control system: UAMC five axis.

MICRO-TOOLING

Micro-tooling is the essential enabler for micro-/nano-cutting processes. It also determines the feature sizes and surface quality of the miniature and micro-components machined. Smaller tools have decreased thermal expansion relative to their size, increased static stiffness from their compact structure, increased dynamic stability from their higher natural frequency, and the potential for decreased cost due to smaller quantities of material utilized [4].

Single-crystal diamond is the preferred tool material for micro-/nano-cutting due to its outstanding hardness, high thermal conductivity and elastic and shear moduli. The crystalline structure of the diamond makes it easy to generate a very sharp cutting edge, e.g. a cutting edge in tens of nanometers can be achieved. More recently, CVD (chemical vapor deposition) diamond-cutting tools have become available, as shown in Fig. 2-15 [24]. They are extremely hard



(a)



(b)

FIGURE 2-15 Cutting tools manufactured by: (a) CVD diamond cutting tools; (b) diamond cutting tools. (Courtesy: Contour Fine Tooling Ltd).



FIGURE 2-16 Micro-milling tools [25].

and can be used to cut tungsten carbide with a cobalt percentage of 6% or greater.

However, diamond is limited to the cutting of non-ferrous materials because of the high chemical affinity between diamond and iron. Micro-tools that are used to machine ferrous materials are normally made from tungsten carbide. As shown in Fig. 2-16 [25], these micro-milling tools are made from tungsten carbide with a diameter from 0.2 mm to 1.5 mm.

Commercially available micro-drills are typically on the order of 50 μm diameter [1]. However, methods for minimizing micro-tools continue to be developed, such as focused ion beam, EDM, WEDG and grinding, etc. Figure 2-17 [26] shows micro-end mills developed by the focused ion beam process, their diameter being less than 25 μm .

Other trends in the development of micro-tools include: the optimization of the geometric and

coating properties of micro-tools for longer tool life and accuracy enhancement; and characterization and condition monitoring of micro-tools.

APPLICATIONS

Micro-/nano-cutting has many applications, which are directly related to the overall application markets of micro-products. For instance, MEMS, as shown in Fig. 2-18, is and will remain one of major driving forces for micro-cutting. It is expected that the MEMS/MST market volume will reach \$24 billion in 2009 from \$12 billion in 2004. Moreover, completely new products such as micro-fuel cells, MEMS memories, chip coolers, liquid lenses for cell-phone zoom and autofocus will be included in this category.

The EU FP6 4M Network has organized the major applications into the following three divisions [28], i.e.:

1. **Micro optics:** telecommunication, bio-technological, instrumentation and medical applications.
2. **Micro-sensors and actuators:** medicine, biomedical field, health and safety, environment and process control.
3. **Micro fluidics:** biological, medical, pharmaceutical and chemical engineering applications.

Micro-/nano-cutting is very promising in the production of micro-products used in the above three divisions, such as sensors, accelerometers, actuators, micro-mirrors, fiber-optics connectors and micro-display, etc. Some typical application samples resulting from micro-/nano-cutting are shown in Fig. 2-19 [29].

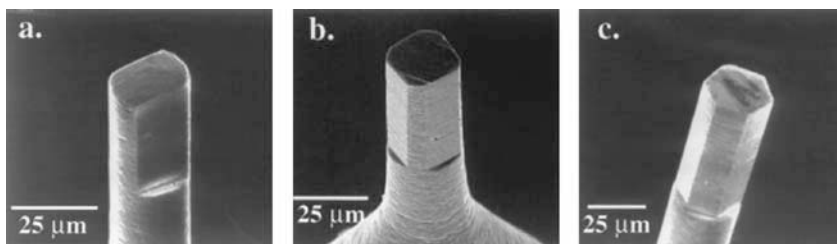


FIGURE 2-17 Micro-end mills made by focused ion beam sputtering having: (a) two cutting edges; (b) four cutting edges; and (c) five cutting edges (scanning electron micrographs).

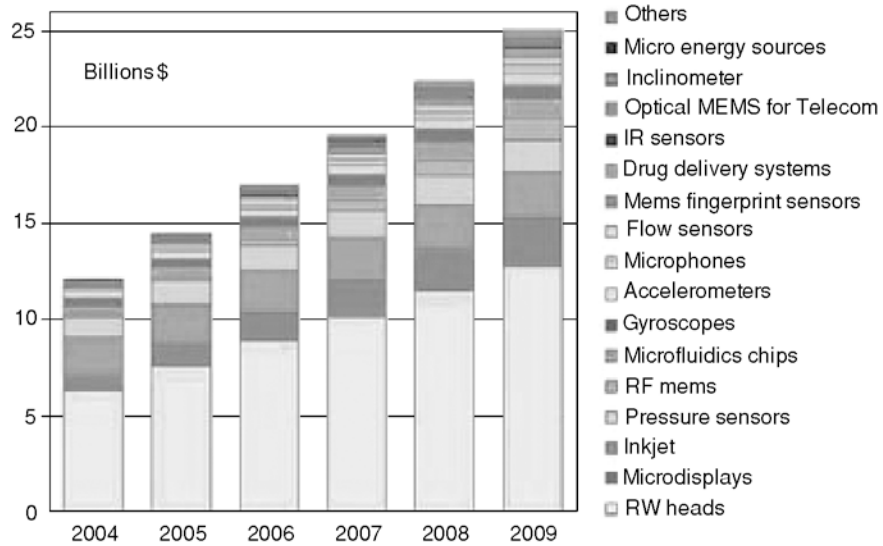


FIGURE 2-18 Market for MST/MEMS products in the future [27].

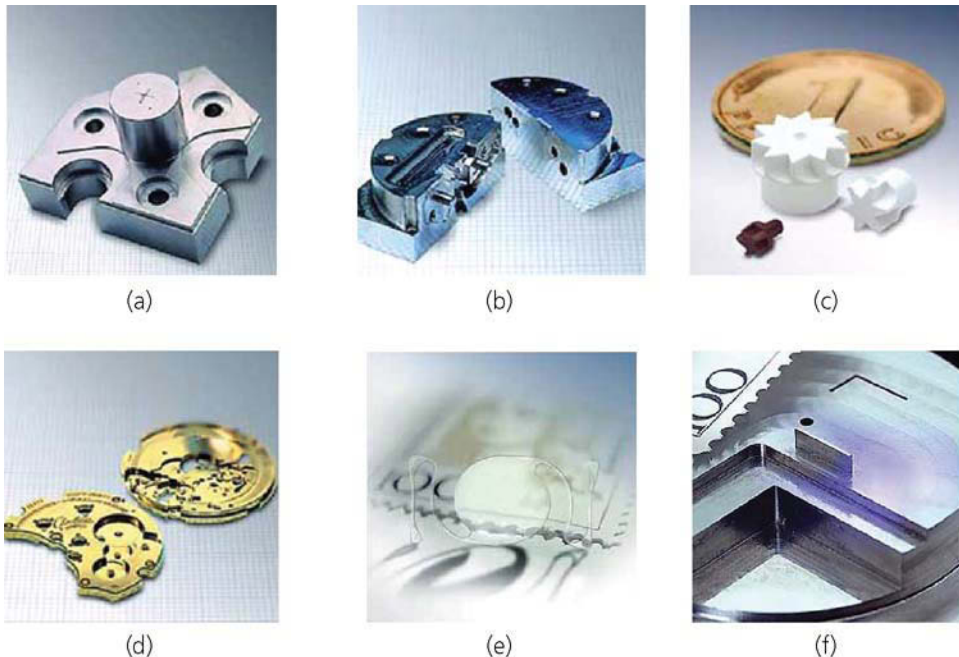


FIGURE 2-19 Micro-product samples (Courtesy: KERN Micro- & Feinwerktechnik GmbH).

Figure 2-19(a) is a joining element (steel) for optical-fiber connections. There are 18 drill holes with a diameter of $0.23 \text{ mm} \pm 5 \mu\text{m}$ and a drilling depth of 1.5 mm. The positional tolerance of the

drill holes is $10 \mu\text{m}$. The complete machining time was 25 minutes.

The part shown in Fig. 2-19(b) is a mixing disc of a rocket motor, produced by five-axes

machining. Six tools were used and precision adjustment on spot faces was required.

Figure 2-19(c) shows three turbine wheels for micro-fluid pumps, produced by five-axes machining. The wheels are made of vespel and ceramic with diameters of 2–7 mm and a circumferential tolerance of 2 μm .

Figure 2-19(d) shows watch base-plates made by fully automatic production using 30 tools including milling, drilling and tapping. The positional tolerances between the drill holes and drill depths are $\pm 3 \mu\text{m}$.

The cataract lens shown in Fig. 2-19(e) has a surface finish of $R_a < 0.2 \mu\text{m}$. Its outside contour is machined with a milling tool (0.4 mm) and the positioning holes are produced by drilling.

The indispensable advantage of micro-/nano-cutting is applicable to the manufacture of 3D complex-shape/form micro-molds. It is anticipated that micro-/nano-cutting will be intensively used in the fabrication of compression molds and injection molds. Figure 2-19(f) shows an injection-molding tool for watch-making, machined by micro-milling. The material of the mold is hardened steel 54 HRC, its position and form tolerance is $\pm 5 \mu\text{m}$, and its surface quality is $R_a > 0.25 \mu\text{m}$.

COMPETITIVE TECHNOLOGIES AND ECONOMIC CONSIDERATIONS

Micro-/nano-cutting brings many potentialities to the fabrication of miniature and micro-products/components with arbitrary geometry. The micro-/nano-cutting process is particularly suitable for the manufacture of individual personalized components rather than large batch sizes, which is largely indispensable for the current vibrant markets. With the high level of machine accuracy of ultra-precision machine tools, good surface finish and form accuracy can be achieved. Micro-/nano-cutting is also capable of fabricating 3D free-form surfaces. The high machining speed of micro-/nano-cutting is another advantage over other micro-manufacturing technologies. Moreover, it can fabricate a huge range of materials, such as steel, aluminum, brass, plastics, ceramic, poly-

mers, etc. Unlike micro-laser beam machining and lithographic techniques, it does not require a very expensive set-up, which enables the fabrication of miniatures at an economically reasonable cost.

ACKNOWLEDGEMENTS

The authors would like to thank all research colleagues in the AMEE research group at Brunel University for stimulating discussions, and relevant research publications and projects to access and refer to. Thanks are also extended to the EU MASMICRO Project Consortium, practically to its RTD 5 sub-group for frequent meetings and discussions which are always very helpful.

REFERENCES

- [1] D. Dornfeld, S. Min, Y. Takeuchi, Recent advances in mechanical micromachining, *CIRP Annals* 55 (2) (2006) 745–768.
- [2] D.A. Lucca, R.L. Rhorer, R. Komanduri, Energy dissipation in the ultraprecision machining of coppers, *CIRP Annals* 40 (1) (1991) 69–72.
- [3] D.A. Lucca, Y.W. Seo, Effect of tool edge geometry on energy dissipation in ultraprecision machining, *CIRP Annals* 42 (1) (1993) 83–86.
- [4] J. Chae, S.S. Park, T. Freiheit, Investigation of micro-cutting operations, *Int. J. Mach. Tools Manuf* 46 (3–4) (2006) 313–332.
- [5] X. Liu, R.E. Devor, S.G. Kapoor, An analytical model for the prediction of minimum chip thickness in micromachining, *J. Manuf. Sci. & Tech., Trans. ASME* 128 (2) (2006) 474–481.
- [6] N. Ikawa, S. Shimada, H. Tanaka, Minimum thickness of cut, *Nanotechnology* 3 (1) (1992) 6–9.
- [7] M.P. Vogler, S.G. Kapoor, R.E. Devor, On the modeling and analysis of machining performance in micro-endmilling, *J. Manuf. Sci. & Tech., Trans. ASME* 126 (4) (2004) 685–705.
- [8] S. Shimada, N. Ikawa, H. Tanaka, G. Ohmori, J. Uchikoshi, H. Yoshinaga, Feasibility study on ultimate accuracy in microcutting using molecular dynamics simulation, *CIRP Annals* 42 (1) (1993) 91–94.
- [9] S. Shimada, N. Ikawa, T. Inamura, N. Takezawa, H. Ohmori, T. Sata, Brittle-ductile transition phenomena in microindentation and micromachining, *CIRP Annals* 44 (1) (1995) 523–526.
- [10] D. Li, S. Dong, Y. Zhao, M. Zhou, The influence of rake of diamond tool on the machined surface of brittle materials with finite element analysis, Proceedings of the 1st International Conference and

- General Meeting of the European Society for Precision Engineering and Nanotechnology, Bremen, Germany (1999) pp. 338–341.
- [11] Y. Ichida, Ductile mode machining of single crystal silicon using a single point diamond tool, Proceedings of the 1st International Conference and General Meeting of the European Society for Precision Engineering and Nanotechnology, Bremen, Germany (1999) pp. 330–333.
- [12] F.Z. Fang, H. Wu, W. Zhou, X.T. Hu, A study on mechanism of nano-cutting single crystal silicon, *J. Mats. Proc. Tech.* 184 (1–3) (2007) 407–410.
- [13] X. Liu, R.E. Devor, S.G. Kapoor, The mechanics of machining at the microscale: assessment of the current state of the science, *J. Manuf. Sci. & Tech., Trans. ASME* 126 (4) (2004) 666–678.
- [14] S. To, W.B. Lee, C.Y. Chan, Ultraprecision diamond turning of aluminium single crystals, *J. Mats. Proc. Tech* 63 (1–3) (1997) 157–162.
- [15] X. Luo, High precision surfaces generation: modeling, simulation and machining verification, PhD thesis, Leeds Metropolitan University (2004).
- [16] K.S. Woon, M. Rahman, F.Z. Fang, Investigations of tool edge radius effect in micromachining: a FEM simulation approach, *J. Mats. Proc. Tech.* 195 (1–3) (2008) 204–211.
- [17] W.G. Hoover, Molecular dynamics, in: *Lect. Notes Phys.* vol. 258, Springer-Verlag, Berlin (1986) 13.
- [18] E.B. Tadmor, M. Ortiz, R. Phillips, Quasicontinuum analysis of defects in crystals, *Philos. Mag. A* 73 (1996) 1529–1563.
- [19] X. Sun, S. Chen, K. Cheng, D. Huo, W. Chu, Multi-scale simulation on nanometric cutting of single crystal copper, *Proc. Inst. Mech. Eng. B, J. Eng. Manuf* 220 (7) (2006) 1217–1222.
- [20] D. Huo, K. Cheng, A dynamics-driven approach to the design of precision machine tools for micro-manufacturing and its implementation perspectives, *Proc. Inst. Mech. Eng. B, J. Eng. Manuf* 222 (1) (2008) 1–13.
- [21] X. Luo, K. Cheng, D. Webb, F. Wardle, Design of ultraprecision machine tools with application to manufacture of miniature and micro components, *J. Mats. Proc. Tech.* 167 (2005) 515–528.
- [22] N. Ikawa, R. Donaldson, R. Komanduri, W. König, Ultraprecision metal cutting – the past, the present and the future, *CIRP Annals* 40 (2) (1991) 587–594.
- [23] L. Alting, F. Kimura, H.N. Hansen, Micro engineering, *CIRP Annals* 52 (2) (2003) 635–657.
- [24] <http://www.contour-diamonds.com/HTML/CVDdiamonds.html> (accessed on Nov. 19, 2007).
- [25] T. Dow, E. Miller, K. Garrard, Tool force and deflection compensation for small milling tools, *Prec. Eng* 28 (1) (2004) 31–45.
- [26] D.P. Adams, M.J. Vasile, G. Benavides, A.N. Campbell, Micromilling of metal alloys with focused ion beam-fabricated tools, *Prec. Eng.* 25 (2001) 107–113.
- [27] H. Wicht, J. Bouchaud, NEXUS market analysis for MEMS and microsystems III 2005-2009. <http://www.suframa.gov.br/minapim/news/visArtigo.cfm?Ident=147&Lang=EN> (accessed on Nov. 19, 2007).
- [28] S.S. Dimov, A.N. Bramley, W. Eberhardt, et al., 4M Network of Excellence, process report 2004-2006. 4M2007 Conference on Multi-Material Micro Manufacture, Borovets, Bulgaria (Oct. 3-5, 2007).
- [29] <http://www.kern-microtechnic.com/2-Sub-Samples.html> (accessed on Nov. 19, 2007).

Micro-EDM

*Eckart Uhlmann, Markus Röhner and Malte Langmack***INTRODUCTION**

Today, micro-electrical discharge machining (μ -EDM) is applied in all kinds of fields concerning micro-machining. Especially in single-part or small batch production μ -EDM can be used economically to produce micro-tools and micro-molds. By combining different process variants of μ -EDM with current machining processes such as micro-milling or laser ablation a cost efficient mass production can be realized [1–4].

Based on a thermal material removal process, μ -EDM is working almost free of process forces. It is also independent of mechanical workpiece properties such as the Young's modulus or hardness. Bringing together huge geometrical freedom and precision, μ -EDM allows the machining of a wide range of electro-conductive materials with a minimal conductivity of $\kappa = 0.01$ S/cm including high temperature alloys, cemented carbide, and electro-conductive ceramics.

WORKING PRINCIPLE**Machining Principle of EDM**

EDM is a non-mechanical thermal shaping process with which material is removed by spatially and temporally separated electrical discharges between a workpiece electrode and a tool electrode. The high frequency discharges cause melting and vaporization of material on the surface of both electrodes. To enhance the material removal EDM operates in a non-conducting fluid, the dielectric fluid (Fig. 3-1).

During machining, the tool and workpiece electrode are positioned in such a way that a working gap s filled with dielectric fluid remains between them. Applying a voltage – depending on the working gap width and conductivity of the dielectric fluid – causes an expanding energetic plasma channel and a current flow after exceeding the dielectric strength of the fluid. Temperatures above $T = 10,000$ K [5] inside the plasma channel effect melting and vaporization processes of the material on the surfaces of both electrodes. By switching off the current, melted material is abruptly erupted due to an implosion of the plasma channel [6–9].

The result of a single discharge is a crater-shaped pit on the electrodes' surfaces, the discharge crater (Fig. 3-2(a)). Depending on the erosion parameters such as the discharge time, discharge current or the type of dielectric fluid, typical crater diameters vary from around $d_c = 1 \mu\text{m}$ [10] to around $d_c = 100 \mu\text{m}$. The EDM-specific surface topography is caused by a multitude of overlapping discharge craters (Fig. 3-2(b)). The removed material mostly consists of ball-shaped particles (Fig. 3-2(c)).

Process Variants

With different variants μ -EDM is a very flexible machining process. Three variants of big industrial relevance are micro-die sinking (μ -die sinking) (Fig. 3-3(a)), micro-wire electrical discharge machining (μ -WEDM) (Fig. 3-3(b)) and micro-electrical discharge drilling (μ -ED drilling)

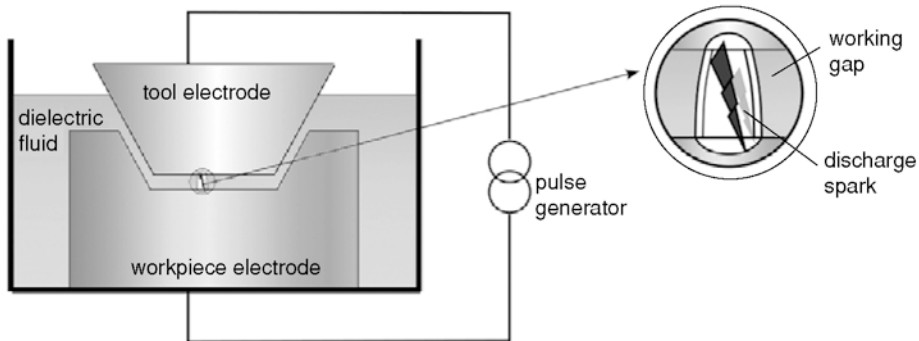


FIGURE 3-1 Principle illustration of the EDM process.

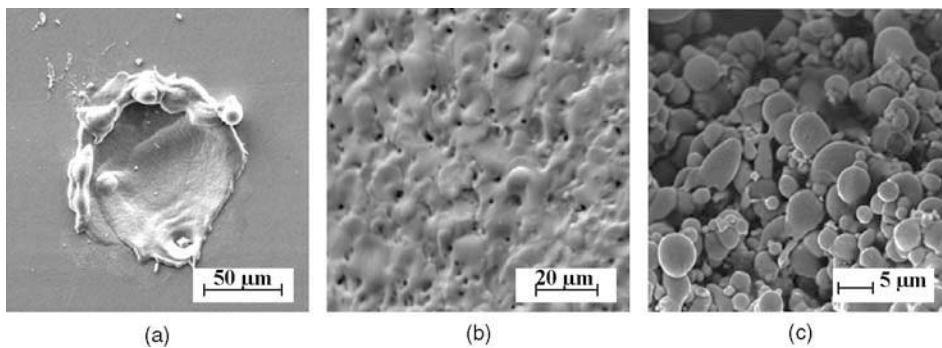


FIGURE 3-2 Single discharge crater (a), surface topography (b), and removed particles (c).

(Fig. 3-3(c)). In μ -die sinking a shaped tool electrode is used for manufacturing three-dimensional shapes and free-forms. μ -WEDM comes into operation for cutting defined contours by using a fine wire electrode. μ -ED drilling, a special

option of μ -die sinking, operates with a rotating pin electrode to produce micro-holes, e.g. as needed in fuel injection systems.

Processes with less industrial relevance are micro-electrical discharge milling (μ -ED milling)

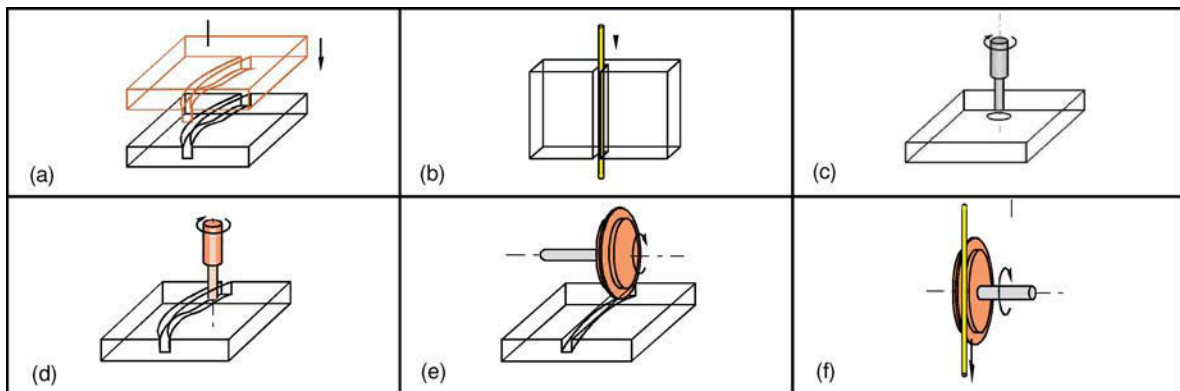


FIGURE 3-3 Process variants of μ -EDM: μ -die sinking (a), μ -WEDM (b), μ -ED drilling (c), μ -ED milling (d), μ -EDG (e), and μ -WEDG (f).

(Fig. 3-3d), micro-electrical discharge grinding (μ -EDG) (Fig. 3-3e), and micro-wire electrical discharge grinding (μ -WEDG) (Fig. 3-3f). μ -ED milling is a further development of μ -ED drilling. In combination with a path controlled motion in three dimensions, free-forms and cavities can be produced. This process variant is gaining in importance for micro-machining because with this option 3D-shaped tool electrodes do not have to be manufactured anymore. In analogy towards the kinematics of conventional grinding processes, μ -EDG is used for producing, e.g. micro-fluidic channels. For manufacturing, e.g. ejector pins, μ -WEDG is applied.

Dielectric Fluid

The dielectric fluid has several main functions in the EDM process. It isolates the tool electrode [11] from the workpiece electrode to achieve a high current density in the plasma channel. It cools down the heated surfaces of the electrodes and exerts a counter pressure to the expanding plasma channel [12]. Flushing with dielectric fluid removes the particles after the discharge process and prevents developing particle linkages causing process interruptions by short circuit, or damage of the electrodes' surfaces [13].

There are two main types of dielectric fluids: deionized water and dielectric fluids based on hydrocarbon compounds, also known as dielectric oil.

Deionized water, mostly tap water which was filtered by deionization resin to decrease electrical conductivity to $\kappa_w \sim 1 \mu\text{S/cm}$, has a higher conductivity and therewith a lower dielectric strength than hydrocarbon-based dielectric fluids with $\kappa_{\text{hdf}} < 0.1 \mu\text{S/cm}$. Due to the lower dielectric strength of deionized water, discharge sparks ignite more easily at bigger working gaps compared to dielectric oil. The higher vaporization heat of water-based dielectric fluids also removes more thermal energy from the process than hydrocarbon dielectric fluids. This especially becomes very important at short discharge durations and high effective pulse frequencies. In comparison to dielectric oil, deionized water effects a higher surface quality [14] and a higher material removal rate [13]. Furthermore, the influence on the subsurface formation, also known as white layer, is much lower using deionized water. Disadvantages of water-based fluids are high tool wear, corrosion of the workpiece, and deionization. Due to the high dielectric strength, dielectric oil can be used for high discharge energies with small working gaps applied for micro-die sinking operations. Special disposal of used oil and contaminated filters, low flash point and hazardous vapors during the machining process are problems when machining with hydrocarbon dielectric fluids [13]. Table 3-1 gives an overview of the properties and technological behavior of hydrocarbon-based dielectric fluids and deionized water.

TABLE 3-1 Differences of Hydrocarbon Dielectric Fluids and Deionized Water

Type of Dielectric Fluid	Hydrocarbon Dielectric Fluids	Deionized Water
Electrical conductivity	$< 0.1 \mu\text{S/cm}$	$\sim 1 \mu\text{S/cm}$
Technological behavior	High material removal rate, small tool wear, big influence on peripheral zone	High material removal rate, high surface quality, high wear
Properties	No corrosion of workpiece, no deionization necessary, special disposal, low flash point, hazardous vapors	Not flammable, no hazardous vapors, no special disposal, corrosion
Application	Micro-die sinking	Micro-wire electrical discharge machining

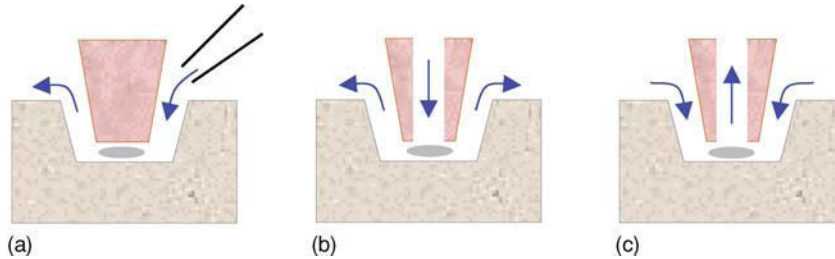


FIGURE 3-4 Illustration of direct flushing strategies: lateral flushing (a), pressure flushing (b) and suction flushing (c).

General Flushing Strategies

To force a circulation of the dielectric fluid and to clean the working gap from removed material particles, different flushing strategies are used. There are direct and indirect flushing strategies (Figs 3-4 and 3-5). Direct flushing, such as lateral flushing (Fig. 3-4(a)), pressure flushing (Fig. 3-4(b)), or suction flushing (Fig. 3-4(c)), is produced by a fluid pump. Flushing can also be pulsatory or intermittent.

In μ -EDM, flushing through the electrode is often impossible because of the small electrode dimensions. Thus, a circulation in the dielectric fluid is realized by indirect flushing strategies (Fig. 3-5). Indirect flushing is a result of a relative motion between the tool electrode and the workpiece that is superimposed onto the tool feed. The relative motion can be generated by a periodic high frequency vibration (Fig. 3-5(a)) or a rotary motion of the tool electrode (Fig. 3-5(b)) created by a high speed spindle.

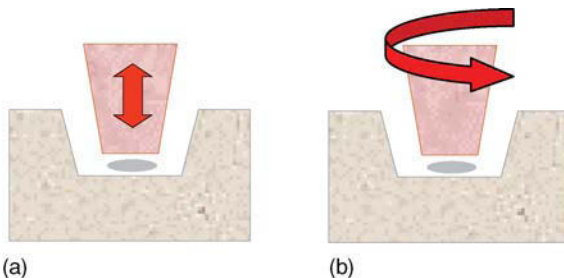


FIGURE 3-5 Illustration of indirect flushing strategies: lift-ing (a) and rotation (b).

PROCESS PARAMETERS AND PROCESS CAPABILITIES

Procedure of a Single Discharge

A single discharge can be differentiated into four phases: the build-up phase, the ignition phase, the discharge phase, and the breakdown phase, as shown in Fig. 3-6.

During the **build-up phase** a voltage, which is called open circuit voltage u_0 , is applied between the tool electrode and the workpiece. The voltage, with a level from $u_0 = 60$ V to $u_0 = 400$ V depending on the machining process [13], causes a strong electrical field in the working gap between the electrodes. An acceleration of existing free charge carriers inside the dielectric fluid takes place along the streamlines of the field [15]. Additionally, the electrical field effects an emission of electrons out of the cathode (field emission). With electrons moving towards the anode and ions that are attracted by the cathode, a current starts to flow. As a consequence, the dielectric fluid is heated above its boiling temperature, then vaporizes, and as a result a plasma channel is formed.

In the **ignition phase** the accelerated electrons prompt an ionization, the so-called impact ionization, of neutral particles or molecules which rapidly increases the number of existing charge carriers. Passing a defined threshold causes the working fluid's dielectric strength to exceed. The ignition phase is directly connected to a change in current and voltage. With building up a discharge channel, the open circuit voltage u_0 drops to discharge voltage u_c which depends on

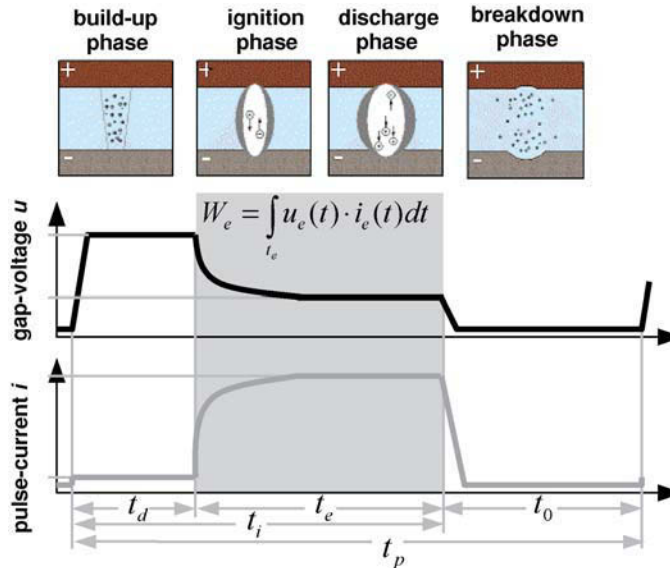


FIGURE 3-6 Illustration of a single discharge.

the ohmic resistance in the working gap, and a discharge current i_e begins to flow on the super-ficiety surface of the plasma channel [12]. Common discharge currents of μ -EDM range from $i_e = 1$ mA to a maximum of $i_e = 1$ A [13]. The time from applying the open circuit voltage u_0 to exceeding the dielectric strength is called the ignition delay time t_d .

During the third phase, named the **discharge phase**, the electrical energy is changed into heat energy because of the kinetic impact of charge carriers on the electrodes' surface. Due to different particle masses the amount of melted material created by impacting electrons on the anode is less compared to that created by ions on the cathode. Furthermore, the material from the anode is mainly removed at the beginning of the discharge phase. For long discharge durations t_e the anodic material removal decreases towards zero, while the cathodic material removal increases and converges towards a specific value. This phenomenon, known as the polarity effect, can also be explained by the different mobility of the charge carriers [15]. Since μ -EDM operates at very short discharge durations from $t_e = 10$ ns to $t_e = 1$ μ s the tool electrode is usually charged as the cathode to reduce tool electrode wear [13].

The primary material removal takes place during the **breakdown phase**. Switching off the discharge current causes a collapse of the plasma channel. An induced low pressure reduces the boiling temperature of the melted material on the electrodes' surfaces and the material is vaporized or explosively erupted by hydro-mechanical forces [6–9]. The amount of removed material mainly depends on the discharge energy W_e which is defined by:

$$W_e = \int_0^{t_e} u_e(t) i_e(t) dt \approx u_e \cdot i_e \cdot t_e \quad (1)$$

After discharge the working gap is deionized and cleaned from particles by flushing with dielectric fluid during the pulse interval time t_0 . The pulse interval time is generally set to be as long as the pulse duration t_i .

Micro-wire EDM (μ -WEDM)

Wire electrical discharge machining (WEDM), a process variant introduced industrially in 1969 [5], is characterized by a path programmed cut of the workpiece contour by a traveling wire electrode. The kinematics of WEDM is comparable to that of a band saw. The wire electrode is fed

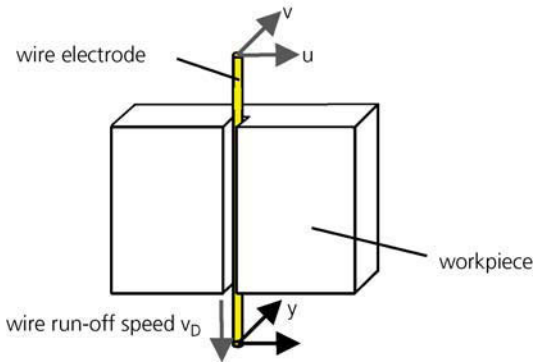


FIGURE 3-7 Illustration of wire-EDM.

from a spool and ‘cuts’ the workpiece along the programmed contour. Either the workpiece or the wire is moved relatively to each other in the x - and y -directions. For this reason, only two-dimensional and no free-form shapes can be machined. Conical shapes can be manufactured by a sloping position of the wire. Hereby the upper guide of the unwinding wire tool electrode is relatively adjustable in the u - and v -directions (Fig. 3-7) to the lower guide. Due to wear and an associated decrease of the wire diameter, the wire electrode can only be used once. A reuse causes an increasing risk of tearing the wire electrode and of deviations in contour.

Multiple Cutting Strategies. To reach high surface quality and geometrical accuracies at efficient cutting speeds, multiple cutting strategies are used. The main cut is applied at the highest available discharge energy. It is related to a maximum material removal rate, low surface quality, and a high thermal influence of the workpiece’s peripheral zones, the white layer. Applying several trim cuts, where the discharge energy, working gap, and tool offset are successively decreased (Fig. 3-8), causes a lower material removal, a thinner white layer ($<1 \mu\text{m}$), and a surface roughness down to $R_a = 0.07 \mu\text{m}$.

Micro-wire Electrodes. In contrast to conventional wire electrodes that are generally made of copper or brass, premium electrodes for μ -WEDM have a more complex build-up, which is also very cost-intensive. Based on a steel or tungsten core which is coated with several layers

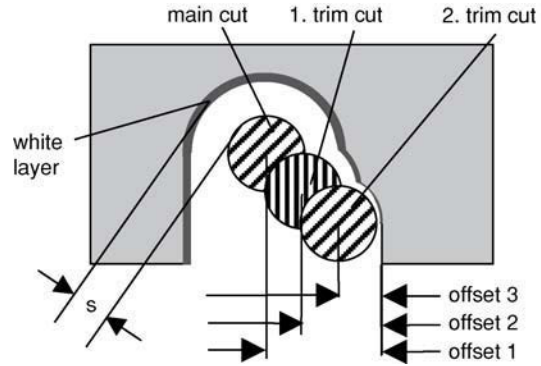


FIGURE 3-8 Multiple cutting strategy.

(e.g. copper, zinc, silver) (Fig. 3-9), it is possible to achieve a combination of high thermal and mechanical stability and high electrical conductivity. Additionally, the soft upper layers decrease abrasive wear of the machine’s wire guiding system. Micro-wires ranging from $d_w = 10 \mu\text{m}$ to $d_w = 100 \mu\text{m}$ have a tensile strength of $\sigma_z = 2000 \text{ N/mm}^2$ to $\sigma_z = 3600 \text{ N/mm}^2$.

Dielectric Fluid and Flushing. As in conventional WEDM, deionized water is also used as a dielectric fluid for μ -WEDM. To minimize the working gap and to increase shape contouring accuracy, the electrical conductivity of the water is reduced to $\kappa_w = 1 \mu\text{S/cm}$. Due to limited mechanical properties of the micro-wire, vibrations easily lead to inaccuracies in shape and a decrease in surface quality. To reduce occurring vibrations and the risk of a damaged micro-



FIGURE 3-9 Build-up of a micro-multi-layer wire electrode.

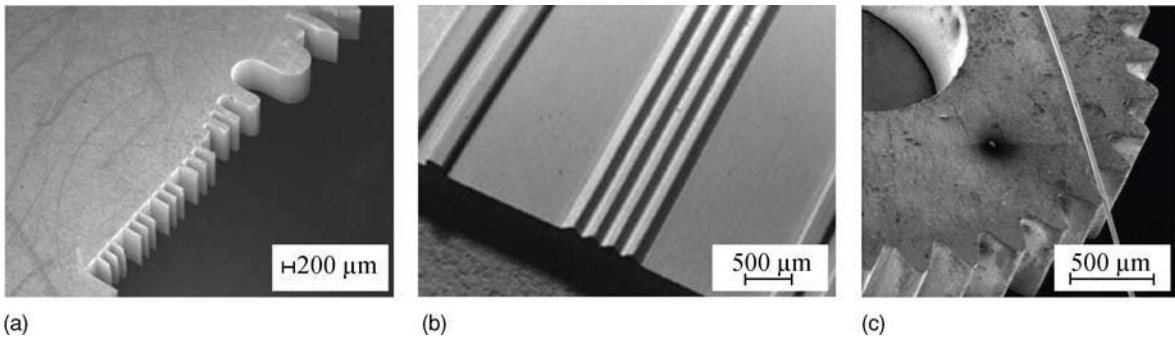


FIGURE 3-10 Micro-structured referential workpiece (a), mold insert for hot embossing micro-opto-electronic connecting plugs (b), and micro-gear of a micro-planetary drive (c).

product, a very low flushing pressure $p_f < 1$ bar or no flushing is used during machining.

Dimensions and Applications. μ -WEDM allows the production of very complex and fine 2D/3D structures (Fig. 3-10(a)). In combination with high precision machines and special relaxation generators, shape accuracies of around $\pm 1 \mu\text{m}$ at high aspect ratios of more than 100 can be machined by using several trim cuts [10]. An aspect ratio is the relation between a characteristic lateral dimension of a micro-structure and its height.

μ -WEDM is mainly used in the field of high precision tool making for micro-mechanical and optical devices (Fig. 3-10(b)). Other applications are micro-gears for the clock and watch industry (Fig. 3-10(c)) and punching dies for electronic components. Micro-tools such as micro-grabbers or components for micro-reactor systems can also be machined by μ -WEDM [11].

Micro-wire Electrical Discharge Grinding (μ -WEDG). A special variant of μ -WEDM is μ -WEDG (Fig. 3-11). In μ -WEDG the wire is moved along two axes of motion through a rotating cylindrical workpiece.

The rotation of the workpiece causes a uniform material removal that allows fabricating pin electrodes with minimal diameters of $5 \mu\text{m}$ or machining disc electrodes with thicknesses down to $7 \mu\text{m}$ used in electrical discharge contouring. Industrial applications of the μ -WEDG process are contact pins for micro-assembly [16], ejector pins for injection molds or micro-single blade

milling tools [17–18]. Other examples are gear shafts that are free of joint patches [18–19] or components for micro-turbines [20].

Micro-die Sinking EDM (μ -die Sinking EDM)

μ -Die sinking EDM is characterized by the replication of the tool electrode's shape into the workpiece. The tool's path motion is basically single axial and the machining is realized in several steps to achieve high surface and geometrical quality. For the finishing of lateral surfaces, planetary machining steps come into operation.

To receive smallest discharge energies for μ -die sinking EDM and high surface quality, generators based on capacities, so-called relaxation generators, are used. Discharge capacitors of $C_c = 10$ pF are able to generate impulses with discharge

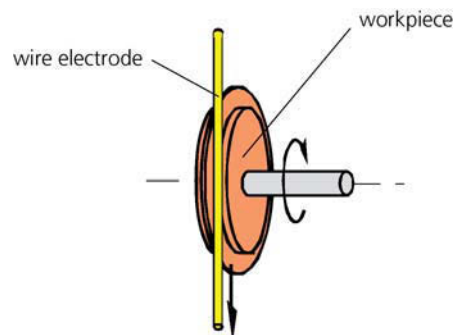


FIGURE 3-11 Illustration of the μ WEDG process.

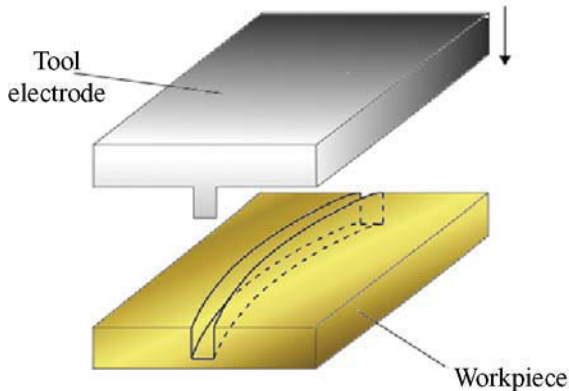


FIGURE 3-12 Illustration of the micro-die sinking process.

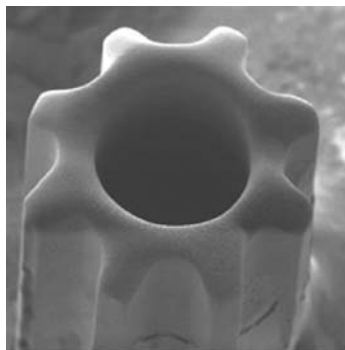
durations of $t_c = 40$ ns at discharge currents of $i_c = 100$ mA to obtain discharge energies of $W_c = 0.1$ μ J [13]. To allow an adequate material removal rate, maximum pulse frequencies of up to $f_p = 10$ MHz are generated [21]. Due to the very short discharge duration, the tool electrode (Fig. 3-12) is charged cathodic and the workpiece is anodic.

Micro-Die Sinking Electrodes. The shape accuracy is mainly influenced by the electrode wear. For this reason suitable materials for micro-die sinking electrodes must offer high electrical conductivity as well as high thermal conductivity and a high melting temperature. Furthermore, these materials should be easy to machine because the main rate of all shaped electrodes is formed by

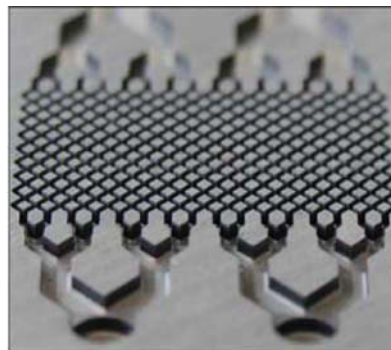
milling processes. Further shaping processes for micro-tool electrodes are μ -WEDM and the LIGA technology (Fig. 3-13). Even though thermally and mechanically resilient materials such as graphite, cemented carbides or tungsten-copper are used for tool electrodes, the relative wear can rise above 30% and is extremely noticeable at structure edges and corners due to increased electric field strength.

Dielectric Fluid and Flushing. Often small dimensions or low mechanical stabilities of the structures on the tool electrode or the workpiece prevent direct flushing strategies. In this case either no or indirect flushing is used. Due to its high dielectric strength, dielectric oil with low viscosity around $\nu_o \leq 1.8$ mm²/s is applied as dielectric fluid in the micro-die sinking process. Compared to deionized water, the oil's higher dielectric strength causes smaller working gaps and therewith higher shape accuracies of the workpiece.

Dimensions and Applications. Today, μ -die sinking is mostly used in single or small batch production. The main application field is the fabrication of tools for micro-embossing (Fig. 3-14 (a)) or micro-injection molding (Fig. 3-14(b) and (c)). Minimal structure widths that can be achieved by μ -die sinking vary from 20 μ m to 40 μ m [5,10]. Also, channels of around 20 μ m and corner radii of 10 μ m at aspect ratios of up to 25 can be produced. Deviations of contouring accuracies are ± 1 μ m [5].



(a)



(b)

FIGURE 3-13 Micro-tool electrodes: gearwheel (a) and fluid mixer (b).

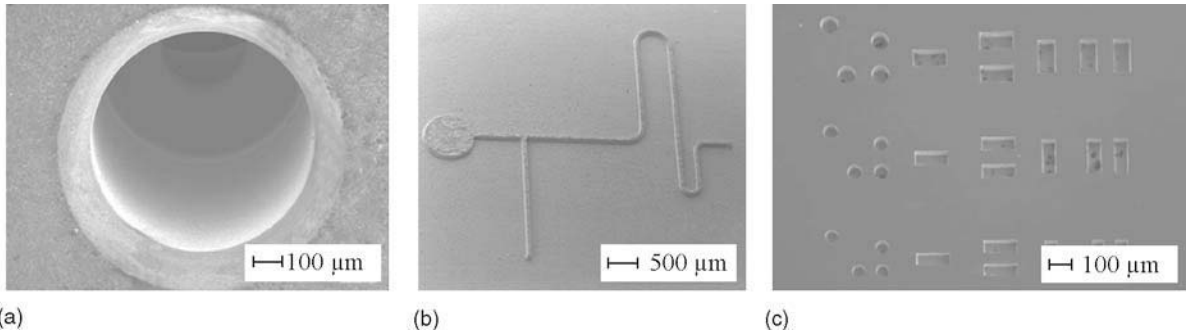


FIGURE 3-14 Micro-fabricated die for shaping small silver pins (a), mold insert for hot embossing fluidic micro-components ('lab-on-a-chip') (b), and mold insert with different referential structures (c).

Micro-electrical Discharge Drilling (μ -ED Drilling)

A special application of μ -die sinking is micro-electrical discharge drilling (μ -ED drilling), which uses small pin electrodes for the manufacturing of boreholes. The rotating or stationary pin electrode is moved single axially into the workpiece (Fig. 3-15).

Micro-drilling Electrodes. Conventional electrodes for μ -ED drilling made from cemented carbide are available with diameters down to $d_p = 45 \mu\text{m}$. Production, handling and positioning (Fig. 3-16) of these electrodes are demanding [10]. Special guiding systems also made from cemented carbide or ceramics are needed for the exact guiding and positioning of the electrode. Tungsten,

tungsten-copper, copper, and brass are used as electrode materials. Pin electrodes with diameters smaller than $d_p = 45 \mu\text{m}$ can be produced using μ -WEDG.

Dielectric Fluid and Flushing. As in μ -die sinking, either deionized water or oil with a low viscosity is used as dielectric fluid. To improve flushing conditions inside the gap and to obtain higher accuracies in roundness, higher aspect ratios and higher material removal rates, the electrodes are rotated at speeds of up to $n_r = 2000 \text{ l/min}$ [10, 22–26]. Additionally, the effectiveness of the flushing is increased by a translatory vibration with an amplitude between $4 \mu\text{m}$ and $20 \mu\text{m}$ and a frequency of 50 Hz to

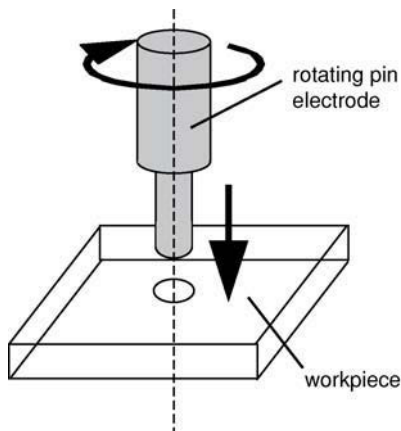


FIGURE 3-15 Illustration of the micro-electrical discharge drilling process.

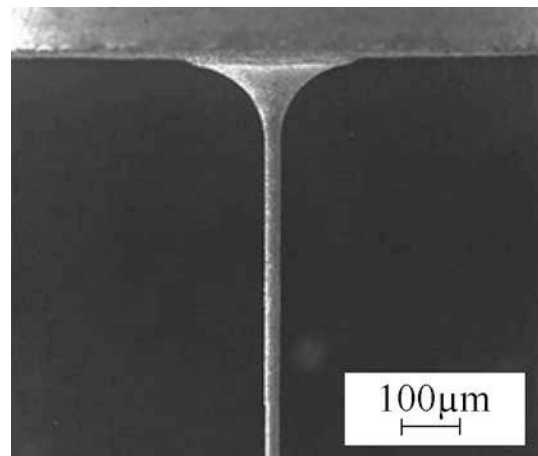


FIGURE 3-16 Electrode for μ -ED drilling made of cemented carbide.

300 Hz which can be superimposed onto the feed of the electrode.

Dimensions and Applications. Boreholes with aspect ratios of 10 to above 50 for tool electrodes with diameters ranging from $d_e = 25 \mu\text{m}$ to $d_e = 100 \mu\text{m}$ can be machined by μ -ED drilling [10]. Reproducible hole diameters of $d_h = 30 \mu\text{m}$ can be produced with a shape accuracy of $\pm 2 \mu\text{m}$. Minimal diameters of $d_h = 6 \mu\text{m}$ [37] and $d_h = 2.9 \mu\text{m}$ [27] have been achieved. μ -ED drilling is mainly used for the fabrication of common rail injection nozzles, cooling boreholes of turbine blades or starting holes for μ -WEDM [10]. Figure 3-17 shows examples for applications like boreholes for ejector pins in embossing tools (Fig. 3-17(a)) or spinning nozzles in a ceramic plate with a depth of 1 mm and a diameter $d_h = 80 \mu\text{m}$ (Fig. 3-17(b)).

Micro-Electrical Discharge Contouring

Using process variants such as μ -die sinking or μ -WEDM the fabrication of large molds with widely spread micro-structures of different heights is sometimes very cost-intensive or not possible at all. Reasons for this are the limited workpiece heights caused by the micro-wire's mechanical and thermal stability, or maximal overall dimensions of the die considering adequate flushing conditions inside the working gap. As an alternative, micro-electrical discharge contouring process variants such as micro-electrical discharge milling (μ -ED milling) or

micro-electrical discharge grinding (μ -EDG) can be used.

In contrast to μ -ED drilling which only works in one direction, μ -ED milling uses a rotating pin electrode that is moved through the workpiece on a defined three-dimensional path (Fig. 3-18(a)). Typical infeed rates of the pin vary from $0.5 \mu\text{ms}^{-1}$ to a maximum of $10 \mu\text{ms}^{-1}$ [28]. Thus, in electrical discharge milling it is possible to produce free-forms and cavities without fabricating a special tool electrode.

μ -EDG (Fig. 3-18(b)) uses a rotating disc electrode instead of a pin electrode. The profile of the disc is reproduced in the workpiece as a channel. Similar to μ -ED milling, the electrode can also be moved in three dimensions which enables the fabrication of long, curved channels of different depths.

Micro-electrical Discharge Contouring Electrodes. Even though high strength materials such as cemented carbide, tungsten or tungsten-copper are applied, the tool wear of the pin electrode with a minimal diameter of $d_m = 45 \mu\text{m}$ is very high. In electrical discharge contouring it is possible to regulate the wear by using special wear compensation algorithms that are superimposed onto the CNC-controlled path. Disc electrodes can be used for the manufacturing of extensive channel structures which cannot be produced by μ -WEDM. A main advantage of disc electrodes is the allocation of the wear on the circumferential length. Disc electrodes made of tungsten copper can either be produced by cutting removal

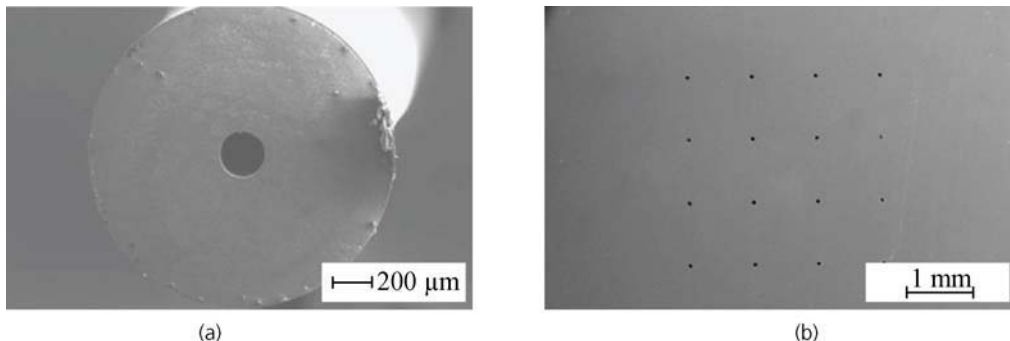


FIGURE 3-17 High precision borehole in an ejector pin (a), spinning nozzles in a ceramic plate (b).

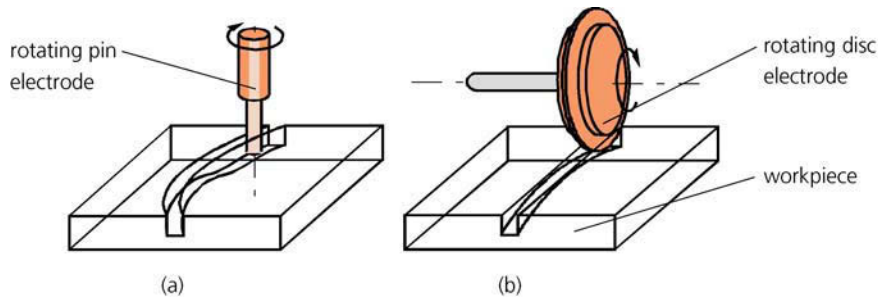


FIGURE 3-18 Illustration of micro electrical discharge milling (a), and μ -EDG process (b).

processes or μ -WEDG. Electrodes with minimal widths of $7\ \mu\text{m}$ have been successfully manufactured by μ -WEDG and have been applied [29,30, 31].

Dielectric Fluid and Flushing. Due to the open shape of the workpiece and the rotating electrode in micro-electrical discharge contouring, the flushing conditions inside the working gap are comparable to micro-die sinking EDM. With regard to the variant of μ -ED milling, flushing through the electrode can be applied to increase material removal and decrease machining time.

Dimensions and Applications. Today, μ -ED milling is used for the fabrication of cavities (Fig. 3-19(a)) or channels in injection molds, reliefs in embossing dies or prismatic micro-molds [28]. Due to its novelty, long machining time and disadvantages regarding finishing strategies, μ -ED milling has only a small relevance in industrial application so far. μ -EDG realizes the fabrication of very long structures which predetermine

this process variant for the production of micro-fluidic channels (Fig. 3-19(b)). Other industrial applications are the post-production of cutting inserts made of polycrystalline diamond or cemented carbides and micro-structuring of grinding wheels [32].

MACHINES AND TOOLS

Machine Design

Basic EDM equipment consists of the machine unit with actuation components, the generator, the dielectric unit including pumps, filters, and cooling (Fig. 3-20), and in the case of WEDM a deionization unit (Fig. 3-21). To ensure the high precision of μ -EDM many components of the system are produced with materials of a long-term thermal and mechanical stability such as ceramics. Also, servo drives with positional accuracies of around $1\ \mu\text{m}$ and high precision clamping systems are used.

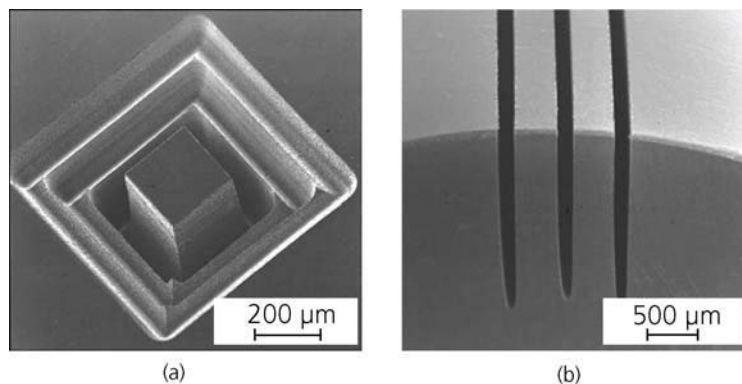


FIGURE 3-19 Cavity fabricated by μ -ED milling (a), μ -EDG produced micro-fluidic channels (b).

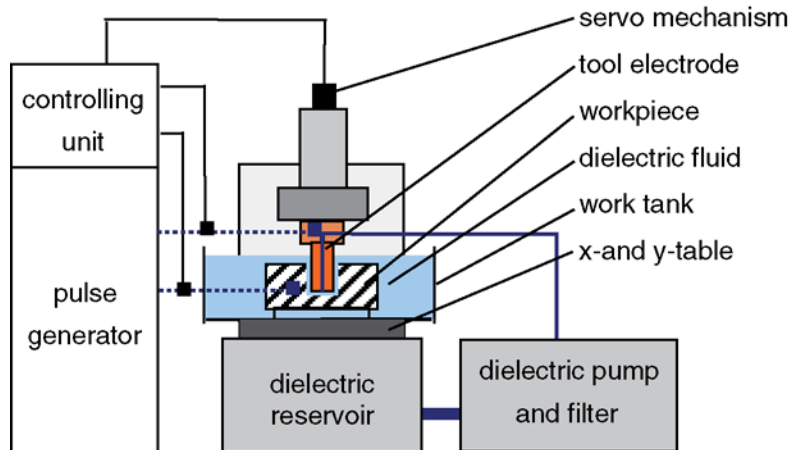


FIGURE 3-20 Die-sinking ED machine tool.

Die-sinking EDM Machine. Die-sinking EDM machines are mainly built as a C-frame construction (Fig. 3-20). The tool electrode is moved along the z -axis by a servo-drive which is controlled by the machine control. The controlling unit is connected to a power supply that provides a pulsed DC output, the so-called pulse generator. The power supply is also controlled. The workpiece, which is immersed in a tank of dielectric fluid, is connected to one lead of the pulse generator. The tool electrode is linked to the other lead of the power supply. The tank is placed on an x - and y -axis table and is moved during the machining process. It is combined with a dielectric pump, a fluid reservoir, and a filter system. The pump provides pressure for flushing the working gap. The filter system refines removed material particles

from the dielectric fluid. The dielectric reservoir stores and cools additional dielectric fluid and provides a container for draining the dielectric fluid between the operations.

Wire EDM Machine. In wire EDM machines (Fig. 3-21), which are built as a C-frame or gantry portal construction, the wire electrode is constantly fed from a spool. It is guided by rolls through an upper and lower nozzle head. The lower nozzle head is fixed. The upper nozzle head can be moved horizontally (u, v) and vertically (z). Thus, in combination with an x - and y -motion of the workpiece, it is possible to machine conical shapes of different heights with angles ranging from 0° to 15° , depending on the machine design. To reduce oscillations caused by electromagnetic, electrostatic or hydromechanical forces, the wire

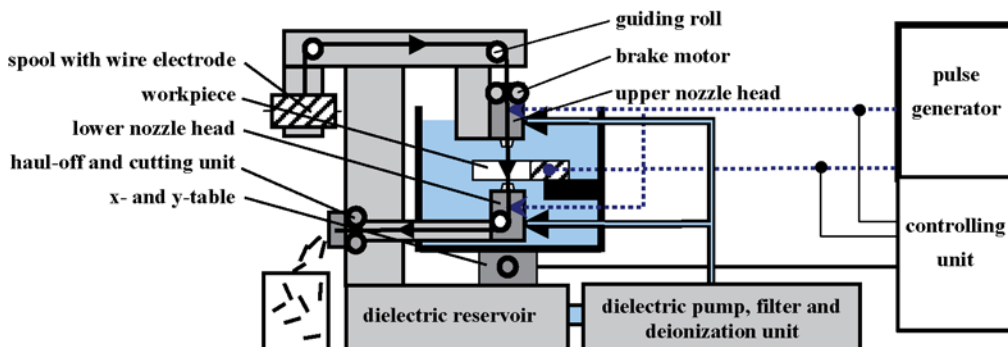


FIGURE 3-21 WEDM system.

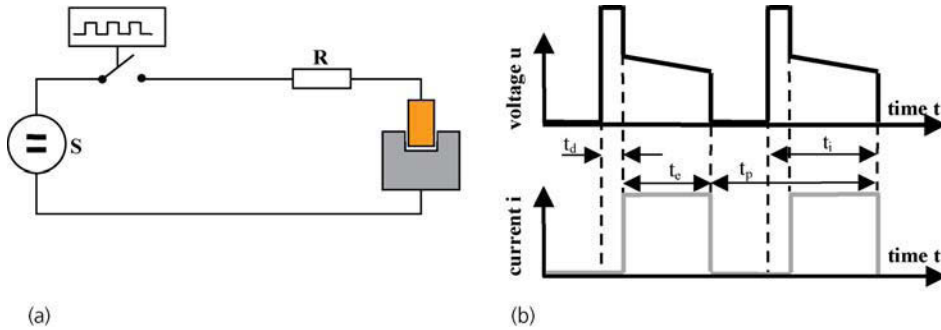


FIGURE 3-22 Static pulse generator: schematic illustration (a), voltage and current diagram including ignition delay time (t_d), discharge duration (t_e), pulse duration (t_i), and pulse cycle time (t_p) (b).

is strained with a defined force that is generated by a brake motor and a haul-off unit. After use the wire is cut, chopped and recycled.

Generator Types

Modern EDM machines provide two different types of generators in order to fit a wide range of different applications: static pulse generators for roughing operations and relaxation generators for micro-structuring and finishing operations.

Static Pulse Generators. Static pulse generators are characterized by a controlled current or voltage source which generates rectangular single pulse discharges [12]. The source is directly connected to the discharge path via electronic switching elements (Fig. 3-22). Pulse shape, pulse duration t_i , and discharge duration t_e can be adjusted and controlled for the realization of a relatively low wear of the working electrode.

In contrast to relaxation generators static pulse generators allow the setting of the discharge duration t_e independently of the discharge current i_e and are normally used for intensive material removal processes with long discharge durations t_e and high discharge currents i_e .

Relaxation Generators. The principle setup of a relaxation generator is a direct current source in combination with different storage elements (RC, RLC or LC circuits) [12] (Fig. 3-23). In case of charged storage elements the gap between the tool electrode and the workpiece serves as a switch. After exceeding the dielectric strength of the dielectric fluid, an oscillating discharge is released. Discharge duration t_e and discharge current i_e depend on the value of the capacity and cannot be controlled independently as this is the case with a static pulse generator. Additionally, the pulse frequency depends on the charging voltage of the capacity. Due to very small discharge

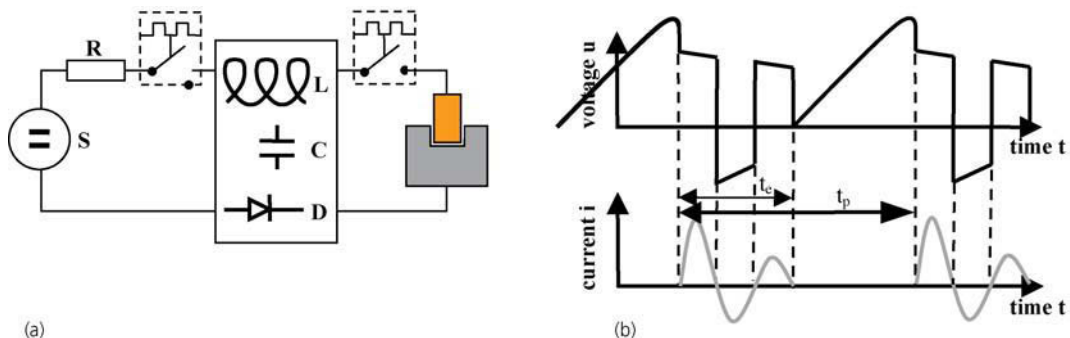


FIGURE 3-23 Relaxation generator: schematic illustration (a), voltage and current characteristic including discharge duration (t_e), and pulse cycle time (t_p) (b).

energies of down to $W_e = 0.1 \mu\text{J}$ at high pulse frequencies of up to $f_p = 10 \text{ MHz}$, relaxation generators are used for micro-machining and precise surface finishing.

Adaptive Feed Control. In contrast to cutting technologies, the feed rate in EDM is adaptively controlled by the control of the EDM machine. A constant feed rate can lead to short circuits, resulting in a destruction of the micro-structures. The adaptive feed control analyzes the measured parameters of the electrical impulse characteristics and classifies them using a pulse detection unit. According to that detection, the feed rate is regulated by a control circuit.

The electrical impulses are classified in four different types (Fig. 3-24) which result from the conditions inside the gap: no-load discharge, normal discharge, arc discharge, and short circuit.

No-load discharges occur when the working gap is oversized. As a consequence the build-up of a plasma channel is prevented and the discharge current does not flow. The adaptive feed control reacts with an increase of the feed rate. At a **normal discharge** the width of the working gap has an optimal size. For the following discharges the adaptive feed control tries to keep a constant feed

rate. An **arc discharge** is characterized by a premature ignition of the spark. The real ignition delay time t_{dr} is far below the set value of the ignition delay time t_d . This type of discharge is caused by a high concentration of electro conductive particles inside the gap. This status is normally followed by a series of normal discharges. The adaptive feed control reacts with a decrease in feed. **Short circuits** can either occur due to contact between the tool electrode and the workpiece or because of remaining particles that form an electrical linkage [13]. To leave that state, the tool electrode is pulled back along the machining path.

Depending on the application, different control technologies and strategies based on fuzzy logic are used in modern $\mu\text{-EDM}$ machines such as adaptive control optimization (ACO) or adaptive control constraint (ACC) are used in modern $\mu\text{-EDM}$ machines.

DESIGN CONSIDERATIONS

$\mu\text{-EDM}$ Optimized Design

In the case of manufacturing a punch and die set, it is beneficial to use identical materials, ideally a

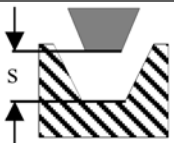
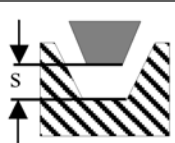
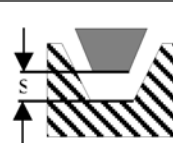

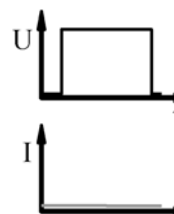
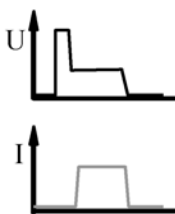
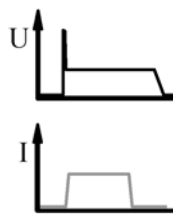
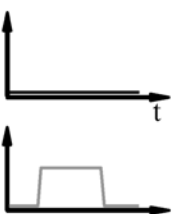
Discharge type	No-load discharge	Normal discharge	Arc discharge	Short circuit
Cause	Working gap is too big	Working gap is optimal	Working gap is too small	Working gap $s = 0$
Illustration				
Effect				
Reaction	Increase of feed rate	Constant feed rate	Decrease of feed rate	Pullback of tool electrode

FIGURE 3-24 Illustration of the principle controlling strategies.

fine grained steel alloy. Especially in the case of μ -WEDM with deionized water as dielectric fluid, it is recommended to use stainless steel. It is necessary to consider clear reference sides and to prevent machining operations from different directions due to multiple clamping and connected inaccuracies. At least one outside surface is needed for electrical touching. If possible, subsequent heat treatment should also be prevented due to risk of shape deviations. If heat treatment is still necessary it should be applied before EDM processing.

In μ -WEDM the workpiece height is limited by the thermal and mechanical stability of the wire electrode which depends on the diameter of the wire. Inside contours generally require a start hole for the wire. For proper insertion of the wire the start hole should be larger than the wire diameter. Modern WEDM machines are able to insert a wire in a start hole with 30 μm oversize automatically.

The main fact to consider during the design of a part to produce with μ -die-sinking EDM is the shape of the tool electrode. The applied shaping process, e.g. micro-milling, laser ablation or μ -WEDM, must be able to produce the negative shape of the workpiece contour. A preferred shaping process for thin contours is μ -WEDM instead of micro-milling due to the smaller structure dimensions and higher accuracy that it allows. In μ -EDM the application of the same clamping

system for the shaping process is needed due to a defined clamping accuracy if a reworking of the electrode is needed.

Material Selection

Every material with an electrical conductivity above $\kappa = 0.01 \text{ S/cm}$ can be machined by EDM (Fig. 3-25). Mechanical properties like Young's modulus, hardness or strength do not have an influence on the process behavior. Consequently, EDM is especially used for the machining of hard and difficult-to-cut materials such as cemented carbides for punching tools, PCD for cutting inserts or high alloy steels for injection molding tools.

The amount of material being removed is influenced by its thermal and electrical properties. Contrary to a high electrical conductivity (Fig. 3-26(a)) that promotes material removal, high thermal conductivity and high melting temperature reduce the material removal (Fig. 3-26(b) and (c)). This is of special importance when selecting wear resistant electrode materials.

Tool Electrodes for μ -EDM

Up-to-date tool electrode materials for μ -EDM are electrolyte copper, tungsten and tungsten composites such as tungsten copper or tungsten carbide.

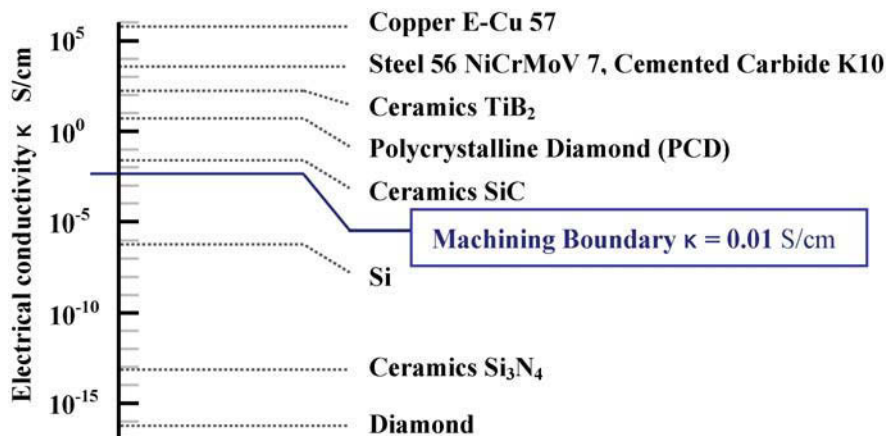


FIGURE 3-25 Machinable and non-machinable materials.

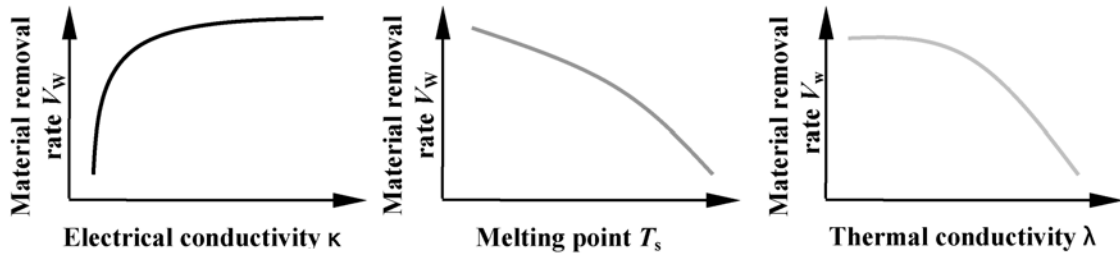


FIGURE 3-26 Influence of thermal and electrical properties on material removal rate.

The attractive attributes of **electrolyte copper** are its high electrical and thermal conductivity. Electrolyte copper is easy to obtain, very consistent in quality, and low in cost. A disadvantage of the material is its limited grindability [12]. Due to mechanical instability, the material's ductility and softness can cause problems when milling small structures. Another problem is the high wear of electrodes made from electrolyte copper.

Tungsten is a metal of very high strength, density and hardness. With a melting point near 3400°C , it resists thermal damaging effects of the EDM process very well. Disadvantages of tungsten are a very high material price. It is also difficult to machine because of its high hardness. To make tungsten more attractive for certain applications it is combined with ductile materials such as copper.

The resulting material, **tungsten copper**, is easier to machine, more conductive than normal copper and extremely wear resistant. Especially in the field of micro-structuring and surface finishing, tungsten copper is used as the tool electrode material.

APPLICATIONS

A final summary of the chapter and the wide application field of μ -EDM are shown in Table 3-2.

TECHNOLOGICAL COMPETITIVENESS AND OPERATION ECONOMICS

In various industrial sectors a number of micro-technical components with a volume of less than

1 mm^3 and structure dimensions in the range of micrometers come into application. The production of these components is usually done by technologies that originated in the semiconductor industry. To avoid the technological limitations of these processes as well as the very high investments, the mass production of micro- or miniature parts is increasingly based on replication technologies such as hot embossing, micro-injection molding or bulk forming. To achieve a sufficient tool life, functional materials like hardened steel or cemented carbide are used due to the high thermal and mechanical loads in the forming process. The mechanical properties of these materials limit the variety of structuring processes which can be applied. Next to micro-cutting, laser machining, and LIGA technology, electrical discharge machining (EDM) is a manufacturing technology which can be applied. Due to the non-contact thermal material removal mechanism, EDM technologies offer a suitable alternative in terms of obtainable structure dimensions and accuracy. Since EDM can be economically applied in single and small batch production, in addition to its use for the primary structuring of micro-parts, it is predetermined for the production of micro-dies and molds [33–35].

Considering the operation economics of μ -EDM, it is necessary to know the workpiece accuracies that are needed. Although most μ -EDM machines include a cooling system for the dielectric fluid and therewith offer adequate thermal long-term stability, an air conditioned installation is needed to achieve the best geometrical accuracy. Despite an air conditioned installation the temperature can change around $T = 1\text{ K}$ which can influence the machine accuracy.

TABLE 3-2 Table of μ -EDM Process Variants According to Performance and Applications

Process Variant	Geometry Complexity	Structure Dimension	Surface Quality	Application Examples
Micro-wire EDM (μ -EDM)	<ul style="list-style-type: none"> – 2{1/2}D – Tapered surfaces with maximal angles of 15° 	<ul style="list-style-type: none"> – Min. inner radii, cutting width, and max. workpiece height depends on wire diameter, e.g. at $d_{wmin} = 0.03$ mm, $s_{min} = 0.005$ mm, $h_{max} = 5$ mm 	$R_a \sim 0.07^{1)}$ $R_z \sim 0.35^{1)}$ ¹⁾ with multiple cutting strategy	<ul style="list-style-type: none"> – Forming tools for opto-electronic components – Lead frame stamping tools – Spinning nozzles – Micro gears
Micro-die sinking (μ -die sinking)	<ul style="list-style-type: none"> – 3D – Freeform surfaces – Undercuts possible by planetary erosion – Limited by electrode manufacturing 	<ul style="list-style-type: none"> – Min. structure width ~ 0.02 mm – Aspect ratio ~ 20 	$R_a \sim 0.1 \mu m^{1)}$ $R_z \sim 0.5 \mu m^{1)}$ ¹⁾ in all directions	<ul style="list-style-type: none"> – Micro-injection molds – Embossing molds for micro-optics
Micro-electrical discharge drilling (μ -ED drilling)	<ul style="list-style-type: none"> – 2D – Boreholes 	<ul style="list-style-type: none"> – Bore hole diameters down to $d_{min} = 0.04$ mm – Aspect ratio from 25–50 	$R_a \sim 0.3 \mu m^{1)}$ $R_z \sim 1.5 \mu m^{1)}$ ¹⁾ lateral	<ul style="list-style-type: none"> – Injection nozzles – Micro-fluid systems – Starting holes for μ-WEDM
Micro-electrical discharge grinding (μ -EDG)	<ul style="list-style-type: none"> – 2{1/2}D – Straight partly vertically curved channel structures – Profile of structure depends on cross-section of disc 	<ul style="list-style-type: none"> – Min. structure widths of 0.07 mm – Aspect ratio ~ 15 – Possible length depends on electrode wear (>50 mm) 	$R_a \sim 0.2 \mu m^{1)}$ $R_z \sim 0.8 \mu m^{1)}$ ¹⁾ in all directions	<ul style="list-style-type: none"> – Embossing and coining tools – Micro-fluid channels
Micro-electrical milling (μ -ED milling)	<ul style="list-style-type: none"> – 3D – Free-form surfaces 	<ul style="list-style-type: none"> – Min. inner radii depend on pin diameter – Applicable electrode diameter $d_{min} = 0.1$ mm 	$R_a \sim 0.2 \mu m^{1)}$ $R_z \sim 0.8 \mu m^{1)}$ ¹⁾ in all directions	<ul style="list-style-type: none"> – Cavities for micro-injection molding – Embossing or coining tools
Micro-wire electrical discharge grinding (μ -wire EDG)	Rotational symmetric structures (discs, pins)	<ul style="list-style-type: none"> – Min. pin electrode diameter $D_{min} \sim 0.02$ mm – Aspect ratio ~ 30 	$R_a \sim 0.15 \mu m$ $R_z \sim 0.75 \mu m$	<ul style="list-style-type: none"> – Pin electrodes – Rolling tools

Therefore, most μ -EDM machines consist of a machine frame made from granite and have ultra-precise linear axes. This drives the price to levels of more than €300,000 for a high end μ -WEDM machine. Considering the tooling costs

of EDM wire electrodes, there are differences regarding the wire diameter. Whereas the price for conventional wire electrodes with diameters from $d = 300 \mu m$ down to $d = 100 \mu m$ is around €8/kg to €15/kg, the price for micro-wires

with diameters $d < 50 \mu\text{m}$ can easily be 3 to 5 times this amount. The operating costs for a μ -EDM machine depend on the dielectric fluid. When applying deionized water additional costs such as for deionization resin need to be considered. In the case of dielectric oil as the dielectric fluid, the costs for renewing the oil have to be considered as well as the costs for wear strained parts in the wire guiding system, debris filter, and electricity (Table 3-3).

As an example, the following listing shows the average costs of a WEDM machine, AGIE Evolution, in a dual-mode operation (roughing, finishing process for cemented carbide/steel up to $R_a = 0.2$ with wires CCA 0.2/0.25) with an average eroding performance of ~ 4000 machining hours per year and the use of the wearing part kit 8000 for 8000 machining hours. Additional peripheral units such as air conditioning, cooling or lighting are not included [36].

Due to the complex machine structure, machine control, and process technologies, it is recommended to train technicians with courses offered from machine suppliers. These courses last one to two weeks and cost between €5000 and 1 €10,000.

THE OUTLOOK

During to the latest development in end mill geometry, micro-milling is able to machine materials with a hardness of up to 60 HRC. Cutting technologies originated for non-conventional machining processes are pushing into the market.

TABLE 3-3	Cost Listing AGIE Evolution/ Classic 2/3 S
Wearing parts	€0.30
Filter	€0.61
Deionization resin	€0.51
Water	€0.06
Electricity	€0.58
Wire costs	€2.52
Total	€4.58

Limiting factors for the application of micro-milling and grinding for structuring micro-parts are the process forces. Therefore, at a comparable cost listing for micro-milling, μ -EDM, as a process that is almost force free and independent of material properties, is predestined for micro-structuring. Even though the process is slower compared to micro-milling, the independence of the material's hardness is a big advantage which will gain in further importance in the future.

Latest machine developments and research activities show a trend toward hybrid processes to combine the possibilities and advantages of different technologies and therewith reach best machining results more efficiently. One example is the 'Hybrid Wire[®]' machine from Sodick[®], which combines water jet cutting and WEDM. Further research activities head toward the combination of laser ablation and EDM technologies, e.g. using laser ablation for roughing operations and ED contouring for finishing. In the field of tool electrodes, research concentrates on developing more wear resistant materials, e.g. electrodes with special diamond coatings. Also extending the spectrum towards new workpiece materials plays an important role. The development of EDM process variants concerning the machining of low conductive high performance materials related to even higher wear resistance and new application fields especially comes into focus. An essential demand for new EDM systems is the fabrication of workpieces with shape accuracies smaller than $1 \mu\text{m}$ at shorter process times. Therefore, new, more precise positioning systems and generators with higher pulse frequencies than the present ones are needed that will turn μ -EDM into nano-EDM.

REFERENCES

- [1] E. Uhlmann, Trennende Fertigungsverfahren für neue Perspektiven in der Mikrotechnik, Forschungspolitische Dialoge in Berlin: MST – Schlüsseltechnologie des 21. Jahrhunderts, Berlin (1998).
- [2] E. Uhlmann, U. Doll, Mikrofunkenerosion zur Fertigung von Mikrosystemen, Jahrbuch Innovative Produktion 2000, Trade & Contact Verlag, Berlin (März 2000).

- [3] A. Wolf, W. Ehrfeld, H.P. Gruber, Mikrofunkenerosion für den Präzisionsformenbau, *wt Werkstattstechnik* (1999) H. 11/12.
- [4] S. Thiel, S. Lehnice, O. Zimmer, D. Grimme, U. Doll and S. Piltz, Abformung von Mikrostrukturen in Glas, VDI-Z Special Werkzeug- und Formenbau VII/2000.
- [5] W. Menz, J. Mohr, O. Paul, *Mikrosystemtechnik für Ingenieure*, Wiley-VCH Verlag GmbH Co, KGaA, Weinheim (2005).
- [6] B.R. Lazarenko, N.I. Lazarenko, *Elektrische Erosion von Metallen*, Cosenergoidat, Moskau (1944).
- [7] B.R. Lazarenko, *Die Elektrofunkenbearbeitung von Metallen*, Vestuik Maschinostroia (1974).
- [8] B.N. Zolotych, *Physikalische Grundlagen der Elektrofunkenbearbeitung von Metallen*, SVT 175 VEB-Verlag Technik, Berlin (1955).
- [9] B.N. Zolotych, *Über die physikalischen Grundlagen der elektroerosiven Metallbearbeitung*, Bd. 1: Elektroerosive Bearbeitung von Metallen, Moskau: Akademie der Wissenschaften der UdSSR (1957).
- [10] E. Uhlmann, S. Piltz and U. Doll, Machining of micro/miniatue die and moulds by electrical discharge machining – recent development, *Journal of Materials Processing Technology*, Elsevier (2005).
- [11] R. Brück, N. Rizvi, A. Schmidt, *Angewandte Mikrotechnik – LIGA – Laser-Feinwerktechnik*, Carl Hanser Verlag München Wien (2001).
- [12] W. König, *Fertigungsverfahren Band 3*, VDI-Verlag GmbH, Düsseldorf (1990).
- [13] S. Piltz, *Grundlagen und Prozessstrategien der Mikrofunkenerosion für die Bearbeitung von Rotationsbauteilen*, Fraunhofer IRB Verlag, Stuttgart (2007).
- [14] F.-J. Siebers, *Funkerosives Senken mit wässrigen Arbeitsmedien*, Grundlagen, Technologie und Wirtschaftlichkeit, Dissertation, RWTH Aachen (1994).
- [15] J. Schönbeck, *Analyse des Drahterosionsprozesses*, Carl Hanser Verlag München Wien (1993).
- [16] H.H. Langen, T. Masuzawa, M. Fujino, Modular method for microparts machining and assembly with self-alignment, *Annals of the CIRP* 44(1) (1995).
- [17] J. Fleischer, T. Masuzawa, J. Schmidt and M. Knoll, New applications for micro EDM, *Proc. of the 14th International Symposium for Electromachining (ISEM XIV)*, March 30–April 1, 2004, Edinburgh, Scotland, UK, published in *J. of Materials Processing Technology* 149 (1-3) (2004).
- [18] J. Fleischer, J. Schmidt, M. Knoll, S. Haupt, C. Müller, R. Förster, A. Gehringer, *Mikrobearbeitung durch Abtragen*, *wt Werkstattstechnik online*, Jahrgang (2004) H. 11/12.
- [19] R. Förster, *Untersuchung des Potenzials elektrochemischer Senkbearbeitung mit oszillierender Werkzeugelektrode für Strukturierungsaufgaben der Mikrosystemtechnik*, Albert-Ludwig-Universität Freiburg, Dissertation (2004).
- [20] T. Masaki, K. Kawata, T. Masuzawa, *Micro electro-discharge machining and its applications*, *Proceedings of IEEE MEMS* (1990).
- [21] T. Masaki, et al. *Micro electro-discharge machining*, *Proceedings of the 9th International Symposium for Electromachining-ISEM IX*, Nagoya (Japan) (1989).
- [22] D. Allen, H. Almond, and P. Logan, A technical comparison of micro-electro-discharge machining, microdrilling and copper vapour laser machining for the fabrication of ink jet nozzles, *Proc. of SPIE Conference on Design, Test, Integration and Packaging of MEMS/MOEMS*, 4019, Paris, France, May 9–May 11, (2000).
- [23] M. Ghoreishi, M. and J. Atkinson, Vibro-rotary electrode, a new technique in EDM drilling – performance evaluation by statistical modelling and optimisation, *Proc. of the 13th International Symposium for Electromachining (ISEM XIII)*, Bilbao, Spain, Vol. II, May 9–May 11, (2001).
- [24] M. M. Ghoreishi, J. Atkinson, A comparative experimental study of machining characteristics in vibratory, rotary and vibro-rotary electro-discharge machining, *J. of Materials Processing Technology* 120 (2002).
- [25] A. Muttamara, Y. Fukuzawa, N. Mohri, T. Tani, Probability of precision machining of insulating Si₃N₄ ceramics by EDM, *J. of Materials Processing Technology* 140 (2003).
- [26] E. Uhlmann, *Funkerosives Feinbohren keramischer Werkstoffe. Abschlussbericht zum DFG-Forschungsprojekt UH 100/22-2*, Technische Universität, Berlin (2002).
- [27] N.N., *Pressemitteilung der Fa. Sodick Europe Ltd*, Coventry, UK, zur Präsentation der AE05 Nano EDM Machine, erschienen in: www.tool-moldmaking.com.
- [28] W. Meeusen, D. Reynaerts, J. Peirs, H. Van Brussel et al., *The machining of freeform micro moulds by micro EDM – work in progress*. *Proc. of Micromechanics Europe Workshop*, Cork, Ireland (MME 2001).
- [29] A. Wolf, W. Ehrfeld, H. Lehr, F. Michel, T. Richter, H. Gruber, O. Wörz, *Mikroreaktorfertigung mittels Funkerosion*, *F&M Fernwerk- und Mikrotechnik* (1997) 6.
- [30] H.-M. Chow, B.-H. Yan, F.-Y. Huang, *Micro slit machining using electro-discharge machining with a modified rotary disk electrode (RDE)*, *J. of Materials Processing Technology* 91 (1999).
- [31] C.-L. Kuo, J.-D. Huang, *Fabrication of series-pattern micro-disk electrode and its application in machining micro-slit of less than 10 µm*, *Int. J. of Machine Tools and Manufacture* 44 (2004).
- [32] S. Appel, *Funkerosive Bearbeitung von ploykristallinem Diamant*, Technische Universität Berlin, Dissertation (1998).

- [33] E. Uhlmann, U. Doll, Application of μ -EDM in the machining of micro structured forming tools, Proceedings of the 3rd Int. Machining & Grinding Conf, Cincinnati (USA) (1999).
- [34] F. Michel, W. Ehrfeld, O. Koch, H.-P. Gruber, EDM for micro fabrication – technology and applications, Proceedings International Seminar on Precision Engineering and Micro Technology, Aachen (Germany) (2000).
- [35] T. Masuzawa, State of the art of micromachining, CIRP Annals – Manufacturing Technology 49(2) (2000).
- [36] AGIE, Cost listing of an AGIE Wire EDM Machine (2003).
- [37] D.M. Allen, Micro electro discharge machining for MEMS applications, IEE Seminar on Demonstrated Micromachining Technologies for Industry, Ref. No. 2000/032 (2000).

Laser Micro-Structuring

Arnold Gillner

INTRODUCTION

In the production of micro-scaled products and micro-replication tools, laser ablation is becoming an ever more important tool, which is able to generate structure sizes in the range of 10–100 μm , not only in metals but also in hard and ultra-hard materials such as tungsten carbide and ceramics. Especially for micro-machining, laser processes qualify for a wide range of materials, from semiconductors in the field of micro-electronics, to hard materials such as tungsten carbide for tool technology, to very weak and soft materials such as polymers for medical products. Even ceramics, glass and diamond can be processed with laser technologies with accuracies better than 10 μm . In comparison to the classical technologies, laser processes are generally used for small and medium lot sizes but with strongly increased material and geometric variability.

Using ultra-short pulsed lasers with durations of 10 ps in bursts of several pulses with a time spacing of 20 ns each and adapted pulse energies, the surface quality of metal micro-ablation has been increased significantly and allows the production of tools and parts with R_a values of less than 0.5 μm . Compared to conventional EDM processing, laser manufacturing of parts and tools can be performed without additional working tools in reasonable times directly from the CAD-CAM system.

Micro-ablation by means of laser-based vaporization of materials has been used in a large variety of applications to produce micro-molds,

functional components in electronics and micro-drilling applications. Most of these processes were focused on small parts, where the laser has its unique position in selectivity and low thermal input without changing the properties of the entire part. Recent developments in solar cell manufacturing, display manufacturing and the manufacture of products based on electrically conducting polymers such as OLEDs have opened a new field in laser micro-manufacturing with laser radiation, where the specific advantages and outstanding properties of laser radiation are highly sought after. Laser micro-ablation and surface fictionalization with:

- micron and sub-micron scale accuracy in ablation depth
- nanometer scale in-depth heat input
- micron scale lateral accuracy and
- sub-micron scale in lateral dimensions with special process techniques

on almost all types of materials allow new manufacturing processes, when the production of components cannot be met by conventional processes. In this way laser ablation and surface fictionalization have been already proven as a non-convertible tool in solar cell and display manufacturing.

BASIC PROPERTIES OF LASER ABLATION

The precision of laser ablation is given by a combination of different effects, which is related to

- the working tool (geometry of the laser beam)

- the process itself (laser/material interaction) and
- the positioning system for the part and the laser beam.

Laser radiation is used as a working tool to structure matter by thermal vaporization with well-defined volumes and high lateral precision. For this, depending on the type of laser and processing technology, laser radiation is focused or projected by objectives onto the surface, and subsequently formed into a specific spatial intensity distribution. Depending on the intensity, the absorption conditions of the materials and the interaction time, several aspects have to be considered, which define the ablation geometry and the precision of the ablation process.

The precision of the resulting structures depends not only on the focus diameter and the positioning stage, but also on the precision of the process resulting from the reactions of the matter during and after irradiation. Thus, the processing diameter depends not only on the beam radius w_0 , but also on the physical properties of the material, such as the reflectivity, absorption, melting and evaporation enthalpy. Depending on the optical properties of the material and on the applied radiation, the precision of the process diameter depends on the absorption of the radiation, which can be linear or non-linear. Additionally, the ablation depends strongly on the pulse duration and on the wavelength.

Absorption Effects on Ablation Geometry

Generally the interaction of photons and matter is based on the absorption of the electromagnetic energy at the free and bound electrons of a material. The electrons are heated and transfer their energy after a characteristic time to the lattice of the material. After transfer of the optical energy to the lattice, the material heats up and starts to melt and subsequently vaporizes with further energy deposition. The laser-induced ablation itself can be distinguished between photo-induced and thermal ablation. The precision is greater for photo-induced abla-

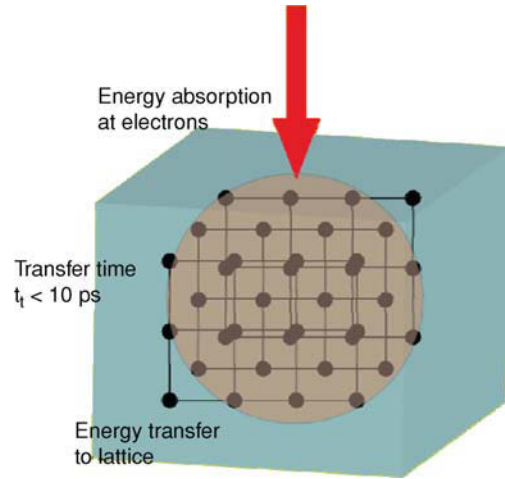


FIGURE 4-1 Principle of laser beam interaction with materials.

tion being comparable to the precision of the working tool, here resulting in the processing diameter. In the case of the thermal ablation, additional processes such as heat diffusion decrease the precision and give rise to a larger processing diameter than the focus diameter.

For most of the materials in laser material processing, surface absorption is the dominating process. Materials absorb laser radiation linearly, when an absorption band at the laser wavelength (Fig. 4-1) or due to free or quasi-free electrons being present (such as metals or graphite) is given. This can be described by Lambert-Beer's law:

$$I(x) = (1 - R)I_0 e^{-\alpha x} \quad (1)$$

where R is the reflectivity, α is the absorption coefficient (cm^{-1}), and I_0 is the threshold intensity for ablation (W/cm^2). Based on this, a logarithmic dependence of the ablation depth h [cm] on the intensity can be found:

$$h = \frac{1}{\alpha} \ln \left(\frac{I}{I_0} \right). \quad (2)$$

The ablation depth defines the precision of the structures in depth.

Applying Gaussian radiation with a focus diameter $2w_0$ the processing diameter can be controlled by the intensity of the radiation, depending on the ratio of the applied intensity to the

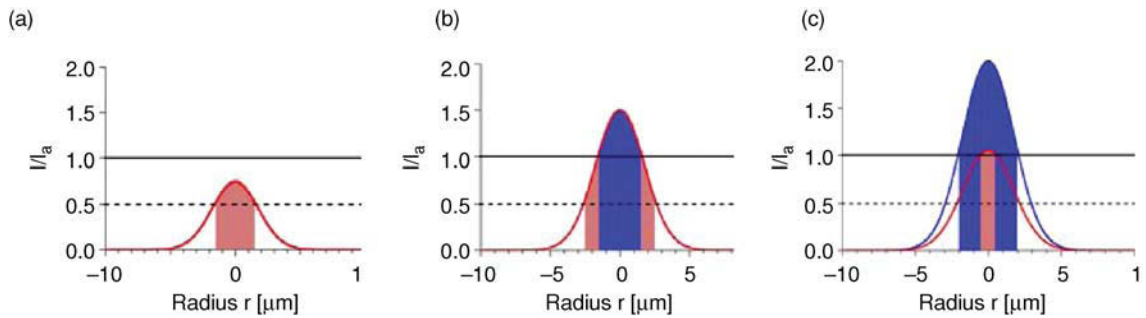


FIGURE 4-2 Extension of the melted (faint) and ablated (dark) region for intensities smaller (a), larger (b), than I_a . For $I \approx I_a$ and $I > I_a$ demonstrates differences in the extension of the ablated region (c).

threshold intensity for ablation. Threshold intensities are given for homogeneous material by the threshold intensity for melting I_m and for evaporation I_v (Fig. 4-2(a)). Solid materials feature a melt enthalpy that is always smaller than the evaporation enthalpy, resulting in larger processing diameters for melting than for evaporation (Fig. 4-2(b) for $I_m = I_v/2$).

The processing diameter of focused Gaussian radiation can be reduced steadily by decreasing the intensity close to the threshold intensity for ablation I_a . Processing diameters much smaller than the focal diameter $2w_0$ are achievable (Fig. 4-2(c)).

Thermal and/or photo-physical processes govern ablation. Thermal processes are represented by heating of matter without change in the chemical constitution, whereas photo-physical processes imply changes in the chemical constitution or irradiated matter.

Thermal Effects on Ablation Precision and Ablation Geometry

Today, for precise laser ablation, single nanosecond pulses with time spacings between the pulses in the range of 10 μ s are used. Ablation rates of between 0.1 and 1 mm³/min are achieved with depth accuracies of 1 to 2 μ m. In the nanosecond range the thermal influence of the laser irradiation results in typical melting depths of several micrometers and a surface quality which is controlled and defined by the melt resolidification and the surface tension of the melt. With this technology, ablation accuracies

of typically 1 μ m can be achieved and a surface roughness of 0.6 μ m can be obtained. Recent investigations using ps-lasers showed even higher accuracy, which is due to a totally different laser interaction regime with significant differing thermal influence and resulting quality. In nanosecond beam interaction the energy deposition and heat transfer in the material is taking place within the pulse duration. In ultra-short pulse processing the energy transfer to the lattice occurs after the entire pulse duration. The temperature increase and thermal behavior are then described by a two-temperature model which takes into account the laser/material interaction that takes place generally between photons and electrons with an overheated electron gas; and an energy transfer to the lattice by a material-specific coupling coefficient.

The effect of the absorbed optical energy on thermal ablation of matter is driven by the pulse duration and is subdivided into four regimes for linearly absorbing matter:

- Absorption of the optical energy by quasi-free electrons ($t_{ye} < 10$ fs);
- Thermalization of the electrons, called the electron system ($t_{ee} < 100$ fs);
- Interaction between the electron and the phonon system ($t_{ep} < 10$ ps);
- Thermalization of the phonon system ($t_{pp} < 100$ ps).

The durations of the single processes within the brackets are exemplary if given for copper. Two limiting cases can be distinguished:

1. **Pulse duration larger than the thermalization of phonons** $\tau > t_{pp}$. For $\tau > t_{pp}$ the times for

absorption of the photons, and the thermalization of the electron and phonon system, are much smaller than the pulse duration, resulting in the description of heating by one temperature for the electron and the phonon system. Ablation affects the subsystems as an instantaneous process. The threshold fluence for ablation (fluence = energy per area) scales with the square root of the pulse duration and a thermal penetration depth can be defined as:

$$\delta_{therm} = 2\sqrt{\frac{\kappa t_p}{c_p \rho}} \quad (3)$$

depending on the thermal property of matter, with κ the thermal conductivity, c_p the heat capacity, ρ the density and t_p the pulse duration of the applied radiation. The thermal penetration depth δ defines the region beyond the focus diameter (tool diameter), which can be thermally modified, such as by the amorphization of crystalline substrate. This regime is called the heat affected zone (HAZ). The processing diameter is given by $2(w_0 + \delta)$.

2. **Pulse duration smaller than the electron–phonon relaxation time $\tau < t_{ep}$.** For $\tau < t_{ep}$ the processes within the electron and the phonon system are decoupled. The temperature development for these systems are described by a two-temperature model representing two coupled differential equations:

$$\begin{aligned} C_e \frac{dT_e}{dt} &= \frac{\partial}{\partial z} \left(\kappa_e \frac{\partial T_e}{\partial z} \right) + S - \mu(T_e - T_p) \\ C_p \frac{dT_p}{dt} &= \mu(T_e - T_p) \end{aligned} \quad (4)$$

C_e and C_p represent the heat capacities of the electron and the phonon system, κ the heat conductivity of the electron system, S the applied optical energy, μ the electron–phonon coupling constant and T_e and T_p the temperatures of the two systems. Ablation of materials is characterized by negligible melt and small mechanical load of the irradiated region. The processing diameter is comparable to the focus diameter.

In nanosecond laser processing this energy transfer occurs during the duration of the laser pulse, whereas in picosecond laser processing the energy transfer occurs after a certain interaction time. For metals, this transfer time is generally in the range of some picoseconds. In this case, the material is heated up after the end of the laser pulse, so that there is no interaction of the photons with melted and evaporated material. The result is a much more accurate ablation because the ablation is mainly due to vaporization of the material and not by melt expulsion. The second reason for the use of picosecond pulse durations in laser ablation is the very high intensity of the pulses. With peak intensities of more than 10^{10} W/cm² all materials are vaporized rather than merely melted. As a consequence of these high intensities, the ablation rate per pulse is quite low, because for vaporization an excessive amount of energy is needed. In Fig. 4-3(a) direct comparison of laser ablated steel with nanosecond pulses and picosecond pulses is shown. It can be seen clearly that in nanosecond ablation the residual melt after ablation is much stronger and the geometry is affected by melt resolidification. In picosecond ablation almost no melt can be found in the ablation area and clean surfaces with a surface roughness of $<0.5 \mu\text{m}$ can be produced by laser ablation.

PROCESS PRINCIPLES FOR LASER ABLATION

Micro-structuring with laser radiation adopts one of the following techniques:

- the mask technique
- the scribing technique.

The mask technique is appropriate for $2^{1/2}$ dimensional structuring, for example application in lithography and the generation of micro-fluidic systems and nano-scaled optical devices such as gratings. The scribing technique is adopted for full 3D structuring and is comparable to mechanical milling.

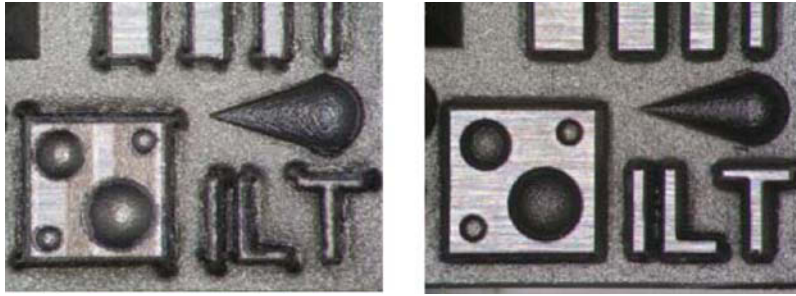


FIGURE 4-3 Comparison of nanosecond laser ablation (left) and picosecond laser ablation (right) of steel.

Mask Technique

For mask-based laser ablation the laser radiation is formed and homogenized by a telescope and projected onto a mask representing the desired intensity distribution. The mask is imaged by an objective to the final intensity distribution. The transversal miniaturization m is given by:

$$|m| = \frac{f}{g - f}, \quad (5)$$

This relation is known from the optical geometry, with the focal length of the lens f and the distance of the mask to the lens g (Fig. 4-4).

The precision of the working tool is described by Abbe's law, which gives the theoretical resolution limit Δx of an objective for non-

coherent radiation:

$$\Delta x = 1.22 \frac{\lambda f}{D_L} = 0.61 \frac{\lambda}{NA} \quad (6)$$

and depends on the objective diameter D_L and on the numerical aperture of the objective NA .

Scribing Technique

Scribing is a common technique for structuring with laser radiation. Similar to milling, the working tool 'laser radiation' is moved relatively to the substrate and removes matter in the focal regime by melting, vaporization or photo-ablation.

The spatial intensity distribution of the laser radiation depends, among other things, on the applied laser resonator. Of special importance for micro-structuring concerning focusability is

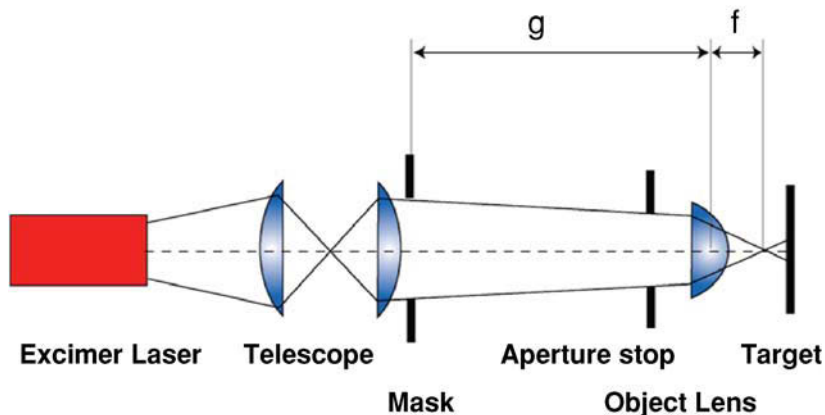


FIGURE 4-4 Principle of mask projection imaging. Laser radiation is collimated and homogenized by a telescope and a homogenizer to illuminate the mask. The mask itself is imaged on the target.

the radiation, which should exhibit a spatial Gaussian intensity distribution. Micro-structuring, applying this radiation, benefits the property of Gaussian radiation to be focused to the smallest possible value, called the diffraction-limited focus, resulting in a beam radius of:

$$w_0 \approx \frac{2\lambda f}{D} \approx \frac{\lambda}{NA} \quad (7)$$

with λ the wavelength of the applied radiation, f the focal length of the objective and D the beam diameter of the radiation close to the objective. The working tool diameter is given by $2w_0$ and defines the working tool precision. The numerical aperture is given by $NA = D/f$ for objectives with large focal length ($f \gg 15$ mm) and by $NA = n \sin \theta$ for microscope objectives ($f < 15$ mm), with the refractive index of the medium between objective and the substrate and θ the aperture angle of the objective.

Microstructures, like a cavity, are generated by ablation with laser radiation displacing the laser radiation relative to the workpiece and carrying out a meander trajectory, removing the material in layers (Fig. 4-5). In general, the laser displacement of the laser beam is realized by high speed galvanometer mirrors. Focusing of the laser beam is made by either adjustable lenses set before the scanning mirrors or by telecentric lenses.

The ablation rate per length depends on the ratio between the applied intensity to the threshold intensity for ablation and on the overlap, o :

$$o = 1 - \frac{v}{2 f_p w_p} \quad (8)$$

where w_p represents the processing diameter, v the relative velocity, and f_p the pulse repetition rate. The processing diameter for mechanical ablation (e.g. milling) is given by the tool diameter whereas the processing diameter for laser ablation is given by the focal diameter (tool diameter) and the process precision, described below. Applying laser radiation for micro- and nano-structuring, the appropriate tool diameter is obtained by reducing the wavelength and increasing the numerical aperture. The last one is obtained by decreasing the focal length of the objective or by increasing the beam diameter close to the objective (example: $\lambda = 355$ nm; $NA = 0.5 \Rightarrow w_0 \approx 0.7$ μ m).

Microscope objectives are often used for focusing laser radiation to small focal diameters < 10 μ m. The focal diameter is varied during processing by changing the objective, or changing the beam diameter in front of the objective, or positioning the laser radiation extra focally. Compared to mechanical milling, laser radiation is contact

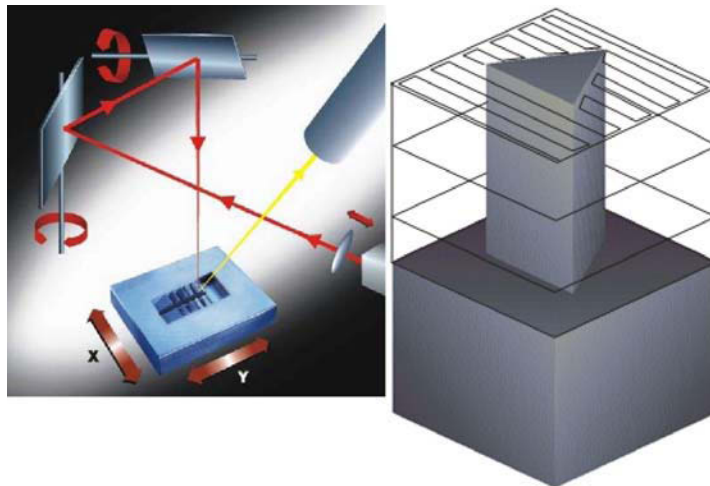


FIGURE 4-5 Principle of 3D laser machining by laser scribing technology.

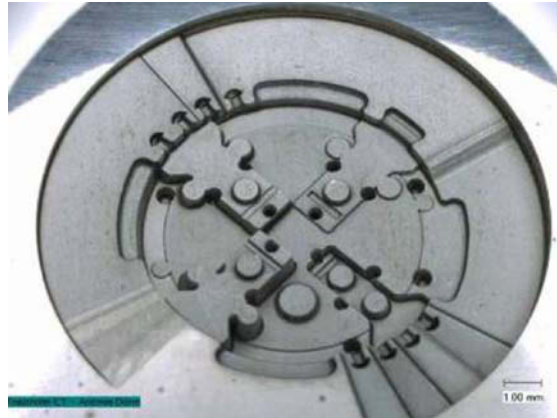


FIGURE 4-6 Laser manufactured micro-injection molding tool insert.

free and mass-less, resulting in reduced delay times for positioning of the working tool. Mechanical micro-milling with a tool diameter $<100\ \mu\text{m}$ exhibits positioning times in the range of minutes whereas laser radiation is positioned within fractions of seconds.

EXAMPLES

In the production of micro-scaled products and products with micro- and nano-scaled surface functionalities, laser ablation becomes an even more important tool which is able to generate structure sizes in the range of $10\text{--}100\ \mu\text{m}$ and with new machining strategies, even within a range smaller than one micrometer. Using ultra-

short pulsed lasers with durations of $10\ \text{ps}$ in bursts of several pulses with a time spacing of $20\ \text{ns}$ each and adapted pulse energies, the surface quality of metal micro-ablation has been increased significantly. With a combination of ultra-short pulses and high resolution interference methods, structures with dimensions of less than $300\ \text{nm}$ can be generated, either in polymer parts directly, or in steel replication tools. For mass replication of those structures to achieve improvements in wetting capabilities or optical properties of surfaces, a new laser supported embossing technology has been developed.

The availability of these new process variants and improved beam sources qualifies the laser as a universal tool, especially in the area of

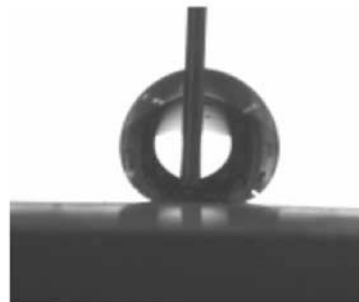
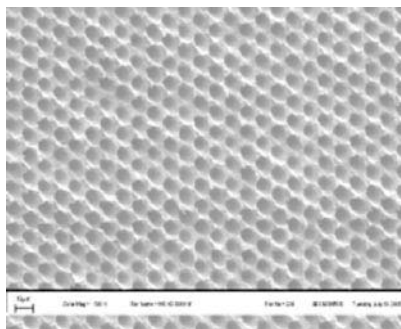


FIGURE 4-7 Micro-structured replication tool for self-cleaning surfaces (left). Super lotus effect on micro-structured polymer surface (right).

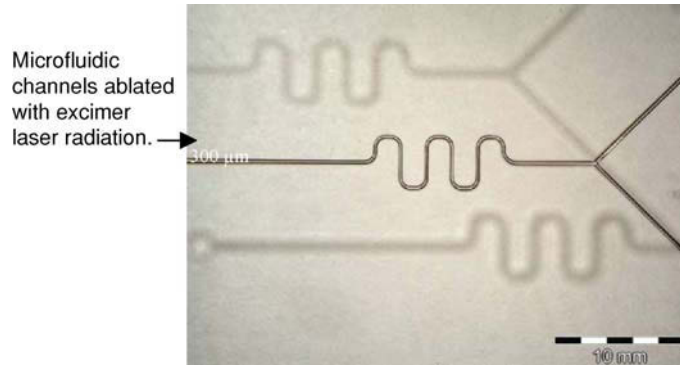


FIGURE 4-8 Micro-fluidic channels ablated with excimer laser radiation.

micro-mold processing (Fig. 4-6). The wide variety of materials processed by lasers range from hard materials such as tungsten carbide for tool technology to ceramics, glass and diamond, with accuracies of better than $10\ \mu\text{m}$, which make the technology useful for the processing of innovative tools, and also for high temperature mass replication processes.

With the newly developed laser ablation technology using ultra-short pulsed lasers in the picosecond range, accuracies of better than $5\ \mu\text{m}$ and surface roughnesses of less than $0.5\ \mu\text{m}$ can be provided for the manufacturing of micro-molding tools.

Using this new laser ablation technology opens a new field in the micro-processing of tools, which allows the manufacture of micro- and even nano-scaled functional structures on polymer, metal and glass components. With laser ablation using picosecond lasers, a machining technology with accuracies $<1\ \mu\text{m}$ is available which can be applied to all kinds of materials. Figure 4-7 shows the surface of a replication tool, whereby laser ablation in tungsten carbide micro-pits with sizes of between 1 and $5\ \mu\text{m}$ have been produced. Due to the process characteristics of laser ablation, sub-micrometer scaled substructures are produced, which further increase the surface area. Tools like this have been successfully tested for the replication of polymers to achieve functional surfaces. In Fig. 4-7 the result of a wetting test shows that by micro-structuring, a super hydrophobic effect can be produced.

By mask technique ablation with UV-excimer lasers, polymer parts especially can be produced in a very flexible way. Among others, micro-fluidic systems (Fig. 4-8) require very small channels and reservoirs in the geometry range of several $10\ \mu\text{m}$. With mask-based excimer ablation a tool for rapid prototyping is available for the manufacture of single parts in small lot sizes [5].

CONCLUSIONS

Laser micro-ablation has been shown to be a versatile tool in the machining and production of micro-parts and micro-replication tools. Using ultra-short pulsed lasers with material-adapted wavelengths the quality of the ablation process can be increased significantly compared to long pulses. With an optimized energy deposition, a significant reduction of the surface roughness down to $R_a < 0.7\ \mu\text{m}$ could be achieved over a wide parameter range, the best achieved roughness being $R_a = 0.5\ \mu\text{m}$. Using this optimized parameter, laser ablation can be used for the generation of micro-replication tools as well as for the direct manufacturing of small parts in different materials such as ceramics, steel and sintered metals showing the potential for high precision tool manufacturing for high accuracy parts.

REFERENCES

- [1] J.-C. Diels, *Ultrashort Laser Pulse Phenomena*, Academic Press, Boston (1996).

- [2] J. Jandeleit, A. Horn, R. Weichenhain, E.W. Kreutz, R. Poprawe, Fundamental investigations of micro-machining by nano- and picosecond laser radiation, *Applied Surface Science* 127 (1998) 885–891.
- [3] F. Korte, et al., Sub-diffraction limited structuring of solid targets with femtosecond laser pulses, *Optics Express* 7(2) (2000) 41–49.
- [4] H.-G. Treusch, *Geometrie und Reproduzierbarkeit einer plasmaunterstützten Materialabtragung durch Laserstrahlung*, Dissertation, TH Darmstadt, (1985).
- [5] M. Wehner, *Excimer Laser Technology*, Ed.: D. Basting, Lambda Physik AG Göttingen (2001).
- [6] R. Poprawe, A. Gillner, D. Hoffmann, J. Gottmann, W. Wawers, W. Schulz, High speed high precision ablation from ms to fs, *Proc. SPIE* 7005, 12 S, 200.
- [7] A. Gillner, J. Holzkamp, C. Hartmann, A. Olowinsky, J. Gedicke, K. Klages, L. Bosse, A. Bayer, Laser applications in microtechnology, *J. of Materials Processing Technology* 167 (2005) 494–498.
- [8] G.J. Schmitz, C. Brücker, P. Jacobs, Manufacture of high-aspectration micro-hair sensor arrays, *J. of Micromechanics and Microengineering* 15 (2005) 1904–1910.
- [9] M. Wehner, S. Beckemper, P. Jacobs, S. Schillinger, D. Schibur, A. Gillner, Processing of polycarbonate by high-repetition rate ArF excimer laser radiation, *Proceedings of Lasers in Manufacturing* 3 (2005) 557–561.
- [10] E. Bremus-Köbberling, U. Meier-Mahlo, O. Henkenjohann, S. Beckemper, A. Gillner, Laser structuring and modification of polymer surfaces for chemical and medical micro components, *Proceedings of SPIE* 5662 (2004) 274–279.
- [11] E. Bremus-Köbberling, A. Gillner, Laser structuring and modification of surfaces for chemical and medical micro components, *Proceedings of the 4th International Symposium on Laser Microfabrication LMP* 4 (2003) 1–5.
- [12] C. Hartmann, T. Fehr, M. Brajdic, A. Gillner, Investigation on laser micro ablation of steel using short and ultrashort IR-multipulses, *LAMP 2006*, Kyoto, Japan (2006).
- [13] C. Hartmann, A. Gillner, Ü. Aydin, et al., Investigation on laser micro ablation of metals using ns-multipulses, *J. Physics* 59 (2007) 440–444.

Hot Embossing

Matthias Worgull

INTRODUCTION

A further distribution of applications with integrated micro-features or micro-systems requires technologies to replicate the corresponding micro-structures. In addition to the structuring of silicon, glass or metals by different structuring processes, the replication of micro-structures is based typically on polymers. Polymers, especially thermoplastic polymers, are commercially available and are characterized by a large bandwidth of properties. Here for most applications a suitable polymer which fulfills the requirements of the application can be found.

Hot embossing is one of the established replication technologies for the replication of a micro-structured master, a so-called mold insert. The available replication processes are listed below [1–4]:

- Micro-reaction injection molding (RIM)
- Micro-injection molding
- Micro-injection compression molding
- Micro-hot embossing
- Micro-thermoforming
- Nano-imprint lithography processes (NIL).

None of these processes are in competition with each other, since they have their own specific characteristics and merits. Therefore, depending on the requirements, like stress in molded parts, flow length, number of replications or cost effectiveness, the replication process can be determined. Nevertheless, the design and arrangement of the structures will define the suitable replication technology. Hot embossing is a technology which is suitable for the replication of a large

bandwidth of structures, especially structures with high aspect ratios. In this chapter such a process is presented. The technology of hot embossing machines, hot embossing tools and examples of typical applications will underline the merits and flexibility of hot embossing.

The replication technique of hot embossing of micro-structures can be traced back to the second half of the 20th century. Already in 1970 hot embossing had been implemented by a group of researchers from RCA laboratories at Princeton, NJ, USA [5]. The objective of their work was to develop a low cost reproduction technique of surface hologram motion pictures for television playback. A master tape was made by electroplating nickel into photo resist patterns. The master was run through heated rollers together with a vinyl tape and, thus, the micro-structure was transferred into the vinyl. The molded structures were characterized by a depth of 0.1 μm and a lateral resolution of 1 μm . In 1978 Gale et al. [6] used a hot embossing technique for the replication of surface relief structures for color and black-and-white reproductions. These relief phase grating structures refer to a recording of light in zero order diffraction. These structures, with a height of 1–2 μm and a spacing of around 1.4 μm , were replicated from a nickel mold insert into transparent PVC by hot embossing at a molding temperature of 150 °C and a pressure of 0.3 MPa. The structures were also replicated in polycarbonate (PC) and acetate.

The structures replicated by hot embossing today are characterized by high aspect ratios,

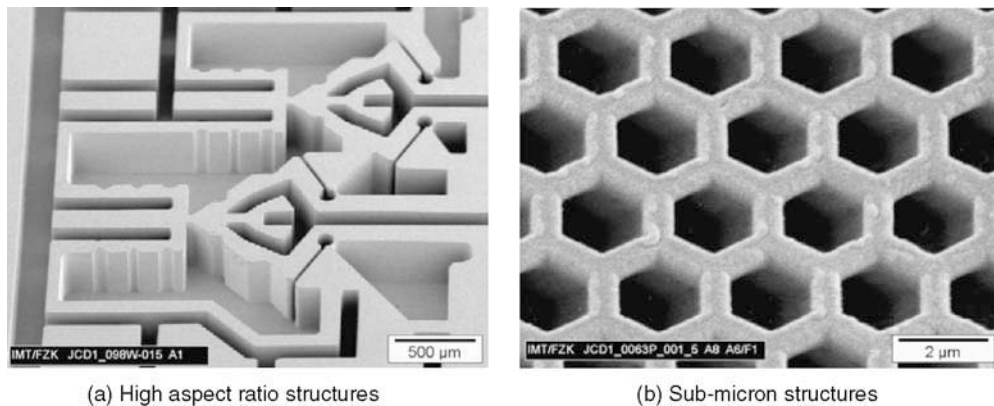


FIGURE 5-1 In PMMA replicated structures with high aspect ratios.

smaller feature sizes down to the nanometer range, and vertical sidewalls with a surface roughness below 40 nm (Fig. 5-1).

Before the hot embossing process was established in micro-structure technology previous experiments were done by reaction injection molding. This process enables injection of mixed liquid monomers and a starter into a micro-structured mold and the molding occurs by polymerization in the mold [7]. Micro-structures of PMMA and PA (polyamide) were molded successfully, but at the beginning of these experiments the filling and the demolding of filigree micro-structures with high aspect ratios was a challenging aspect. Nevertheless, because of the difficulties in controlling the polymerization and the high shrinkage of the molded part, the hot embossing technique based on polymer foils was investigated. Beside fundamental tests with micro-injection molding, basic experiments in 1989 with an embossing technique of PMMA material marked the start of the use of micro-hot embossing for the production of LIGA structures [8] (LIGA is a German acronym for lithography, electroplating and molding – Lithographie, Galvanik, Abformung). With the further development of the LIGA technique the development of the hot embossing technique also proceeded. At the beginning the technique was based on laboratory machines with a low grade in automation which required the control of every molding step by the user. The precision of the molding machine regarding the

press force, the molding velocity, and the temperature distribution was also improved. A milestone in the development was the use of computer controlled tensile testing machines for hot embossing applications. Such machines, already available in many material testing laboratories, can fulfill the requirements for micro-hot embossing, including high stiffness of the machine, precise motion, the control system for force and velocity combined with a measurement system, and an interface to the user. An integration of a molding tool with a heating and cooling system completed the required components for hot embossing. Subsequently, this concept was further developed into commercially available machines. Together with further development of the hot embossing technique, these kinds of machines are now part of state-of-the-art hot embossing technology [9]. Apart from the developments based on the use of tensile testing machines, new concepts based on the use of the hydraulic drives were also established [10]. There are also other types of machines existing in various research laboratories and industry, as a result of independent development and/or customized applications.

On the basis of the hot embossing technology available at the present time, hot embossing is a well-established process in industry and science with a large bandwidth of process variations. The replication of Fresnel lenses for overhead projectors or concentrating solar systems [11] is also established, like the replication of CDs by the

related process of injection compression molding. The development of nano-imprint lithography with thermal and UV curable materials opens a way for hot embossing technology to be extended to nano-structuring methods. A new level of different applications, such as surface modifications in the nano-range or the replication of structures in the wavelength dimensions of light, will pave a way to a new class of applications. The development of the hot embossing technique is closely linked to the development of structuring techniques for the fabrication of mold inserts. Today, structures of mold inserts in a range below 10 nm can be fabricated. The hot embossing process in combination with polymers is well suited for the replication of these structures and it can make contributions to the volume production of new applications based on nano-structuring. One of the key merits is its flexibility in set-up, which allows for convenient changing of the mold and molding material. Therefore, hot embossing is also a popular process in laboratories for micro-structuring. The process is characterized by a large bandwidth of possible process variations, such as double-sided aligned molding, molding of through-holes, molding of polymer stacks, thermoforming by polymer melts or structuring by hot punching. These variants offer attractive characteristics for micro- and nano-replications and for the development of micro- and nano-systems.

HOT EMBOSsing PROCESS

To illustrate the fundamentals of the process, the case of single-sided hot embossing is described below. The principle of a one-sided hot embossing cycle is represented schematically in Fig. 5-2. Between the micro-structured mold insert and a metal plate with a rough surface, the so-called substrate plate, a semi-finished product, i.e. a polymer foil, is positioned. The thickness of the foil exceeds the structural height of the tool. The surface area of the foil covers the structured part of the tool. The tool and substrate are heated under vacuum to the polymer molding temperature. When a constant molding temperature is reached, the two steps of the molding cycle are initiated. In a first step, the mold insert and substrate are moved towards each other (in the range of 1 mm/min) until the preset maximum embossing force is achieved. In a second step, the embossing force achieved is held at a constant value for a defined holding time. To generate a constant force, the relative movement between the tool and substrate has to be controlled. The force is now kept constant over an additional time period (packing time, holding time). During this period, the plastic material flows in the radial direction and the residual layer will be reduced under the acting constant force (packing pressure). At the same time, the tool and substrate move further towards each other, while the thickness of the

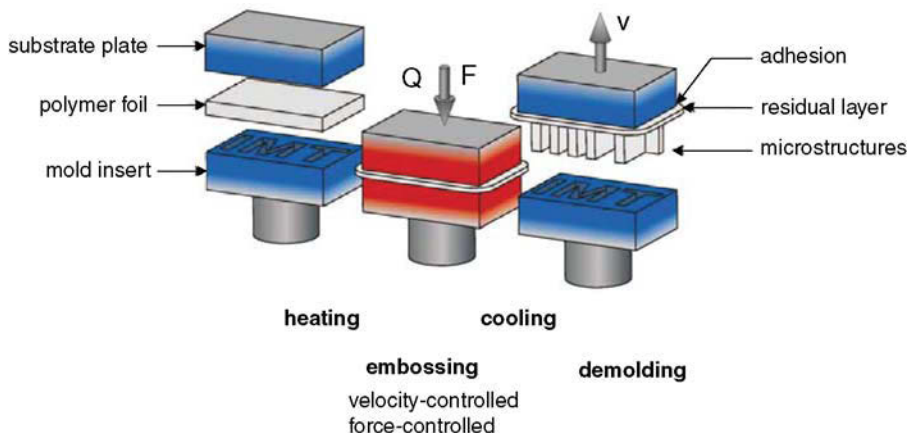


FIGURE 5-2 Schematic view of the hot embossing process.

residual layer decreases with packing time. During this molding process, the temperature remains constant. This isothermal embossing under vacuum is required to fill the cavities of the tool completely. Air inclusions or cooling during mold filling may result in an incomplete molding of the microstructures, in particular at high aspect ratios. Upon the expiry of the packing time, cooling of the tool and substrate starts, while the embossing force is maintained. Cooling is continued until the temperature of the molded part drops below the glass transition temperature or melting point of the plastics. When the demolding temperature of the polymer is reached, the molded part is demolded from the tool by relative movement between the tool and the substrate. Demolding only works in connection with an increased adhesion of the molded part to the substrate plate. Due to this adhesion, the demolding movement is transferred homogeneously and vertically to the molded part. Demolding is the most critical process step of hot embossing. Depending on the selected process parameters and the quality of the tool, demolding forces may vary by several factors. In extreme cases, demolding is no longer possible; the structures are destroyed during demolding.

Apart from the one-sided molding described, the process is also used for double-sided positioned embossing. The principle of the process remains the same. Instead of the substrate, however, another tool is applied. To demold the molded part from one of the two tool halves, special demolding mechanisms, such as ejector pins or pressurized-air demolding, are used. For a better understanding, the schematic representation of embossing in Fig. 5-2 is limited to the major process steps. Depending on the tool and the polymer used, the process and process parameters have to be adapted to any changes.

The characteristics and merits of hot embossing may be summarized as follows:

- The molding process is characterized by short flow paths, only from the molten polymer film into the micro-cavities.
- Because of the moderate molding velocities in the range of 1 mm/min only moderate shear

stress in the polymer will be generated. This results in comparative low residual stress in the molded parts.

- If the molding temperature is set to the range where the relaxation times of a polymer correspond to the cycle times of molding, the stress induced by molding can be decreased by relaxation processes. This option requires knowledge of the temperature dependent relaxation behavior of the polymer.
- The use of standardized mold inserts allows for the quick change of a micro-structured mold, which underlines the flexibility of the technology.
- Beside the quick change of the mold insert, the polymer can also be changed quickly. Only a new polymer foil has to be placed between the mold insert and the substrate plate (Fig. 5.1). This allows for replicating a mold insert into several polymers in a short time.
- The technology allows for a variety of process variations, for example double-sided molding, molding of through-holes, multi-layer molding and also thermoforming of a high temperature polymer foil by a low temperature polymer melt.
- Compared to injection molding, the process may be characterized by longer cycle time. Although the development shows that with an effective technology the cycle times could be reduced, the process is economically well suited for small and medium series production. Nevertheless, because of the high flexibility this process can be adapted to several requirements and it, therefore, is of high potential for the development of prototypes within laboratories.

PROCESS VARIATIONS

As mentioned above, hot embossing is not limited to the case of a single-sided molding cycle. The concept of hot embossing allows for the process to be modified according to the requirements of further applications of the molded parts. Representative of a large number of modifications, the concepts of double-sided molding, multi-layer molding, the molding of through-holes, and roller embossing, are described in this section.

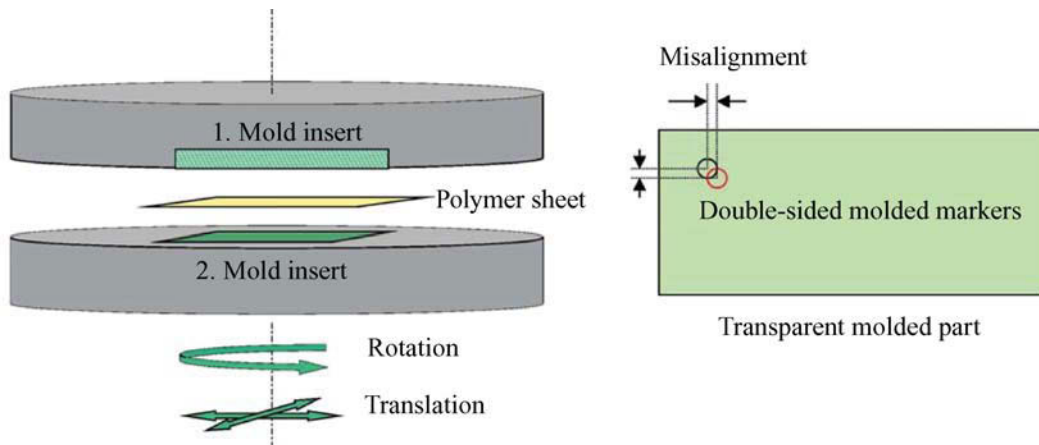


FIGURE 5-3 Principle of alignment for double-sided molding.

Double-sided Molding

Double-sided molding paves the way to a further large family of molded parts. For example, double-sided structured parts are part of micro-fluidic systems where through-holes are essential features. Although fraction lines with thin residual layers can be designed to separate molded parts, in general, with double-sided molding, the possibility of three-dimensional structuring could be enabled. A precondition for such designs is the correlation of two mold inserts which are positioned opposite each other and adjusted laterally relative to each other. Use of markers or the orientation on characteristic structures of the design is recommended. After a coarse adjustment of both mold inserts, a first part should be molded. In a second step the differences in the lateral dimension between the markers on the top side and the bottom side of the molded part have to be measured. Transparency of the polymer is helpful, because it enables the determination of the misalignment of the markers with an optical measurement system, focusing on the top and bottom of a thin molded part. The misalignment can be split into a transversal (x,y) direction and a rotational (in the perpendicular axis of the part) misalignment. With this measured data the alignment of both mold inserts can be corrected by an alignment system integrated in a hot embossing

tool. The alignment can be done separately in the transversal and rotational directions (Fig. 5-3). These alignment systems are optional components of commercial hot embossing machines (for example, Jenoptik Hex03) and are a precondition for double-sided molding.

Multi-layer Molding

Another illustrated approach [12], e.g. for the fabrication of through-holes, is the use of a polymer composite, a stack of two different polymer films (polymer 1 and polymer 2). The structured part with through-holes will be molded onto a layer of a second polymer (polymer 2) (Fig. 5-4). After demolding of the molded composite the first polymer can be separated from the second polymer, in this case the carrier layer, by peeling. The advantage of this method is the maintenance of the adhesion on the substrate plate. This allows for demolding the molded composite in the vertical direction by the precise movement of the hot embossing machine. The adhesion between the first polymer and the second polymer has to be high enough to withstand the tensile forces during demolding. Additionally, a form closed connection, effected by the penetration of the mold insert into the second polymer, will support the connection of both polymers. This approach is only suitable for selected material combinations,

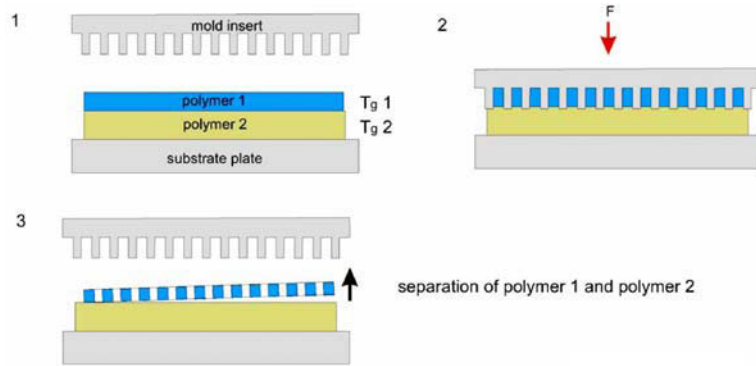


FIGURE 5-4 Principle of two-layer molding for molding through-holes.

because of the required adhesion and further separation.

Through-holes

In micro-system technology the need for molded parts with through-holes is increasing; micro-fluidic components like micro-pumps, micro-valves or fluidic components for lab-on-a-chip systems are common examples. The fabrication of through-holes is, therefore, an actual aspect in fabrication of micro-system components. To reduce the post-processing steps, through-holes should be fabricated already during molding. Because of the molding principle, this requirement is difficult to achieve. As mentioned above, hot embossing is characterized by a squeeze flow of a polymer melt. Typical molded parts are therefore characterized by a residual layer. On the one side, this residual layer is necessary to obtain the pressure for filling micro-cavities; on the other side, for the fabrication of parts with through-holes, this residual layer should be completely displaced. The methods for fabrication of these holes can be split into the post-processing methods to remove thin residual layers and methods that are characterized by the selected substrate plates allowing for fabricating through-holes already during molding. Finally, a new development is discussed – a principle that allows for fabricating through-holes with a two-step

process, a molding cycle and a cutting cycle which gives the name of this process – hot punching.

To avoid any post-processing of molded parts, through-holes should be fabricated already during the embossing cycle. This can be achieved by the use of a combination of modified mold inserts and selected substrates [13]. The principle refers to a complete displacement of the residual layer in selected areas, achieved by embossing free-standing structures of the mold inserts into modified substrates. This enhanced molding principle requires a sensitive set-up of the process parameters and a proper selection of the substrate materials, because of the relatively high load on the structures during molding. The risk of damaging filigree structures of the mold insert increases, especially when the diameter of the through-holes decreases.

Representative of the process variation of molding through-holes, the approach of molding onto a stack of foils is described here. In this approach, in addition to the conventional metal substrate plate, a flexible layer is put on top. This layer consists typically of a polymer layer and a metal film. By the selection of the materials and film thickness, the flexibility of this combination can be influenced. Figure 5-5 illustrates the principle. Because of the flexibility of the layer, in selected areas the polymer melt can be displaced completely from the top side of the mold insert. By using this technique it is possible to retain the

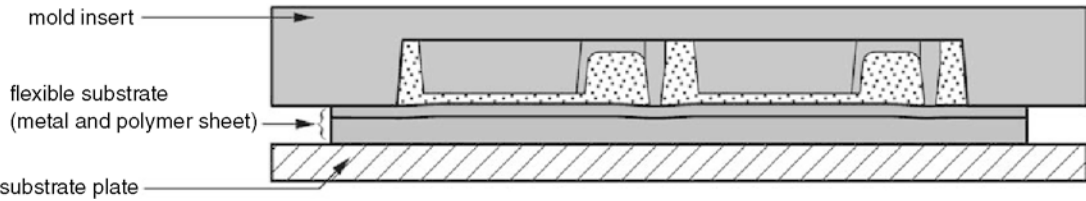


FIGURE 5-5 Schematic view of a configuration for the molding of through-holes with the use of a stack of foils.

residual layer in large contact surfaces, e.g. at the margin regions of the mold insert, and to completely displace the residual layer in small contact areas. During the cooling state the desired dwell pressure will be generated by the flexible layer and not by the residual layer.

Hot Punching

The principle of hot punching is a two-step method for molding through-holes (Fig. 5-6). In the first step a selected mold insert will be replicated in an amorphous polymer with high glass

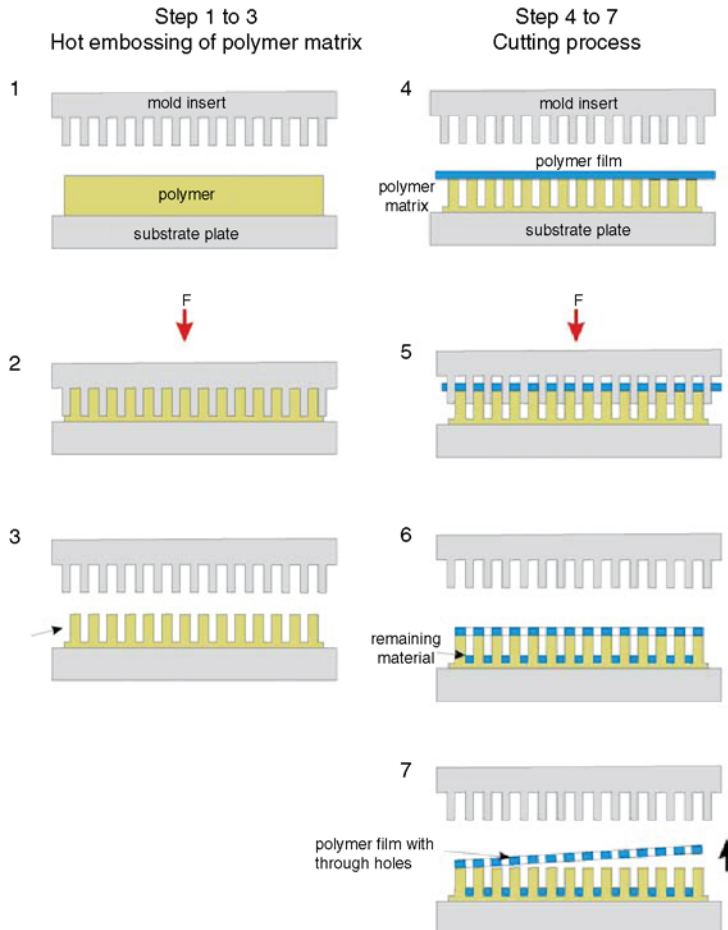


FIGURE 5-6 Principle of hot punching for molding through-holes.

transition or a semicrystalline polymer with high melting temperature. The replication refers to a single molding on a rough substrate plate. Instead of peeling off the molded part from the substrate plate, the replicated part remains on the residual layer after demolding. The molded part will be used as a second to the first mold aligned mold insert, here the so-called matrix. In the second process step a thin film of another polymer with a lower glass transition temperature than the matrix is positioned between the mold insert and the molded part. The mold insert and substrate are heated to a temperature in the range of the glass transition temperature of the thin polymer film which should be significantly below the glass transition temperature of the matrix. The third step of this method is simply another embossing cycle structuring the thin film of polymer between the mold insert and the remaining matrix. Because of the high accuracy of the alignment of the previously molded matrix compared to the mold insert, the structures of the mold insert will match the inverse structures of the matrix properly. Differences of thermal expansions will be compensated for by the relative flexibility of the polymer matrix, compared to that of the mold insert of metal. During the second molding step the mold insert now cuts holes inside the thin polymer film. This principle can be seen as a shearing process. The punched areas will remain in the matrix, where the matrix has to be renewed after several punching steps. Depending on the design and the thickness of the polymer film, the demolding of the punched polymer film from the matrix can be difficult to achieve and should be accomplished carefully, otherwise damage to the polymer film will occur. To help the process a release agent may be used [14].

The advantage of this method is the use of a wide range of mold inserts without any modifications. The material combinations are manifold. Besides the differences in softening temperatures, no adhesion between the used polymers is a precondition. Because of the two-step molding, this method is more time consuming. For series production the method has to be improved.

Thermoforming of High Temperature Polymers by Hot Embossing

In accordance with the molding of through-holes the concept of two-layer molding can also be used for the thermoforming of thin films of semicrystalline high temperature materials like LCP or PEEK. Thermoforming refers to the straining of a polymer, typically by air pressure. The gas pressure is substituted with a polymer melt. The starting point refers to a combination of two polymer films, a thin film of a high temperature polymer and a second film of a material with lower softening temperature. A suitable combination is, for example, PMMA as molding material and PEEK as thermoforming material on top. Similar to multi-layer molding, the combination of materials has to be selected carefully. The molding temperature has to be set such that the low temperature polymer is in the melting range and the semicrystalline high temperature polymer foil is in a temperature range above the transition temperature but below the melting temperature. In this temperature range the amorphous part is softened which reduces the elastic modulus of the high temperature semicrystalline polymer which supports the straining of the polymer film. A characteristic of this method is the combination of a molding step (PMMA) and a simultaneous thermoforming step of the high temperature polymer foil (PEEK).

The achievable thickness of the foils depends on the process parameters and the necessary molding force. Experiments show that good results for this kind of thermoforming can be achieved up to a film thickness of 100 μm . The thickness of the polymer film has to be selected in relation to the size of the cavities. To obtain a three-dimensional shape the thickness of the polymer foils has to be much lower than the lateral dimensions of the mold cavity, otherwise the polymer foil will not fill the cavity completely. Further, the material combination has to be selected in such a way that only a moderate adhesion is effective between both foils after molding, because the thin foil has to be separated from the molded low temperature polymer manually

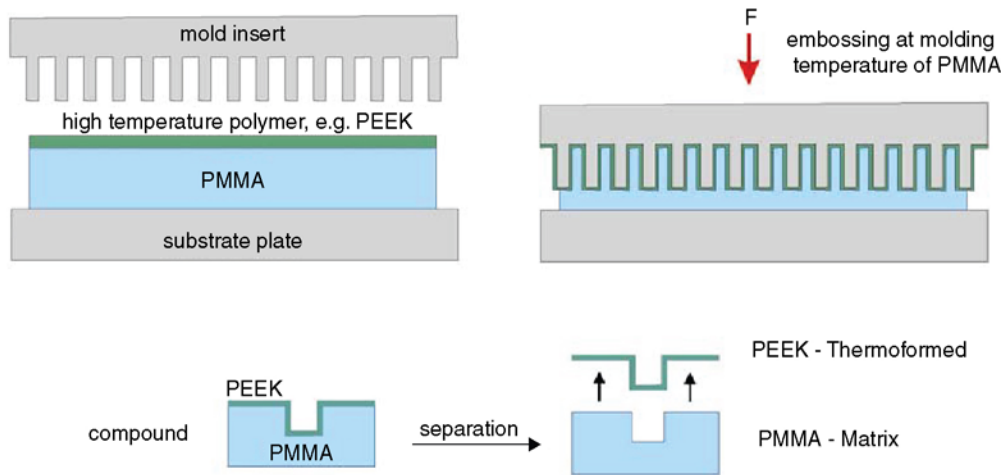


FIGURE 5-7 Principle of thermoforming of a thin polymer film by hot embossing.

by peeling. With this method a three-dimensional structuring is possible, the rear side of the thin polymer foil showing the inverse structure of the front side that is similar to the mold insert (Fig. 5-7).

Roller Embossing

Roller embossing or roll-to-roll embossing is a well-established modification of the hot embossing process. Using rolls instead of plates,

a continuous molding can be achieved with advantages regarding the molding times and disadvantages regarding the height and the aspect ratio of the molded structures (Fig. 5-8). Tan et al. [15] used this approach, so-called roller nano-imprint lithography, to fabricate sub-100 nm patterns. Two methods were investigated. The cylinder mold method refers to a thin structured metal film bent around a smooth roller. In particular, a compact disc master with a thickness of 100 μm was used. The second

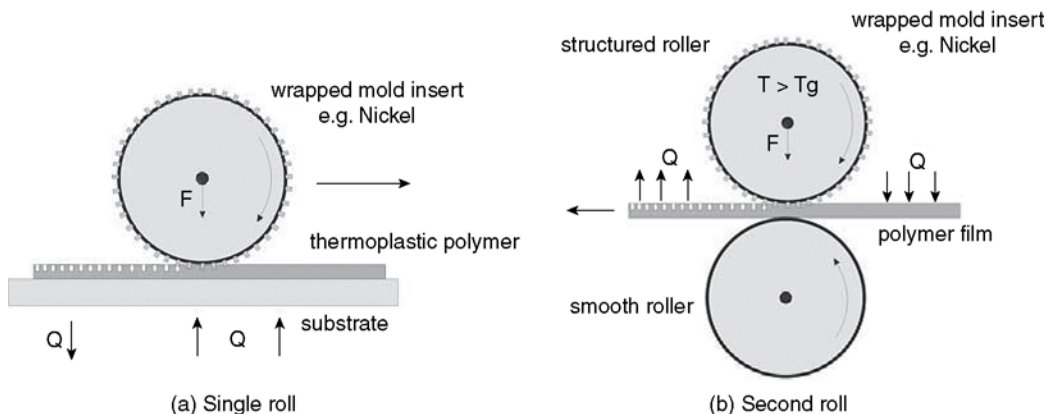


FIGURE 5-8 Thermal roller hot embossing.

method, the so-called flat mold method, refers to a structured silicon wafer mold placed on a polymer substrate. A smooth roller mold is rotated over the mold and the deformation of the mold under the pressure of the roll imprints the structures into the polymer. In both methods the roller temperature is set significantly above the glass transition temperature. For PMMA the roller temperature is set in a range between 170 and 200 °C and the platform temperature in a range between 50 and 70 °C. Roller speeds from 0.5 up to 1.5 cm/s were investigated, the pressure being set in the range between 300 and 4800 psi.

MATERIALS FOR HOT EMBOSSING

Most applicable materials for hot embossing are thermoplastic polymers. During a molding cycle a thermoplastic polymer undergoes several temperature dependent aggregate states. Switching to another aggregate state changes the material properties significantly. Based on the molecular structure of amorphous and semicrystalline polymers different aggregate states and different transition ranges can be determined. The thermal behavior of thermoplastic polymers may be described with the time dependent shear modulus over temperature.

Based on the shear modulus temperature diagram, typical molding windows for embossing amorphous and semicrystalline polymers can be specified. Amorphous polymers show, theoretically, a wide temperature range for hot embossing, beginning at the glass transition temperature and ending before the decomposition range. In practice the molding window depends on several other parameters and has to be set dependant of the design, the molding area and the technique used in the embossing machine. Due to these factors, the actual molding window is smaller than the theoretical window and can be set approximately in the range of 20 up to 100 K above the transition temperature. In contrast to the amorphous polymers, semicrystalline polymers show only a small gap of temperature suitable for hot embossing. As described above,

the decrease in the shear modulus occurs in a small temperature gap in the melting range. At the beginning of this range the stiffness of the polymer is too high for molding. The risk of damage to a micro-structured mold is high. At the end of the range, marked by a low shear modulus, semicrystalline polymers show typically a behaviour like a fluid with low viscosity, which is not suitable for hot embossing because the pressure needed for embossing with freeflow fronts cannot be achieved. Therefore, the molding window can be found approximately in the middle of the small gap of the melting range. In practice, an exact temperature has to be set during molding. The temperature range of amorphous polymers is considerably larger than that for semicrystalline polymers, which in practice makes it easier to mold amorphous polymers in hot embossing (Fig. 5-9).

HOT EMBOSSING TECHNIQUES

Components

The technology components for micro-hot embossing mainly include four groups:

- **The embossing machine** – this is responsible for delivering the press force and the accurate molding velocity. The challenge of the technology is to obtain a high stiffness at high force and also a precise relative motion between the mold and the substrate plate. These requirements result in a stiff frame design consisting of two crossbars and mostly four massive guiding pillars. To obtain a press force, one of the crossbars is fixed. Another crossbar is moved by a precise motion system, like a spindle drive or a hydraulic drive.
- **The tool** – this is mounted between the two crossbars and is responsible for the heating and cooling of the mold, substrate plate and polymer sheet. A typical tool consists of two halves, the top half fixed onto the top crossbar and the bottom half fixed at the lower crossbar, each with a single heating and cooling system. With an approximation of both halves, an integrated vacuum chamber will

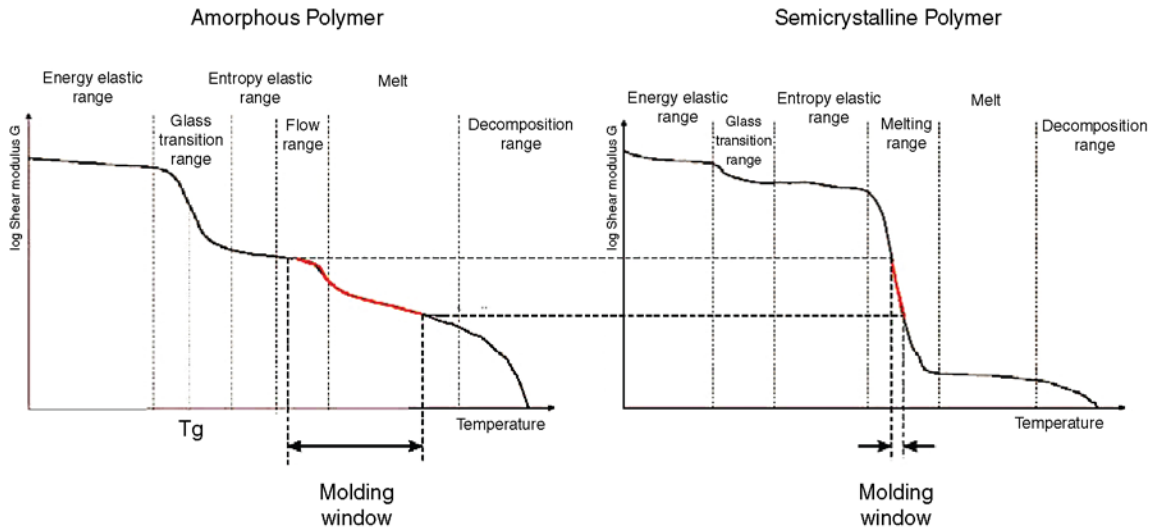


FIGURE 5-9 Thermal molding windows for hot embossing.

be closed and isolates the micro-structured mold insert and the substrate plate against the ambient pressure. Optionally, an alignment system is integrated that allows the adjustment, for example, of two mold inserts against each other or to mold on pre-structured substrates.

- **The micro-structured mold insert** – this is reversibly fixed onto the tool. Opposite the mold insert another mold insert or a substrate plate will be positioned. A wide range of micro-structured mold inserts can be used, for example inserts produced by mechanical machining or mold inserts fabricated by lithographic techniques.
- **A precise controlling system** – the precise control of the press force, the motion of crossbars and the temperature is one of the technological challenges. Besides the control of the process parameters, the measurement of the press force, temperatures inside the mold inserts and the distances between the mold insert and the substrate plate are tasks for the control unit. As an interface to the user, it is also a task to prepare and visualize all data, allowing the user to set up and control the process in an effective way.

Hot embossing machines have been developed to different levels, beginning with simple

manually controlled hot embossing machines, for example for general laboratory use, up to high-level machines with a high grade in automation, used in industry and scientific research.

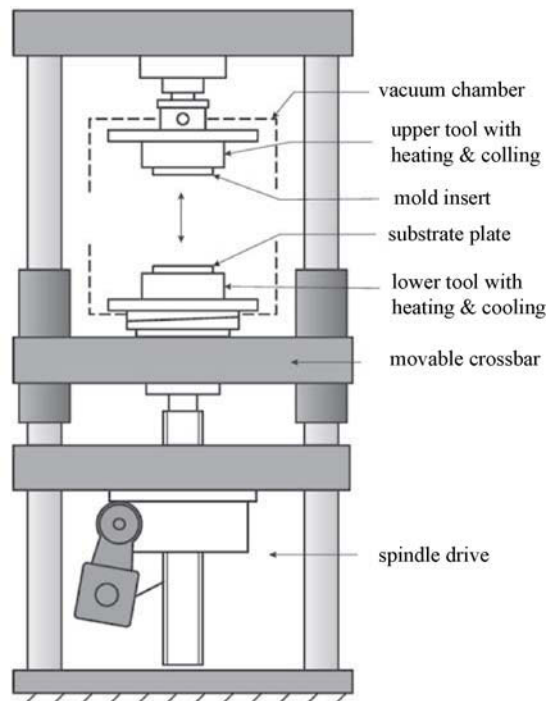


FIGURE 5-10 Schematic view of the components of a hot embossing machine.

Commercial Available Machines

The commercially available hot embossing machines market is comprehensive. The first hot embossing machine suitable for hot embossing of high aspect ratio was developed in Karlsruhe at FZK in cooperation with Jenoptik Mikrotechnik.

Jenoptik Mikrotechnik. Jenoptik Mikrotechnik [9] was one of the first companies providing a complete family of hot embossing machines. Each member of the hot embossing machine family is suited for different kinds of embossing tasks. The machine HEX01 is the smallest machine, compact and with a maximum force of 100 kN already suitable for most molding tasks, especially up to a molding area of four inches. If larger areas are to be molded the machine HEX02 fulfills the requirements regarding molding forces up to 200 kN and molding temperatures up to 300 °C. If double-sided molding is required, the machine HEX03 is equipped with an addition precise alignment system and an integrated microscope that allows the alignment of the tool to be accomplished very easily. The latest machine, HEX04, is especially designed for large area replication under high molding forces of up to 600 kN. All these machines are characterized by an electrical heating unit, a convective cooling system, a spindle drive and flexible controlling by a macro-language. The family of hot embossing machines is shown in Fig. 5-11.

Wickert Press. Another company that manufactures hot embossing machines is Wickert Maschinenbau [10]. In the past this company built the first machine 'MS1' used in industry for hot embossing of micro-spectrometers. In 2003 a new generation of hot embossing machines was developed. The machine WMP1000 (Fig. 5-12) is characterized by a hydraulic drive, a molding area larger than 8 inches and a maximum force of 1000 kN. The machine was developed particularly for industrial use, therefore an automatic handling system was integrated with the machine. In parallel an optimized molding tool was developed to reduce the heating and cooling times, which finally resulted in a significant reduction of cycle times. Further, a user-friendly control

panel was integrated, allowing the control of the machine in an effective way. Nevertheless, the realized concept requires more infrastructure for the operation of the machine. For example, a separate room for the hydraulic pumps and a solid foundation for the heavy machine which also has a large overall height will be required.

EVGroup. The company EVGroup [16] offers two hot embossing machines with different levels of automation [17]. The hot embossing machine EVG520HE is characterized by a semi-automatic molding process, while the hot embossing machine EVG750 is, in contrast, fully automated (Fig. 5-13). This high level of automation is suited for large serial production. The machines are compatible with standard semiconductor manufacturing technologies and allow molding on substrates up to 200 mm. The hot embossing system EVG520HE includes a vacuum chamber, a drive unit with a high press force up to 600 kN, and a heating system which allows the molding of a wide range of polymers. Both machines are equipped with an alignment system.

HOT EMBOSsing TOOLS

Apart from the molding press and the micro-structured mold insert, hot embossing tools are essential components for any hot embossing system. The hot embossing tool may be defined as an interface between the molding press that is responsible for applying the molding force and molding velocity and the micro-structured mold insert to be replicated in polymers. Compared to macroscopic molding tools, such as tools for injection molding, where the structures are part of the tool, tools for micro-replication are characterized by a reversible integration of a micro-structured mold insert. This concept results from the different and incompatible fabrication processes of the macroscopic tool and microscopic structures. On the one hand, the tasks of a hot embossing tool are similar to tasks known from macroscopic molding tools. On the other hand, the embossing tool has to fulfill tasks that are specific to the molding of micro-structures, such as the



(a) HEX01



(b) HEX02



(c) HEX03



(d) HEX04

FIGURE 5-11 The hot embossing family of Jenoptik.

generation of a vacuum. In detail, a hot embossing tool has to fulfill the following tasks.

- Heating and cooling of the polymer film by heat conduction of the mold insert and substrate plate;
- Fixation of different kinds and sizes of mold inserts;
- Hermetic sealing of the mold insert, polymer, and substrate plate against ambient pressure;
- Generation of a vacuum to fill the micro-cavities completely;

- A demolding unit which allows the demolding of the embossed parts in the vertical direction at a controlled demolding velocity;
- Optional alignment of both mold halves, if double-sided molding or positioned molding is desired.

From these tasks, the requirements to be met by a molding tool can be deduced, including minimum requirements for molding and optional requirements for specific tasks.



FIGURE 5-12 Hot embossing machine Wickert WMP1000.

Basic Tools for Hot Embossing

The requirements and concepts underlying the design of tools for hot embossing were described above. An example of a hot embossing tool with an optimized heating and cooling concept was developed at the Institute of Microstructure Technology at the research center of Karlsruhe. In this case, thermal mass is reduced, while the stability and evenness of the surfaces needed for molding micro-structures on large areas of a thin residual layer are maintained (Fig. 5-14).

The functioning of this tool is illustrated in Fig. 5-15. To reduce the heated masses by the

largest possible extent, the hot and cold areas of the tool are separated thermally. Hence, such a tool is divided into a heating plate and a so-called cooling block (Fig. 5-15). In the basic state of the tool, both functional units are insulated thermally by an air gap produced with the help of springs (Fig. 5-15(a)). This air gap is retained when melting the polymer. The contact force is generated by the springs only (Fig. 5-15(b)). Due to thermal insulation, the relatively thin heating plate and the mold insert can be heated rapidly. In the displacement- and force-controlled embossing process, the molding force presses the heating plate onto the massive cooling block, which results in a mechanically stable set-up, by means of which homogeneously thin residual layers may be produced even on large areas (Fig. 5-15(c)). As soon as the heating plate is in contact with the cooling block, heat is removed from the heating plate to the comparably large and permanently cooled cooling block. As the cooling block acts like a heat sink, the heating plate and the mold insert can be cooled down rapidly. Subsequently, the components can be demolded (Fig. 5-15(d)). Except for the vacuum chamber, the tool halves are designed symmetrically and consist of a water-cooled cooling block and a heating plate each. The heating plate is lifted off the cooling block by prestressed disc spring packages. Mold inserts of 250 mm in diameter can be fixed onto the heating plate, and



(a) EVG520HE



(b) EVG750

FIGURE 5-13 Nano-imprint machine EVG520HE and EVG750.

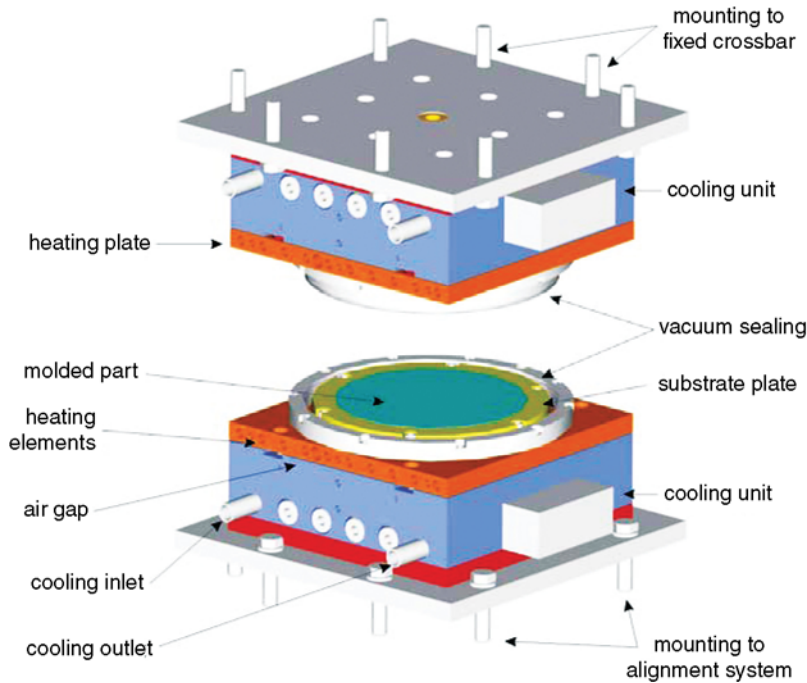


FIGURE 5-14 Schematic view of a basic molding tool with reduced thermal mass.

the maximum molding temperature is 300 °C. In this tool, the heating plate can be clamped to the cooling block using a magnetic clamping system. A tolerance-free opening movement of the hot embossing machine thus allows for offset-free demolding. As in conventional hot embossing tools, substrate plates roughened by lapping or sand blasting may be used for demolding. The demonstration tool is presented in Fig. 5-16.

For precise temperature control, the heating plates of the basic tool are divided into four zones each, which are controlled separately and may be set to various temperatures. In this way, a highly homogeneous temperature distribution can be achieved in the mold insert. In the hot embossing process, three different temperatures can be input for each tool half: the molding temperature is the temperature to which the heating plates are heated, while the embossing temperature is the temperature at which the embossing force starts to build up. At the demolding temperature, demolding of the embossed component starts. The molding temperature is measured directly in

the individual zones of the heating plates, and the embossing and demolding temperatures are measured in the mold insert and substrate plate, respectively. As the mold insert cools quickly when the embossing force is generated, it may be reasonable to select a molding temperature far above the embossing temperature. As a result of the thermal inertia of the heating plate and the cooling block, cooling of the polymer melt is then slowed slightly: this allows the fabrication of very thin components of low stress.

The heating concept based on a spring was also implemented by Schiff et al. [18] for the molding of wafer-type substrates. A clamped stack of the stamp and substrate was preassembled in an alignment system, and it was not in contact with the heating plate, under action of the spring system. The gap was closed by the acting of force, pressing the stack onto the heating plate. After embossing, the force was set to a low value which results in the separation of the stack from the heating plate under action of the springs. The molded part is cooled and can be demolded manually.

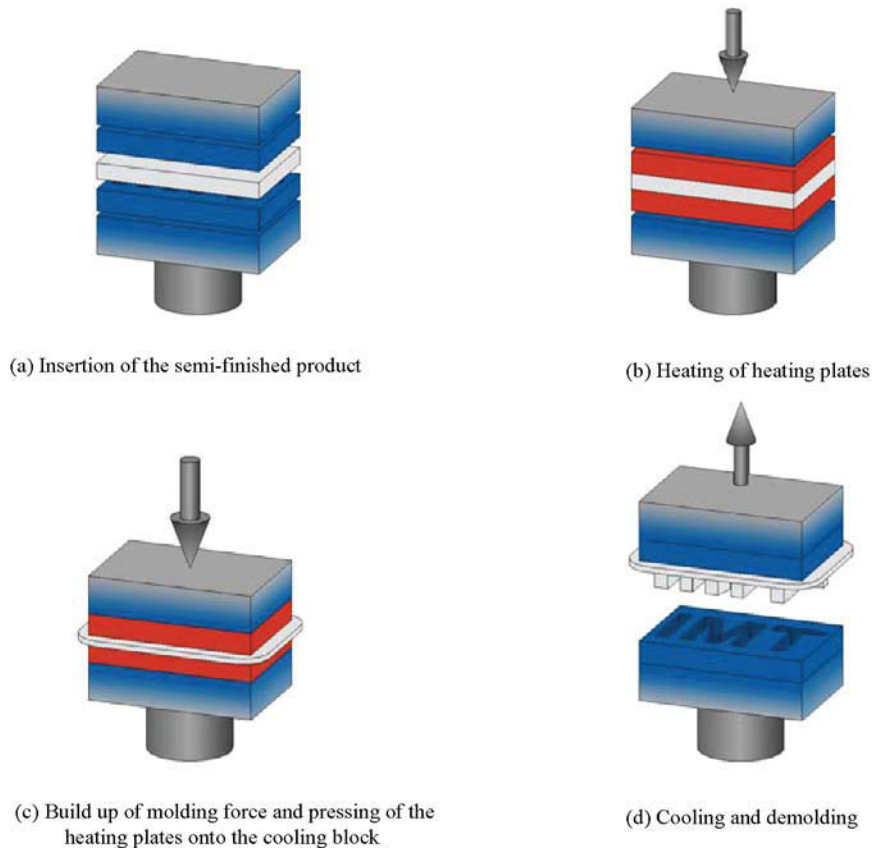


FIGURE 5-15 Schematic view of the process steps of hot embossing with the basic molding tool.

Micro-structured Mold Inserts

For every replication process a mold or so-called master is necessary to copy the structures of the mold into a molding material. The mold is split into the tool and the mold insert with the micro-structured surface. In theory every micro-structured surface can be used as a mold insert. A precondition is that the mold material and the micro-structures will withstand the temperature and mechanical load during molding. Nevertheless, for successful molding, and especially demolding, the mold insert has to fulfill the following requirements:

- The yield stress of the mold material at the maximum molding temperature has to be



FIGURE 5-16 Lower half of a basic molding tool with a moldable surface area of up to 250 mm diameter.

significantly higher than the stress effected by the molding force.

- To avoid any bending and to ensure the greatest possible evenness of the mold, the residual stress inside the mold, caused by the fabrication process, should be reduced to a minimum.
- The mold material should show chemical resistance against the polymer.
- There should be a high heat conductivity of the mold material to reduce the heating and cooling times.
- For cost effectiveness the lifetime of the mold should be extended over many cycles.
- To support successful demolding, the surface roughness, especially of vertical sidewalls, should be reduced to an unavoidable minimum.
- Demolding angles are advantageous because they facilitate demolding. In contrast, undercuts prevent the successful demolding of micro-structures. Even small undercuts in the

sub-micron range can increase demolding forces significantly.

Regarding the requirements, especially the requirement of high yield stress, it is obvious that mold inserts, fabricated in metals, are well suited. The technique of micro-structuring of metals is therefore essential for mold fabrication, but also glass or polymers like UV-transparent PDMS or high temperature resistant PEEK can be used for selected replication tasks. Nevertheless, regarding the lifetime of a mold insert, high stiffness molds fabricated from metals are widely used for replication. An overview of the different mold fabrication processes is shown in Fig. 5-17.

The structuring processes can be split into two groups: direct structuring methods like mechanical machining, electric discharge machining (EDM) or laser structuring [19]; and lithographic methods like E-beam lithography and UV-lithography. For structures with high aspect ratios,

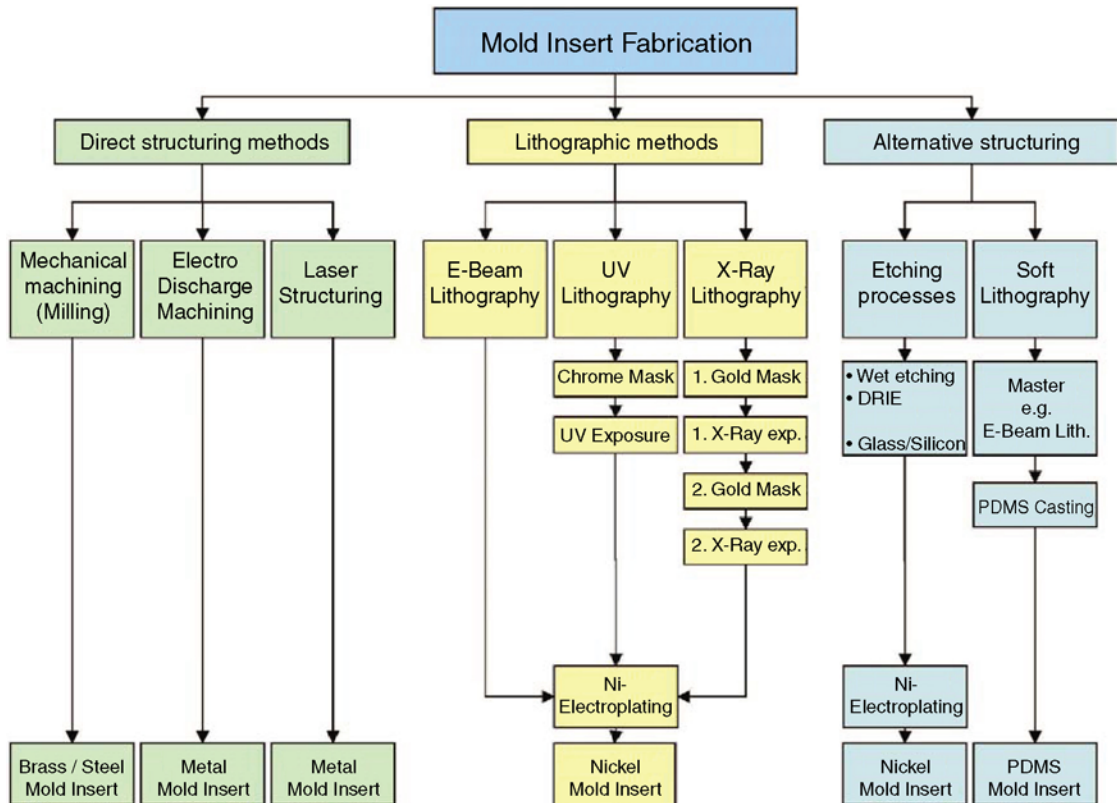
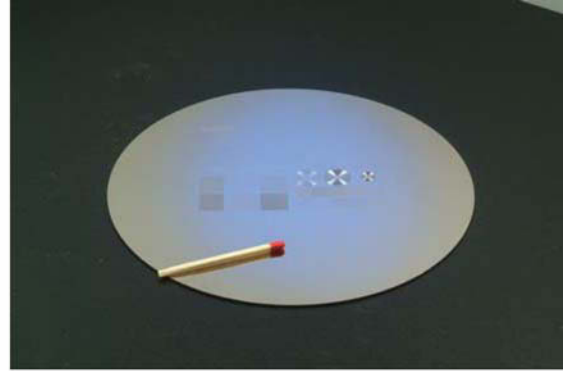


FIGURE 5-17 Overview of the mold fabrication processes.



(a) LIGA mold insert



(b) Nickel Shim mold insert

FIGURE 5-18 Electroplated LIGA mold insert, structured by X-ray lithography.

X-ray lithography is also used to structure the mold inserts. All lithographic processes require the step of electroforming to obtain a metal mold insert. Each structuring method has different characteristics and is therefore suitable for different kinds of applications.

Representative of the large number of suitable mold inserts are two electroplated mold inserts shown in Fig. 5-18: a typical LIGA mold insert with high aspect ratio structures with dimensions of $28 \times 66 \text{ mm}^2$ and a thickness of 5 mm and as an alternative for larger structured areas a 4 inch nickel shim mold insert with a typical thickness of approximately 300 up to 500 μm .

The height of the structures is 750 μm . Nickel shims are characterized by a thickness in the range of several hundred micrometers and are well suited for the replication of structures with low aspect ratios on large areas, typically 4 or 6 inches.

APPLICATIONS

This section presents some applications where hot embossing plays an important role for their fabrication.

Micro-optical Devices

Micro-optical devices are one of the main applications in micro-system technology. The devices that can be replicated by hot embossing are

manifold, beginning at micro-optical components like lenses, mirrors, optical benches or waveguides, up to micro-systems like micro-spectrometers, DFB-laser systems, optical switches, fiber connectors, photonic crystals or anti-reflection films [20–21]. Because of the requirements regarding structure sizes, surface quality and accuracy of lateral distances, the mold inserts for hot embossing are typically fabricated by lithographic processes.

Optical Waveguides. For optical interconnection the replication of polymeric waveguides opens a new field of applications. Depending on the application, monomode or multimode waveguides with different sizes are required, beginning with lateral dimensions of approximately 6 μm [22] up to 500 μm [23]. Sufficient for most applications is an aspect ratio in the vicinity of unity, but typically a guiding path over several millimeters or centimetres is desired. The design refers typically to free-standing rectangular shapes without any additional supporting structures, which makes it necessary to reduce internal stress inside the structures to avoid any deformation of the shape of the waveguides. Several techniques allow the modification of the refractive index of the material, for example the UV-radiation of PMMA, which makes this material suitable for the replication of waveguides. Representative for a variety of polymer waveguides, replicated rectangular

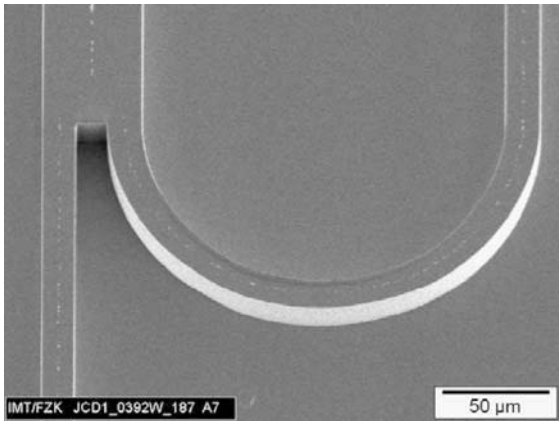


FIGURE 5-19 Molded optical waveguides with a cross-section and height of approximately $6\ \mu\text{m}$ [22].

waveguides and further optical splitters are presented in Fig. 5-19.

The electroplated nickel shim mold was fabricated by UV-lithography and replicated into PMMA. The refractive index of the molded waveguides was modified after replication by UV-radiation. The basic optical waveguide elements allow further the development of interactions between waveguides for subsequent applications

Micro-fluidic Devices

Micro-fluidic systems are part of life science technology and diagnostic and therapeutic biomedical

engineering. Passive micro-components like capillary micro-channel structures and so-called wells, reservoir areas or miniaturized sample chambers can be part of micro-total analysis systems or lab-on-a-chip systems [24]. Representative for passive micro-fluidic systems are, for example, capillary electrophoresis chips. Active micro-fluidic components like pumping systems or valve systems are mostly part of complex total analysis systems.

Capillary Analysis Systems. The functioning of a capillary electrophoresis system can be explained principally by Fig. 5-20. The system consists of two intersecting micro-channels with wells at the beginning (buffer) and at the end (waste). The first shorter channels will contain the sample material which should be analyzed, the longer channels contain a buffer solution. To achieve a flow an injection of the sample fluid into the buffer fluid is made at the intersection point; a difference in potential has to be obtained by electrodes integrated in the wells. By electric switching the sample volume located in the intersection area can be injected into the longer separation channel. In this channel the plug is separated into its components, depending on molecule size and electric charge [25]. Characteristic for micro-fluidic structures are grooves typically with an aspect ratio in the vicinity of unity and a flow path of up to several centimeters which can be arranged in a

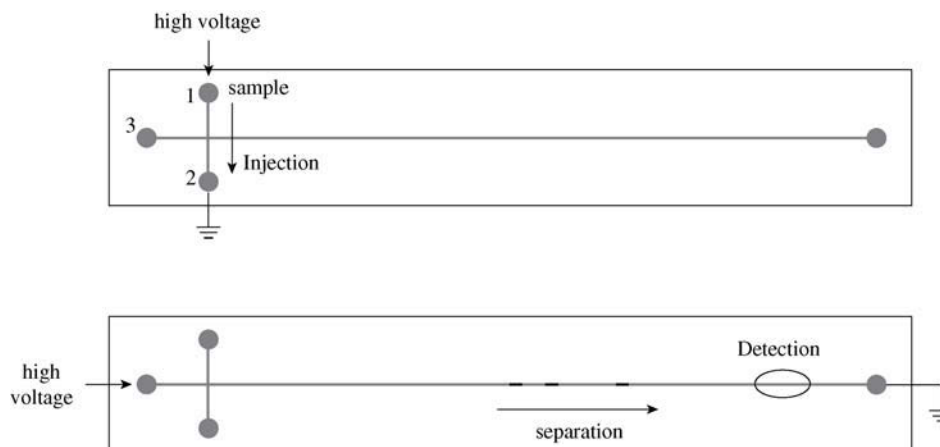
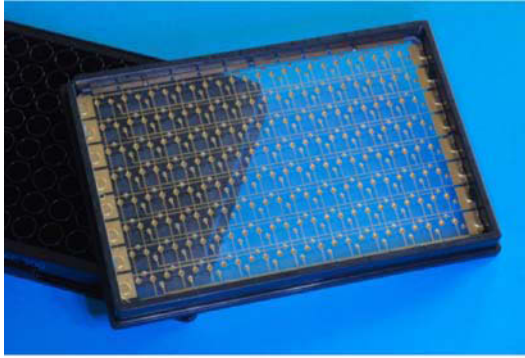
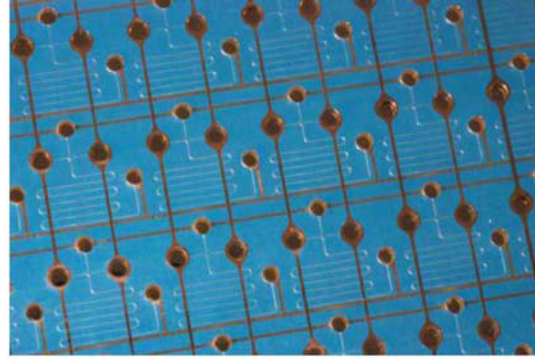


FIGURE 5-20 Principle of a capillary electrophoresis system.



(a) Microtiterplate with 96 CE-systems



(b) Microfluidic channels with electrical connections

FIGURE 5-21 Microtiterplate with 96 CE systems [24,25].

shape of a meander to achieve compact systems. For easy handling of these structures it is recommended to arrange such CE systems onto standardized platforms, for example microtiterplates with an area of 125 mm × 85 mm. On this area, for example, 96 CE systems could be integrated (Fig. 5-21).

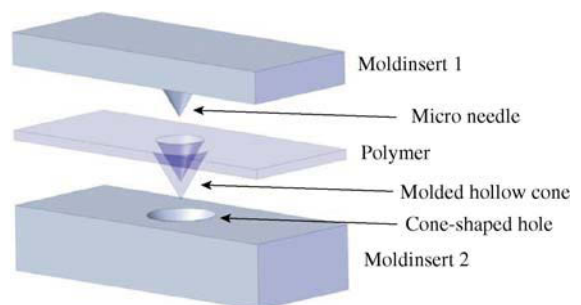
The principle refers to an intersection of two micro-channels where a small volume of the sample fluid is injected into the long fluid channel with a buffer fluid inside. During the flow the sample volume will be separated into its components, which can be detected at the end of the flow path. The injection and the flow are supported by a high voltage difference between the buffer and the waste with electrical connections.

Micro-needles

Another application for the hot embossing technique is an example of a medical technique, in particular in drug delivery. Micro-needles are one of the minimal invasive drug delivery systems entering the body through the skin. Therefore the outer layer of the skin (stratum corneum) with a typically thickness in a range between 10 and 20 μm has to be disrupted. The thickness of this layer determines the minimum height of the needles. The biocompatibility of selected polymers and the fabrication of an array of micro-needles for the drug delivery make this application well

suited for polymer replication processes. One of the requirements is a hollow needle which makes it necessary to integrate a fluid channel inside the polymer needles.

A suitable fabrication method is the replication of micro needles by double-sided, positioned hot embossing. In this case a cone shaped needle on the one side hits a cone shaped hole in the other side of a two-sided molding mold insert (Fig. 5-22). The achievable accuracy regarding the homogeneous thickness of the sidewalls depends here on the overlay accuracy of both mold halves. The advantage of this method is that only a thin residual layer on the tip of the cone has to be disrupted. This can be done easily, for example, by laser structuring. The fabrication of the mold inserts, the positive cone and the negative cone-shaped hole can be done by mechanical machining.

**FIGURE 5-22** Double-sided molding of micro-needles.

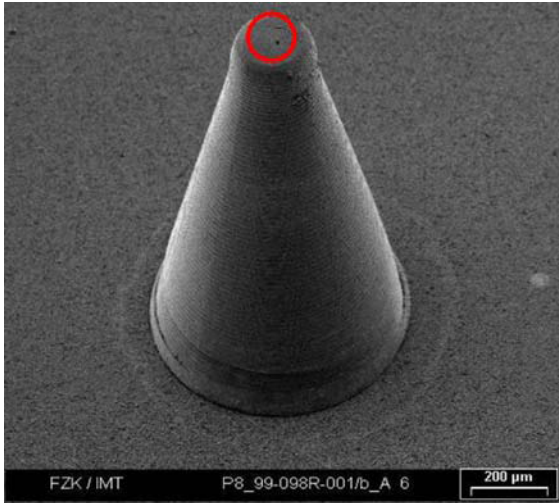


FIGURE 5-23 Molded micro-needles with a through-hole on top of the cone-shaped needle.

To achieve hollow cone-shaped needles double-sided positioned molding of a cone-shaped needle into a cone-shaped hole is required.

Finally, the residual layer of the needle has to be eliminated. In this case the residual layer is beside the carrier layer of the needle, also located in the tip of the cone. To achieve a fluid channel through the needle, the residual layer has to be removed. A molded micro-needle with a fine hole in the tip is shown in Fig. 5-23.

THE OUTLOOK

The examples presented above are only part of a pool of applications, but they underline the relevance of the hot embossing or thermal nano-imprint process as an established replication technology. Further developments in hot embossing and nano-imprinting will be supported by new applications, especially if large series are required. Here the kind of automation and standardization of, e.g., molding formats will also help to establish this technology in the industry as replication technology. Especially, the cycle times have to be minimized in future, which corresponds to an efficient heating and cooling system. Optimized molding

tools are therefore a key issue for cost-effective molding. In combination with already well-established handling systems in macroscopic processing the process times can be minimized and hot embossing can be established as an industrial replication technology. A cost-effective replication also requires large molding areas. These molding areas correspond to the fabrication methods of the mold inserts which are limited individually. To overcome these limits, molding tools with multiple mold inserts can be used. These aspects are mainly in the foreground of interest for a cost-effective use of hot embossing. Independently of the potential to optimize the cost effectiveness, hot embossing will still be a well-suited process for the first replications of prototypes. In this case the future may shift the replication to structures with smaller structure sizes in the nano-range in combination with high aspect ratios, e.g. larger than 5. Further, those structures will be replicated over large areas such as 8 inches or more. Nevertheless, all replication processes are inspired by the requirements of the further applications and these applications will finally determine the structure sizes, the molding areas and the kind of automation.

REFERENCES

- [1] H. Becker, C. Gärtner, Polymer microfabrication technologies for microfluidic systems, *Anal. Bioanal. Chem.* 390 (2008) 89–111.
- [2] H. Becker, U. Heim, Hot embossing as a method for the fabrication of polymer high aspect ratio structures, *Sensors and Actuators* 83 (2000) 130–135.
- [3] M. Hecke, W. Bacher, K.D. Mueller, Hot embossing—the moulding technique for plastic microstructures, *Microsystem Technologies* 4 (1998) 122–124.
- [4] M. Hecke, W.K. Schomburg, Review on micro moulding of thermoplastic polymers, *J. of Micromechanics and Microengineering* 14 (2004) R1–R14.
- [5] R. Bartolini, W. Hannan, D. Karlsons, M. Lurie, Embossed hologram motion pictures for television playback, *Applied Optics* 9 (10) (1970) 2283–2290.
- [6] M.T. Gale, J. Kane, K. Knop, Zed images: embossable surface-relief structures for color and black-and-white reproduction, *J. of Applied Photographic Engineering* 4 (2) (1978) 41–47.

- [7] E.W. Becker, W. Ehrfeld, P. Hagmann, A. Maner, D. Münchmeyer, Fabrication of microstructures with high aspect ratios and great structural heights by synchrotron radiation lithography, galvanofforming and plastic moulding (ligaprocess), *Microelectron. Eng* 4 (1986) 3556.
- [8] M. Harmening, W. Bacher, P. Bley, A. El-Kholi, H. Kalb, B. Kowanz, W. Menz, A. Michel and J. Mohr, Moulding of three-dimensional microstructures by the liga process. In *Proc. MEMS' 92*, Trarvumünde, Germany, p. 202. IEEE (1992).
- [9] Jenoptik Mikrotechnik, <http://www.jo-mt.de> (2008).
- [10] Wickert Press, <http://www.wickert-presstech.de> (2008).
- [11] Fresnel Optics, <http://www.fresnel-optics.de> (2008).
- [12] K.D. Mueller, Herstellung von beweglichen metallischen Mikrostrukturen auf Siliziumwafern, Scientific report FZKA 6254. Forschungszentrum Karlsruhe (1999).
- [13] Ch. Mehne, Grossformatige Abformung mikrostrukturierter Formeinstze durch Heissprägen, PhD thesis, University of Karlsruhe, Institute for Microstructure Technology (2007).
- [14] B. Rapp, M. Worgull, M. Hecke, A.E. Guber, Mikro-Heissstanzen-Erzeugung von Durchlochstrukturen in ebenen Kunststoffsubstraten, In *Conference in Microsystem Technology*, Freiburg i. Br, Germany (2005).
- [15] H. Tan, A. Gilbertson, S.Y. Chou, Roller nanoimprint lithography, *J. Vac. Sci. Technol. B* 16 (6) (1998) 3926–3928.
- [16] EVG, <http://www.EVGroup.com> (2008).
- [17] Ch. Schaefer, S. Farrens, T. Glinser, P. Lindner, N. Roos, State of the art automated nanoimprinting of polymers and its challenges, In *7th International Conference on the Commercialization of Micro and Nano Systems (COMS)* (September 8–12, 2002).
- [18] H. Schiff, S. Bellini, J. Gobrecht, F. Reuther, M. Kubenz, M.B. Mikkelsen, K. Vogelsang, Fast heating and cooling in nanoimprint using a spring-loaded adapter in a preheated press, *Microelectronic Engineering* 84 (2007) 932–936.
- [19] J. Fleischer, J. Kotschenreuther, The manufacturing of micro moulds by conventional and energy-assisted processes, *Int. J. Adv. Manuf. Technol.*(2006).
- [20] C.J. Ting, M.C. Huang, H.Y. Tsai, C.P. Chou, C.C. Fu, Low cost fabrication of large-area anti-reflection films from polymer by nanoimprint/hot-embossing technology, *Nanotechnology* 19 (2008) 1–5.
- [21] J. Seekamp, S. Zankovych, A.H. Helfer, P. Maury, C.M. Sotomayor Torres, G. Böttger, C. Liguda, M. Eich, B. Heidari, L. Montelius, J. Ahopelto, Nanoimprinted passive optical devices, *Nanotechnology* 13 (2002) 581–586.
- [22] M. Bruendel, Herstellung photonischer Komponenten durch Heissprägen und UV-induzierte Brechzahlmodifikation von PMMA, PhD thesis, University of Karlsruhe (TH), Institute for Microstructure Technology (2008).
- [23] H. Mizuno, O. Sugihara, T. Kaino, N. Okamoto, M. Hosino, Low-loss polymeric optical waveguides with large cores fabricated by hot embossing, *Optics Letters* 28 (23) (2003) 2378–2380.
- [24] A.E. Guber, M. Hecke, D. Herrmann, A. Muslija, V. Saile, L. Eichhorn, T. Gietzelt, W. Hoffmann, P.C. Hauser, J. Tanyaniwa, A. Gerlach, N. Gottschlich, G. Knebel, Microfluidic lab-on-a-chip systems based on polymers-fabrication and application, *Chemical Engineering J* 101 (2004) 447–453.
- [25] A. Gerlach, G. Knebel, A.E. Guber, M. Hecke, D. Herrmann, A. Muslija, Th. Schaller, Microfabrication of single-use plastic microfluidic devices for high-throughput screening and DNA analysis, *Microsystem Technologies* (2002) 265–268.

Micro-Injection-Molding

Guido Tosello and Hans Nørgaard Hansen

INTRODUCTION

The essential condition for the market success of micro-systems is the cost-effective production of micro-structures on a large scale. In recent years plastic molding techniques such as injection molding, which is a suitable process for medium- and large-scale fabrication, have been adapted for the necessities of micro-components fabrication. Injection molding is a process technology that has been well established in the production of polymer parts in the macro-dimensional range for decades. Therefore, vast know-how and machine technology is available to be made use of in micro-injection molding as well.

Moreover, the fabrication costs of molded micro-parts are only slightly affected by the complexity of the design. Once a mold insert has been made, several thousands parts can be molded with little effort. The cost of raw material in most cases is negligibly low, because only small material quantities are required for micro-components. Therefore, parts fabricated by micro-injection molding, even from high end materials, are suitable for applications requiring low cost and disposable components [1]. The result is that plastic products manufactured by micro-injection molding have made successful entry into the market. In fact, peculiar characteristics such as production capability, disposability, biocompatibility, optical properties, just to mention a few, pose plastics as the best choice for numerous micro-products. Fields of application of micro-molded products are: micro-optics (waveguides, micro-lenses, fiber connectors), micro-mechanics (micro-gears,

micro-actuators, micro-pumps, micro-switches), information storage and data carrier devices (CDs, DVDs, sensor discs), micro-fluidic systems (blood analysis, DNA analysis), medical technology (hearing aid, components for minimal invasive surgery).

When downscaling systems, products, and their components, the limits of conventional manufacturing techniques are reached. This initiated the improvement of conventional techniques and the further development of new ones, as in the case of the micro-injection molding process. Lateral dimensions in the micrometer range, structural details in the sub-micrometer dimensional level and high aspect ratio (aspect ratio = depth/width) of 10 and above are achieved. There are a variety of applications already known for the micro-molding of thermoplastic polymers and many more are expected to arise in the future.

MICRO-INJECTION MOLDING SCENARIO

Injection molding is one of the most versatile and important operations for the mass production of complex plastic parts. Injection-molded parts typically have good dimensional tolerance and require almost no finishing and assembly operations. In addition to thermoplastics and thermosets, the process is also being extended to such materials as fibers, ceramics, and powder materials, with polymer as binders. Among all the polymer-processing methods, injection molding accounts for 32% by weight of all the polymeric

material processed [2]. Innovations of the conventional injection molding process have been continuously developed to further extend the applicability, capability, flexibility, productivity, and profitability of this versatile mass-production process.

In particular, micro-injection molding is an innovative technology for replication on the medium-to-large scale of micro-components. Micro-injection molding introduces additional design freedom, new application areas, unique geometrical features, and sustainable economical benefits, as well as material properties and part quality that cannot be accomplished by the conventional injection molding process.

Micro-injection molding (or μ IM, also called micro-molding) refers to the production of parts that have:

- Weight in the range of milligrams, overall dimensions, functional features, and tolerance requirements that are expressed in terms of micrometers, as well as miniaturized gate and runner system (see Figure 6-1, left).
- Overall dimensions in the macro-range, weight of the order of grams, and areas with micro-features. Such micro-structures have dimensions, functional features, and tolerance requirements that are expressed in terms of micrometers down to nanometers (see Figure 6-1, right).

On the basis of these definitions, micro-molding can be also regarded as a type of molding technology recently defined as ‘Precision Injection Molding’ [3].

Among the various micro-manufacturing processes, micro-injection molding possesses the advantage of having a wealth of experience available in conventional plastics technology, standardized process sequences, and a high level of automation and short cycle times.

Due to the miniature characteristics of the molded parts, however, a special molding machine and auxiliary equipment are required to perform tasks such as shot volume control, process parameters control, injection, ejection, plastification, inspection, handling, packaging of molded parts, etc. Furthermore, micro-machining technologies are needed to produce the micro-cavity.

MICRO-INJECTION MOLDING TECHNOLOGY

The development of micro-injection technology entered a first phase between 1985 and 1995 [5]. During that period, injection molding technology for macro parts with micro-structured details started and no appropriate machines were available. Only modified commercial units, hydraulically driven and with a clamping force of usually 25 up to 50 tons, could be applied for

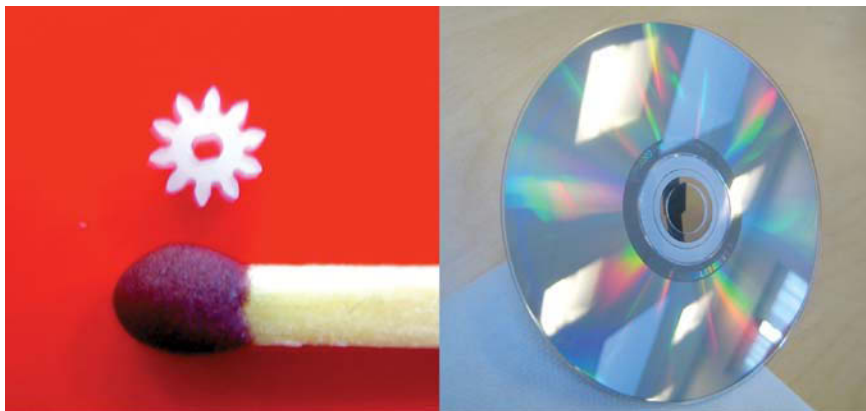


FIGURE 6-1 Example of a micro-molded part (micro-gear, on the left) and a macro-part with a micro-structured region (DVD disc, on the right).

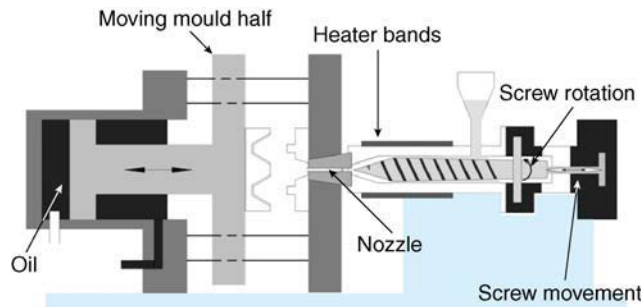


FIGURE 6-2 Schematic view of a hydraulic injection molding machine with its main components [7].

the subtle way of replicating micro-structured mold inserts with high aspect ratios by injection molding. Then a second stage occurred from 1995 to 2000 when, with the collaboration between mechanical engineering companies and research institutes, special micro-injection units or even completely new machines for the manufacturing of real micro-parts were developed. The task was to reduce the minimal amount of injected resin, which is necessary to guarantee a stable process (i.e. improve the process repeatability) and increase replication capabilities of very small features (down to 20 μm).

Following this intense developing stage a number of machines equipped with special features for micro-injection have been produced by leading manufacturers. Minimum shot weights down to 25 mg are now feasible, micro-features can be replicated in a short cycle time, and three-dimensional micro-products are produced, which can now successfully enter the market.

Micro-molding with Conventional Injection Molding Machine

The fabrication of micro-molded parts becomes a challenge when conventional injection molding machines (see Figure 6-2) are used for the replication of very small parts. If such machines are adapted to the direct production of a micro-product, i.e. parts with a part weight down to a milligram (mg), they produce precise but large sprues to achieve the minimum necessary shot weight to perform the process properly. Very often over 90% of the polymer is wasted and this

waste can be an important cost factor (considering, e.g., plastic material for medical applications, it is not unusual for 1 kg of special material, e.g. polyaryletheretherketone, to cost €100). Moreover, the large sprue increases the cooling time and, simultaneously, the cycle time [6].

In conventional injection molding, an injection cycle is composed of the main phases described in the following (see Figure 6-3).

1. **Plastification** – during the plastification phase, the screw is rotating to build up the melt polymer necessary for the injection phase. The pressure pushes the screw backwards. When sufficient polymer has built up (i.e. shot volume is plastificated) rotation stops.
2. **Injection, filling and packing phase** – when the mold is closed, the screw is advanced (injection). The melt polymer fills the sprue, the runners and the mold cavity (filling). The screw begins rotating again to build up more polymer (packing).
3. **Cooling and ejection** – after the polymer is solidified (cooling), the mold opens and ejector pins remove the molded part (ejection).

A problem which occurs with the small shot weight typical of micro-parts is related to the size of pellets used in standard injection molding. Conventional injection molding machines utilize screws with diameters down to 14 mm. Thus the depth of the screw channels should have at least the dimensions of a single grain. Hence, when the screw moves just 1 mm, about 185 mg of plastic are injected. For example, even one single pellet of poly(methylmethacrylate) (PMMA) weighs 24 mg. This exceeds the part

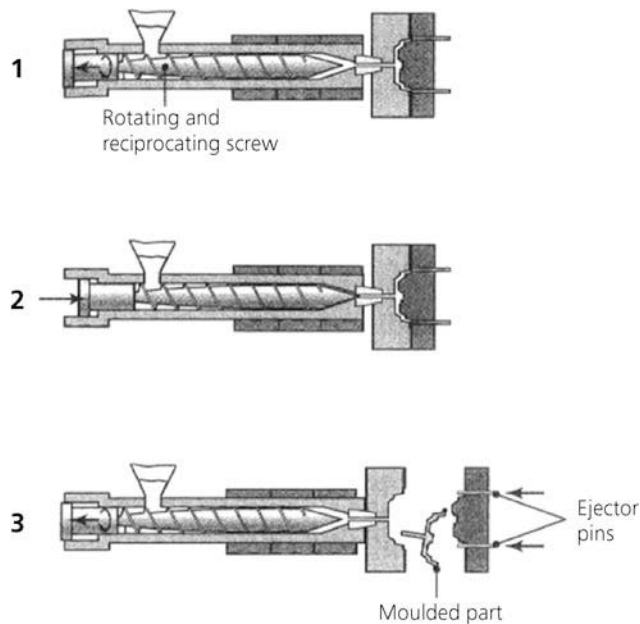


FIGURE 6-3 Phases of the injection molding process.

weight of, e.g., gears for the watch industry of 0.8 mg. Again, to produce such gears, relatively huge runner systems are used to compensate for this issue (Fig. 6-4).

It is clear that these data represent a limit for correct processing of an injection molded micro-part: the minimum shot weight for a stable production lies in the range of tenths of a gram. When producing parts at the lower limit of the machine

capacity, problems such as dwelling time of the material will appear, with risk of polymer degradation [7].

A screw for melting and injecting polymers combines four functions in one single unit:

- Plastification and homogenization
- Metering
- Locking
- Injection.

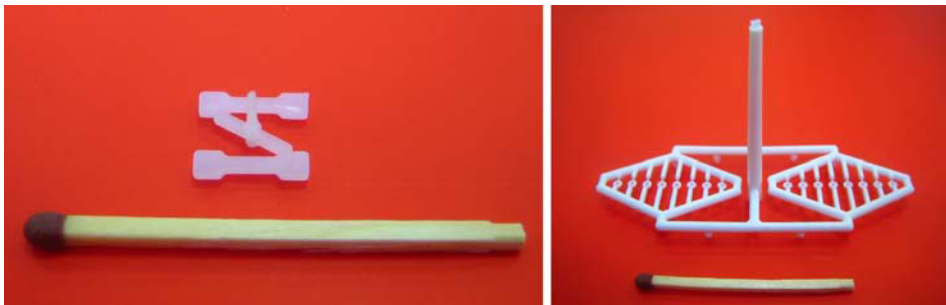


FIGURE 6-4 Comparison of runner systems to mold micro-part with conventional injection molding machines (right) and with micro-injection molding machine (left) [4].

A conventional reciprocating screw used in macro-machines presents the following problems when it is employed on molding micro-parts:

- It is difficult to control the melt metering accuracy as a result of the screw structure and the limitation to reduce screw size.
- Because of the channel configuration there is a melt backflow when high injection pressure is applied to fill small and micro-cavities.

For further downscaling of the injection molding process, these issues have to be solved by dividing the four functions of the screw at least in two different units:

- A screw for plasticizing and homogenizing
- A piston for metering and injection.

Micro-injection Molding Machine

In order to control the metering accuracy and the homogeneity of the very small quantities of melt in the micro-injection molding process, a new micro-molding machine that uses an injection system comprising a screw extruder and a plunger injection unit has been developed over the last ten years.

The main difference between the new micro-molding machine design and the conventional reciprocating screw injection system is that by separating melt plastification and melt injection, a small injection plunger of a few millimeters in diameter

can be used for melt injection to control metering accuracy. At the same time, a screw having sufficient channel depth to properly handle standard plastic pellets and yet provide the required screw strength can be employed in micro-molding machines.

The typical solution provided by a micro-injection molding machine consists of the splitting of the four functions of the reciprocating screw (plastification, metering, locking, injecting) into different components (see Figure 6-5).

The plastification takes place in a dedicated functional part of the machine, which is separated from the injection unit:

- The very small amount of plastics needed is plasticized either by a plasticizing small screw (diameter of 14 mm, see Figure 6-6) or in an electrically heated cylinder, and then fed into the injection cylinder by a plunger (diameter of 5 mm).
- A second plunger with a diameter of just 5 down to 2 mm, depending on the machine configuration, injects the molten material into the cavity. It is driven by an electric motor and a precise linear drive. Typically, the shot weight can be varied between 5 and 300 mg.

The micro-injection molding process steps are the following (see Figure 6-9):

1. Plastic pellets are plasticized by the fixed extruder screw and fed into the metering chamber.

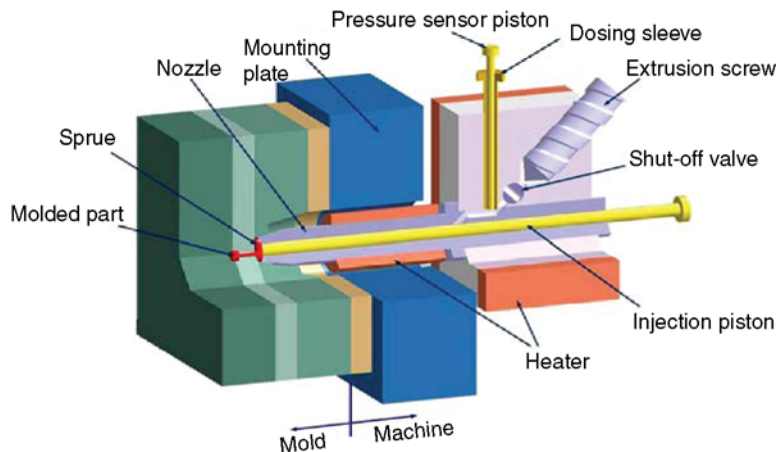


FIGURE 6-5 Injection unit of a micro-injection molding machine [4].



FIGURE 6-6 Comparison of dimensions between screw and injection plungers for μM (left) and a screw for conventional injection molding (right).

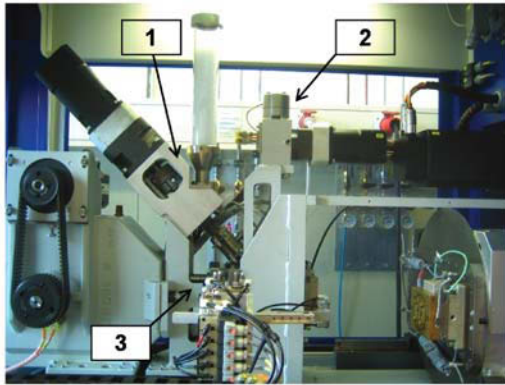


FIGURE 6-7 Micro-molding machine and the three-stage unit: plastication (1), metering (2) and injection (3) [8].

2. The shut-off valve closes in order to avoid backflow from the metering chamber.
3. After the set volume has been achieved, the plunger in the dosage barrel delivers the shot volume to the injection barrel.
4. The injection plunger then pushes the melt into the mold.
5. Once the plunger injection movement is completed, a holding pressure may be applied to the melt. This is achieved by a slight forward movement (maximum 1 mm) of the injection plunger.

The injection piston is usually capable of a maximum injection speed of 500 to 1000 mm/s and it was able to inject up to the parting line of the micro-cavity (i.e. the pin-point gate); in this way no sprue is attached to the molded part (see Figure 6-8). This design feature is particularly suitable for the mass production of micro-injection molded components for the following reasons: it allows shorter filling time due to the lower volume to be filled, it avoids short shots due to

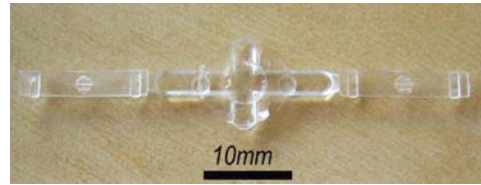


FIGURE 6-8 Micro-molded components and runner systems [10]: thin tensile bar test part ($15 \times 3 \times 0.3 \text{ mm}^3$) including three micro-features (width = $300 \mu\text{m}$, length = from $1500 \mu\text{m}$ up to $2000 \mu\text{m}$), material = polystyrene, weight complete molded part = 119 mg (17% for each of the two parts and 64% for the miniaturized runner system)[8].

premature melt freezing allowing better micro-features replication, and it decreases the cycle time due to shorter cooling time.

PROCESS CONTROL AND ANALYSIS

Micro-injection molding is a process which enables the mass production of polymer micro-products. In order to produce high quality injection molded micro-parts, a crucial aspect to be fully understood and optimized is the filling of the cavity by the molten polymer. As a result, the relationships between filling performance and the different process parameter settings have to be established.

Characterization of the filling phase during micro-injection molding is a challenging task, mainly due to the dimensions of the cavity (typically in the sub-millimeter range, and even down to a few micrometers) and the filling time of the cavity (in the order of a few tens of milliseconds).

Different approaches have been recently applied in order to accurately describe the filling of the micro-cavity depending on the process parameter settings. For example, methods for

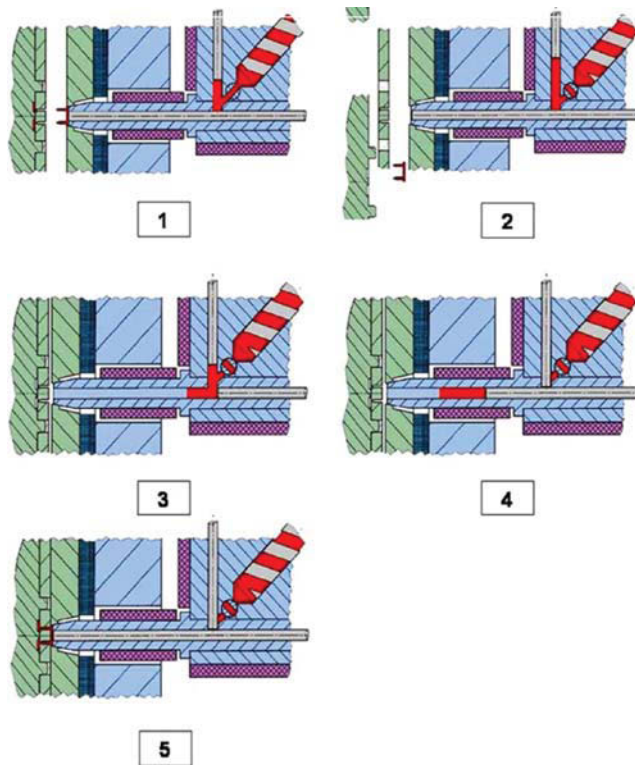


FIGURE 6-9 Micro-injection molding steps [4].

the analysis of filling performance are: the short shots method, the flow-melt visualization method, and the flow length test.

Micro-cavity Filling Analysis

Different approaches can be employed for the analysis of the filling stage of the micro-injection molding process. In particular, three methodologies can be applied in order to characterize filling performances:

- Short-shots, where partial filling is obtained by means of part-filled moldings of increasing volume.
- Flow visualization, used to show the progress of the melt front in the cavity during the injection phase.
- The length flow test, used to evaluate the filling capacity of the molding system in terms of achievable flow length and aspect ratio.

Short Shots Method. In conventional injection molding (i.e. in the macro-dimensional range), a common approach to study the development of the melt flow inside the cavity is the short shot analysis. This consists of the injection of a fraction of the molten polymer volume necessary to completely fill the cavity (see Figure 6-10).

The application of the short shots method to micro-injection molded parts has been shown to be possible when using a micro-injection molding machine provided with an injection plunger [3, 8]. One of the main conditions for the applicability of such a method is that the resolution of the machine (i.e. the smallest shot volume that can be injected in a controlled manner) has to be smaller than a fraction of the part which is significant to give information about intermediate stages of the filling. This condition can be fulfilled by injection molding machines having an injection unit with a plunger. On the other hand, small injection

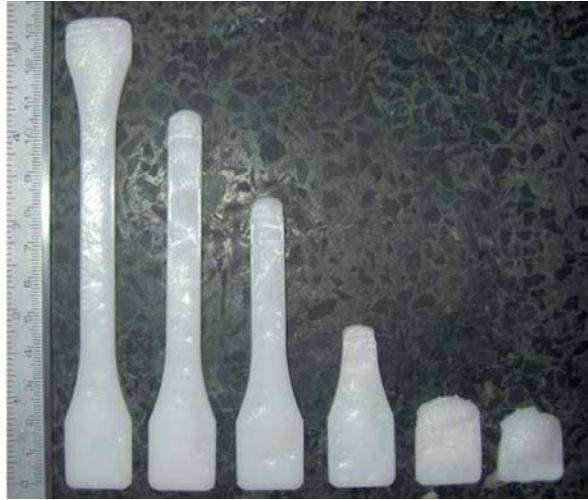


FIGURE 6-10 Short shots of an injection molded dog bone (material: polyoxymethylene, POM).

molding machines with the conventional plastification unit with a reciprocating screw cannot provide controlled short shots in the order of a fraction of 1 mm^3 (typical volume of polymer micro-parts and/or micro-features). Furthermore, in conventional machines, the acceleration of the screw may not be high enough to provide the required injection speed in the very short time needed to produce micro-short shots. As a result, despite the fact that it is actually possible to injection mold micro-parts with conventional injection molding machines (especially if electrically driven and capable of high injection speed), with such machines it is not possible to produce reliable micro-short shots. Process condition repeatability in terms of actual speed and injection pressure at the beginning of the screw movement is lower than when it has reached a steady state injection movement. Moreover, the produced incomplete micro-parts present free surfaces with a deformation due to stress relaxation and thermal contraction. This causes an approximation on the dimensional accuracy of the determination of the actual flow front during the filling, especially if the target is accurate in the micrometer range. On the other hand, the short shots method has been proven to be a feasible method to represent the evolution of the filling stage when performing micro-injection molding (see Figure 6-11).

Flow Visualization Tests

Flow visualization can also be used to describe the advancement of the flow front into the cavity during the filling stage. It consists of the use of a high speed camera capable of actually recording at high frame rates (in the order of 10^3 – 10^4 frames per second) the flow advancement inside the micro-cavity. In order to achieve such results, the mold has to be provided with a lateral opening (camera access to the mold) and one side of the cavity made of glass [11–12] (see Figure 6-12). By subsequent image processing of the recorded film of the cavity filling, it is possible to perform a time-dependent analysis on the displacement of the melt-flow front depending of different setting of process parameter such as melt temperature, mold temperature and injection speed.

The flow visualization method offers a better resolution than the short shots method. Furthermore, it can be applied not only to micro-injection molding machines but also to conventional reciprocating screw machines (mainly because the high resolution is provided by the high speed camera). On the other hand, the construction of the mold itself is quite complicated due to the presence of a perfectly aligned optical glass and an optical mirror conveying the image from the cavity, through the glass and on to the external camera. As a



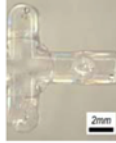






Experimental short shots	Parameters	Experimental short shots	Parameters
	Inj. Vol. = 55 mm ³ Inj. Time = 21 ms Weight = (52.1 ± 0.4) mg		Inj. Vol. = 105 mm ³ Inj. Time = 38 ms Weight = (96.9 ± 0.2) mg
	Inj. Vol. = 65 mm ³ Inj. Time = 25 ms Weight = (61.0 ± 0.5) mg		Inj. Vol. = 110 mm ³ Inj. Time = 41 ms Weight = (101.2 ± 0.2) mg
	Inj. Vol. = 75 mm ³ Inj. Time = 26 ms Weight = (7.0 ± 0.4) mg		Inj. Vol. = 125 mm ³ Inj. Time = 51 ms Weight = (114.4 ± 0.2) mg
	Inj. Vol. = 90 mm ³ Inj. Time = 29 ms Weight = (84.0 ± 0.3) mg		Inj. Vol. = 130 mm ³ Inj. Time = 83 ms Weight = (118.8 ± 0.2) mg
	Inj. Vol. = 95 mm ³ Inj. Time = 31 ms Weight = (88.0 ± 0.2) mg		

FIGURE 6-11 Series of short shots of a thin wall micro-molded part with micro-features [8].

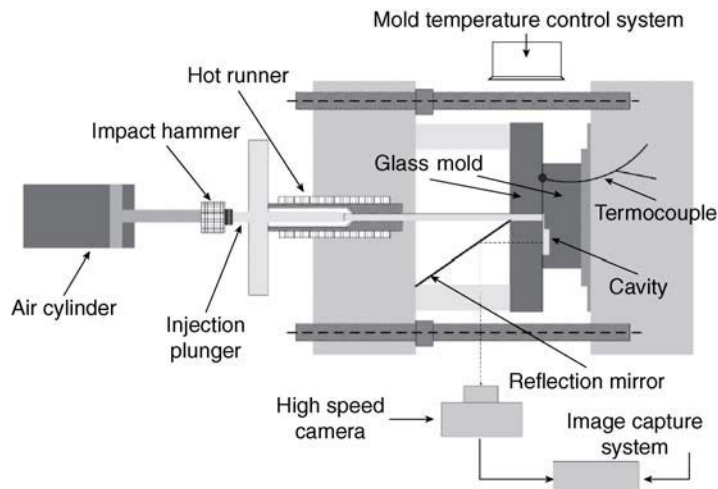


FIGURE 6-12 Schematic diagram of a machine equipped with a glass mold cavity and a flow visualization set-up.

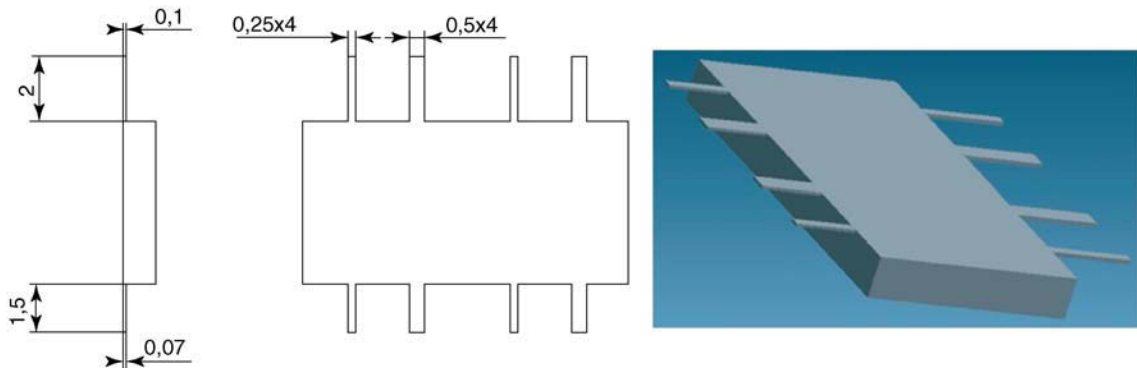


FIGURE 6-13 Part design for process analysis based on flow length test [14].

consequence, the method appears to be of difficult implementation in an industrial environment.

Length Flow Tests

Length flow tests are used to evaluate the filling capacity of the molding system in terms of flow length in the cavity and aspect ratio. Usually a test

cavity having constant cross-section and a dominant dimension parallel to the flow front advancing direction is used for the purpose; typically, aspect ratios above 10 are desired. Downscaling of such an approach, commonly employed on conventional injection molding, has been proposed for the investigation of filling behavior and processability during micro-injection molding

	Processing parameters				
Polymer		D _{1A}	D _{2A}	D _{1B}	D _{2B}
POM	T _{melt} = 220°C				
	T _{mould} = 120°C				
	V _{inj} = 200mm/s				

FIGURE 6-14 Flow length evaluation of micro-injection molded features for different ($D_1=70 \mu\text{m}$, $D_2=100 \mu\text{m}$), widths (250 μm , 500 μm) and features distance from the injection location (A, B) thickness.

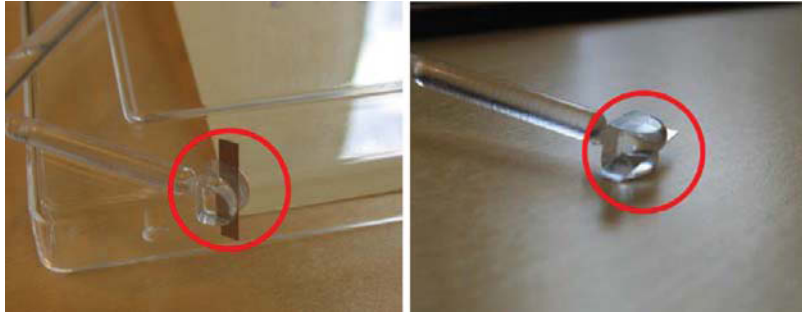


FIGURE 6-15 Weld lines formation due to the presence of an insert in the cavity during insert molding [8].

of semi-crystalline polymers (i.e. polypropylene and polyoxymethylene) as well as amorphous polymer (i.e. acrylonitrile-butadiene-styrene) [13]. Investigations are usually carried out by performing injection molding under different process factors affecting the replication capabilities and the filling performance of the process. Then, the achieved flow lengths in miniaturized channels, defined as the actual length reached by the melt during the molding, are determined and compared in order to establish the relation between flow lengths and process parameter settings.

Filling Analysis in μ IM using Weld Lines as Flow Markers

In injection molding, during the filling of cavities, when two or more flow fronts meet, an imperfection observable as a line is created. This defect

of injection molded parts is referred to as a weld line. Weld lines are influenced by material composition, mold design and process conditions [15]. Particularly related to mold design, the basic situations that are conducive to weld line formation that are conducive to weld line formation are the presence of [16]: inserts in the cavity (i.e. insert molding, see Figure 6-15), two or more gates for the part filling, the presence of regions of varying depths, features in the mold (e.g. pins all through the thickness of the cavity). Weld lines are visible on the surface of the part (their depth was measured with the atomic force microscope and found to be in the range between 500 and 1500 nm [17]) and they are a clear trace of the development of the flow melt during the filling of the cavity (see Figure 6-16).

Therefore, weld lines can be used as flow markers and, in particular, represent the position of the flow front at the end of filling. The analysis of

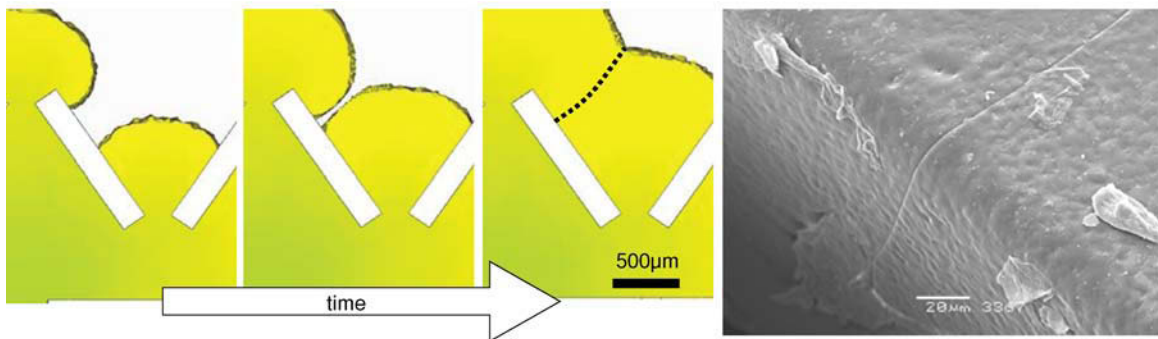


FIGURE 6-16 Simulation of the formation of a weld line due to the presence of a micro-feature (width = 200 μ m) in the cavity (left). Scanning electron microscope images of the actual weld line shown in the simulation (polymer = polystyrene) (right) [8].

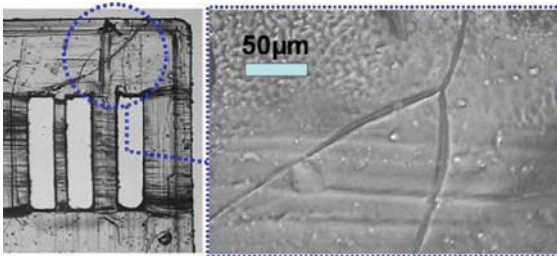


FIGURE 6-17 Optical image of weld lines due to melt flow front separation [8].

the positions of weld lines permits study of the influence of different processing conditions on the filling capability of the micro-molding process.

In fact, the different paths of weld lines obtained with the different settings of process parameters can be employed to study the effect

of different process parameters and determine the conditions for better cavity filling conditions [18]. In particular, a variation of mold temperature and of injection speed produces modification of the path of the weld lines, pushing towards the end of micro-features as the polymer melt flows. For example, in the case of polystyrene, the effect of melt temperature and packing pressure was extremely limited.

The flow front depth of filling (i.e. the ease of the melt flow to fill micro-structures) increases with the width of the structures to be filled. The meeting points of weld lines out of channels 200 μm and 300 μm wide, as well as the horizontal weld line in the channel 150 μm , show such behavior (see Table 6-1).

Complete filling of micro-injection molded features (i.e. a good filling performance) can be

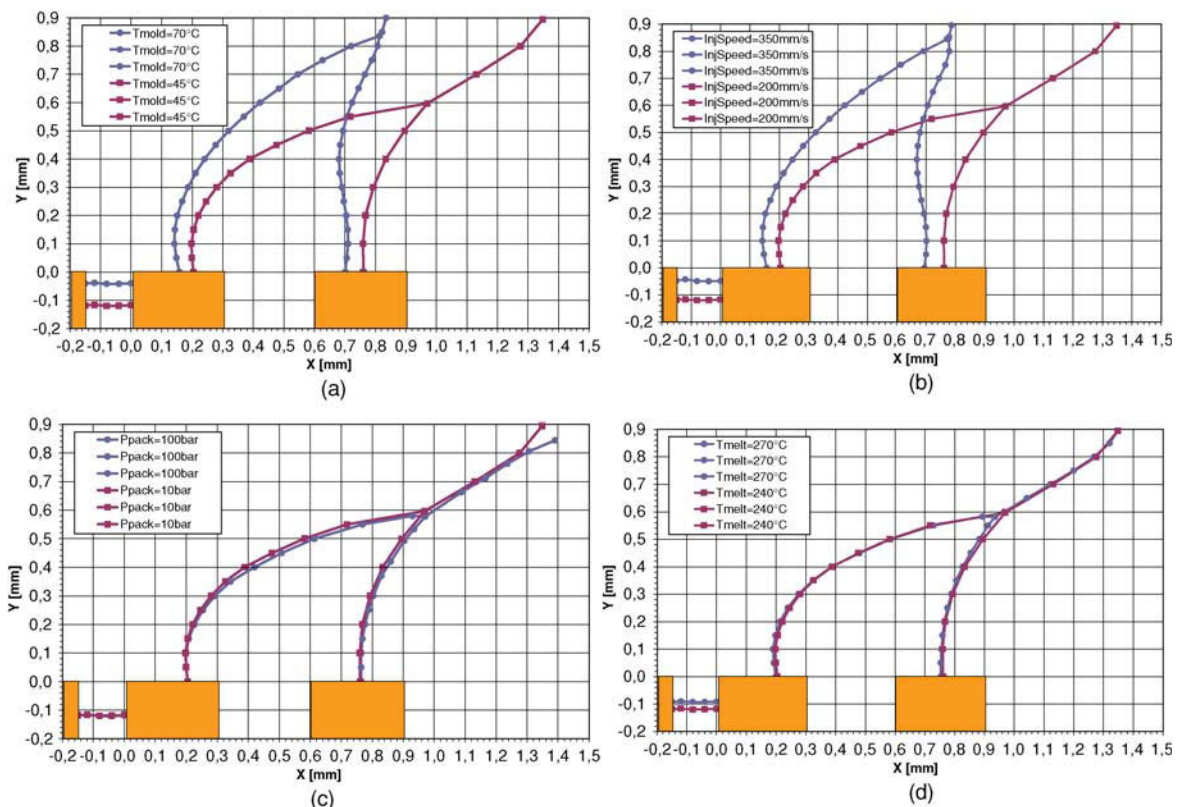


FIGURE 6-18 Effect of mold temperature (a), injection speed (b), packing pressure (c), and melt temperature (d) on the positions of weld lines shown in Figure 6-17 [8].

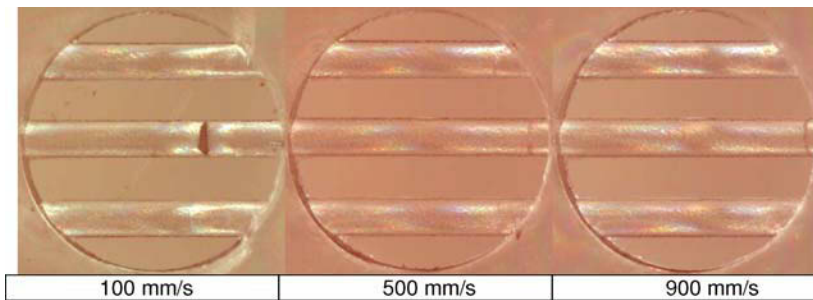


FIGURE 6-19 Injection molding of 300 μm wide micro-features: optical microscope images of the flow front position shift due to an increase of injection speed (injection direction from left to right, $T_{\text{melt}} = 220^\circ\text{C}$, $T_{\text{mold}} = 55^\circ\text{C}$) [8].

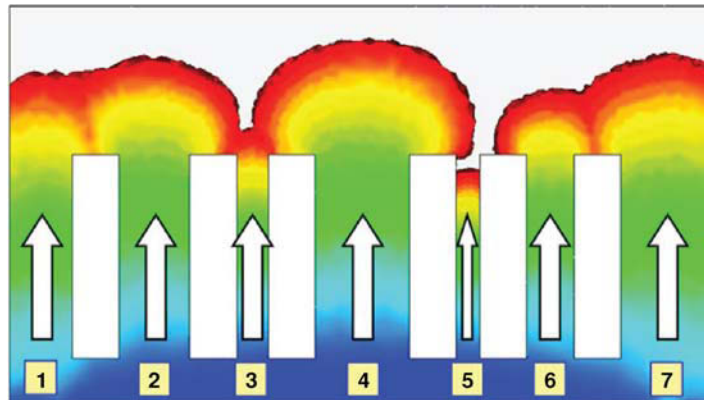


FIGURE 6-20 Simulated flow front pattern to be compared with weld lines used as flow markers [8].

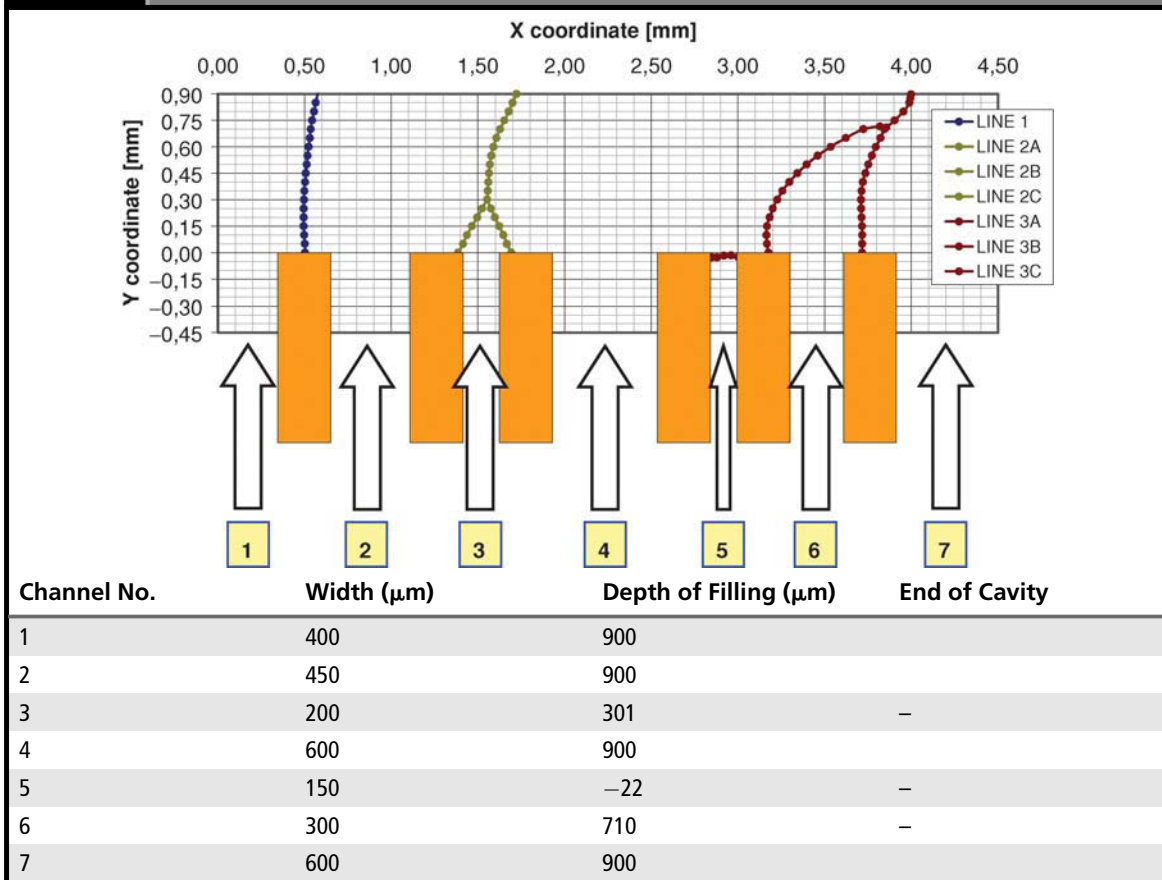
therefore obtained by using a high temperature of the mold (which decreases the viscosity of the melt and prevents premature solidification) and high injection speed (which also decreases the viscosity of the melt due to viscous thinning and viscous heating, as well as decreasing the injection time, thus avoiding premature short shots and incomplete filling). On the other hand, it is not convenient to increase the temperature of the melt, first due to the limited benefit on the filling performance, and second to avoid material degradation due to material overheating. An elevated packing pressure is also not advantageous because it can produce high internal tension on the polymer matrix as well as induce high stress on the mold itself.

Micro-injection Molding Process Control and Analysis

The reliable manufacturing of polymer-based micro-components on a mass production perspective is directly connected to the capability of controlling the micro-injection molding process. The influence of process parameters on μ -injection molding (μIM) can be investigated with a mold with a sensor applied at injection location. It can be used to monitor actual injection pressure and to determine the cavity filling time.

At the injection location where the melt is pushed into the cavity (see Figure 6-21, detail A) by the injection piston, a piezoelectric pressure sensor is usually placed (see Figure 6-21, detail B).

TABLE 6-1 Experimental Depth of Filling Depending on the Channel Width



The recording of the in-cavity pressure at injection location over time is one of the methods to monitor conventional and micro-injection molding processes. It allows comparative studies to be performed on different process conditions and evaluation of the process repeatability when molding under the same process conditions. Moreover, especially in the case of micro-molding, it is a powerful method to calculate the cavity filling time which would not be possible by other means, since filling of micro-cavities takes place in times in the order of tens of milliseconds.

The cavity pressure profile, in μIM as well as in precision injection molding, is a factor directly correlated to the quality of the part [20]. The cavity pressure control, expressed in terms of both

absolute value and repeatability (i.e. standard deviation), is fundamental for an optimized part and process realization and it is the critical process parameter for the precision molding of high accuracy thermoplastic parts [21] as micro-molded components. For example, an excessive value of the cavity pressure will lead to defects such as flashes (see Figure 6-22); whereas a large value of the standard deviation of the pressure indicates a poor cycle-to-cycle process repeatability (i.e. different filling conditions) and therefore different properties of the molded part.

Analysis of the cavity injection pressure shows that an increase of the temperature of the melt causes an increase of the cavity injection pressure. This is due to the fact that higher temperature

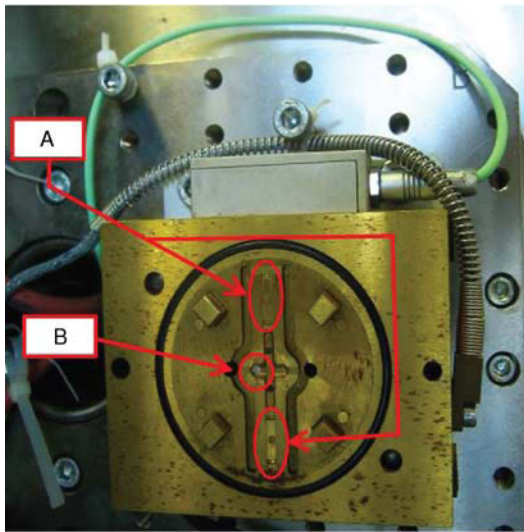


FIGURE 6-21 Two-micro-cavity mold (A) equipped with in-cavity pressure sensor at injection location (B) [8].

reduces the melt viscosity, which has as a consequence the reduction of the pressure drop through the nozzle and runners, resulting in higher cavity injection pressure. To attain higher injection speed, a higher injection pressure must be applied, which in turn increases the cavity injection pressure. The influence of the temperature is also of importance. At higher mold temperature,

close to the glass transition temperature of the polymer, the melt viscosity is decreased, which in turn reduces the pressure drop, resulting in a higher cavity injection pressure.

The cavity injection pressure cycle-to-cycle repeatability can provide a valuable parameter to determine the process stability. In micro-molding, a standard deviation in the order of 10–50 bar, which corresponded to a coefficient of variation between 1% and 5%, can be obtained.

The injection pressure rise at the injection location and the subsequent reaching of the maximum cavity pressure can be employed to determine the cavity injection time (see Figure 6-24) under different process conditions. Due to the very short filling time in micro-molding (of the order of a few tens of milliseconds), sampling rates of the order of 5–25 kHz are recommended to be employed. Experimental results show that an increase of both the temperature of the mold and of the injection speed lead to a shorter cavity injection time, with injection speed having the greatest influence. The cavity injection time can be used also to estimate the cycle-to-cycle repeatability of the micro-molding process. Standard deviation values in the range between 1 and 3 ms are usually encountered during micro-molding (which correspond to a coefficient of variation of below 1%).

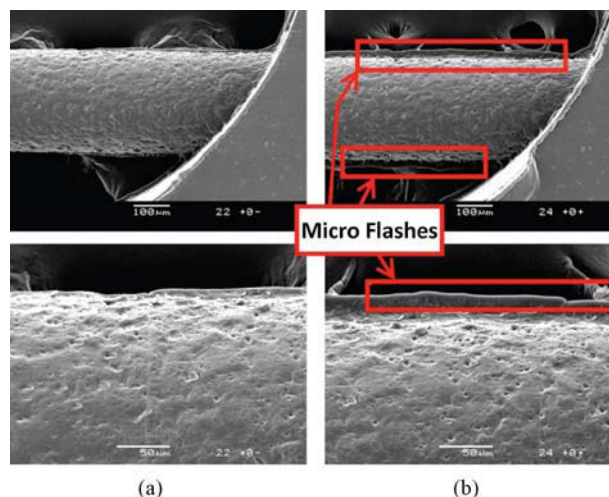


FIGURE 6-22 Effect of cavity injection pressure: micro-flashes do not occur at lower pressure (553 bar, (a)) and appear at higher pressure (778 bar, (b)). Melt temperature, mold temperature and injection speed were: (a) 260°C, 70°C, 100 mm/s and (b) 260°C, 70°C, 900 mm/s [8].

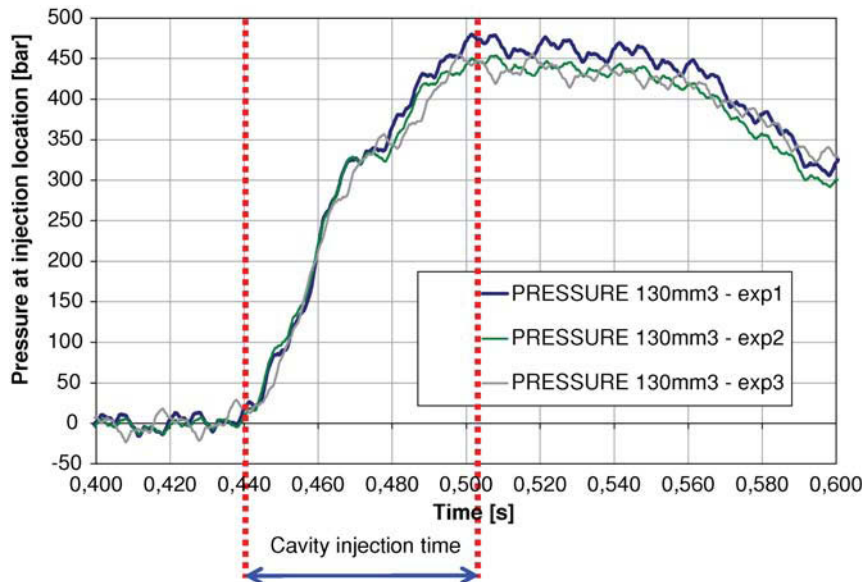


FIGURE 6-23 Cavity injection time determination from the cavity pressure vs. time plot [8].

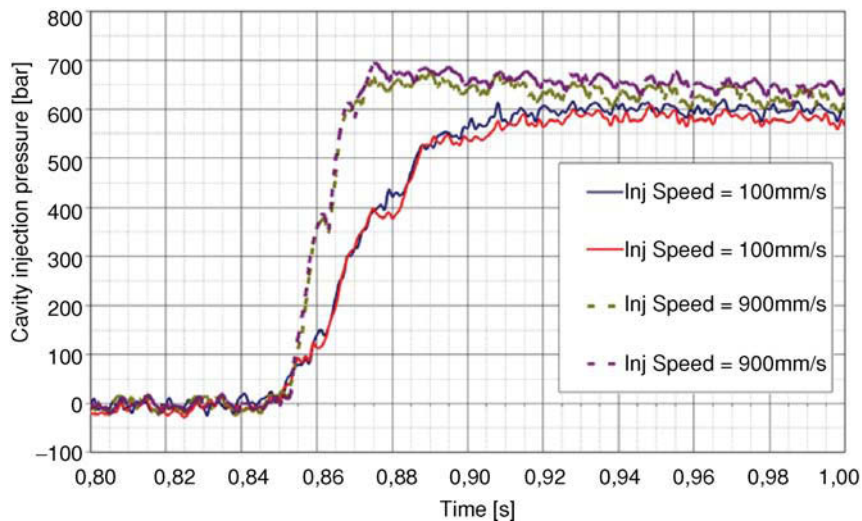


FIGURE 6-24 Pressure vs. time curves from the in-cavity sensor. Moldings at two different injection speeds (100 mm/s and 900 mm/s) are shown. Temperatures of the melt and of the mold were 220°C and 55°C, respectively. In the chart, two curves sampled from the same molding, carried out under the same processing conditions, are shown. The increase of the injection speed produced a decrease of the average cavity injection time from 67 ms to 30 ms and an increase of the average maximum cavity injection pressure from 612 bar to 672 bar [8].

DEFECTS OF MICRO-INJECTION MOLDED PARTS: WELD LINES

Weld lines are a reality of the injection molding of complex parts. Multiple gating, splitting of the melt flow due to inserts in the cavity or through-

holes, as well as changes of thickness give rise to points within the structure where the flowing fronts will recombine and weld. An imperfection is observed as a line on the surface of the molded part (see Figure 6-25). In the molding of very

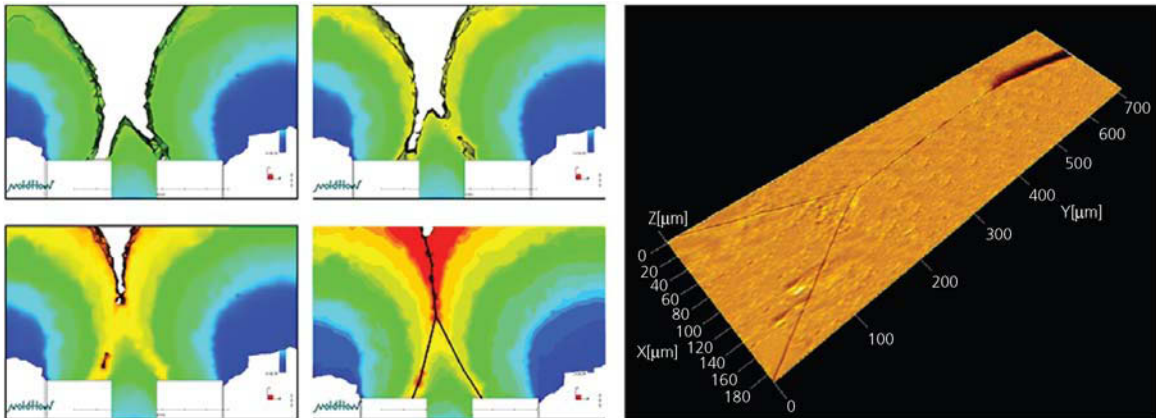


FIGURE 6-25 Simulation of the formation of a weld line due to the presence of two micro-features and the meeting of three melt flow fronts (left) and large-range AFM scanning of the actual meeting area on a polystyrene micro-molded part (right). The large range scanning of $700\ \mu\text{m} \times 200\ \mu\text{m}$ was obtained using a software tool for stitching three-dimensional surface topography data sets [20]: 18 different scanings $50\ \mu\text{m} \times 100\ \mu\text{m}$ were employed for the reconstruction [8].

complex components a multiplicity of weld lines is generated. The weld lines are formed as the mold is being filled. Weld lines reduce the mechanical strength of components in the macro- [22] as well as in the micro- [15] dimensional range. In particular, an area where the properties are different from the bulk is created. Weld-line factors (defined as the ratio between the strength of workpieces containing a weld line and workpieces with the same geometry but without weld lines) as low as 20% were found on micro-injection molded tensile strength specimens. The main causes are incomplete molecular entanglement or diffusion, the formation of V-notches at the weld surface, the presence of contamination of micro-voids at the weld-line interface, and unfavorable molecular or fiber orientation at the weld [15].

It is therefore of great importance to optimize the injection molding process, and especially the filling phase, in order to decrease such defects. In particular, injection speed and mold temperature set at a convenient level can be beneficial in order to decrease the depth and width of weld lines (see Figs. 6-29 to 6-31). A higher temperature of the mold allows a higher molecular mobility (i.e. lower viscosity) which permits obtaining of smaller weld lines. Higher injection speed causes a

decrease of the injection time, which has the consequence of avoiding premature freezing of the polymer melt, allowing higher mobility of the polymer at the interface melt front/mold surface. As a conclusion, higher temperature of the mold and higher injection speed are preferable when molding micro-components with polystyrene polymer grade in order to decrease the importance of weld lines.

Furthermore, the position of the gate with respect to a considered area of the part with weld lines is also important. In particular, the longer the flow length, the larger the weld lines that will form. Increase of width and depth of 30% were observed when measuring weld lines far from the gate compared with weld lines near to the gate. To this respect, multi-gating solutions can be employed to shorten the flow length along the part of the polymer melt during the filling of the cavity (see Figure 6-32).

PROCESS SIMULATION

Simulation programs in polymer replication micro-technology are applied with the same purposes as in conventional injection molding. To avoid the risks of costly re-engineering, the functions of the final products as well as

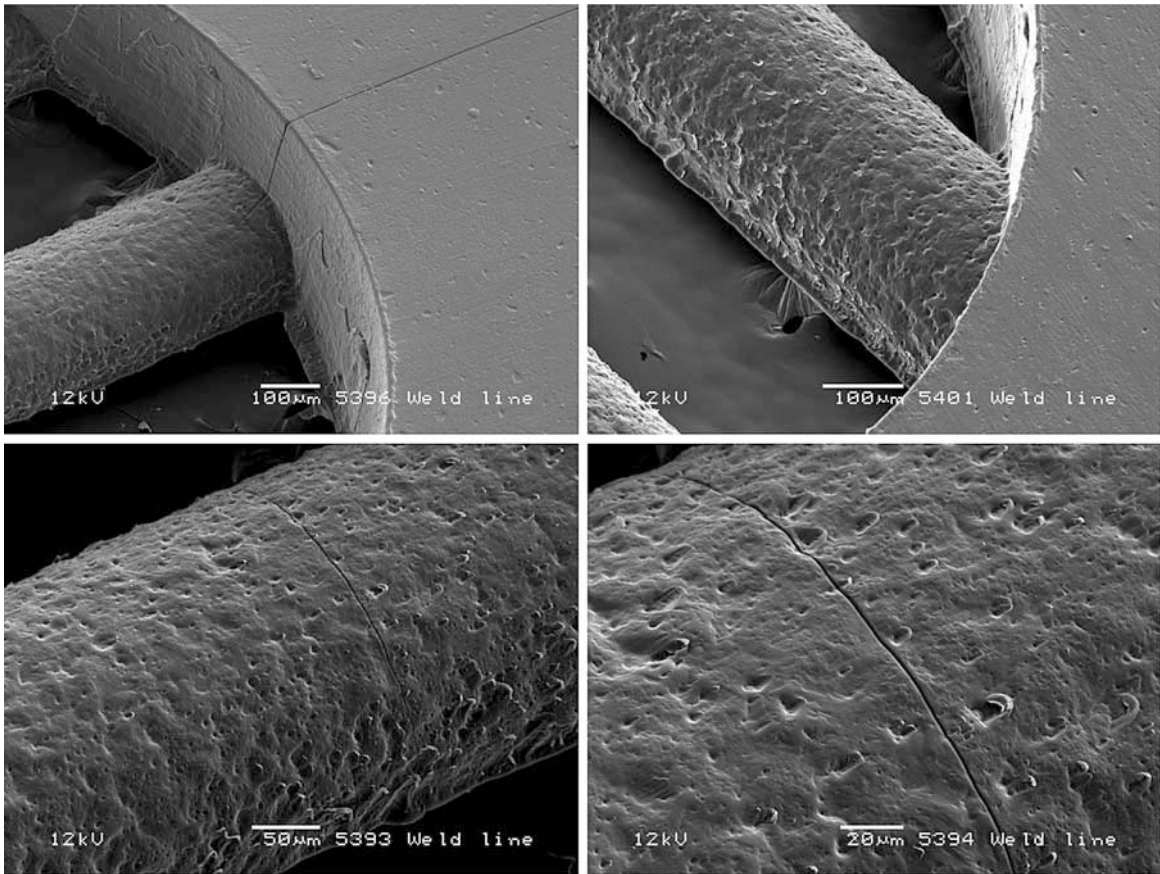


FIGURE 6-26 Scanning electron microscope (SEM) images of weld lines on the surface of the 300 µm wide micro-features [8].

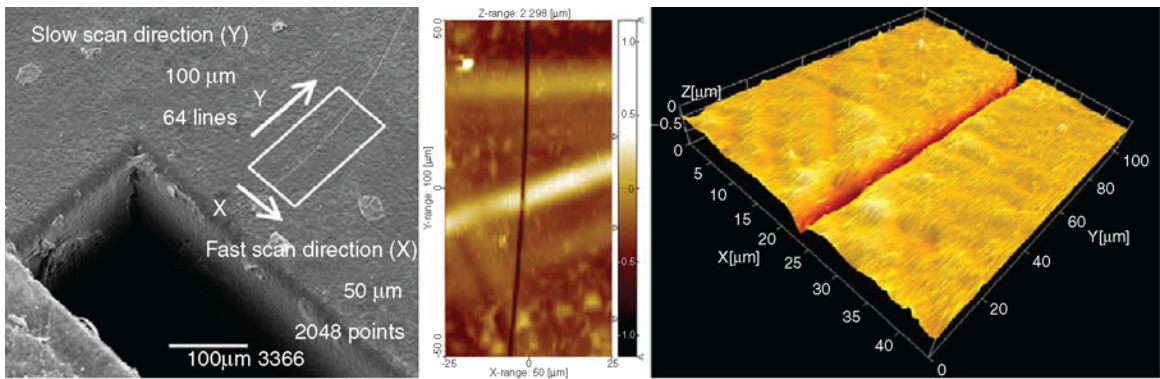


FIGURE 6-27 Atomic force microscope measurement of weld lines produced at the meeting area of two flow fronts [8].

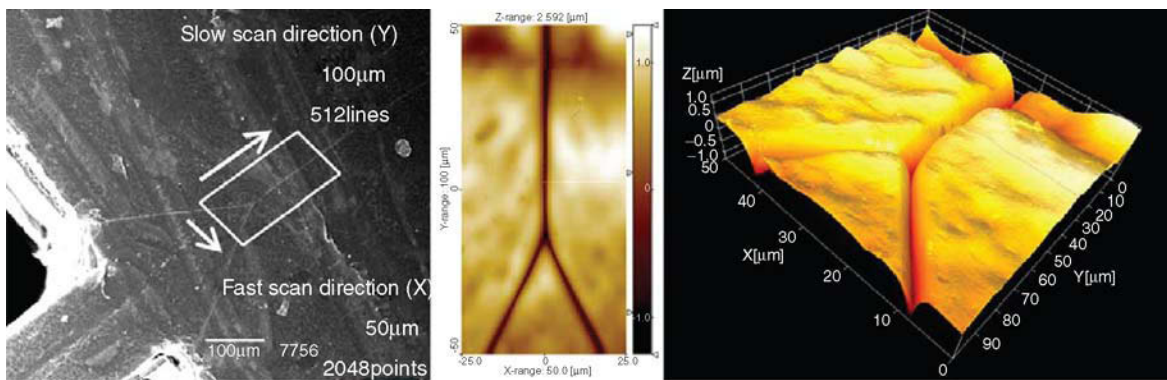


FIGURE 6-28 Atomic force microscope measurement of weld lines produced at the meeting area of three flow fronts [8].

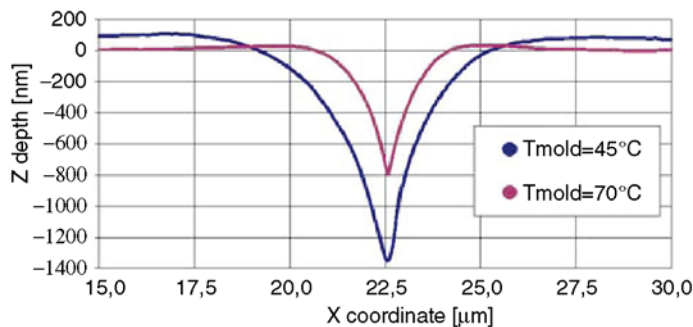


FIGURE 6-29 Effect of the temperature of the mold on the weld line profile [8].

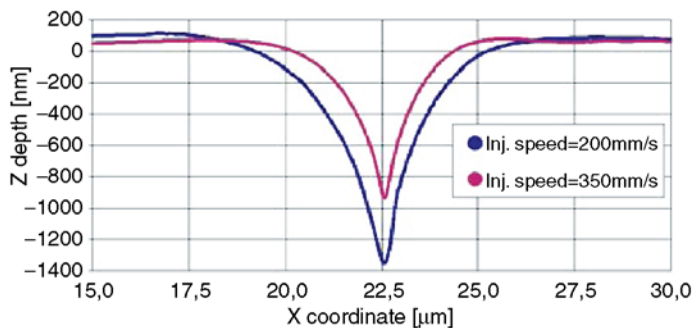


FIGURE 6-30 Effect of the injection speed on the weld line profile [8].

the manufacturing steps are simulated extensively before starting the actual manufacturing process: important economic factors are the optimization of the molding process and of the tool, using different simulation techniques.

In polymer micro-manufacturing technology, software simulation tools adapted from conventional injection molding can provide useful assistance for the optimization of molding tools, mold inserts, micro-component designs, and process parameters.

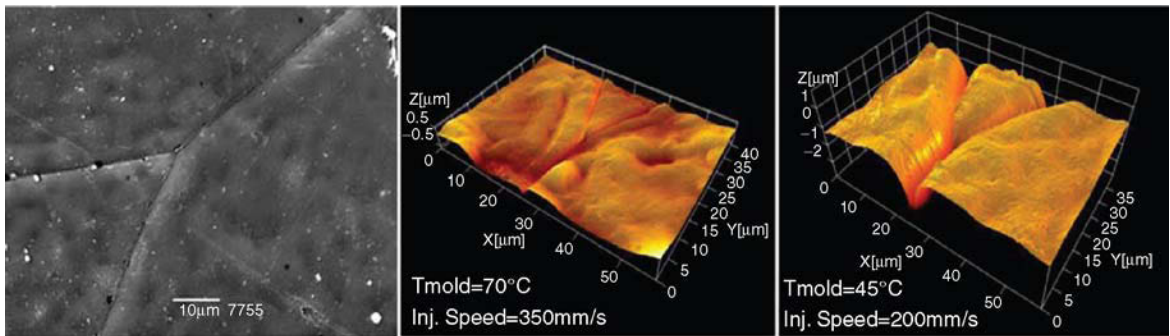


FIGURE 6-31 Three-dimensional visualization of the effect of temperature of the mold and of injection speed on weld line topography [8].

At present, commercially available simulation tools can work adequately from a qualitative point of view but numerical values cannot be calculated as precisely as necessary [25] and therefore simulation is not integrated in the product development process as extensively as for

macro-products. In addition to this, most programs have difficulties in simulating exactly the filling of micro-structures with high aspect ratio. The reason is that commercial software tools developed for macroscopic applications do not consider microscopic aspects properly.

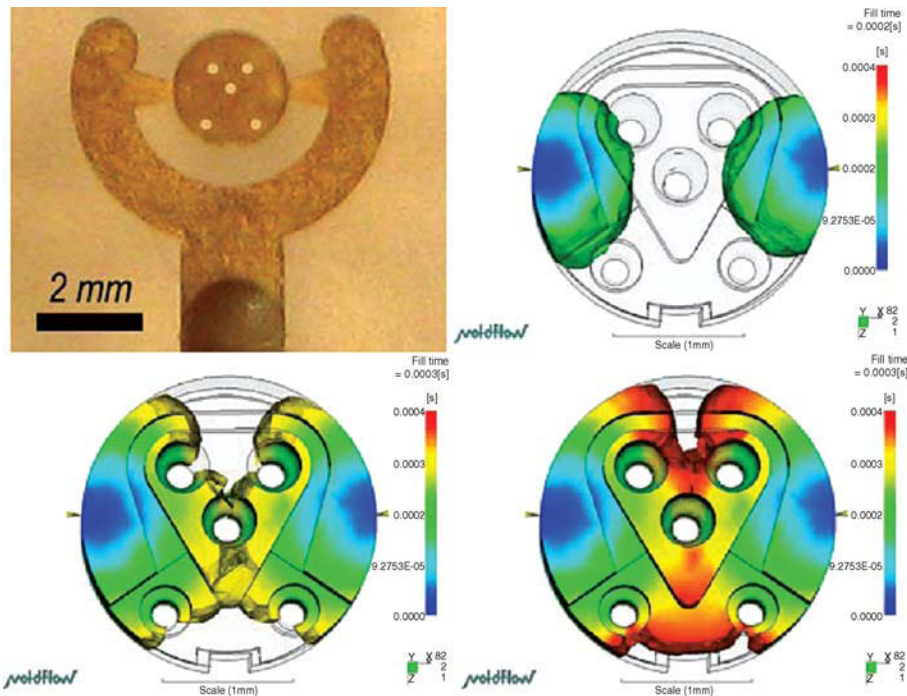


FIGURE 6-32 Multi-gating design of a polymer micro-product produced by injection molding (hole diameter is 300 μm) [8].

The main limitations encountered are related to the fact that the rheological data used in current packages are obtained from macroscopic experiments and that a no-slip boundary condition is employed, with the consequence that wall slip cannot be predicted [26]. Moreover, surface tension is not taken into account, but plays a role on the filling of micro-structures [27]. Usually a constant heat transfer coefficient (HTC) is assumed, but it cannot describe the flow through micro-channels [26, 28] and its standard value suitable for the simulation of macro-parts differs substantially from values indicated for μ IM [28–29]. Moreover, rheology data provided by the software's database are obtained at shear rates and pressures typical of capillary rheometers (i.e. over significantly lower ranges if compared with those of micro-molding), and therefore are not directly applicable and not suitable for micro-scale polymer flow applications.

However, a proper implementation strategy employed during the set-up of the simulation can improve the quality (i.e. the accuracy) of the simulated results. There are a number of aspects to be considered in order to improve existing software packages' results:

- **At the machine/software interface boundary:** the implementation of the actual injection speed profile during the filling stage of the cavity, the implementation of the actual cavity injection pressure profile developed during the filling stage, the use of the actual cavity injection time [27].
- **Concerning part modeling and meshing:** three-dimensional modeling of the whole molded component including sprue, runner, gate, part and micro-features, to consider the meshing tolerance compared to the actual dimensions of the micro-features and therefore using an element size down to at least a few tens of micrometers, to optimize meshing accuracy for high precision modeling of part and micro-features with surface and edge definition within at least 5 to 10 μm [19].
- **Regarding the material characterization:** the use of experimental micro-rheological data of the polymer material instead of the default rheology available in the software database, to use experimental data obtained with micro-sized cavities (see Figure 6-33) and high speed rheometry experiments (at higher shear rates of 10^6 1/s and higher) [8] [28].

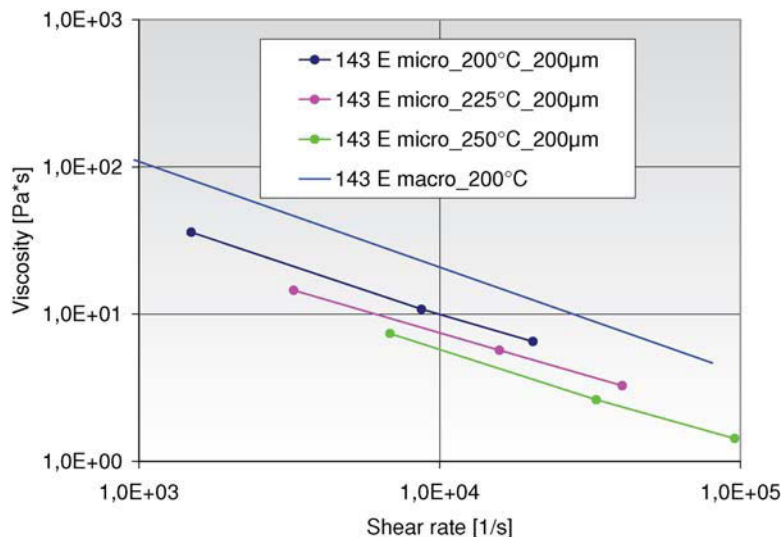


FIGURE 6-33 Polystyrene 143 E micro-rheology curves for a channel 200 μm wide at melt temperatures of 200°C, 225°C and 250°C and 143 E macro-rheology at 200°C (i.e. obtained with conventional capillary rheometer). Viscosity of polymer melt flowing in micro-channels is lower than in the macro-dimensional range due to the wall-slip effect [8].

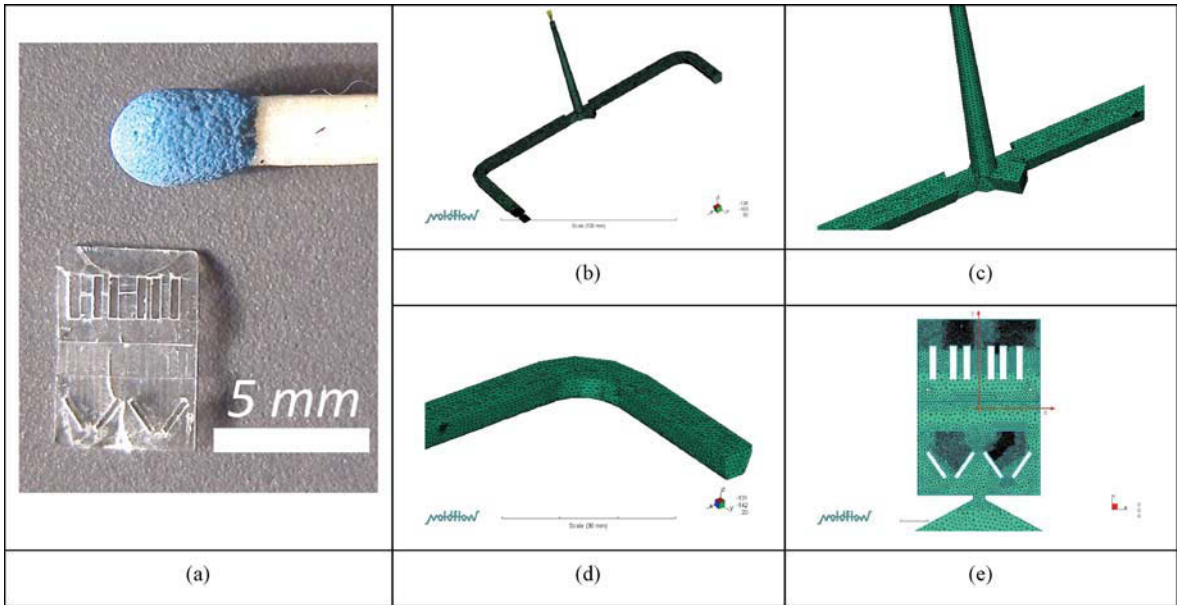


FIGURE 6-34 Micro-injection molded parts (a) (material = polystyrene) and complete three-dimensional meshing of the model (b), including: sprue (c), runner (d), gate and part (e) [8].

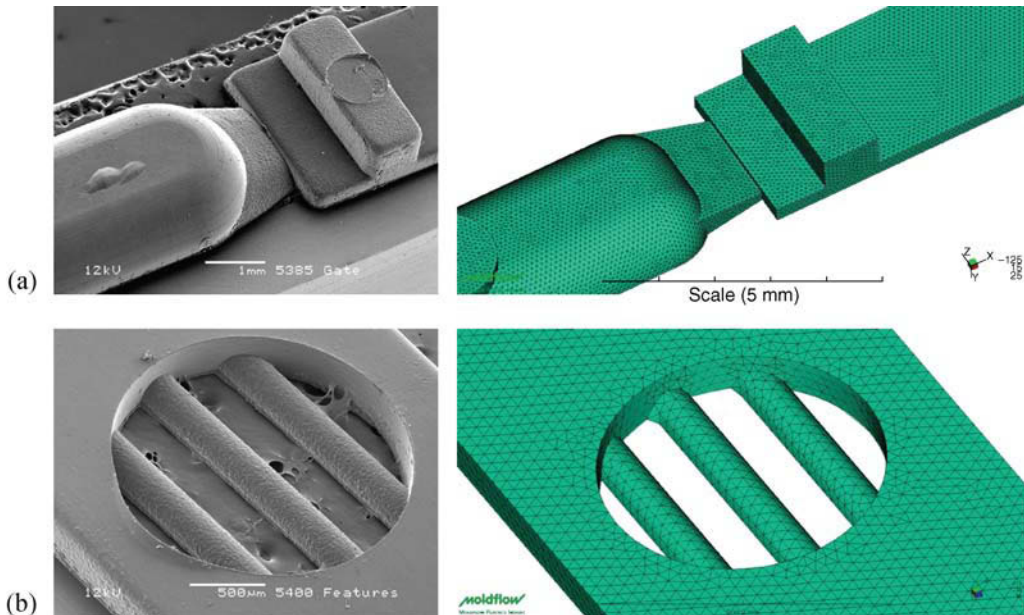


FIGURE 6-35 Accurate 3D meshing (right) of gate (a) and micro-features (b) (width = 300 μm) of micro-injection molded part (left) [8].

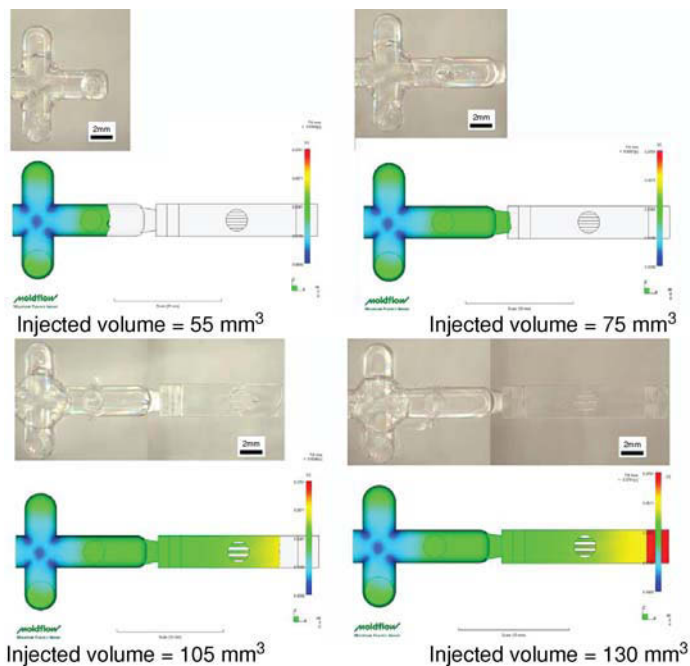


FIGURE 6-36 Experimental and simulated short shots method [8].

CONCLUSIONS

Micro-injection molding is recognized as a manufacturing process enabling the mass fabrication of polymer micro-components. Fundamental process parameters for the control of both the micro-product and the process are the temperature of the melt, the temperature of the mold, the injection speed, and the cavity injection pressure. Process simulation can be used for polymer micro-product and process design, and can provide at the present time mostly qualitative input to the designer and the process engineer. Further, process analysis methods and optimization tools are being used in order to provide reliable validation of both process and simulations.

REFERENCES

- [1] M. Hecke, W.K. Schomburg, Review on micro molding of thermoplastic polymers, *J. of Micromechanics and Microengineering* 14(3) (2004) R1–R14.
- [2] L.-S. Turng, Special and emerging injection molding processes, *J. of Injection Molding Technology* 5(3) (2001) 160–179.
- [3] B.R. Whiteside, M.T. Martyn, P.D. Coates, Introduction to Micromolding, *Precision Injection Moulding*, Greener, J., and Wimberger-Friedl, R. (eds.) (2006) Hanser, Munich, Germany 239–264.
- [4] M. Ganz, Micro Injection Moulding and Compression Moulding, Workshop at the 1st International Conference on Multi-Material Micro Manufacture (4M): Polymer Technology toward Nano, future technology for Europe, Karlsruhe (Germany) (June 29–July 1, 2005).
- [5] V. Piottter, W. Bauer, T. Benzler, A. Emde, Injection molding of components for microsystems, *Microsystem Technologies* 7(3) (2001) 99–102.
- [6] W. Michaeli, A. Spennemann, R. Gärtner, New plastification concepts for micro injection moulding, *Proceedings of the Conference of Micro System Technologies* 8 (2002) 55–57.
- [7] W. Michaeli, A. Spennemann, Micro injection moulding – improving the efficiency of a classical processing technology, *Proceedings of International Conference on Microtechnologies: MICRO.tec 2000* 2 (2000) 593–596.
- [8] G. Tosello, Precision moulding of polymer micro components, PhD thesis, Department of Mechanical Engineering, Technical University of Denmark, ISBN 978-87-89502-77-9 (2008).
- [9] S.Y. Yang, S.C. Nian, I.C. Sun, Flow visualization of filling process during micro-injection molding,

- International Polymer Processing 17(4) (2002) 354–360.
- [10] X. Han, H. Yokoi, Visualization analysis of the filling behaviour of melt into microscale V-groove during the filling stage of injection molding, *Polymer Engineering and Science* 46(11) (2006) 1590–1597.
- [11] B.R. Whiteside, R. Spares and P.D. Coates, Rheological measurements in micromoulding, Society of Plastics Engineers – 67th Annual Technical Conference (ANTEC2009), Chicago (Illinois, USA) (22–26 June 2009) 1803–1810.
- [12] B. Sha, S. Dimov, C. Griffiths, M.S. Packianather, Micro-injection moulding: factors affecting the achievable aspect ratios, *Int. J. of Advanced Manufacturing Technology* 33 (2007) 147–156.
- [13] C.H. Wu, W.J. Liang, Effect of geometry and injection-molding parameters on weld line strength, *Polymer Engineering and Science* 45(7) (2005) 1021–1030.
- [14] S. Fellahi, A. Meddad, B. Fisa, B.D. Favis, Weld lines in injection molded parts: a review, *Advances in Polymer Technology* 14(3) (1995) 169–195.
- [15] G. Tosello, A. Gava, H.N. Hansen, G. Lucchetta, F. Marinello, Micro-nano integrated manufacturing metrology for the characterization of micro injection moulded parts, 7th International Conference of the European Society for Precision Engineering and Nanotechnology (Euspen), Bremen (Germany) (May 20–24, 2007) 377–380.
- [16] G. Tosello, A. Gava, H.N. Hansen, G. Lucchetta, Study of process parameters effect on the filling phase of micro injection moulding using weld lines as flow markers, *Journal of Advanced Manufacturing Technology* DOI: 10.1007/ s00170-009-2100-1 (2010) 81–97.
- [17] A.E. Varela, Self-tuning pressure control in an injection moulding cavity during filling, *Chemical Engineering Research and Design – Trans IChemE* 8:A (2000) 79–86.
- [18] D. Kazmer, P. Barkan, The process capability of multi-cavity pressure control for the injection molding process, *Polymer Engineering and Science* 37(11) (1997) 1880–1895.
- [19] G. Tosello, A. Schoth, H.N. Hansen, Implementation strategies for the optimization of micro injection moulding simulations, 4th International Conference on Multi-Material Micro Manufacture (4M2008), Cardiff (United Kingdom) (September 9–11, 2008) 271–274.
- [20] F. Marinello, P. Bariani, L. De Chiffre, H.N. Hansen, Development and analysis of a software tool for stitching three dimensional surface topography data sets, *Measurement Science and Technology* 18 (2007) 1404–1412.
- [21] G. Tosello, A. Gava, H.N. Hansen, G. Lucchetta, F. Marinello, Characterization and analysis of weld lines on micro injection moulded parts using Atomic Force Microscopy (AFM), *Wear* 266 (5–6) (2009) (Metrology and Properties of Engineering Surfaces) 534–538.
- [22] V. Piottter, K. Mueller, K. Plewa, R. Ruprecht, J. Hauselt, Performance and simulation of thermoplastic micro injection molding, *Microsystem Technologies* 8 (2002) 387–390.
- [23] O. Kemann, L. Weber, C. Jeggy, O. Magotte, F. Dupret, Simulation of the micro injection moulding process, SPE-ANTEC Tech. Papers (2000).
- [24] W. Cao, O. Hassager, Y. Wang, Surface tension effect on micro injection molding, *Polymer Processing Society (PPS) 24th Annual Meeting Proceedings* S08 (2008) 141.
- [25] L. Yu, Experimental and numerical analysis of injection moulding with microfeatures, PhD thesis, Ohio University (2004).
- [26] A. Gava, G. Tosello, G. Lucchetta, H.N. Hansen, M. Salvador, A new approach for the validation of filling simulations in micro injection moulding, *Proceedings of 9th International Conference on Numerical Methods in Industrial Forming Processes (NUMIFORM)* (2007) 307–312.
- [27] G. Tosello, A. Gava, H.N. Hansen, H. Reinecke, G. Lucchetta, A. Schoth, Influence of different process settings conditions on the accuracy of micro injection molding simulations: an experimental validation, Society of Plastics Engineers – 67th Annual Technical Conference (ANTEC 2009), Chicago (Illinois, USA) (22–26 June 2009) 787–1793.
- [28] R.D. Chien, W.R. Jong, S.C. Chen, Study on the rheological behaviour of polymer melt flowing through micro-channels considering the wall-slip effect, *J. of Micromechanics and Microengineering* 15(8) (2005) 1389–1396.

Micro-Bulk-Forming

*Mogens Arentoft, Rasmus Solmer Eriksen
and Hans Nørgaard Hansen*

INTRODUCTION

Forming of metals is a well-established process, dating back more than a thousand years. During the early colonization in Europe, the village blacksmith formed fittings and weapons using hammer, anvil and forge.

The idea of plastically deforming metals into a desired shape makes good use of the material and can even enhance the performance of the material [1, 2]. In the ancient Asian cultures the forging of the Samurai sword was considered to be a black art. By forging steel alloys with different carbon content into a sword blade, it was possible to combine the ductility of low carbon steel with the hardness of high carbon steel into a blade which was both flexible and sharp. The subsequent heat treatment of the sword blade included the addition of a mixture of water and clay to the cutting edge of the blade in order to reduce the cooling gradient in this area. Only by mastering the craftsmanship of forming, and using his knowledge of materials and empirical skills for the hardening procedure, was the Samurai sword maker able to make the ultimate weapon [3].

BASIC COLD FORMING PROCESSES

Today bulk forming is used extensively in a wide range of industrial applications. Within the production of transmission elements for the automotive industry, the bulk forming process is the standard. Huge tonnages of rack, axles and other components are manufactured by the bulk forming process, either into near-net components that

subsequently undergo light machining or net shape components which are finished after the forming process.

A typical forming process requires multiple forming steps and comes in a wide range of variants. Each of the variants can, however, be categorized into the eight basic bulk forming operations depicted in Fig. 7-1.

The industrial popularity of the bulk forming process still relies on the underlying theory of material flow and behavior, something that has not changed since the early days of forging. Even with the employment of numerical simulation and modern computer aided design systems, a well-functioning bulk forming system requires extensive knowledge of the strain hardening of the material and its flow behavior as well as of friction and lubrication conditions (tribology). These parameters generally dictate the forming limits of the bulk forming process and thereby also the achievable geometry of the components.

A medium advanced bulk forming process often consists of 3–5 consecutive forming steps, either mounted in the same press system or as individual operations. This means that a typical bulk forming process actually is a process chain of several forming operations, each carefully designed and analyzed to arrive at the best possible end result for the finished component.

Micro-bulk forming is the utilization of the bulk forming process to form micro-components. Compared to more traditional micro-manufacturing processes, such as turning and milling, this process holds the potential of producing high quality

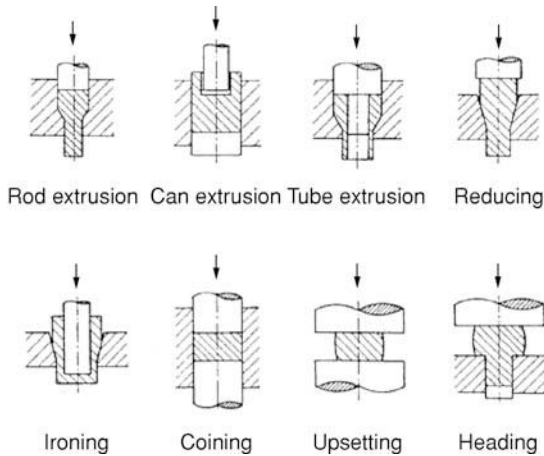


FIGURE 7-1 Basic cold forging processes [4].

components, faster and with no or only little material waste.

THE SIZE EFFECT

By definition, a micro-component is a component with one or more geometrical dimensions or functional features of less than one millimeter in size [5]. By decreasing the size of the components in small mechanical systems, the weight and volume of the device can be reduced without sacrificing functionality, and often the micro-component technology is the enabler of a new miniaturized product. Micro-components are often a central part of the mechanical systems in consumer products such as hearing aids, computer drives or mobile phones. The medical sector is another important application for micro-components. Here the components are used as parts of dental implants, in spine fracture repair kits or as elements in drug delivery systems. These applications often require low failure rate in combination with high functionality; giving rise to strict quality and tolerance requirements on the components making up the system. It is not uncommon to see 100% inspection rate requirements for these types of components, something that is incompatible with mass production at low cost.

Size effect is a term for the deviation from the linear continuum theory, when the scale is

reduced to micro-size. That is, when the scale is reduced to the micro-level, some of the rules change and a new set of theories have to be applied. Or putting it in another way, when the size on the component is within orders of magnitude of the physical elements of the process, e.g. material grain size, the linear theory of the macro-domain breaks down [6].

The contributors to size effects can be put into three groups: density, shape and structural effects.

Density effects relate to the inhomogeneity of materials at small scale. If the average grain size of a material is considered to be of the order of $40\ \mu\text{m}$, a macro-size component would contain millions of grains, meaning that the material could be modeled as homogeneous. Going to the micro-domain, a $500\ \mu\text{m}$ feature would only contain about 12 grains over the cross-section, resulting in the properties of the individual grains influencing the forming process.

Shape effects are closely related to the surface-to-volume ratio of the component. Consider a dice with a scalable side length of α . The volume then scales with the third power α^3 , whereas the surface area scales to the second power α^2 , meaning that a small component will have a higher surface-to-volume ratio, by α , when compared to its larger equivalent. The surface-to-volume ratio is an important parameter when considering an ejection or handling situation, where the friction is a factor of the component surface area and the component strength is related to the material volume. Designing an ejector system to remove a micro-component from the forming die is challenging, due to the risk of collapse or reverse forming during ejection. Further, small components are prone to the sticking effect, where adhesive forces between the gripper and the component outweigh gravitational forces. These adhesive forces primarily consist of surface tensions, van der Waals, and electrostatic forces, and can be the limiting factor of a handling system for micro-components.

The third effect contributing to the size effect is the group of micro-structural effects. This group of effects is made of physical elements which either experience a physical length limitation,

where it is not practical to scale the micro-geometry or where secondary scaling effects come into play. Surface roughness is an example of a quantity that, in practice, is not fully scalable. The roughness topography of a tool is often an inherent property of the manufacturing process and is only scalable within a certain window, resulting in higher relative roughness at smaller size.

Manufacturing tolerance is another important property prone to the size effect. High precision tooling machines are costly with an approximately exponential correlation between achievable precision and machine cost. However, the machine precision is independent of workpiece size and is strictly bound to the precision of the tooling machine itself. However, when the overall size of the component is reduced to the millimeter scale, it is seldom acceptable to inherit the tolerance band of the macro-scale, which is normally within a few orders of magnitude of a millimeter.

Figure 7-2 depicts prominent scaling effects affecting the micro-forming process; the boundary roughness characteristics, the fixed tolerances inherited from the tool manufacturing process, the grain size determined by the physics of

metallurgy and the geometrical non-linearity of the surface/volume ratio.

WORKPIECE MATERIALS

Material knowledge is central for the bulk forming process, which fundamentally relies on differences in flow stress between two materials. These two materials are often termed ‘workpiece material’ and ‘tooling material’, relating to their respective functional purpose in the bulk forming process. Properties such as price, flow stress, ductility and strain hardening are important for the forming material, whereas the yield strength, machinability and ductility are performance parameters for the tool material.

In order to accurately analyze and simulate the forming process, workpiece material data are needed. These data can be acquired by performing an upsetting test, where the mechanical strain/stress curve of the material can be acquired using length and force transducers connected to a data acquisition device. The resulting data can be fed into a numerical simulation program and the forming process can be simulated.

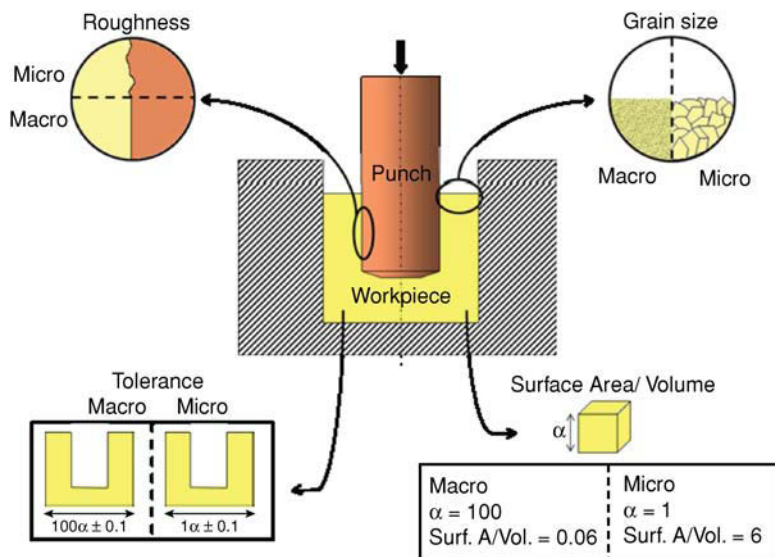


FIGURE 7-2 Overview of dominant size effects in micro-bulk forming, the influence of roughness scaling, grain size scaling, tolerance scaling the non-linear scaling for surface-to-volume ratio.

The selection of workpiece material is normally a trade-off between requirements set by the component application and formability performance. Materials with a high strength are generally desirable, leading to lower mass and a more compact design; however, these materials are often difficult to form in a bulk forming process. On the other hand, a soft material is easier to extrude or form but the strength of the finished component is often not adequate for high performance applications. The choice of workpiece material further influences tool life expectancy, forming temperature, the choice of lubricant, coating and the number of forming operations required.

Amorphous Metals

Amorphous metals are a new range of non-crystalline materials with interesting properties for manufacturing of micro-metallic components. The amorphous structure of the materials is generally realized by combining alloying metallic elements of considerably different atom sizes with rapid cooling when transitioning from the liquid to the solid phase. By rapid cooling the alloy is frozen in the amorphous state, thereby not allowing the metallic atoms to combine into the well-known lattice structure characterizing conventional metals. The required critical cooling rate generally sets limits on the achievable forms in which amorphous metals can be realized, typically thin ribbons, foils and wires. However, recent development has enabled the casting of amorphous metals with dimensions exceeding one millimeter: these are known as bulk metallic glasses.

Bulk metallic glasses are interesting for the forming of micro-components because the material is not subject to the grain size forming limitations, dislocations and sliding planes of normal crystalline materials and can be formed at the micrometer scale with good results. The forming of bulk metallic glasses takes place between the glass transition temperature T_g and the crystallization temperature T_x . At T_g the BMG becomes a super-cooled viscous liquid exhibiting decreasing

flow stress with increasing temperature. A second dependent parameter of the forming temperature is the crystallization time t_{cryst} , at which the amorphous structure is lost and the material turns crystalline. There is a time/flow stress trade-off when selecting the forming temperature; a higher temperature equals low flow stress and low viscosity but limited forming time due to the decreasing crystallization time. On the other hand, a lower forming temperature results in increased flow stress and viscosity of the BMG, resulting in longer process time and increased tool loads, whereas the window of amorphous processing time increases.

Further, BMG materials are generally very strain rate dependent and fast processing results in high flow stresses. It has been claimed that BMG above the glass transition temperature behaves like asphalt on a summer's day, since the viscosity of both BMG and asphalt is strongly dependent on temperature and strain rate. Figure 7-3 depicts the flow stress dependency of Mg60Cu30Y10 bulk amorphous alloy in comparison to a conventional crystalline magnesium–aluminum alloy.

Figure 7-4 depicts a micro-component formed by bulk forming in BMG and a soft aluminum alloy. By comparison it is observed that there is better form filling in the case of the BMG material (a) even though the forming process is not fully completed. As marked by the arrows, the outer rim of the component is subject to rounding in the case of the aluminum material whereas the BMG case exhibits sharp edges.

The forming of BMG material is not trivial and remains a topic of research [7, 8]. Some of the issues yet to be solved relate to fracture strength and high temperature tool development. Low temperature BMG, with a glass transition temperature below 200°C, is brittle with fracture strength as low as 500 MPa and may easily fracture during ejection or use. Zirconium and iron-based BMGs are formed at between 360 and 600°C and have a higher yield and fracture strength, but here the design of the tooling set-up becomes challenging due to the high temperature that gives rise to

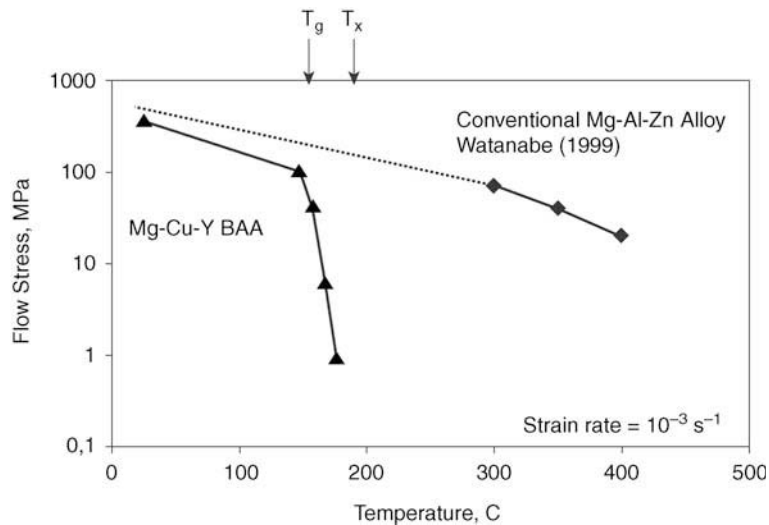


FIGURE 7-3 Flow stress for Mg60Cu30Y10 bulk amorphous alloy.

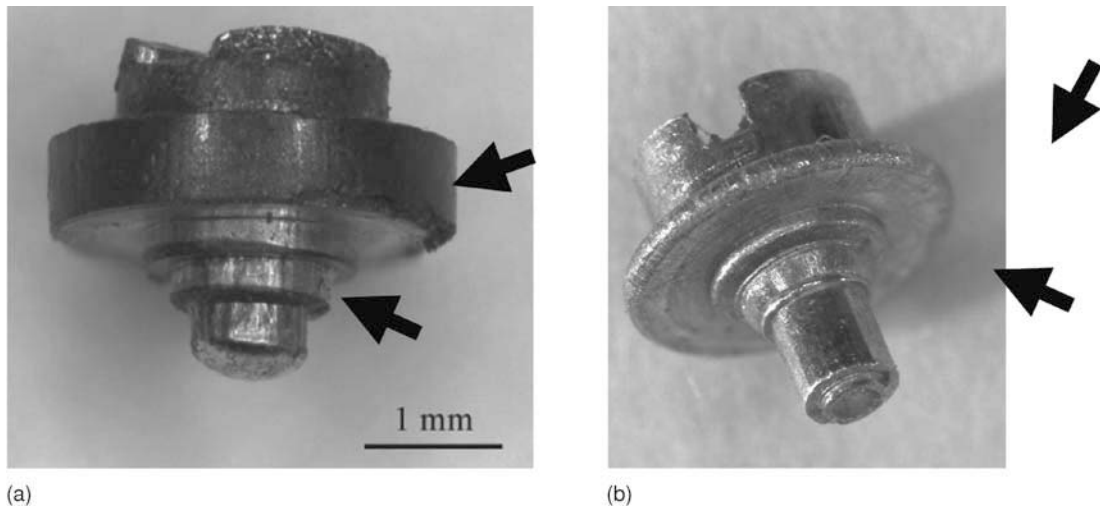


FIGURE 7-4 Side-by-side comparison of a potentiometer axle for a hearing aid bulk formed in: BMG Mg60Cu30Y10 (a); and in an annealed aluminum EN AW-6060 (b).

thermal deflection, oxidation and lubrication breakdown.

TOOL MATERIALS

The most dominant tool steels for bulk forming tools are state-of-the-art powder metallurgical steels with high toughness, hardness and metallurgical homogeneity. Due to the high surface pressures

involved in bulk forming, a tool material hardness of greater than 50 HRC is normally required. The tool steels used to be cut in their soft state and subsequently heat treated to their maximum hardness and ultimately polished or surface treated. However, modern tooling machines can directly cut hardened steel, allowing for better tolerances of the finished tool by avoiding the inevitable geometrical deflections arising during heat treatment.

In micro-bulk forming the geometrical tolerances of the tool are very narrow and deflections of the tool during heat treatment often exceed the total allowable tolerance deviation of the tool. Thus tooling materials for micro-bulk forming need to be hardened already from bulk and will be machined in their hard state using grinding, hard micro-milling or electro discharge machining. Owing to the small size of the tools it can be time and cost effective to use known prefab elements such as standard industrial punch needles or bushings as a starting point for a bulk forming tool, as these ISO standardized machine elements are cost effective, easy to source and have the mechanical properties required.

Hard metal, ceramics or solid tungsten carbide materials are other options for tooling materials. The cost of these materials is often much higher than traditional tool steel but since the amount of material used for a micro-bulk forming die is small, the solid tungsten carbide can be an economically viable tool material. The benefits of using tungsten carbide as tool material are the increased hardness of 62–70 HRC and a very low elasticity. The drawbacks of using tungsten carbide are the limited available machining processes, normally only electrical discharge machining, and the low tensile fracture strength of the material (as low as 400 MPa). Especially, the presence of tensile hub stress is unwanted for hard metal dies because of the crack initiation risk. With a correctly dimensioned pre-stress system, in the form of conical stress rings, it is possible to superimpose compressive stresses onto the hard metal forming die. As a result, the stress rings counteract the tensile stresses arising from the forming process, thereby eliminating any effective tensile stresses on the hard metal die. This is also touched upon in the next section dealing with machine and tool design.

MACHINE AND TOOL DESIGN

The design and manufacturing of machine and tooling elements play an important role in the overall performance of a micro-bulk forming process. Ideally the machine should scale accordingly,

meaning that the micro-bulk forming could take place on small mobile table-top machines. This vision has been proposed by several researchers as the factory lines of the future. In order to realize this vision, several technologies have to work together to form a fully working micro-bulk forming plant, from raw material to the final component.

Billet Preparation

Workpiece material is delivered in bulk, typically as rods. These have to be split into billets with the right volume for the subsequent bulk forming operation. A straightforward way to split the bulk material is by machining. This is, however, not very appealing for the reasons of cost and time. Rightfully, a claim could be made that if the billets have to be machined, the whole component should be finished when the part is in the cutting machine.

By cropping billets from rods the machining operation is avoided. Cropping is a process where the bulk material rod is divided into smaller pieces by a static and a moving cutting edge. Cropping is not a high precision process and some volume deviation is to be expected between the final billets. An investigation of the cropping quality of an Ø1.9 mm aluminum rod has been made and the results are depicted in Fig. 7-5 [9]. It is clear that the cut in Fig. 7-5(b) exhibits only little scatter in volume among the cut billets due to the high quality cut. It was further found that the billet was geometrically deformed in the high speed cutting scenario, where the faces of the cutting dies move with speeds exceeding 10 m/s, Fig. 7-5(c).

It was further found that cropping is a fast and inexpensive way of manufacturing billets for micro-bulk forming. The best results are achieved using a cropping process where the bulk material is kept under axial stress, close to the yield strength of the material, while the billet is sheared from the bulk.

Press System

Conventional macro-size hydraulic or excenter presses are not suitable for micro-bulk forming processes due to their size, and their low load

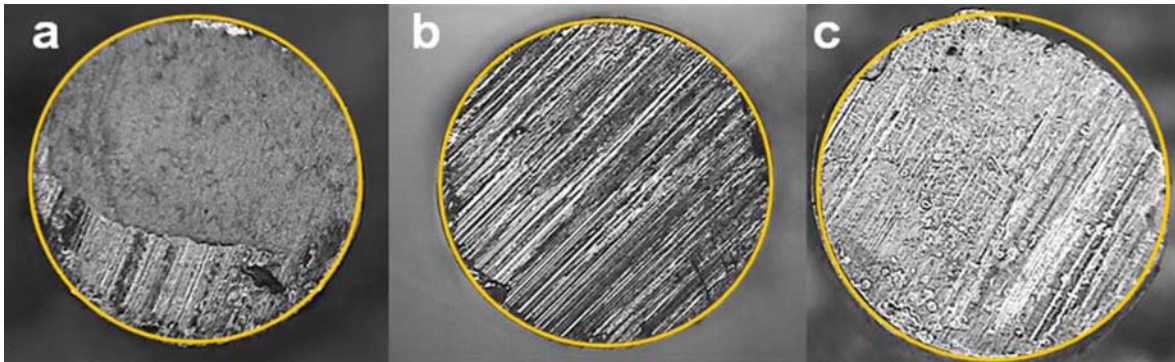


FIGURE 7-5 Cropping quality comparison of an $\text{\O}1.9$ mm aluminum rod with three different cropping scenarios. (a) conventional cropping, (b) cropping under hydrostatic pressure and (c) high speed cropping.

control capability. Bulk forming of high quality components requires high stiffness of the press frame, high speed and good load and position control of the press. The load requirements often range between 5 and 30 kN, depending on the component and the material. With these requirements in mind a number of micro-bulk forming press systems have been built [9–11]. By using a servomotor as the actuator for the press movement, the required speed and force can be delivered while maintaining good control over the position of the press axis. The actuator itself can be a direct drive linear motor, where a linear rod is moved by the magnetic field of surrounding coils. This solution offers very high speeds and accelerations of up to 40G while having a peak force output at about 0.5 kN. Another commonly used set-up is a configuration with a nut and roller screw driven by a servomotor, through a gearbox. The roller screw solution is capable of positioning to within a few micrometers while delivering high loads at moderate speed. The press frame should be designed for high stiffness in order to minimize elastic deflections of the frame and the consequent positional inaccuracy and lateral deflections. The press frame system is normally not prestressed, as deflections can be kept within tolerable limits.

The Tool Die System

Due to the required precision on tooling elements and the machine in general, manufacturing process chain design decisions will have to be

made in order to keep tolerances within acceptable limits. Examples of such process chain design decisions include machining several tooling elements in the same run, thereby eliminating inaccuracies arising from fixation and long-term deflections of the tooling machine.

Precision and Alignment of Tooling Elements

In general the precision requirements of a tooling system for micro-bulk forming can be divided into precision issues relating to the precision of the individual tooling element, such as the die and the punch, and the precision of the relative alignment of the individual parts, relating to the framework of the tooling system.

Achieving the required tolerances on the individual tooling parts is relatively easily done by an appropriate choice of tooling machine and process chain. Here high speed milling and turning, and electro discharge machining (EDM), are processes of choice. These processes can work directly in hardened material and can achieve good precision down to about $5\ \mu\text{m}$. With subsequent surface treatment such as polishing or micro-spraying, high quality tooling components can be achieved with a short lead time and at low cost.

When considering the alignment of the individual tooling elements, there are a number of approaches to achieving the alignment of the tooling parts. The straightforward way of ensuring the alignment of tooling elements is by a

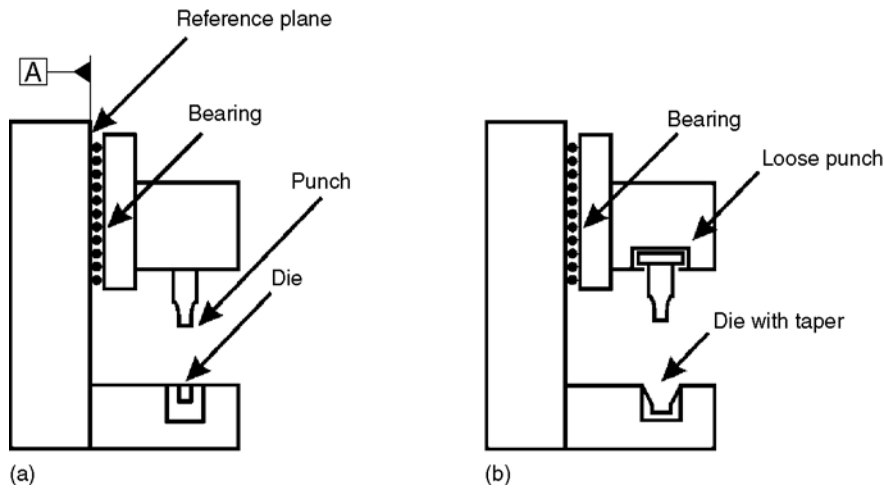


FIGURE 7-6 (a) Example of a bulk forming set-up where the back-plate is used as a reference for the tooling elements. (b) A die with a tapered inlet and a flexible punch fixture is used to form a self-aligning bulk forming tool.

framework supporting the tooling elements. This could be the utilization of a standard die set where ball-cage bearings ensure the alignment of the upper and lower part of the die set. The use of a reference plane, as depicted in Fig. 7-6(a), such as a ground flat back plate, is another way of ensuring good alignment. By placing the high accuracy reference element in the middle of the tolerance chain, it is possible to reference all other tooling elements to this element. This approach requires strict control of the tool tolerance chain to ensure that alignment errors are within an acceptable level. It is often challenging to ensure that the macro-size framework tooling elements, such as the stand and the base-plate, are within the precision required for the alignment of the micro-size forming tools. In Fig. 7-6(b), the punch is loosely fitted into a slot of the moving fixture allowing the punch to center on the die during closure. It is important that the alignment occurs before any load is applied to the punch, meaning that this property should be included into the design of the forming tools. This alignment approach is simple and self-contained, but is generally only suitable for simple forming operations of rotationally symmetrical components.

A hybrid solution for the alignment of tooling elements is depicted in Fig. 7-7. Here the punch holder fixture is spring loaded with a micrometer

screw, allowing for adjustment of the punch position. With this flexible solution it is easy to achieve good alignment and long-term stability, and re-establishing the alignment is tolerable.

Flexibility of Tool System. With the vision of small desktop style factories of the future in mind, flexibility and low changeover times are important factors of focus. With the trend towards smaller production series and more customized products, several components should be produced on the same set-up with a quick change of only the central forming dies and handling fixtures. This idea of modularization is easy to grasp and has been widely adopted in the manufacturing

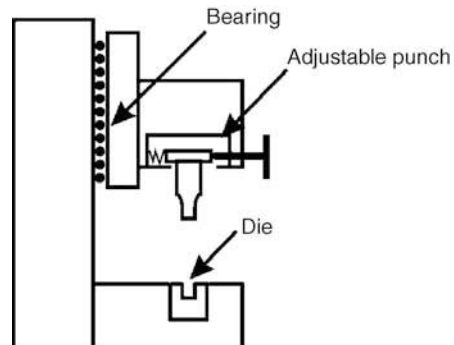
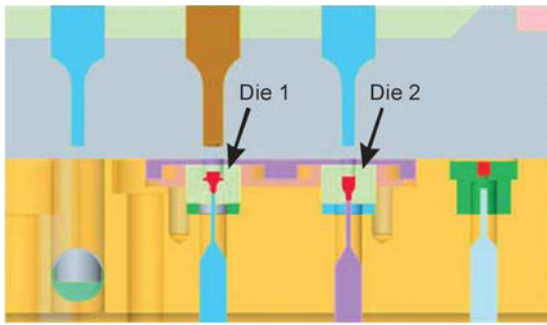
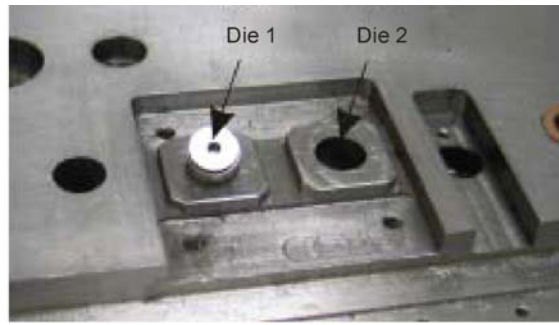


FIGURE 7-7 An adjustable punch fixture allows for the alignment of the punch and die through an adjustment screw.



(a)



(b)

FIGURE 7-8 Sectional view of a two stage micro-bulk forming machine.

industry. When considering micro-bulk forming, it is suggested to realize a flexible bulk forming system through the utilization of modified normal machine elements.

Figure 7-8(a) depicts an example of a two-step flexible micro-forming set-up. The forming dies, punches and ejectors are manufactured from standard punch needles. By standardizing the diameter and tooling material and allowing for easy set-up, the central tooling elements can easily be changed and the machine can manufacture different components with low change times. With an outer diameter of 8 mm and a ground surface finish, the forming dies in Fig. 7-8(b) can be easily interchanged.

Warm Forging of Micro-components

Micro-components are often manufactured using precious metals such as alloys of palladium, titanium or magnesium. The choice of material is often given by the end applications, where the environment of use can be humid, corrosive or have special demands for strength or biocompatibility. Also new age materials, such as bulk metallic glasses, are expected to find wide use within micro-bulk forming. With some of these advanced materials it can be beneficial to utilize warm forging, where the central forming tool elements are operating at elevated temperature. The main benefits of warm forging are a decreased tooling load, increased ductility of the workpiece material and elimination of the heat treatment

process prior and post to forging. For some materials, such as bulk metallic glasses or high grade titanium, it is required to warm the forming tools in order to have an acceptable lifetime of the tooling elements. Warm forging is defined as forging at elevated temperatures above the ambient temperature and below the material recrystallization temperature, typically in the range 100–400°C. The use of warm forming tools requires an advanced tooling set-up with good thermal isolation, heat shields and possible external cooling. It is essential to control the temperature gradient between the warm forging tool elements and the cold framework elements to minimize thermal deflections and the following misalignment and possible tool damage. Figure 7-9(a) depicts a prototype tool system for warm forging of a dental implant in titanium.

The system consists of a central heated core including die, punch, ejector supporting elements and heaters. The framework die set is thermally isolated from the warm core by a calcium silicate-based ceramic material with a thermal conductivity of 0.4 W/mK. Heat shields, with an optical reflective finish, are placed around the upper and lower heated tooling elements. These heat shields prevent heat transfer to the frame by radiation and have a secondary function as a simple safety measure for avoidance of touching of the warm tool parts. Figure 7-9(b) illustrates the steady state temperature distribution of the tool system when heated to 200°C. It can be observed that the tool frame is kept cold with only an

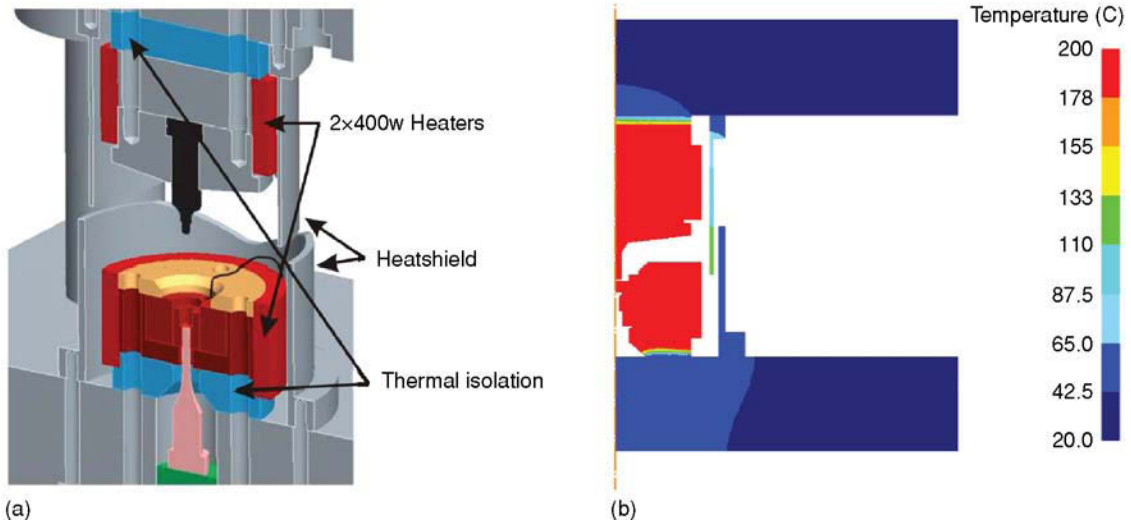


FIGURE 7-9 (a) A prototype tool system for warm micro-bulk forming of a dental implant in titanium. (b) Steady state thermal analysis of tool system including external die set for alignment.

insignificant temperature gradient over the supporting tool frame, thereby keeping thermal deflections to an acceptable level. In an industrial set-up it is usually necessary to apply external temperature control as known from tools for thermoplastic injection molding.

The elevated temperature in warm forging imposes some additional design challenges on the tooling parts located in the heated zone of the tool. For an open-die forging scenario the primary adjacent factors to handle are more challenging tribological conditions. The tribological conditions can be controlled by applying suitable coatings to the punch and die, and matching the workpiece material and the lubricant: the section on tribology later in the chapter touches more on these issues. Further, periodically cleaning of the punch and die might be needed to remove residues of lubricant and workpiece material pickup. For closed-die forming the tribological challenges remain and are followed by oxidation and lubricant entrapment issues. When tempering the punch and die at temperatures near to the recrystallization point, oxides will form on the surface of these parts. The oxide layer, having a high friction coefficient, will give rise to a narrowing of tool clearances and increased friction between the tool pieces and between the tool and work-

piece. This can lead to tool breakdown and should be avoided. Further, pickup due to lubricant breakdown and lubricant entrapment is more dominant at elevated temperatures. Most lubricants are unfit for warm forging because the base liquid components become volatile, leaving solid lubricant residues in the forming die and on the workpiece surface. However, by application of the right coatings in combination with the right type and amount of lubricant, it is possible to realize a micro-bulk forming process at elevated temperature.

Handling and Ejection System

Today, most industrial machines handling micro-components are based on conventional circular vibrating screeners. These screeners are cross-vibrating vessels that are able to align a specific component geometry by means of a custom-built mechanical gate system allowing only components that are rightly aligned to pass through. Depending on the component geometry, material and the crafted design of the gate system, the mean failure rate of a vibrating screen system is usually around $\lambda = 1\text{E-}2$ to $\lambda = 1\text{E-}6$ pieces, meaning that one in every hundred to every million components will jam the system so that an

operator will have to inspect the system. Further, the vibrating screeners are bulky, noisy and inflexible, making them unsuitable as a handling system for a multi-stage micro-manufacturing machine. The sticking of matter is another issue that influences the handling of micro-components. With the increased surface-to-volume ratio for these small components, the van der Waals forces will cause sticking of the components. Primarily, the components will tend to stick to each other, requiring a strategy capable of both handling and separation. For this reason handling concepts of micro-components have been studied intensively in recent years [12,13]. The use of robot cells, advanced gripper systems and self-assembly systems have been proposed, but none have been widely employed within micro-manufacturing because of the unfavorable combination of cost, complexity and speed of these systems.

Figure 7-10 depicts a handling system for the micro-bulk forming process. A cut-out of the transfer system is illustrated in Fig. 7-10(b), where the components can be ejected into the container fixture, moved laterally to the next station and inserted into the succeeding forming die. This system is capable of transferring components at high

speed and is simple to monitor for failure. The container is a precision element used to hold and transport the components from one forming station to the next. For the container depicted in Fig. 7-10(a), the component is held in place by a combination of friction forces and surface tension forces. In order for the surface tension forces to overcome the gravitational forces and keep the component in the container, a specific clearance in the order of micrometers between the component and the container wall must be realized. Furthermore, wear of the container, production tolerances and lubrication quantity must be under control.

Another concept for the component to be held in place in the transfer container is shown in Fig. 7-10(b). In this design an O-ring is placed inside the container die and primarily functions as a friction gate. Secondly the O-ring also has a centering function because the rubber O-ring will absorb minor misalignment and center the component in the container. The proposed transfer system is only capable of handling rotationally symmetrical components, but could be made to function for free-form workpiece geometries also.

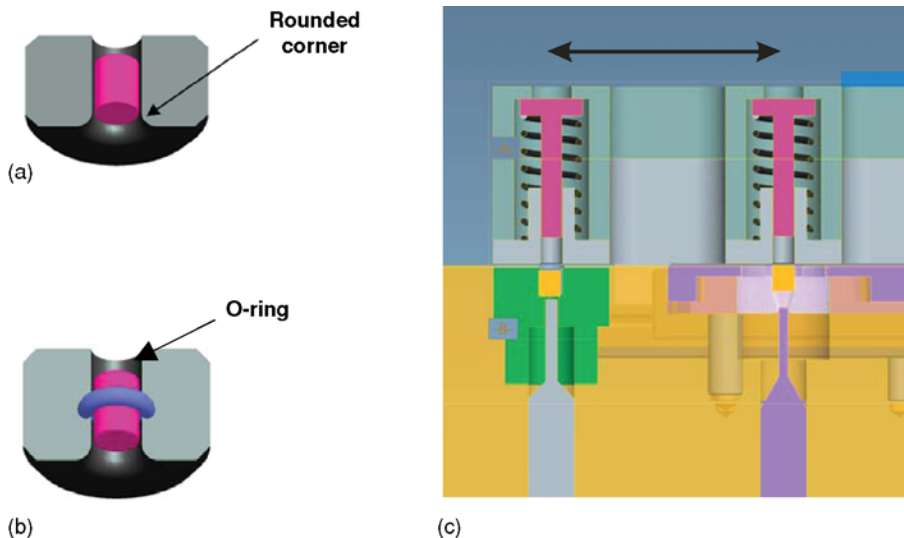


FIGURE 7-10 (a) Gripper for cylindrical micro-component functioning by a combination of friction and sticking forces. (b) Gripper with integrated rubber O-ring. The billet is centered in the carrier and is held in place by the friction of the O-ring. (c) Sectional drawing of a micro-bulk forming tool with an integrated ejector and transfer system.

Process Supervision

Intelligent process supervision is an area of increasing interest within manufacturing technology. By online monitoring of different process parameters and real-time comparison with *a priori* values or values acquired through earlier processing, it is possible to make sure that the process is performing correctly. Some common parameters that are monitored in a bulk forming process are the load/stroke curve for each forming cell, the tool temperature, the workpiece weight, and the position of the transfer rig.

The micro-bulk forming tool shown in Fig. 7-11 employs online measurement of load on the individual forming cells by piezo force sensors. The tool set-up is equipped with two piezo-type force transducers which measure the forming and ejection forces on each of the two forming cells. By correlating the forming force with the stroke length, given by the actuator position encoder, the load/stroke curve can be determined and the curve can be compared with some pre-established curve envelopes. With this type of set-up it is possible to detect machine errors such as tool breakdown, stuck workpieces and misplaced aligned workpieces due to transfer errors. Secondary faults such as inconsistency in workpiece material, lubricant breakdown and tool wear can also be monitored.

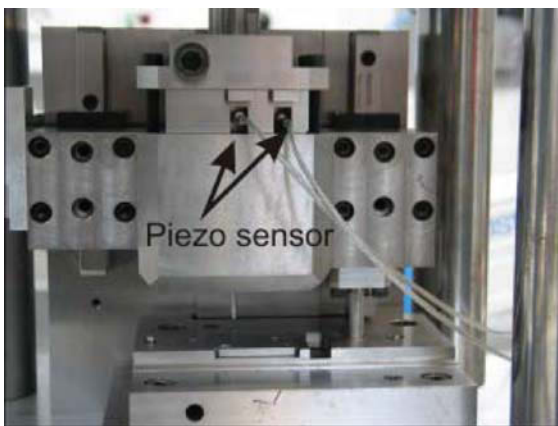


FIGURE 7-11 Online measurement of load on the individual forming cells by piezo force sensors.

Data logging of the monitored values can serve as a quality assurance parameter of the manufactured components. As it is not uncommon to encounter inspection requirement rates of 100% within micro-manufacturing, the addition of traceability and online quality inspection can be valuable. Furthermore, the ability to stop the bulk forming machine in case of misalignment of workpiece or general tool malfunction can avoid machine breakdown, save tooling costs and help to minimize production downtime.

MICRO-TRIBOLOGY

Tribology is the science and technology of interacting surfaces in relative motion. This includes the study of the phenomena of friction, lubrication and wear phenomena. Micro-tribology is the subcategory of tribology dealing with the interaction of micro-size surfaces. As mentioned in the earlier section on the size effect, the laws of friction and lubrication are prone to the size effect. The main reason for this can be found in the underlying surface roughness (or surface asperities, as it is usually termed when referring to tribology), which only scales to a certain extent. This means that the relative surface roughness of a micro-component will be greater in the case of a micro-component compared with macro-size. However, the main parameter of interest in bulk forming is friction, which is dependent on surface load, lubrication and surface characteristics, including surface roughness. Amortons' law of friction dictates a linear dependence between load and friction force: $F_f = \bar{\mu} \cdot L$, where F_f denotes the friction force, $\bar{\mu}$ is the friction coefficient and L is the load. It can be noted that the friction force is independent of contact area, something that was later challenged by the Bowden and Tabor law of friction. Here the friction force F_f is expressed at the product of the effective shear stress, denoted by $\bar{\tau}$, and the sum of the areas of the asperities in contact: $F_f = \bar{\tau} \sum A_{asp}$. In bulk forming, the friction coefficient $\bar{\mu}$ is often established on the basis of experiment and there is seldom an explicit formulation for this quantity. The double-cup extrusion test (DCE test) is a recognized way of establishing

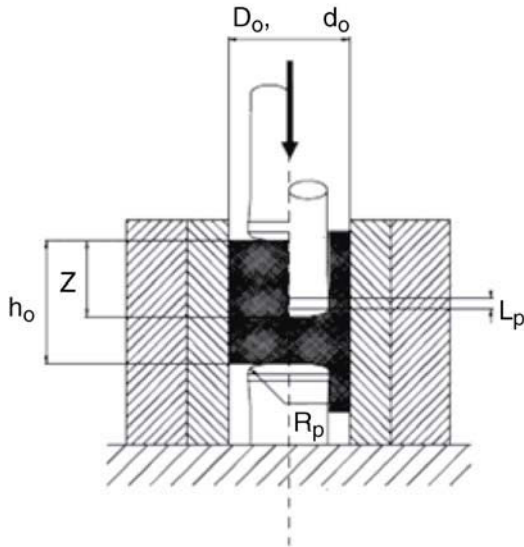


FIGURE 7-12 Sectional illustration of the double-cup extrusion test.

the friction coefficient experimentally. The experimental set-up, depicted in Fig. 7-12, is based on a double-cup pressed between two punches with equal geometry. In the case of zero friction, the height ratio between the upper and lower cup will be unity, while no lower cup will be formed in the case of infinite friction.

A number of micro-scaled DCE tests were carried out by Engel and it was found that the

measured friction coefficient depends on the scale of the experiment [14]. It was further found that the friction coefficient would increase by a factor of 20 when the experiment was scaled by a factor of 8. According to Engel, this is due to the fact that for micro-scale surfaces, more surface asperities reside close to the boundaries of the workpiece where they are less likely to form lubricant pockets under hydrostatic pressure. This influences the surface contact area, leading to an increase in friction force, as observed from the Bowden and Tabor law of friction. More studies of friction behavior can be found in references [15,16].

The influence of increase in friction coefficient when working in the micro-size domain brings about challenges for the handling and ejection of the bulk formed micro-components. Considering the increase of the surface-to-volume ratio, by the scaling factor α , while keeping in mind that surface area promotes friction and volume of material brings strength, this is an important frictional challenge encountered within micro-bulk forming. Further, with the increase in friction due to open lubricant pockets for the micro-size domain, it is evident that friction is a key challenge to be overcome in micro-bulk forming.

Figure 7-13(a) illustrates a simulation of a pre-form for a component to be manufactured by micro-bulk forming. In this case the lower pin

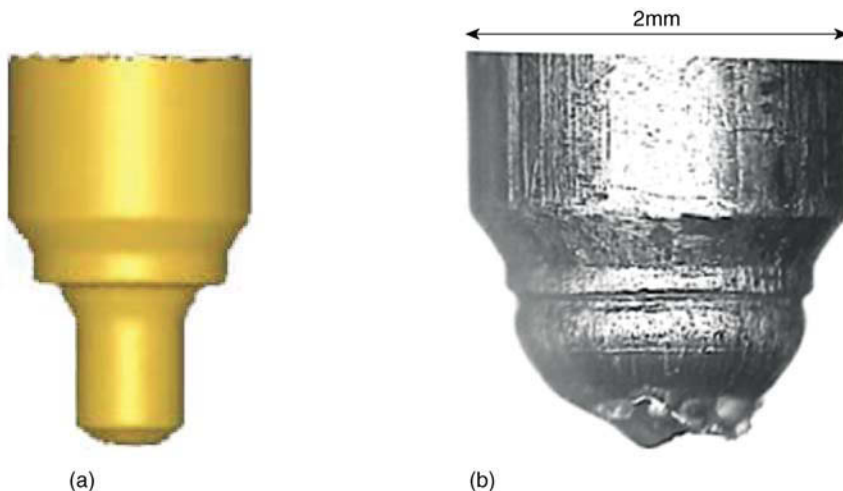


FIGURE 7-13 (a) 3D simulation of pre-form for a micro-axle. (b) Photograph of the formed component where unwanted reverse forming has occurred during ejection from the forming die.

extrusion, with a diameter of about 0.5 mm, must be able to withstand the total friction force during ejection. If the friction force is greater than the yield strength of the component the pin will collapse and reverse forming will occur. The photograph in Fig. 7-13(b) presents an example of reverse forming of the component: this component is the realization of the simulation illustrated in Fig. 7-13(a) where the forward rod extrusion has collapsed during ejection. The problem was resolved by a reduction of the press load, change of lubricant and polishing of the forming die. The use and application of lubricants for micro-bulk forming is at the present time not very well researched. In conventional bulk forming, soaped-phosphate lubricant has been the lubricant of choice for several decades. Unfortunately this lubricant is unsuitable for micro-bulk forming due to the chemical properties of the lubricant layer, allowing scaling down only to a certain thickness. In the example discussed above and other micro-bulk forming experiments at ambient temperature, the use of a commercial silicon paste showed good results. However, the application and removal of the lubricant as well as unintended confinement of lubricant in the forming die have been identified as challenges.

For warm forging and the forming of bulk metallic glasses, a commercial sprayable lubricant based on MoSO₂ has been utilized. This lubrication approach worked fairly well and is suitable for forming at elevated temperatures. A drawback of utilizing a MoSO₂-based lubricant is the undesirable interaction with the workpiece surface. This will leave a dark-colored, rough surface which is difficult to remove and is generally unsuitable for use in any advanced or medical applications.

PROCESS ANALYSIS

The analysis of the bulk forming process normally takes place in a dedicated finite element method (FEM) computer simulation environment. In practice, the software is solving the underlying partial differential equations by doing incremental integration of an approximate set of equations. Due to the severe deformation of the workpiece in

bulk forming, the software must be capable of doing accurate remeshing while retaining volume constancy. The process analysis is initiated by establishing the material parameters. The workpiece material flow curve is typically acquired by doing a tensile test or performing an upsetting test in a universal testing machine. Once the material data are known, these can be fed into the material model of the FEM software together with the tool geometry. If the material is strain-rate dependent or the process needs to run at high strain rates, this influence will have to be included in the model also. This forms the physical basis of the simulation and the simulation process proceeds by selection of simulation parameters.

The choice and analysis of simulation parameters depend on the type of forging process, tolerances, simulation accuracy and several other influencing factors. The most important factor, however, is the number of elements in the simulation, N . The N -factor determines the number of nodes in the mesh and is thus responsible for the simulation accuracy. The number of calculations to be done by the computer increases linearly with N , and thus the number of elements becomes a trade-off between calculation workload and simulation accuracy. It is possible to use a zoned mesh where the user can define zones of the workpiece to have a more refined mesh, typically in areas of severe deformation.

Another important simulation parameter is the simulation step size. This is the time (or punch travel distance) between successive simulation steps. As in the case of number of elements, a large number of steps indicate a large calculation workload, while a low number of simulation steps will affect simulation accuracy. However, by taking notice of the rate of convergence of the simulation it is possible to choose the right step size within a few iterations.

For rotationally symmetrical workpieces, such as bolt, axle or cup geometries, it is possible to cut down on the calculations by doing a two-dimensional simulation while retaining the full validity of the simulation. Even in the case of three-dimensional geometries it is often possible to impose symmetry constraints and cut down on

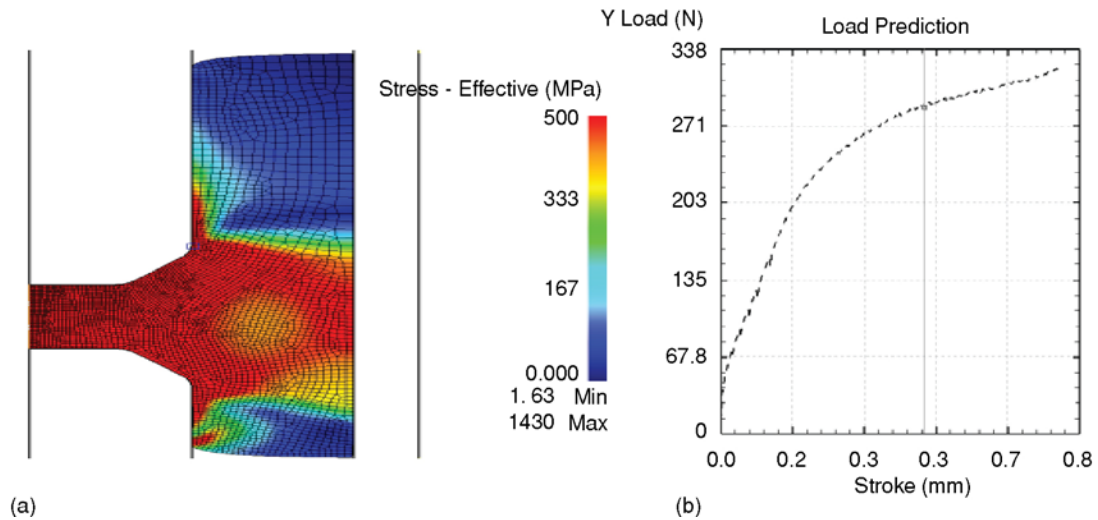


FIGURE 7-14 FE simulation of a double-cup extrusion: (a) stress distribution, and (b) load/stroke curve.

the amount of calculations or increase the accuracy of the simulation. Figure 7-14(a) illustrates the achieved geometry and stress distribution of a two-dimensional simulation of a double-cup extrusion. The simulation was done with a billet diameter of 1 mm of CuZn15 material and a friction coefficient $\mu = 0.15$ between the billet and container wall. Figure 7-14(b) is a plot of the corresponding load/stroke curve where the exponential progress of the envelope can be attributed to the work hardening of the workpiece material.

The benefits of simulations are manifold and simulations of traditional bulk forming processes often have exhibited a geometrical accuracy of better than 0.5%. If the simulation parameters are chosen carefully it is possible to predict the

press load, unwanted forming folds and tool stress without having to prepare costly prototype tools.

The micro-bulk forming process can be simulated in the same way as conventional macro-size bulk forming process with a few important exceptions. Most simulation models hold an underlying assumption of a continuous and isotropic material model. This means that the grain structure of the material is not taken into account, meaning that the model is only valid down to a certain size. Within normal limits, a material can be modeled as continuous and isotropic if it is indeed isotropic and the number of grain structures across all features is greater than 8–10 grains [15].

Figure 7-15 illustrates a forming experiment where a small copper pin was extruded.

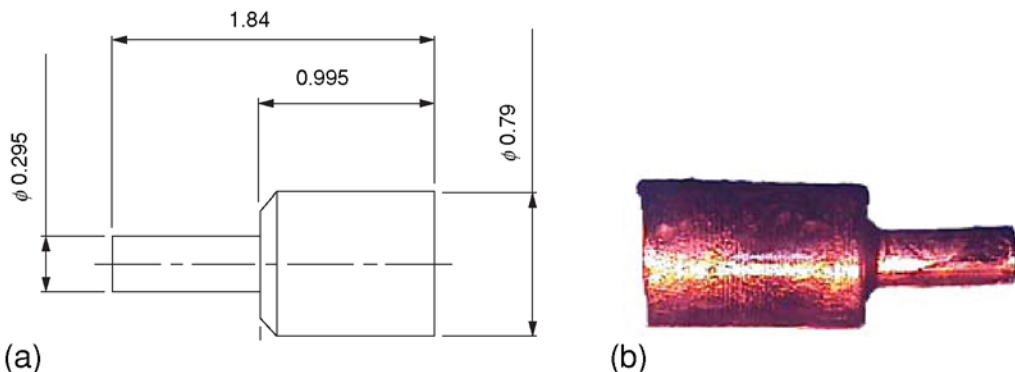


FIGURE 7-15 A sample of the extruded micro-pin (dimensions: mm).

The original specification is reproduced in Fig. 7-15(a). With an average grain size of about 80 μm , there are less than four grains across the pin, thereby invalidating the assumption of isotropy of the material. A photograph of the bulk formed pin is shown in Fig. 7-15(b) where a clear side tracing of the extruded pin can be noted. This behavior has been the topic of several research projects, and a range of new material models trying to incorporate the inter-grain behavior have been proposed. By choosing a material with a fine grain structure or by changing the grain size by heat treatment or mechanical remodeling, it is possible to form micro-size components while keeping the assumption of homogeneity and isotropy in the material intact.

REFERENCES

- [1] R.B. Cruise, L. Gardner, Strength enhancements induced during cold forming of stainless steel sections, *J. of Constructional Steel Research* 64 (11) (2008) 1310–1316.
- [2] M. Ashraf, L. Gardner, D.A. Nethercot, Strength enhancement of the corner regions of stainless steel cross-sections, *J. of Constructional Steel Research* 61 (1) (2005) 37–52.
- [3] T. Inoue, The Japanese sword: the material, manufacturing and computer simulation of quenching process, *Materials Science Research International* 3 (1997) 193–203.
- [4] L.S. Nielsen, S. Lassen, C.B. Andersen, J. Grønbaek, N. Bay, Development of a flexible tool system for small quantity production in cold forging, *J. Mater. Process. Technol.* 71 (11/1) (1997) 36–42.
- [5] U. Engel, R. Eckstein, Microforming – from basic research to its realization, *J. Mater. Process. Technol.* 125–126 (2002) 35–44.
- [6] M. Geiger, M. Kleiner, R. Eckstein, N. Tiesler, U. Engel, Microforming, *CIRP Ann. Manuf. Technol.* 50 (2001) 445–462.
- [7] J.A. Wert, C. Thornsens, R.D. Jensen, M. Arentoft, Forming of bulk metallic glass microcomponents, *J. Mater. Process. Technol.* 209 (2009) 1570–1579.
- [8] J. Schroers, T. Nguyen, S. O’Keeffe, A. Desai, Thermoplastic forming of bulk metallic glass – applications for MEMS and microstructure fabrication, *Materials Science and Engineering: A* 449–451 (3/25) (2007) 898–902.
- [9] N.A. Paldan, M. Arentoft, R.S. Eriksen, Production equipment and processes for bulk formed micro components, *AIP Conference Proceedings* 907 (04/07) (2007) 463–468.
- [10] Y. Okazaki, N. Mishima, K. Ashida, Microfactory – concept, history, and developments, *J. Manuf. Sci. Eng.* 126 (November 2004) 837–844.
- [11] J. Cao, N. Krishnan, Z. Wang, H. Lu, W.K. Liu, A. Swanson, Microforming: Experimental Investigation of the extrusion process for micropins and its numerical simulation using RKEM, *J. Manuf. Sci. Eng.* 126 (November 2004) 642–652.
- [12] H. Van Brussel, J. Peirs, D. Reynaerts, A. Delchambre, G. Reinhart, N. Roth, M. Weck, E. Zussman, Assembly of microsystems, *CIRP Ann. Manuf. Technol* 49 (2000) 451–472.
- [13] T. Eriksson, H. Hansen, A. Gegeckaitė, On the use of industrial robots in microfactories, *Int. J. of Advanced Manufacturing Technology* 38 (08/01) (2008) 479–486.
- [14] U. Engel, Tribology in microforming, *Wear* 260 (2006) 265–273.
- [15] N. Krishnan, J. Cao, K. Dohda, Study of the size effects on friction conditions in microextrusion – Part I: Microextrusion experiments and analysis, *J. Manuf. Sci. Eng.* 129 (August 2007) 669–676.
- [16] Y. Mo, K.T. Turner, I. Szlufarska, Friction laws at the nanoscale, *Nature* 457 (2009) 1116–1119.

Forming of Micro-Sheet-Metal Components

Yi Qin, Andrew Brockett, Jie Zhao, Akhtar Razali, Yanling Ma and Colin Harrison

INTRODUCTION

Sheet metal components are used extensively in various applications such as vehicles, aircraft, electronics products, medical implants and packaging for consuming goods, typical parts/components including car panels, aircraft skins, cans for food and drinks, frames for TV/computer screens/monitors/displays, etc. Concerning miniature/micro-products, sheet metal parts include electrical connectors and lead frames, micro-meshes for masks and optical devices, micro-springs for micro-switches, micro-cups for electron guns and micro-packaging, micro-laminates for micro-motor and fluidic devices, micro-gears for micro-mechanical devices, casings/housings for micro-device assembly/packaging, micro-knives for surgery, etc. Therefore, miniature/micro-sheet metal parts are closely associated with everyday life.

Basic process configurations for the forming of macro-products include shearing, blanking, bending, stamping, deep drawing (including mechanical and hydromechanical), hydroforming, stretching forming, super-plastic forming, age forming, spinning, explosive forming, incremental forming, etc. Some of these processes may be equally applied to the forming of miniature and even micro-products, if the issues related to 'size effect' can be handled successfully [1–8]. General challenges associated with the manufacture of micro-products have been described in [Chapter 1](#) of this book.

The forming of small/thin metal parts has been undertaken by industry for many years. New challenges arise when the overall sizes reduce to sub-millimeters, or local features reduce to tens of microns, or the precision requirements for macro-/miniature parts reduce to less than a few microns. Studying the research reported previously and recent research conducted in-house resulted in the following observations:

1. Conventional metal-forming process configurations may be equally used for the forming of miniature/micro-parts, although the process capabilities are likely to be constrained more, due to additional material, interfacial and tooling considerations in micro-forming.
2. The types of materials which could be formable at micro-levels are prescribed more significantly than for forming at macro-levels by the micro-structures and grain-boundary properties of the materials. The forming limits for these materials are, therefore, somewhat different, compared to those for the forming of macro-parts.
3. Size effects may exist in material/property and tool/material interfacial property characterization, depending largely on the micro-structures of the materials, which leads to the requirement of the definition of these parameters with reference to the actual materials and interfaces to be used.

Regarding micro-sheet-forming production, the following are the particularities which need to be paid attention, especially for the forming of sheets of less than 100 microns in thickness and feature sizes less than sub-millimeters, the reasons for which will be explained in the following sections of this chapter, wherever appropriate:

1. The need to use proper materials which are micro-formable, either under cold, warm or localized heating conditions;
2. Special care in the handling of the raw materials (e.g. guiding thin strip, holding the strip during forming, etc.) and in collecting scrap, parts/components effectively;
3. Constraints on the tool layouts due to the limited space and closeness of miniature/micro-tools, and, hence, constraints on tool design;
4. The process capabilities, which are prescribed largely by the tool fabrication capabilities, including tool coatings and the assembly of miniature/micro-tools;
5. Miniaturization of the forming machinery and improving the precision of the machinery at the corresponding scales;
6. Tool cost issues, including process chains for micro-tooling, effective tool life affected by susceptibility to wear, fragile structures, damage to the tools caused by manufacturing, etc.

MANUFACTURING PROCESSES AND FUNDAMENTALS

Traditionally, sheet metals may be defined as metal having a thickness of between 0.4 and 6 mm, while micro-sheet forming usually deals with sheet metals of which the thickness is usually below 0.3 mm. Therefore, thin strips or coils may be proper words for defining these materials. As with conventional sheet metal forming, major material conversion mechanisms in micro-sheet forming include shearing/cutting, bending, unbending, stretching, compressing, stress relaxation, etc., and their combinations.

Being the same as for conventional sheet metal forming, the mechanical properties of the materials such as elasticity, plasticity, stress strain relations, strain rate, work hardening, temperature effect,

anisotropy, grain size, residual stress, etc., are very important for understanding material deformation/separation mechanisms. The effects of grain sizes and orientations, and grain-boundary properties, are especially significant in micro-sheet forming, considering their effects on the definition of the overall stress/strain relationships, sheared-section qualities, bending curvatures, springback phenomena, stress relaxation, etc. For given micro-structures, the effects are more significant, in terms of the relative ratios between the grain sizes and the strip thickness/feature sizes/part dimensions.

The following sheet-forming processes may be used in micro-sheet forming.

Manufacture of Sheet Metal Parts by Blanking/Punching

Cutting may be used to separate large sheets into smaller pieces, to cut out a part perimeter, or to make holes in a part, and can be accomplished by shearing action between two sheared-cutting edges through the following stages of the material: (a) plastic deformation, (b) fracture initiation, and (c) separation (Fig. 8-1). The parameters that

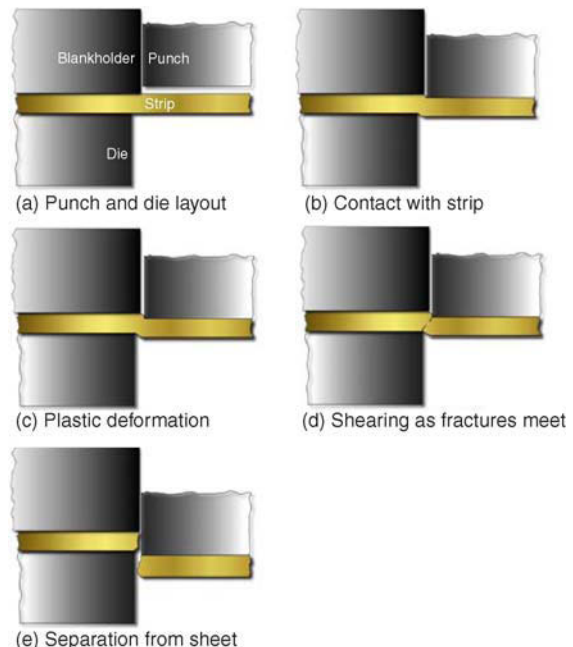


FIGURE 8-1 Stages of a shearing/cutting process.

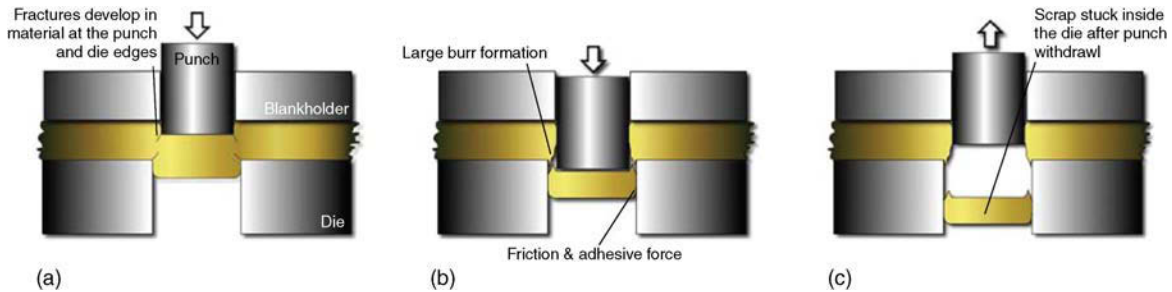


FIGURE 8-2 Illustration of the influence of the punch/die clearance.

influence the shearing/cutting quality significantly include: punch-die clearance, punch velocity, sheet metal materials, cutting tools, lubrication, alignment of the tools, strain rate, etc.

The clearance between the punch/cutting tool and the die is a very important parameter (Fig. 8-2). For the clearance in conventional sheet metal forming, 4–8% of the sheet thickness is recommended. With too small a clearance a greater cutting force is required; and the fracture lines tend not to intersect, while with too large a clearance excessive burr sizes develop. The best clearance value depends on the sheet metal type and thickness. The recommended clearance may be calculated from $C = a t$, where t is the sheet thickness and a is a factor (provided from different sources).

The value of a for micro-blanking/punching needs to be determined by addressing actual cases because of the large influence of the micro-structure (size, orientation and grain-boundary properties) relative to the overall scale of the part dimensions and/or cut geometries. For example, due to the size effect, the formation of edge draw-in, shear/plastic deformation and fracture/burr (Fig. 8-3) will be affected more significantly than that in a macro-blanking/punching process, by the micro-structure of the material. The level of the effect depends largely on the number of grains, the grain orientation, the possible number of sliding planes, etc., at the cutting areas. It was observed that the shearing resistance actually increases as the process/part dimensions are scaled down, but not in a linear manner [1]: this may be due to the limited number of sliding planes and the constrained position in which the shearing

is taking place. A small number of grains may not be able to allow shear deformation to the same extent as would a poly-crystal which has a large number of grains and grain boundaries [9]. The strain rate in shearing/cutting plays an important role, especially on the cutting quality, e.g. burr formation. It has been established that high velocities in blanking can lead to a decrease in the blanking force and improved quality of cutting sections [10]: a dynamic fracturing mechanism and increase of the temperature locally for a short period of time may contribute to this. The same principle can be seen in high speed chopping of metal billets for forging/forming. Considering that in micro-forming, the sheet metal is relatively thin, how the temperature factor could contribute to this is not clear. However, as a general

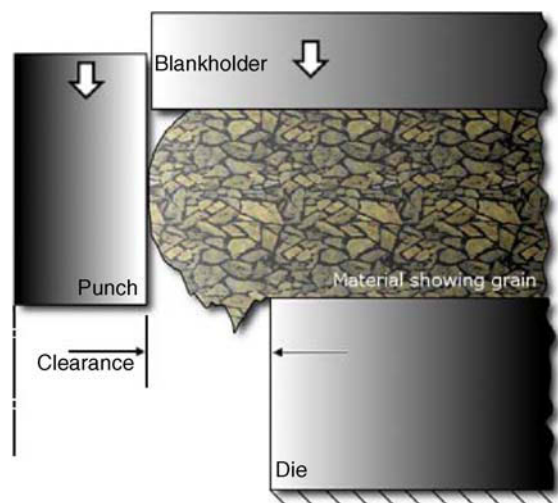


FIGURE 8-3 Illustration of the influence of grains on the sheared section.

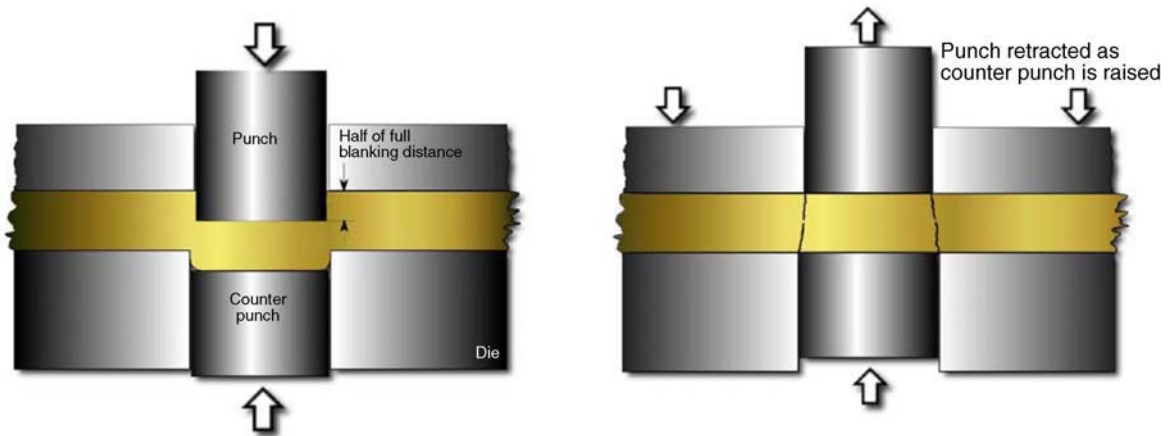


FIGURE 8-4 Illustration of a ‘burr-free’ punching process.

principle, using a higher speed in cutting should normally help to improve the cutting quality.

A practical problem associated with micro-blanking/punching is that the punch/die clearance required may not always be met. For example, for the stamping of a $20\ \mu\text{m}$ thick sheet metal strip, the ideal clearance would be $1\text{--}2\ \mu\text{m}$. This would be a challenge to tool making and to the guiding of the tools (machine set-up and tooling). Even if it is possible to achieve this in fabrication and assembly, the dynamics characteristics of the machine and tooling, including the resulting deflections, are very likely to cause an offset of the punch or the die of more than $1\text{--}2\ \mu\text{m}$. As a consequence, damage to the tools is likely to occur constantly. When using larger clearance values than the ideal values, burr formation in micro-forming of thin sheets may not be avoidable, if conventional process configurations are employed.

For micro-sheet metal parts, especially those to be used in important electronics products and MEMS, the presence of burrs may not be acceptable. Therefore, a post-process for burr removal may be necessary, e.g. laser ablation or mechanical methods. Burr-free blanking/punching processes have been explored in the past for the forming of thick sheet metals, and recently there were also attempts to use these to form thin metal strips [11]. The process of using half-distance piercing without separating the material, then using a

counter-punch to effect a counter-direction piercing (pushback) to complete the blanking/punching (Fig. 8-4), is feasible for eliminating burr formation for strips as thin as $50\ \mu\text{m}$. The several stages, including two stages shown in Fig. 8.4, can be accommodated using a progressive die design in micro-stamping, e.g. punching for producing pilot holes, half-blanking (which may also be supported with a soft counter-punch), push-back blanking to complete the blanking operation, and, finally, clearing the cutting or cutting off the parts, etc. For micro-forming, e.g. where the sheet metal thickness is less than $50\ \mu\text{m}$, controlling the half-blanking depth precisely will be crucial, and involves the control of not only the machine ram and the punch motion with the tooling, but also guiding and holding the metal strip inside the tooling.

Another useful process configuration called laser-assisted micro-stamping may be used for improving the quality of the cut section and extending the capabilities of the process such as the stamping of greater aspect ratios (the ratio of the cutting thickness to the cutting area dimensions) and high strength materials, including brittle/difficult stamping materials. The process is described in Chapter 10. The laser heating will provide a reduction in the strength of the local material and improve the flowability of the material at the cutting section.

Manufacture of Sheet Metal Parts by Bending

Bending in sheet metal forming may be defined as the straining of the metal around a straight axis. A neutral axis plane exists for the sheet metal around which the top section of the material may be stretched during bending while the bottom section is compressed (Fig. 8-5). Bending operations may be performed using punches, rolls, wipe dies, the downward movement of the bending tools, depending on the bending processes, i.e. V-bending, U-bending, edge bending, etc., that are normally used in conventional sheet metal working. The manufacture of micro-sheet metal products, such as those used in electronics products and MEMS, often needs bending to produce 3D profiles/sections. Typical applications include micro-electric contacts/fingers/switches, 3D profiles for mechanical and thermal-mechanical sensors and 3D sheet metal frames/housing for optical devices and micro-sensors. The manufacture of these items may also require photo-chemical etching to produce fine geometry, while using bending to complete the 3D profiles/sections.

In employing bending for making micro-products the bend angle, bend radius, bend allowance, length of bend, etc., are still key process parameters (Fig. 8-5). The calculation of the strain value in bending, the minimum bend radius, the bend allowance, etc., may still be effected with the

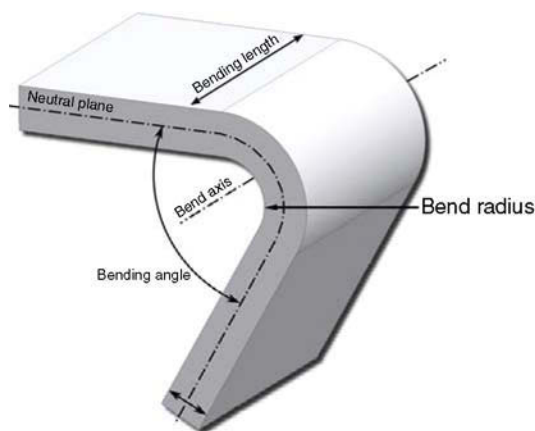


FIGURE 8-5 Illustration of a sheet metal bending process and parameters.

simplified equations that are normally used for macro-/miniature parts. These, however, need to include considerations concerning size effects. Similarly to the case of blanking/punching, the relative grain size to the sheet metal thickness, grain distribution and grain-boundary conditions at the bend section will have significant influences on the bending process and bending quality: a universal definition in terms of the level of these influences does not exist.

One of the main challenging issues in the bending of thin sheet metals is to prevent the distortion of the sheet and to overcome springback-related problems (Fig. 8-6). Sheet metal may recover

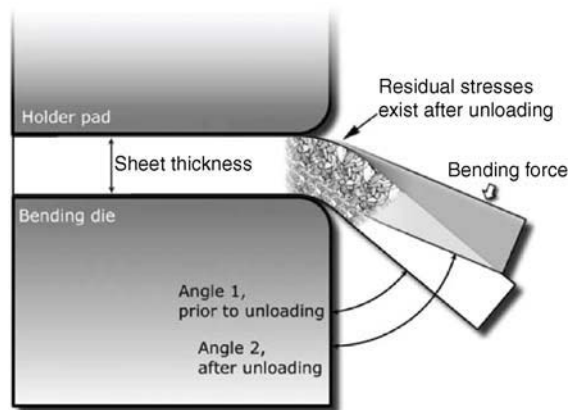
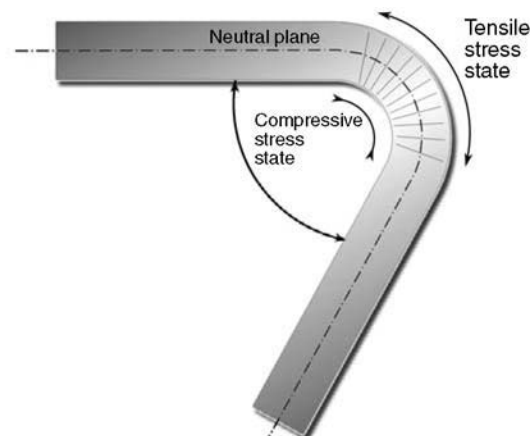


FIGURE 8-6 Illustration of the springback phenomena in sheet bending.



elastically after manufacturing, not only after bending, but also due to possible changes of the state of the stresses during/after secondary processes, e.g. after trimming, i.e. the cutting of neighboring material which affects the stress balance in this or another section. This often occurs when micro-parts with condensed features or cutting/bending sections are produced with a progressive die-forming/stamping configuration. The springback may occur immediately after the release of the forming force, or occur due to the subsequent release of the residual stresses, and results in the distortion of the shape of the part or instability of the dimensions of the part under service conditions. The amount of springback in bending is dependent on the ratio of the bending radius to the sheet metal thickness, the yield strength and Young's modulus of the material, the micro-structure in the bending sections, and the closeness of the forming/cutting features.

The component form errors resulting from the springback may be compensated for by properly designing the die and the bending parameters, or introducing extra processes. Rebending, overbending, bottoming or stretch bending are the techniques often used to eliminate the errors caused by the springback in conventional sheet metal forming. It may be difficult to employ some of these techniques in micro-sheet forming, either due to the complexity of the geometry in small areas, or due to the difficulty in adding extra tools or forming stages in the limited tooling space, etc. Other limitations are those due to cost considerations. Feasible compensation measures include optimization of the bending stroke, bending angle, tool shape, punch/die clearance, etc. In-process measurement of springback plus adjusting the bending angle or bending speed is possible, if proper sensing (e.g. displacement and angular sensors, non-contact sensors such as laser-based sensors, etc.), an effective feedback loop and analysis, and control of the actuators can be ensured. This is achievable mainly for simple bend geometry, not for a complex stamping process.

To avoid difficulties in handling micro-components/parts and in the fabrication of micro-tooling, non-contact processing approaches such

as laser-assisted bending may be introduced to achieve accurate bend geometries [12]. For example, short-pulse excimer laser radiation is able to result in a required level of thermally induced stress in very thin surface layers of a sheet metal, and the deformation of the thin sheet in the radiated area may be effected in the forms of bending by the released stresses. Laser heating can also assist in forming of 3D micro-sheet structures effectively, e.g. combining bending and twisting [13].

Deep Drawing of Sheet Metal Parts

Deep drawing is a sheet metal-forming process used industrially to produce cup-shaped, box-shaped and other complex-curved hollow-shaped sheet parts. Micro-cups/micro-boxes may be produced with similar process configurations (Fig. 8-7) for micro-housing applications, such as for the packaging of micro-sensors and micro-actuators. As for conventional deep drawing, the major parameters which influence the process and product quality include the dimensions of the blank, the punch and die dimensions, especially the punch corner radii, the clearance between the punch and the die, as well as the blank-holder geometry, the interfacial conditions and the holding pressures. Deep drawing is a more complex process than shearing/cutting and bending because it usually combines processes such as bending, unbending, stretching, compression and shearing, depending on the part geometry to be produced. These processes become more complex when the micro-structure of the sheet metal becomes a dominant factor as the scale decreases [2].

The drawing ratio ($DR = \text{diameter of the blank}/\text{diameter of the punch}$) achievable is usually about 2.0 (the limiting drawing ratio (LDR)), depending on the sheet material thickness and micro-structure. With fine-grain sheet metals, controlled friction at the contact surface of the blank-holder with the sheet, the sheet with the die, the punch to sheet metal interfaces, and possibly providing counter-pressures under the sheet, the LDR value could be increased. A major challenge faced in micro-deep drawing is to achieve these DR values within a limited space, which

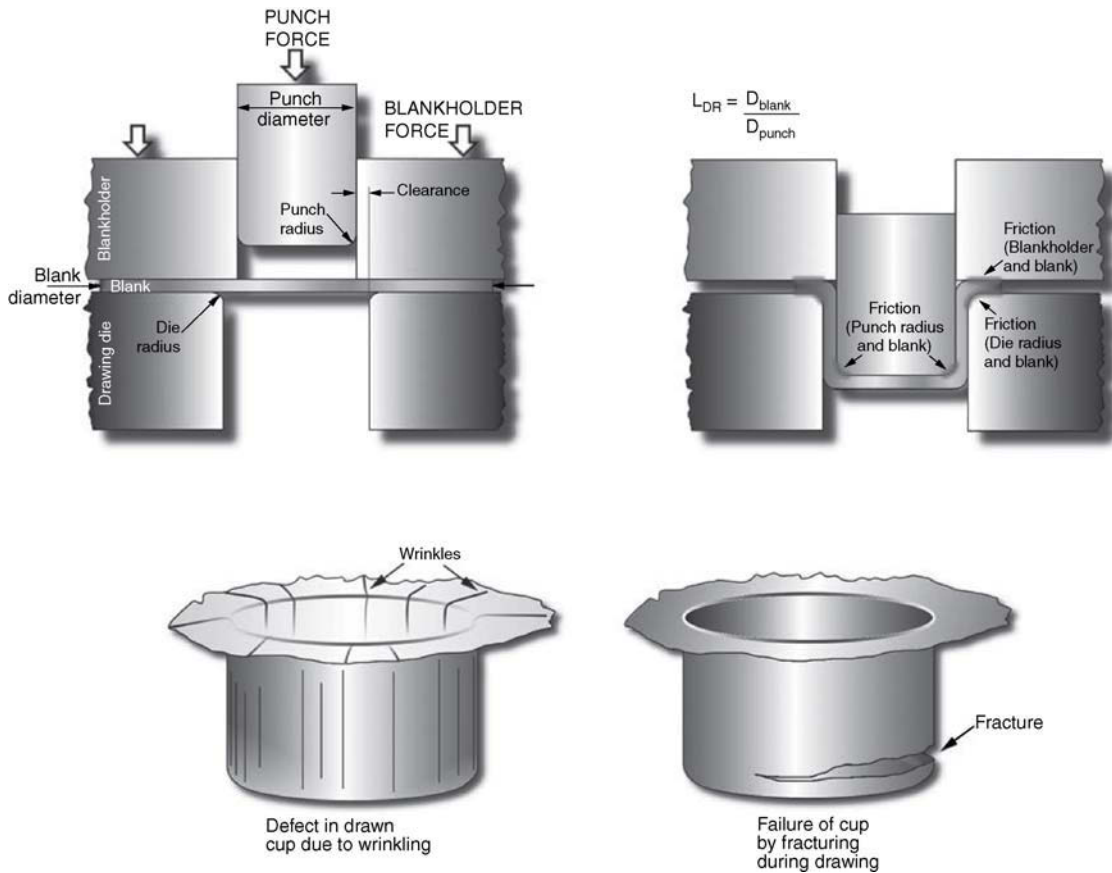


FIGURE 8-7 Illustration of the deep drawing process, influential parameters and part failure forms.

usually limits the tooling arrangement. Control of the interfacial conditions is even more difficult. Ideally, no other media should be used, and enhanced complexity of the tool/material interface conditions should be avoided. The actual LDR achievable in micro-deep drawing production also depends on how the blanks and the formed cups will be toggled with the sheet metal strips in the forming/stamping layout design, since the blanks and the finally formed cups are unlikely to be detached from the strip during forming/stamping due to the difficulties associated with handling these small objects, while a reasonable production rate may have to be maintained. This is a special issue to be addressed, compared to the laboratory-based prototype process development.

Common defects in drawn thin-sheet parts include the formation of wrinkles (due to buckling), material fracturing (especially at the punch and die corners), and surface scratching (Fig. 8-7). Wrinkles often occur when very thin sheet metals are to be drawn (the material most likely buckles), such as 20 μm thick sheets. Blank-holding will be crucial, but it may not be easily arranged due to the limited space for tool components in micro-deep drawing. Fine-grain materials and materials with superplastic flow characteristics will be helpful in overcoming the fractures which often occur at the punch corner (small radius) and the flange/cup wall interface. Smaller cups with thin sheet metals may not be achievable, due either to excessive springback for shallow geometries or due to

the initiation of fractures arising from the use of small punches, similar to what can occur in a piercing process. Again, the avoidance of these features will also depend on how the blanks are to be toggled with the strip.

Redrawing is usually necessary, due to the limitation in the achievement of a feasible reduction value of a cup, in one stroke. Redrawing or reverse redrawing, even introducing an annealing process and ironing, is possible for miniature cups. These steps are unlikely to be introduced in the forming of a micro-cup, due to the difficulties occurring in the handling and alignment of the workpiece, etc. Ideal processes would be those without the need to reposition the workpiece while the tools are being changed.

Other Micro-sheet Metal-forming Processes

Other micro-sheet metal-forming processes include: (a) incremental (or dieless) forming – micro-sheet metal parts or micro-features on sheet metals can also be produced in incremental forming forms, such as by using CNC-controlled hammering, piezo-electric actuated micro-probes for dimpling (high frequency vibration actuated), by which micro-features in small and large areas of thin sheet metals (down to 10 to 20 microns thickness) can be produced [14]. (b) Isostatic pressing – ultra-thin metal foils may be pressed into a die with grooved surfaces to produce micro-channels. Foils as thin as several microns can be formed to produce such channels within the range of several to tens of microns [15]. (c) Embossing/coining is also possible for use in producing surface micro-textures on the thin sheet metals, e.g. using silicon tools, on thin aluminum sheets, fine-grained alloy, amorphous alloy, in the cold and hot state, etc. [1,4].

GENERAL CONSIDERATIONS FOR MANUFACTURING

Similarly to the planning for conventional sheet forming, the following aspects may have to be checked with a view to implementing micro-

forming processes (some details concerning these issues being described in the next sections):

- Whether the maximum stamping-force requirements, machine static/dynamic characterization can be met with the available machines;
- Whether the machine strokes and manufacturing precision requirements can be met with available machines and tools;
- Whether the production rates achievable are acceptable, also considering the thickness of the sheet metals to be dealt with, the precision requirements and tool life factors;
- Whether the raw materials obtainable meet the requirements, in terms of mechanical properties, grain sizes and dimensional tolerances for production;
- What the stock/tool layout for progressive die design will be, including how the scrap and the parts will be despatched;
- Whether the tool design/manufacturing capabilities meet the requirements (especially micro-tooling capabilities, involving the whole process chains);
- Whether the punch/die clearance (recommended) is achievable by toolmaker(s);
- Whether a burr-removal process is required (for high quality/performance parts);
- What extra care for handling fragile thin strips and the structural parts stamped will be required, including that for careful strip/blank-holding designs;
- Whether a push-pull set-up with two feeders or just a single feeder is to be used for pulling/feeding the sheet metal;
- What extra measures for dealing with springback and distortions of the sheet parts with dense geometrical features will be required;
- How the scraps and parts will be collected from the tool system and the machine;
- How the process monitoring will be implemented (force, velocity, energy, etc.);
- How the tool condition, e.g. wear, breaking, damage to the coating, will be monitored;
- Whether a cleaning process is needed and a clean environment should be maintained;
- How the parts will be packed/transported;

- How the parts/products will be inspected (off-line or online, or both), etc.

FORMING TOOLS

General considerations for tool design and manufacture for micro-sheet-forming production include: the scheme for progressive die forming/stamping or transfer die forming/stamping (need to give careful consideration to the part sizes, features and sizes, use of the strip material, etc.); the availability of the die-working space provided by the machine as well as the connection to the feeder(s); the stock layouts considering micro-forming characteristics (especially the closeness of the features) as well as transport requirements; the blank-holding design considering limited spaces and precision; the feasible punch penetration distance (taking into account the punch diameter/free length ratio); the punch/die clearance achievable with micro-tooling capabilities; web formation and limitation due to space arrangements and its potential effect on the distortion of the parts; the ejection/removal of the small/thin parts and scraps (if needed); burr generation and removal; punch stiffness/strength and assembly requirements (with limited spaces); the transport of the thin part/scrap ribbon at high speed; maintaining the flatness of the thin strip during transport; considerations for the implementation of a dry stamping process and its effects; the micro-tooling process chains and capabilities in dimension tolerances and surface finish; tool materials and cost; micro-tooling cost (considering the process chains); assembly and inspection techniques for micro-tools; the interfaces with the machine; special arrangements for the guiding of the punches/moving parts of the tooling; the proper selection of bearings and guides, prestressing parts, if possible; tool surface polishing; tool surface coating, etc.

Forming tool design and manufacturing is a particularly challenging area for micro-sheet forming, and is mainly associated with the size effects induced as the scaling factor decreases:

1. Punch-die clearance in micro-stamping needs to be redefined (closely relating to the material

properties qualified at micro-scales and to the micro-structures at the deformation/shearing sections). The recommended clearance (4–10% of the sheet thickness, Fig. 8-2) for conventional stamping may not be correct. Increasing the punching velocity would affect the shearing section quality positively, which would, in turn, relax the clearance requirements.

2. For cutting thinner strips, tight clearances down to one to several microns may be needed, which may be achievable but at high cost. Constraints to this include whether the tool-fabrication capabilities are able to achieve one to several microns accuracy in manufacturing individual tool parts, to align these within a similar accuracy after assembly, and whether the dynamic characteristics of the tooling are able to maintain the tool bending, the tool offset due to loading eccentricity and clearance between the bearings and guiding pillars to be within a similar precision range (a tool system is illustrated in Fig. 8-8). Tool damage/breaking could be easily caused by these factors.
3. The reduced sizes of the cutting geometry restrict the punches to only a very short free length (to maintain sufficient stability). As a consequence, it may be difficult to punch the scrap out of the die exit (Fig. 8-2(c)), if the punches are too short. It also requires extremely accurate control of the punch stroke to ensure that the stamping operation is completed.
4. Due to the limited space available, the number of tool parts/elements for constructing the tooling may have to be reduced to avoid difficulties in fabricating these parts/elements and assembling them in tiny spaces, as well as reducing the assembly errors accumulated. Using compound tool designs may be considered.
5. The design of the pilot pins for positioning thin strip needs to be carefully done, by which the pins could correct the position of the strip (Fig. 8-9), and help to reduce the positional errors significantly, thereby relaxing the stringent requirements on the strip feeder(s), in terms of feeding accuracy.

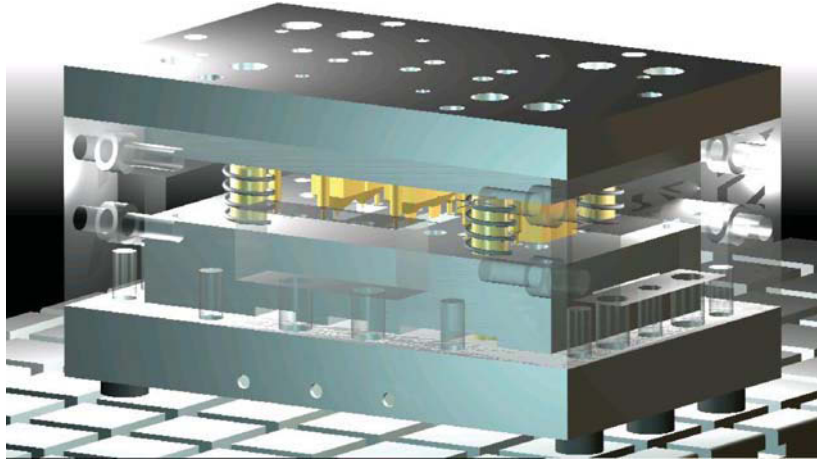


FIGURE 8-8 A tool system for micro-sheet forming.

6. To prevent damage to the workpiece surfaces (e.g. coated strips for electronics applications) and to prevent sticking of the scrap and micro-parts to the tool surfaces, dry stamping will be needed, for which special tool materials such as ceramics tools and self-lubricated tool coatings, etc. should be considered.
7. In micro-sheet forming, gravity cannot be considered as the main force being applied to the part. Unwanted surface forces such as van der Waals, electrostatic and surface-tension forces are dominant at such a scale. As a result, concepts for handling parts/scrap deployed in conventional forming (largely considering the gravity force of the parts) do not usually work. Parts may not drop out automatically and connecting these to the strip may be feasible in some cases. However, separation may still be needed, depending on the end uses and customer's requirements. A vacuum system directly connected to the dies or proper locations within a tool system will be helpful for collecting the scrap and even micro-parts.

Micro-tooling capabilities and process chains (e.g. mechanical cutting, EDM, laser treatment, coating, electro-forming, chemical etching, etc.) are especially important, which significantly prescribe the feasibility of realizing the processes and achievability of the required scales of the micro-parts, while maintaining proper production rates

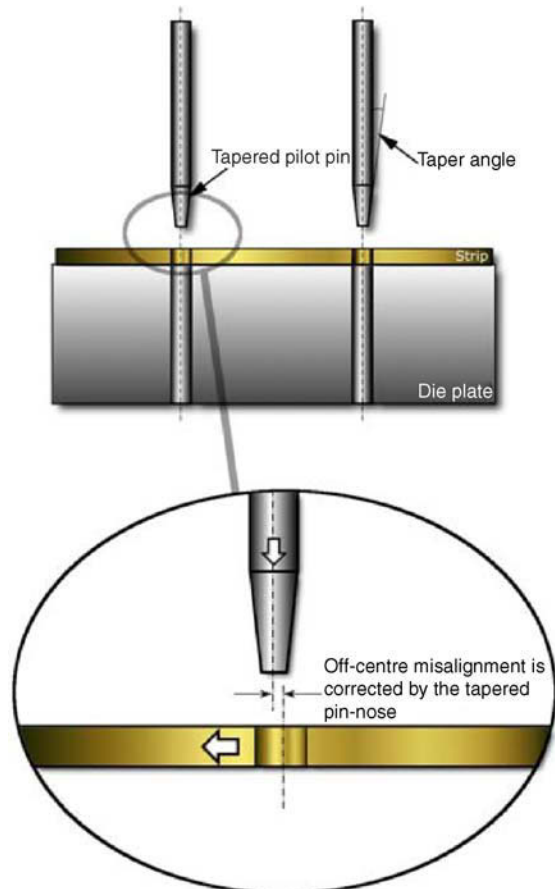


FIGURE 8-9 Illustration of the function of the pilot pins.

and product quality, and low manufacturing cost. These are addressed in several other chapters of this book.

MANUFACTURING PRESSES/ MACHINES

Traditionally, sheet metal forming may be effected either with mechanical presses or hydraulic presses, the latter usually being of large scale. These presses are usually not of sufficient precision for micro-forming applications, and they are not compatible, in terms of scale, for the forming of the miniature/micro-sheet metal parts. Conventional, large-scale presses may be optimized/upgraded for the manufacture of miniature/micro-sheet metal parts with the required enhanced precision. Their manufacture may also be achievable through the use of delicately designed and fabricated forming tools. Conventional forming tools may be designed primarily for manufacturing metal parts with precisions in the millimeter range. However, with some specific engineering modifications implemented in these machines they could be optimized for micro-forming applications. BSTA from Bruderer is a machine which can operate at up to 1400 spm and a press force of 300 kN [16]. Incorporated in the machine are specific modifications such as guides that are insensitive to thermal influences, additional features to secure high precision, and a counterbalance system 'acting irreversibly' to the movement of the ram with a view to keeping the machine free from vibration. The guides and levers that control the ram movement are arranged in such a way that the tilting of the ram due to the application of an eccentric load does not affect the position of the punch: this is achieved by placing the theoretical center of gravity of the ram at the tip of the punch.

Machines of smaller size such as bench-top machines may be built with newly enhanced elements/parts and/or designs particularly for micro-forming applications. This category of machine is of normal size but incorporating new concepts dedicated to micro-forming. A high-precision stamping press was developed jointly by Schuler,

PtU Darmstadt, ILT, IPA and other partners [17]. The machine has a modular arrangement and a high rigidity design. In this machine, linear motors are used for driving the ram. Linear driving has the advantage of high and reproducible accuracy. Lubrication is not needed and maintenance can be avoided, hence it is an attractive option for clean-room manufacturing. Other beneficial features include low noise emission and high reliability and endurance.

A new, low cost, bench-top machine dedicated for micro-sheet forming is being developed at the University of Strathclyde [8], in collaboration with its EU MAMSMICRO consortium partners (Fig. 8-10). A linear-motor driving mechanism is used. The maximum frequency of the machine is 1000 strokes per minute (spm), the maximum force is 5.3 kN, the vertical position resolution is 0.1 μm , and the load measurement resolution is 0.1 N.



FIGURE 8-10 A bench-top micro-sheet-forming machine, designed by the University of Strathclyde.

The machine enables the micro-stamping/forming of sheet-metal parts (ideally for sheet metals of a thickness of less than 100 μm). The machine has a maximum working space of 400 mm \times 400 mm with a flexible set-up, due to its modular design (the ram-driven form/power is changeable, without the need to change other machine set-ups; four machine-frame columns and supports to the ram guiding bridge can be repositioned according to the requirements, as well as the sheet metal feeder, and the part carrier). The bridge for guiding the ram is separated from the main machine frame, and hence it is not affected significantly by the deflection of the main frame and by vibration. Other innovations include monitoring the displacement directly on the tooling (therefore the punch stroke can be controlled more accurately), transporting the miniature/micro-parts directly out of the dies by a part carrier, a new vacuum/compression air chamber design, a new sheet metal holding design, etc. The machine design was supported by finite element dynamics analysis, which led to the development of a bench-top machine that has very good dynamic performance and machine stability (no connection to the bench is needed, and no significant vibration is felt on the shop floor).

Micro-forming may also be effected with micro-machines or similar set-ups, especially for research purposes. This category of machines is of much smaller size, compared to that of conventional, large-scale presses. The development of this type of machine has attracted much interest from researchers during the last ten years [18–19]. Various new concepts are being experimented with to design and fabricate prototypes of new micro-machines. Force may be effected with linear-motor actuation, piezoelectric actuation, piezoelectric/hydraulic actuation, electromagnetic launch and impact, etc. A micro-machine prototype using a working principle of incremental micro-forming has also been developed in Japan [14]. Small dents in sheet metal can be generated by hitting the metal with a small punch installed at the end of a swinging arm. By repeated hammering, incremental deformation can be achieved across small areas of thin sheets. Other

developments include the use of combinations of piezo-actuating with hydraulic devices to amplify the punch stroke [20–21], e.g. the piezoelectric-driven press developed by Zentrum Fertigungstechnik Stuttgart (ZFS), Germany. A mechanical micro-press has been developed by the Mechanical Engineering Laboratory [22], Ministry of Trade and Industry, Japan. The machine has a size of 111 mm \times 66 mm \times 170 mm, and is powered by an AC servo motor of 100 W rated power which can generate a force of up to 3 kN. The transmission is effected by a ball screw/nut structure, plus timing pulleys and belts. A micro-progressive die enables four blanking and two bending strokes. The stroke and speed of the machine can be controlled and 60 strokes per minute achieved.

DESIGN CONSIDERATIONS FOR MICRO-SHEET METAL PARTS FOR FORMING

Various metals are possible for making micro-sheet parts, including copper, brass, stainless steel, low carbon, mild and high strength steel, aluminum, nickel, etc. Fine grain sheet metals are preferable for micro-sheet forming, due to the reasons explained in Manufacturing Processes and Fundamentals, above. The description/characterization of material properties has to refer to the scaling factor for a particular part, material, process and tooling, the values of which are normally expected to be obtained through a series of tests/measurements. The strength, relationship of stress and strain, anisotropy factor, rate-dependent properties, springback behavior, thermal properties, etc. of the metal to be used are required to be corrected from the descriptions/definitions, which are based normally on a macro-scale.

General product design considerations include:

1. Thin sheet metal parts/structures should have sufficient strengths and stiffness, in relation to the functional and performance requirements;
2. Thin sheet metal parts should have good dimensional accuracy, with reference to the applications;

3. Thin sheet metal parts should have good surface finish, and precoating may be needed, depending on the application;
4. Relatively low cost manufacturing may be a key factor to be considered;
5. The design should consider the manufacturing constraints to the smallest features and tolerances, taking tool-making and tooling construction capabilities into account;
6. The design should consider the manufacturing constraints to the closeness of neighboring smaller features (minimum web sizes) and the number of features;
7. The design should consider the specific aspect ratios achievable in stamping, considering size effects in micro-stamping;
8. The design should consider specific bending radius, considering size effects in micro-bending;
9. The design should consider the limiting specific drawing ratios for deep drawing, and the feasibilities of redrawing, considering size effects in micro-deep drawing;
10. The design should consider the specific embossing/coining/denting ratios achievable in embossing/coining/incremental forming, considering size effects in these processes; and
11. The design should consider proper material selection and the availability of suitable materials, together with the 'size-effects' associated with their mechanical properties, surface/interface properties, and their influence on process design and tool design.

MICRO-SHEET FORMING – A CASE STUDY

In the following case study, the forming of a micro-sheet part – a sheet metal spring (Fig. 8-11), is described. The part has overall dimensions of 2.4 mm × 3.0 mm, a sheet thickness of 50 μm, and it is used in a micro-device. First, the part design was assessed and individual features identified for punching, blanking and bending/forming. Subsequently, the stamping techniques were examined in detail before developing a suitable strip layout for progressive die stamping of the part. Five-stage stamping was employed, which included:

1. Punching to create carrier tabs and holes for pilot pins;
2. Blanking to create two side slots;
3. Forming of a center curve (bending);
4. Forming of edge features (bending/bottoming);
5. Blanking of the final part.



Deformation
x 1e-1 mm
Max: 1.138e-002
Min: 0.000e+000
22/01/2007 13:18

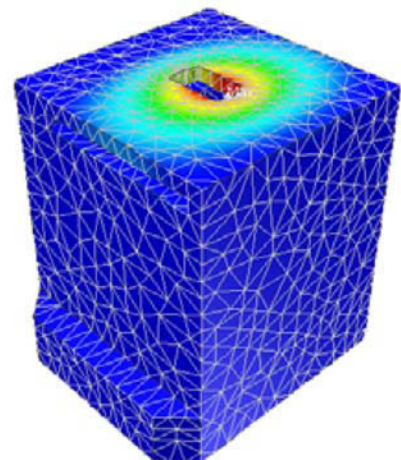
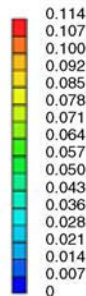


FIGURE 8-11 The sample part (left) and an FEA study on one of the micro-dies (right).



FIGURE 8-12 The micro-forming tool (left) and the micro-forming machine (right), developed at the University of Strathclyde.

The punch and die designs were supported with FE analysis (Fig. 8-11). A high speed tool steel (hardened to a value of 62-64 HRC) was selected to fabricate the individual punches and dies, which were created using mechanical milling, followed by μ -EDM, and then precision grinding to allow the required tolerances to be achieved. A dedicated micro-forming tool system with a footprint of 250 mm \times 160 mm was designed and fabricated (Fig. 8-12), with the individual punches and dies designed as inserts. The tooling incorporates a specially designed blank-holder to hold the strip during the stamping and four high precision ball race guide units as the primary means of aligning the punches and dies. The formed features were generated using polyurethane pads and profiled punches. The pads under pressure adopt the negative feature of the solid punch and form the material of the strip.

The micro-forming tool was designed for use in a dedicated micro-forming machine (Fig. 8-12), capable of providing high stamping rates (up to 1000 strokes per minute) while providing accurate control over the ram position. A load cell and positional encoder are integrated into the machine to allow for data collection from the stamping

process and, additionally, for monitoring of the punch force to indicate breakages or problems in the system.

Brass and stainless steel were both used to produce the micro-spring (Fig. 8-13). The scrap was collected through a vacuum system which is connected to the die blocks directly, while the parts were transported out of the final-stage die via a tape/reel transport arrangement [8].

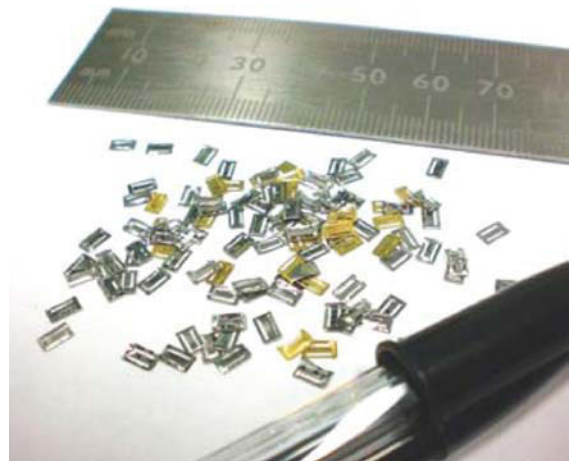


FIGURE 8-13 Samples of the formed micro-components in brass and stainless steel

TECHNOLOGICAL COMPETITIVENESS AND OPERATIONAL ECONOMICS

Micro-fabrication in the past dealt with largely silicon-based materials due to economic considerations and the unique properties of these materials for micro-devices and systems. There are now increased demands on non-silicon materials, e.g. polymers and metals, due to the need of multi-functional materials for the evolution of multi-functional micro-systems and devices. There are various technologies available for the micro-fabrication of metals, among these micro-sheet forming renders unique advantages over other technologies. At the same time, micro-sheet forming also competes with other technologies in the manufacture of micro-sheet metal parts, including photonic etching and electro-forming technology, electron-beam lithography etching, laser micro-machining. It will be difficult for micro-sheet forming to compete with photo-chemical etching/electro-forming, in the areas of fabricating 2D and 2.5D parts with smaller dimensions and finer features such as several to tens of microns in size, and thinner metal sheets, e.g. below 10 to 20 microns. Micro-sheet forming of these may be extremely expensive, or almost impossible to achieve. It is also difficult to compete with laser machining, in terms of the flexibility of the process set-up, the type of materials that can be processed, and when finer geometries are involved. Micro-sheet forming, however, is able to produce metal parts with better integrity, and less deleterious effects on the properties of the material. It is also ideal for producing various 3D structured parts and connections. Most importantly, it can be implemented at a mass production scale (for suitable component

forms) for which other processes/technologies cannot compete, if corresponding tooling technologies and machine capabilities are able to meet the manufacturing requirements. Good examples of applications include the high speed stamping of lead frames for electronics products and the stamping of micro-laminates for micro-motors, etc.

Table 8-1 presents a comparison of the costs quoted for using photo-chemical etching and micro-stamping, to produce a 2D flat sheet metal part.

Without considering other merits of micro-sheet forming, just referring to the manufacture of this particular part, the data presented in this table suggests that the investment on tooling for the first batch production is extremely high for micro-sheet forming. However, for producing over one million pieces of this part, micro-sheet forming does have an advantage. Considering the feasibility of producing 1000 pieces of such a part (simple micro-blanking) per minute with micro-stamping, the advantage of micro-sheet forming in mass production is evident. Such an example does, however, not suggest a general calculating principle, in terms of comparison of costing. It should depend on the actual component form to be considered. Currently, there is a trend in combining photo-chemical etching, laser machining and micro-sheet forming, in a process chain, to achieve the greatest efficiency of manufacturing.

The engineering applications of micro-sheet forming are not isolated issues. To enable realization of the potential of micro-sheet forming, in terms of its technological competitiveness and economic advantages, one should be able to manage the whole manufacturing and operation chain properly, including, in the chain, material supply and characterization of the material properties,

TABLE 8-1

Company	Technology	Quality	Quotation	Other Costs
A	Photo-chemical etching	10,000	£600	Tooling £125
B	Photo-chemical etching	10,000	£488	Tooling £395
C	Micro-stamping	10,000	£349	Tooling £20,000 (first batch)

stock preparation, forming process selection/design, forming tool selection/design and fabrication, machine selection/set-up, process/machine/tool control, material/parts/tool handling, post-processing, linking to other processes/equipment, etc. The quality of the sheet metal and the quality of the tooling are extremely important, especially for the forming of thin sheet metals (thickness below 100 microns), smaller part sizes (several millimeters) and finer features (sub-millimeters). Fine grain sheet metals could be expensive and the tooling cost could be extremely high, while the tool life could be very short, due to the fragility of the small tools employed, such as slender punches, etc. Therefore, the development of overall consideration for the manufacture of a particular part is needed, which should take a balanced view of the manufacturing economics.

REFERENCES

- [1] M. Geiger, M. Kleiner, R. Eckstein, N. Tiesler, U. Engel, *Microforming*, *Annals of CIRP* 50(2) (2001) 445–462.
- [2] F. Vollerston, Z. Hu, H. Schulze Niehoff, C. Theiler, State of the art in microforming and investigations into micro-deep drawing, *J. Mats. Proc. Tech* 151 (2004) 70–79.
- [3] U. Engel, S. Geißdörfer, *Microforming technology – on the way to industrial application*, Keynote paper, Proc. 1st Int. Conf. on Micro-Manufacturing, Urbana-Champaign, USA (Sept. 2006) 21–30.
- [4] EU Masmicro Consortium, *Project Technical Reports (2004-2008)*, NMP2-CT-2004-500095.
- [5] Y. Qin, *Micro-forming and miniature manufacturing systems – development needs and perspectives*, Keynote paper, 11th Int. Conf. of Metal Forming, Sept. 2006, *J. Mats. Proc. Tech.* 177 (2006) 8–18.
- [6] Y. Qin, *Development of an integrated manufacturing facility for mass-manufacture of miniature/micro-products*, Keynote paper, Proc. 1st Int. Conf. on Micro-Manufacturing, Urbana-Champaign, USA (Sept. 2006) 35–40.
- [7] Y. Qin, *Advance in micro-manufacturing research and technological development, and challenges/opportunities for micro-mechanical machining*, Keynote paper, The Cutting Tool Congress 2007, Milan (Nov. 2007) 1–8.
- [8] Y. Qin, Y. Ma, C. Harrison, A. Brockett, M. Zhou, J. Zhao, F. Law, A. Razali, R. Smith and J. Eguia, *Development of a new machine system for the forming of micro-sheet-products*, Proc. of the ESA-FORM Conf.
- [9] M. Geiger, F. Vollertsen, R. Kals, *Fundamentals on the manufacturing of sheet metal microparts*, *Annals of the CIRP* 45(1) (1996) 277–282.
- [10] M. Grünbaum, J. Breitling and T. Altan, *Influence of high cutting speeds on the quality of blanked parts*, Report No. ERC/NSM-S-96-19 (1996) The Ohio State University.
- [11] S.S. Kima, C.S. Hana, Y.-S. Lee, *Development of a new burr-free hydro-mechanical punching*, *J. of Mater. Process. Technol* 162–163 (2005) 524–529.
- [12] N. Matsushita, *Laser micro-bending for precise micro-fabrication of magnetic disk-drive components*, Int. Sympo. on Laser Precision Microfabrication, No. 4, Munich 5063 (2003) 24–29.
- [13] H.-W. Jeong, S. Hata, A. Shimokohbe, *Microforming of three-dimensional microstructures from thin-film metallic glass*, *J. of Microelectromechanical Systems* 12(1) (2003) 42–52.
- [14] Y. Saotome, T. Okamoto, *An in-situ incremental microforming system for three-dimensional shell structures of foil materials*, *J. Mats. Proc. Tech* 113 (2001) 636–640.
- [15] S.I. Oh, S.H. Rhim, B.Y. Joo, S.M. Yoon, H.J. Park, T. H. Choi, *Forming of micro channels with ultra thin metal foil by cold isostatic pressing*, 5th Japan-Korea Joint Symposium on Micro-Fabrication (2005) 50–54.
- [16] <http://www.bruderer.com/bruderer-high-performance-presses/bsta-300>, visited in May 2009.
- [17] http://www.schulergroup.com/de/05_Extras/02_Publikationen/Broschueren_Anlagen_Herstellung_Elektrobleche/Download_Anlagen_Herstellung_Elektrobleche/extras_download_flyer_schnell-laeuferpressen_stanzrapid_linearantrieb_d.pdf.
- [18] N. Mishima, K. Ashida, T. Tanikawa, H. Mae-kawa, *Design of a microfactory*, Proceedings of the ASME Design Engineering Technical Conference – 7th Design for Manufacturing Conference, Sept. 29–Oct. 2, Montreal, Que., Canada 3 (2002) 103–110.
- [19] Y. Okazaki, N. Mishima and K. Ashida, *Microfactory and micro machine tools*, presented in the 1st Korea-Japan Conference on Positioning Technology, Oct. 15-17, KIMM, Daejeon, Korea (2002) 1/6-6/6.
- [20] J.H. Park, K. Yoshida, Y. Nakasu, S. Yokota, *A resonantly-driven piezoelectric micropump for microfactory*, Proc. ICMT20002, Kitakyushu (2002) 417–422.
- [21] A. Hess, *Piezoelectric driven press for production of metallic microparts by forming*, ACTUATOR 2000, 7th International Conference on New Actuators, June 19-21, Bremen (2000) 427–430.
- [22] <http://www.mel.go.jp/>.

Micro-Hydroforming

Christoph Hartl

INTRODUCTION

Hydroforming is a metal forming technology based on the application of pressurized liquid media to generate defined workpiece shapes from tubular materials or sheet metals. Numerous industries, for example the manufacturers of automotive components and the piping industries, which are providing mass products, apply this technology productively today [1]. This successful adoption of hydroforming technology results from the advantages that hydroforming offers in comparison to conventional techniques such as the assembly of stampings by welding. Hydroforming provides the possibility to form hollow complex-shaped components with integrated structures from single initial workpieces, combined with improvements in stiffness and strength behavior due to the reduction of welding seams, and with reduced assembly costs [1].

Due to an increasing integration of micro-system technology into products of electronics, telecom and medical devices for an ever-growing market, efficient and timesaving production technologies for micro-components become increasingly more important. Against this background, metal forming plays a decisive role for the mass production of respective components because it can offer the required productivity and accuracy. Concerning the mass production of hollow-shaped micro-components, this applies to hydroforming technology in cases where the manufacture of such parts currently still largely relies on time-consuming techniques

based on the removal of material, either by chemical or mechanical means. Important existing technologies for the manufacture of complex-shaped hollow miniature and micro-components made from metals are, for example, techniques using electrodeposition of metal materials on subsequently removed mandrels (electroforming) [2] or rapid manufacturing techniques such as selective laser melting of metal powder (SLM) [3]. Although these processes can offer the fabrication of high precision components, their application is limited to small and low volume production due to a comparatively high cycle time. Techniques working with the assembly of micro-surface structured component halves (for example, structured by laser or etching processes) which are used for the production of hollow-shaped metal parts are predominantly restricted to planar workpieces. Also micro-injection molding techniques (MIM) [4] enable the manufacture of complex-shaped components; however, these are limited to those with comparatively simple hollow inner shapes due to restricted possibilities in core design.

The design and optimization of micro-hydroforming processes require knowledge of the fundamentals to determine the necessary process loads, to estimate feasibility, and to obtain an improved comprehension of influences on the reliability and quality of component manufacturing. Additionally, size effects have to be taken into account when scaling down conventional hydroforming processes to micro-size. The objective of

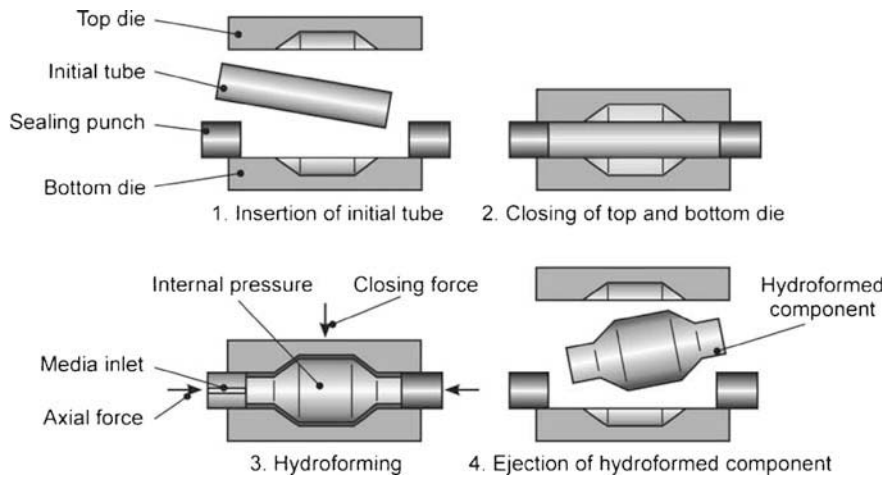


FIGURE 9-1 Hydroforming principle.

this chapter is to provide an overview of the respective hydroforming fundamentals and detailed information relevant for the practical application of micro-hydroforming.

PRINCIPLE OF HYDROFORMING AND PROCESS VARIANTS

Concerning existing hydroforming processes, a general distinction is to be drawn between the forming of tubular material such as straight as well as bent tubes or profiles, and the forming of sheet material, for example single or multiple sheets. Currently, tubular material is predominantly applied for the manufacture of hydroformed components. The principle of these hydroforming processes is represented in Fig. 9-1. At the beginning of the process the initial part is placed into a die cavity which corresponds to the final shape of the component. The dies are closed with the closing force F_c while the tube is internally pressurized by a liquid medium with internal pressure p_i to effect the expansion of the component. Additionally the tube ends are axially compressed by sealing punches with axial force F_a to force material into the die cavity. The component is formed under the simultaneously controlled action of internal pressure and axial force. Water/oil emulsions are typically used media to apply the internal pressure, which is usually

increased to 1200 up to 4000 bar. The necessary amount of internal pressure is influenced significantly by the wall thickness of the component and the material strength and hardening, as well as by the component shape [1].

Further mechanical loads can be applied to the workpiece, depending on the part and process type. An example is the hydroforming of T-shaped components, as shown in Fig. 9-2. This process requires an additional counter-punch with a suitable control of the counter force F_g during the forming process. The counter-punch acts on the end of the expanded protrusion and is displaced by the workpiece when the hereby exerted force achieves the current level of the counter-force.

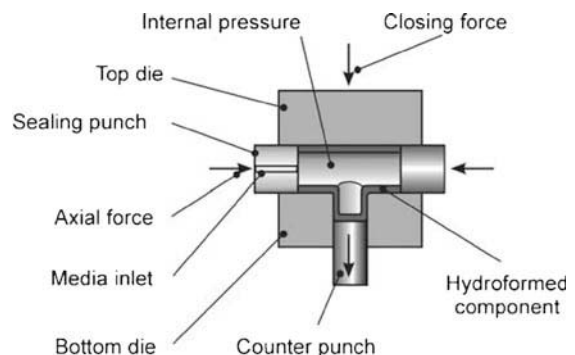


FIGURE 9-2 Principle of T-piece hydroforming.

Regarding the currently applied hydroforming process types, in [5] a first classification has been developed considering the acting stress state within the formed workpiece region and the specific characteristics of the expanded geometry. Based on this work, classifying engineering standards have been enhanced and updated regarding the description of hydroforming processes, for example the engineering standard of manufacturing technologies DIN 8580, published by the German Institute for Standardization (DIN).

For conventional hydroforming processes the integration of additional manufacturing operations in the hydroforming process itself is used to improve productivity. Industrial hydroforming tools are often equipped with numerous piercing units to create holes for bolts, drain holes, reference points, collar formed holes, etc. [6]. Additionally, assembly operations within the hydroforming process have been shown to be feasible, for example, cam shafts [7,8].

SEMI-FINISHED PRODUCTS AND MATERIALS

Currently, predominantly steel alloys and aluminum alloys are used as materials for the required semi-finished products in hydroforming production. Copper and brass alloys are used for hydroformed products in the piping and sanitary industry. The applied alloys correspond in the majority of cases to materials which are used for common cold forming processes such as deep drawing or mass forming. In principle, all metal materials with sufficient formability are suitable for semi-finished products in hydroforming processes. A fine-grained structure combined with large amounts of uniform elongation and elongation at fracture and a large strain-hardening coefficient are advantageous in the feasible expansion of the initial workpiece, achievable without the occurrence of material instabilities. The strength of the final component is improved by a distinctive work-hardening of the formed material; however, work-hardening also causes an increase in the required forming loads.

Steel alloys used or tested for conventional hydroforming components are ductile low carbon steels, case-hardened steels, heat treatable steels, ferritic and austenitic stainless steels as well as high strength and ultra-high strength steels, for example [9]. In general, tubular steel materials which are used for hydroforming applications are produced from flat sheet material by continuous roll forming and longitudinal high frequency welding to close the roll formed tubular cross-section. Tubes with circular cross-section as well as profiles which differ from a circular shape are able to be generated by the roll forming process using appropriate roll forming tools. However, predominantly semi-finished products with circular cross-sections are currently in use for the hydroforming production of steel components. Typical dimensions of conventionally hydroformed steel tubes are outer diameters d_0 between about 20 mm and 140 mm with ratios of wall thickness to outer diameter t_0/d_0 between about 0.012 and 0.16. Regarding micro-hydroforming, the market currently provides roll formed and welded metal micro-tubes with minimal outer diameters of about 0.2 mm and minimal wall thickness of about 0.03 mm.

When selecting appropriate tubes for hydroforming processes, a distinction is to be drawn between tubes without an annealing process after cold forming by roll forming or drawing, tubes drawn with a small resulting strain after a preceding annealing process and tubes annealed after the final cold forming operation. Drawing processes, following the roll forming operation, serve for the adjustment of the final tube diameter and/or wall thickness as well as providing an increase in strength due to work-hardening effects.

Drawn and non-annealed tubes commonly provide reduced formability in hydroforming processes, depending on the characteristics of the steel alloy used and the amount of strain induced by the drawing operation. Tubes which have been drawn with a small resulting strain after annealing show a cold formability within certain limits. The most extensive cold formability is obtained by the use of tubes which have been annealed after

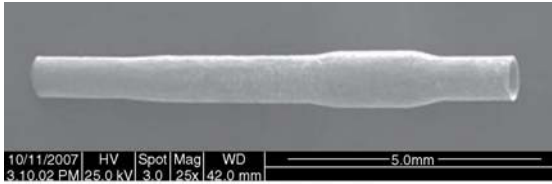


FIGURE 9-3 Micro-hydroformed component.

the final cold forming operation such as roll forming or drawing.

To avoid premature bursting of the workpiece within the hydroforming process, a highly satisfactory weld seam quality is required for roll formed and welded tubes. It is recommended to avoid locating the weld seam in the final hydroformed component within areas where excessive tensile stresses due to the expansion are acting on the component during the hydroforming process.

Figure 9-3 shows an example of a hydroformed micro-prototype part made from a solution annealed stainless steel tube. The initial tube with an outer diameter of 0.8 mm and a wall thickness of 0.04 mm had been manufactured by continuous roll forming and subsequent drawing and annealing processes.

Concerning the use of aluminum alloys for conventional hydroforming applications, work-hardening aluminum 5000 alloys are currently used when priority is given to a high amount of formability and corrosion resistance, whereas precipitation-hardening aluminum 6000 alloys are applied for components requiring high strength, e.g. [10]. In general, tubes made from aluminum 5000 alloys are manufactured from flat sheet material by continuous roll forming with longitudinal welding, whereas aluminum 6000 alloys are produced as extruded profiles. Extruded profiles offer advantages in design flexibility for complex cross-sections with sharp corners, multiple hollows and flanges. However, the reduced formability of these semi-finished products has to be considered when designing a respective hydroforming component. Additionally, the selection of extruded material for hydroformed micro-components is currently restricted by the minimal cross-sectional dimensions that

can be produced by the relevant industries. Currently, the manufacturing of micro-extruded profiles as semi-finished products is the subject of several investigations, for example [11].

Due to their high strength-to-weight ratio, magnesium alloys offer a great potential for weight-reduced components. However, the use of these alloys in forming processes working at room temperature is limited due to their hexagonal atomic structure. An improvement in formability is achieved by the use of increased temperatures, above about 200 °C, when additional gliding planes become activated. Against this background, various investigations into the conventional hydroforming of semi-finished products made from magnesium alloys by the use of an elevated temperature have been carried out during the last few years, e.g. [12].

The design of hydroforming processes as well as the monitoring of semi-finished product quality in hydroforming production require suitable and reliable methods to obtain material parameters characterizing the forming behavior. Concerning conventional tube hydroforming, predominantly traditional material-testing methods are currently in use, such as tensile tests, mechanical expansion methods, and grid analysis. However, the suitability of these methods is often limited, as the typical biaxial stress state in hydroforming processes is not, or is only approximately, reproduced.

Most common in use to characterize the forming behavior of the applied tubular material is the tensile test which is a standardized uniaxial material test method. A distinction is to be drawn between the application of this test to the initial sheet material before roll forming and the application to the roll formed and welded workpieces. Testing the initial sheet material means that changes in material properties due to the manufacturing process of the tube remain unconsidered.

A method for strain analyses in hydroformed components consists in the application of circular or quadratic grids on the surface of the initial semi-finished product. The measured distortion of the individual grid elements at the hydroformed workpiece enables the determination of local

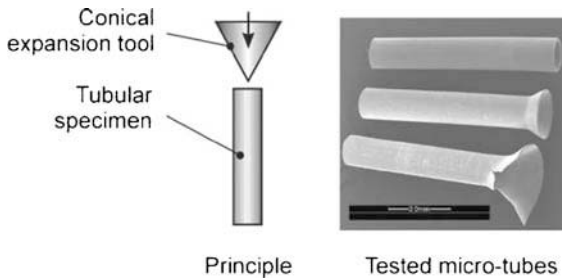


FIGURE 9-4 Expansion cone test and experimental results.

strains, which provides an assessment of the hydroforming process when comparing the analyzed strains with the forming limit curve of the respective tube material, e.g. [13]. There are restrictions in the use of this method in micro-hydroforming processes due to the minimal applicable grid size on micro-tubes.

An example of a standardized mechanical expansion testing method is the cone test, where the end of the investigated tube is expanded by a conical punch until fracture occurs. This test enables the principal determination of formability, for example to compare different batches of tubular material. Also, failures at the tube surface or within the weld seam are able to be detected. When applying this test method it has to be taken into consideration that variations in friction conditions or unequal prepared surface roughness at the tube end face influence the initiation of fracture of the expanded tube section. Figure 9-4 shows results of mechanically expanded micro-tubes made from stainless steel AISI 304. These solution-annealed tubes with an outer diameter of 0.8 mm and a wall thickness of 0.04 mm showed

a possible expansion of the initial tube diameter by this test method of about 33% [14].

To improve methods for the characterization of tubes for hydroforming applications, several investigations have been carried out into tube expansion tests working with an inner pressurization of the tested tube, which is clamped at its ends according to Fig. 9-5. This bulge test enables the determination of the bursting pressure p_b , the pressure-dependent expansion diameter $d(p_i)$ and the achievable expansion diameter d_r under the biaxial tensile stress state. Strategies to determine the material properties of tubes as well as their yield curves based on the bulge test have been developed, for example in [15] and [16]. When applying the bulge test, it has to be taken into consideration that the ratio of the expanded tube length l_d to the tube diameter d_0 influences the required pressure to expand a tubular specimen, if the ratio l_d/d_0 is below a certain limit [17,18]. The bulge test device shown in Fig. 9-5 has been developed for the testing of micro-tubes with outer diameters below 1 mm and is suitable to apply up to 4000 bar of internal pressure [19].

PROCESS CHAIN FOR PART PRODUCTION

Depending on the component design, the industrial production of hydroforming parts requires several additional manufacturing steps in addition to the hydroforming process itself. Figure 9-6 shows schematically a typical process chain for the manufacture of hydroformed components.

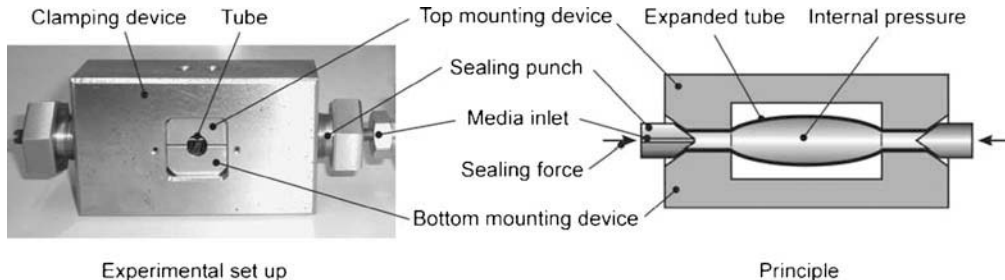


FIGURE 9-5 Bulge test device for micro-tubes.

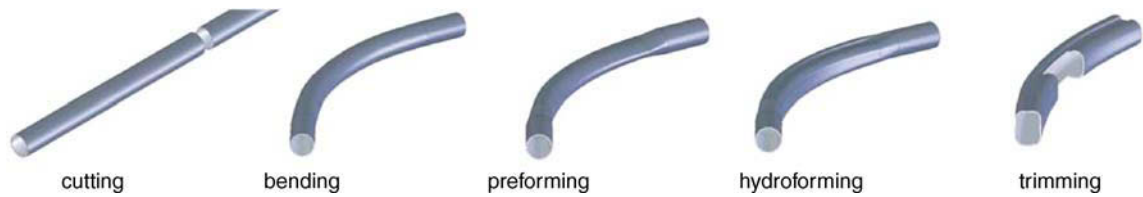


FIGURE 9-6 Typical process chain for the production of hydroformed components.

The basic part of the process is the tube, which has to be cut to length in a first step. A comparatively high standard of quality for the cut tube ends is required to ensure reliable sealing during the hydroforming process. In general, tubes with conventional dimensions are cut and machined by sawing or mechanical cutting. However, the damage-free machining of thin-walled structures such as micro-tubes and micro-hydroformed components requires processes with a minimum of forces for clamping and processing. In general, lasers are predestined for the here-required operations because of their contact-free function. Also, cutting by wire EDM provides reliable cut surfaces.

In the majority of cases the complexity of the components requires that additional forming operations are to be applied preceding the hydroforming process. These operations can consist of bending and mechanical forming (preforming) of the initial component to enable its insertion into the hydroforming die or to obtain an optimized material distribution. Typical bending processes are in general rotary draw bending for complex

bent components and press bending for less complex shapes with large bending radii [6]. However, it has to be taken into account that due to a preceding bending process of the initial tube, the wall thickness is decisively reduced within the outer bent areas and formability is exhausted to a large extent [20]. As a consequence, these workpiece areas tend to fail prematurely by necking and bursting. The increase of corner radii and/or the reduction of the overall expanded cross-sectional circumference are recommended to avoid the appearance of these instabilities.

In cases where the initial tube diameter d_0 is larger than the die cavity width w a preforming operation is necessary to enable the reliable insertion of the initial workpiece into the hydroforming die. The preforming operation induces the reduction of the tube dimension within these areas in the direction of w . Typically used methods for preforming operations are shown schematically in Fig. 9-7. For the preforming of straight as well as bent tube sections, methods working with beveled dies according to Fig. 9-7(a) are suitable to be

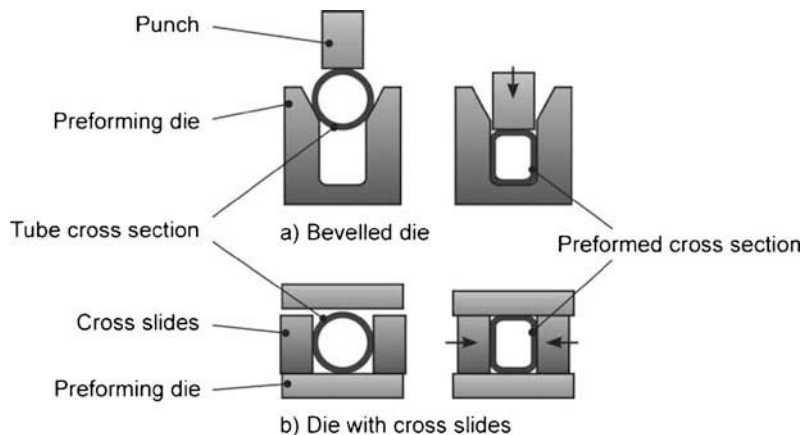


FIGURE 9-7 Principles of performing.

applied. In contrast to this, methods using cross slides for local workpiece reduction are limited when bent tube sections are to be preformed, Fig. 9-7(b). In certain cases preforming is also used to flatten tube sections, for example when a flattening by closing of the hydroforming tool is not reliably feasible. Limits of preforming can consist in shape deviations which are caused by this operation and which remain after the hydroforming process, for example wrinkles due to an inappropriate material distribution or excessive small radii generated by local folding of the tube wall. Also excessive elastic springback of flat workpiece sections can occur due to an insufficient forming degree within the hydroforming process.

The following hydroforming of the preformed workpiece takes place by the controlled application of the forming loads p_i and F_a . Commonly, these process parameters are determined versus the time of the forming process. The suitable variation of internal pressure and axial force depends predominantly on the material properties and strain-hardening behavior, on the tube wall thickness, on the sizes of intricate sections of the component such as small corner radii, and on the potential occurrence of instabilities.

Further operations such as trimming, notching or additional forming may need to be performed subsequent to the hydroforming process, for example to enable the connection to other components by welding. For hydroformed parts with conventional dimensions, trimming operations consist in sawing, milling, mechanical cutting or laser machining, depending on the required shape and quality of the component ends. Regarding micro-components, similarly to the cutting of the initial micro-tubes, lasers are suitable for final trimming and cutting operations due to their contact-free and flexible processing method.

HYDROFORMING PROCESS DESIGN

The design of process control for the forming loads during the hydroforming operation should be suitable to obtain the required forming result due to a continuously achieved yield stress of the

material under the avoidance of failures such as wrinkling, buckling and bursting. The internal pressure p_i and the axial force F_a are the decisive parameters of the process control.

Currently, fundamentals to determine the correlation between applied loads and forming result have been developed predominantly for the conventional hydroforming of straight rotationally symmetrical workpiece shapes and of T-piece components, for example [17,21–24]. The methods used to derive applicable solutions have been the Membrane Theory, the Theory of Shells and the Continuum Theory of Plasticity in the majority of cases. Due to the further development of commercial programs based on the finite element method within the last few years the detailed and efficient analysis of forming processes where the component shape differs from parts with round cross-sections and a straight axis is feasible currently [20].

However, the predominant part of investigations conducted up to the present considered conventional dimensions of formed tubular material and component geometry. From fundamental research work into the miniaturization of manufacturing processes it is known that size effects have to be taken into account when scaling-down forming processes [25]. Hence, common correlations for the determination of process loads existing for conventional hydroforming processes have to be verified and possibly adapted when being applied to micro-hydroforming processes. The use of scale factors is one option to consider such size effects in forming processes [26]. Investigations into the influence of size effects in micro-hydroforming processes are being carried out currently [14]. To provide here a general basis to determine process parameters for micro-hydroforming, correlations are given in the following, which have been proven for conventional hydroforming.

Based on the Membrane Theory, which considers a biaxial stress state, the condition for the initiation of yielding of a cylindrical straight tube under axial force F_a and internal pressure p_i and the resulting stress state can be derived [17]. The circumferential stress σ_θ and the axial stress σ_z

within a thin-walled straight tube can be determined accordingly with:

$$\sigma_{\theta} = p_i \frac{d_0 - t_0}{2t_0} \quad (1)$$

$$\sigma_z = \frac{1}{\pi(d_0 - t_0)t_0} \left(p_i \frac{\pi}{4} (d_0 - 2t_0)^2 - F_a \right) \quad (2)$$

for an initial outer tube diameter d_0 and an initial tube wall thickness t_0 . Plastic yielding of the tube starts when the effective stress σ_{eff} , which results from the combination of axial and circumferential stresses, corresponds to the local yield strength σ_Y of the tube material with:

$$\sigma_{eff} = \sqrt{\sigma_{\theta}^2 + \sigma_z^2 - \sigma_{\theta}\sigma_z} \quad (3)$$

according to the von Mises Yield Criterion. These equations enable the derivation of the correlation between the internal pressure p_i and the resulting axial force F_a , which is suitable to induce plastic deformation of the tube as follows [17]:

$$F_a = \pi(d_0 - t_0)t_0 \left[\sqrt{\sigma_Y^2 - \frac{3}{16}p_i^2 \left(\frac{d_0 - t_0}{t_0} \right)^2} - p_i \frac{d_0 - t_0}{4t_0} \right] + p_i \frac{\pi}{4} (d_0 - 2t_0)^2 \quad (4)$$

To ensure the sealing of the workpiece ends during the overall process a minimum axial force is required which can be determined with:

$$F_p = p_i \frac{\pi}{4} (d_0 - 2t_0)^2 \quad (5)$$

If the axial force F_a is less than F_p , leakage between the hydroformed tube ends and the sealing punches occurs and with this a pressure loss.

In the final stage of the hydroforming process the tube wall has to be formed into the corner radii of the die cavity, which was not formed during the main expansion of the tube. This is achieved by raising the internal pressure up to its maximum value p_k . Several theoretical and experimental investigations have provided correlations to determine this necessary calibration pressure, for example [27]. An empirically deduced equation suitable

for a first estimation to determine the maximum necessary internal pressure is as follows [28]:

$$p_k = 1.2\sigma_{UTS} \frac{t_0}{r_c} \quad (6)$$

with the ultimate tensile strength σ_{UTS} of the formed tube material, the tube wall thickness t_0 , and the minimal outer radius r_c which has to be formed.

The axial force F_a throughout the hydroforming process up to its end can be generally made up of three individual forces [29]:

$$F_a = F_z + F_p + F_f \quad (7)$$

The force F_z is the axial force component which is initiated in the tube wall and maintains, together with the action of the internal pressure, the plastic flow of the tube wall. F_p is the minimum sealing force according to Equation (5). The force F_f is the frictional force that must be overcome throughout the forming process due to the contact between the tube ends with the hydroforming tool.

For practical use the required force F_z can be estimated by:

$$F_z = (1.2\sigma_{UTS} + p_i)\pi t_0(d_0 - t_0) \quad (8)$$

with the initial tube dimensions d_0 and t_0 and the ultimate tensile strength σ_{UTS} .

When Coulomb's frictional behavior is taken as a basis, the following correlation to determine the friction force F_f in practical cases can be used:

$$F_f = \mu p_i d_0 \pi l_f \quad (9)$$

with the coefficient of friction μ , the tube diameter d_0 in the feeding zone and the length l_f where frictional movement occurs.

The maximum values for the axial force and the internal pressure are commonly applied at the end of the forming process when the workpiece is calibrated with an increase in the internal pressure up to the magnitude of the calibration pressure p_k . Component-specific correlations to determine the axial force have been derived, for example in [17], for the hydroforming of rotationally symmetrical

components and in [24] for the forming of T-shaped parts.

The occurrence of failures limits the applicable forming loads F_a and p_i and with this the feasible workpiece geometries produced by hydroforming processes. These instabilities are predominantly local necking and bursting of the workpiece wall, local or extensive wrinkling of the workpiece, and buckling of the initial tube [5].

Necking is caused by a locally exceeded formability of the workpiece material and introduces the bursting of the hydroformed workpiece. To predict the internal pressure p_b at the moment of the bursting of straight tubes within the state of free expansion, the correlation investigated in [17]:

$$p_b = \sigma_{UTS} \frac{2t_0}{d_0 - t_0} \quad (10)$$

has shown to be applicable for conventional tube hydroforming. Regarding the expansion of straight tubes, the bursting pressure p_b should not be exceeded within a hydroforming process as long as the tube is not in contact with the surrounding die cavity. Only if large areas of the expanded tube received alignment to the die cavity, can internal pressure be increased beyond p_b . Bursting and preceding necking predominantly occur within the area of largest expansion. In general, an increase in axial force F_a , within certain limits, raises the feasible expansion until necking and bursting are induced due to the resulting increase of axial compressive stress within the tube wall [2,17,22,23]. However, it has to be taken into consideration that long feeding sections and bent workpiece areas, where workpiece material has to be transported by the axial force into the area to be expanded, impedes the material flow due to friction forces and additional bending forces [29]. In the case of complex-shaped components with varying cross-sections along the workpiece axis, bursting induced by necking predominantly occurs within the areas of cross-section corners. Additional to the influences from the process control and hydroformed component geometry, the occurrence of necking and

bursting can also be induced by the properties of the applied semi-finished product which result from their manufacturing process. Welding seams at longitudinally welded tubes or extruded profiles can be the starting points of these failures, for example.

Wrinkling of the component wall results predominantly from excessive axial load. Due to this possible failure case, the applicable axial stress to reduce the decrease in wall thickness during the hydroforming process is limited. An adapted control of axial force and internal pressure has to be applied to avoid this instability. Wrinkles in the longitudinal direction of the workpiece can be caused during closing of the hydroforming tool when improper dimensions for the semi-finished product or for the preformed component geometry have been selected.

In cases of comparatively long free-tube length, unsupported by surrounding tool surfaces, buckling of the workpiece can occur due to an excessive axial load. Also here, the application of an adequate control of axial load and internal pressure is required to avoid this failure case. In [30] an iterative method is presented to determine suitable load paths for the hydroforming of rotationally symmetrical workpieces with a maximum of compressive stress, derived on the basis of the determination of buckling with plastic material behavior.

The geometric parameters of the initial tube, the workpiece and the tool as well as the tube material properties and friction conditions influence the range of failure-free process controls for the forming loads F_a and p_i . Figure 9-8 shows schematically the range for feasible process controls for a hydroforming process limited by the occurrence of instabilities, the initiation of yield of the workpiece and the minimum required force to seal the tube, according to investigations reported in [17].

In [31] and [32] examples of achievable workpiece geometries within the here-discussed forming limits, considering comparatively satisfying formability of the component material and reliable and economic production, have been presented for conventional hydroforming.

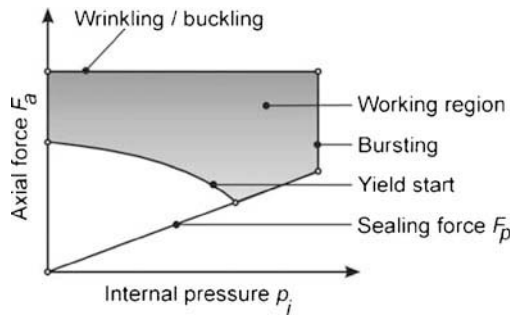


FIGURE 9-8 Range of feasible process controls (schematic).

DESIGN CONSIDERATIONS AND POTENTIAL APPLICATIONS OF MICRO-HYDROFORMING

Attributes which micro-components should have to be appropriate for a hydroforming production consist of:

1. a tubular shape with hollow cross-sections;
2. changes in circumferences along the axis which are below the limits of possible expansion;
3. material properties which provide a reasonable formability;
4. a geometry which enables smooth die cavities with large corner radii to be formed by the hydroforming process to avoid uneconomic high internal pressures and high stresses within the tool elements;
5. an adequate ratio of wall thickness to tube diameter t_0/d_0 between 0.05 and 0.16 to ensure an economic amount of necessary internal pressure and to enable handling of the workpieces free of damage; and
6. comparatively rough tolerances demanded for inner dimensions [14].

For materials with a comparatively good formability an expansion of 10% in circumference is feasible without an axial feeding of material and up to 30% is to be expected when axial forces are applicable to the component ends. However, corresponding to forming limits in conventional hydroforming [6], expansions within pre-bent tube sections should be avoided.

Micro-hydroforming offers the potential for the production of a wide range of products from

the fields of *medical engineering* (e.g. needles and microtubes for drug delivery, micro-pipettes, tubular parts for endoscopes or elements for surgical tools), *micro-fluidics* (e.g. components for micro-fluidic chips, elements for micro-dosage or pipe connections and housings), and *micro-mechatronics* (e.g. shafts and elements for micro-actuators, components for micro-sensors or connection pins). However, certain design changes of such products with an adaptation to the micro-hydroforming process will be required to enable a failure-free and reliable production by hydroforming.

TOOLS AND MACHINES

In addition to the applied process parameters and the quality of the tubular blanks used, the final quality of the hydroformed components is decisively influenced by the design of the hydroforming tool and the hydroforming machine. Also, production parameters such as cycle time, production reliability, equipment availability and production costs depend on their design.

One important difference between hydroforming and other forming processes is the comparatively high level of loads acting on the tooling due to the closing force F_c and the internal pressure p_i . The minimum closing force which is required throughout the forming process to ensure that the hydroforming tool remains closed can be determined as follows:

$$F_c = p_i A_p \quad (11)$$

with the projected component surface A_p perpendicular to the closing direction, and the applied internal pressure p_i .

The acting loads generate elastic deformation of the tool elements which crucially influences part quality and tool lifetime. Figure 9-9 presents a schematic drawing and an example of hydroforming tooling for mass production with its essential components. The tool inserts, which contain the die cavity, are in general made of heat-treated tool steel to ensure a sufficient lifetime and wear resistance of these elements. The

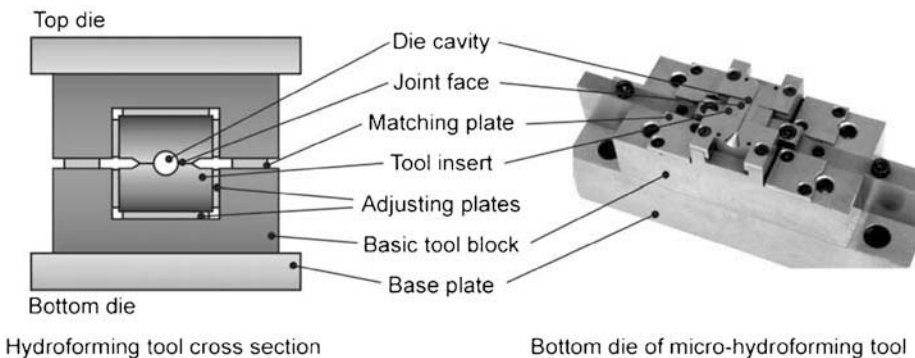


FIGURE 9-9 General design of micro-hydroforming tools.

stresses within die inserts, resulting from the acting loads, are essentially influenced by the size of the corner radii of the die cavity, the positioning of the joint face between the top and bottom die, which determines the depth of the die cavity, and the surface quality of the die cavity [6]. On principle, the design of die inserts with deep cavities, small corner radii and rough surfaces should be avoided. Due to these factors the stresses within the inserts increase and, if a critical stress state is exceeded, fracture after a low number of cycles is the consequence. When positioning the joint face in the course of the tool design, it has to be taken into consideration that: (a) the initial component is able to be inserted into the bottom die without problems; (b) no undercuts exist within the die cavity; and (c) the hydroformed component is able to be removed failure free from the die cavity.

In general, part handling in automated conventional hydroforming production processes is done by robots equipped with grippers for the insertion of the initial tube into the tooling and to remove the hydroformed part from the tooling. Both actions, insertion and removal, are in most cases supported by so-called ejectors which are integrated into the top and bottom hydroforming tool halves [33]. These ejectors can be lifted and moved inwards when the initial tube is inserted and they can be lifted to eject the part. Through lifting the part, a space is opened for the grippers to reach the workpiece. The disadvantages of ejectors are that they produce markings on the workpiece and that they reduce the stiffness of the

tooling due to the necessary cut-outs within the die in which to place the necessary drives. Additionally, micro-hydroforming tools often allow a limited space for the integration of ejectors. Alternative concepts for efficient part removal for micro-hydroforming can consist in grippers which take the component at its ends out the tooling while the tool is set in vibration to reduce the friction between the tool and the component and, with this, the forces for removal.

Adjusting plates, covering the contact areas between the basic tool blocks and the integrated tool inserts, serve to adjust the correct position of the die insert elements relative to each other and to the axis of the sealing punches. The basic tool blocks are commonly made of heat-treatable steel with a strength that is lesser in comparison to the strength of the tool insert.

Figures 9-10 shows examples of several design principles for the sealing of tubes during hydroforming from conventional practical applications and research works. In general, axial sealing punches are made from hardened tool steel. Punches working with rubber elements, Figs. 9-10(c) and (d), have shown an insufficient wear resistance in practical use for series production. Conical punches, as presented in Fig. 9-10(b), show good behavior regarding sealing and wear resistance but do not enable the axial feeding of tube material into the die cavity. A suitable punch design proved in a practical series production is represented in Fig. 9-10(a). Here the sealing occurs mainly due to a sharp corner surrounding the contact area between the punch and

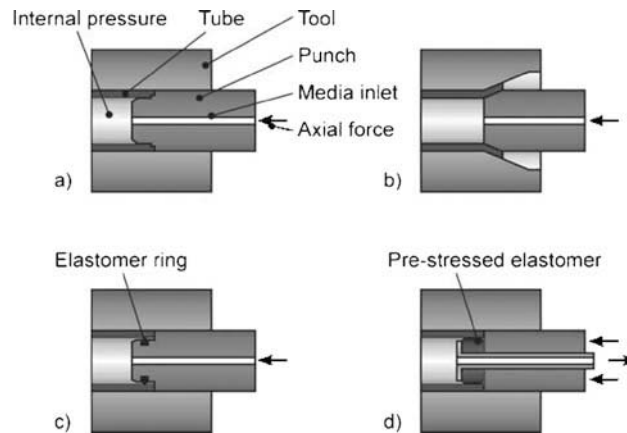


FIGURE 9-10 Sealing principles.

the tube end. When the punch comes into contact with the tube end, this corner is pressed into the tube front and thereby creates the sealing. A general problem of axial sealing punches is their reduced durability due to the high level of stresses generated by the applied loads. The lifetime is mainly influenced by the level of loads, the tool material used, the surface roughness of the punch, the size of corner radii at the punch in critical areas, the size of the bore to feed the pressurizing media into the tube, and by additional bending moments acting on the punch which can result from elastic tool deflection caused by the closing force.

The hydroforming tool is mounted on the hydroforming machine, which performs the required actions and movements to conduct the forming process. The main tasks of this machine are:

1. to open and close the tool for part insertion and removal;
2. to provide the required closing force F_c during the forming process;
3. to close the component ends using the axial sealing punches;
4. to fill the component with the pressurizing media;
5. to apply the internal pressure p_i according to a specified pressure/time curve;
6. to move the component ends for material transport by means of the axial sealing punches by applying the force F_a according to a specified stroke/time curve; and

7. to communicate with the handling system for component handling.

According to the tasks to be executed, hydroforming machines consist of corresponding sub-assemblies, as shown schematically in Fig. 9-11. The predominant part of these sub-assemblies is mounted on the press frame, which has to provide sufficient stiffness against the loads to resist deformation and displacement of the structure and an adequate accessibility for part handling and die changing.

The opening and closing of the tool as well as the application of the closing force is in general conducted by one single drive. The requirements of this drive are a sufficiently high translational speed to enable short production times, and enough force to close the hydroforming tool. It is recommended to synchronize the level of the required closing force with the currently applied internal pressure. This control strategy reduces tool deflection and improves with this the quality of the component produced. Hence, precision for force control of the drive is expected to be comparatively high whereas precision of stroke control is secondary. When selecting a suitable drive it has to be taken into consideration that the maximum force is applied without movement. Under these conditions hydraulic cylinders are suitable for use as drives. Additionally, the overall stroke of the drive should be able to afford sufficient space for comfortable and fast tool changing

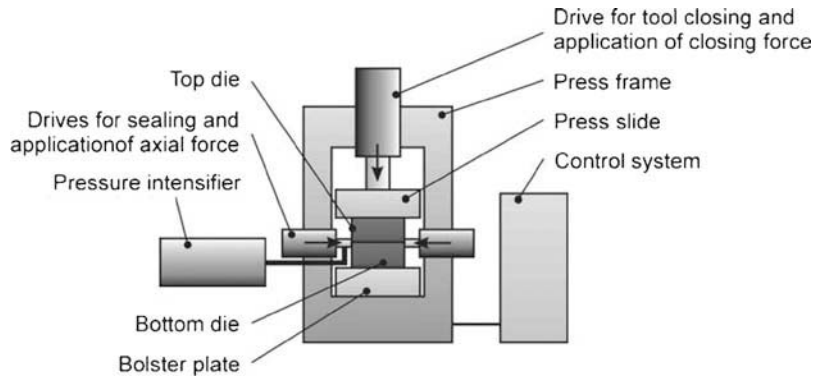


FIGURE 9-11 Elements and functions of the hydroforming machines.

and part handling. It should be mentioned here that for conventional hydroforming applications also, machine concepts exist which use one drive for a fast movement of the top die and a second drive with short stroke to apply the closing force [1].

The internal pressure p_i is applied by a pressure intensifier which is integrated into the high pressure system, consisting of valves, piping, equipment for media supply and maintenance such as filters and tanks, and of the pressurizing medium. Due to the reduced volume of hydroformed micro-components, the required volume flow of the intensifier is comparatively small. However, depending on the component to be formed and its material, the required pressure is reasonably high. Pressure intensifiers can be driven mechanically, e.g. a spindle-driven plunger with an electric motor, by hydraulic power, or by air pressure. The systems differ in minimum and maximum provided volume flow, achievable maximum pressure, and control accuracy.

Regarding the applied pressurizing media, predominantly water/oil emulsions, solutions based on water and in a few cases pure oil, are in use as the pressurizing media. The applied water/oil emulsions and the solutions consist in general of about 95% to 98% water. The water-based systems have the advantage of a negligible compressive behavior whereas oil shows comparatively high compression under high pressure, which can influence the process control. Solutions show an improved resistance against micro-organisms

in comparison to emulsions. Pure oil provides immunity against micro-organisms and good corrosion protection. Additionally, a crucial criteria for the decision of a suitable pressurizing medium is the pressure loss of the fluent liquid medium under increased pressure flowing through narrow bores, as is necessary for micro-hydroforming when providing the medium through the axial sealing punch into the workpiece [34]. In general, liquids with higher viscosity show an increased pressure loss.

The primary function of the axial driving system is the axial movement of the sealing punches toward the tube ends to ensure leakage-free sealing of the pressurized tube during the hydroforming process. The secondary function comprises the axial feeding of the tube material into the die cavity during the forming process to enable an extended formability of the tube. For example, linear actuators with a gear spindle can be used to drive the sealing punches. Hydraulic drives, as used in common hydroforming processes, generally deliver unnecessarily high levels of load for micro-hydroforming processes.

The control systems of industrial used hydroforming machines are based on conventional programmable logic controller systems, customary for press controls. Common sensors are used for measuring the strokes, speeds and forces of all axes and for measuring the pressures of the hydraulic system and the forming high pressure.

Figure 9-12 shows as an example a prototype micro-hydroforming press which was

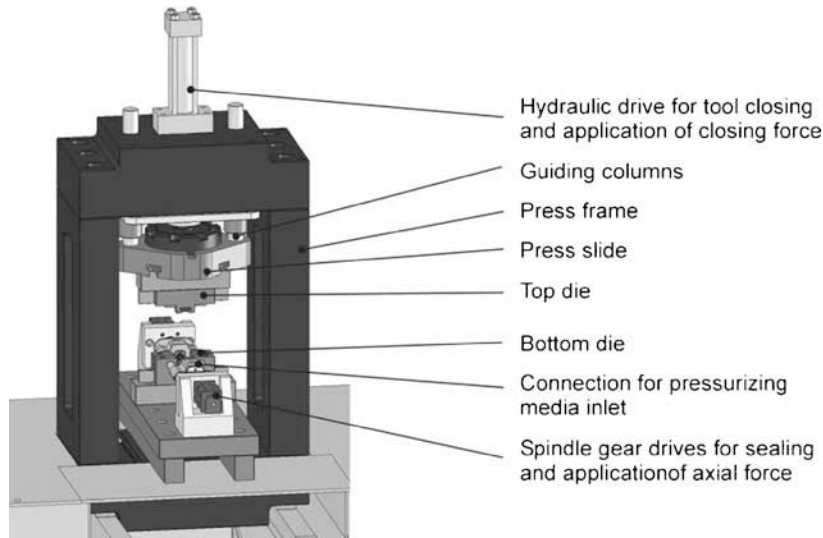


FIGURE 9-12 Micro-hydroforming prototype machine.

designed for investigations into the mass production of micro-components. This machine enables the micro-hydroforming of components with cross-sectional dimensions between 0.2 and 1 mm. It is equipped with a spindle-driven pressure intensifier which enables the application of up to 4000 bar internal pressure, the closing force being realized by a hydraulic drive, and the axial punches being moved by linear actuators with spindle gears. The investigation into this prototype machine served for the development of the first serial production micro-hydroforming machines [19].

CONCLUSIONS

Micro-hydroforming is a new manufacturing method for the mass production of tubular complex-shaped metal micro-components with integrated structures. It is based on the forming of initial tubes by internal pressurization with a liquid medium. Potential applications concern the production of corresponding components for medical devices, micro-fluidic and micro-mechatronic technology. Important advantages of micro-hydroforming consist in the possibility to generate complex geometries with reduced

effort in machining and joining operations as well as in process time, compared to methods used until now for the manufacture of such components. As micro-hydroforming is characterized by comparatively high forming loads and pressures, the application of this forming technology implies an enhanced knowledge of an adequate process design to obtain economic and reliable production. This chapter provided an overview of hydroforming fundamentals adapted to gain insight into the essential requirements for the development and execution of micro-hydroforming processes. Besides the description of the hydroforming principle and necessary additional manufacturing steps to obtain the required component shape, this concerns the determination of forming loads, the choice of suitable tube materials, the definition of feasible component geometries as well as details on tool and machine design for mass production.

REFERENCES

- [1] Ch. Hartl, Research and advances in fundamentals and industrial applications of hydroforming, *J. of Materials Processing Technology* 167 (2005) 283–392.

- [2] J.A. McGeough, M.C. Leu, K.P. Rajurkar, A.K.M. De Silva, Q. Liu, Electroforming process and application to micro/macro manufacturing, *Annals of the CIRP* 50(2001) 499–514.
- [3] I. Yadroitsev, L. Thivillon, Ph. Bertrand, I. Smurov, Strategy of manufacturing components with designed internal structure by selective laser melting of metallic powder, *Applied Surface Science* 254 (2007) 980–983.
- [4] V. Piottter, T. Gietzelt, L. Merz, R. Ruprecht, J. Hausselt, Powder injection molding in micro technology, *Proceedings of PM2TEC, Advances in Powder Metallurgy & Particulate Materials*, Orlando, US (2002) 43–48.
- [5] F. Dohmann, Innenhochdruckumformen. In: K. Lange, *Umformtechnik*, Vol. 4, Springer, Berlin (1993) 252–270.
- [6] Ch. Hartl, Case studies in hydroforming, *Proceedings of Int. Conf. Recent Development on Tube and Sheet Hydroforming*, Columbus, OH (2003).
- [7] M. Schroeder, Herstellung von PKW-Rahmenstrukturteilen und Abgaskomponenten durch IHU, *Proceedings of Int. Conf. on Hydroforming*, Stuttgart (1999) 403–419.
- [8] A. Sterzing, R. Neugebauer, M. Putz, Verfahren-sintegration beim Innenhochdruck-Umformen – Schneiden, Ziehen, Fügen, *Proceedings of 3rd Chemnitz Car Body Colloquium*, Chemnitz (2002) 277–292.
- [9] T. Flehmig, S. Schwarz, Hydroforming complex hollow sections, *Steel Grips* 1(6) (2003) 408–412.
- [10] C. Schuster, C. Loretz, F. Klaas, M. Seifert, Potentials and limits with hydroforming of aluminium alloys, *Proceedings of Int. Conf. on Hydroforming*, Stuttgart (2005) 113–136.
- [11] A. Rosochowski, P. Wojciech, O. Lech, M. Richert, Micro-extrusion of ultra-fine grained aluminium, *Int. J. of Advanced Manufacturing Technology* 33(1–2) (2007) 137–146.
- [12] M. Geiger, M. Merklein, M. Celeghini, H.-G. Haldenwanger, M. Prier, Sheet and tube hydroforming at evaluated temperature, *Proceedings of Int. Conf. on Hydroforming*, Stuttgart (2003) 259–278.
- [13] D.E. Green, Experimental determination of tube forming limits, *Proceedings of Int. Conf. on Hydroforming*, Stuttgart (2003) 299–314.
- [14] Ch. Hartl, J. Lungershausen, H. Biedermann, J. Conzen, Study of hydroforming processes for the production of micro-components, *Proceedings of 1st Jubilee Scientific Conf Manufacturing Engineering in Time of Information Society*, Gdansk (2006) 137–140.
- [15] P. Groche, G. Breitenbach, Influence of tube manufacturing processes on hydroforming, *Proceedings of Int. Conf. on Hydroforming*, Stuttgart (2005) 219–240.
- [16] T. Altan, M. Koc, Y. Aue-u-lan, K. Tibari, Formability and design issues in tube hydroforming, *Proceedings of Int. Conf. on Hydroforming*, Stuttgart (1999) 105–122.
- [17] F. Klaas, Aufweitstauchen von Rohren durch Innenhochdruckumformen, *VDI*, Duesseldorf (1987).
- [18] C. Hielscher, Tube testing for the production of complex hydroforming parts, *Proceedings of Int. Conf. on Hydroforming*, Stuttgart (2001) 63–84.
- [19] Ch. Hartl, J. Lungershausen, J. Eguia, L. Uriate, P. Lopes Garcia, Micro hydroforming process and machine system for miniature/micro products, *euspen 7th Int. Conf.* Bremen 2 (2007) 69–72.
- [20] F. Dohmann, Ch. Hartl, Hydroforming applications of coherent FE-simulations to the development of products and processes, *J. of Materials Processing Technology* 150(2004) 18–24.
- [21] S. Fuchizawa, Influence of strain hardening exponent on the deformation of thin-walled tube of finite length subjected to hydrostatic internal pressure, *Adv. Tech. Plasticity I* (1984) 297–302.
- [22] D.M. Woo, Tube-bulging under internal pressure and axial force, *J. of Engineering Materials and Technology* 10 (1973) 219–223.
- [23] W.J. Sauer, A. Gotera, F. Robb, P. Huang, Free bulge forming of tubes under internal pressure and axial compression, *Proceedings of 6th North American Metal Working Research Conf*, Gainesville (1978) 228–235.
- [24] J. Chalupzak, L. Sadok, The problem of forces and stresses in the hydromechanical process of bulge forming of tubes, *Metalurgia I Odlewnictwo – Tqm* 9 – Zeszyt 1 (1984) 57–66.
- [25] F. Vollertsen, Size effects in manufacturing, *Proceedings of 1st Colloquium Process-scaling*, Bremen (2003) 1–9.
- [26] O. Pawleski, Beitrag zur Aehnlichkeitstheorie der Umformtechnik, *Archiv für das Eisenhüttenwesen* 35 (1964) .
- [27] M. Koc, Development of guidelines for tube hydroforming, *Doctoral dissertation*, Columbus, OH (1999).
- [28] M. Braeutigam and H. Rutsch, Hydroformen – als Ausweg aus der Investitionsklemme, *VDI Berichte Nr 946*, VDI, Duesseldorf (1992).
- [29] Ch. Hartl, Theoretical fundamentals of hydroforming, *Proceedings of Int. Conf. on Hydroforming*, Stuttgart (1999) 23–36.
- [30] F. Dohmann, A. Boehm, K.-U. Dudziak, The shaping of hollow shaft-shaped workpieces by liquid bulge forming, *Adv. Tech. Plasticity* (1993) 447–452.
- [31] F. Klaas, Innovations in high-pressure hydroforming, *Proceedings of 2nd Int. Conf. on Innovations in Hydroforming Technology*, Columbus, OH (1997) 1–31.
- [32] F. Dohmann, Ch. Hartl, Hydroforming components for automotive applications, *The Fabricator* (2) (1998) 30–38.

-
- [33] Ch. Hartl, T. Abbey, Product development of complex hydroformed parts and requirements regarding tool manufacture, Proceedings of Int. Conf. on Technology of Plasticity, Nuremberg (1999) 1183–1188.
- [34] R. Cousin, CFD-simulation of fast filling procedures in small fluid chambers for hydroforming processes, Proceedings of 1st Jubilee Scientific Conf. Manufacturing Engineering in Time of information Society, Gdansk (2006)75–80.

Laser-Assisted Micro-Forming

Jens Holtkamp

INTRODUCTION

Forming is one of the basic production technologies, and due to the potential and low costs of the process is widely spread in industrial applications. Nevertheless, there are specific limitations regarding the workpiece materials and the maximum strain within the forming operation. Brittle and high strength materials cannot be accommodated without high process complexity or low product quality.

By heating the used materials prior to the forming process, with the corresponding change of their material properties, these drawbacks can be eliminated.

The use of laser radiation as the heat source enables short heating times, due to the associated high energy density. In addition, there are other advantages such as contactless heating, good focusability and good controllability lasers are therefore becoming a promising alternative to existing technologies such as induction or conductive heating.

In principle, every forming technique can be enhanced by laser technology. The basics for its integration and some exemplified processes are described in the following sections.

SYSTEM TECHNOLOGY

Heating of the workpiece can be achieved by different methods: conductive through the contact of a heated tool, convective within a convection oven, or inductive by swirling currents generated in the material.

Pre-process heating of the workpiece outside of the tool leads to an increase of temperature within

the whole part. Temperature gradients are not adjustable; therefore, local heating of selected areas of the part is not possible. Heating of micro-components is difficult due to their low mass. This low heat capacity leads to a cooling down after the transport into and the contact with the tool.

The disadvantage of methods based on heat convection is the bad controllability of the forming temperature and the resulting long cycle times. Similarly to the pre-heating method, the heating of local areas of the workpiece is not possible.

By using a laser as the heat source, the induced energy and the resulting temperatures can be easily controlled by laser power. Heating of selected areas is possible by forming the laser beam. The high energy density of the radiation and the direct absorption enable short cycle times. Therefore, a laser is a promising tool to achieve the potential of micro-forming at elevated temperatures.

The laser system causes the main additional cost in comparison to the cost of conventional machinery. Due to its low price in comparison with that of other laser systems, a diode laser is often favored, but there are also other effective systems such as fiber lasers. If absorption within transparent workpieces is intended, the wavelength of the laser has to be adapted.

The machinery used for laser-assisted processes is based on conventional forming machines. The system is then, beside the laser itself, enhanced with components for the integration and control of the laser. One basic additional element is an optical system which is placed inside the tool. Adapted to a fiber which connects the

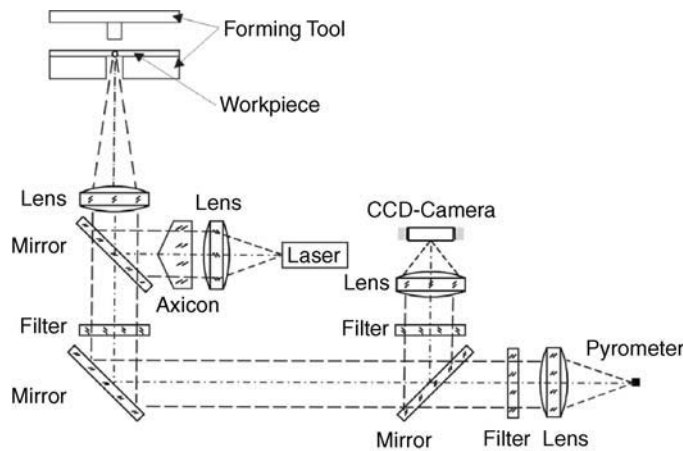


FIGURE 10-1 Example of an optical path.

laser with this system, it guides the radiation through the forming tool onto the surface of the workpiece to be heated. If necessary, the shape of the radiation can be adapted to the geometry of the workpiece.

Figure 10-1 presents a schematic drawing of an exemplified configuration.

The laser radiation is first collimated and then reflected on a dichroic mirror through a focal lens towards the sheet metal surface.

By means of an additional camera, which is arranged coaxially with the optical path, the position of the laser radiation can be displayed on a monitor. This enables an easy adjustment of the tool to the optical system and the possibility of process monitoring.

Knowledge of, and the possibility to control, the process temperatures arising are important for reproducible and accurate process results. Additional sensors can be used such as thermocouples or pyrometers to detect these temperatures and, if necessary, to submit them to a controller. The value of a pyrometer depends on the emittance of the material and its surface properties. Therefore, it is necessary to ‘teach’ the system before using new materials.

Filtering is necessary to divide the radiation into the wavelengths that are important for the corresponding detectors: while the camera requires wavelengths in the visible range, the pyrometer detects a range just above $1\ \mu\text{m}$.

If metal is used as the workpiece material, a circular shape of the laser focus leads to a non-uniform temperature distribution. Hot spots are generated in the middle of the area to be heated, whereas the border area remains cold due to the high thermal conductivity of metals. By using an Axicon within the beam bath, this drawback can be substantially eliminated.

An Axicon is a rotationally symmetric optical element which consists of a cylindrical part and a cone, as shown in Fig. 10-2. The Axicon creates an annulus as the focus geometry. As a result, a more homogeneous temperature distribution can be achieved. Depending on the angle of the Axicon and the focal lengths of the lenses used, the ring diameter can vary.

In addition to the optical system, the forming tool also has to be adapted, in such a way that the radiation can be guided onto the workpiece or the punch, depending on the workpiece material. For stamping operations the radiation can be easily

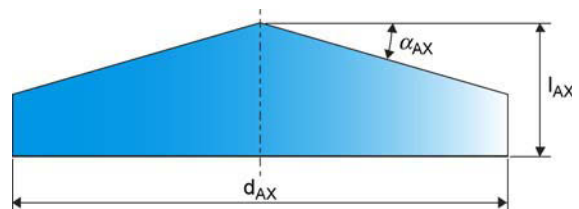


FIGURE 10-2 An Axicon.

guided through the tool matrix. No additional elements are necessary, but it is important to remove the punched parts from the optical path at the end of the operation. Other forming processes require ‘tool windows’. These can be made of sapphire or fused silica which are both, on the one hand, hard enough for the occurring process forces and, on the other hand, transparent for the laser radiation (as long as it is not in the infrared range). Through a breakout in the tool frame, the laser radiation is transmitted through the sapphire/glass onto the workpiece or the punch.

All devices – the laser and the press – are controlled by software which controls the laser, depending on the position of the punch relative to the tool and the required temperature, and switches it off after a defined distance or time has been reached.

In order to obtain short heating times and to maintain a constant temperature, a temperature controller can be used. The controller compares the signal of a thermal sensor with the demanded temperature and determines an according value for the laser system.

PROCESSES

Stamping

Stamping is a well-established process which enables the production of sheet metal or plastic parts in very short cycle times (up to 40 parts per second). In addition, the production of precise and complicated contours is possible. The process is characterized by a high material utilization [3].

The main components of a stamping tool usually consist of the punch and the female die (the matrix), sometimes with an additional pressure pad to build up compressive strength in the workpiece. The cutting forces are transferred from the surface of the punch and the female die to the sheet metal, which leads to an elastic deformation. With increasing force the deformation resistance is overcome and the elastic limit of the material is reached, whereupon the punch penetrates into the sheet metal [7]. This plastic deformation without separation leads to the rounded edges at the material surface [3]. Due to the plastic deformation in the cutting direction, the material yields in lesser-loaded areas and leads to roll-over. With increasing punch displacement, the roll-over passes into a smooth shearing zone. Within zones of high material stressing, cracks appear. This leads to cleavage fracture and the creation of the fracture zone [7].

Figure 10-3 shows the three phases of the stamping process [5].

The process, the workpiece material and the production accuracy of the tool are crucial for the quality of the stamped part. While a high shearing zone is intended, different defects occur on nearly every part. Figure 10-4 shows the different defects of the cut edge.

The height of the roll-over depends on the cutting clearance and the yield/stress ratio. This ratio is defined as the quotient of the yield stress and the tensile strength. The roll-over increases with increasing cutting clearance and yield/stress ratio. Moreover, increase in cutting clearance also affects the fracture zone.

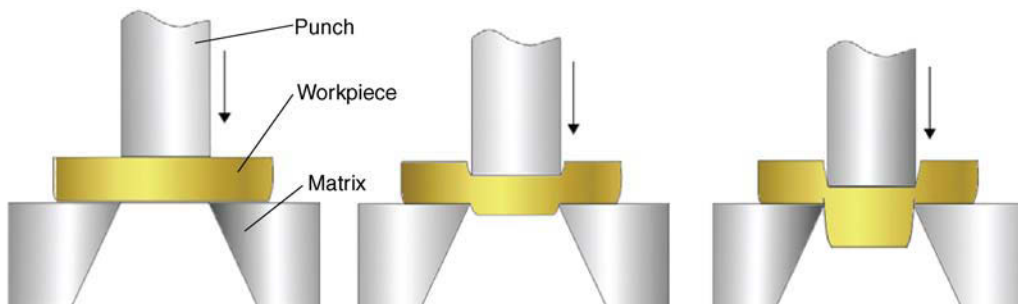


FIGURE 10-3 Process sequence.

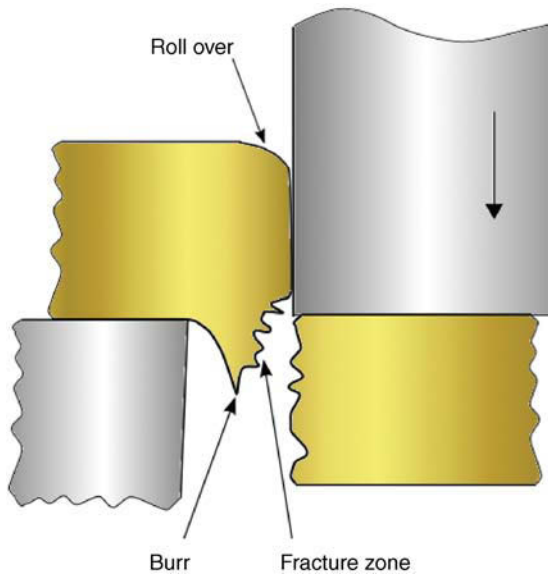


FIGURE 10-4 Defects of the cut edge.

The height of the burr, an indication of the manufacturing quality, depends on the properties of the workpiece material. Whereas ductile materials, due to their formability, create a high burr; the burr is smaller on brittle materials [5]. Figure 10-5 shows the active tool parts for the stamping operation of gearwheels.

Depending on the temperature of the metal workpiece, the processes are divided into cold, warm and hot forming. Cold forming takes place at ambient temperature. During the process the mechanical properties of the workpiece materials

change, with the strength being most affected. The formability decreases, while the forming resistance increases, with a reduced cross-section.

Within the hot-forming processes the temperature of the workpiece is above the recrystallization temperature, which is estimated to be around 40 to 50% of the melting temperature [8] according to the Tamman rule. Hereby, the formability can be increased, whereas the required forming forces are lower.

Warm forming takes place close to, but below, this recrystallization temperature. Even a small temperature increase leads to a reduction of the yield strength within the material [9]. Higher temperatures lead to higher flexibility of dislocation and crystal regenerations, which causes a reduction of the dislocation density and the strain hardening of the crystal lattice. In comparison to recrystallization, the size and the position of the crystallites remain unchanged.

The influence of different forming temperatures on the material properties are shown in Fig. 10-6. The yield stress and maximum strain are displayed for room and for elevated temperatures. This points out that greater working temperatures ease plastic forming by reducing the yield stress. The reduction of the yield stress can be explained with the oscillation of atom crystals. The possibility to move is constricted at room temperature but increases at elevated temperatures until the melting point is reached [6].

Hot forming enables processes to be carried out that cannot be implemented at room temperature.

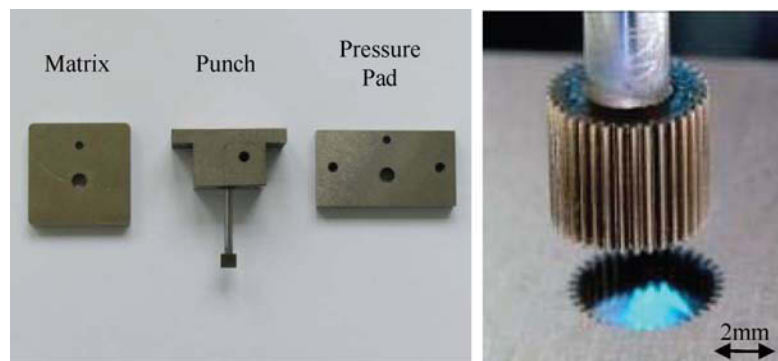


FIGURE 10-5 Active tool elements (manufactured by Fraunhofer IPK).

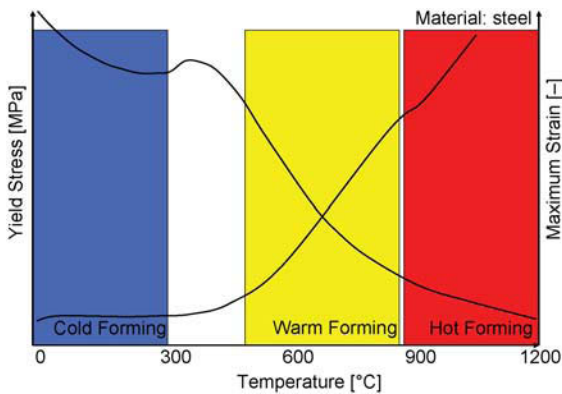


FIGURE 10-6 Forming temperature versus yield stress and maximum strain.

Nevertheless, it is not an entirely satisfactory alternative to cold forming due to its disadvantages: e.g. bad surface quality, inaccuracy in size and high tool loading because of the high temperatures. Since the whole tool is heated and not just the forming zone, the whole component is thermally loaded [10].

Warm forming uses the potentials of both the cold- and hot-forming processes. These potentials are the constant strain hardening and good surface quality of cold forming and the low process forces and the high formability of hot forming [2]. High-alloyed steels are then plastically formable with constant quality and high accuracy in size.

As an example, the magnesium alloy AZ31 (MgAl_3Zn ; 3.5312) is chosen as the test material. The main alloying additions are aluminum and zinc. Due to their addition, the tensile strength

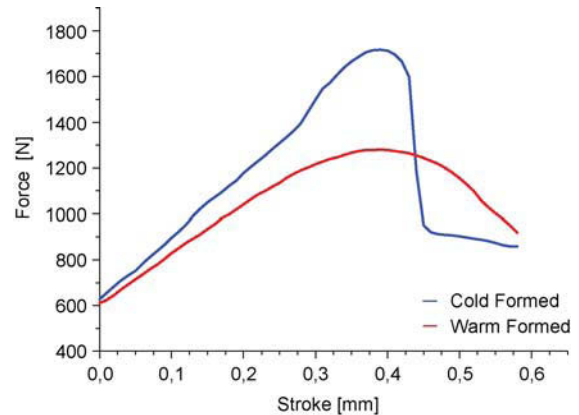


FIGURE 10-7 Force path.

and hardness are increased. However, the increased micro-porosity is disadvantageous [4] for forming operations.

Due to the hexagonal arrangement of the crystals of magnesium, the formability at room temperature is very low. Above 225°C the formability increases through the activation of additional gliding planes [1].

The measured force/displacement curves confirm the influence of the elevated workpiece temperatures. The maximum punching force can be reduced by 30% (Fig. 10-7).

Figure 10-8 shows two pictures made by a scanning electron microscope. The quality of both parts can be assessed concerning defects of form. The cold-formed part has significant defects. Many teeth are roughly removed, rather than smoothly sheared. The burr and the large fracture zones are indicators of bad quality. The warm-

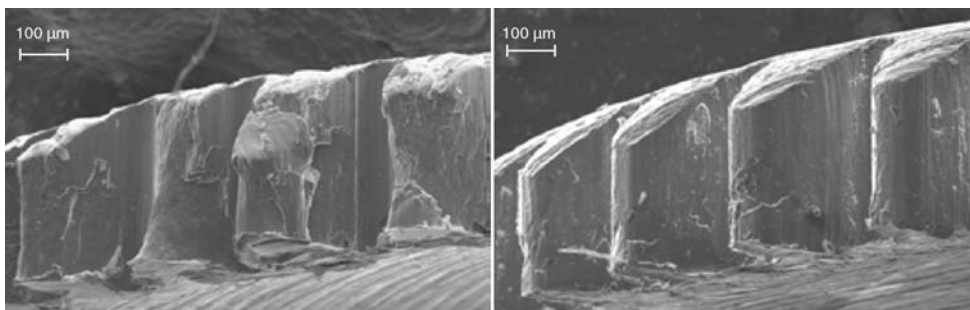


FIGURE 10-8 Gearwheels stamped without (left) and with (right) laser assistance.

formed gearwheel has nearly no burr and fracture zones, but has a high shearing ratio.

Embossing

Conventional technologies for the manufacturing of micro-structured components with geometries below $100\ \mu\text{m}$ are injection molding and hot embossing. Both technologies are mainly limited to polymer materials and require long cycle times due to different temperatures during forming and mold release. These drawbacks can be eliminated by laser-assisted hot embossing, where high energy density laser radiation is used for a selective and fast heating of the tool and the workpiece. Using controlled irradiation of the tool surface, tool temperatures of more than 500°C can be achieved within seconds. At these temperatures even glass and metals can be structured with this technology. In comparison to other heating technologies such as induction heating, laser-assisted embossing enables the use of tool materials with low thermal and electrical conductivity such as ceramics.

In the use of transparent workpiece materials such as glass or polymers, the laser radiation heats the structured die which, after achieving the required temperature, is then pressed onto the workpiece and heats it via heat conduction. In the case of non-transparent workpiece materials such as metals, the radiation is directly absorbed within the workpiece. The cold die then penetrates into the heated metal workpiece. With this technology micro-structures from $200\ \text{nm}$ to several tens of micrometers can be created at cycle times of below one minute.

The process sequence for transparent materials is shown in Fig. 10-9.

The laser radiation is guided onto the structured surface of the punch. Transparent tool inserts, integrated into the lower tool part, enable the radiation to directly access through the tool onto the die.

The workpiece is heated to the forming temperature, which is between the glass-transition temperature and the melting point. The tool then applies pressure on, and penetrates into, the workpiece. During the holding time, the material yields to the punch structure. The de-embossing phase is the most critical during the process: the structures are often destroyed in this phase due to tearing or overstretching. After the laser is switched off, the punch cools down again to below the heat-transition temperature. Since only the structured face side is heated, the cooling phase is shorter in comparison to that for conventional technologies.

The advantages of laser-assisted hot embossing can be summarized as follows:

1. Tooling materials are independent of thermal or electrical conductivity;
2. Short heating times due to high energy density of laser radiation;
3. Short cooling times by heating the near-surface area only;
4. Accurate measurement of the embossing temperature;
5. Selective heating of single areas of the component.

Metals. As an example, the magnesium alloy AZ31 is used. A step-like structure with an edge length of $100\ \mu\text{m}$ is pressed into the material both

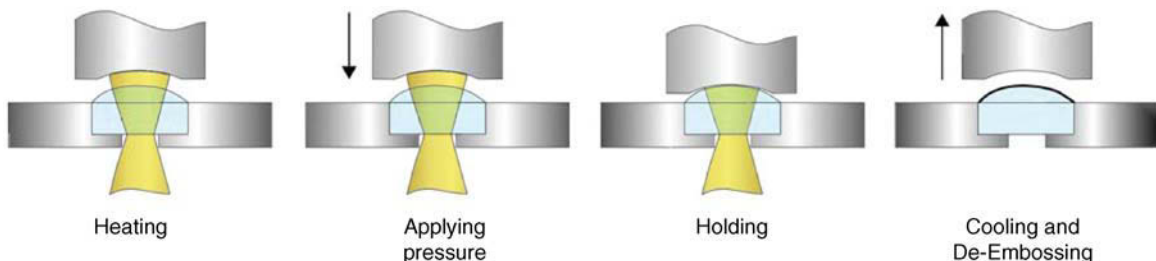


FIGURE 10-9 Process sequence in hot embossing.

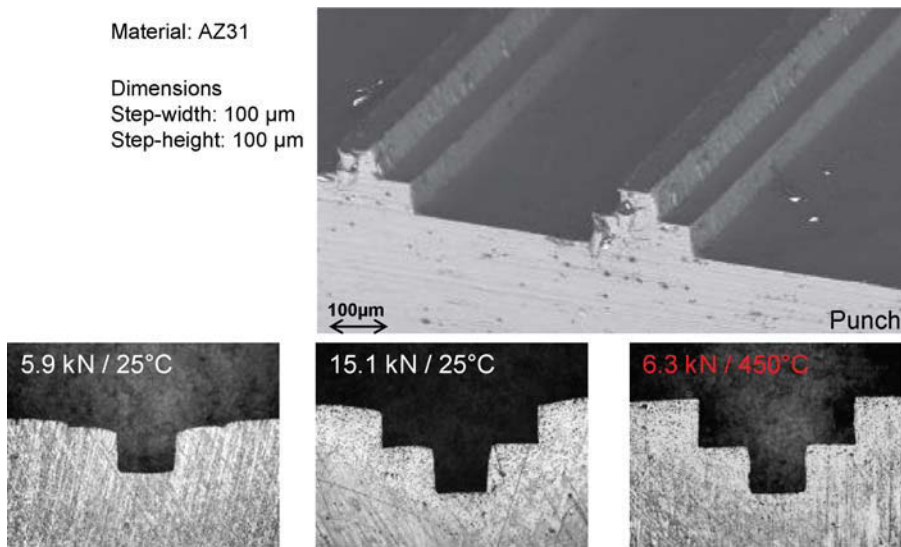


FIGURE 10-10 Hot embossing of magnesium (AZ31).

at room and elevated temperature. [Figure 10-10](#) shows the top of the punch and the resulting metallographic cross-sections of the embossed geometry.

Starting with a force of 5.9 kN, only the top of the geometry can be formed in the sheet metal. With increasing punch force, the penetration depth also increases. Even at 15.1 kN it is not possible to reproduce the hole structure in the sheet metal, as shown in the middle picture. When the pressing force is increased further, the tool breaks. By heating the sheet metal with laser radiation, it is possible to reproduce the structure with just 6.3 kN of applied force. In addition, the roll-over that occurred in the cold-formed part can be avoided. Thus, highly precise parts used for micro-fluidic applications, for example, can be produced.

Plastics. Amorphous thermoplastics are hard and brittle at room temperature. Above the softening or the glass-transition temperature they transform into a plastic condition in which they can be formed.

The tooling requirements are low due to the low embossing temperatures of 150–250°C. Different technologies can be used for tool manufacturing, such as lithography, whereby

structure sizes in the nanometer range can be obtained with high flexibility regarding the geometry. [Figure 10-11](#) shows two imprints into acrylic glass, both embossed with cycle times of below one minute. The left-hand side picture has an overall size of 6 × 6 mm. It consists of pins with a structure size of around 15 microns. The picture on the right-hand side has a diameter of 7 mm. The structure size of 200 nm leads to the colored effects visible on the picture.

Glass. In comparison to plastics, the material glass has a higher optical quality, which is important for different applications such as camera lenses, sensors or innovative lighting systems where aberration has to be avoided. The characteristic properties of glass are, among others, high mechanical strength, and environmental and temperature resistance, as well as joining ability. Due to its hardness and brittleness, this material is difficult to process. The mass manufacture of precise glass components is done by blank molding, but it is not possible to manufacture micro-optical functions such as diffractive optical elements on 3D components with this technology.

Laser-assisted hot embossing is a suitable process for the cost-efficient processing of glass within short cycle times. Tool materials with high

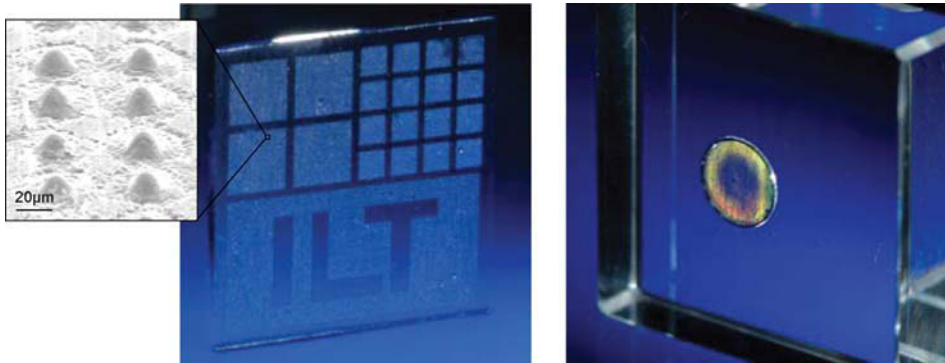


FIGURE 10-11 Hot embossing of acrylic glass.

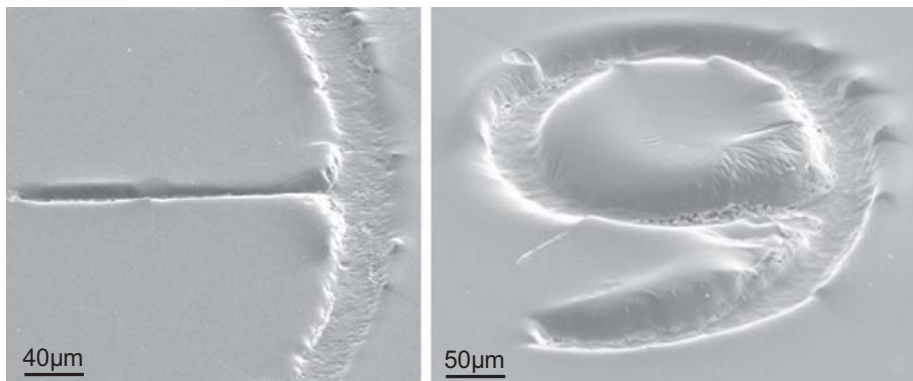


FIGURE 10-12 Hot embossing of glass (SK57).

temperature stability are necessary, which can be carbides, ceramics or high alloy HSS.

If high temperature gradients appear on the glass surface, the risk of glass breakage increases. A plane heat input is therefore necessary. Glass material SK57 is a low melting point glass with a transition temperature of $T_g = 493^\circ\text{C}$. Starting at this temperature, imprints are possible with heating times of below one minute.

Figure 10-12 shows embossed imprints made with this technology with structure sizes of between 30 and 80 microns.

Bonding of Plastic with Metal and Ceramic – LIFTEC[®]

The ongoing trend regarding an increased level of integration in many technical products and the increased use of plastics as construction material

is a challenge for many manufacturers regarding the connection of dissimilar materials, such as plastics with metals. The requirements for consumer products as well as for technical components are a flexible joining technique with short cycle times and a broad field of application.

Until now, the connection of these materials has been performed by gluing, screwed fastening or the so-called mold-in technique. Hereby the properties of the particular process define the area of application. Clamped or screwed joints enable a detachable connection while form-closed connections are able to transmit high power free of clearance. Gluing is applied for large areas. A complex preparation of the components is necessary for all mechanical connections. The most commonly used connection technique for plastics with metal is the mold-in technique during injection molding. The mechanical component is

Process	+ good o average - bad	Properties				
		Strength	Backlash	Tolerance requirement	Additional joining part	Reversibility
Screwed Joint	+	+	+	-	+	-
Press Fit	o	+	-	+	o	o
Glueing	o	o	o	+	-	+
Multi-Component-Injection-Moulding	+	+	-	+	-	o
Snap Connection	o	o	o	+	+	-
Riveting	o/+	+	+	-	o/-	-
In-Mould-Connection	+	+	-	+	-	o
LIFTEC®	+	+	+	+	-	o

FIGURE 10-13 Comparison of different joining techniques.

placed in an adapted tool prior to the injection-molding process. An optimal process result requires tight tolerances of the tool and high precision components. The part handling is difficult. A subsequent joint of plastic with metal is not possible.

A process for a subsequent joint is the so-called post-molding technology, which is mainly used for thread inserts which are heated by induction and then pressed into the plastic component. However, the whole component may be heated, and ceramics cannot be processed. The positioning of the inductor is often difficult and the heat input not sufficient for small structure sizes.

Figure 10-13 displays a comparison of LIFTEC® with other joining techniques.

LIFTEC® – an acronym for ‘laser-induced fusion technology’ – is a newly developed process. It is based on every thermoplastic being transparent or at least translucent in the unpigmented state. Based on this fact, a metal or ceramic component or a part of it is heated with laser radiation through the plastic part. The component is pressed onto the plastic part and heats this by heat conduction. After reaching sufficient plasticity the component penetrates into the plastic part. By choosing an appropriate geometry, a form-closed connection can be obtained. This can be a bump, a drilling or a groove, for example. The material displaced upwards leads to unwanted bulging on the surface of the part. This can be eliminated or at least reduced by an additional cavity or by drilling within the part where the plastic can yield.

An inevitable element of this technology is a component with a higher melting point in comparison to the plastic join partner. Possible materials are mainly metals and ceramics, but can also be a temperature-resistant plastic such as Teflon or even wood.

Advantages of the technique are:

1. Short cycle times;
2. High mechanical strength;
3. Non-loosening connection, free from backlash;
4. Low requirements regarding tolerances and positioning accuracy;
5. No pre- or post-processing necessary;
6. Post-process assembly;
7. Synergy effects by material combination.

Figure 10-14 shows the sequence of this process:

1. Positioning and applying pressure;
2. Heating the metal part through the plastic component with laser radiation;
3. Penetration into the plastic component after exceeding the glass transition temperature;
4. Cooling down and the creation of positive locking.

When plastics are used that are not transparent for the laser radiation, the process can be adapted in the way that the radiation does not transmit through the plastic part, but is guided laterally to the component, as shown in Fig. 10-15.

Heating with laser radiation is, in comparison to heating concepts already in use, quasi-independent of the heat conductivity and the electrical conductivity of the material used. This means that, in addition to metal, ceramic materials can

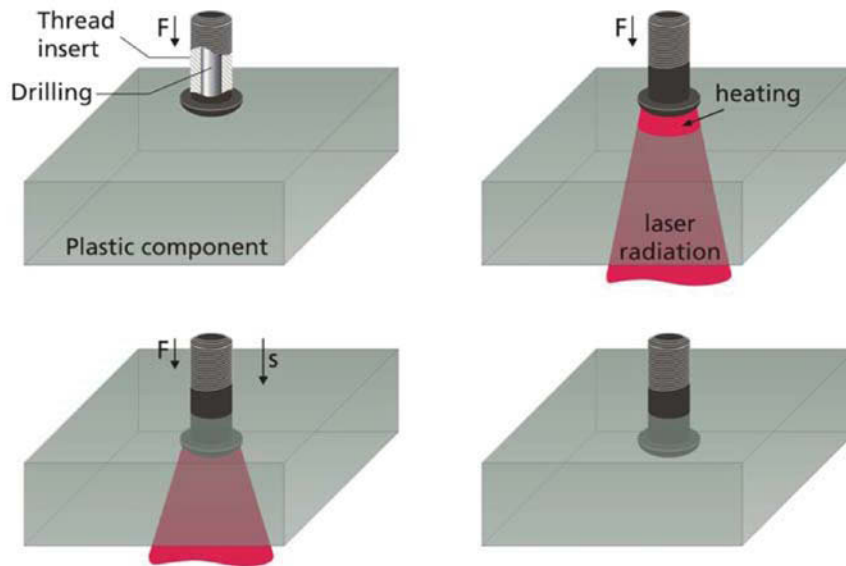


FIGURE 10-14 Process sequence.

also be joined with plastics. The combination of the properties of these hybrid components offers high mechanical strength, resistance to wear, high temperature stability with, at the same time, reduced weight and variable shape forming.

Due to the high energy density of laser radiation, quick heating is possible. If necessary, selected regions alone can be heated to limit the total amount of absorbed energy. The temperature of the part can be measured by a pyrometer to control the accurate joining temperature, depen-

dent on the materials and geometries used. Thus, a stress-minimized insertion of the components is possible and damaging overheating does not occur.

Transparent plates made of sapphire or fused quartz integrated into the tool enable the irradiation within the closed tool directly onto the surface of the metal even during the forming operation.

An essential process parameter is the joining temperature. When too high temperatures are applied, bubbling and discoloration occur. If the temperature is too low, cracks open due to high induced stress.

To reduce the cycle time a peripheral software control for regulation of the power output is used, which allows reducing the heating time by a time-dependant power modulation.

A high power output is applied to reach the intended temperature, then the power is reduced to keep the temperature constant. An example of a temperature/time curve is shown in Fig. 10-16.

In the present case there is a heating period of 4 seconds at 25 watts to achieve a temperature of 135°C. Afterwards the laser power is reduced to 16.5 watts.

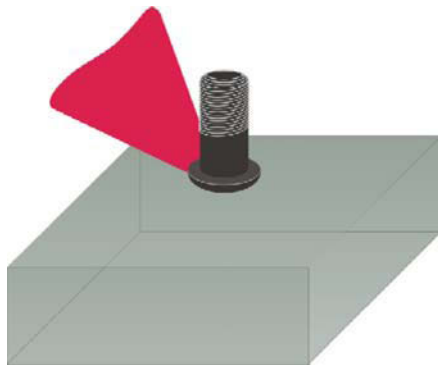


FIGURE 10-15 Alternative irradiation strategy for non-transparent plastics.

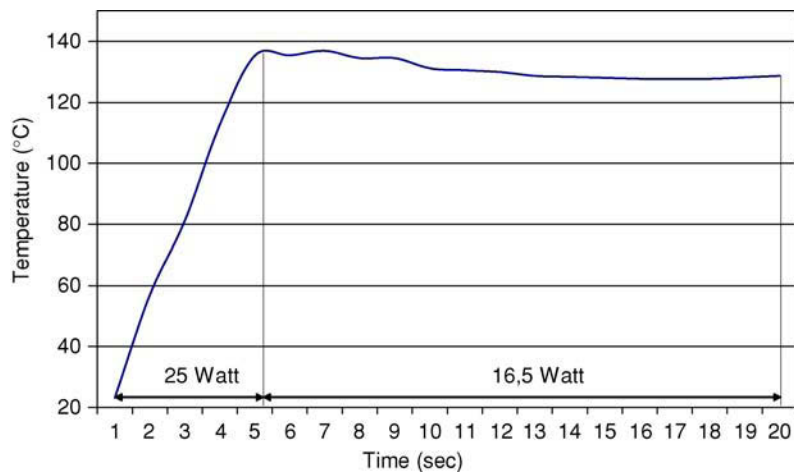


FIGURE 10-16 Reduction of heating time by modulation of laser power.

Plastic components can easily be formed, which thereby enables many design possibilities. Low density and chemical resistance are additional reasons for the increased application of this material. On the other hand, the high strength is a characteristic and important advantage of metals and ceramics. The combination of the materials results in the combination of their positive properties.

Principal fields of applications are anywhere where this combination of properties is reasonable. These are, for example:

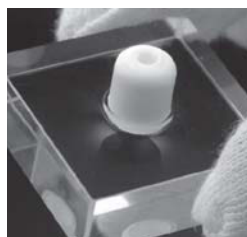
1. Joining of rimless plastic eyeglasses with the arm. Besides higher strength of the bond and the security against loosening, new designs are possible. No pre- or post-processing such as pre-drilling for screwed connections is necessary.

TABLE 10-1



Metallic Thread Insert

- Material: steel, PMMA
- Thickness of plastic plate: 10 mm
- Screw diameter: M4
- Form closure by a bump



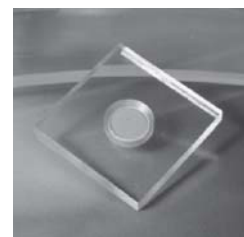
Plastic-Ceramic Bond

- Material: ZrO_2 ; PMMA
- Thickness of plastic plate: 10 mm
- Diameter of cylinder: 8 mm
- Form closure by surface roughness
- Additional drilling to avoid throw-offs



Plastic-Plastic Bond

- Material: Teflon, PMMA
- Thickness of plastic plate: 10 mm
- Diameter of cylinder: 10 mm
- Form closure by a groove



Plastic-Silicon Bond

- Material: silicon; PMMA/PC
- Thickness of plastic plate: 3 mm
- Diameter of silicon plate: 7 mm
- Thickness of silicon plate: 0.3 mm

2. Joining of plastic windows with metal frames with high leak tightness.
 3. Metallic pins at heavily and often loaded hinges in plastic components, e.g. cell phones. Besides having improved durability, the joint also ensures higher product quality.
 4. Mounting of plastic components on metal components.
 5. Plastic components with metallic inserts. The mechanical load can be absorbed by the mechanical part to reinforce the compound.
- The main considerations of the process are:
1. Accessibility of the laser radiation to the component to be heated;
 2. Different temperature stability of both components;
 3. Maximum size of the components;
 4. Geometry with positive locking.
- Table 10-1 shows some exemplified bonds.

CONCLUSIONS

Warm forming with laser radiation is a promising technique to enable new processes or enlarge the processing limits of conventional processes. In comparison to other production technologies like lithography, no additional operations are necessary. Elevated temperatures of the workpiece material lead to a reduction of the yield stress and an increase of the forming-ability. As heat source laser radiation is applicable, making a fast heating of selected areas of the workpiece is possible. The demand towards reproducible and high

quality process results requires the accurate measurement of occurring temperatures during the forming operation, which can be achieved by the employment of a pyrometer. The system technology, the process basics as well as exemplified applications have been shown for the processes of stamping, hot embossing and LIFTEC®.

REFERENCES

- [1] E. Doege, St. Janssen, J. Wieser, Kennwerte für die Magnesiumumformung am Beispiel von AZ31 (2001).
- [2] E. Egerer, T. Neudecker, U. Engel, Grundlagenuntersuchungen zum Halbwarmmikroumformen, Tagungsband zum DFG-Kolloquium in SPP 1074 (2001).
- [3] W. Hellwig, Spanlose Fertigung: Stanzen. Friedl, Vieweg & Sohn Verlagsgesellschaft mbH, Braunschweig, Wiesbaden (2001).
- [4] S. Kleiner, Magnesium und seine Legierungen, Feinstbearbeitung technischer Oberflächen – 6, Internationale IWF-Kolloquium (2002).
- [5] W. König, F. Klocke, Blechbearbeitung, Fertigungsverfahren Band 5, VDI Verlag, Düsseldorf (1995).
- [6] H. Lüpfer, Metallische Werkstoffe, Akademische Verlagsgesellschaft Geest & Portig K.-G, Leipzig (1958).
- [7] A. Pöllmann, Prozessparameter beim Scherschneiden von Karosserieblechteilen, Druckhaus Berlin-Mitte GmbH, Berlin (1997).
- [8] H. Schmann, H. Oettel, Metallographie, Wiley-VCH Verlag GmbH, Weinheim (2005).
- [9] K. Sieber, Werkstoffe, Fertigungsverfahren und Maschinen der Massivumformung, VDI-Verlag GmbH, Hamburg (1969).
- [10] F. Vollersten, M. Schilf, T. Seefeld, Verbesserung der Umformbarkeit von Aluminiumlegierungen, in: UTF Since 4 (2006) 1–5.

Micro-Mechanical-Assembly

*Hans Nørgaard Hansen, Mogens Arentoft,
Guido Tosello and Asta Gegeckaitė*

INTRODUCTION

This chapter gives an introduction to micro-mechanical assembly and proposes a classification and characterization of micro-mechanical assembly methods. Micro-mechanical assembly is defined as assembly methods on a micro-scale, where the relative position of components is retained by exchange of contact forces provided by mechanical constraints. Based on this definition, the current chapter will not deal with solid bonding, welding, gluing, etc.

In view of the high quality and accuracy requirements on the mechanical assembly of miniaturized products in the precision mechanical engineering industry, manual methods still prevail. Manual micro-assembly procedures are extremely demanding on the human operators performing them, time-consuming, costly and frequently they give rise to quality problems in terms of uniformity. Automatic procedures with a low level of flexibility have been adopted only where high product volumes occur [1–3]. Hence, highly automated systems for micro-assembly are not suitable for medium/small production batches due to their not respecting the minimum cost of manufacturing principle. These problems are rendered more severe by the trend towards further miniaturization of mechanical components and by the increasing variety of products and models.

Forms of flexibility have been developed in classical macro-scale assembly technology which can also be adopted in principle when assembling micro-components. Assembly systems can be

adjusted to various models by means of a modular product design which uses easily interchangeable product-specific system components. Furthermore hybrid micro-systems to be assembled should be constructed on a modular principle, dependent on the particular application, by using standard components [1,3].

The actual mechanical assembly function can be divided into the following constituent functions:

- Handling and positioning.
It has the function of putting two or more objects into a particular mutual position and orientation. Handling comprises processes of selection and preparation of components for composing or checking and transportation to the following production, assembly or packaging systems.
- Mechanical assembly.
It has the function of ensuring the mutual relationship between components against outside effects. By mechanical assembly, connections between the components can be created by means of mechanical constraints. The assembly process can be achieved by means of shape, material, force, etc.
- Quality control.
It has the function of ascertaining whether the mechanical assembly process has been carried out as specified. Checking represents those processes by which the component's presence and position are checked in addition to the quality of the finished product.

Assembly becomes particularly challenging when dealing with micro-products. A first approach may be to miniaturize macro-scale solutions by simple downscaling of dimensions. This approach reaches a limit with respect to obtainable tolerances in manufacturing processes and handling solutions. Another natural approach is then to try to reduce as much as possible the mechanical manipulation of micro-components, through a higher level of integration as compared to that of conventional size products. This involves a high degree of integration with the design phase when the product development is still in the early stage as well as the choice of materials, which obviously determines the process choice itself [1].

Finally it should be considered that the assembly of two or more components may result in a sub-assembly which will then be subject to further processing or assembly (Fig. 11-1).

Mechanical assembly of micro-components presents quite a few challenges because of the reduced dimensions [3]:

- In the micro-world, submicron precision is often required, comparable to wafer stepper precision. This degree of precision is beyond the calibration range of conventional open-loop precision assembly devices used in

mechanical industry. Closed-loop strategies are required to compensate for poor kinematic models and thermal effects: real-time vision feedback is perfectly suited for this application.

- In the micro-world, forces other than gravity dominate due to scaling effects. Surface-related forces, such as electrostatic, van der Waals and surface tension forces, become dominant over gravitational forces.
- Manual handling of micro-parts shows the problem of the loss of direct hand/eye coordination. It implies a series of interconnected problems: because of the dimensions in the micro-range, microscopes for vision and micro-grippers for manipulation are suitable. In order to achieve a good resolution, high magnification is used, but then problems related to restriction of field of view (smaller than the object), very short depth of focus (an unclear image) and short working distance arise. Magnification could be reduced, but then issues of trade-off between field of view and resolution emerge. Furthermore, micro-grippers have less degree of freedom than the human hand and lack of force feedback.
- Manual handling is time consuming because operators can handle only one or a few objects at a time, which implies high production costs.

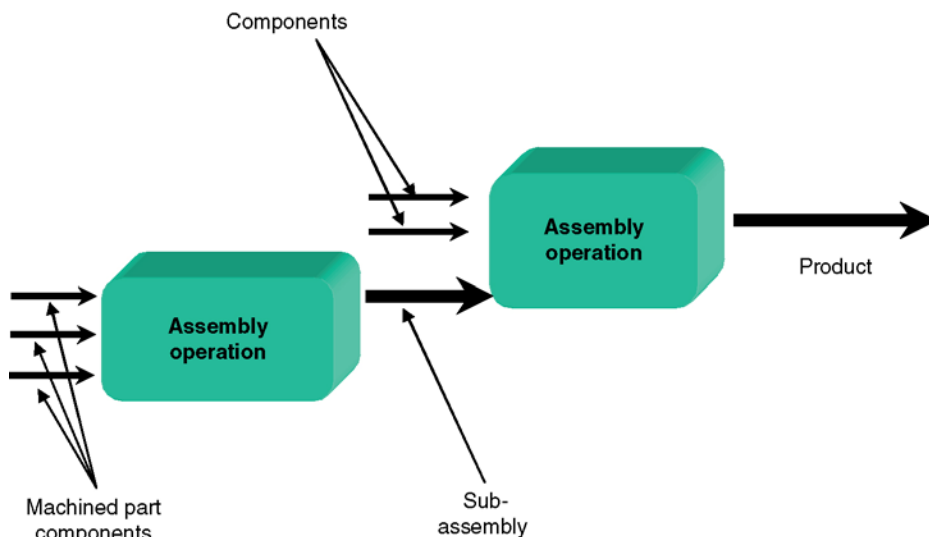


FIGURE 11-1 Levels of micro-assembly.

CLASSIFICATION OF MICRO-MECHANICAL ASSEMBLY METHODS

Micro-mechanical assembly methods can be classified according to the mechanical constraint and the way the material is processed in order to achieve this constraint (Table 11-1). The mechanical constraint is divided into two categories: possibility for disassembly or no possibility for disassembly. The material conditioning characteristics are no deformation, elastic deformation, plastic deformation, flow and solidification. The micro-mechanical assembly methods listed in the table are those typically found in the literature when searching for micro-assembly. This implies that methods and technologies may exist which are not mentioned in this chapter. However, it is believed that the most relevant technologies are mentioned in Table 11-1. A more specific description of the single technologies will be given in the following sections.

Micro-snap Fits

Micro-snap fit is a mechanical joining method, based on the elastic deflection of joint features on one micro-part that are inserted into a mating feature on another micro-part, to obtain an elastic interference.

Complicated micro-structures consisting of multiple components can be assembled using snap fasteners. They also have great potential when

being lifted out of plane and used as vertical plug-in connectors.

A snap fastener consists of a mating pair of an anchor and flexible latches. As an example, it may have two outer latches and a central anchor. The latches are supported on flexible beams. In its disengaged state, the anchor and the latches can move freely with respect to each other.

In this type of assembly only a linear movement is required to engage the components. The relative positioning accuracy required depends on the absolute dimensions, but is relatively large due to the self-aligning nature of the joint. The design can be modified in such a way that the required force for engagement is small. See [4–8] for examples of micro-snap fits.

Micro-screwing

Screws are components with a thread (a uniform cross-section following a spiral or helical path) either on the inside or outside surface. Threads may be right handed or left handed. The screw may be cylindrical or tapered. Cylindrical screws need a counterpart geometry, whereas tapered screws usually create the geometry in the counterpart. Assembly operations involving screws require a combined translational and rotational movement. Furthermore a certain alignment accuracy of the screw with respect to the counterpart is required. The level of this accuracy depends on screw dimensions and tolerances.

TABLE 11-1 Overview of Mechanical Assembly Methods at the Micro-Scale

	Characteristic			Material Constraint		
	No Disassembly	Disassembly Possible	No Deformation	Elastic Deformation	Plastic Deformation	Flow and Solidification
Snap fit	X			X		
Screw		X		(X)	X	
Velcro	X			X		
Joinery		X	X			
Injection molding	X					X
Riveting, folding, clinching	X	X			X	

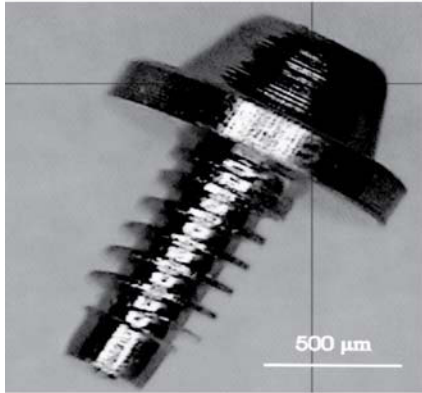


FIGURE 11-2 Example of micro-screw with non-ISO dimensions and geometry [9].

Very little literature exists on micro-screwing although it is extensively used, for example in the watch industry. ISO standard geometries are not necessarily scaled down to micro-scale (metric screws according to ISO 68-1) in these applications (Fig. 11-2). Micro-screws are used in medical devices (e.g. hearing aids) as one of the simplest fastening components. In some of the products, the screw has another functionality, namely creating an electrical connection.

Micro-Velcro

Micro-Velcro is a micro-mechanical fastening system, based on silicon micro-machining technology, which results in a strong, permanent bond without chemical adhesives (Fig. 11-3). The working principle is based on arrays of micro-mechanical mating structures, which act as mechanical adhesives.

The joining principle of micro-Velcro is based on the matching of silicon wafers with highly density micro-structured surface, with an areal density of approximately 200,000 units/cm². The micro-structures on two identical surfaces will self align and interlock with each other under application of adequate external pressure. A tensile strength per unit interlocked area of the order of 0.2 MPa has been achieved [10].

The principle of bonding is a button snap, or a zipper, but in a two-dimensional configuration. The bonding principle is depicted by the schematic cross-section in Fig. 11-3. Under application of adequate external pressure, the tabs of the structures deform and spring back, resulting in an interlocking of the two surfaces. In this way, a permanent bond is achieved. Other examples are reported in [11,12].

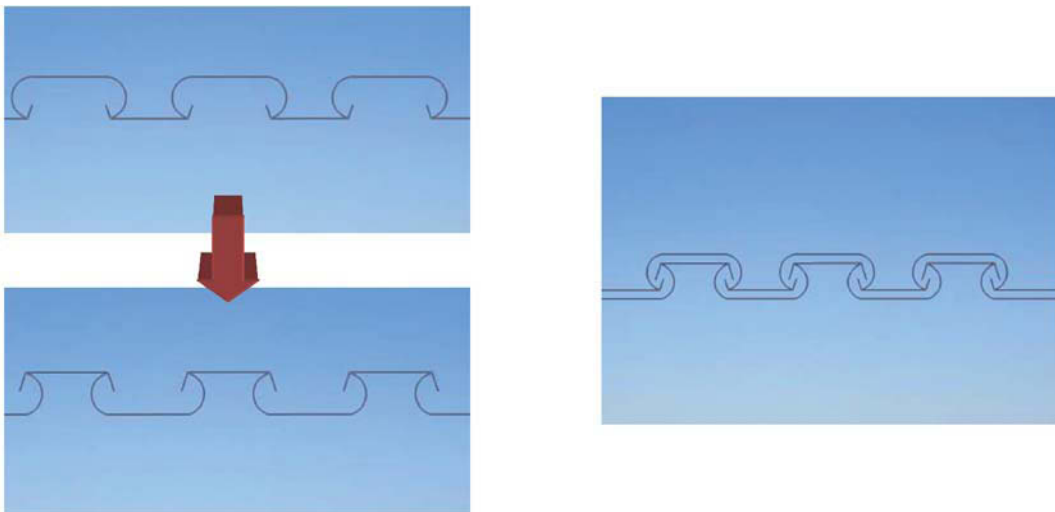


FIGURE 11-3 Principle of a micro-Velcro assembly. Left: two initial parts. Right: assembled unit.

Micro-joinery

Micro-joinery is the fabrication and assembly of micro-joints to realize three-dimensional micro-structures. Each micro-joint contains two or more mating surfaces which join the various parts together as a single unit. This technique involves primarily silicon but virtually any single crystalline material of virtually any crystalline orientation (GaAs, Ge, quartz, metals, etc.) is suitable [13]. In macro-scale mechanical assembly this technique is well known. It is therefore also applicable for metallic, ceramic or polymer micro-components providing that adequate processing technologies exist and can be applied. A critical point is, of course, the tolerances of the parts. On the one hand, they should ensure mating, and on the other hand, they should be as small as possible in order to secure the assembly. The surface area to volume ratio favors the strength of the joint on micro-scale but it also is a potential challenge in terms of actual assembly.

The dovetail micro-joint is a particular adaptation of the micro-joinery concept and it is commonly used in 3D (x , y , z) positioning devices requiring linear translation – see Fig. 11-4 for an example.

The slot joint is similar in function to the dovetail micro-joint in that it also has constrained translation, but method and geometry are slightly different. The slot joint has a rectangular-shaped

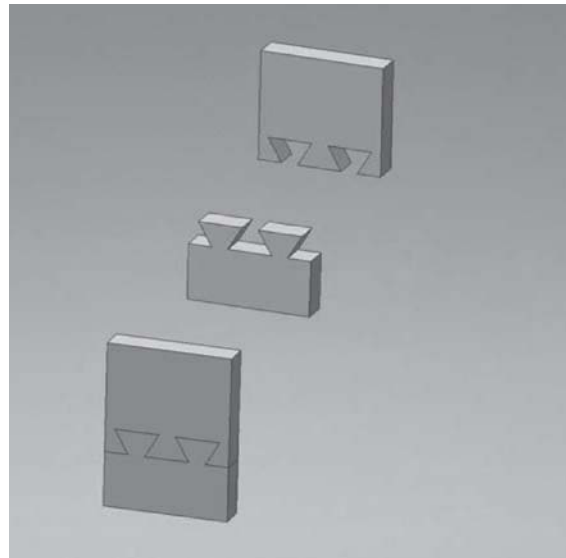


FIGURE 11-4 Dovetail assembly.

cross-section (Fig. 11-5). A number of techniques are suitable for the fabrication of a slot joint: micro-milling, sawing, LIGA or anisotropic etching of silicon wafers. Finger joints are interlocking structures that feature a periodic assembly of mating fins as shown in Fig. 11-5. Finger joints are used to attach two substrates rigidly together, paying attention to the fact that large mating surfaces of the finger impart considerable strength and stability to the joint.

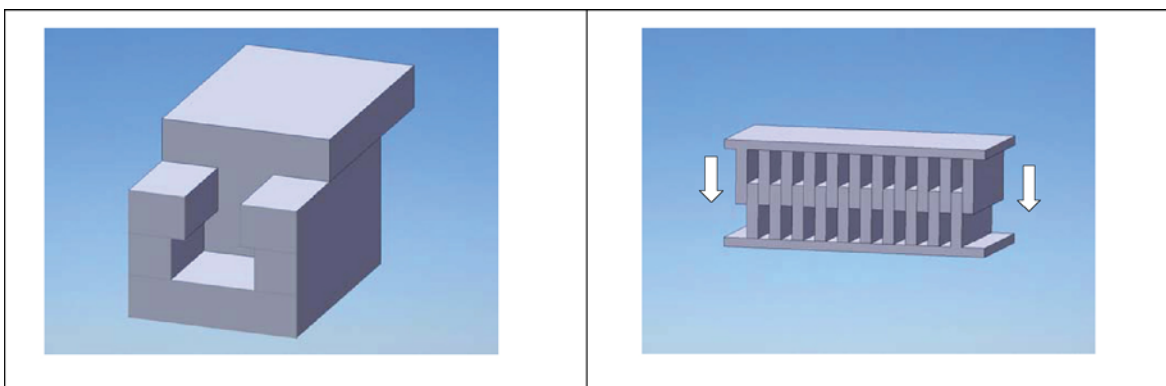


FIGURE 11-5 Slot joint (left) and finger joint (right).

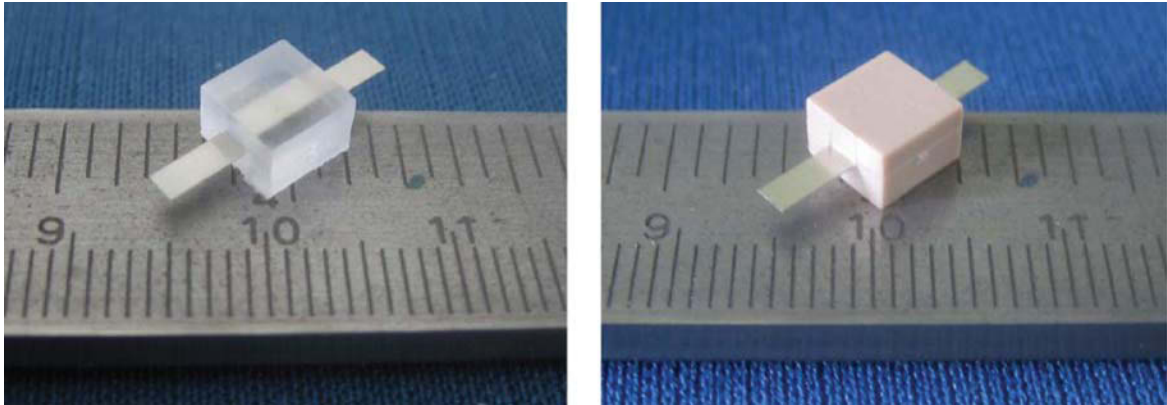


FIGURE 11-6 Hybrid (metal/polymer) structures manufactured by injection molding. Material: PS (left) and PA66 + GF50% (right). Metal foil thickness up to 100 μm [16].

Micro-injection Molding

Micro-injection molding is a manufacturing technique that can be used not only for the production of monolithic micro-structures but also for the assembly of hybrid structures. As components and functional structures become smaller, they cannot be regarded in terms of steps in a single process, but as an integrated production concept. A process called micro-assembly injection molding has been developed and combines the joining of hybrid elements with the generation of functional structures [14,15].

Micro-injection molding allows the production of movable micro-structures by using incompatible polymers, soft/hard combinations of materials, the generation of fluidic hollow structures by lost core technology and the overmolding of wires and optical systems like optical fibers.

The differences of materials used, the temperature layout of the process and the mechanical strain of inlay parts play a fundamental role. Most of all, the precision in positioning of inlay parts and the demolding of hybrid structures have a relevant importance. For these reasons, a mold technology with flexibility, precision and special processing equipment is required. The mold is characterized by using a special system for positioning of inlay parts and complex sensor

equipment for measuring pressure and temperature, which are relevant process parameters. Thus, a new mold concept has to consider the possibility of various thermal processes, such as heating the cavity before injection, cooling down again before demolding. It has to be characterized by acceptable cycle times and the possibility to evacuate the cavity. Figure 11-6 illustrates hybrid micro-structures produced by injection molding. Overmolding of other polymer parts is used in two-component micro-injection molding, for example for the creation of molded interconnect devices [17].

Micro-riveting, Folding and Clinching

Riveting, folding and clinching are mechanical assembly processes based on plastic deformation of the materials involved. This excludes brittle materials from these particular processes although MEMS-based riveting has been reported [18]. In macroscopic assembly processes these technologies are used in metal joining/assembly. They require the use of molds/dies and tools and are based upon sheet metal operations: reference can be made to a relevant chapter for the basis of these technologies. Figure 11-7 illustrates a micro-rivet which was produced by a micro-cold forging operation.

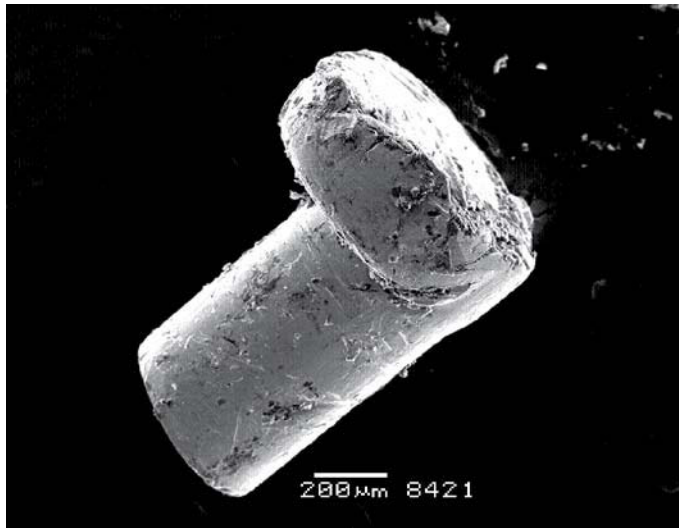


FIGURE 11-7 Micro-rivet in Ag.

SYSTEMATIC APPROACH TO MICRO-MECHANICAL HANDLING AND ASSEMBLY

The handling of the small parts has been studied for almost half a century and different micro-handling principles are summarized in [1]. A classification scheme for the quantified analysis of micro-gripping principles has been proposed in [3] and describes basic features of the gripping operation on micro-scale. Different handling classification schemes have been introduced in recent years. Different realizations of micro-grippers have been reported (their diversity is large) addressing different handling situations, materials and dimensions.

However, when developing solutions for micro-mechanical handling and assembly, a systematic approach is beneficial. Figure 11-8 illustrates the contents of a proposed methodology. Object characteristics (material, weight, dimension, geometry) are considered as the basic information of the problem. Depending on what should be done with the objects (referred to as functionality) a choice of gripping principle and assembly method can be made. The description of the desired functionality is important due to the fact that the resulting feedback may also involve a

redesign of the component to make it more suitable for the assembly operation.

It is not the methodology to automatically result in an optimized overall handling and assembly process. However, by considering all the points in the methodology a characterization of the entire situation is possible and an identification of the most important steps in the process is possible. The systematic consideration of what exactly is needed in terms of operations will hopefully result in gripper designs that are tailor-made. The next section will illustrate how the methodology has been applied.

APPLICATION EXAMPLE: MECHANICAL ASSEMBLY OF PUSH BUTTON PARTS

As an example of mechanical assembly, a hearing aid push button will be taken. The push button consists of seven different parts both geometrically and in respect of the material (see Fig. 11-9). All parts have an axis-symmetrical geometry but different diameters and shapes. The screw is shown in detail in Fig. 11-2. Different geometrical dimensions of the parts are up to

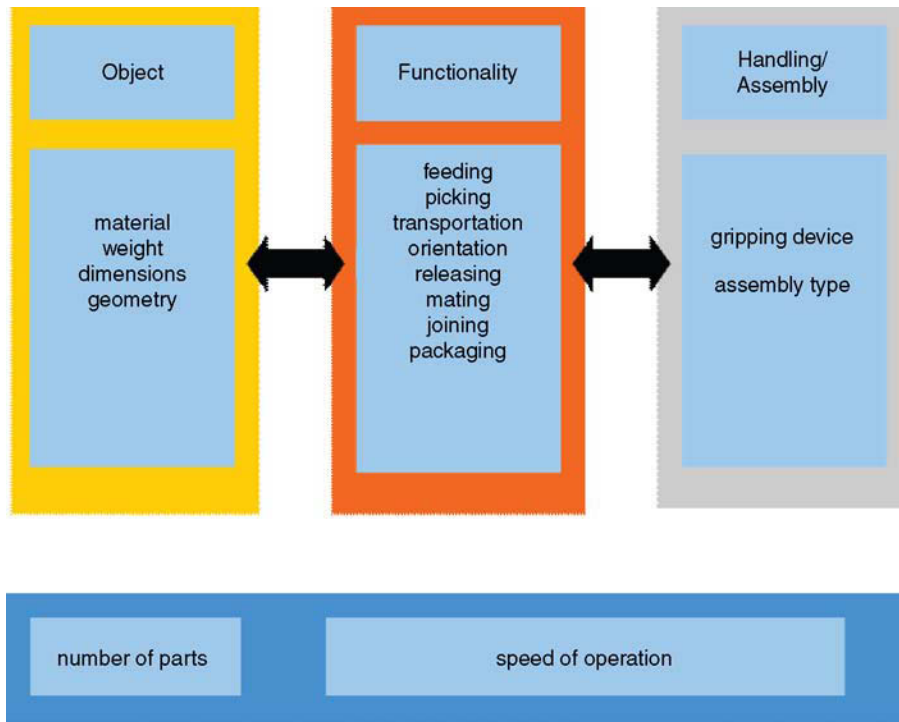


FIGURE 11-8 Systematic approach to micro-mechanical handling and assembly [9,19].

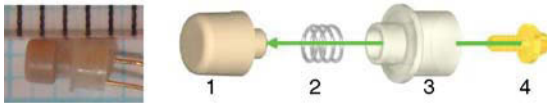


FIGURE 11-9 Schematic view of push button parts: 1 – knob, 2 – spring, 3 – holder and 4 – screw. Scale on left picture in mm.

2 mm, but dimensions of the functional structures are less than 1 mm, therefore these parts are known as micro-objects. Assembly of these parts is usually done by putting parts 1–3 onto each other, then screwing a screw through part 3 to part 1. A lid with two wires is placed on top and fastened by thermal heating and gluing, for sealing purposes: the lid and wires are not used in this example. Presently these assembly operations are performed manually or on semi-automatic stations involving manual labor.

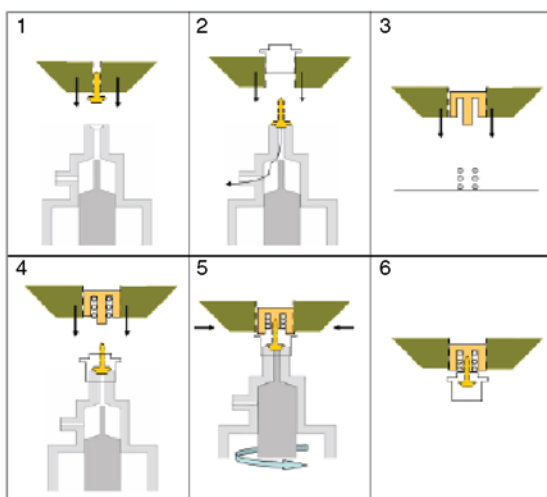
The requirements of the handling and assembly process can be summarized as follows:

- The assembly operations should be performed using a small standard industrial robot.

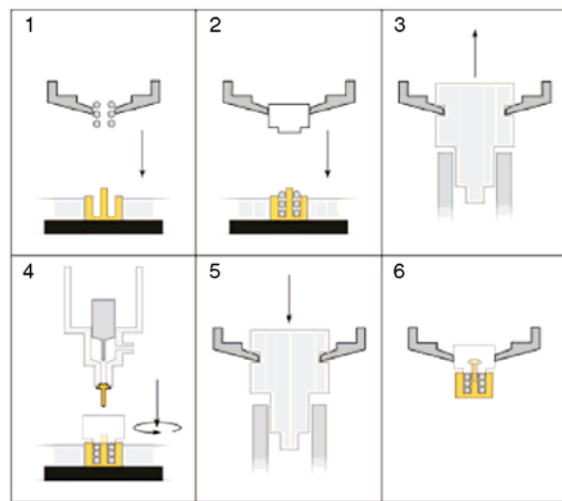
- The parts (all axi-symmetrical) need to be aligned with respect to each other.
- The screwing process must be achieved by a combined rotational and translational movement using a certain torque. In this process, either the screw or its counterpart should be moving while the other is kept in a fixed position.

It was chosen to work with small pallets as carriers for the components because the industrial company already had good experience with this type of system. The parts were therefore placed in separate fixtures and then picked and placed during the assembly process. Two types of tools were needed for handling and assembly: one capable of executing a combined rotational/translational movement and one capable of picking and releasing axi-symmetrical parts.

Two assembly scenarios were considered (Fig. 11-10): In Fig. 11-10(a) a screwdriver is fixed and the parts are manipulated one by one using a mechanical gripper. In the first step, the screw is



(A)
Fixed screwdriver



(B)
Moveable screwdriver

FIGURE 11-10 Assembly scenarios of push button [20–22].

fixed in the screwdriver by means of vacuum. Subsequently, the remaining parts are fitted over the screw one by one, and finally the screwing process is performed. In the second scenario (Fig. 11-10(b)) three of the parts are picked and placed on top of each other by a mechanical gripper. Then a screwdriver is used to pick and screw the small screw into place and to perform the screwing operation [9].

The design of the mechanical gripper is a subject of high importance. On the one hand, the gripper should match the shapes of the objects – preferably of all the objects – and on the other hand, a custom-made design for each part would ensure a better picking and releasing operation. As a compromise, a two-finger gripper design was investigated (see Fig. 11-11). Various angles of the slots as well as surface textures were

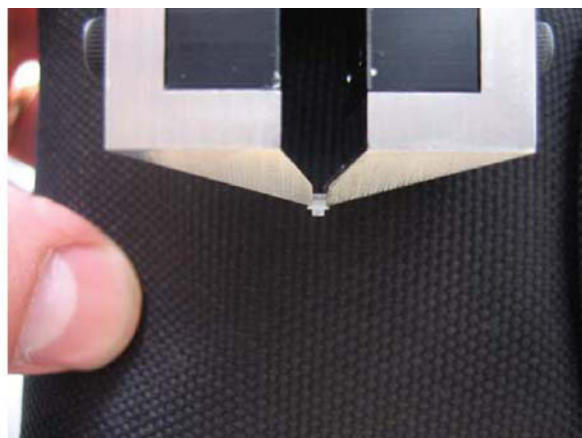
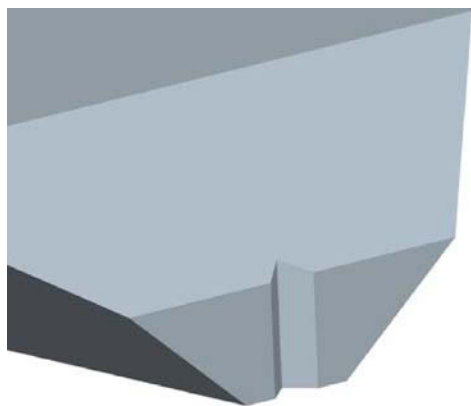


FIGURE 11-11 Mechanical gripper. V-groove design (left) and mounted on robot (right).

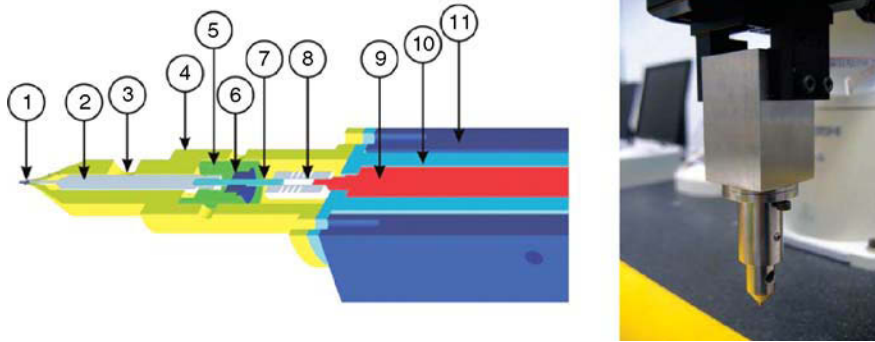


FIGURE 11-12 Detailed screwdriver design. 1 – micro-screw, 2 – shaft, 3 – vacuum connection place, 4 – corpus, 5 – holder, 6 – bearings, 7 – shaft, 8 – shaft coupling, 9 – motor and gears, 10 – motor holder and 11 – corpus.

investigated in order to optimize the design. It was concluded that a flexible design with a V-groove would accommodate all the various diameters of the parts. Furthermore, the use of micro-structured surfaces facilitates the release of objects, especially in case of the plastic parts, which have weights ten times smaller than that of the screw [23].

The detail-designed screwdriver (Fig. 11-12) is composed of two different mechanisms. The first is an air suction-based mechanism [3] (11 shows where it has to be connected) for picking up the screw (1) and holding it in the required position while transporting it. The vacuum system consists of a pump, tubes and a manipulator (not shown in the figure). The second mechanism is a screwing mechanism that is composed of a screwdriver (2), a screwdriver shaft holder, bearings, a hexagonal key, a coupling and a motor with a gearbox (9). The remaining parts are designed for supporting the screwdriver. The corpus consists of two parts: 4 and 11. The corpus has a chamber for air and air connection place (3), the motor is kept in the corpus, and fastened to a motor holder (10). The screwdriver shaft holder and the motor are kept in place by two screws. Four screws connect both parts of the corpus and the motor holder. The corpus is fastened by (11) holes on the sides, by which it is held by a robot hand [24].

With the use of the described gripping and screwing device, the relative limited accuracy of the robot was compensated for. The described assembly process was successfully tested in a

laboratory environment, and is currently considered for industrial implementation.

CONCLUSION

Mechanical micro-assembly methods are among the most highly relevant in micro-manufacturing. They allow the assembly of different materials, primarily non-silicon, and potentially they can incorporate possibilities for disassembly. The challenges related to micro-mechanical assembly include the almost total lack of guidelines (i.e. standards, best practice, etc.) and the need for tailor-made tools for the processes. This often is used as an argument against the automation of such processes.

REFERENCES

- [1] L. Alting, F. Kimura, H.N. Hansen, G. Bissacco, Micro engineering, *Annals of the CIRP* 52 (2) (2003) 1–23.
- [2] G. Reinhart, M. Hohn, J. Milberg, Growth into miniaturization: flexible microassembly automation, *Annals of CIRP* 46 (1) (1997) 7–10.
- [3] H. Van Brussel, J. Peirs, D. Reynaerts, A. Delchambre, G. Reinhart, N. Roth, M. Weck, E. Zussman, Assembly of Microsystems, *Annals of the CIRP* 49 (2) (2000) 451–472.
- [4] R. Prasad, K.-F. Bohringer, N.C. MacDonald, Design, fabrication, and characterization of single crystal silicon latching snap fasteners for micro assembly, *Proceedings of the 1995 ASME International Mechanical Engineering Congress and Exposition* 57 (2) (1995) 917–923.

- [5] N. Dechev, W.L. Cleghorn, J.K. Mills, Tether and joint design for microcomponents used in microassembly of 3D microstructures, *Proceedings of the SPIE – The International Society for Optical Engineering: MEMS/MOEMS Components and their Applications* 5344 (1) (2004) 134–146.
- [6] R. Yeh, E.J.J. Kruglick, K.S.J. Pister, Surface-Micromachined Components for Articulated Micro-robots, *J. of Microelectromechanical Systems* 5 (1) (1996) 10–17.
- [7] Y.S. Oh, W.H. Lee, H.E. Stephanou, G.D. Skidmore, Design, optimization, and experiments of compliant microgripper, *Proceedings of 2003 ASME International Mechanical Engineering Congress* 5 (2003) 345–350.
- [8] D. Koester, A. Cowen, R. Mahadevan, M. Stonefeld, B. Hardy, *PolyMUMPs Design Handbook – a MUMPs[®] process, MEMSCAP, Revision 10.0* (2003).
- [9] A. Gegeckaitė, Handling and assembly of microproducts, PhD thesis, Department of Mechanical Engineering, Technical University of Denmark (2007) ISBN 978-87-89502-73-1.
- [10] H. Han, L.E. Weiss, M.L. Reed, Micromechanical Velcro, *J. of Microelectromechanical Systems* 1 (1) (1992) 34–43.
- [11] University of Limerick website, Ireland, <http://www.plato.ul.ie/academic/Vincent.Casey>, (January 2005).
- [12] H. Han, L.E. Weiss, M.L. Reed, Mating and piercing micromechanical structures for surface bonding applications, *Proceedings of IEEE Micro Electro Mechanical Systems: An Investigation of Micro Structures, Sensors, Actuators, Machines and Robots* (1991) 253–258.
- [13] S.D. Collins, C. Gonzalez, R.L. Smith, D.G. Howitt, 1998, MicroJoinery: concept, definition, and application to microsystems development, *Sensors and Actuators – A: Physical* 66 (1–3) (1998) 315–332.
- [14] W. Michaeli, A. Rogalla, C. Ziegmann, 2001, Micro assembly injection moulding of hybrid microsystems, *Journal of Polymer Engineering* 21 (2) (2001) 99–109.
- [15] W. Michaeli, C. Ziegmann, Micro assembly injection moulding for the generation of hybrid microstructures, *Microsystem Technologies* 9 (6) (2003) 427–430.
- [16] G. Tosello, Precision moulding of polymer micro components, PhD thesis, Department of Mechanical Engineering, Technical University of Denmark (2008) ISBN 978-87-89502-77-9.
- [17] A. Islam, Two component micro injection moulding for moulded interconnect devices, PhD thesis, Department of Mechanical Engineering, Technical University of Denmark (2008) ISBN 978-87-89502-75-5.
- [18] B. Shivkumar, C.J. Kim, 1997, Microrivets for MEMS packaging: concept, fabrication, and strength testing, *J. of Microelectromechanical Systems* 6 (3) (1997) 217–225.
- [19] A. Gegeckaitė, H.N. Hansen, A methodology for characterization and categorization of solutions for micro handling, *Proc. of the 5th International Conference of Euspen, Montpellier* (2005) 397–400.
- [20] T. Erikson, H.N. Hansen, A. Gegeckaitė, M. Arentoft, Automated assembly of micro mechanical parts in a microfactory setup, *Proc. of the 5th international workshop on microfactories, Besancon, France* (October 2006) .
- [21] A. Gegeckaitė, H.N. Hansen, Automation of 3D micro object handling process, *7th International Conference of the European Society for Precision Engineering and Nanotechnology (Euspen), Bremen (Germany), May 20–24* (2007) 2 (2007) 233–236.
- [22] A. Hansen, C. Langhans, D. Ingham, H.K. Dahl-Hansen and M.H. Olsen, Automated assembly of micro components, Student report (in Danish), Department of Mechanical Engineering, Technical University of Denmark (2008).
- [23] A. Gegeckaitė, H.N. Hansen, L. De Chiffre, P. Pocius, Handling of micro objects: investigation of mechanical gripper functional surfaces, *7th International Conference of the European Society for Precision Engineering and Nanotechnology (Euspen), Bremen (Germany), May 20–24* (2007) 2 (2007) 185–188.
- [24] A. Gegeckaitė, H.N. Hansen, T. Eriksson, A screwing device for handling and assembly of micro screws, *7th International Conference of the European Society for Precision Engineering and Nanotechnology (Euspen), Bremen (Germany), May 20–22* (2007) 2 (2007) 481–484.

Laser Beam Micro-Joining

Felix Schmitt and Alexander Olowinsky

INTRODUCTION

The joining processes in electronic device manufacturing are today still dominated by conventional joining techniques such as press fitting, crimping and resistance welding. Laser beam joining techniques have been under intensive investigation and subsequently new processes for mass manufacturing and high accuracy assembling have been established. With the newly developed SHADOW[®] welding technology, technical aspects such as tensile strength, geometry and precision of the weld can be improved. This technology provides the greatest flexibility in weld geometry with a minimum welding time as well as new possibilities in using application adapted materials. Different parts and even different metals can be joined by a non-contact process. The application of a relative movement between the laser beam and the part to be joined at feed rates of up to 60 m/min produces weld seams with a length of 0.6 mm to 15.7 mm using a pulsed Nd:YAG laser with a pulse duration of up to 50 ms. Due to the low energy input, typically 1 J to 6 J, a weld width as small as 50 μm and a weld depth as small as 20 μm have been attained. This results in low distortion of joined watch components.

In the field of micro-production a variety of materials with individual product-specific dimensions are commonly used. Especially, the manufacturing of hybrid micro-systems, built up from different functional groups, affords variable joining technologies tailored to the specific demands of each component or material combination. Soldering with metal solder alloys is an

established and well-known process in electronic industries [1].

LASER BEAM SOLDERING

During the soldering process a liquid phase is caused by melting of a solder alloy or by diffusion processes within the intermediate layer. In principle, the joining process is based on interaction reactions between the joining partners and the melted solder. Therefore, a direct, oxide- and contamination-free, contact between the metal surfaces of the joining partners and the solder alloy is one of the most important process requirements. If the melting temperature of the additional material is below 450 °C (840 °F) the process is called soldering, while when above 450 °C the process is called brazing. Characteristic features of soldering include [2]:

- The melting temperature of the joining partners is higher than the melting temperature of the solder alloy.
- In most cases the service temperature of the assembly must be lower than the melting temperature of the solder alloy. In a diffusion soldering process, called transient liquid phase (TLP) bonding, the service temperature can be higher than the soldering process temperature.
- Prior to the joining operation, the surfaces have to be cleaned to remove oxides and organic films. The use of a flux can avoid prior processing. However, there are some constrictions associated with the use of flux, e.g. the residues that they leave behind, which are often corrosive and can be difficult to remove.

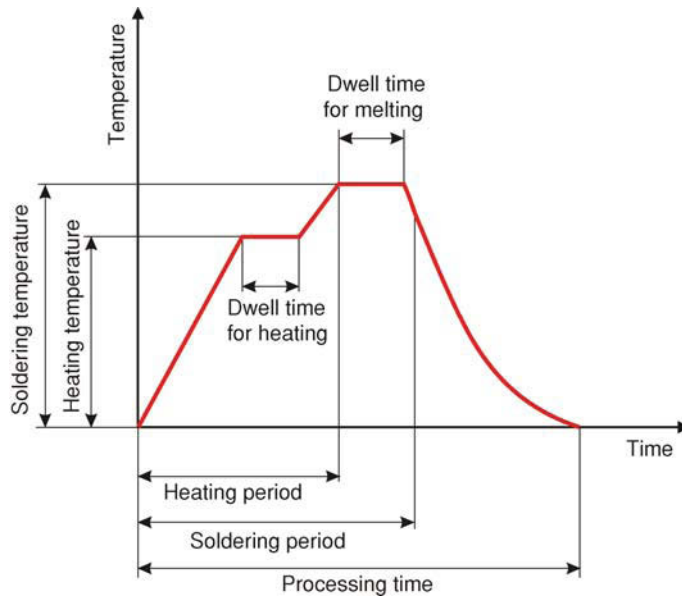


FIGURE 12-1 Heating cycle for soldering.

- Complex assemblies can be produced with low distortion, high fatigue resistance and good resistance to thermal shock.
- Joints tend to be strong if well filled, unless embrittling phases are produced by reaction between the solder alloy and the components.
- By using a broad variety of solder alloys it is possible to match the solder with the required process temperature and to reduce the melting temperature by using elements with a low melting point (e.g. indium, bismuth).
- Compensation and gap bridging can be achieved by using an additional filler material as solder alloy.
- For a molten solder alloy to wet and bond to a metal surface, the surface has to be free from non-metallic surface films. Despite a pre-cleaning process and ensuring this condition at the beginning of the process, significant oxidation will occur if the components are heated in air. An active flux fulfills the following functions [2]:
 - Removal of oxides and other films on surfaces by either chemical or physical means.
 - Protection of the cleaned joint from oxidation during the soldering process.
 - Wetting the joint surfaces, but being displaced by the molten solder as the latter spreads.
 - Reducing the surface tension between the solder alloy and the joint surface, thereby enhancing spreading.
- The heating cycle involves four important parameters: the heating period with heating rate and dwell time for heating, the peak soldering temperature, the dwell time above the melting point of the solder alloy and the cooling rate (Fig. 12-1). In general, it is desirable to use a high heating rate but the maximum heating rate is normally constrained by the form of the energy input. By means of laser energy and its high energy density it is possible to realize a maximum heat rate. The dwell time for heating is necessary for the evaporation of vapor and constituents of the flux and for the uniform heating of the joining partners up to the wetting temperature. This temperature is below the melting temperature of the solder alloy. The soldering temperature should be such that the solder alloy is certain to melt, but at the same time the solder alloy should not be overheated so that it degrades through the loss of

constituents. The peak temperature is normally set at about 20–30 °C above the melting point. The minimum time that the joint geometry is held at this temperature must be sufficient to ensure that the solder alloy has melted over the entire area of the joint. Extended holding times tend to result in excessive spreading of the molten solder alloy, possible oxidation gradually taking place, and deterioration of the properties of the parent materials. The cooling stage of the cycle is not controlled by the operator but normally governed by the thermal mass of the joint geometry. For laser processing it is very fast because of the instantaneous switch-off of the laser power, resulting in a fine-grained micro-structure of the joint.

Apart from light beam soldering and electron beam soldering, laser beam soldering is a soldering technique using radiation as an energy source (DIN 8505 1979). In contrast to other conventional selective soldering techniques, laser beam soldering features a contactless, temporally and spatially well-controllable energy input. Because of these characteristics, laser beam soldering is predestined for joining tasks where miniaturization and reduced thermal and mechanical stresses are required. Special features of laser beam soldered joints are fine-grained micro-structure and a low amount of intermetallic phases due to the high heating and cooling rates of this process. In principle, laser beam soldering is characterized by temporally and spatially selective energy input by surface absorption in the joining area, successive heat conduction and interface processes. The joining process is determined by characteristics of the laser beam source, the chosen process parameters and the thermo-physical properties of the joining partners.

The first tests on soldering with laser radiation were conducted in 1974 by C.F. Bohmann [3]. Here, a continuously emitting CO₂ laser was used for selective contacting of electronic components, the influence of laser power, irradiation time and geometry of laser beam interaction zone on the quality of the joints being explored. Although different research teams were working on the industrial implementation of this process, the CO₂ laser

did not become a widely accepted tool for soldering tasks despite the good automation possibilities [4,5]. There are some technological and economical reasons which are inhibiting the use of CO₂ lasers as a laser source for soldering applications. Widely used basic materials in electronic production (e.g. FR4) have an absorption of more than 90% at the emission wavelength of CO₂ lasers ($\lambda = 10,600$ nm), but soldering alloys (e.g. tin-lead) have a reflection of about 74% at the same wavelength [6]. In consequence, the risk of burning or partial carbonization of the circuit board is high by primary or diffused scattered laser radiation. Apart from these process-specific drawbacks, the investment and operation costs, maintenance effort and dimensions of this laser source are not an advantage compared to the use of technological alternatives.

Nd:YAG lasers were used for the first time for soldering applications in the 1980s [7,8]. Compared to CO₂ lasers, these laser sources have different positive features and emit light at near infrared ($\lambda = 1064$ nm). Apart from smaller dimensions, the shorter emission wavelength enables flexible and cheaper beam shaping and guidance. Here, fiber optics is used for beam guidance and optical components need not be made from materials such as germanium, zinc-selenium or cadmium-tellurid but can be made of cheaper optical glasses. Metallic materials have a higher absorption in the near infrared, resulting in a more efficient and reproducible process. The main applications for laser soldering systems based on Nd:YAG lasers are electrical and mechanical joints from sectors which require a greater level of reliability. Here, precision applications are known from civil fields, e.g. computer technology, automotive, aviation, aerospace, but there are also applications from military fields [6,9]. Because of high investment and operational costs, even laser beam soldering with solid-state lasers is only established in small market segments compared to competing selective soldering technologies.

Since the development of high power diode lasers, laser beam soldering has become increasingly more important in industrial applications.

Diode lasers feature a simple layout, a high electrical efficiency factor and small dimensions and are appropriate for manifold industrial applications on this account. In combination with not requiring maintenance, being of simple operation and having long lifetimes, these laser sources fulfill the requirements of industry due to providing an economic operation by lasers [10].

The latest developments in laser technology have resulted in fiber lasers becoming a versatile tool for laser-based production processes. Even if they are currently not used for soldering, very often it can be seen that they will penetrate laser beam soldering applications within the next few years. Due to their excellent beam quality, only these laser sources provide minimal focus geometries meeting the requirements for further miniaturization. Furthermore, these laser sources feature continuous emission, small emission wavelengths ($\lambda = 1030$ nm) and high anticipated lifetimes, combined with small dimensions.

Table 12-1 shows the important characteristics of these four laser sources for soldering applications.

Although the beam quality of high power diode lasers cannot be compared to that of conventional laser sources, these laser sources excel at flexibility. The decisive factor in this is the dimension ratio between the single different laser beam sources. The beam generating dimensions of a high power diode laser are smaller by a factor of 100 compared to an Nd:YAG laser at the same power. For the CO₂ laser this difference is even greater (a factor of 1000). Compactness of

semiconductors and the higher efficiency resulting in smaller and low power consumptive peripheral devices are responsible for the small system design. This saves space in the production environment and increases the mobility of these laser sources. Therefore, it is possible to integrate diode lasers directly into production cells. With respect to economical aspects, modern high power diode lasers are an attractive alternative to Nd:YAG and CO₂ lasers. Investment costs related to the optical output are at the lower range of competitive laser sources. Due to the epitaxial layout, diode lasers offer the possibility for cost-efficient mass production. Hence, forecasts see a decreasing price for diode bars so that high power diode lasers will gain an advantage compared to other laser beam sources [10]. With an electro-optical efficiency of about 50%, diode lasers work much more efficiently compared to Nd:YAG (<17%) and CO₂ lasers (<15%), resulting in lower power consumption as well as in required cooling power: this influences directly the operational costs. Diode lasers work almost maintenance free because there are no components wearing out (e.g. flash lights in Nd:YAG).

Due to the demands for high quality soldered joints, many process control mechanisms have been examined over the last few years. An essential requirement for laser beam soldering is the stability of the material and geometry conditions due to the energy input into the materials being independent of environmental conditions. Compared to other selective soldering methods, laser beam soldering enables temporally and spatially

TABLE 12-1 Comparison of Different Laser Sources for Laser Beam Soldering

	Diode Laser	Fiber Laser	Nd:YAG Laser	CO ₂ Laser
Dimension (ratio)	1	1	100	1000
Electro-optical efficiency	40–50%	30%	3–17%	10–15%
Emission wavelength	800–1000 nm	1030–1090 nm	1064 nm	10,600 nm
Lifetime	>100,000 h	>100,000 h	>1000 h	~10,000 h
Maintenance	Low maintenance	Low maintenance	200–1000 h	every 500 h
Investment/power	10–50/W	15–30/W	50–100/W	10–50/W
Beam guiding (fiber optics)	yes	yes	yes	no



FIGURE 12-2 System design for laser beam soldering based on a galvanometric scanner: Production cell (left) and laser processing optics (right).

adapted energy input by pyrometric process monitoring. The development of a closed-loop feedback of process information by thermal radiation gives the possibility of process control.

There are numerous different application-specific solutions available commercially for laser beam soldering machines. In principle, they are based on flexible beam shaping and guidance using galvanometric scanners or axis systems. For fiber-guided systems the processing optics are moved but there are also systems where the entire laser beam source is being moved. In Fig. 12-2 a production cell and laser processing optics are shown based on a galvanometric scanner.

The machine is designed for the laser beam soldering of an automotive micro-electronic module (an alternator regulator realized in thick-film technology) with solder pads printed on an alumina substrate (Fig. 12-3). The housing has seven terminal leads to be soldered to the substrate. The entire alumina substrate is glued by a heat conducting adhesive to an aluminum base-plate [11,12].

The diode laser system has a maximum optical output power of 500 W, which can be modulated by controlling the pump current. The collimated laser beam passes through a galvanometer scanner and is focused by an f-theta lens onto the lead/solder pad area to generate the joint. The circular

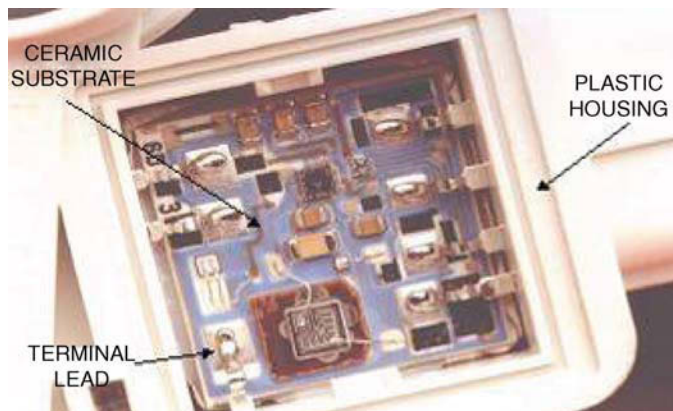


FIGURE 12-3 Automotive microelectronic module in a plastic housing – alternator regulator. Major components of the production cell are a fiber coupled, continuous wave (cw) diode laser system and a processing head with integrated pyrometric and power sensors.

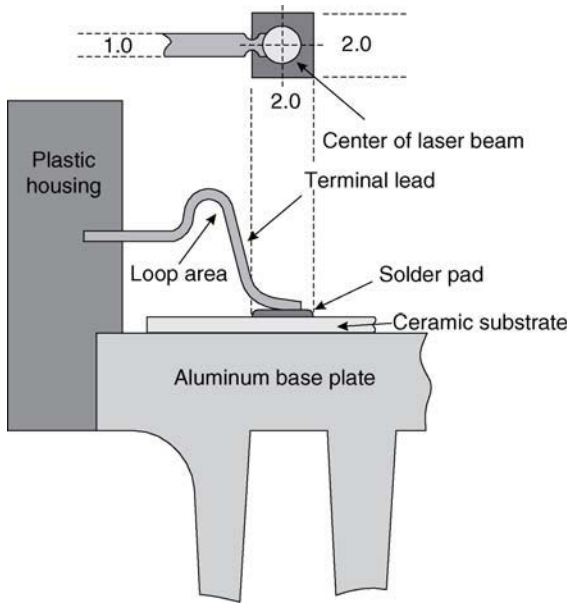


FIGURE 12-4 Solder joint configuration (dimensions in mm).

focus geometry of the laser beam is aligned to the center of the semicircle at the end of the terminal lead (Fig. 12-4). The working distance between the optics and the laser beam interaction area is about 80 mm. With an image projection ratio of 1:2 the minimum focal diameter is 1.2 mm, which is double the fiber core diameter of 0.6 mm.

Thermal radiation emitted from the surface follows the beam delivery system of the galvanometer scanner and passes through a dichroic mirror, which is transparent for this wavelength range. After passing the dichroic mirror the thermal radiation is focused by a lens on a photo detector (Ex. InGaAs, peak wavelength 2.3 μm). The output signal of the detector is conditioned by a logarithmic amplifier circuit. The integrated pyrometric sensor is conditioned for laser beam applications with process temperatures in the range of 150 $^{\circ}\text{C}$, e.g. welding of plastics or soldering. The pyrometric sensor is calibrated by means of a standardized black body and the response time of the sensor is about 1 ms at 150 $^{\circ}\text{C}$.

The surface of the lead/solder pad area is imaged onto a CCD camera via a deflecting mirror.

Apart from interconnection requirements, a high production rate has to be ensured for the process to remain attractive for mass production. For this reason the total process period, especially the irradiation time, has to be as short as possible. However, to achieve an adequate solder joint with reduced irradiation time the laser power has to be increased. To avoid the hazard of superheating, the laser power has to be limited and controlled. Therefore the thermal radiation from the interaction zone is detected and analyzed in more detail. In a series of experiments the following features could reproducibly be observed in the recorded pyrometric signal. A typical profile is presented in Fig. 12-5, where the laser is switched on at time $t = 0.2$ s. At point A the reduction of the ascending slope indicates the initial activation of the applied adipic acid. The second change in the pyrometric signal at point B is related to the onset of localized melting of the solder pad and outgassing of volatile components. Due to the continued energy input by the laser beam, the terminal lead reaches the wetting temperature (point C). In the next phase there is a sudden improvement in heat dissipation due to the wetting of the terminal lead, which often results in a temperature decrease (points C to E). At point D a gas bubble consisting of volatile components leaves the molten solder. The variation of the signal curve following point E is induced by self-optimization of the surface

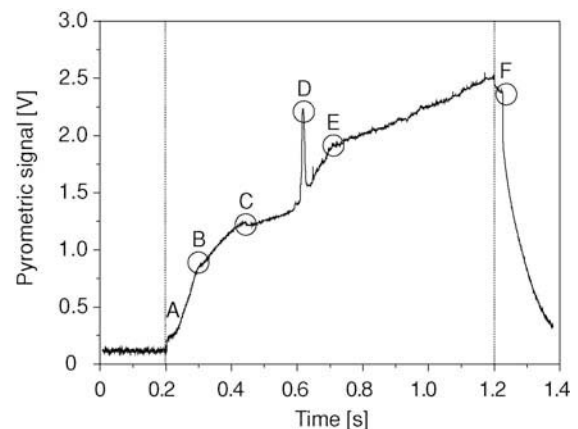


FIGURE 12-5 Pyrometric signal detected during soldering; irradiation time: 1000 ms.

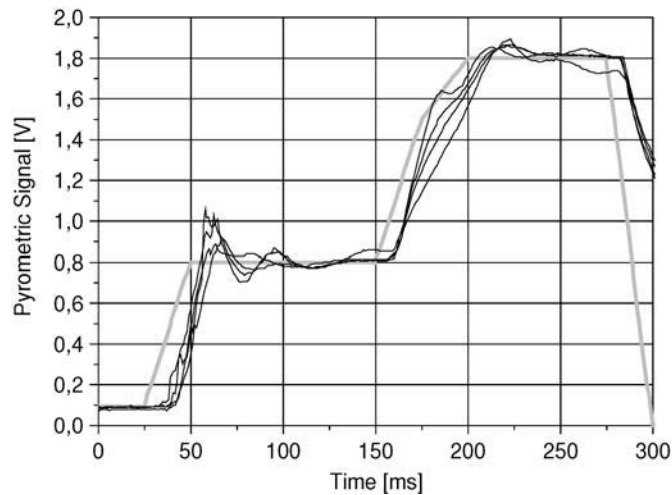


FIGURE 12-6 Array of pyrometer signals recorded during different closed-loop controlled LBS processes. The gray curve represents the defined set point settings.

tension and by superheating of the molten solder pool. After the laser beam is switched off at $t = 1.2$ s, very high cooling rates are observed. This high rate is caused by the optimized heat transfer into the aluminum base-plate. At point F the solder solidifies. The change of the descending slope in the signal curve at the crystallization point F is known from the thermal analysis of solidification reactions in the literature [13,14].

Based on a set of characteristic curves, benchmarks can be determined and by changing specific process parameters a thermal and temporal optimized profile can be generated. Using these analytic profiles as set point settings for a closed-loop control system, the energy input can be controlled

individually for each joining application or product (Fig. 12-6).

Figure 12-7 shows a detailed view of two solder joints and a cross-section of a laser soldered joint.

An innovative application for laser beam soldering is the electrical contacting of solar cells for photovoltaic module production (Fig. 12-8). Due to the decreasing thickness of the solar cells (at the present time $220\ \mu\text{m}$ but in future likely to be below $150\ \mu\text{m}$) the demand for a soldering method without any mechanical contact has led to the development of the laser beam soldering process. The process is controlled by pyrometric sensors to avoid thermal damage of the thin silicon wafer.

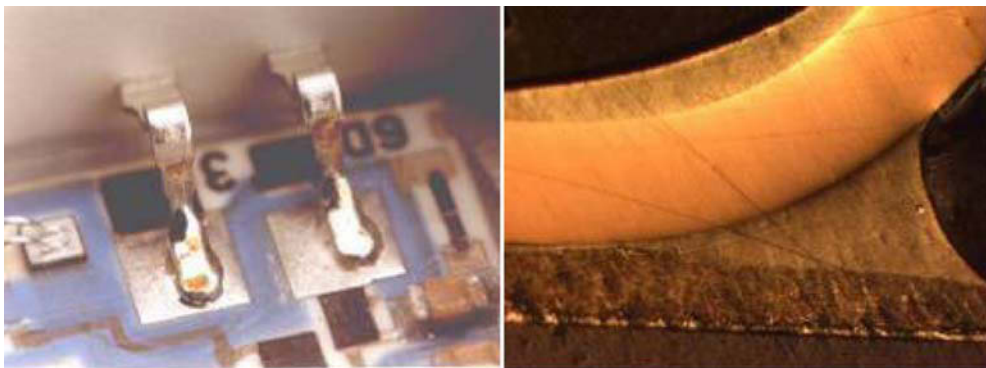


FIGURE 12-7 Detailed view of two solder joints (left) and cross-section of a laser-soldered joint (right).

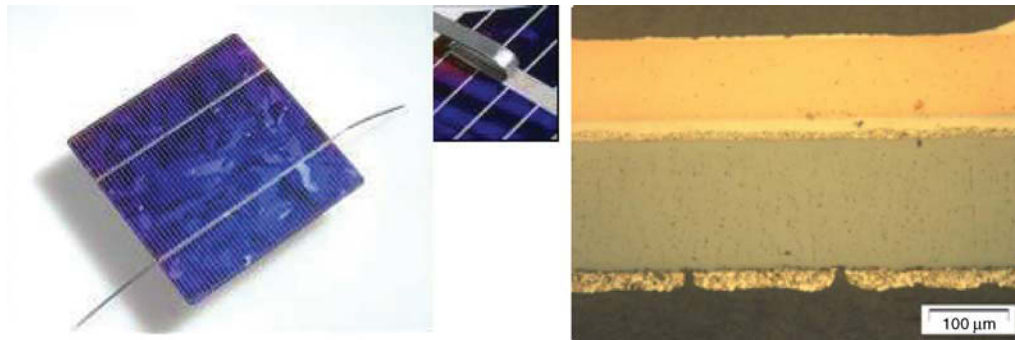


FIGURE 12-8 Electrical contacting for solar cell interconnection.

Laser soldering is playing an increasingly important role as an alternative to the gluing or clamping of micro-optical components into metallic mountings (see Fig. 12-9 left). In contrast to laser soldering, the energy input by induction is difficult for miniaturized optics with a diameter smaller than 1 mm and mounting widths below 50 μm because of the smaller amount of material for heating. Similarly, manual soldering using a soldering iron raises problems because of the small dimensions and therefore the resulting insufficient reproducibility. An alternative to these processes is soldering by using a high power diode laser or a fiber laser. For these experiments the joining components consist of a gold metallized stainless steel mounting and sapphire optics, also metallized with gold. An AuSn solder alloy with a melting temperature of 280 $^{\circ}\text{C}$ is used. By using a fluxing agent, the surfaces are cleaned of oxides before soldering and the joining area is prevented from oxidation during the soldering process. This flux causes pores in the soldering joint and there-

fore pores can be detected. By means of a pyrometer it is possible to set a controlled process and a two-step temperature profile, as recommended in the literature for soldering. At the beginning of the laser soldering process the flux is activated at a lower temperature ($\sim 150^{\circ}\text{C}$), while in the second step the necessary energy for the melting of the solder alloy is applied. This process management reduces the number of pores within the soldered joint significantly (Fig. 12-9 right).

The gap is filled homogeneously with the solder by capillary forces: excessive solder does not wet the surfaces of the sapphire but wets the mounting on the laser facing side. Both diode lasers focused to 1 mm and fiber lasers collimated to 1 mm diameter or lower can be used as laser sources. The advantage of the fiber laser is that the focal position does not have to be aligned because of the Rayleigh length of greater than 1600 mm.

Application areas of selective laser beam soldering using high power diode lasers are manifold and are not confined to a special branch of

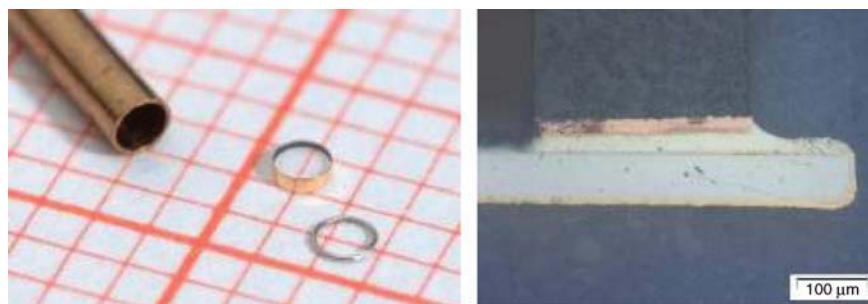


FIGURE 12-9 Joining components: bushing, sapphire optics, solder preform (left) Cross-section of a soldering joint (right).

industry. Currently industrial applications are focused on electronics assembly, especially for the automotive sector. Discrete mounting of critical components, soldering of cable strands, soldering and brazing of micro-electronic and micro-mechanical components and cable assemblies are industrial applications of laser beam soldering.

LASER BEAM MICRO-WELDING

Laser beam micro-welding is a versatile and flexible manufacturing technology, which has found its way into various industrial applications. Electron guns for CRT displays have been produced using Nd:YAG lasers since the 1970s. Such an electron gun contains more than 150 spot welds to assemble the different parts. This adds up to 15 million laser pulses per day. In many other industrial fields laser beam welding tends to become a standard manufacturing technology for small products.

In the watch industry, gear wheels and arbors will no longer be joined in a press fit process, but by means of laser beam welding. In the automotive industry increasingly more sensors and components such as relays and control units are being mounted directly under the hood and have to undergo heavy vibrations and high temperatures. The joints in these components have to survive these stresses with a long estimated lifetime and a very low failure probability, as they are part of the safety equipment.

As a variety of different geometries and different accessibilities have to be joined securely, only a joining technology with high flexibility at reasonable cost and the ability to provide short cycle times can be used. Alternative joining methods often reach their limits in terms of product quality and reliability (Table 12-2).

Laser beam micro-welding is a non-contact process without any tool wear-out. The process duration is shorter than that of comparable techniques. The joining process may be finished within a few milliseconds, whereas the whole cycle time is determined by loading and unloading of the components to be joined as well as by the specifications of the laser source.

Joining method	Disadvantage in comparison to laser beam welding
Adhesive bonding	Elaborate surface pre-conditioning Lower bond strength Long process time
Swedging or border crimping	Tool wear-out Additional forces
Resistance welding	Two-sided accessibility Limited material choice
Soldering	Reduced high temperature strength

One main advantage of laser beam welding is its flexibility: part geometry, material and material combinations can be changed very easily because the energy input can be controlled and the intensity and the power can be adapted to the task over a wide range. Spot welds as well as continuous weld seams can be applied. Process monitoring as a main requirement in industrial production lines can easily be integrated as inline weld monitoring or offline inspection of the weld.

Laser beam welding requires good contact between the joining partners. To obtain good results the joint geometries in Fig. 12-10 have been established.

Processes and Results

The most commonly used laser source is a pulsed flashlamp pumped Nd:YAG laser at a wavelength of $\lambda = 1064 \text{ nm}$ with a low absorption in nearly all

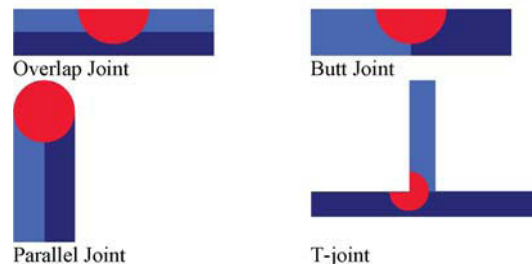


FIGURE 12-10 Joint geometries for micro-welding.

TABLE 12-3 Typical Specifications of Pulsed Nd:YAG Laser Sources and Fiber Lasers

	Pulsed Nd:YAG	Fiber Laser
Average power	10–400	100–200
Pulse power (kW)	1–7	–
Pulse energy (J)	1–50	–
Pulse duration (ms)	0.1–20	Cw
Beam quality (mm mrad)	8–16	0.4
Beam diameter (μm)	50–400	35
Fiber diameter (μm)	100–500	10–50

material. Typical data of commercially available laser sources are listed in Table 12-3.

Pulsed flashlamp pumped Nd:YAG lasers offer some advantages compared to continuously emitting (cw) Nd:YAG lasers:

- High maximum pulse power at moderate average power;
- Better beam quality;
- Affordable investment costs and low cost-of-ownership;
- Lower requirements for cooling;
- Steeper slopes for pulse rise time;
- Pulse forming capability.

The applicability of optical fibers to guide the laser light offers new possibilities for industrial use within manufacturing equipment. The separation of the laser source itself and the working head inside the machine or even the possibility of using one laser source for different machines by energy-sharing or time-sharing mechanisms. By means of this the use of lasers becomes more economic.

The new sources, e.g. fiber lasers, now combine better beam quality with reduced costs.

Beam Delivery

For Nd:YAG lasers, there are two possible ways for beam delivery: direct beam and fiber delivery [10]. The beam quality of a direct beam (BPP 8–20 mm mrad) is better than the beam quality of a fiber guided system (BPP 15–30 mm mrad). The intensity distribution of a direct beam is normally a Gaussian distribution, whereas the fiber guided

system has a top-hat distribution. Thus the Gaussian distribution can be focused better to smaller beam diameter.

A disadvantage of Nd:YAG rod lasers is the influence of the thermal lens. Beam quality and intensity distribution are dependent on duty cycle, pulse duration and laser power. They also can change from pulse to pulse as well as within one pulse. Therefore a laser beam guided through an optical fiber by multiple reflections is homogenized. Beam quality and intensity distribution are predetermined by the diameter of the fiber and its NA and vary only slightly. Furthermore, the maximum temperature of the weld bead using a Gaussian distribution is normally higher, so the top-hat distribution is normally more appropriate for laser beam welding.

The positioning of the beam can be made, by using a Cartesian positioning system, to move the workpiece or by moving the beam by means of a galvanometer scanner (Fig. 12-11).

Typical applications of laser beam micro-welding are dealing with wires and thin sheets ranging from several tens of microns to 1 millimeter in thickness. The diameter of the laser beam should be of the dimension of the thickness of the parts to be welded, although in certain applications it can be larger. Sometimes the parts are already placed in a polymer housing (e.g. a pre-molded package). Here it has to be taken account that the housing material must not be influence by diverging laser radiation or by the heat created by the joining process. The main materials are steel and coated and uncoated copper alloys.

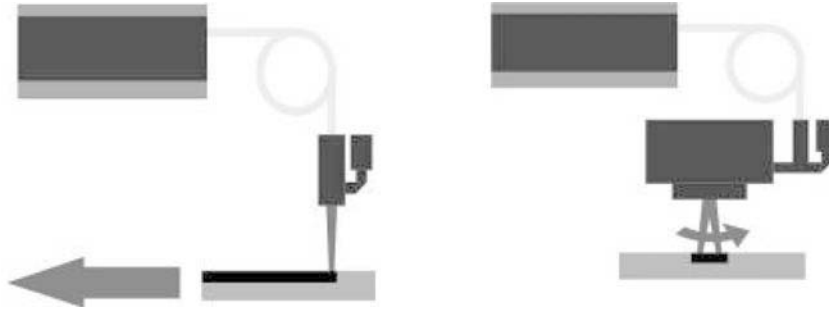


FIGURE 12-11 Positioning of the laser beam for micro-welding.

Often combinations of materials have to be joined, e.g. steel/copper or steel/brass. In this situation the joint geometry determines the weldability. As the joining tasks differ greatly in terms of geometry, dimensions and material, attention has to be paid to the heat conduction in the parts. Sheets with a thickness of below $500\ \mu\text{m}$ cannot be treated as semi-infinite bodies. Therefore, heat accumulation at the back face of the sheet influences heavily the welding as well as the heat losses into the surrounding material of the parts and the clamping devices.

In micro-technology three different types of joining methods are applied: spot welding, spaced spot welding to create lines and continuous seam welding (Fig. 12-12).

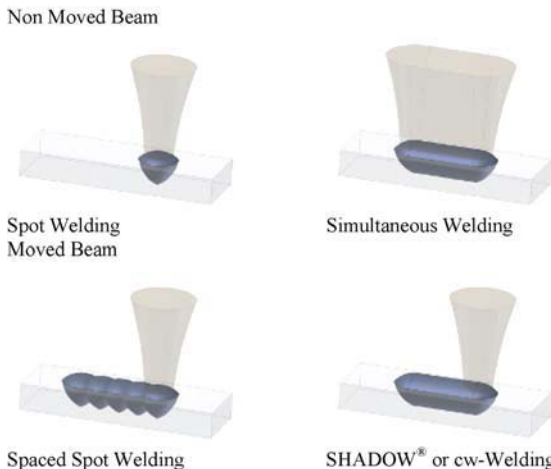


FIGURE 12-12 Classification of laser beam micro-welding.

Spot Welding

Spot welding will be applied if only small connection cross-sections are needed or if the available space is not sufficient for elongated weld seams. The diameter ranges from 100 to $800\ \mu\text{m}$ depending on the beam diameter, the material and the laser power. The spot welding process can be divided into four phases: heating, melting, melt flow dynamics and cooling. Depending on the intensity, evaporation of material may occur.

By means of pulse forming, the intensity can be adapted to the sequence of the process phases. A typical pulse form is given in Fig. 12-13.

For some materials a pre-heating, as shown on the left in Fig. 12-13, is favorable. Other materials such as copper alloys require high intensities at the beginning of the pulse in order to crack existing oxide layers and to ensure stable uncoupling of the laser energy.

Post-heating with well-controlled cooling conditions may reduce the risk of cracks. Therefore a pulse form as shown on the right in Fig. 12-13 can be used. Typical pulse durations range from 1 to $15\ \text{ms}$.

For pure heat conduction welding, the weld depth amounts to the radius of the weld spot diameter. Increasing the intensity leads to evaporation of material and to the establishing of a capillary. The presently developing keyhole welding process creates deeper weld depths. The discrimination between pure heat conduction welding and keyhole welding cannot be given for micro-parts due to the given facts of heat accumulation and the dimensions of the parts.

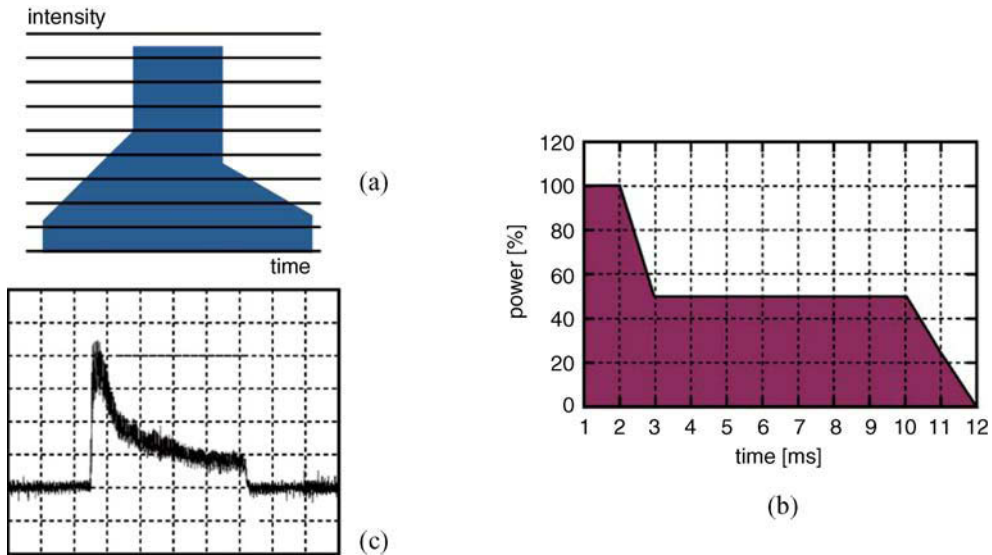


FIGURE 12-13 Typical pulse form.

Spaced Spot Welding. Spaced spot welding is realized by placing several spot weldings at a certain overlap in order to achieve a seam weld. The length of the seam is scalable, but the heat input is very high because for each spot all process phases of spot welding have to be passed through. This may lead to distortion or thermal damage of the parts. Fig. 12-14 shows a cover of a battery housing for a pace-maker.

Important process parameters beside pulse power and pulse duration are pulse repetition rate and feed rate. The latter two determine together with the spot diameter the overlap of two consecutive spots, which is usually in the range of 60%.

Continuous Welding

Continuously emitting lasers are seldom used in micro-technology to realize weld seams because of the large beam diameter.

Up to the present time, cw laser welding has been used only for longer joints and for larger parts. A high average laser power, $P_{av} > 500$ W, and a high processing velocity, $v > 5$ m/min, are required for cw laser welding. Above all, cw laser sources are more expensive than pulsed laser sources. Nevertheless the joints obtained by cw laser welding show a smooth surface and an optimized micro-structure almost entirely without pores. The energy per length is less for cw laser welding than for pulsed laser welding.



FIGURE 12-14 Typical application for spaced spot welding.
(Source: Lasag.)

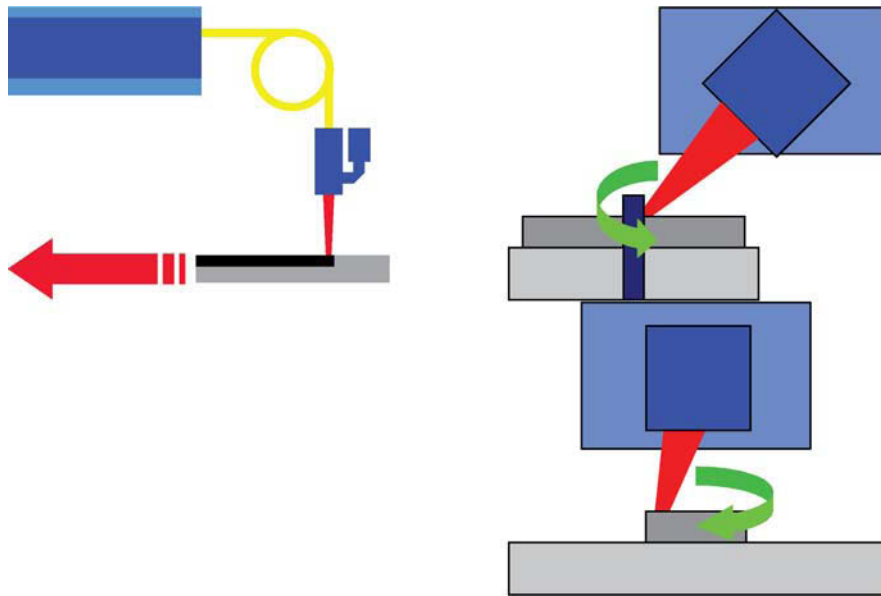


FIGURE 12-15 Schematic drawing of the set-up.

The idea is to apply continuous wave welding to micro-parts with a part geometry of less than $500\ \mu\text{m}$ and a weld width of less than $100\ \mu\text{m}$. The use of pulse forming (temporal shape of the laser pulse) enables the joining of dissimilar materials such as steel to copper. As the length of the weld seam will be very short, continuous wave lasers tend to be off rather than being used for welding. In a typical application until a welding time of 20 ms and a part cycle time of 1 part per second the duty cycle amounts to 0.02 and the use of a continuous laser tends to be very inefficient. Therefore a new technique called SHADOW[®] was developed to realize extended weld seams with a pulsed laser using one single pulse and sweeping the laser beam over the surface during the duration of the pulse.

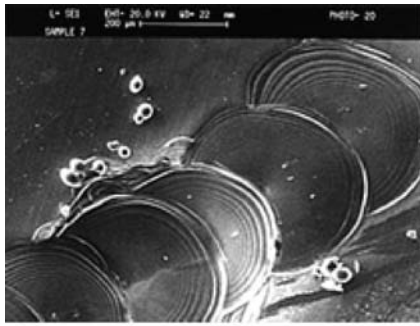
SHADOW[®] stands for Stepless High Speed Accurate and Discrete One Pulse Welding. It was invented to weld small axi-symmetric parts which can be rotated quickly during one single laser pulse. This technique combines the advantages of continuous wave welding, such as a smooth surface and a high process speed, with the possibilities of the pulsed laser systems, such

as lower costs and the capability of forming the temporal lapse of a pulse. Since the parts are small the latter advantage of the process enables the application in micro-technology, where the thermal load of the assembled parts has to be well controlled (Fig. 12-15).

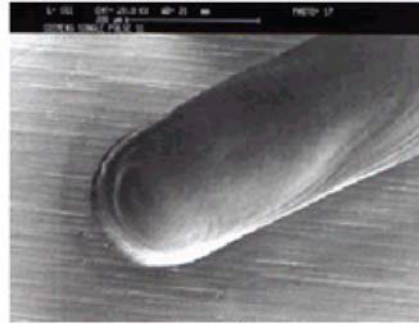
Pulsed laser sources at present are able to generate a maximum pulse duration of $\tau_{H,\text{max}} = 20\ \text{ms}$. To weld parts over a length of $l = 2\ \text{mm}$ a processing velocity of $v = 6\ \text{m/min}$ is therefore required.

Comparing the energy input ($E_{H,\text{SHADOW}} = 6\ \text{J}$) to the energy input for a similar joint using the multi-pulse technique where ten pulses without overlap are needed ($E_{H,p} = 10 \times 2.4\ \text{J} = 24\ \text{J}$), it is seen to be less by a factor of 4. Moreover, the joined parts show less debris or pollution on the surface and neglecting the time needed to accelerate the process, and the processing time is dramatically reduced.

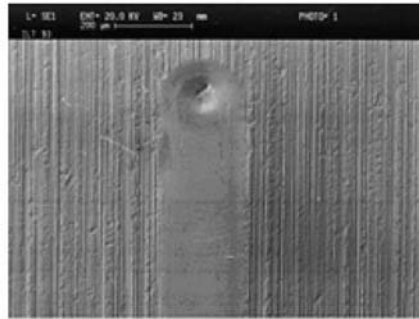
The effect of reduced energy input can be seen in Fig. 12-16. As the transition from solid to liquid is limited to the initial instant of the process, no particles or melt ejections occur. The result is a smooth and even surface of the weld seam.



Stainless steel, pulsed mode



Stainless steel, SHADOW®



Brass, SHADOW®

FIGURE 12-16 Examples of the weld seam with SHADOW®.

SHADOW® can be used for welding difficult materials and to improve the weld quality. The applications are shown in the following section.

Applications of SHADOW® in fine Mechanics and Electronics. The accuracy of a mechanical watch depends on the quality of the rotating spring assembly (balancer). For high-end watches this balancer consists of a ring with four pins. Here SHADOW® is used to weld the pin to the ring. As the outer surface is diamond turned after the welding process the weld seam can no longer be seen. The diameter of the annular weld seam can be adjusted to achieve either a ring around the pin or, by reducing the diameter, the pin can be molten in total (Fig. 12-17).

Instead of moving the laser beam by means of a scanning head the complete part can be turned, especially for the joining of a wheel to an axis or, as shown in the following example, the inner cage of a ball bearing. The axis in the middle of the part

prohibits the use of a scanning head where the beam comes from the center of the field of view. This application is done with a high speed rotating workpiece with a tilted beam targeting from the outside to the center of the part at an inclination angle of 45° (Fig. 12-18).

Comparison of Conventional Pulsed Mode Welding to SHADOW®. The already mentioned advantages of the SHADOW® technique can be discussed in an example from the watch industry. The application is the second hand of a gear wheel. The typical combination of steel and brass with its problem of evaporation of zinc is shown in Fig. 12-19. Two different methods are applied and the results are discussed in the following.

In pulsed mode, 130 pulses with a pulse energy $Q = 0.1$ J are applied. The total energy amounts to 14 J. In comparison, the SHADOW® technique only uses one pulse with an energy $Q = 1.3$ J. The reduction of the energy results in a smooth surface without any ejection or particles on the part.



Material		Parameter	
Ring	CuBe2	$Q = 2.0 \text{ J}$	
	$h = 700 \text{ }\mu\text{m}$	$\tau_{II} = 6.5 \text{ ms}$	
Pin	CuBe2	$v_f = 35 \text{ m/min}$	
	$d = 350 \text{ }\mu\text{m}$	$N = 3$	
		$\alpha = 0^\circ$	

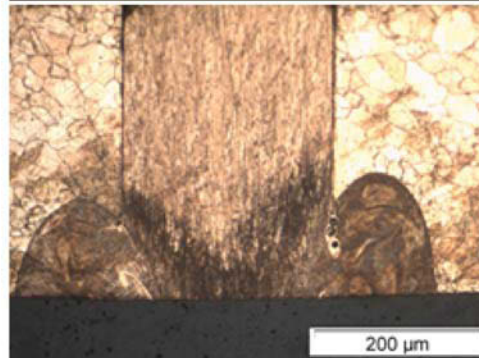
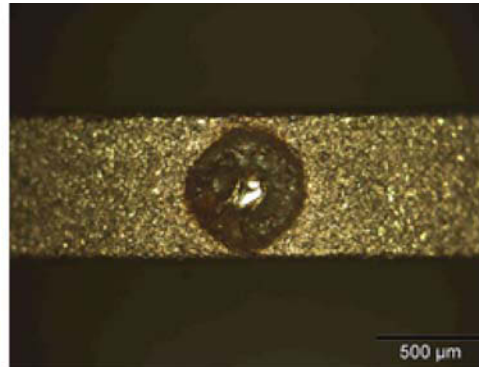


FIGURE 12-17 Balancer for mechanical watches.



Material		Parameter	
Inner Cage	CuBe2	$Q = 1.3 \text{ J}$	
	$d = 600 \text{ }\mu\text{m}$	$\tau_{II} = 20.0 \text{ ms}$	
Outer Cage	CuBe2	$v = 5.6 \text{ m/min}$	
	$d = 3\,000 \text{ }\mu\text{m}$	$N = 1$	
		$\alpha = 45^\circ$	

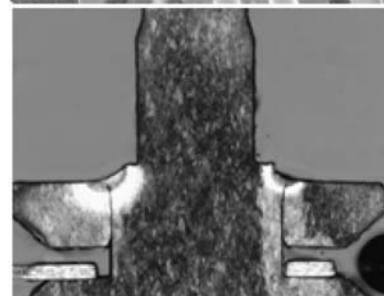
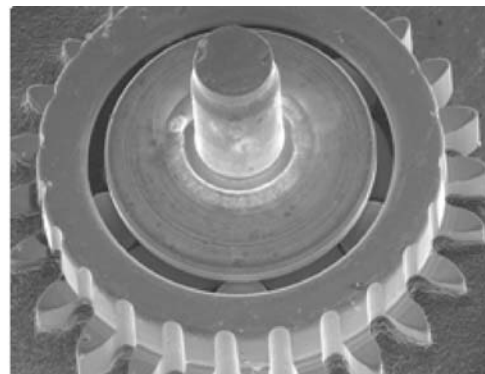


FIGURE 12-18 Ball bearing.



$P_H = 112 \text{ W}$, $\tau_H = 1.0 \text{ ms}$, $f_p = 100 \text{ Hz}$, $Q = 1.3 \text{ J}$, $\tau_H = 20 \text{ ms}$, $v = 3.3 \text{ m/min}$
 130 pulses

Low contamination of the surface

FIGURE 12-19 Comparison of conventional pulsed mode (left) welding to SHADOW® (right). Material: axis S20AP; \varnothing 0.3 mm wheel CuZn37.

Pre-conditions and Limits of Laser Beam Micro-welding

To determine the applicability of laser beam micro-welding for a specific joining problem, there are some crucial points that have to be investigated.

Offsets in the butt joint configuration and gaps at all instances commonly create kerfs at the edges of the weld seam, which decrease the stability and strength of the joint. Furthermore, the surface conditions such as oxidation or contamination with lubricants due to preceding manufacturing steps, e.g. stamping, change the absorption and therefore the welding result. As a consequence more pores may occur.

Reproducible clamping conditions are one major precondition to assure reproducible weld results. The thermal mass and the dimensions of the parts are so small that differences in the positioning within the clamping, varying gaps or clamping forces may not be compensated for.

Furthermore, the position of the focal plane with respect to the surface of the workpiece is crucial for the weld result. Defocusing due to misalignment will lead to broadening of the weld seam, taking into account that the intensity distribution may seriously change the process behavior. Finally, the mode of operation of the laser source itself influences the weld results. At the limits of the working range the focusing conditions vary from pulse to pulse in terms of pulse power, pulse form and intensity distribution.

CONCLUSIONS AND REMARKS

Laser beam joining offers the advantage of well-controlled energy input into the parts with low effects on the surrounding material.

When welding micro-parts, two different kinds of laser sources can be chosen: diode pumped systems such as fiber or thin disc lasers for longer weld seams and flashlamp pumped rod lasers used for the SHADOW® technique. Fiber laser systems of up to 200 W are able to weld stainless steel as well as copper up to thicknesses of at least 250 μm . It is also possible to weld dissimilar metals in an overlap configuration. The beam diameter has to be small to obtain a keyhole. However, the Rayleigh length of a laser beam with 15 μm beam diameter is smaller than 200 μm , so the requirements for beam positioning are quite high.

The flashlamp pumped rod laser used for the SHADOW® technique is more economic for weld seams length of up to several half centimeters. The SHADOW® welding technique combines the advantages of continuous welding such as low contamination and smooth weld beads with the lower investment costs of a pulsed solid state laser, with its capability of pulse forming and the good focusability due to its comparable beam quality. As most micro-parts need only short weld seams, the SHADOW® technique is often the more economic welding technique.

Fiber lasers with their unique beam quality at reasonable cost and extremely small footprints are at their point of entry into industrial use. The possibility to realize very small weld seams

due to their achievable focus diameter opens up new fields of use in micro-mechanics and micro-electronics, such as the replacement of thermo-sonic ribbon bonding for high power electronics.

REFERENCES

- [1] L. Bosse, N. Göbbels, A. Olowinsky, A. Gillner, R. Poprawe, Production cell for laserjoining of micro-systems with modular Pick-&-Join-tools, Proc. Third Int. WLT-Conf. on Lasers in Manufacturing LIM (2005) 785–789.
- [2] G. Humpston, D.M. Jacobson, Principles of Soldering, ASM Int, Materials Park (2004).
- [3] C.F. Bohmann, The laser and microsoldering, SME Technical + Paper No. 10: AD74-810 (1974).
- [4] F. Burns, C. Zyetz, Laser microsoldering, Electronic Packaging & Production(1981).
- [5] D. Chang, Experimental investigation of laser beam soldering, Welding J. 65 (10) (1986) 33–41.
- [6] F.G. Meyer, Laserlöten unter besonderer Berücksichtigung der SM-Technologie und des Lötens an schwer zugänglichen Stellen, DVS-Verlag Düsseldorf (1989) 122 70–71.
- [7] R. Vanzetti, A.S. Dustoomian, Intelligence comes to laser soldering, Electronics(July 1986) 75–77.
- [8] F.G. Meyer, B.H. Klimt, Laser soldering of surface mounted devices, Proc. SPIE 744 (1987) 8–90.
- [9] R. Keeler, Lasers for high-reliability soldering – for soldering military, computer, and other high-rel products lasers surpass mass-soldering methods, Electronic Packaging & Production 27 (10) (1987).
- [10] M. Haag, M. Brandner, Diodenlaser – innovatives Werkzeug für die Produktion, Proc. LaserOpto 3 (2000) .
- [11] L. Bosse, A. Koglin, A. Olowinsky, V. Kolauch, M. Nover, Laser beam soldering – an attractive alternative to conventional soldering technologies, Proc. SPIE 4977 (2003) 473–480.
- [12] L. Bosse, A. Gillner, R. Poprawe, Temperature controlled selective soldering with laser radiation, Proc. of the 6th International Symp. on Laser Precision Microfabrication (2005).
- [13] L. Bosse, A. Schildecker, A. Gillner, R. Poprawe, High quality laser beam soldering, Microsystem Technologies 7 (2002) 215–219.
- [14] L. Bosse, A. Gillner, R. Poprawe, Adapted time-power profile for laser beam soldering with solder paste, Proc. SPIE 4406 (2001) 76–81.

Deep X-Ray Lithography

Pascal Meyer, Joachim Schulz and Volker Saile

INTRODUCTION

By far the leading technology for the manufacturing of MEMS devices is silicon micro-machining with its various derivatives. However, many applications of micro-systems have requirements in respect of materials, geometry, aspect ratio, dimensions, shape, accuracy of micro-structures, and number of parts that cannot be fulfilled easily by mainstream silicon-based micro-machining technologies. LIGA, a German acronym for Lithography (Lithographie), Electroplating (Galvanoformung), and Molding (Abformung) enables the highly precise manufacture of high aspect ratio micro-structures with large structural thickness ranging from hundreds to thousands of microns. These tall micro-structures can be produced in a variety of materials with well-defined geometry and dimensions, very straight and smooth side walls, and tight tolerances. LIGA technology is also well suited for the mass fabrication of parts, particularly in polymers. Many micro-systems benefit from the unique characteristics and advantages of the LIGA process in terms of product performance. In this chapter the strengths of the manufacturing method and its main fields of application are emphasized, with examples taken from various groups worldwide, especially in micro-mechanics and micro-optics.

Several micro-fabrication technologies are available at the present time and are used to fabricate micro-components and -systems. The most successful micro-machining technologies have been developed as extensions of standard IC and micro-electronics planar silicon-based processing.

Others are based on advanced precision engineering and laser structuring. However, individual technologies including Si micro-machining or laser structuring are far from being sufficient to fulfill the needs of the variety of problems posed by:

- the great variety of functions of most of the devices to be made;
- the conditions of the surroundings in which they will operate;
- the optimum cost/performance ratio for the targeted application.

Interest in a number of non-Si-based machining methods stems from major deficiencies of IC-based machining techniques:

- the need for using application-specific materials to optimize the functions and performance of various devices;
- the need to reduce cost by choosing low cost materials;
- the difficulty in constructing truly 3D objects with planar-based processing, which continues to be a challenge.

Precision and ultra-precision mechanical, electro-discharge, LIGA-based, and laser-based, micro-machining techniques, to mention the most current, are such alternative techniques, each with its specific application domains and relative merits. LIGA-based processing, a sequence of micro-fabrication steps combining a step of deep X-ray lithography (DXRL), also called by some authors 'deep etch X-ray lithography', and subsequent additive processing of plating-through-mask and molding, has moved from the position of emerging from micro-fabrication technology to become

a well-established non-silicon alternative micro-fabrication technology for MEMS.

LIGA technology provides unique advantages over other manufacturing methods in the fabrication of micro-structures. LIGA-based technologies are used and are being further developed in a number of R&D institutes around the world. Spin-off companies and commercial companies have also evolved around large-scale synchrotron facilities. Also, commercial applications of the LIGA process are on the market. LIGA technology has been developed over the rather long time span of two decades [1–4]. During this time other high aspect ratio technologies such as UV photolithography in thick resist, for example as SU-8, often referred to as UV-LIGA, and Deep Reactive Ion Etching (DRIE) of silicon have also evolved and challenged LIGA successfully in some specific application areas. For planning the role of LIGA in future manufacturing, a review of potential applications may serve as a useful basis. The basic LIGA process and some aspects of the process are recalled here to illustrate its strengths and discuss still existing challenges.

THE LIGA PROCESS AND ITS STRENGTHS

The basic LIGA process is described in Fig. 13-1. In the first step of the process, an X-ray-sensitive polymer (resist) layer of up to several millimeters thickness is coated onto a conductive or non-conductive substrate. Typically polymethylmethacrylate (PMMA) is used as positive resist and an epoxy-based resist SU-8 [5–9] as negative resist. A pattern from a mask is then transferred into the thick resist layer via a 1:1 shadow-proximity printing scheme using hard X-rays from a synchrotron radiation source. After exposure, selective dissolution of the chemically modified irradiated parts of the positive resist (or dissolution of the non-irradiated parts of the negative resist) in a chemical developer results in a polymeric relief replica of the mask pattern.

Then, depending on the material, number of parts selected for the final product, accuracy, quality and price, different fabrication routes

can be chosen, which may include further steps of micro-replication through electroforming and/or a variety of molding techniques (injection molding, embossing, casting, compression molding, etc.). The polymeric micro-structure can be used:

- simply as it is;
- as a lost mold for the formation of ceramic micro-parts;
- as an electroplating template to generate metallic micro-parts;
- as an electroplating template to produce a metallic master-mold, which can then be used many times to mold cost-effective replicas in other materials, primarily polymers. When producing large numbers of electroplated components, the molded polymer parts are used as lost molds for a second plating process.

The unique processing feature that enables the manufacture of thick micro-structures characterized by very steep walls and very tight tolerances is the creation of a high precision resist template by deep X-ray lithography using X-ray photons from a synchrotron radiation source.

LIGA MANUFACTURING STEPS

Resist Technology

The resist technology consists of applying a resist onto a substrate, the substrates that can be used depend on the product to be made (for example, a mold insert), but they should meet the following criteria:

- a high planarity;
- the substrate and resist should have good adhesion;
- the substrate surface should be conductive if an electroplating step is needed;
- the resist developer should not etch the substrate.

Concerning the resist, a distinction should be made between positive and negative resist. In the first case, the radiation will damage the polymer by reducing its molecular weight; the most commonly used being polymethylmetacrylate (PMMA); the irradiated parts becoming soluble

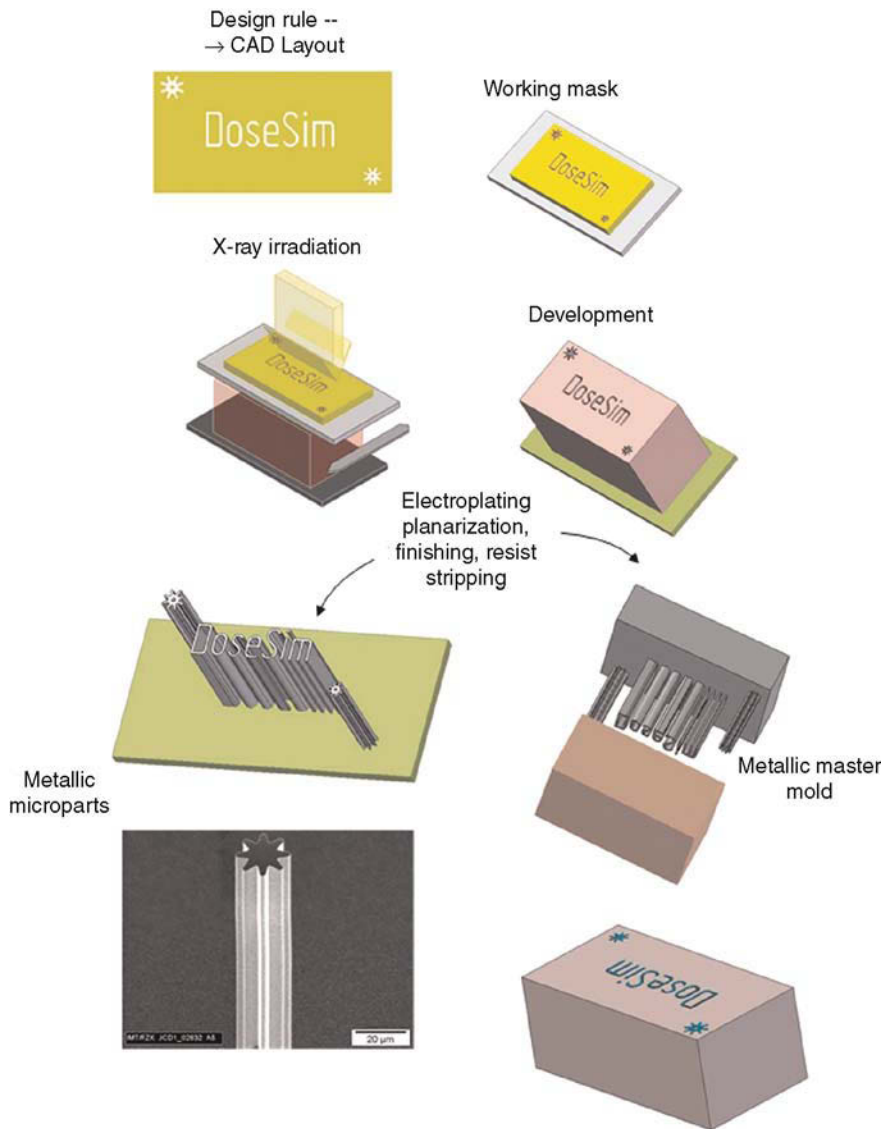


FIGURE 13-1 Illustration of basic LIGA process steps.

in a developer. In the case of a negative resist, the radiation will ‘damage’ the polymer by increasing its molecular weight (curing/cross-linking); the irradiated volume being insoluble in a developer; the most commonly used of which is an epoxy-based resin: the SU-8. In the first case, it is necessary to know the dose to apply to the resist so that it becomes soluble in the developer; while the developer must have a negligible influence on

the non-irradiated parts; in the second case, it is necessary to know the dose to apply to the resist so that the exposed part becomes insoluble in the developer. PMMA is still the resist of choice for many applications; this resist offering very high resolution and stable processing parameters. Its sensitivity is low, which means high exposure costs. SU-8 is a very attractive resist; its sensitivity is high, reducing exposure times by a factor of 100

compared to PMMA. However, SU-8 actually offers an unreliable performance due to the high sensitivity of processing parameters' fluctuation.

Resist Deposition

Concerning PMMA, two possibilities exist:

1. **Gluing a commercially available PMMA sheet with a glue consisting of PMMA dissolved in methylmetacrylate (MMA).** Prior to gluing, the PMMA sheet is cut and milled to the desired dimensions, the stress so induced being removed by annealing under controlled ramping conditions (the max temperature is slightly above the glass transition temperature of the PMMA used). The positioning of the sheet and the dispersing of the glue can be made using a robotic dispenser combined with a pick-and-place machine. This method is generally used for PMMA thicknesses greater than 100 μm .
2. **Casting.** A resin consisting of PMMA dissolved in MMA is mixed with di-benzoylperoxide and dimethylaniline, and is applied to the substrate and hardened under a pressure of 4 bar at room temperature for 4 h; the dispensing can be effected using a robot dispenser. Subsequently, the resist-coated substrate is annealed under ramping conditions.

This method is generally used for PMMA thicknesses of less than 100 μm .

The SU-8 is spin coated. Experimental results indicate that the coating qualities of SU8 are affected by several factors, including the spinning speed, the photoresist viscosity, the initial acceleration and the duration. After the resist has been applied to the substrate, it must be soft baked to evaporate the solvent and densify the film.

Irradiation Technology

LIGA technology needs a synchrotron beam-line to perform the resist exposure, a scanner to move the sample through the line shaped beam, and a computer program to calculate the dose.

Synchrotron Source – Scanner. At the heart of a synchrotron (see Figs. 13-2 and 13-3) is a storage ring: a huge donut-shaped vacuum chamber. Electrons are accelerated and confined to travel around the storage ring at nearly the speed of light [10–12]. Because the electrons are constantly forced to travel in a closed loop they are accelerated, and accelerated electrons lose energy in the form of synchrotron light. A synchrotron produces light of exceptional quality and brightness: a million times more intense than that of a hospital X-ray machine. A



FIGURE 13-2 Schematic view of a synchrotron (source: Soleil).



FIGURE 13-3 View of the synchrotron ANKA.

charged particle that is constrained to move in a curved path experiences centripetal acceleration. Due to this acceleration, the particle radiates energy according to the Maxwell equations. A non-relativistic particle emits radiation primarily at its frequency of revolution. However, as the speed of the particle approaches the speed of light, the radiation pattern is distorted by relativistic effects and changes to a narrow cone of radiation with angular spread. The total energy E for a particle of mass at rest m_0 moving at velocity v is:

$$E = \gamma \cdot m_0 \cdot c^2 \quad (1)$$

with

$$\gamma = 1 / \sqrt{\left(1 - \frac{v^2}{c^2}\right)} \quad (2)$$

The opening angle $\Delta\varphi$ of the radiation cone can be expressed, for high values of γ , as:

$$\Delta\varphi \cong \gamma^{-1} \quad (3)$$

Synchrotron radiation sources produce photons with a continuum of energies, from the infrared to the X-ray region. The spectral range of

photons produced by electrons (energy $E_e(\text{GeV})$) in a bending magnet (radius of curvature: R_b , magnet field: B (T)) can be characterized with the critical energy E_c , where:

$$E_c = \frac{3\hbar c \cdot \gamma^3}{2 \cdot R_b} \quad (4)$$

In practical units, the critical photon energy is also given by:

$$E_c(\text{KeV}) = 0.6650 \cdot E_e^2(\text{GeV}) \cdot B(\text{T}) \quad (5)$$

E_c is defined in terms of the spectral power radiated by a relativistic particle: half of the power spectra is radiated at energies below E_c and the other half at energies above it. A wiggler (a series of magnets designed to periodically horizontally deflect the charged particle) and an undulator (a series of magnets designed to periodically vertically deflect the charged particle) are also used to produce synchrotron radiation, the differences of which are indicated in Fig. 13-4.

Presented in Table 13-1 is a non-exhaustive list of synchrotrons with install LIGA beam-lines.

For example, the synchrotron ANKA in Karlsruhe (Germany) is a third-generation, medium-

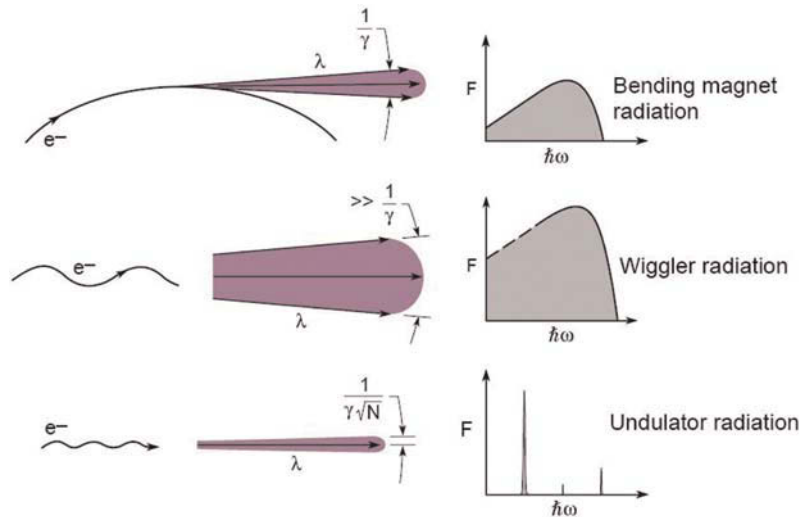


FIGURE 13-4 Different sources of synchrotron radiation with some of their characteristics.

energy source, with an electron beam energy of 2.5 giga electron volts. The X-rays are sent into the various beam-lines (the straight lines branching out of the synchrotron). A typical LIGA beam-line is presented in Fig. 13-5. All of the beam-lines are equipped with a scanner (see Fig. 13-6), and optical elements which modify the spectrum of the source. In fact, the synchrotron spectrum should be adapted to the needs of the user. The synchrotron ANKA has three LIGA beam-lines (LIGA1, LIGA2, LIGA3) sited on a bending magnet (1.5 T) with different optics. The characteristics of the beam-lines are given in Table 13-2. The spectra of the lines after the front end window and optics are given in Fig. 13-7. The X-rays produced are highly parallel and to conserve this property

for the lithography aspect, the diffraction (Fresnel) effect should be as low as possible and also the absorption of the photons should take place only in the designed volume. In X-ray lithography, typically X-rays in the $0.5\text{--}5 \cdot 10^{-10}$ m region are used, which interact with matter by the photoelectric effect, the Compton effect, and Rayleigh scattering. The total effect depends on the cross-section of the different possibilities of interaction. The primary dose, which is about 95% of the deposited dose, is due to the photoelectric effect in PMMA. Incident photon energy will be dissipated ultimately by secondary electrons generated by impact ionization; the distance over which the energy is spread should be as small as possible. The resolution limit of X-ray lithography is a

TABLE 13-1 Synchrotron Location and Operating Energy (this is a Non-Exhaustive List)

Name	BESSY	ANKA	ELETTRA	CAMD	AURORA
Country/City	Germany/Berlin	Germany/Karlsruhe	Italy/Trieste	USA/Baton Rouge	Japan/Kyoto
Operating energy (GeV)	1.7	2.5	1.7	1.3	0.575
Nb. of LIGA beam-lines	2	3	1	4	4

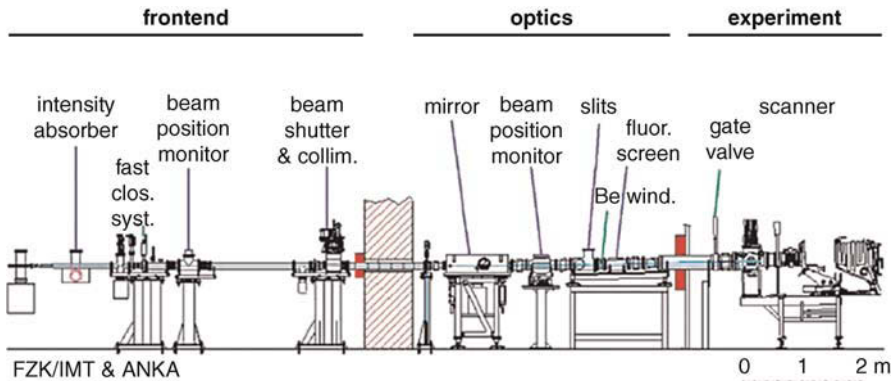


FIGURE 13-5 Schematic diagram of an X-ray lithography beam-line (ANKA-LIGA2).

function of diffraction in the mask-to-sample gap, and the effective range of the photo and auger electrons related when an X-ray is absorbed. In Fig. 13-8, it is shown how the spectrum (source synchrotron ANKA; beam-line LIGA3) is attenuated during the exposure of a 1400 μm PMMA sample. The carbon and aluminum filters absorb the low energy radiation to prevent overexposure of the top surface; the primary dose to be deposited in the resist should be situated in the region D_{bottom} to D_{top} . This region has been determined by many tests and is the best compromise between exposure and development time. The mask membrane (beryllium) is quasi-transparent, as it is required. The absorber thickness should be a

minimum, defined by the threshold dose at which the resist starts to dissolve.

PMMA Degradation. During X-ray irradiation of PMMA, synchrotron light is absorbed in the exposed PMMA area, which results in a chemical modification; a scission of the polymer chain leads to a radiation-induced degradation of the molecular weight and becomes soluble in an organic developer. By increasing the dose of radiation, the average molecular weight decreases from an initial value $M_{W(D_{\text{dose}}=0)}$ (about $1.5 \cdot 10^6$ g/mol) to a minimum limiting value of between 2500 g/mol and 3000 g/mol at a very high dose of radiation. The degradation mechanism of radiation-excited PMMA depends on the chemical structure of the



(a)



(b)

FIGURE 13-6 (a) Side and front (scanner open) view of the Jenoptik scanner – beam-line: ANKA-LIGA3, and (b) side and front (scanner open) view of the Jenoptik scanner – beam-line: ANKA-LIGA3.

TABLE 13-2 Some Characteristics of the Three LIGA Beam-lines of the Synchrotron ANKA

Beam-line	LIGA1	LIGA2	LIGA3
Window	175 μm beryllium	225 μm beryllium	350 μm beryllium
Optics	single Cr mirror	single Ni mirror	no optics
Dedicated to	X-ray lithography	deep X-ray lithography	Ultra-deep X-ray lithography
Structure height	up to 100 μm	100 to 600 μm	600 to 2500 μm

resist and the exposure energy. The radiochemistry of PMMA is a complex mixture of consecutive reactions including excitations, fissions, cross-linking, recombinations, disproportions, rearrangements and transfer reactions. The most important step of degradation is the scission of the methyl ester group, which is responsible for the major amount of the gases evolved. The remaining polymer chain stabilizes after hydrogen abstraction by formation of a double bond or by chain scission. Radio-chemical degradation of PMMA is categorized into two schemes:

1. About 80% of the main-chain scissions have been observed after preceding side-chain degradation. The radiation-excited polymer molecule splits off an ester side-chain. The remaining chain radical stabilizes after hydrogen abstraction by the formation of a double bond, or reacts by way of a main-chain scission. In the case of stabilization by hydrogen

abstraction, the molecule has one ester side-chain less than before irradiation.

2. The remaining 20% of the main-chain scissions are due to the direct decomposition of the polymer into two macro-molecules. Recombination of these fragments results in the primary polymer molecule.

PMMA Development. The dissolution rate is a function of molecular weight, which is related to the initial PMMA molecular weight, the dose and the main-chain scission yield [13–21]. This reduction of the average molecular weight causes the solubility of the resist in the developer to increase dramatically. A developer suitable for PMMA in X-ray lithography, commonly referred to as the GG developer, is composed of 15 vol% deionized water, 60 vol% 2-(2-butoxyethoxy)ethanol, 20 vol% tetrahydro-1-4-oxazine and 5 vol% 2-aminoethanol. For X-ray lithography process simulation to calculate

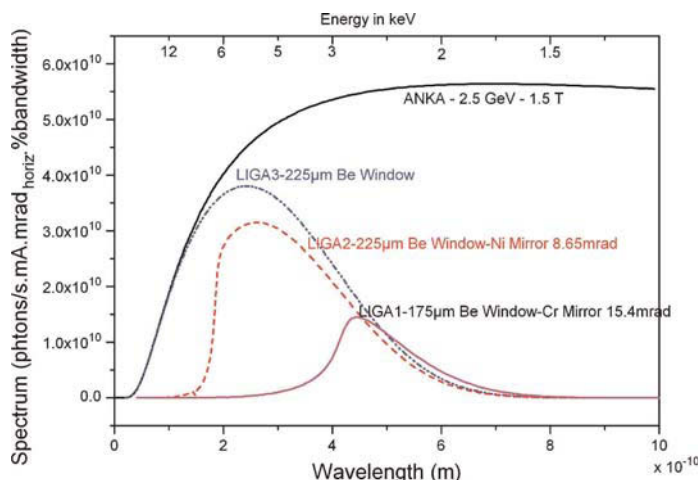


FIGURE 13-7 Spectrum of the three LIGA beam-lines at ANKA, Germany.

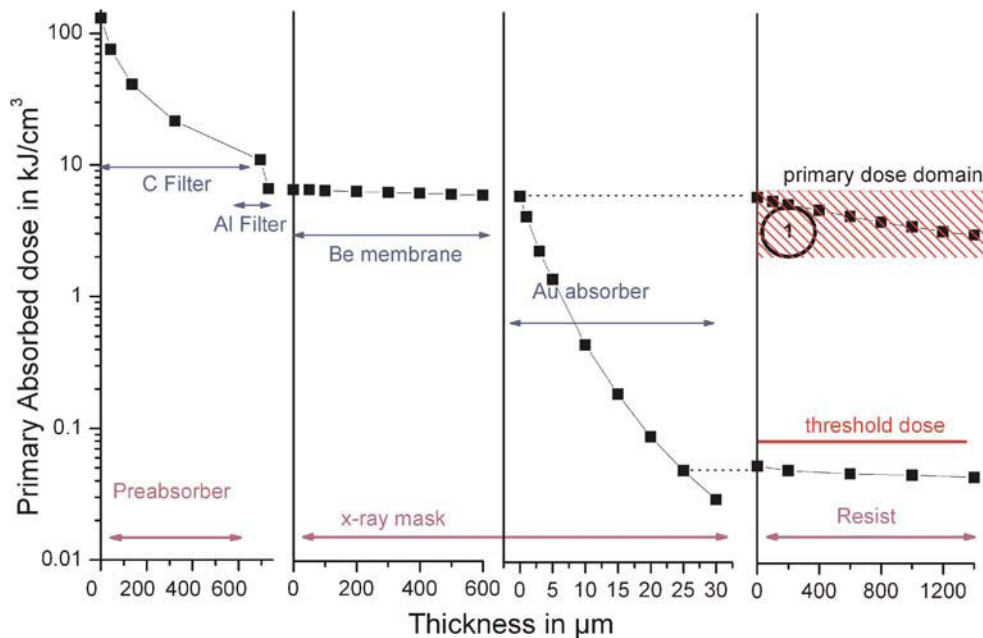


FIGURE 13-8 Primary absorbed dose along the X-ray trajectory, including a 1400 μm thick PMMA foil X-ray mask with a 550 μm beryllium membrane and carbon and aluminum filters. The source is ANKA; the beam-line is LIGA3.

high aspect ratio micro-structures and realistic MEMS devices of the size order of mm, a macroscopic resist dissolution and an easily measurable approach are required, rather than to describe the very complicated problem of microscopic resist dissolution. In chemistry, many models concerning polymer dissolution may be found. Due to the fact that a dose profile is deposited during X-ray lithography and the GG developer consists of four components, these models cannot be applied easily. The dissolution rate is described by the following equation (all other parameters being constant):

$$R(D) = R_0 + C \cdot (M_{W(Dose=D)})^{-\beta} \quad (6)$$

R_0 corresponds to the development rate of an unexposed resist $M_{W(Dose=0)}$ (R_0 is negligible in the case of the PMMA-GG system), and C and β are characteristic constants of the polymer and solvent.

In reality, the relationship between the dissolution rate and the dose is influenced by a large number of parameters related to chemical reac-

tion at the liquid (GG developer) – solid (PMMA) interface, e.g. the PMMA molecule weight, the developer temperature and the development apparatus.

Special Computer Programs for X-ray Lithography. Different computer programs have been developed, which meet the requirements of a LIGA X-ray beam-line [22,23]. The code currently permits the computation of synchrotron radiation from bending magnets, the effects of the optical properties of materials, and the necessary parameters for the resist exposure. The basic calculations needed for synchrotron beam-line design are related to the spectral characteristics and to the modeling of the optical elements (mirrors, filters, beam-stop). For example, the following calculations are performed: the dose rate, the dose profile from the top to the bottom of the resist, the exposure dose (the parameter which should be given to the scanner which moves the sample) and the time needed to develop an irradiated resist sample. In Table 13-3 are listed computer programs especially dedicated to deep X-ray lithography.

TABLE 13-3 Deep X-ray Software Packages Available: (a) <http://www.ipal.sandia.gov/ip-details.php?ip=4874>; (b) <http://www.kit.edu>; and (c) tabata@se.ritsumei.ac.jp

Program	& Platform	Status	Possibility
LEX-D ^a	Dos	Commercial	Source: bending magnet Optics: mirror, double mirror, beam-stop Dose: primary and secondary Development: 4 dimensions
DoseSim ^b	Windows	Freeware	Source: bending magnet Optics: mirror, double mirror, beam-stop Dose: primary Development: 1 dimension
X3D ^c	LINUX	Freeware	Source: bending magnet Optics: Dose: primary Development: 4 dimensions

MICRO-ELECTROPLATING TECHNOLOGY

Electroplating is the key step in the fabrication of metallic micro-components and tools such as masks and molding tools. Established routine processes are often referred to by simply giving the name of the plating solution. However, every user performs the basic process with differences in electrolyte formulation and operation due to specific fabrication environments such as the plating apparatus or specific material properties. Nevertheless, some general aspects in micro-electroplating will be pointed out next. From the standpoint of a lithographic pattern, an ideal plating solution has the following properties:

- the resist structures are not changed (no swelling, no thermal loading introduced);
- the mechanical stress remains very low (a few tens of MPa);
- the grain structure does not change with height;
- small and large areas grow at the same rate.

Some limiting aspects arise from the desire to plate fairly thick layers in excess of 10 μm . This is usually referred to as electroforming and many commercial solutions can already be excluded.

The complexity of LIGA electroplating can best be described using a sketch of the current-density vs. voltage relationship (Fig. 13-9) [24].

At the onset of the net current density (1 and 2), the rate is limited by the kinetics at the surface. The growth rate depends exponentially on the voltage, so this is not a robust working point. Furthermore, this corresponds to very low growth rates and unacceptably long plating times. In region 4, the current density is limited by diffusion of some species of which the concentration at the cathode becomes zero. To keep the diffusion zone small, both strong convection and high ion concentrations in the electrolyte are usually employed. Both aspects will raise the diffusion-limited current density.

From the electroplating point of view, the lithographic pattern is a nuisance. First, it distorts the flow across the surface (Fig. 13-10(a)). On the one hand, eddy currents may form and on the other hand, convection into the structures, particularly for high aspect ratios, may be completely inhibited. In the latter case, the diffusion length corresponds to the total resist height while, for good convection, the diffusion length may be as small as a few micrometers. This means that locally, the current-density-potential relationship will vary

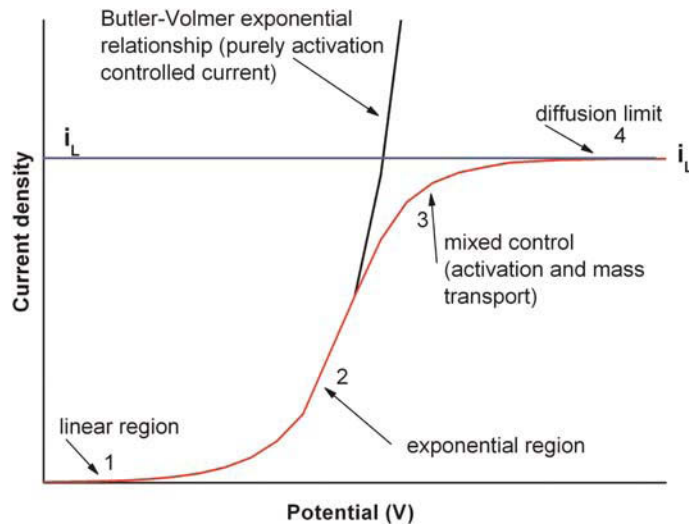


FIGURE 13-9 General current-density-potential relationship [24].

significantly. Second, the pattern distorts the homogeneity of the electrical field, with stronger fields corresponding to greater potentials on the current-density-potential curve. This effect is sketched in Fig. 13-10(b).

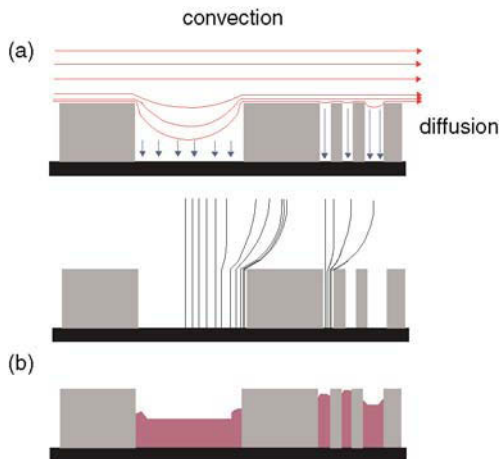


FIGURE 13-10 (a) Mass-transport phenomena in micro-electroplating. The lithographic pattern may have a strong influence on the length of the diffusion zone which, in turn, will result in locally differing current densities, and (b) inhomogeneous field distribution due to the lithographic pattern. Isolated small features focus the field lines and grow faster than wider structures. The same effect leads to higher rates near to resist edges.

The art of electroplating therefore involves finding the right chemical composition that gives the desired properties of the deposited layers and making/keeping the solution stable against changes associated with the electrochemical reactions during plating. The lithographic pattern introduces the requirement of low sensitivity to local variations in potential and local variations in mass transport. The use of additives alters the performance of the plating process drastically. Additives may be employed to change the current-density-potential curve, where a leveler typically makes the curve near to the operating point flatter, an inhibitor reduces the current density at high voltages and a brightener reduces the potential for the same current density by facilitating the nucleation of new grains. The finer grains usually are related to a greater hardness of the deposit. The electroplating procedures used in the LIGA process chain are gold plating for X-ray mask fabrication and nickel plating for molding tools and metallic micro-components. Further alloys may be deposited in resist molds such as Ni-Co, Ni/P or Ni-Fe. Different plating solution properties (bath temperature; composition; thickness accuracy; aspect ratio), which produce a range of hardnesses of between 280 and 680 Vickers, are listed in Table 13-4.

TABLE 13-4 F&S Plating Solution Characteristics

Property	Nickel	Nickel/Cobalt	Nickel/Iron
Composition	100	80/20	95/5
Bath temp.	40°C	40°C	52°C
Plating rate	12 $\mu\text{m/h}$ (1 A/dm ²)	12 $\mu\text{m/h}$ (1 A/dm ²)	10 $\mu\text{m/h}$ (1 A/dm ²)
Hardness (Vickers)	280–330 (0.1)	450–500 (0.1)	580–630 (0.1)
Thickness accuracy	$\pm 50 \mu\text{m}$	$\pm 50 \mu\text{m}$	$\pm 100 \mu\text{m}$

The parts are typically ‘overplated’ to ensure complete filling; an electroplating step is not able to deliver a homogeneous thickness all over the substrate and a polished surface, which is sometimes needed. The top surface (electroplating front) is typically lapped and polished to the final part thickness and aspect. Other techniques are also available:

1. **Ultra-precision milling.** This involves cutting with a milling tool while the workpiece is rotating. Using natural-diamond cutting tools, a broad range of materials such as, for example, non-ferrous metals (NiCo, NiP, Ni, Au, etc.) or plastics, can be machined with a surface roughness of below 5 nm R_a . Only the diamond can be sharpened to the required level of accuracy. Cutting-edge sharpness and roundness are crucial to the manufactured quality of the workpiece.
2. **Turning.** This involves cutting with a rotating milling tool while the workpiece is fixed. Actually, only hard Au can be turned using this technique;
3. **Grinding and polishing.** The polishing can be effected electrolytically or chemically. All of the techniques should meet the following criteria:
 - A. to deliver a good thickness-accuracy ($\pm 5 \mu\text{m}$);
 - B. to avoid burr formation;
 - C. to deliver a specified surface quality (for example, optical quality).

DESIGN RULE – MASK TECHNOLOGY

A complete LIGA process database does not yet exist. Nevertheless, the LIGA centers (CAMD,

BESSY, IMT) have accumulated working design rules that enable them to advise customers on the feasibility of their needs. As an example, numerous parameters influence the quality of the final parts in terms of lateral dimensions, and roughness of the side wall, some of the most important being listed here [25,26]:

- **Secondary radiation.** Divergence of the electrons and photons; fluorescence emitted by the membrane, the absorber and the substrate; secondary electrons emitted by the membrane, the absorber and the substrate; and the Fresnel diffraction; it will deposit a certain dose in the unwanted parts of the resist.
- **Thermal distortion.** The mask, resist and substrate get heated during irradiation. This leads to thermal distortion which affects the

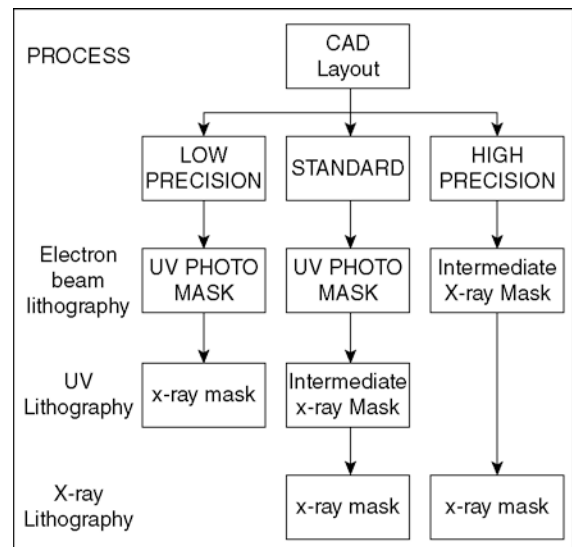


FIGURE 13-11 Different mask technology.

TABLE 13-5 Typical Mask-Blank Characteristics

Material	Typical Thickness (μm)	Young's Modulus (GPa)	Thermal Expansion Coefficient ($10^{-6}/\text{K}$)	Thermal Conductivity (W/mK)	Density (g/cm^3)	Price
Titanium	2	116	9	22	4.5	++
Silicon	100	240	2.3	157	2.32	–
Beryllium	500	318	12	230	1.85	++
Polished carbon	150	11	8.8	96	1.8	–
Vitreous carbon	200	28	2.6	6.3	1.4	–
Diamond	30	30	1.2	1000	3.51	++

accuracy of the copy. Cooling of the mask and the substrate is very important.

- **Swelling and thermal expansion of the resist.**

X-ray masks are not available from commercial mask shops as is the case for Cr masks. Therefore the LIGA centers have developed their own technology to produce them. A variety of options exist (see Fig. 13-11) requiring different tools using different mask membranes providing different performances for different costs (see Table 13-5). Nevertheless, a standard exists; it is limited to the characteristics of the support ring. X-ray masks consist of absorber patterns (generally Au)

supported by highly X-ray transparent membranes, the characteristics of which are given in Table 13-5.

In Fig. 13-12 is shown a standard X-ray mask (the membrane being a polished carbon membrane, the layout area having a diameter of 80 mm).

METROLOGY

Micro-system technology requires 3D coordinate measurements to be performed with measurement precision and accuracy to within $0.1 \mu\text{m}$. Two-dimensional parts can be measured using

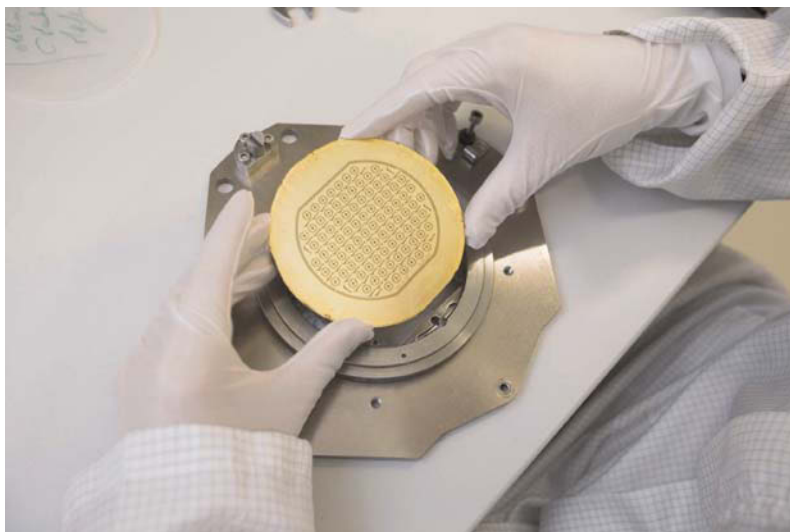


FIGURE 13-12 A standard X-ray mask ($25 \mu\text{m}$ Au absorber supported by a $160 \mu\text{m}$ polished carbon membrane).

one-dimensional measurement devices. Three-dimensional parts require 2D information, or a picture, to describe them. A gear, for instance, requires multiple measurements, including hub diameter, pitch, addendum and dedendum circles, involutes, top- and bottom-surface finish, side-wall finish, side-wall angle and tooth thickness, radius of curvature, and circularity. In addition, for reliability, information about the internal structure of the part is of great importance. Metrology for micro-features is one of the most active areas in dimensional metrology. Different techniques are possible [27]; the most commonly used being the employment of a coordinate-measurement machine (CMM) equipped with an optical-fiber probe [28,29].

UNIQUE FEATURES OF THE LIGA PROCESS

Features characterizing this process are listed below:

1. As a result of their high energy, these X-rays are capable of deeply penetrating thick (e.g. hundreds of micrometers or even millimeters) layers of polymeric resist, allowing the formation of tall micro-structures in one exposure step. Very precise shape definition of parts, both laterally in terms of dimensional control and in term of the straightness and planarity of side walls, are available.
2. The short wavelengths of X-ray photons provide high resolution for patterning due to low diffraction effects. Smallest lateral dimension of a few micrometers with structural details in the sub-micrometer range can be manufactured.
3. The very small vertical angular divergence of the X-ray beam achieves high accuracy in pattern transfer from the mask. Due to their excellent collimation, the X-rays penetrate thick resists with extremely low horizontal run-out (less than $0.1 \mu\text{m}/100 \mu\text{m}$ thickness), thereby producing the substantially vertical walls for which LIGA structures are well known.
4. The almost parallel (well-collimated) light of X-ray beams produced by synchrotron radiation sources also allows printing with a large depth-of-field. A large working gap between the mask and the substrate can then be used in non-traditional pattern transfer as for the manufacture of slanted structures or for pattern formation on substrates presenting a large topography.
5. The vertical side walls are optically smooth with a typical local roughness of the order of 10 nm and longer-range waviness such as slope errors or steps determined solely by the accuracy of mask writing.

MARKET SITUATION OF DEEP X-RAY LITHOGRAPHY

As mentioned earlier, the LIGA technique offers the possibility to manufacture micro-structures with a number of unique features. With these properties, LIGA is on the leading edge of micro-fabrication. This is a well-known issue to most participants in the micro-sector. However, most of them consider LIGA to be very expensive, to employ much time from design-to-realization, and to invoke a number of quality problems. They therefore try to avoid LIGA, and only consider LIGA if the alternative fabrication methods fail to fulfill the requirements. These requirements, however, are often very challenging, even for LIGA, resulting in long development times, high failure rates, and, of course, high cost. This reinforces the above-described perception, resulting in a sort of vicious circle.

The LIGA road-map (see Fig. 13-13) defined by IMT (Institut für Mikrostrukturtechnik

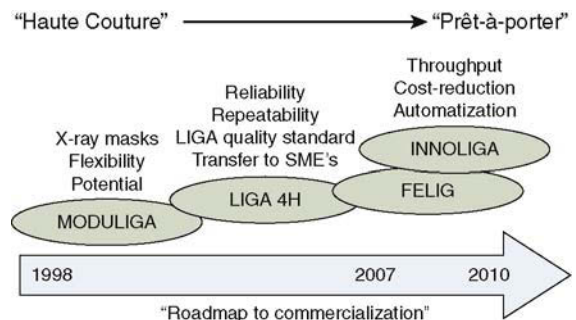


FIGURE 13-13 Road-map to commercialization.

Karlsruhe Institute of Technology) consists of continuous process innovation and the ability to continually improve internal processes in the direction of greater economy, productivity and cost effectiveness, so that products can be offered at lesser cost. Products that are complex and intricately designed are often produced initially in a prototype, low volume mode. This is especially true if the end product is very expensive. A project named MODULIGA (modular production method using the LIGA process) [30] linked together the activities of the German LIGA centers: IMT, IMM (Institut für Mikrotechnik, Mainz), and BESSY (Berliner Elektronenspeicherring-Gesellschaft für Synchrotronstrahlung, Berlin). The LIGA process steps were standardized and interface specifications were defined to establish a modular production method. The aim of a project named LIGA 4H (High aspect ratio, High structure height, High dimensional accuracy and high sidewall quality), was to obtain a stable manufacturing process. The next step consists of increasing the production and of decreasing the cost, and theoretically it should be a simple procedure then to move from the low volume prototype production to high volume production by simply adding equipment and

labour. However, the transition is much more complex. A fully automated fabrication line (FELIG) for direct LIG(A) parts in a cleanroom environment has been built up to demonstrate the high throughput potential of LIGA at the ANKA synchrotron.

COMMERCIAL APPLICATIONS

Three examples are now given of commercial products representing the different uses of the process. For a more complete review of applications, see [4].

Polymer Compound Refractive X-ray Lenses – Direct Resist Structure [5]

For hard X-rays the refractive index n in matter is slightly less than unity. This implies a focal length F (given as $F = R/2N\Delta n$ where R is the radius of the lens) of a single concave lens ($N = 1$) in the range of some 10 meters. A compound refractive lens, consisting of a linear arrangement of N single lenses (see Fig. 13-14), significantly reduces the focal length and thus can overcome this problem. For 14 keV photons a focal spot of $0.32 \mu\text{m}$

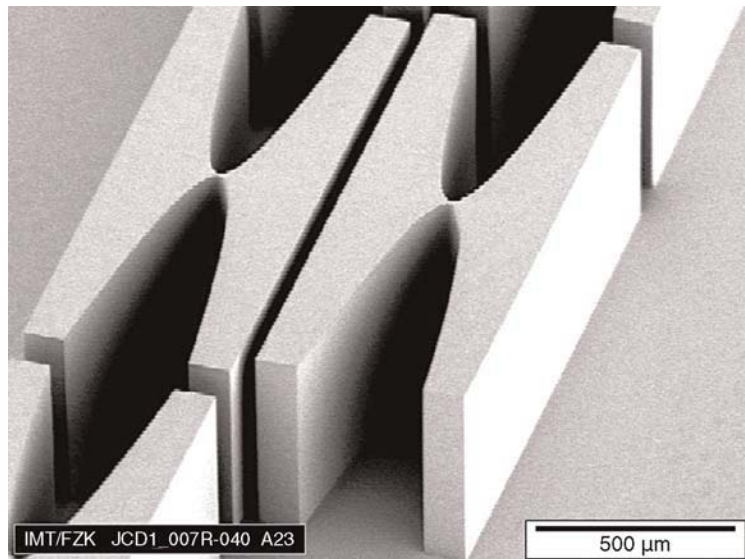


FIGURE 13-14 Compound refractive lens for focusing X-rays in one direction.

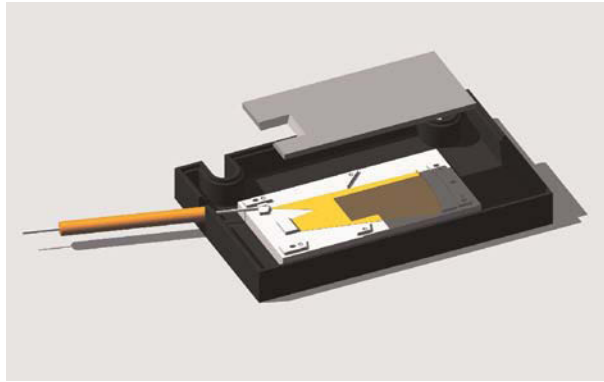


FIGURE 13-15 Microspectrometer.

(FWHM) was achieved using a focal distance of 242 mm.

Micro-spectrometer [31] – Mold

The spectrometer, as shown in Fig. 13-15, consists of a molded base-plate where the central hollow area, the gating profile, the location of the input fiber and the 45° mirror surface, are produced with a single pressing. The molded part is then placed in a vacuum chamber and an aluminium film is deposited on both the grating surface and the mirror surface. This is then assembled into the complete spectrograph by the fitting of the input fiber, the central hollow being filled with a polymer of different refractive index to that of the molding and a lid of the same refractive index as that of the base that is glued into place. The assembly is then aligned with, and glued to, the diode array.

Micro-gears – Direct Metal Parts [32]

The search for the perfect product is one of the major preoccupations of the luxury watch-making industry. The combination of lithography with electroforming offers unparalleled machining precision and extended design freedom for the manufacture of fine parts. The SU-8-based UV LIGA technology undoubtedly attracts interest, in particular when competing technologies fail to meet the precision and quality requirements. Deep X-ray lithography

enables greater precision, better side-wall quality and fewer restrictions, as almost any design can be realized. As an example, the quality of the production of gearwheels (thickness: 180 μm) in nearly pure, but sufficiently hard, gold was addressed. From a fabrication point of view, dimensional quality refers to all of the parts that can be produced, the deep X-ray LIGA process showing a process reproducibility of better than 1 μm in the case of the example gearwheel. In Fig. 13-16, the reproducibility of the measurement process of a gear (in PMMA) used as a reference is presented: it is excellent, the standard deviation being 0.1 μm

In Fig. 13-17, the variation between about 20 wafers is presented. The diameter range min-max is 2 μm. The FT for all the measurements is better than 0.5 μm. The process shows a reproducibility of better than ±1 μm (standard deviation: 0.5 μm). Measurements of side-wall roughness R_a were performed using an atomic-force microscope: all the data (R_a) obtained are of better than 50 nm accuracy.

CONCLUSIONS

Being invented in the 1980s, the potential of LIGA became evident in the 1990s when numerous examples of structures and devices were presented. The lead in MEMS technologies, however, was taken by silicon micro-machining, and not by LIGA, despite its technical superiority for many applications. The main reasons for this are the required technical infrastructure,

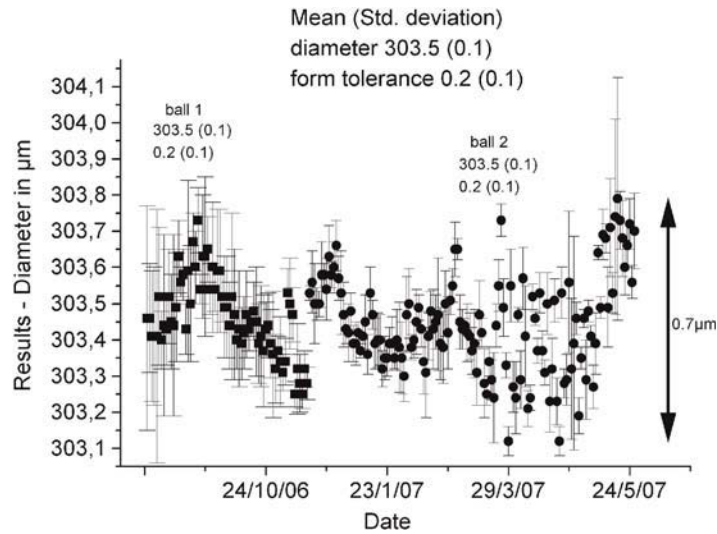


FIGURE 13-16 Reproducibility of the measurement process of a gear.

process knowhow, and cost issues. Silicon-based technologies could exploit the vast technology base developed for chip-making, with billions of dollars invested. LIGA, on the other hand, was new and confined to research laboratories. Furthermore, as a key process step, LIGA required access to a synchrotron-radiation facility, again a research laboratory provision, and often unacceptable for industries establishing manufacturing plants. Neverthe-

less, and this is a demonstration of the technical strength and superiority of LIGA, several industrial LIGA products have been launched by industries and synchrotron-radiation facilities are currently widely used for micro-fabrication. In addition to the described efforts to make LIGA acceptable as a manufacturing technology for a large variety of industrial products, cutting-edge research in, and with, LIGA remains a topic of serious interest. The goals include

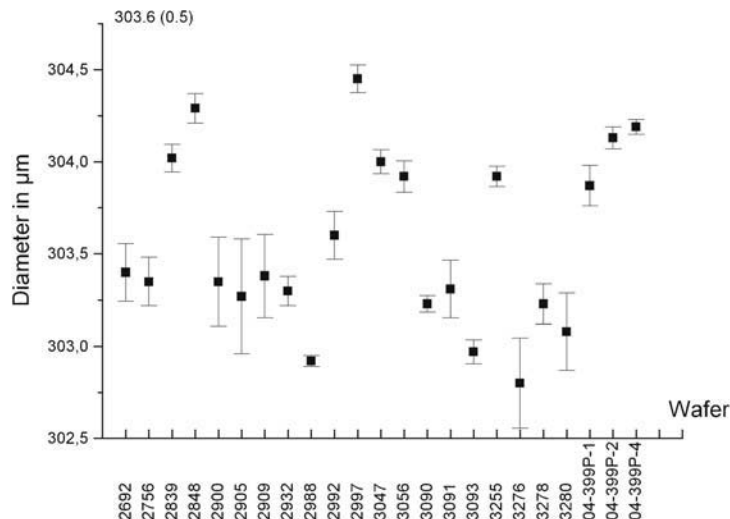


FIGURE 13-17 Variation between about 20 wafers.

research into new materials, new replication techniques, and new lithographic approaches exploiting the short-wavelength nature of X-rays. Questions such as ‘how small can we really get?’ and ‘can we overlap our top-down technologies with the typical bottom-up approach in nano-technology? At which dimensions?’ are currently being addressed. Making devices much smaller than is possible today will open up entirely new fields in research and applications.

REFERENCES

- [1] E.W. Becker, W. Ehrfeld, P. Hagmann, A. Maner, D. Münchmeyer, Fabrication of microstructures with high aspect ratios and structural heights by synchrotron radiation lithography, galvanofarming, and plastic moulding (LIGA process), *Microelectronic Engineering* 4 (1986) 35–36.
- [2] R.K. Kupka, F. Bouamrane, C. Cremers, et al., Micro-fabrication: LIGA-X and applications, *Appl. Surf. Sci.* 164 (2000) 97–110.
- [3] J. Hruby, LIGA technologies and applications, *MRS Bulletin* 26 (4) (2001) 337–340.
- [4] C.K. Malek, V. Saile, Applications of LIGA technology to precision manufacturing of high-aspect-ratio micro-components and -systems: a review, *Microelectronics J.* 35 (2004) 131–143.
- [5] V. Nazmov, E. Reznikova, J. Mohr, A. Snigirev, I. Snigireva, S. Achenbach, V. Saile, Fabrication and preliminary testing of X-ray lenses in thick SU-8 resist layers, *Microsystem Technologies* 10 (2004) 716–721.
- [6] C. Becnel, Y. Desta, K. Kelly, Ultra-deep X-ray lithography of densely packed SU-8 features: I. An SU-8 casting procedure to obtain uniform solvent content with accompanying experimental results, *J. Micromech. Microeng.* 15 (2005) 1242–1248.
- [7] L.J. Guerin, The SU8 Homepage, <http://www.geocities.com/guerinj/>.
- [8] C. Cremers, F. Bouamrane, L. Singleton, R. Schenk, SU-8 as resist material for deep x-ray lithography, *Microsyst. Technol.* 7 (2001) 6–11.
- [9] M. Stewart, H. Tran, G. Schmid, T. Stachowiak, D. Becker, G. Willson, Acid catalyst mobility in resist resin, *J. Vac. Sci. Technol. B* 20 (2002) 2946–2952.
- [10] H. Winick, *Synchrotron Radiation Research, Chapter 2: Properties of synchrotron radiation*, Plenum Press, New York (1980).
- [11] G. Margaritondo, *Introduction to Synchrotron Radiation, Chapter 2.2: Bending magnet radiation*, Oxford University Press, New York, Oxford (1988).
- [12] D. Attwood, Univ. California (Berkeley), *Intro Synchrotron Radiation, Bending Magnet Radiation*, EE290F (Feb. 8, 2007).
- [13] A. El-Kholi, P. Bley, J. Göttert, J. Mohr, Examination of the solubility and the molecular weight distribution of PMMA in view of an optimised resist system in deep etch x-ray lithography, *Microelectronic Engineering* 21 (1983) 271–274.
- [14] M. Gad-el-Hak, *The MEMS Handbook*, CRC Press, New York, USA (2001).
- [15] O. Schmalz, M. Hess, R. Kosfeld, Structural changes in poly(methyl methacrylate) during deep-etch X-ray synchrotron radiation lithography. Part II: Radiation effects on PMMA, *Die Angewandte makromolekulare Chemie* 239 (1996) 79–91.
- [16] W. Glashauser and G.V. Ghica, German patent, 3039110 (1982).
- [17] J.S. Greeneich, Developer characteristics of poly-(methyl electron resist methacrylate), *J. Electrochem. Soc.* 122 (1975) 970–976.
- [18] Z. Liu, F. Bouamrane, M. Rouillay, R. Kupka, A. Labeque, S. Metgert, Resist dissolution rate and inclined-wall structures in deep x-ray lithography, *J. Micromech. Microeng.* 8 (1998) 293–300.
- [19] P. Meyer, A. El-Kholi, J. Mohr, C. Cremers, F. Bouamrane, S. Metgert, Study of the development behavior of irradiated foils and microstructure, *SPIE* 3874 (1999) 312–320.
- [20] P. Meyer, A. El-Kholi, J. Schulz, Investigations of the development rate of irradiated PMMA microstructures in deep X-ray lithography, *Microelectronic Engineering* 63 (2002) 319–328.
- [21] F.J. Pantenburg, S. Achenbach, J. Mohr, Influence of developer temperature and resist material on the structure quality in deep x-ray lithography, *J. Vac. Sci. Technol.* 16 (1998) 3547–3551.
- [22] P. Meyer, J. Schulz, L. Hahn, DoseSim: MS-Windows Graphical User Interface for using synchrotron X-ray exposure and subsequent development in the LIGA process, *Review of Scientific Instruments* 74 (2) (2002) 1113–1119.
- [23] S. Hafizovic et al., X3D: 3D X-ray lithography and development simulation for MEMS, *Transducers’03* (2003) 1570–1573.
- [24] M. Paunovic and M. Schlesinger, *Fundamentals of Electrochemical Deposition*. The Electrochemical Society Series, John Wiley and Sons 2nd edition (2006).
- [25] S.K. Griffiths, J.M. Hruby, A. Ting, The influence of feature sidewall tolerance on minimum absorber thickness for LIGA x-ray masks, *J. Micromech. Microeng.* 9 (1999) 353–361.
- [26] S.K. Griffiths, Fundamental limitations of LIGA x-ray lithography: sidewall offset, slope and minimum feature size, *J. Micromech. Microeng.* 14 (2004) 999–1011.
- [27] D. Chinn, P. Ostendorp, M. Haugh, R. Kershmann, T. Kurgess, A. Claudet, T. Tucker, Three dimensional imaging of LIGA-made microcomponents, *J. of Manufacturing Science and Engineering* 126 (2004) 813–821.

- [28] S. Cao, U. Brand, T. Kleine-Bestent, W. Hoffmann, H. Schwenke, S. Bütefisch, S. Büttgenbach, Recent developments in dimensional metrology for microsystem components, *J. Microsystem Technologies* 8 (2002) 3–6.
- [29] U. Brand, J. Kirchhoff, A Micro-CMM with metrology frame for low uncertainty measurements, measurement science and technology, *Meas. Sci. Technol.* 16 (2005) 2489–2497.
- [30] L. Hahn, P. Meyer, K. Bade, H. Hein, J. Schulz, B. Löchel, H. Scheunemann, D. Schondelmaier, L. Singleton, MODULIGA: the LIGA process as a modular production method-current standardization status in Germany, *Micr. Tech.* 11 (2005) 240–245.
- [31] C. Müller, J. Mohr, Microspectrometer fabricated by the LIGA process, *Interdisciplinary Science Reviews* 18 (3) (1993) 273–279.
- [32] P. Meyer, J. Schulz, L. Hahn, V. Saile, Why you will use the deep X-ray LIG(A) technology to produce MEMS? *Microsystem Technologies* 14 (9–11) (2008) 1491–1497.

Surface Engineering and Micro-Manufacturing

Gonzalo G. Fuentes

INTRODUCTION

Surface Engineering

Advanced surface technology or surface engineering is a key knowledge-based sector of great relevance for several manufacturing processes and consumer goods production. Surface engineering encompasses those technologies capable of modifying the surfaces of solids to provide them with superior performance or new functionalities.

During recent decades, part of the surface engineering sector has been devoted to the protection of the surfaces of manufacturing tools and industrial components working under severe conditions of friction, wear, oxidation or corrosion. These phenomena are usually considered as catalysts of surface degradation, and yearly they cause huge production costs mainly related to tool reshaping or replacement, as well as component rejection. It is estimated that, in developed economies, surface degradation might cause losses of up to 4% of the GDP. For the USA these features represent approximately \$280 billion/year. Moreover, other studies estimate that in Germany alone, the consumption of oil-derived lubricants for wear prevention represents up to \$1–2 billion/year [1] for manufacturing industries. Additional costs related to surface protection are those caused by the generation of residues derived from galvanic techniques (e.g. hexavalent chromium).

Surface engineering is facing new and exciting challenges from the advent of micro- and nano-manufacturing technologies (MNT), and surface modification processes will have a major role in enabling the industrialization of several technologies in the near future, such as micro-forming, micro-machining, or micro-nano-texturing. Moreover, new and emerging technologies need to find novel functional surfaces which could introduce new products able to outperform those already existing from classical concepts. Some examples are: (1) bio-materials, which require advanced techniques for surface bio-functionalization; or (2) renewable energy, through the engineering of functional membranes and other functional coatings for H₂ fuel cells.

Surface Contact Phenomena and Tribology

The study of tribology (friction, wear and lubrication) is a major, ongoing, priority for every manufacturing process. In fact, it is generally accepted in mechanical engineering that numerous failure cases in manufacturing are related to these surface-degradation mechanisms. Tribology addresses the contact interactions between two surfaces in relative motion, and the physical-chemical response of such surfaces against the degrading action of the environment. A deep knowledge of the basic mechanisms of friction,

wear and lubrication is a major requirement to better understanding of the benefits of surface engineering and its role in improving the surface performance of tools and components. There exists an extensive amount of literature about tribology in general [2–3], and tribology in micro-manufacturing processes in particular [4–5]. A detailed revision over these studies and the reference therein will provide the reader with a better insight about surface-related failure mechanisms in manufacturing and the strategies for their prevention.

Characterization Techniques

Understanding the principles of surface functionalities and the strategies for their modification requires the utilization of purposely designed advanced characterization techniques. In fact, a good background on surface characterization enables mechanical engineers to better solve surface-related problems during prototype design, simulation or process testing. In the specific case of manufacturing tools and component surface protection, the related characterization techniques focus on the chemical composition, the mechanical properties (hardness, fracture toughness, coefficient of friction, wear rate), the thermal-chemical stability (oxidation, corrosion) and the surface topography (roughness, texturing). It is noteworthy to remark that several of the existing characterization techniques are today approved as validation standards under national and international standardization agencies, e.g. the American Society for Testing and Materials (ASTM) and the International Standards Organization (ISO) (www.astm.com and www.iso.org, respectively).

This chapter aims to provide the reader with a general and concise overview of the *surface engineering* field and its relevance for micro-manufacturing. In the first section, the fundamentals of the most extended advanced techniques for surface modification will be addressed, with special focus on those technologies which, due to their specific characteristics, might be more applicable in micro-manufacturing. The last section addresses different case studies where surface engineering plays a decisive role.

FUNDAMENTALS OF ADVANCED SURFACE ENGINEERING PROCESSES FOR TOOLING PROTECTION

In this section, different advanced surface modification processes for tooling protection will be overviewed. Surface protection technologies have been developed during recent years in order to accomplish optimal material protection, depending on the environment, the working conditions, and the compatibility between the treatment itself and the substrate material. There exists a large variety of surface treatment techniques which have demonstrated their performance for surface protection or other functionalization purposes, and therefore they are already implemented at industrial scale. In general terms, all surface treatments can be classified within three main categories: *physical–chemical functionalization*, *mechanical-structural functionalization*, and *surface coating*, as illustrated in Figs. 14-1.

In the case of micro-manufacturing, tools of sub-millimeter dimensions exhibit special features which limit the applicability of several of these techniques for surface protection. For instance, surface techniques must in this case prevent changes of the net-shape of a tool which could reduce its performance or precision. Analogously, treatments carried out at excessive temperatures might degrade the bulk mechanical properties of the tool. In this context, this section presents a series of particular techniques which have proven their effectiveness in protecting small-size manufacturing tools. These techniques are framed within the groups of *physical–chemical functionalization*, including gas and plasma nitriding, ion implantation, and *coating techniques*, including electro-deposition, chemical vapor deposition (CVD), and physical vapor deposition (PVD).

Physical–Chemical Functionalization I: Thermal and Plasma Nitriding

Nitriding is a surface technique to harden the surfaces of several types of cold- and hot-work steels for forming operations. Metal nitriding is a high

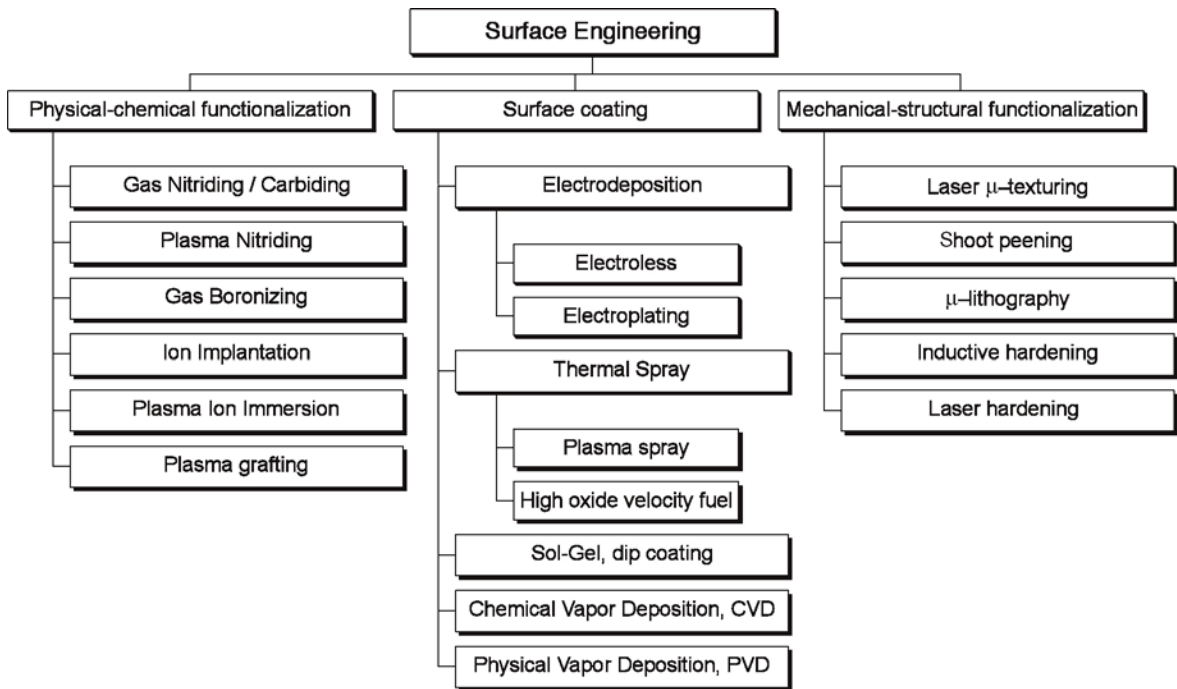


FIGURE 14-1 Classification of surface modification techniques in terms of: physical–chemical functionalization, surface coating and mechanical–structural functionalization.

temperature surface treatment based on the incorporation of nitrogen species into metallic surfaces by different mechanisms of *thermal diffusion* or *plasma-activated thermal diffusion*. The nitrogen diffusion process in steels has two main effects. On the one hand, it induces the formation of a shallow layer (2–5 microns thick) containing hard metal

nitrides such as Al-N, V-N or Cr-N. The formation of small precipitates of these nitrides provides high alloyed steels with high hardness and toughness. On the other hand, nitriding produces the so-called *diffusion layer* (10–100 microns thick) in which nitrogen atoms occupy interstitial sites in the crystalline lattice of the host metal, producing an

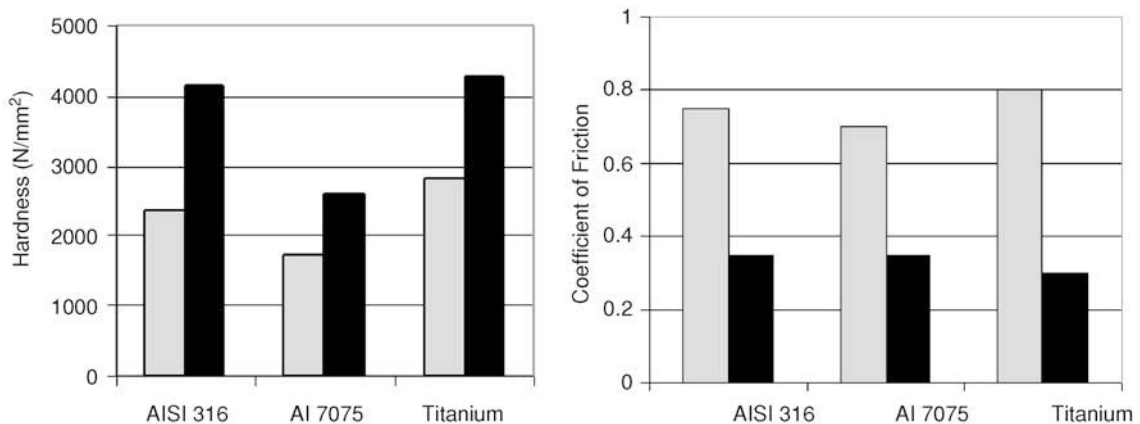


FIGURE 14-2 (left) Universal hardness. (right) COF of three different metallic compounds AISI316, Al 7075 and titanium before (gray) and after (black) nitrogen ion implantation treatment [1].

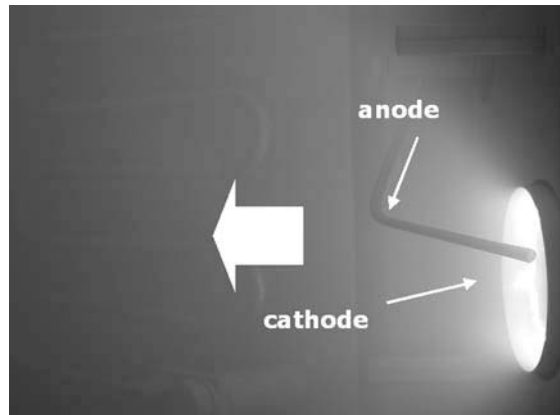


FIGURE 14-3 The reactive cathodic arc discharge PVD working. The anode tip is a high temperature resistance metal alloy rod located near the surface of the target (glowing part of the photograph). The presence of ionized nitrogen provokes the red-like glow. The arrow indicates the vapor stream direction from the cathode.

induced lattice-expansion effect. This expansion is well reported to cause compressive stresses, which leads to superior toughness and wear resistance properties. These effects have already been observed in different metallic alloys such as AISI H11-13 series steels [6], AISI-316L[7], Ti4Al6V [8], V5Ti[9] and others. The nitriding of steels often forms a shallow overlayer of iron nitrides (ϵ -Fe_{2,3}N, γ -Fe₄N, typically), denoted as *white layer*. It is usually recommended to remove such films by mechanical means (sand blasting, polishing) due to their brittleness, which can induce catastrophic crack propagation into the bulk component under normal or shear overloading.

Thermal nitriding of tool steels requires temperatures above 500°C and the use of reactive nitriding precursors such as pure N₂ or NH₃. Additionally, processing times could be of the order of 1–2 days to achieve a diffusion layer thickness of some hundreds of microns. The plasma activation permits the nitriding of tool steels at slightly lower processing temperatures (i.e. 400–500°C) due to the larger reactivity of the ionized gases to penetrate the surface-to-bulk barrier of the material.

Physical–Chemical Functionalization II: Ion Implantation

Ion implantation is a surface bombardment treatment widely implemented for tribological appli-

cations as well as for other technologies requiring special surface functionalities (e.g. micro-electronics, optics, bio-materials). The technique consists of the bombardment of ionized species and their implantation into the first atomic layers of a solid. Ion implantation essentially requires an ion-generation source, an electrostatic acceleration system, and a vacuum chamber for the target housing. Ions are generated by physical means in a discharge chamber, using precursors appropriately converted to the vapor phase. There exist two main operative modes of ion implantation: *charge/mass selective mode* and *linear acceleration mode*. In *charge/mass selective mode*, the ionized species are pre-accelerated until they reach a quadrupole magnet working as a charge/mass ion filter. The filtered beam is then post-accelerated and focused onto the target component. In the *linear acceleration mode*, all ionized species produced in the discharge chamber will be accelerated towards the target component. This latter implantation mode is less accurate, as the generated beam may contain some impurities from the different process stages.

The implantation process does not modify the net-shape of sharp-edged tool features. On the other hand, ion implantation is a *line-of-sight* technique, meaning that all surfaces under treatment need to be directly exposed to the ion beam, which restricts the applicability of the technique to non-complex surface geometries. To overcome

this feature, new sources of plasma immersion ion implantation (PIII) are being successfully developed. This technique allows the high energy bombardment of inhomogeneous surfaces with a variety of ionized atomic species.

For hardness-enhancement purposes on metallurgical components, nitrogen ion implantation has been found the most universal solution at industrial scale. Implanted nitrogen species (typically, N_2^+ and N^+) on transition metal surfaces form nitride phases that increase the hardness and toughness of the targeted surfaces. Some examples of hardness and coefficient of friction measurement of Aluminum Titanium an AISI 316 after Nitrogen ion implantations are depicted in Figure 14-2. In addition, implanted nitrogen induces crystalline lattice expansion at the surface of the bombarded metals. This effect is usually observable by the appearance of new diffraction peaks shifted to lower diffraction angles with respect to those of the original lattice structure. This lattice distortion provokes high compressive stress of the implanted surfaces and hence increases the hardness and toughness.

Nitrogen ion implantation increases the surface hardness of several alloyed steels, titanium or aluminum alloys [10] or even some thermoplastics such as polyethylene [11] (PE) and polycarbonate (PC). Moreover, the hardness of Ni alloys can also be increased by the implantation of metal species such as Cr, Ti or Al. Finally, the corrosion protection of some alloys is improved upon gaseous and light atomic weight metals implantation.

Coating Techniques I: Electro-deposition

Electro-deposition is a well-implemented technology in the surface treatment sector for its relatively easy installation and high performance. The technique is based on the chemical reduction of metallic precursors and the precipitation of a solid thin film onto the cathode (component) by either galvanic-induced (*electroplating*) or self-catalytic processes (*electroless*). The electroless process exhibits lower deposition rates than electroplating. Conversely, electroless coatings show larger homogeneity than electro-deposited films

due to the absence of electric field lines during the process. The deposition parameters which drive the properties of electro-deposited coatings are: the electrolyte composition and its chemical stability, the deposition speed, and the surface geometry of the substrates. Hard-chromium, nickel, copper and zinc are typical materials deposited by electro-deposition methods for tooling and component protection.

Hard-chromium, produced by the galvanic reaction of CrO_3 , H_2SO_4 in the presence of catalyst compounds which produce a metal Cr precipitation, leads to the formation of highly compact, porous-free films exhibiting high hardness and low COF. Hard-chromium exhibits excellent wear resistance against abrasion and a very low adhesive COF. Nickel is also a widely utilized coating for tooling and component surface protection against wear and corrosion that can be precipitated by electroplating and electroless methods. Nickel is additionally used as a base material for electro-formed tools, e.g. micro-embossing or micro-plastic injection molds. Ni-electroplated films show high hardness (see Table 14-1) and low COF, achieving efficient anti-wear properties. Moreover, this material shows excellent protection against corrosion.

Electroless nickel-M (where M can be an atomic, molecular or micro-particle additive) might show excellent anti-wear properties and low COFs. Ni-phosphor and Ni-boron exhibit a hardness between 500 HV and 1300 HV. Ni-Teflon (Ni-PTFE) exhibits a very low COF in combination with hardness values of around 500 HV.

Coating Techniques II: Chemical Vapor Deposition

Chemical vapor deposition (CVD) is a vacuum-plating technique by the precipitation reactions of gaseous precursors onto a given surface. Depending on the temperature and the presence or absence of plasma assisting processes, CVD can be classified into *thermal CVD* and *plasma-assisted CVD* (PACVD).

In thermal CVD, the surfaces should be kept to temperatures of between 800°C and 1000°C,

TABLE 14-1 Vickers Hardness and COF for Different Electroplated Engineered Coatings

Coating	Hardness HV	COF*
Hard – chromium	1300–1500	0.15–0.25
Ni – electroplated	200–500	0.15–0.3
Electroless Ni	800–800	0.2–0.3
Ni-B	1300–1400	0.08–0.2
Ni-P	500–700	0.08–0.2
Ni-PTFE	400–500	0.05–0.1
Ni-W	900–1000	0.15–0.3

*COFs measured against chromium steels, using a ball-on-disc configuration.

hence limiting the type of materials suitable to be coated by this technique due to thermal-degradation effects. In fact, the high temperatures reached during CVD cycles often produce size distortions of the tools. A typical thickness of thermal CVD coatings for tooling protection could vary between 5 and 20 microns depending on the specific application and nature of the deposited material. Thermal CVD films exhibit very high adhesion strength, due to temperature-induced atomic diffusion at the coating/substrate interfaces. This fact converts thermal CVD into a recommended technique to be applied to tools subjected to strong normal and shear forces (cold/hot forging, metal forming). In addition, CVD coatings show low residual stresses and hence greater toughness and fatigue resistance.

The most commonly utilized coating materials for tooling protection are titanium nitride (TiN), titanium carbon nitride (TiCN), and chromium nitride (CrN). Other transition metal carbon nitrides such as hafnium or vanadium can be deposited by CVD, showing a good combination of hardness and low COF.

An alternative to thermal CVD is the plasma activation of the precursor gases, which can promote precipitation of dense thin films, even at deposition temperatures as low as 200–300°C, which limits the size distortion effects on steel tools. These processes are named *plasma activated CVD* (PACVD) [12], and represent a feasible alternative to deposit films onto a larger

variety of substrate material. Other CVD activating processes can be found in the literature, such as hot-filament assisted CVD, hollow cathode CVD or microwave RF plasma-assisted CVD.

CVD is a well-implemented coating technique to deposit low friction carbon-based films containing different ratios of sp^3 – sp^2 carbon-carbon bonds [13]. Highly containing sp^3 carbon films exhibit hardness values close to those of natural diamond, although they show a high tendency to brittleness and are difficult to implement in the form of thin films. Diamond-like carbon films (DLC) constitute a valid alternative as a protective coating due to their low COFs (as low as 0.1 against bearing steels) and high hardness (1500–3000 HV). DLC can be deposited even at relatively low temperatures of around 300°C with high adhesive strength using adequate bonding layers. Presently, silicon-based films produced by PACVD are pre-deposited to enhance the adhesion of DLCs on steel and hard-metal substrates.

Coating Techniques III: Physical Vapor Deposition

Physical vapor deposition (PVD) is a high vacuum coating technique used for tooling protection as well as for several technological applications (optics, photovoltaic conversion, decorative). PVD deposition is the result of producing a vapor stream in-vacuum from a solid material (usually named the *target*) by physical means (arc

discharge, sputtering, heat transfer by laser or electron beams, etc.). *Cathodic arc evaporation* (CAE), *magnetron sputtering* (MS) and *electron beam* (EB) at the present time constitute the core group of PVD techniques for industrial tooling protection. In fact, there exists a great variety of PVD techniques, but those of the core group alone share more than 95% of the PVD market, in terms of both equipment sales and services.

Cathodic arc evaporation (CAE) sources are probably the most widely utilized technique for industrial tooling protection. In CAE, a high electron current density is discharged onto a target material, producing a fast evaporation rate at its surface. The energy dissipated during the process sprays the evaporated atoms towards the substrate at energies of tens to some hundreds of eV (refer to Fig. 14-3). This feature, and the high ionization produced during the electron discharge (up to 90% of the evaporated species), produce uniform and dense films, with compressive residual stresses. The deposition of metal compound films can be obtained by introducing reactive gases such as N_2 , O_2 or C_2H_2 during the discharge process.

Part of the energy dissipated on the target surface during CAE is able to produce micro-sized particles (*micro-droplets*) that can also be sprayed towards the substrate. In general, these micro-droplets are barely detrimental for conventional machining tools provided the net-shape of cutting edges remains unchanged upon deposition. The presence of these micro-particles, however, can be strongly detrimental for precision tools. In these cases, a surface repolishing process needs to be performed after a PVD CAE treatment. To avoid an excessive deposition of micro-particles, different arc sources design strategies are in use, such as the *lateral arc rotating cathode* (LARC) configuration, or the filtered arc.

Magnetron sputtering sources are based on the confinement of a low pressure plasma around an evaporation target by an appropriate configuration of static or alternating electric/magnetic fields. The confined plasma bombards the target material, producing the sputtering of atoms from the target towards the substrate. The energy of the

sputtered atoms is usually not greater than a few eV, and their ionization rate is generally poor (below 5% of the total sputtered atoms). Both factors, low ionization and energy, make necessary the post-ionization and acceleration of the sputtered species in order to achieve sufficient impact energy during the deposition process. This can be accomplished by polarizing the substrate with a negative potential (bias potential) of some tens of volts. Under these conditions, the deposition of sputtered atoms is produced simultaneously to the bombardment of ionized inert species (typically Ar ions) onto the growing film. This combined process, so-called *ion beam assisted deposition* (IBAD), provides sufficient energy per arriving atom to form dense and well-adhered films. The ionization and energy of the sputtered atoms can also be increased using high power impulse magnetron sources (HIPIMS) [14]. HIPIMS utilizes high energetic electromagnetic mega-watts/cm² millisecond pulses during the sputtering process to achieve ionization rates of almost 100% of the depositing species.

Sputtering techniques are able to deposit *low friction* coatings or *solid lubricant*. This family gathers the Me:C [15] coatings, where Me is a metal and :C represent a variety of carbonaceous phases present in the film. In addition, MoS_2 or WS_2 low COF films can also be deposited in the form of thin film by sputtering techniques (see Table 14-2).

Electron beam evaporation is based on the heat generated in a target material by the bombardment of an electron beam onto its surface. The technique retains the same principles as that of CAE and sputtering, in terms of vacuum process, coating thickness, reactive deposition, etc. Electron beam deposition is, in addition, currently used in industrial applications due the surface finish properties achieved, along with good mechanical properties, such as those presented in Table 14-2. Plasma activation systems of the vapor stream are reported to contribute to the achievement of dense film growth, increasing hardness and toughness properties. A scheme of a *hollow cathode arc activated deposition* (HAD) is shown in Figs. 14-4, the trajectory of the electron beam from the source to the target, and the

TABLE 14-2 Deposition Parameters and Properties of Common PVD Coating Materials for Mechanical Engineering Applications

Coating	PVD Process*			Processing T°C	Hardness (GPa)	COF (ASTM G99-5)	Max Working T°C
	CA	EB	MS				
TiN	x	x	x	450–550	20–25	0.6–0.8	500
TiCN	x	x	x	450–550	25–30	0.3–0.5	300
TiAlN	x	x	x	450–550	25–30	0.6–0.8	500–700
AlTiN	x	x	x	450–550	30–35	0.6–0.8	600–800
nc-ALSiTiN**	x		x	450–550	35–40	0.6–0.8	800–1000
CrN	x	x	x	200–500	18–22	0.6–0.8	600–800
ZrN	x		x	450–550	25–28	0.5–0.7	400–500
WC/C			x	200–250	10–15	0.2–0.4	200–250
MoS ₂			x		10–15	0.1–0.3	200–300
DLC***			x	200–300	10–40	0.1–0.2	200–300

*CA = cathodic arc-discharge; E-B = electron beam evaporation; MS = magnetron sputtering. **nc denotes a nano-composite phases, as produced by *Spinodal* decompositions of non-soluble phases.

***In the case of DLCs there is a large dispersion of results derived from the sp^3/sp^2 bonding relations.

plasma activation area, are indicated on the right of this figure.

The main application of PVD coating for mechanical engineering is in machining/cutting tooling protection against wear and oxidation, this application representing almost 70% of all coating services worldwide. Forming tools, steel stamping dies, injection molds, cold- and hot-forging dies

constitute another important niche sector for PVD. Finally, a smaller ratio of the PVD market is devoted to solid lubricious films, especially for the protection of bearing parts in machines or engines.

The most common industrial PVD coatings for anti-wear purposes are TiN, TiCN, AlTiN, and CrN, all deposited at processing temperatures of between 450 and 550°C, in the presence of

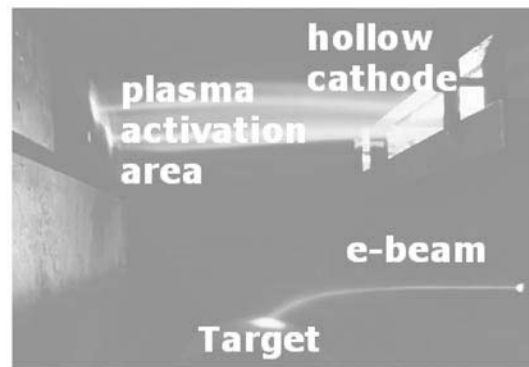
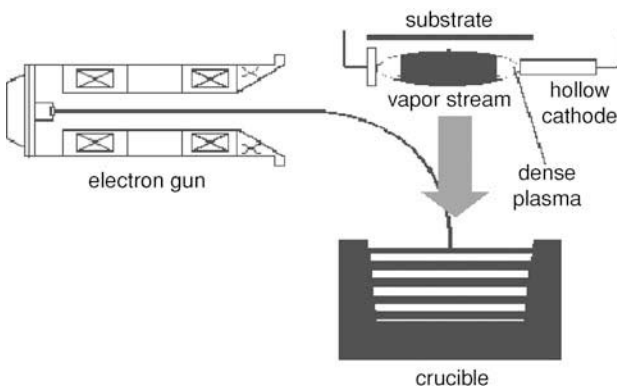


FIGURE 14-4 (right) Schematic representation of the hollow cathode arc activated electron beam deposition. (left) Picture of the running process (courtesy of Dr C. Metzner, Fraunhofer Institute for Electron Beam and Plasma Technologies).

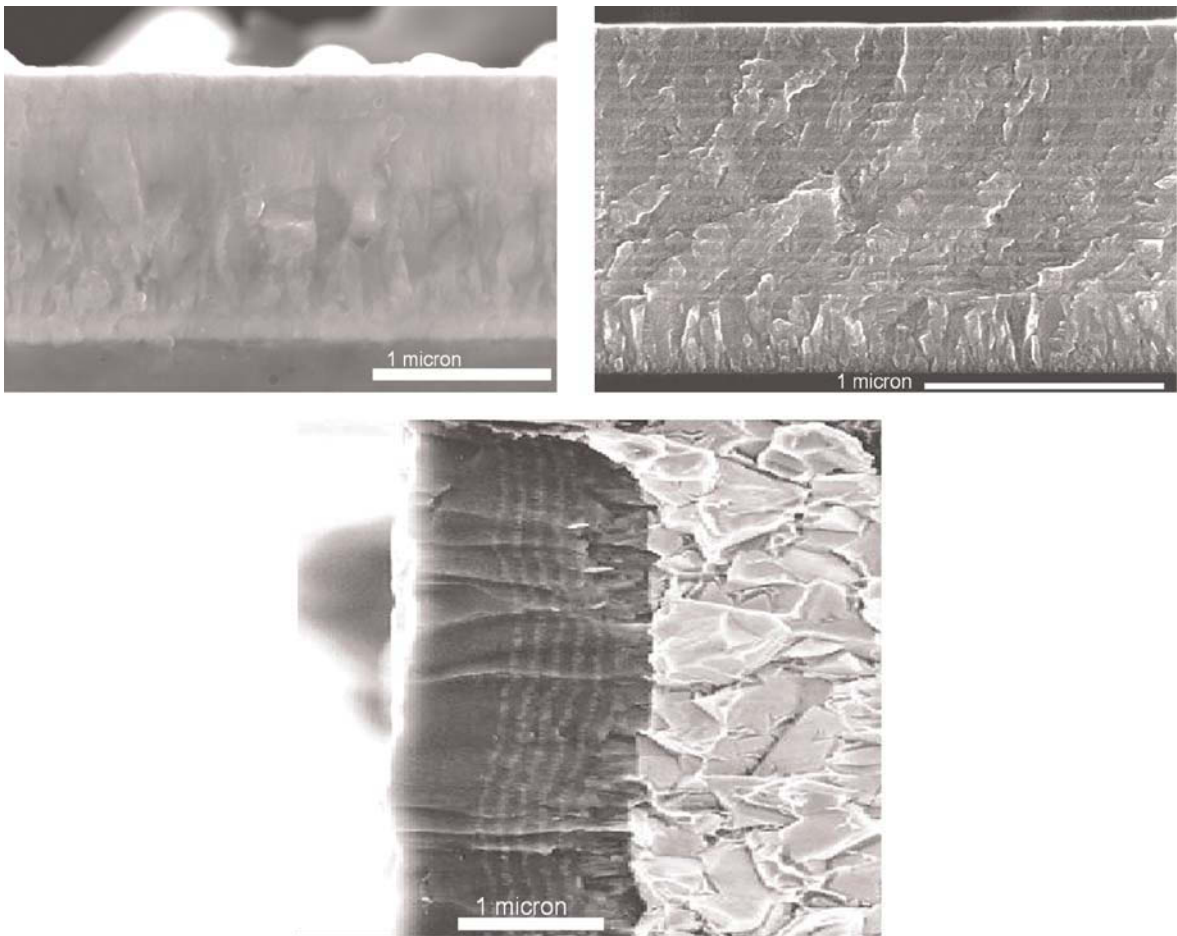


FIGURE 14-5 Different multi-layer structures developed at AIN Surface Engineering Centre using the cathodic arc PVD technique. (left) Gradient CrCN, (center) damping coating AlTiN, (right) nano multi layer TiN/CrN ($\lambda \sim 40$ nm).

gaseous precursors, N_2 , O_2 or hydrocarbons (see Table 14-2). The deposition temperatures are in general compatible with those in the tempering of tool steels (HSS, cold- and hot-work steels, etc.). Powder-metallurgical tool steels additionally exhibit an excellent support to PVD hard coatings. Analogously, sintered hard-metal cutting tools show excellent load support and adhesive strength for PVD hard coatings.

Titanium nitride (TiN) [16] is the most commonly used coating for cutting and forming tools due to its high hardness, low friction coefficient and toughness. Additionally, its golden-like color makes TiN a suitable film for decoration/protection in household items and other consumer

goods. Titanium carbon nitride (TiCN) shows a higher hardness and lower COF than TiN [17–18], but reduced thermal stability. In fact, this coating requires oil lubrication, especially during high speed machining operations, to avoid its premature oxidation by overheating. Aluminum titanium nitride (AlTiN) coatings [19] were implemented for industrial products in the 1990s and are used widely at the present time for high speed and dry-machining tools due to their high hardness (greater than that of TiN) and elevated thermal stability. Chromium nitride (CrN) [20] shows inferior hardness to that of TiN but very low adhesive COF, permitting its application in plastic injection molding and other forming

operations where galling needs to be attenuated. This is due to the low tendency of CrN to stick to the working material during processes requiring high contact stresses at the tool/material interface. At present, recently developed CrCN [21] coatings are found to exhibit even lower adhesive COF to those of CrN when sliding on stainless steels. Zirconium nitride (ZrN) exhibits a similar hardness to that of CrN and has a very low affinity for aluminum. This characteristics enables ZrN to be a recommended coating for Al-transformation dies (extrusion, injection), as well as for the machining of non-ferrous alloys. Analogously to TiN, its brass-like color enables ZrN to be used as a decorative coating. Finally, the family of solid lubricious coatings WC-C [22–23] or MoS₂ [24] is utilized on bearing parts, as these are usually not subjected to excessively high temperatures.

PVD permits the design of a variety of film architectures with the aim to outperform the protective characteristics of single-layer configurations. Figures 14-5 show different multilayer structures developed at AIN Surf. Eng Center using the cathodic arc PVD technique. A common strategy to enhance the mechanical performance of PVD films is the design of load-adaptive layers [25]. Gradient composition films containing a hard layer at the interface and a low COF outer layer is a well-developed solution for several applications in the manufacturing sector [24]. A hard nitrided layer by nitriding processes can be an excellent load support surface for a PVD coating [26–28] (duplex processes).

Nanometer scale thin films are postulated [29]. Nano-multilayered coatings made of two different compounds (usually hard ceramic-ceramic or metal-ceramic) are found to exhibit the highest hardness/toughness when the nominal bi-layer thickness ranges between 10 and 15 nm.

The deposition of immiscible phases in the form of thin film can lead to the formation of finely grained coatings (denoted as *nano-composites*). This variety of coatings shows superior values of hardness and toughness than the characteristics of their single counter-phases. It is commonly found that the incorporation of silicon in TiN [30–31], or AlTiN films [32], in quantities of

around 8–10 at.%, increase their hardness values by a factor of 1.5 to 2. In addition, (Al,Si)TiN nano-composites retain their mechanical properties even after annealing temperatures of above 800–900°C [33]. These outstanding properties have allowed these nano-composites to be utilized for the high speed and dry cutting of difficult-to-machine materials.

APPLICATIONS OF SURFACE-ENGINEERING PROCESSES IN MICRO-MANUFACTURING

Advanced Surface Treatments for Micro-cutting Tools

As addressed in this chapter, micro-cutting technologies are one of the most important pillars of micro-manufacturing. With regards to tool design and development, strong efforts are being focused on the investigation of new materials and design concepts [34–37]. Nevertheless, few studies focus specifically on the problem of tool surface wear, which to some extent constitutes one of the main degradation mechanisms at this scale.

Some attempts to protect diamond tools have been made using DLC films deposited by CVD methods. DLC films were tested on diamond-based micro-cutting tools with different grain refinement, from coarse- to fine-grained structures [38]. Figure 14-6 compares the appearance of the drill point for two different cases: (a) DLC on coarse-grain diamond after 1800 holes had been processed; (b) DLC on fine crystal diamond after 15,500 holes had been processed. The results provide evidence that a DLC coating deposited on fine-grained diamond single-crystal end-mills enhances the cutting performance of the system.

Yao et al. [39] investigated the wear properties and drilling precision of PVD-coated metal carbide micro-drilling tools. In particular, two different coating architectures were investigated: single hard TiN, and nano-multi-layered hard TiN/AlN coatings. The two architectures revealed different anti-wear performances under the same working conditions. The TiN/AlN nano-multi-layer exhibited greater protection against wear on both the

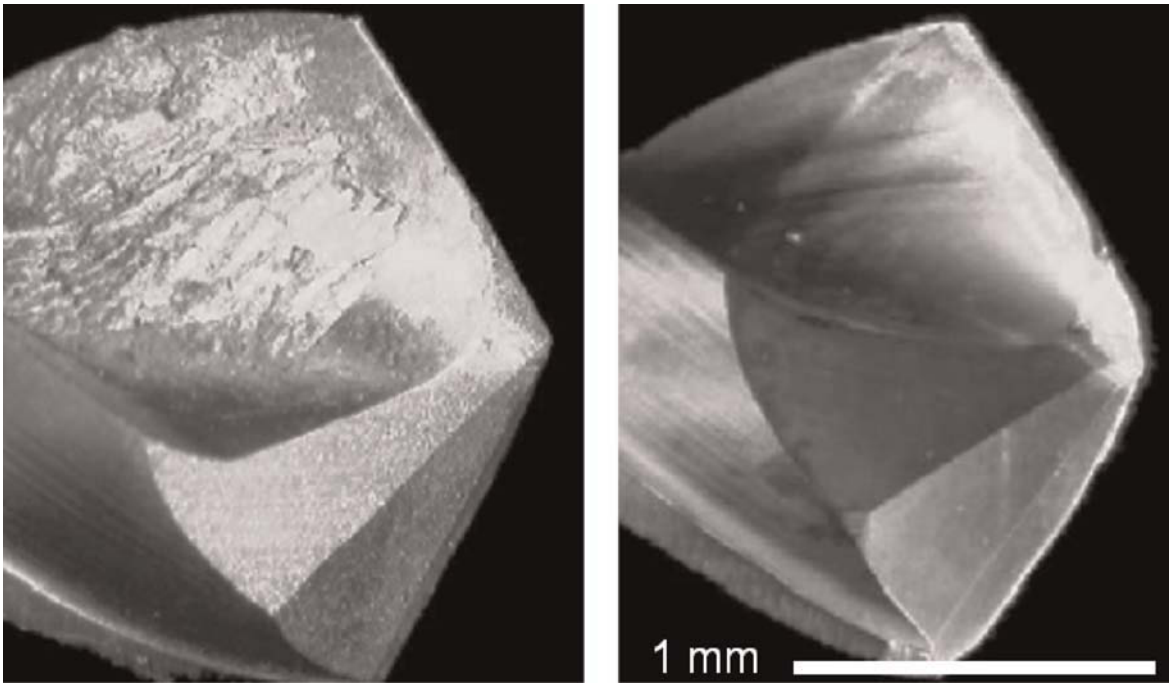


FIGURE 14-6 The appearance of drill points (width of chamfer 0.05 mm) ((a) DLC coated on coarse grain diamond after 1800 holes processed, and (b) DLC coated on fine crystal diamond after 15,500 holes processed).

tool flank and the rake faces than those shown by TiN films in the single layer configuration, as depicted in Fig. 14-7(a)–(d). Single TiN layers on the tool flank often tend to fail due to both the abrasion by hard particles and the accumulation of compressive stresses which originate from coating delamination.

Alternatively, nano-multi-layered TiAlN/TiN-coated carbide end-mills were found to outperform a single TiAlN coating, during the cutting of Cr-Mo alloyed steels. In this study, different wear mechanisms were reported, depending on the cutting speed. At low cutting speed, built-up edge (BUE) formation was identified, caused by pressure-induced welding. High cutting speeds increased the temperatures at the contact zone, resulting in the diffusion of oxygen and enhancing the oxidation of the tool surface. It was observed that a metal-nitride PVD coating prevented both premature BUE and oxidation of the tool edge under low and high cutting speed respectively [40]. Additional studies were reported on the cutting performance of different magnetron sputter-

ing-coated carbide precision tools in terms of the flank wear resistance.

Multilayered Cr/TiAlN and Mo-doped CrTiAlN coatings as deposited by magnetron sputtering exhibited the lowest flank wear rate during the micro-cutting of NiCrMoV alloyed steels, and CrCo alloys. The low wear rate obtained by these coated tools was attributed to the magnetic field configuration utilized for their deposition process, the so-called *close-field unbalanced magnetron sputtering* [41]. Analogously, the coating thickness distribution between the tool rake and the flank faces was considered to have a significant influence on the cutting performance of carbide micro-end-mills [42]. More specifically, a lesser coating thickness on the tool rake with respect to the tool flank strongly diminishes the performance of the whole system due to uneven heat dissipation. In fact, when the coating on the rake is totally worn off during cutting, the tool base metal might come into contact with the working material, thereby increasing the COF and hence producing overheating at the tool/material interface. Thus thermal energy cannot be dissipated

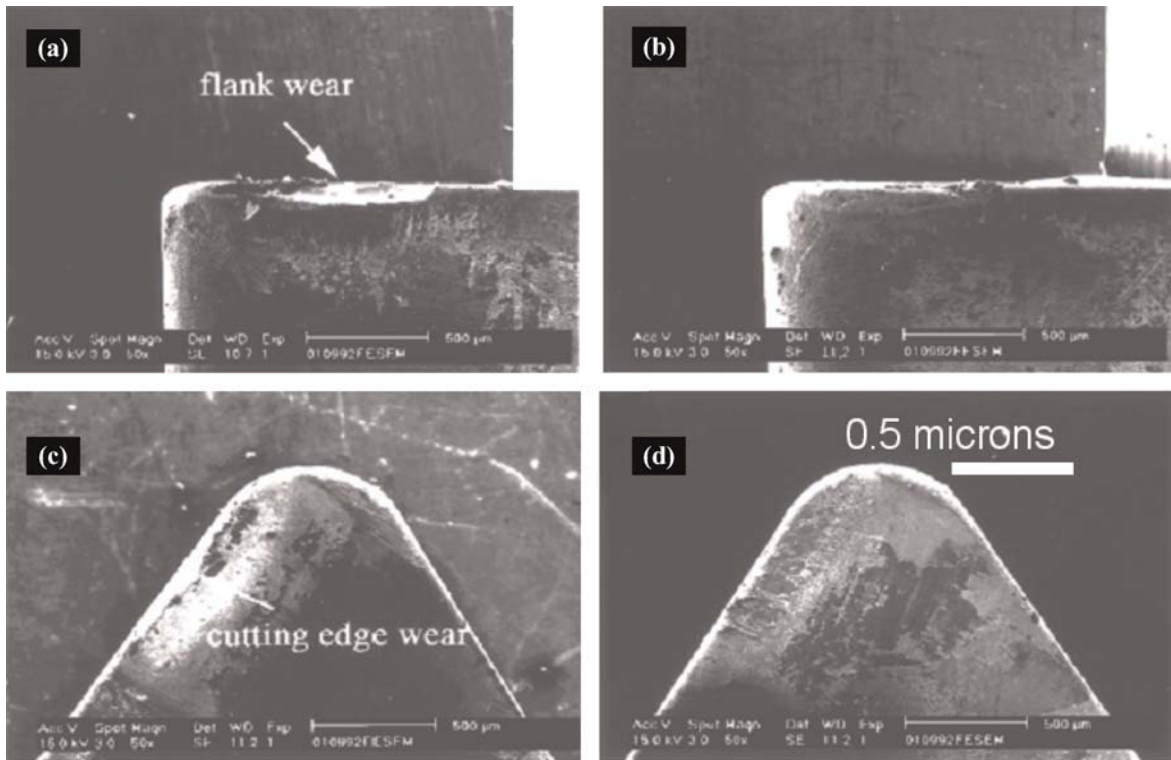


FIGURE 14-7 SEM wear morphology images of hard metal cutting tools with different coatings after running tests: flank wear for (a) single-TiN layer and (b) nano-multi-layer TiN/AlN film, and edge wear for (c) single-TiN layer and (d) nano-multi-layer TiN/AlN film.

out of the tool due to the thermal-barrier effect of the remaining unworn coating at the flank, causing rapid tool degradation. The optimal situation was identified when the coating thickness distribution was similar on the tool rake and the tool flank.

A new generation of nano-structured PVD coatings was attempted in micro-end-mills for hardened steel precision cutting. Figure 14-8(a)–(b) shows SEM pictures of a PVD-coated micro-tool (coating trade name nACRO[®]): (a) as coated and (b) after 14,000 holes had been drilled on PCB plates. The tool-blank total wear during the drilling tests for uncoated, PVD-nACO[®] coated and PVD-nACRO[®] coated is presented in Fig. 14.8 (c) in the form of blank diameter evolution as a function of the number of drillings. The horizontal line represents the size tolerance of the tool. Figure 14.8(c) shows how the wear rates of PVD coated micro-drills decrease significantly with

respect to those of uncoated tools. Thus, whereas uncoated tool blank wear reaches the size tolerance limit after 5000 drillings, nACO- and nACRO-coated tools reached the size tolerance limit after a number of drillings of around 10,000 and 15,000, respectively, indicating an increase of tool life by a factor of 3 with respect to that of untreated tools (courtesy of Metales-talki – PLATIT ACS Ltd).

Anti-adhesion and Wear Resistance Coatings on Micro-molding Tools

The adhesion of the surface-forming materials (plastics, ductile metals, etc.) to the surface of the molding tool during demolding is a common feature in manufacturing which causes several problems of tool adhesive wear and workpiece quality. Additionally, waste production due to

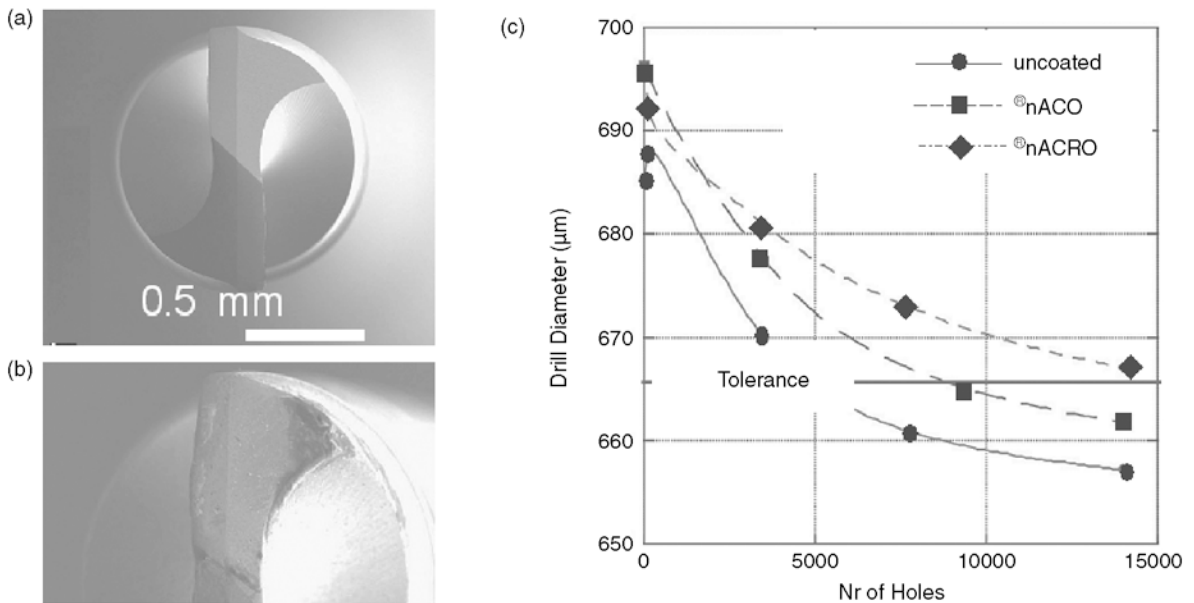


FIGURE 14-8 SEM pictures of a PVD-coated micro-tool blank (coating trade name nACRO[®]), (a) as coated and (b) after 14,000 drills on PCB plates. Figure 14.8(c) represents the tool wear during the drilling tests for uncoated, PVD-nACO[®] and PVD-nACRO[®] in the form of blank diameter, as a function of the number of drills. The horizontal line represents the tolerance of the tool (courtesy of Dr Ibon Azcona, Metalestalki – PLATIT ACS Ltd).

the use of oil lubricants or other wet demolding products is a common drawback associated with this surface-interface problem [43–44].

The reduction of the specific tool/material contact area in sub-millimeter micro-forming processes implies the loss of effective lubrication caused by a small lubricant retention capacity in the so-called closed valleys of the tool surface [5,45–46]. This fact leads sub-millimeter-scale contact interfaces to register COFs of up to one order of magnitude greater with respect to the same interface systems scaled at macroscopic level. Micro-stamping, micro-embossing, and sub-millimeter metal bulk forming are a few examples where a high COF may provoke surface failures during component plastic deformation or workpiece demolding.

Different solutions are currently under development in this area. Polytetrafluoroethylene [47] (PTFE or Teflon) coatings are a standard solution for anti-adhesive purposes in plastic injection molding. Silane and fluorinated silane were proposed as anti-adhesive single films on electro-

plated Ni micro-featured molds for embossing or imprint operations. Different chemical formulations are able to produce self-assembled monolayers of silane derivatives which exhibit extremely low surface energy, therefore preventing the adhesion of plastic during demolding operations. The mechanical stability of silane-based films can be enhanced by depositing support SiO₂, NiO or TiO₂ films [48–49] by vacuum plasma techniques such as plasma enhanced CVD.

Teflon- or silane-based films, however, have poor mechanical stability and high wear rates, making them unable to support mass production. In order to design mechanically stable surfaces on Ni-based micro-molds, other approaches are required. Ion beam-assisted DLC and SiO_x doped coatings are proposed due to their self-lubricious properties, low surface energy, mechanical stability and mimicking ability to replicate complex surfaces [50].

Chromium nitride-based PVD coatings with different stoichiometries and lattice structures

have been investigated for their application in high precision plastic injection molding. It was found that the hexagonal Cr_2N phase deposited by magnetron sputtering exhibited the lowest surface energy among the most common transition metal nitrides [51], and therefore this film is proposed as an anti-adhesive coating for Ni-based micro-embossing tools and other shape micro-replication processes.

Nano-multi-layer coatings TiAlN/ZrN deposited by the magnetron sputtering technique have been applied on silicon micro-featured molds for the production of glass-based optical components. The tested coatings replicated well the original surface micro-pattern of the molds, and exhibited an excellent thermal stability during the stamping of molten glass at 700°C . Additionally, their good anti-oxidation behavior retarded the sticking of glass onto the coated Si molds [52].

Low friction coatings such as MoS_2 , amorphous carbon (a-C:H) and WC-C deposited by magnetron sputtering were tested on Ni-electroplated tools providing different wear rates under sliding against steels [53]. In general, low friction coatings improve the wear rate of Ni molds for

plastic micro-embossing, imprinting or other surface-replication purposes.

DLC coatings deposited by PECVD techniques were reported to prevent the sticking of aluminum to the surfaces of hard-metal molds during sliding in a ball-on-disc configuration at temperatures of between RT and 150°C [54]. While the sticking of aluminum to the uncoated mold is found to occur at very early stages of the sliding contact, DLC inhibited the galling of aluminum on the surface of the hard-metal tool even for temperatures greater than 120°C .

Me-C:H PVD coatings have been used to enhance the tooling service of EDM-produced micro-compression molds for imprinting applications on aluminum surfaces [55]. Figure 14-9(a) shows an SEM image of a coated compression Ni-based micro-mold containing a series of parallel inserts in the form of cylinders. The applied coating was a hybrid CVD/PVD Ti-C:H film (2.5 microns thick). Figure 14-9(b) shows the imprinted hole produced in a one-step stamping stroke.

The results of the Al-imprinting tests at different temperatures showed that the as-fabricated Ni

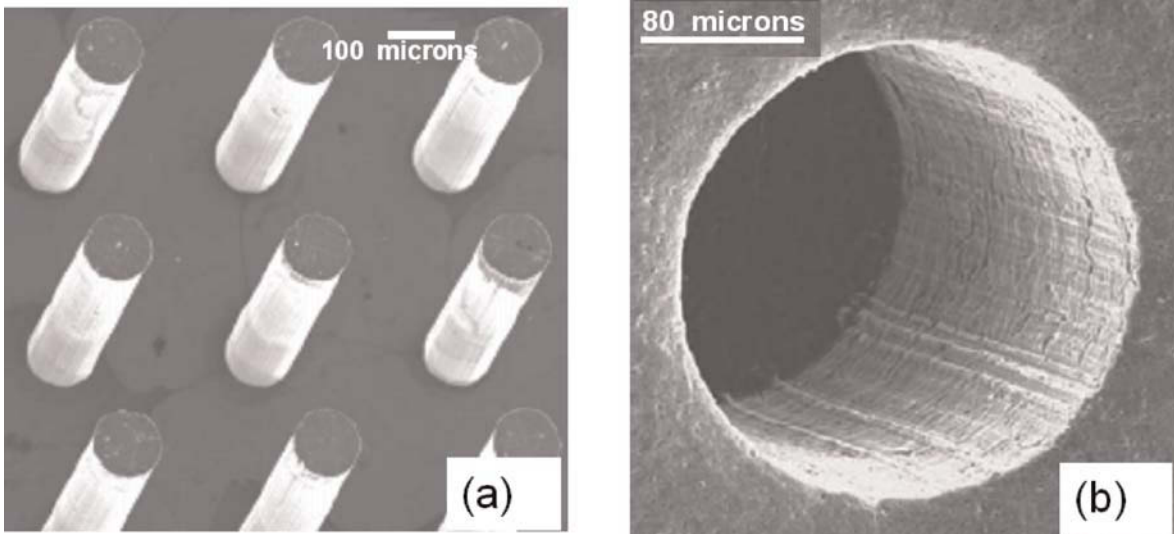


FIGURE 14-9 (a) SEM image of compression Ni micro-molds containing a series of parallel inserts in the form of cylinders, and (b) imprinted hole produced by one-step stamping insert on aluminum plates at 450°C . The inserts are coated with a hybrid CVD/PVD Ti-C:H overlayer (2–3 microns thick).

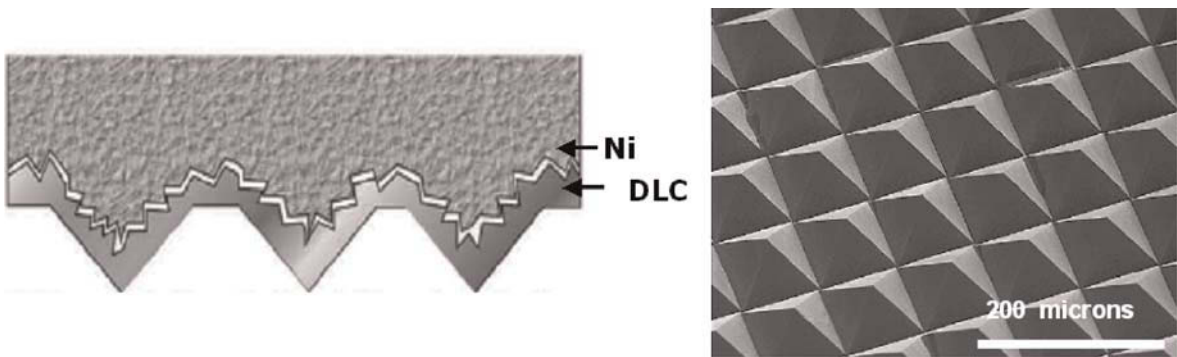


FIGURE 14-10 (top) Scheme of the design of a DLC-deposited Ni mold. (bottom) SEM image of micro-textured molds encompassing a well-defined pattern of indenter pyramids of 100 microns base side (courtesy of U. Petterson et al. *Tribology International* 39 (2006) 695).

inserts were not suitable for Al micro-molding due to strong abrasive surface wear. On the other hand, Ti-C:H deposition over Ni inserts enabled the Al micro-molding process to be carried out with near 100% shape replication.

Micro-forming Tool Fabrication using Surface-engineering Processes

Micro-manufacturing tool production at large scale represents a technological challenge due to the inherent difficulties found in the replication of sub-millimeter features in a reproducible manner. In this context, the increasing demand for smaller micro-components or micro-patterned surface textures has led researchers to explore new alternatives in the design and production of higher precision tool systems where such precision cannot be achieved by traditional manufacturing processes.

Downscaling traditional tool production methods is a well-known approach to achieve micro-tools, e.g. micro-cutting or micro-erosion by electro-discharge machining (EDM) techniques. However, mechanical removal processes by cutting often cause excessive burr formation, especially when the cutting process is made at sub-millimeter scale. On the other hand, the surface finishing of micro-forming molds as produced by micro-cutting or EDM is often too poor, and usually electro-polishing post-treatments are required. Surface engineering has recently been

emerging as a feasible method to fabricate custom-designed ultra-precision tools both for mass manufacturing as well as for flexible production systems.

Surface patterning by photolithography and electro-forming are well-developed techniques within the family of surface engineering. Traditionally employed for the production of plates for ICs, these technologies offer a great potential for the production of ultra-high precision micro-tools, e.g. molds for micro-embossing, micro-stamping, and end-mills for micro-cutting. Moreover, the combination of photolithography, in its different resolution ranges, visible light, UV, or X-ray, with electro-forming is well suited for manufacturing with a high degree of repetitiveness and rapidity, thus permitting its scalability to industrial production. As a drawback, photolithography technologies generate large amounts of residuals, which might compromise environmental regulations on waste production. Analogously, electro-forming is limited to a small set of materials, often with low to medium hardness, having high wear rates in some applications. To overcome this problem, further engineered coatings might provide appropriate hardness values in combination with low coefficients of friction.

The production of Ni-based micro-embossing molds by using surface engineering methods [56] has been proposed, in which hard micro-textured DLC deposited Ni plates are produced following a

six-step chain according to Fig. 14-10. In steps 1 to 3 a pattern of oxidized Si is produced by photolithography and chemical etching, leaving sharp cavities, of which each shape depends on the different etching speed of each family of crystalline planes. In step 4, the patterned Si surfaces are coated with a DLC hard film of 1–2 microns thickness, the DLC replicating accurately the original texture formed. In step 5, an electro-deposited Ni film of 1 to 2 millimeters thickness is deposited on top of the DLC. Interface-bonding films such as Ti could eventually enhance the adhesion strength between the DLC and the electroplated Ni film. Finally, the Si template is removed, and the Ni surfaces polished, leading to a master DLC-coated Ni-embossing tool.

These prototype embossing masters are successfully applied for texturing purposes on thermoplastics such as polymethylmethacrylate (PMMA), polyethylene-terephthalate (PET) or polystyrene (PS). Additionally, the hardness and toughness provided by the DLC film enables these masters to perform well on certain steels.

Figure 14-11 illustrates the result of stamping the DLC-Ni-embossing tool on steel plates. The grooves imprinted on the steel plates resemble those of a Vickers indenter (Fig. 14-11 left). The presence of prominent ridges is caused by the plastic flow of material during the indentation process. Such ridges are easily eliminated by a smooth polishing (Fig. 14-11 right). On the other hand, industrially scalable molds should eventually work over non-planar surfaces. In consequence, the mechanical performance of the molds depends strongly on the appropriate optimization of the Ni electro-deposition method and the adhesion and mechanical stability of the coating, in order to avoid premature crack failure under tool deflections.

Micro-textured DLC-based films were also produced by plasma-based ion implantation [57]. The procedure encompassed the imprinting of micro-patterns on a sacrificial aluminum foil, which is coated afterwards by a thin DLC coating. The aluminum foil is then eliminated by chemical methods, leaving a free-standing DLC-textured

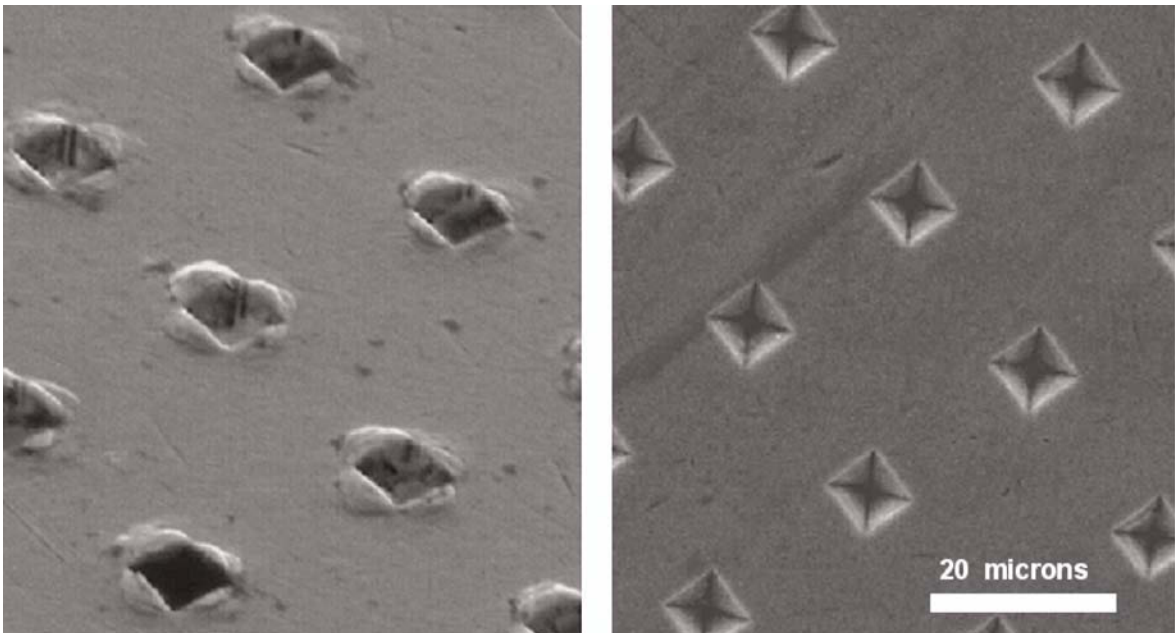


FIGURE 14-11 SEM images of flat steel plate grooves produced by DLC-coated Ni embossing tool molds – (left) ridges caused by the plastic flow of material during the indentation process and (right) ridges can be removed by a smooth polishing process.

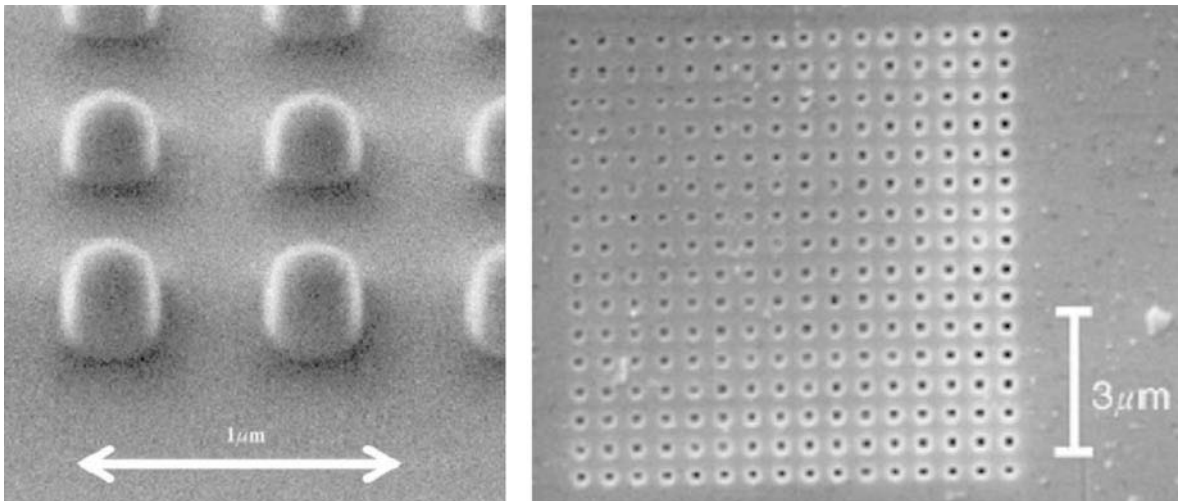


FIGURE 14-12 SEM images of: (left) nano-structured diamond tool produced by FIBs techniques, and (right) imprinted pattern on glass by the prototyped micro-molding tool.

film. The process provides the rapid production of these films, thus enabling mass production upscaling.

Ion beam bombardment methods are under development for the production of extremely fine precision micro-cutting and molding tools. The process of ion beam etching provides excellent precision in the design of micrometer-sharp structures by the so-called focused ion beam (FIB) techniques. Conversely, the process is slow and somewhat expensive as it requires advanced vacuum facilities and ion-acceleration sources, presently available within research laboratories. Ultra-precision diamond micro-shaped end-mills for glass micro-cutting were produced by focused ion beam etching for the prototyping of a new micro-array

chip for DNA assembly [58]. Micro-structured glass surfaces were produced using micro-embossing tools previously prototyped by FIB techniques (Fig. 14-12). The textured surfaces provided the micro-array chip with the functional properties required for their performance: low surface energy, low COF, and high transparency.

Micro-featured punches for sheet micro-forming tools have been semi-finished by FIBs methods and finally coated with low friction DLC films deposited using ion beam-assisted deposition [59] (see Fig. 14-13 for 0.15 mm diameter punches, after different ion beam regrinding cycles). Micro-forming tool finishing is a complex process which requires non-conventional polishing techniques, such as electrochemical etching,

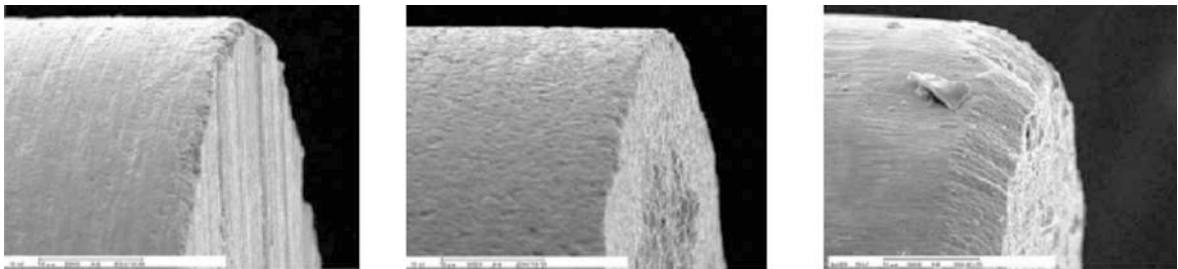


FIGURE 14-13 Surface finish of micro-dies by ion irradiation – (left) before ion irradiation, (center) ion irradiation with 45° beam incidence, and (right) ion irradiation with 10° beam incidence with respect to the tool parallel axis.

which become difficult to control at the micrometer scale, and is strongly dependent on the properties of the tool material. Contrarily, net-shape finishing by FIB mostly depends on the ion beam properties and less on the intrinsic properties of the tool material.

SUMMARY

In this chapter a concise review of recent progress in surface engineering for tooling protection has been presented, with particular focus on applications in micro- and nano-production technologies. As a general conclusion, it can be stated that surface engineering has the potential for great impact in the further development of miniature and micro-manufacturing. In this context, research and development in this field should focus on new concepts of flexible surface modification systems, in order to achieve an optimal performance on non-standard tooling elements. Moreover, the implementation of reliable testing tools and standards needs to be addressed in detail. The development of surface/interface modeling tools is envisaged to help in the integration of both process design and surface engineering for micro-manufacturing. Substantial integrative endeavors need to be undertaken between the scientific community and the relevant industrial stakeholders to obtain the full potential of surface engineering and to convert it in a true enabling technology for micro-manufacturing.

ACKNOWLEDGEMENTS

The author gratefully acknowledges the support of the European Commission for Research and Development through the FP6 funded project MASMICRO NMP-500095. The Ministry of Education and Science of Spain is also acknowledged through its co-funding action (MAT2007-66550-C2). Finally, the author wishes to acknowledge the support of the Regional Initiative INTERREG IIB SUDOE for its support on dissemination activities of surface engineering topics, in the frame of the CHES SO2/1.3/E47 project.

REFERENCES

- [1] S. Veprek, The search for novel superhard materials, *J. Vac. Sci. Technol. A* 17 (1999) 2401–2420.
- [2] Y. Xie, J.A. Williams, The prediction of friction and wear when a soft surface slides against a harder rough surface, *Wear* 196 (1996) 21–34.
- [3] S.C. Tung, M.L. McMillan, Automotive tribology overview of current advances and challenges for the future, *Tribology International* 37 (2004) 517–536.
- [4] U. Engel, Tribology in microforming, *Wear* 260 (2006) 265–273.
- [5] J.-M. Lee, W.-H. Jin, D.-E. Kim, Application of single asperity abrasion process for surface micro-machining, *Wear* 251 (2001) 1133–1143.
- [6] S.-Y. Lee, Mechanical properties of $\text{TiN}_{0.7}/\text{Cr}_{1-x}\text{N}$ thin films on plasma nitriding-assisted AISI H13 steel, *Surface and Coatings Technology* 193 (2005) 55–59.
- [7] S.D. de Souza, M. Olzon-Dionysio, E.J. Miola, C.O. Paiva-Santos, Plasma nitriding of sintered AISI316L at several temperatures, *Surface and Coatings Technology* 184 (2004) 176–181.
- [8] R. Wei, T. Booker, C. Rincon, J. Arps, High intensity plasma ion nitriding of orthopaedic materials, Part I: Tribological study, *Surface and Coatings Technology* 186 (2004) 305–313.
- [9] J.A. García, G.G. Fuentes, R. Martínez, R.J. Rodríguez, G. Abrasonis, J.P. Rivière, J. Rius, Temperature-dependent tribological properties of low-energy N-implanted V5Ti alloys, *Surface and Coatings Technology* 188–189 (2004) 459–465.
- [10] R. Rodríguez, A. Sanz, A. Medrano, J.A. García-Lorente, Tribological properties of ion implanted aluminium alloys, *Vacuum* 52 (1999) 187–192.
- [11] R.J. Rodríguez, A. Medrano, J.A. García, G.G. Fuentes, R. Martínez, J.A. Puertolas, Improvement of surface mechanical properties of polymers by helium ion implantation, *Surface and Coatings Technology* 201 (2007) 8146–8149.
- [12] C. Mitterer, F. Holler, D. Reitberger, E. Badisch, M. Stoiber, C. Lugmair, R. Nöbauer, Th. Müller, R. Kulmer, Industrial applications of PACVD hard coatings, *Surface and Coatings Technology* 163–164 (2003) 716–722.
- [13] A. Erdemir, Genesis of superlow friction and wear in diamondlike carbon films, *Tribology International* 37 (2004) 1005–1012.
- [14] J. Böhlmark, in *Fundamentals of High Power Impulse Magnetron Sputtering*, Dissertation No. 1014, Linköping Institute of Technology, Sweden.
- [15] G.G. Fuentes, M.J. Díaz de Cerio, R. Rodríguez, J. C. Avelar-Batista, E. Spain, J. Housden, Yi Qin, Study on the sliding of aluminium thin foils on the PVD-coated carbide forming-tools during micro-forming, *J. Mat. Proc. Tech.* 177 (2006) 644–648.

- [16] L. Hultman, Thermal stability of nitride thin films, *Vacuum* 57 (200) 1–30.
- [17] G.G. Fuentes, D. Cáceres, I. Vergara, E. Elizalde, J.M. Sanz, Elastic properties of hard TiC_xN_y coatings grown by dual ion beam sputtering, *Surface and Coatings Technology* 151–152 (2002) 365.
- [18] S.J. Bull, D.G. Bhat, M.H. Staia, Properties and performance of commercial TiCN coatings. Part 2: Tribological performance, *Surface and Coatings Technology* 163–164 (2003) 507–514.
- [19] S. PalDey, S.C. Deevi, Single layer and multilayer wear resistant coatings on (Ti,Al)N: a review, *Material Science and Engineering A* 342 (2003) 58–79.
- [20] G.G. Fuentes, R. Rodríguez, J.C. Avelar-Batista, J. Housden, F. Montala, L.J. Carreras, A.B. Cristóbal, J.J. Damborenea, T.J. Tate, Recent advances in the chromium nitride PVD process for forming and machining surface protection, *J. of Materials Processing Technology* 167 (2005) 415–421.
- [21] G.G. Fuentes, M.J. Díaz de Cerio, J.A. García, R. Martínez, R. Bueno, R.J. Rodríguez, M. Rico, F. Montalá, and Yi Qin, Gradient Cr(C,N) cathodic arc PVD coatings, *Thin Solid Films* DOI: 10.1016/j.tsf.2008.08.005.
- [22] M. Arndt, T. Kacsich, Performance of new AlTiN coatings in dry and high speed cutting, *Surface and Coatings Technology* 163–164 (2003) 674–680.
- [23] R.J. Rodríguez, J.A. García, R. Martínez, B. Lerga, M. Rico, G.G. Fuentes, A. Guette, C. Labruguere, M. Lahaye, Tribological metal-carbon coatings deposited by PVD magnetron sputtering, *Applied Surface Science* 235 (2004) 53–59.
- [24] S. Carrera, O. Salas, J.J. Moore, Performance of CrN/MOS₂ (Ti) coatings for high wear low friction applications, *Surface and Coatings Technology* 167 (2003) 25–32.
- [25] A.A. Voevodin, S.D. Walck, J.S. Zabinski, Architecture of multilayer nanocomposite coatings with superhard diamond-like carbon layers for wear protection at high contact loads, *Wear* 203 (1997) 516–527.
- [26] R. Hoya, J.-D. Kammingaa, G.C.A.M. Janssen, Scratch resistance of CrN coatings on nitrided steel, *Surface and Coatings Technology* 200 (2006) 3856–3860.
- [27] J.C. Avelar-Batista, E. Spain, G.G. Fuentes, A. Sola, R. Rodríguez, J. Housden, Triode plasma nitriding and PVD coating: a successful pre-treatment combination to improve the wear resistance of DLC coatings on Ti6Al4V alloy, *Surface and Coatings Technology* 201 (2006) 4335–4340.
- [28] K.S. Klimek, H. Ahn, I. Seebach, M. Wang, K.-T. Rie, Duplex process applied for die-casting and forging tools, *Surface and Coatings Technology* 174–175 (2003) 677–680.
- [29] K. Holmberg, A. Matthews,[†] H. Ronkainen, Coatings tribology - contact, mechanisms and surface design, *Tribology International* 31 (1998) 107–120.
- [30] M. Diserens, J. Patsheider, F. Lévy, Improving the properties of titanium nitride by incorporation of silicon, *Surface and Coatings Technology* 108–109 (1998) 241–246.
- [31] F. Vaz, L. Rebouta, S. Ramos, M.F. da Silva, J.C. Soares, Physical, structural and mechanical characterization of $\text{Ti}_{1-x}\text{Si}_x\text{N}_y$ films, *Surface Coatings Technology* 108–109 (1998) 236–240.
- [32] S.K. Kim, P.V. Vinh, J.H. Kim, Deposition of superhard TiAlSiN thin films by cathodic arc plasma deposition, *Surface Coatings Technology* 200 (2005) 1391–1394.
- [33] E. Ribeiro, L. Rebouta, S. Carvalho, F. Vaz, G.G. Fuentes, R. Rodríguez, M. Zazpe, E. Alves, Ph. Goudeau, J.P. Rivière, Characterization of hard DC-sputtered Si-based TiN coatings: the effect of composition and ion bombardment, *Surface and Coatings Technology* 188–189 (2004) 351–357.
- [34] F. Vollertsen, H. Schulze Niehoff, Z. Hu, State of the art in micro forming, *Int. J. of Machine Tools and Manufacture* 46 (2006) 1172–1179.
- [35] G.M. Robinson, M.J. Jackson, A review of micro and nanomachining from a materials perspective, *J. of Materials Processing Technology* 167 (2007) 316–337.
- [36] J. Chae, S.S. Park* and T. Freiheit, Investigation of micro-cutting operations, *Int. J. of Machine Tools and Manufacture* 46 (2006) 313–332.
- [37] Y. Qin, Forming-tool design innovation and intelligent tool-structure/system concepts, *Int. J. of Machine Tools and Manufacture* 46 (2006) 1253–1260.
- [38] H. Hanyu, S. Kamiya, Y. Murakami, Y. Kondoh, The improvement of cutting performance in semi-dry condition by the combination of DLC coating and CVD smooth surface diamond coating, *Surface and Coatings Technology* 200 (2005) 1137–1141.
- [39] S.H. Yao, Y.L. Su, W.H. Kao, T.H. Liu, On the micro-drilling and turning performance of TiN/AlN nano-multilayer films, *Materials Science and Engineering A* 392 (2005) 340–347.
- [40] J. Kopac, M. Sokovic, S. Dolinsek, Tribology on coated tools in conventional and HSC machining, *J. Mat. Proc. Tech.* 118 (2001) 377–384.
- [41] S. Yang, E. Wiemann, D.G. Teer, The properties and performance of Cr-based multilayer nitride hard coatings using unbalanced magnetron sputtering and elemental metal targets, *Surface and Coating Technologies* 188–189 (2004) 662–668.
- [42] K.-D. Bouzakis, S. Hadjiyiannis, G. Skordaris, I. Mirisidis, N. Michailidis, G. Erkens, Wear development on cemented carbide inserts, coated with variable film thickness in the cutting wedge region, *Surface and Coatings Technology* 188–189 (2004) 636–643.
- [43] Y. Guo, G. Liu, Yi. Xiong, Y. Tian, Study of the demolding process – implications for thermal stress,

- adhesion and friction control, *J. of Micromechanics and Microengineering* 17 (2007) 9–19.
- [44] M. Hecke, W.K. Schomburg, Review on micro molding of thermoplastic polymers, *J. Micromech. Microeng.* 14 (2004) R1–R14.
- [45] A. Erdemir, Review of engineered tribological interfaces for improved boundary lubrication, *Tribology International* 38 (2005) 249–256.
- [46] J. Bech, N. Bay, M. Eriksen, Entrapment and escape of liquid lubricant in metal forming, *Wear* 232 (1999) 134–139.
- [47] J. Tallal, M. Gordon, K. Berton, A.L. Charley, D. Peyrade, AFM characterization of anti-sticking layers used in nanoimprint, *Microelectronic Engineering* 83 (2006) 851–854.
- [48] K.-J. Byeon, K.-Y. Yang, H. Lee, Thermal imprint lithography using sub-micron sized nickel template coated with thin SiO₂ layer, *Microelectronic Engineering* 84 (2007) 1003–1006.
- [49] S. Park, H. Schiff, C. Padeste, B. Schnyder, R. Köt, J. Gobrecht, Anti-adhesive layers on nickel stamps for nanoimprint lithography, *Microelectronic Engineering* 73–74 (2004) 196–201.
- [50] Š. Meškiniš, V. Kopustinskis, K. Šlapikas, S. Tamulevičius, A. Guobienė, R. Gudaitis, V. Grigaliūnas, Ion beam synthesis of the diamond like carbon films for nanoimprint lithography applications, *Thin Solid Films* 515 (2006) 636–639.
- [51] S.M. Chiu, S.J. Hwang, C.W. Chu, D. Gan, The influence of Cr-based coatings on the adhesion force between epoxymolding compounds and IC encapsulation mold, *Thin Solid Films* 515 (2006) 285–292.
- [52] M. Hock, E. Schäffer, W. Döll, G. Kleer, Composite coating materials for the moulding of diffractive and refractive optical components of inorganic glasses, *Surface and Coatings Technology* 163–164 (2003) 689–694.
- [53] O. Wänstrand, M. Larsson, A. Kassman-Rudolphi, Mechanical and tribological properties of vapour deposited low friction coatings on Ni plated substrates, *Tribology International* 33 (2000) 737–742.
- [54] M.J. Díaz de Cerio, G.G. Fuentes, R. Martínez, R. Rodriguez, E. Spain, J. Housden, Y. Qin, W. Hörnig, Temperature dependent contact phenomena of PVD and CVD deposited DLC films sliding on aluminium thin foils, *Int. J. Adv. Manuf. Technol.* 47 (2010) 931–936.
- [55] D.M. Cao, J. Jiang, W.J. Meng, Metal micromolding with surface engineered inserts, *Microsystem Technologies* 10 (2004) 662–670.
- [56] U. Pettersson, S. Jacobson, Tribological texturing of steel surfaces with a novel diamond embossing tool technique, *Tribology International* 39 (2006) 695–700.
- [57] R. Yamamoto, K. Miyashita, H. Hayashi, K. Inoue, Preparation of microstructure bodies in freestanding diamond-like carbon foil prepared using plasma-based ion implantation, *Diamond and Related Materials* 16 (2007) 292–295.
- [58] M. Yoshino, T. Matsumura, N. Umehara, Y. Akagami, S. Aravindan, T. Ohno, Engineering surface and development of a new DNA micro array chip, *Wear* 260 (2006) 274–286.
- [59] K. Fujimoto, M. Yang, M. Hotta, H. Koyama, S. Nakano, K. Morikawa, J. Cairney, Fabrication of dies in micro-scale for micro-sheet metal forming, *J. of Materials Processing Technology* 177 (2006) 639–643.

Polymer Thin Films – Processes, Parameters and Property Control

Bertrand Fillon

INTRODUCTION

Over the last 10 years, the use of polymer thin films has increased significantly in various domains of application: in traditional industries (e.g. papers and metal strips), in the automotive industry, in packaging, etc. Moreover, emerging markets such as consumer electronics and photovoltaic energy use polymer thin films also. This growth has been driven mainly by important advances in the properties of polymer thin films (better barrier properties (water, oxygen, etc.), wear resistance, optical properties, etc.) and a much more extensive range of applications (solvent-based coatings, water-based coatings, plasma deposition, emulsions, etc.). It would indeed be very ambitious to attempt to cover all the properties of polymer thin films in the space of a few pages. Nevertheless, there are two major families of parameters which influence the properties of these thin films:

- Type of the polymer deposited;
- Implementation conditions.

Clearly, the properties of these thin films depend mainly on the type of polymer and its thickness. Certain polymers are better for improving barrier properties, while others offer very good sealing functions. As for the implementation conditions, three processes are used to produce

most of these thin films: extrusion coating, deposition in solution with radiation cross-linking (thermal, UV, electron beam), and physical deposition involving plasma. The ranges of polymer thickness generally deposited by these three process types are respectively: $>5 \mu\text{m}$, $1 < t < 5 \mu\text{m}$ and $<1 \mu\text{m}$. Note that extrusion coating is at the upper limit of the range defined for the thin films.

Generally speaking, a key technological requirement is to provide all the desired functions of the coating (optical, barrier, adhesive, electrical, catalytic, etc.) while controlling the interfaces and micro-structures (film, charge dispersion, orientation, crystallinity, porosity, etc.).

This chapter is broken down into three major sections. Each section will focus on one of the three implementation processes mentioned above. The objective is to briefly describe these processes, indicating the most widely used polymers, and to show how thin film properties can be improved by the type of polymer deposited, but also through control of the interactions between process parameters and material parameters. Each of these sections will be illustrated by examples of applications requiring specific properties, e.g. water or oxygen barrier properties, optical properties, sealing properties or surface properties.

THIN FILMS OBTAINED BY EXTRUSION COATING

The process of extrusion coating (Fig. 15-1) enables covering a flexible substrate with a very thin polymer film. In industry, polyethylene is generally used to cover commercial substrates such as paper, cardboard, polyester and other polymeric films, metal foils including aluminum foil, textiles, etc. The polymer deposited is often a semi-crystalline polymer such as polyolefin (polyethylene, copolymers such as EMA, EBA, etc.), polyesters, PVC, etc.

The objective is to coat a substrate with a polymer, combining the best properties of the two materials. The advantages of this process are a heat-sealable surface, improved resistance to tears and wrinkling, an excellent barrier against moisture, oxygen and odors, enhanced optical properties (dullness, gloss) and an imprintable surface.

Principle of Extrusion Coating

Polymer granules are extruded using a slot die to obtain a thin film of molten polymer. The role of this coating die is to present the molten polymer in a form similar to its final form (coating film), to keep it at a constant temperature, to obtain a stable flow of polymer and to coat the desired

width of the substrate with it. The molten polymer travels over the distance between the slot die and the substrate: this distance is often called the air gap. The air gap value may vary depending on the desired extrusion conditions.

The film of molten polymer is pressed through two rollers positioned directly below the die. The first of these, coated with neoprene, is the pressure roll. It draws the substrate to be coated and presses it against the molten polymer film. This is the precise moment at which the extruded polymer adheres to the substrate. The pressure roll is cooled by internal water circulation with adjustable temperature. This prevents its temperature from rising too rapidly.

The second roller is chrome plated and called the chill roll. It is also cooled by internal water circulation with adjustable temperature. Its role is threefold:

- It must cool and solidify the polymer in a fraction of one rotation.
- Its rotational speed controls the quantity of polymer deposited on the substrate (coating thickness or grammage).
- Its surface (polished, matte, etc.) determines the surface appearance of the polymer coating.

The resulting complex is then directed towards the system's draw roll and winder.

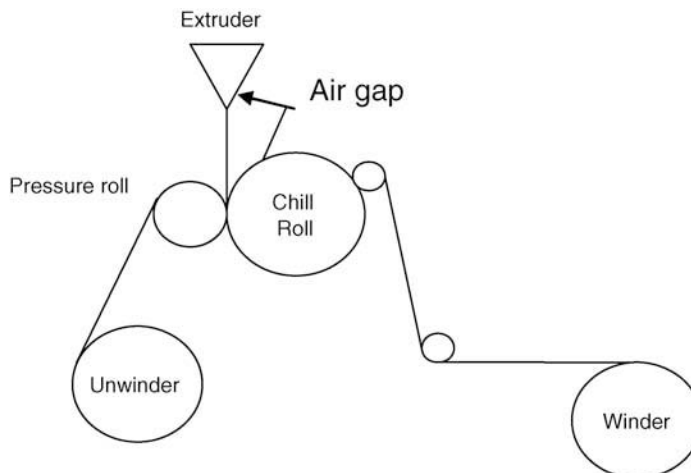


FIGURE 15-1 The process of extrusion coating.

Process Parameters and Influences

Polymer suppliers and converters must deal with a growing market demand for low cost ‘deposited film/substrate’ complexes which still offer high performance properties. Manufacturers, polymer and substrate suppliers, and converters must work together to reach these objectives. Various studies have enabled improving polymer performance while at the same time optimizing process parameters. For example, in the packaging industry, several complexes such as aluminum/polyethylene, paper/PE, etc., are used with low density polyethylene (LDPE) without a binder layer. These various structures are produced using extrusion coating. Good adhesion between the LDPE and the substrate is clearly vital. However, the adhesive strength is generally very weak between the substrate and the LDPE, due to the lack of polar or reactive functions in LDPEs. Likewise, following the extrusion coating process, the complexes alu/LDPE, paper/LDPE, etc., maintain the sealing properties of polyethylene.

Example: Adhesive Properties of an Aluminum/LDPE Structure. For adhesion to occur between LDPE and the aluminum foil, the LDPE has to oxidize during the extrusion process. This functionalization of the LDPE primarily occurs during the molten polymer’s dwell time between the die’s opening and the point of contact with the substrate, i.e. in the air gap. Adhesion between the LDPE and the substrate is affected by several factors, which can be categorized into three groups: extrusion parameters (melt temperature, air gap, etc.), polymer parameters (melt index, density, etc.) and substrate parameters (type, surface roughness, etc.). Over the last 20 years, the practical problem of ensuring good adhesion between the LDPE and various substrates during extrusion coating has been the subject of much interest, both from a technical and a scientific point of view [1–7]. Whereas some parameters (corona treatment, ozone, post-treatment, etc.) generally increase adhesion, it is difficult to draw a single conclusion for process parameters overall, but most authors agree that interactions do exist between these parameters. The main process

parameters with the greatest effect on adhesion between the polymer and the substrate are: temperature of the molten polymer, thickness of the film deposited, pressure of the rollers, extrusion speed, and air gap.

It is very difficult to separate the last two parameters: increasing the substrate speed effectively reduces the dwell time (d_t) in the air gap and LDPE oxidation becomes difficult, resulting in poor adhesion. If the air gap is increased, the dwell time d_t (or freeze time t_f) and LDPE oxidation will also increase, but the LDPE will cool and its viscosity will increase, reducing its wettability relative to the substrate’s roughness. This in turn reduces mechanical adhesion. These two phenomena conflict with one another; hence the need for a compromise. According to most authors, line speed and air gap can be expressed as a single parameter, that of freeze time t_f :

$$t_f = \frac{H}{V_t - V_0} \times Ln \frac{V_t}{V_0}$$

where V_t = line speed, V_0 = material through P and H = air gap.

Figure 15-2 illustrates the interactions between the process parameters and the polymer, which lead to changes in adhesive strength. At low temperatures ($T = 285^\circ\text{C}$), the adhesive strength (F_p) of the LDPE increases with dwell time, attaining a maximum value then falling. This increased adhesion is correlated with an increase in the LDPE’s carboxylic functions and, as a result, in its surface energy (Y_p). The drop in adhesion at high t_f values is related to cooling of the LDPE, which becomes more viscous on contact with the substrate; as a result, the LDPE does not mold as well to the substrate’s surface. At high temperatures ($T = 315^\circ\text{C}$), adhesion of the LDPE is very strong despite short dwell times. This adhesion decreases with high t_f values. Oxidation of the LDPE becomes excessive and initiates its degradation, resulting in a high number of ruptured chains and a drop in its surface energy (Y_p). This leads to a layer with poor cohesion at the surface of the LDPE film, in turn provoking the drop in adhesion.

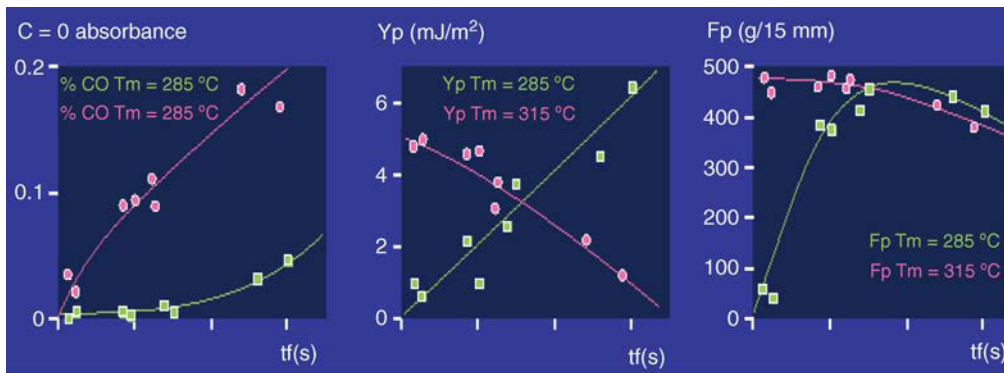


FIGURE 15-2 Freeze time (t_f) dependent changes in the oxidation rate, polar function (Y_p) and peel strength (F_p) of a low density polyethylene extruded on aluminum foil at two temperatures (285°C and 315°C). The thickness of the LDPE film and the pressure between the rollers were constant ($e = 10 \mu\text{m}$; $P = 6 \text{ bars}$).

Achieved through controlling process parameters, LDPE oxidation is necessary to attain good LDPE/aluminum adhesive strength.

Example: Sealing Properties of an Aluminum/LDPE Structure. Besides the adhesion between the aluminum foil and the polyethylene, the LDPE film should have good sealing properties. Figure 15-3 illustrates the changes in the seal strength of one alu/LDPE complex compared to another alu/LDPE complex, both obtained by extrusion coating. The sealing capacity of a polymer is most often linked to its melt index (MI). A high MI results in a high degree of fluidity and improves interfacial diffusion during sealing, allowing the polymer to attain a high seal strength

at low temperatures. This is illustrated by Fig. 15-3; the LDPE2 sealing curve (MI = 7) starts at a lower temperature than that of LDPE1 (MI = 3). Extruded at low pressure and a low rate (45 kg/h), LDPE1 attained a seal strength of 300 g/15 mm at a temperature of 100°C. Under the same conditions, LDPE2 attained a seal strength of 700 g/15 mm.

Process parameters clearly have an influence on sealing properties as well as on adhesion. Figure 15-3 illustrates the effect of extrusion rate on seal strength. Within the operating range for the selected process parameters, when LDPE2 is deposited on aluminum foil at a lower rate (45 kg/h), seal strength goes from 300 g/15 mm

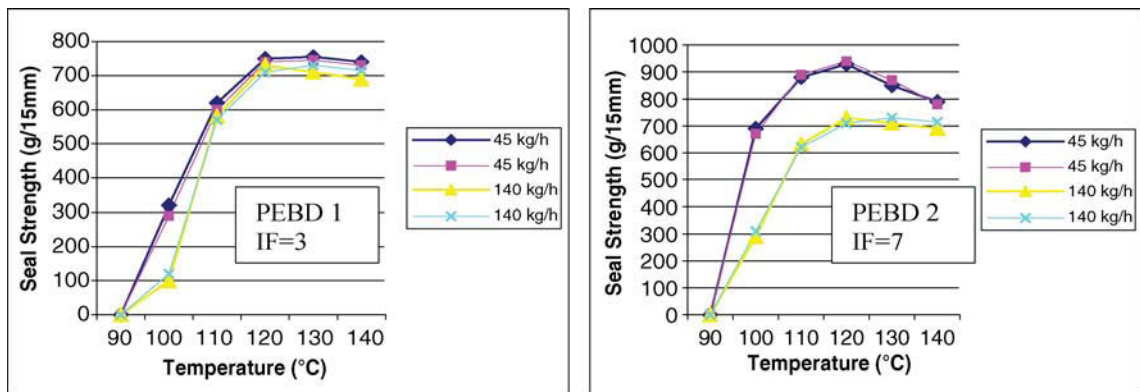


FIGURE 15-3 Changes in seal strength of two LDPEs (LDPE1: MI = 3; LDPE2: MI = 7) according to sealing temperature. The alu/LDPE complexes were obtained by extrusion coating at two different rates (45 and 140 kg/h) and at two different pressures (90 and 150 bar). The low pressure curves are represented by dotted lines.

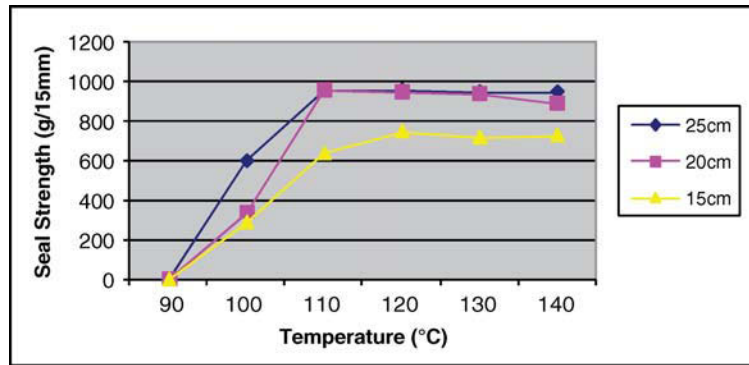


FIGURE 15-4 Changes in seal strength according to temperature for alu/LDPE complexes extruded with various air gaps.

to 700 g/15 mm. Likewise the air gap has an effect on seal strength, which is weaker when the air gap is reduced (Fig. 15-4). Sometimes these process/material interactions do not exist; this is the case for pressure during the extrusion process [3].

Summary on Extrusion Coating

Variation in process parameters can have a significant impact on the final properties of film complexes such as alu/PE, paper/PE, alu/EVA, etc. Final products with excellent performance can be obtained at low cost through polymer selection and adjustment of the process parameters. In the section above, the examples presented for adhesive and sealing properties clearly illustrate the interactions between material and process parameters. Whatever the target property – barrier, optical, etc. – these interactions between process/material parameters will always play an important role in determining the final properties of the product [8].

ORGANIC COATINGS DEPOSITED IN SOLUTION

Organic coatings deposited in solution (i.e. using wet methods) are found in very diverse areas. They are commonly produced by coating substrates with thin layers of a liquid or suspension, which are then transformed into solids by gelation, drying or cross-linking. Such structures are

vital elements for an extremely broad range of industrial products. They are developed for paper, steel, aluminum, polymer films, printed materials, selective membranes, photographic film, photosensitive coatings, adhesives, microelectronics, integrated circuits, etc. However, deposition technologies may differ greatly depending on the final application. For example, the manufacture of microelectronic components uses spin coating, whereas varnish is generally deposited on steel foil using roll or spray coating.

This chapter focuses exclusively on organic coatings deposited with the roll coating technique; this covers a large majority of the polymer thin films produced industrially. Most of the deposition processes based on this technique involve a series of rollers producing polymer thin films which can have thicknesses below one micron. These varnishes offer an effective protective barrier for metal substrates (aluminum, steel), paper substrates or polymer films. These coatings may also be used for decorative or aesthetic purposes (glossy or matte effects, colors, etc.), or act as sealants, etc. They must also offer specific characteristics of durability and resistance to temperature, solvents or UV radiation depending on the final application of the coated product:

- Exterior applications (pre-finished steel and aluminum for construction);
- Decorative interior elements, household appliances, etc.;
- Packaging for food products, cosmetics, etc.

The composition of the varnishes or paints, the choice of substrate, and the conditions under which organic coatings are applied, dried and cured are inextricably linked in determining the properties of the end product [8].

Main Polymers used in Roll Coating

As in extrusion coating, the polymer used to coat the substrate will strongly influence the quality of deposition and the final properties. The most commonly used coatings are indicated in Table 15-1. Note that the molecular weights of polymers deposited in solution are lower than those of polymers deposited by extrusion.

In general, six categories of basic polymers (Fig. 15-5) are used in roll coating [9]. The different categories are based on:

- Solid state (amorphous or crystalline);
- Solubility in common solvents;
- Swellability of crystalline or cross-linked polymers.

Amorphous and soluble polymers (A), for example polyesters, epoxies or acrylics, produce liquid varnishes and paints which are 30% to 70% non-volatile. Amorphous and insoluble polymers (B), which are primarily polyesters, can be used in powder coating technology. Semi-

crystalline polymers (C), which form the basis of the extrusion coating films listed in the previous chapter, can also be used in roll coating after a process of precipitation or grinding to produce fine powders.

Dispersing these fine powders in other basic polymer solutions produces organosols (E), which are 40% to 60% non-volatile. Examples of organosols include PVDF films and polyester polyurethane systems modified by polyamide fine powders.

Organosols can also be formulated with cross-linked polymers (D) in the form of micro-gels or ground into fine powders. Certain applications use these substances, specifically cross-linked amine polymers, acrylics and unsaturated polyesters.

A plastisol (F) is obtained if a fine and crystalline powder polymer is dispersed in a plasticizer that homogeneously dissolves it at temperatures above the crystallite melting point, forming a gel after cooling. Plastisols are more than 90% non-volatile. Little solvent is needed.

Note that in addition to the specific characteristics for roll application and ‘flash’ forming or curing of the film, the varnishes or paints for the pre-finishing of flat steel or aluminum must offer excellent flexibility, e.g. meeting the post-forming requirements for drawing food cans.

TABLE 15-1 Performance of Main Coatings used in Solution

Polymer Family	Polyester/ Amine	Polyester/ Polyurethane	Epoxy	PVDF	PVC
Flexibility	Good	Very good	Poor	Good	Very good
Hardness	Good	Average	Very good	Average	Poor
Adhesion to metal	Good	Good	Very good	Poor	Poor
Corrosion protection	Good	Good	Very good	Average	Very good
Weather resistance	Good	Very good	Poor	Very good	Average
Temperature resistance	Good	Good	Good	Good	Poor
Recyclability	Very good	Good	Good	Poor	Poor

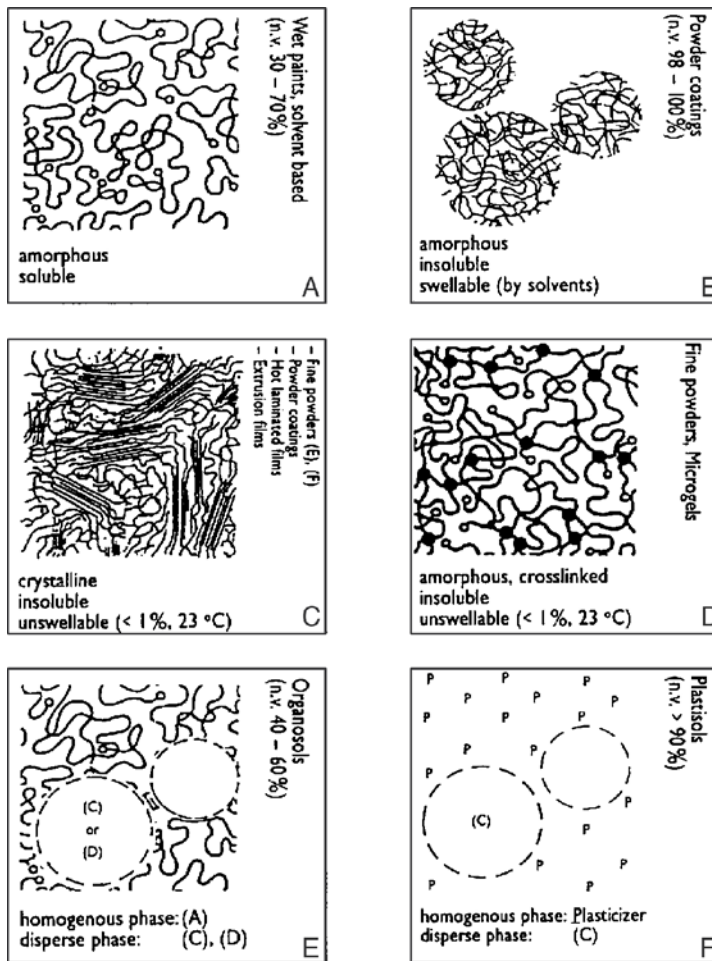


FIGURE 15-5 Morphology of basic resins [13].

Principle of Organic Coating Deposition in Solution

Applying organic coatings to reels of flat substrate offers major technical and financial advantages due to the following:

- Increased productivity and yield of finishing systems (with linear speeds of up to 1000 m/min), reducing the cost of varnish and paint application.
- Flexibility of roll coating; rapid changes can be made without stopping the application process.
- Various curing temperature levels (80–250°C), enabling a wide range of binder systems to be used via various film formation processes (flash

cross-linking, gelation or fusion). Cross-linking increasingly involves the environment-friendly techniques of UV radiation or electron beams.

- Efficient effluent treatment systems (e.g. incineration of solvent vapors).

Generally, the process of roll coating includes three phases:

- **Surface preparation and treatment:** corona surface treatments are widely used on various substrates, e.g. chromate treatment of steel (no-rinse process) which helps to control film weight and eliminate releases.
- **Roll coating of the polymer:** can be performed on both sides of the reel simultaneously.

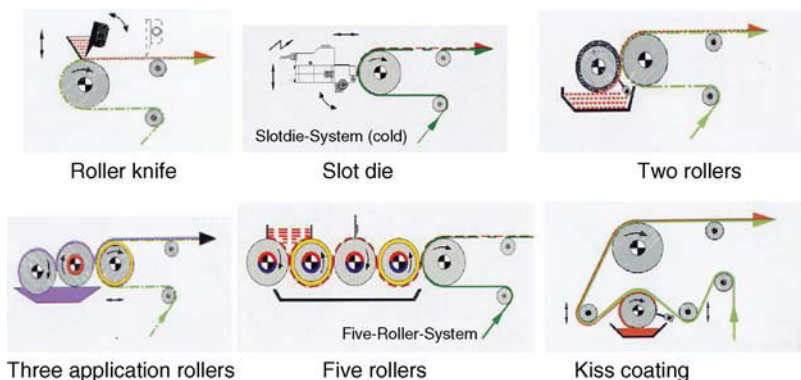


FIGURE 15-6 Various systems for varnish deposition [10]. Diagrams from Coatema sales documentation.

Various approaches can be used for this step (Fig. 15-6). More than 35 systems are available on the market to coat a variety of substrates [10]. The varnish properties, surface appear-

ance and thickness ranges differ according to the process used.

- **Solvent evaporation and flash curing:** necessary for forming the binding network.

TABLE 15-2 Three Varnish Deposition Processes most Commonly Encountered

Type of Process	Characteristics	Main Comments on the Process
Knife coating	Thickness range: 5–500 μm Viscosity: 5000–50,000 mPas Maximum speed: 100 m/mn	Very dependent on varnish and substrate. A very smooth film can be obtained with 4% precision over the full width of the substrate. For low viscosity varnishes, there may be problems with deposition uniformity. Solvent evaporation during the implementation process may lead to the appearance of agglomerates.
Slot die	Thickness range: <1–200 μm Viscosity: <1000 mPas Maximum speed: 1000 m/mn	Possible to work with minimum contact. Substrate does not have a big influence. Precision is on the order of 1%. The low viscosity (<200 mPas) often results in very good precision.
Roll coating	Thickness range: 2–100 μm Viscosity: <2000 mPas Maximum speed: 1000 m/mn	Very dependent on the surface of the deposition roller (very smooth with very good precision, or gravure roller). A very smooth film can be obtained. The precision of deposition depends on the parameters of the application roller and the roller opposite to it. For film thickness, precision is on the order of 2%.

The choice of technology is based on the application, but there are some country-specific trends emerging in the technologies chosen [11]. With the process of varnish deposition, it is possible to influence precision, coating weight and also surface appearance (Table 15-2).

Most often, the coating is applied to the substrate using a series of application rollers. The reasons cited for using such a system are as follows: the ability to transmit shear to a liquid, to smooth the coating before its deposition, to attain an acceleration between the slow movement of the rollers and the speed at which the substrate passes through them (i.e. line speed) and to produce thin films by multiplying the separation phases at each roller. The configurations are selected based on the deposition thickness and precision. In the two-roller configuration, there is only one gap for adjusting and controlling the thickness deposited. In a three-roller configuration, the additional gap allows this thickness to be optimized. Each roller has two functions. First, rollers act as a divider by reducing the thickness and uniformly spreading the varnish between all the rollers. Second, they create the necessary shear to provoke Newtonian behavior in the varnish. There are few publications [12–15] explaining how these deposits form, how a thin film is created, how good the sensitivity is and how to per-

fectly control coating weight based on roller speed, gap, and varnish properties.

But obviously there will always be interactions between the varnish type, its viscosity and the additives (size of charges, chemical nature, form, etc.). Note that for certain production processes, the central chemical treatment and coating section is isolated from the unwinding and winding sections by accumulators, allowing for uninterrupted operation during reel changing.

Process Parameters and Influences

Example: Optimizing Optical Properties.

There is a great deal of demand for coatings with specific visual or optical properties (transparency, gloss, matte finish). By adjusting the parameters of the implementation process, it is possible to influence a coating's surface appearance as well as its thickness and precision.

As the varnish is applied to the substrate, the shear rate changes abruptly, potentially attaining very high values (Fig. 15-7), but this intense shear strain lasts only a short time (<0.01 s). Use of an elastomer roller can be estimated to increase the dwell time and reduce shear by a factor of around 10 compared to a rigid roller. The viscosity of the varnish will thus have a non-negligible effect on its thickness and visual qualities, and it will

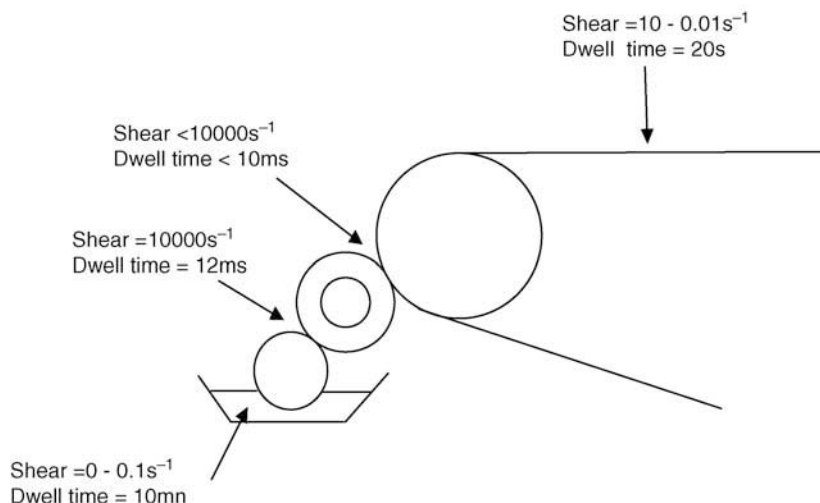


FIGURE 15-7 Timescale and typical values of process parameters for wet deposition.

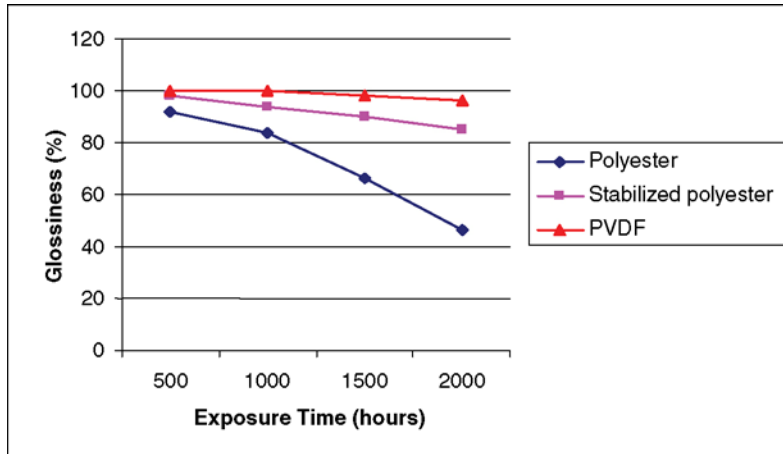


FIGURE 15-11 Variation in the glossiness of different polymer thin films according to exposure time under a mercury lamp.

of varnish. Polyester varnish demonstrates poorer durability than PVDF under mercury lamp exposure [9].

Example: Barrier Properties. Another property in great demand for thin films deposited in liquid form is protection of the substrate by barrier properties or protection against corrosion. In the previous section, it was shown that the substrate's surface energy plays an important role in determining the optical properties of the thin film

deposited. Figure 15-12 illustrates that surface energy is also important for water vapor barrier properties, obtained by depositing a film of polyvinyl alcohol (PVA) on a paper substrate [21–22]. Applying the corona treatment to the paper before PVA deposition increases the substrate's surface energy, while improving deposition quality and therefore the water barrier properties [21]. This surface energy activation benefits calendered papers as well as non-calendered papers. Note that

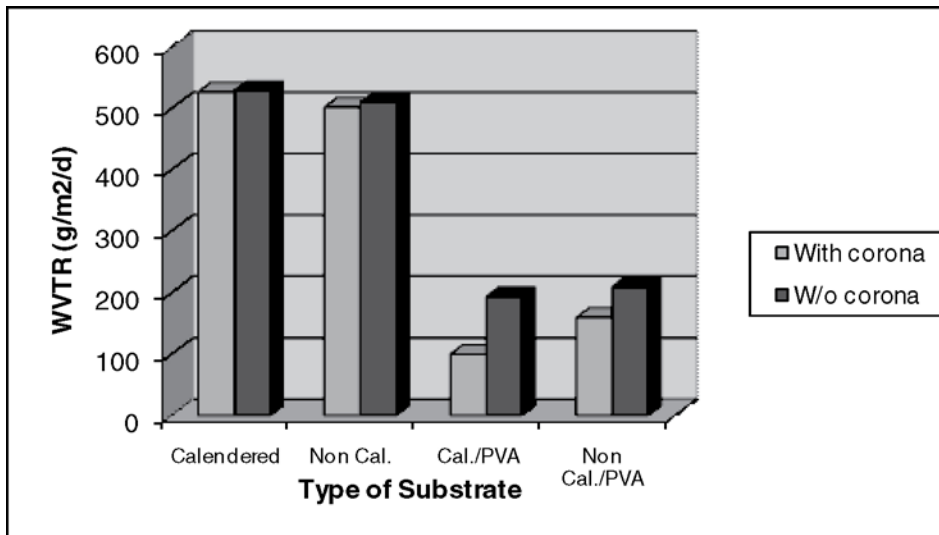


FIGURE 15-12 Changes in water barrier properties (WVTR) according to the type of paper and its surface treatment (with and without corona treatment). Calendered and non-calendered paper, with and without PVA.

the substrate's surface roughness also influences the uniform appearance of the film deposited [22].

A new generation of polymer thin films is currently being developed and involves integrating nano-fillers taken from sheet silicates (clays). Much work has been done on these nano-composites made from platelet nano-fillers, particularly in the packaging and automotive industries. These materials, with nanometric stiffeners that are strongly anisotropic (form factor of 200), offer very attractive properties, in terms of mechanical behavior under high temperatures as well as barrier properties, compared to materials with traditional stiffeners (talc, silica, etc.). Used on polymer, metal and paper substrates, these thin film materials are opening up new possibilities for food-grade and cosmetic packaging, where additional requirements apply in terms of oxygen and odor barriers and resistance to heat and abrasion [23–24]. The industrial development of such impermeable structures, with their enhanced mechanical properties compared to standard thin films, depends on controlling nano-filler dispersion and exfoliation. Figures 15-13 and 15-14 illustrate the difference in nano-filler dispersion depending on the type of polymer matrix and the type of the nano-filler.

The filler in Fig. 15-14 is not sufficiently polar and the filler/polymer interactions are not sufficiently strong to allow perfect exfoliation and dispersion of the platelets in the polymer matrix.

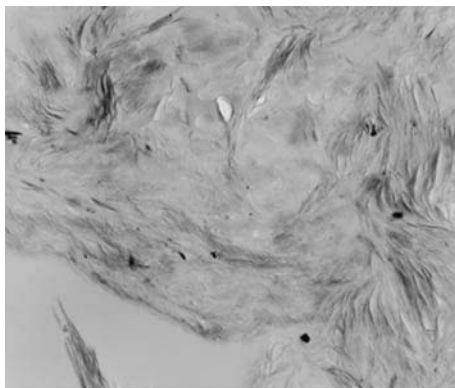


FIGURE 15-13 Homogeneous dispersion of the filler 2MHBT in a vinyl varnish.

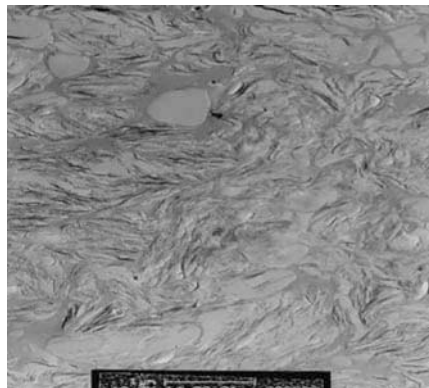


FIGURE 15-14 Inhomogeneous dispersion of 2M2HT in a vinyl varnish.

TABLE 15-3 Families of Sealing Varnish According to Type of Substrate

Varnish Family	Type of Substrate
Acrylic	Film or sheet of polystyrene or bi-oriented polypropylene (BOPP)
Vinyl	Aluminum foil, PVC
Polyester	Polyester, PVC
Modified acrylic on olefin	Film or sheet of polystyrene or bi-oriented polypropylene (BOPP)

Example: Sealing Properties. Certain polymer thin films deposited in solution offer very attractive sealing properties, especially for substrates such as aluminum foil or paper. For example, Table 15-3 indicates which family of sealing varnishes will be effective based on the substrate, for packaging applications such as seals, pouches, etc.

Summary on Organic Coatings

Depositing polymer thin films in solution is a widely used technique for diversifying the surface appearance and functionality of flat substrates. Selecting the binder system for the organic coating is decisive for substrate performance, whether in

terms of appearance, moisture or gas barrier properties, corrosion protection, resistance to photochemical ageing or the capacity to undergo forming without cracking.

Pre-finishing technologies offer diverse possibilities for new development, thanks primarily to the following:

- Coatings are constantly being improved;
- New developments in the area of organic coatings and their implementation.

For exterior applications, the use of new-generation flexible organic coatings with high or ultra-high durability is enabling the development of wet thin films which are affordable and particularly effective. These new thin films meet the requirements of the final application domain and can ensure aesthetic qualities for over 15 years in some cases. In sectors such as household appliances, new, slightly thicker thin films offer better scratch resistance, for example.

It should be noted that other methods of applying organic coatings without a solvent are expanding rapidly, notably radiation cross-linking techniques (UV, electron beam).

VACUUM-DEPOSITED COATINGS

Over the past several years, vacuum deposition techniques have been developed for the industrial manufacture of high quality products. Some of these techniques can be used in-process (ultra-thin films for integrated circuits, magneto-optical films for magnetic discs or tapes, glass coatings for thermal insulation, electrical conductivity or UV filtering for cars or construction, etc.). The main product objectives are as follows:

- Wide variety of deposition materials: pure metals, metal alloys, oligomers, ceramics.
- Deposits with composition gradients are possible, as well as multilayer deposition.
- Single or double-sided coatings are easy to obtain for various purposes.
- Reduced cost of finished products (productivity, energy, etc.).
- Environment-friendliness (low releases, little material used).

Since the end of the 19th century, it has been known that organic compounds in a discharge plasma form a solid deposit. These deposits were initially considered undesirable by-products and little attention was paid to their properties. It wasn't until the 1960s that the material formed in plasma was recognized as a polymer and the process was named 'plasma polymerization'. During its early development, plasma polymerization was considered an exotic method of polymerization. It is now considered an important process for producing entirely new materials. The materials formed by plasma polymerization are very different from conventional polymers and inorganic materials, falling somewhere between the two. This technique is not limited to the production of organic materials, instead opening a broad field of possibilities including metals and inorganic components.

Principle of Vacuum Polymer Deposition

Generally speaking, there are three components to the technology of dry coating processes:

- A precursor, which can be the crucible in a vacuum evaporator, a bombardment target or an effluent producer containing one or several precursor gases. The material to be deposited leaves this source in the form of ions, atoms, atom groupings or molecules.
- A substrate, i.e. the part to be coated and the site of deposition, during which the source species develop progressively (growth), resulting in a more or less well-ordered film.
- An environment, which separates the source from the substrate and is the site of the vapor-phase transfer.

Various deposition methods are used:

1. Physical vapor deposition (PVD), for species produced by a purely physical phenomenon, such as thermal evaporation or ion bombardment.
2. Chemical vapor deposition (CVD), for species produced by a chemical reaction (e.g. reduction of a volatile halide by hydrogen) or by the decomposition of a molecule (hydrocarbon).

In this case, the reactions are essentially surface reactions involving heat activation.

Physical vapour deposition (PVD), one of the most commonly used ‘dry’ processes for inorganic coatings, includes two methods. The first is sputtering, involving bombardment of a solid to obtain a vapor phase, which is then condensed on a cold substrate to form another compound. The other method is vapor deposition (VD), sometimes called thermal evaporation, which produces inorganic or organic thin films through evaporation of the source. In the case of polymer sources, the source is heated or irradiated. However, the deposition process (PVD) may decrease the molar mass of the resulting film.

Chemical vapor deposition (CVD), a process in which a thin film is synthesized from a gas phase precursor that undergoes a chemical reaction (decomposition, grafting reaction) at the substrate’s surface. These reactions distinguish CVD from physical deposition processes, such as evaporation, bombardment or sublimation. CVD is a well-known process used to produce high purity inorganic and organic thin films.

This chapter examines chemical deposition, which is very relevant today. Thin film polymer coatings made from precursors using PECVD (plasma-enhanced chemical vapor deposition) are now common and can be found in a growing number of applications [25] (optics, mechanics, chemical protection, nano-systems, microelectronics, etc.). The success of these coatings in surface functionality is related to their high potential for innovation and their ‘clean’ technology, which is environment-friendly with low material consumption.

In PECVD, ‘cold’ plasmas are used because they are very thermodynamically unbalanced ($T_e \gg T_i$ and T_n , where T_e , T_i and T_n are electron, ion and neutral temperatures, respectively). Plasma is an electrically neutral environment composed of ions, neutrals, radicals, electrons and photons [26]. The gas precursors are dissociated in a controlled-pressure reactor (from a few millitorr to atmospheric pressure) in which an electrical discharge is applied. This partially ionizes the gas. In these plasmas, the electrons

have high kinetic energy (1–10 eV or more); the ions, radicals and neutrals have lower kinetic energies (around 0.5 and 0.1 eV, respectively). This is the advantage of plasma; the active species are produced in the plasma phase before contact with the surface, allowing the energy of the ions to be controlled when they reach the surface. The numerous collisions between neutrals and electrons generate active species at ambient temperature. This enables treatments on all types of substrate, with numerous reaction paths due to the large quantity of active species created. There are several ways to obtain these plasmas. However, thin film deposition techniques mainly use a capacitive discharge obtained by applying an alternating electrical field between two electrodes. There are three categories of excitation frequency: low frequency discharges (where $20 \text{ kHz} < f < 200 \text{ kHz}$) resulting in very low density plasma (low electron density), capacitive radiofrequency (RF) discharges (where $f = 13.56 \text{ MHz}$) resulting in electron density of around 10^{10} cm^{-3} , inductive RF discharges (where $f = 13.56 \text{ MHz}$) and microwave discharges (where $f = 2.45 \text{ GHz}$) for which the electron density is much larger, i.e. greater than 10^{10} cm^{-3} .

For polymerization to occur, the precursors must contain atoms capable of forming chains, such as carbon, silicon or sulfur. Plasma polymerization is very different from conventional polymerization. Chemically speaking, polymerization is the reaction of activated monomers, producing a long repeating chain. During plasma polymerization, the notion of monomers does not really apply beyond the precursor stage. In fact, all the species created in the plasma participate in the reaction. In other words, activated radicals interact at the surface of the substrate and in the plasma, mainly through termination reactions. The terms ‘plasma polymerization’ and ‘plasma-induced polymerization’ are used because plasma produces free radicals and molecules with unsaturated bonds. The structure of the monomer (precursor) is not preserved and the product obtained is more or less disorganized, with variable cross-linking.

The very broad selection of precursors gives rise to a multitude of materials known as plasma polymers.

In summary, the growth of the films obtained by PECVD involves a series of elementary steps:

- Creation of reactive species (ions, excited neutral molecules, radicals).
- Migration of these species to the substrate.
- Absorption at the surface, followed by chemical reactions which produce new species that will form the thin film.

Figure 15-15 provides a general idea of how these processes work, and details of the various phenomena involved (plasma physics and chemistry, thermal hydraulics and thermal kinetics of the gas- and solid-phase reactions, role of operational parameters) will not be given here. H. Yasuda [27], H. Biederman [28] and R. d'Agostino [29] provide an excellent overview of these topics. Because this technique introduces numerous interactions between process parameters and thin film properties, a few examples will be presented below.

The deposits obtained with these techniques offer interesting properties which depend on the substrate and the process conditions used. These properties include chemical and mechanical sta-

bility (adhesion, hardness, etc.) and optical, electrical and gas barrier properties. Moreover, it is easy to obtain films with a gradient of chemical or physical properties by modifying the process parameters during the deposition cycle [30]. Numerous industrial machines are capable of processing reels of plastic film, often exceeding two meters in width, on which they deposit thin SiO_x films, with thicknesses of just a few dozen nanometers and substrate speeds of more than 100 meters per minute.

Major Precursor Families

By analogy with traditional polymerization, the term 'monomer' is also used for the precursor gas that reacts with the plasma. However, this term is inappropriate because there is no growth and no repetition of polymer chains in thin film deposition.

The various categories of common precursors are as follows:

1. **Hydrocarbons.** There is no need to have the traditional polymerizable groups. Thus, ethane, methane and cyclohexane can be polymerized by plasma but with lower growth rates than acetylene, ethylene and benzene [31].

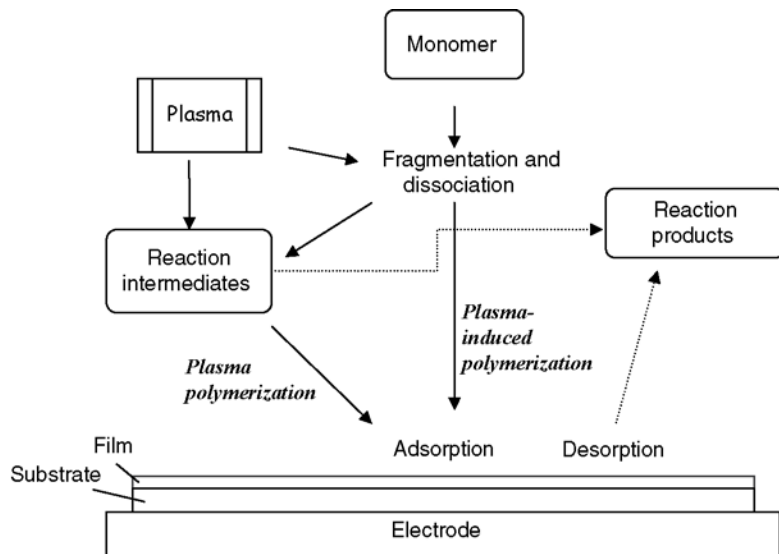


FIGURE 15-15 Schematic diagram of plasma polymerization.

Hydrocarbons contain polar groups, which can be used to produce far more polar films than hydrocarbons by themselves. Pyridine and amines are included in this group of precursors. Note that using nitrogen with a comonomer such as acetylene will produce very polar thin films with hydrophilic properties.

2. **Fluorocarbons.** These precursors are cited in the literature very frequently and are used in micro-electronics for plasma etching. However, depending on the precursor's C/F ratio, deposits with very anti-adhesive properties may be obtained (e.g. C₄F₈ with F/C = 2).
3. **Siloxanes.** These are the most used precursors due to their ease of implementation. They include a broad range of siloxanes, silazanes and linear or cyclical silanes. For example, hexamethyldisiloxane (HMDSO) with the chemical formula OSi₂C₆H₁₈ (162 g.mol⁻¹) is liquid at ambient temperature ($\theta_f = -66^\circ\text{C}$) and very volatile (vapor pressure of 56 mbar at 25°C). With this precursor, polymer deposits containing polysiloxanes (SiO_xC_yH_z) or SiO_x can be easily obtained with PECVD by adding oxygen to the gas phase. Figure 15-16 is a schematic diagram of the molecule and Fig. 15-17 shows its various bond energies.

Adding molecular oxygen to the discharge clearly modifies the composition of the film obtained. The atomic oxygen produced has an

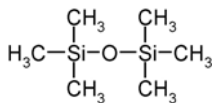


FIGURE 15-16 HMDSO molecule.



FIGURE 15-17 Bond energies of HMDSO.

etching effect on the carbon compounds in the growing film. At high oxygen levels, this makes it possible to obtain SiO₂ films having practically no carbon.

Table 15-4 lists the main precursors used in PECVD, with the type of thin films produced and their properties.

Process Parameters and Influences

In recent years and for diverse applications (packaging, electronics, etc.), the development of low temperature deposition of polymer thin films using the PECVD process has experienced very strong growth. Target properties currently include barrier properties [30–34] (oxygen, water, etc.), optical properties, hydrophobic or hydrophilic properties, anti-adhesion, and abrasion resistance [35–36].

When the precursor is introduced into the plasma, the deposition rate and the physico-chemical nature of the resulting polymer thin film will be affected by the main implementation parameters, such as:

- Excitation frequency of the plasma;
- Driving power;
- Flow rate of the precursor gas;
- Pressure in the chamber;
- Substrate temperature;
- Substrate polarization;
- Dwell time;
- Geometric factors (gas injection point, shape of gas nozzles, reactor dimensions, etc.).

In other words, the properties of a plasma polymer depend on the type of the precursor used, the implementation conditions in the plasma reactor, including its geometry, and the substrate on which the thin polymer film is deposited.

There is not yet complete understanding of the properties of PECVD films (prepared using given conditions and processes), including the range of possible interactions between all the parameters, but various publications describe the key roles of each parameter individually.

In this section, only the well-understood characteristics of polymer thin films will be presented.

TABLE 15-4 A Few Precursors and the Polymer Deposits Obtained using PECVD. The Main Properties of the Resulting Films are also Presented

	Surface Energy	Barrier Properties	Porous Films	Optical Properties
Precursors	Siloxanes: Fluorocarbons C ₃ F ₈ , C ₄ F ₈	Siloxanes, silazanes, tetrafluoroethylene perfluorobutene, ethylene, etc.	Fluorocarbons, perfluoro-1- methyldecaline, octamethylcyclo- tetrasiloxane, pentafluorostyrene, etc.	Hydrocarbons, fluorocarbons, vinyltrimethylsilane, perfluorobutene, tetrafluorobutene
Polymer thin films obtained	Polysiloxane (SiO _x) Teflon-like films (CF _x)	Polysiloxane (SiO _x), (SiO _x C _y H _z) polysilazane (SiN _x) amorphous carbon Teflon-like films	Tetramethylsiloxane	Amorphous carbon Teflon-like films, etc.
Target properties	Anti-adhesive, wettability, hydrophobic, hydrophilic	Corrosion protection, water and oxygen barrier for plastic, paper and other substrates	Gas separation, permeable membrane	High refractive index, transparency, low extinction coefficient, etc.

Example: Barrier Properties. Improved barrier properties for plastic or paper substrates are certainly among the most sought-after characteristics. This can be achieved with PECVD thin films. Figure 15-18 illustrates changes in the moisture barrier of a polyethersulfone according to the power used during deposition. First of all, increas-

ing the reactor's power accentuates disassociation in the gas phase. A higher driving power can increase the deposition rate by creating a greater number of active species. Density saturation may also be observed at higher powers, which suggests that film production is limited by the supply of active species [32,37–38].

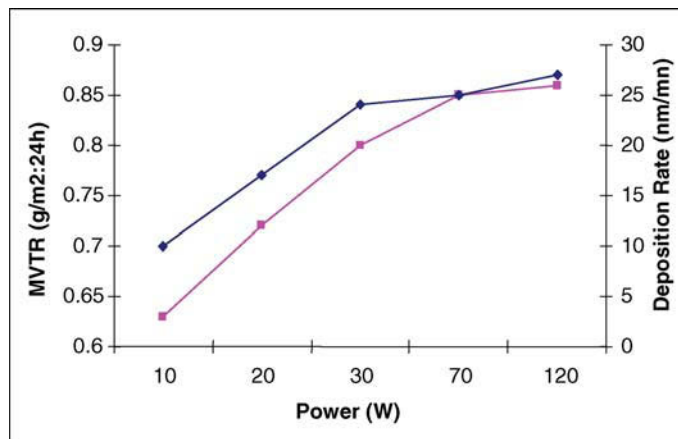


FIGURE 15-18 Changes in the moisture barrier (MVTR) and the rate of deposition according to the reactor's RF power, for a precursor composed of a mixture (N₂O/SiH₄) [32].

Figure 15-18 illustrates the increased deposition rate of an SiO_2 film obtained from a mixture of $(\text{N}_2\text{O}/\text{SiH}_4)$ as the precursor.

The decrease in the MVTR (moisture vapor transmission rate) is due to the polymer thin film and its very high internal stress level, resulting in the formation of defects such as pores, micro-holes and cracks. When power increases, the energy of the plasma generates a significant number of oxygen radicals [39]. The faster deposition rate does not leave atoms enough time to reach low energy sites; this in turn increases the level of etching and, consequently, the surface roughness. In this manner, increased power causes a drop in the moisture barrier (MVTR).

For another commonly used precursor such as the mixture HMDSO/ O_2 , the driving power may have another effect on barrier properties. Figure 15-19 illustrates how increased power improves the oxygen barrier. This Figure also shows that the concentration of silanol groups decreases at higher powers, resulting in better densification of the film. High energies lead to stronger ion bombardment and facilitate the formation of Si–O–Si bridges to the detriment of Si–OH [40].

This barrier property depends not only on the film's chemical nature and the power used during the process, but also on temperature and several other implementation parameters. For example, high substrate temperature generally leads to

greater mobility of the species at the surface during deposition, and if there is also pyrolysis of the film, this leads to a decreased rate of growth. However, in both cases polymer cross-linking is increased, which modifies the thin film's barrier properties. For a deposit obtained with the precursor HMDSO, the chemistry of SiO_2 and $\text{SiO}_x\text{C}_y\text{H}_z$ formation at low temperatures differs significantly from that observed at high temperatures. Si–O–Si bonds are dominant at high temperatures, favoring the formation of SiO_2 thin films. In contrast, at low temperatures the formation of Si–OH (silanol) dominates under certain conditions and a great number of these groups can be incorporated in the thin layer obtained, producing a more flexible film with diminished barrier properties [41–42].

Thermal stability is an important parameter to control. Temperature plays a direct role in film thickness; generally, a drop in thickness is observed from a certain temperature, representing the film's stability limit.

Thus to obtain excellent barrier properties, the deposition thickness and the structure (chemical and physical) of the thin film must be perfectly controlled. The limitation of high barrier values, between 0.1 and 0.5 $\text{cc}/\text{m}^2 \cdot \text{d} \cdot \text{atm}$ in the literature, can be explained by these various defects. The general permeation behavior of a polymer thin film system according to its thickness is

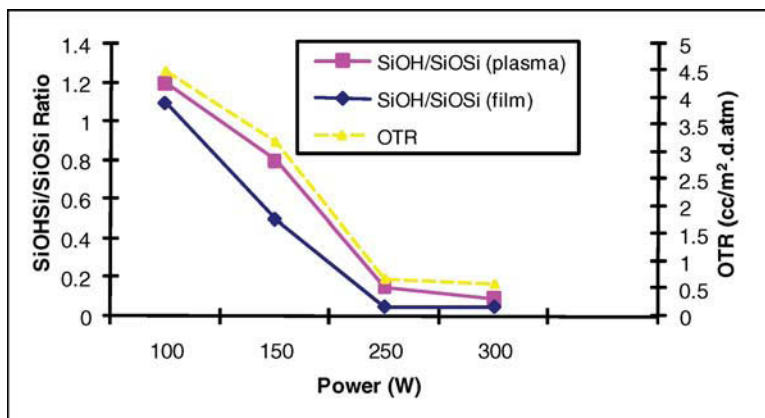


FIGURE 15-19 Changes in the oxygen barrier (OTR: oxygen transmission rate) and silanol groups, measured in the plasma and on the film according to the reactor's RF power [40].

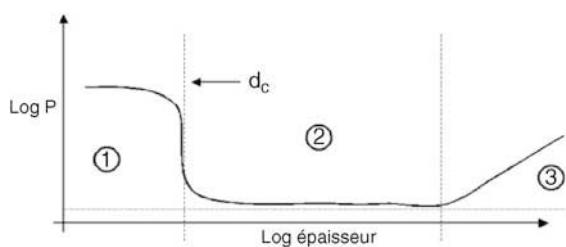


FIGURE 15-20 Variation in the permeability of the film-polymer system according to the thickness of the barrier film.

schematically illustrated in Figure 15-20. It can be divided into three distinct phases.

Phase 1. Until the thickness of the barrier film reaches a critical value (d_c) commonly expressed as d_c , there is practically no barrier effect. This is particularly problematic in certain cases where d_c may reach several nanometers. The value of d_c varies strongly, depending on the type of film deposited and the type of polymer substrate. For example, in the case of PECVD SiO_x on PET using radio frequency this value is 12 nm, whereas for PECVD SiN it does not exceed 8 nm [39].

The following explanation has been proposed for this phenomenon: the substrate is initially coated with patches of material, which coalesce at d_c . In other words, a uniform layer would only be present at this precise time, explaining the drastic drop in P once d_c is reached.

Phase 2. In this phase, permeability decreases slightly until reaching an asymptotic value that remains non-zero, even though the oxides used as barrier films are impermeable at high molecu-

lar weights. A.S. da Silva et al. [39] systematically and statistically demonstrated the presence of defects in PECVD SiO_x coatings on PET [44]. They arrived at the conclusion that a film's barrier performance is strongly correlated to the number of defects, n , it contains (Fig. 15-21), thus proving that performance limits can be explained by the simple presence of holes in the film and the substrate. These defects can have various causes: e.g. coating defect due to an anti-blocking agent in the substrate; coating defect due to the presence of a dust particle on the substrate surface during deposition.

Phase 3. If the film's thickness becomes too great, the barrier effect disappears and permeability increases exponentially. This phenomenon is usually attributed to the mechanical strain present within films. When film thickness is too great, the relaxation of this strain is not plastic; the film then becomes brittle and breaks. Permeant gases rapidly flow through the resulting holes. The thickness at which these breaks appear depends on the substrate, the type of barrier film and the deposition method. For a system of PECVD SiO_x on PET, this thickness is around 200 nm.

Research in the area of thin barrier films is focusing more and more on developing super barriers whose oxygen permeation must not exceed $5 \cdot 10^{-3} \text{ cc/m}^2 \cdot \text{d} \cdot \text{atm}$. Recently, J. Affino [45] proposed a very strong barrier ($< 10^{-5} \text{ cc/m}^2/\text{d}$) based on the concept of a multi-layer organic/inorganic structure obtained using PECVD. This concept of

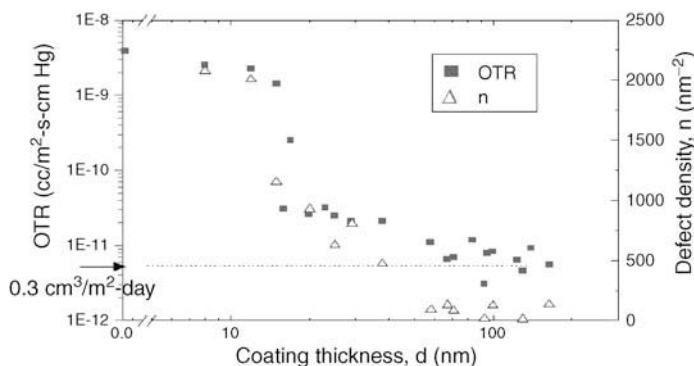


FIGURE 15-21 Correlation between OTR and the number of defects, n , in a PECVD SiO_x film on PET [45].

a series of nano-layers is receiving increasing attention and support [46]. A structure with three layers is often proposed [47]: the first polymer layer acts to reduce the surface roughness of the substrate, the second acts as a barrier and the third serves to protect this barrier layer.

These various examples show that it is difficult to draw a single conclusion on how to control barrier properties. These characteristics are strongly dependent on the precursor type and the PECVD parameters used during the implementation process.

Example: Surface Properties. Even though the surface properties of the polymer thin film obtained using PECVD depend on process parameters, they are very strongly tied to the chemical nature of the precursor used. Low surface energy is obtained with fluorinated precursors, or with mixtures containing perfluorohydrocarbons or silanes. Surface energy for a hydrocarbon thin film is generally higher than that of a standard hydrocarbon polymer because carboxylic groups often appear at the surface during the deposition process. In contrast, it is more difficult to prepare a very high energy surface using the plasma process than a low energy surface. The reason is that organic precursors, which can be used to make very hydrophilic thin films, have very high evaporation temperatures due to their high polarity molecules and are thus difficult to use as precursors. Those with oxide groups lose a very significant portion of these functional groups during plasma polymerization.

In the literature, several strategies have been employed to obtain super-hydrophobic surfaces. Washo describes contact angles close to 170° with PTFE deposited under process conditions (high temperature, high power) leading to the formation of powders. Another approach is to deposit PTFE and use plasma etching to structure the surface so as to obtain a contact angle very close to 170° . A great deal of research is currently underway on the PECVD process conditions necessary to obtain these very hydrophobic films all while structuring the surface [48].

Note that these PECVD deposits can be carried out in a localized manner using a masking technique. Figure 15-22 shows a surface that has undergone both hydrophobic and hydrophilic treatments [30].

These different localized treatments are very important for applications in biology and microfluidics.

The material in contact with physiological substances such as blood or cells has chemical properties that influence the organization of the protein layer, which is adsorbed at the liquid/material interface within a few seconds of contact [48]. A good strategy for controlling the morphology and physiology of cells in contact with a biomaterial is to control the adsorption of proteins at its surface. Many applications such as diagnostic tools, implants, etc., call for substrates which are very or totally repulsive with regard to proteins or cells. Deposition techniques have been proposed to obtain polyoxymethylene

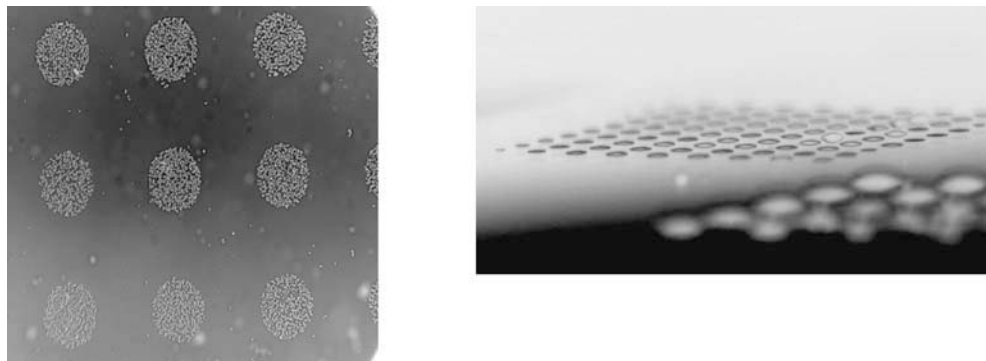


FIGURE 15-22 Localized hydrophobic and hydrophilic deposits obtained by PECVD with a masking technique.

thin films [49], which may offer anti-adhesive properties in relation to cells.

Structured by multiple layers, texturing or by the addition of nano-fillers, these new-generation polymer thin films are currently being developed and will give plastic, paper and steel substrates high performance properties.

Summary on Vacuum-deposited Coatings

Polymer thin films obtained by PECVD have a great deal of relevance for various industrial applications today, mainly due to their lower cost. Moreover, their structure is now very well controlled. This has given rise to systems with excellent new chemical and physical characteristics, such as barrier, friction and hydrophobic properties, etc.

The chemical nature of the precursors and their chemical reaction mechanisms are two significant factors in the vapor-phase deposition process which in turn affect reactor architecture.

Process parameters strongly influence the PECVD process. These parameters, including power, temperature and pressure, allow modifications to film structure that can be controlled. The resulting properties can be very powerful. Numerous studies have been conducted on how to apply the final materials.

The application areas include packaging, with a focus on high barrier films, as well as steel, where the accent is on corrosion protection or adding properties such as high surface energy. A large number of emerging applications are also incorporating such films. Uses include biological, physical and chemical sensors along with electronic, molecular and non-linear optical systems. Despite multiple studies in this area, these materials have only been successfully used for a small number of electronics and optical applications. This is primarily due to the low thermal and chemical stability of thin films as well as their weak mechanical solidity. Hence the relevance of creating high quality polymer thin films for a broad range of technological applications. The next generation of organic flat screens requires drastic encapsulation of their systems, which in

turn necessitates jumping at least three to four orders of magnitude in barrier efficiency compared to the requirements of traditional industries such as packaging.

Today these thin films and the associated processes are used for the electronics market. Certain micro-electronics manufacturers, such as Applied Materials, are trying to push these processes to their limits, but when production of 65 nm transistors starts, they may no longer be satisfactory. A competing technology known as ALD (Atomic Layer chemical vapor Deposition) seems very promising. For example, it should be possible to deposit 2 nm barrier films using ALD. Another emerging technology, electrografting, will be a competitor as well. Electrografting is an electrochemical technique. The chemical species present in a liquid bath migrate between an electrode and the part to be coated. Deposition is controlled through the electrical conditions.

CONCLUSIONS

There are various processes for producing polymer thin films, but whatever the deposition process (extrusion coating, wet or dry methods), the properties of the resulting film will depend strongly on the chemical nature of the polymer used. However, the numerous interactions between the process and material parameters significantly influence the final properties. Also it is very important to control the process parameters for maximum optimization of the target properties.

With control of these processes becoming more and more developed, films with an increasingly fine structure can be obtained (e.g. nanometric scale for PECVD). This in turn produces properties with very high performance.

The resulting thin films are used by traditional industries such as packaging and steel, but because there is enormous progress in the area of structure and properties, new emerging markets are focusing on the latest generation of polymer films. There are new products in optics, electronics, batteries and micro-sources for which precision, multiple layers and much localized

deposition with micro-structures and texturing are required to attain the desired properties.

REFERENCES

- [1] D. Briggs, D. Brewis, M.B. Koniecko, X-ray photoelectron spectroscopy studies of polyethylene-aluminium laminates, *European Polymer J.* 14 (1) (1978) 1–4.
- [2] L. Ulren, T.J. Hjertberg, *The Journal of Adhesion* 31 (2–4) (1990) 117–136.
- [3] A. Strålin, T.J. Hjertberg, Adhesion between LDPE and hydrated aluminium in extrusion-coated laminates, *J. of Adhesion Science and Technology* 7 (11) (1993) 1211–1229.
- [4] B. Fillon, Optimisation of aluminum/polyethylene adhesion with extrusion coating process, *Polyethylene Maaack Business Conference*, Zurich (1995).
- [5] B. Morris, Prediction of polymer/metal adhesion, *Polymer Lamination & Coating Conf.*, Tappi Proc. 191 (1996).
- [6] J.M. Butruille, B. Fillon, J.R. Frier, Analysis of polyethylene/aluminium adhesion mechanism, *European Congress on Applied Surface and Interface Analysis*, Montreux (1997).
- [7] B. Brentley, Coating laminating PFFC, *Paper, Film & Foil Converter* Mar. 01 (2001).
- [8] B. Morris, Tappiconf, San Diego, Reducing curl in multilayer blown film, Part 1: Experimental results, model development and strategies, Part 2: Application of predictive modeling to barrier cereal line film, 2001 *Polymers Laminations & Coatings Conference Proceedings*, Technical Association of the Pulp and Paper Industry, 15 Technology Parkway South, Norcross, GA (2001) 112–113.
- [9] M. Schmitthenner, *European Coating J* 9 (1998) 618.
- [10] A. Glawe, Varnish deposition with various processes, *Kuntsoffe Conf.*, Coatema (2004).
- [11] Dr D. Urban, Dr K. Takamura (editors), *Polymer Dispersions and their Industrial Applications*, Wiley (2002).
- [12] H.H. Hull, The theoretical analysis and practical evaluation of roller ink distribution systems, *TAGA – Technical Association of the Graphic Arts* (1968) 228–315.
- [13] J. MacPhee, An engineer's analysis of the lithographic printing process, *TAGA – Technical Association of the Graphic Arts* (1979) 237–277.
- [14] D. Benjamin, J. Todd, L.E. Scriven, Fluid mechanics and transport phenomena multiple roll systems: steady-state operation, *AIChE J.* 41 (5) (1995) 1045–1060.
- [15] M. Owens, L.E. Scriven, C.W. Macosko, Technical session 5 – Coating technology rheology and process control minimizes misting, 12th International Coating Science and Technology Symposium, Rochester, New York (2004).
- [16] D. Benjamin, M.S. Carvalho, T.J. Anderson, Forward roll film-splitting: theory and experiment, in *TAPPI Proceedings, 1994 TAPPI Coating Conference*, May 1–5, 1994, San Diego, 109, California (1994).
- [17] D.W. Bousfield, P. Salminen, R. Urscheler, J.A. Roper III, Wetting line in high-speed free jet coating, 1999 *Coating Conference Proceedings*, Proc. TAPPI Coating Conference, TAPPI Press, Atlanta, GA (1999), 129–143.
- [18] D.J. Coyle, The fluid mechanics of roll coating: steady flows, stability and rheology, PhD thesis, University of Minnesota, Minneapolis, MN (1984).
- [19] S. Spadafora, H. Leidheiser, Jr., Water disbondment characterization of polymer coating/metal substrate systems, *JOCCA* 71 (9) (Sept. 1988) 276–285.
- [20] H. Leidheiser, W. Funke, Water disbondment and wet adhesion of organic coatings on metals: a review and interpretation, *JOCCA* 70 (5) (1987) 121–132.
- [21] T. Schuman, M. Wilström, M. Rigdahl, Coating of surface-modified papers with poly(vinyl alcohol), *Surface and Coatings Technology* 183 (1) (2004) 96–105.
- [22] T. Schuman, M. Wikström, M. Rigdahl, The effect of hot calendaring of the substrate on the barrier properties of poly(vinyl alcohol)-coated papers, *Nordic Pulp & Paper Research J.* 18 (1) (2003) 81–89.
- [23] D. Burgentzle, J. Duchet, B. Fillon, A. Jupin, J.F. Gerard, Role of clay/solvent interactions for nanocomposite varnishes formulations, *INSA Lyon, Cebal (France)*(2003).
- [24] D. Burgentzle, J. Duchet, J.F. Gérard, B. Fillon, A. Jupin, Study of clay/solvent interactions for varnish formulations, *Laboratoire des Matériaux Macromoléculaires, Institut National Des, Sciences Appliquées de Lyon, Villeurbanne, University of Alicante, France* (2003).
- [25] H. Biederman, D. Slavinska, Plasma polymer films and their future prospects, *Surface and Coatings Technology* 125 (1–3) (2000) 371–376.
- [26] B. Held, *Physique des plasmas froids*, Masson, Paris (1994).
- [27] H. Yasuda, *Plasma Polymerisation*, Academic Press, New York (1985).
- [28] H. Biedermann, (Ed.), *Plasma Polymer Films* Imperial College Press, London (2004).
- [29] R. D'Agostino, *Plasma Deposition, Treatment and Etching of Polymers*, Academic Press (1990).
- [30] B. Fillon, Polymer very thin film deposition, *Hanst-007 Conference, Besançon* (2007).
- [31] N. Morosoff, R. D'Agostino, *Plasma Deposition, Treatment and Etching of Polymers*, Academic Press (1990).

- [32] D.S. Wu, W.C. Lo, L.S. Chang, Properties of SiO₂-like barrier layers on polyethersulfone substrates by low-temperature plasma-enhanced chemical vapor deposition, *Thin Solid Films* 468 (1–2) (2004) 105–108.
- [33] M. Creatore, F. Palumbo, R. D'Agostino, IUPAC, Diagnostics and insights on PECVD for gas-barrier coatings, *Pure and Applied Chemistry* 74 (3) (2002) 407–411.
- [34] S. Sahli, S. Rebiai, P. Raynaud, I. Segui, Y. Segui, R. Wertheimer, Deposition of SiO₂-like films by HMDSN/O₂ plasmas at low pressure in a MMP-DECR reactor, *Plasmas and Polymers* 7 (4) (Dec. 2002) 327–340.
- [35] Y. Wu, H. Sugimura, Y. Ionue, O. Takai, Preparation of hard and ultra water-repellent silicon oxide films by microwave plasma-enhanced CVD at low substrate temperatures, *Thin Solid Films* 435 (1–2) (2003) 161–164.
- [36] E. Sardella, R. Gristina, S. Senesi, R. D'Agostino, P. Favia, Homogeneous and micro-patterned plasma-deposited PEO-like coatings for biomedical surfaces, *Plasma Processes and Polymers* 1 (1) (2004) 63–72.
- [37] K. Takahashi, A. Itoh, T. Nakamura, K. Tachibara, Radical kinetics for polymer film deposition in fluorocarbon (C₄F₈, C₃F₆ and C₅F₈) plasmas, *Thin Solid Films* 374 (2) (2000) 303–310.
- [38] T. Shirafuji, A. Kamisawa, T. Shimasaki, Y. Hayashi, Plasma enhanced chemical vapor deposition of thermally stable and low-dielectric-constant fluorinated amorphous carbon films using low-global-warming-potential gas C₅F₈, *Thin Solid Films* 374 (2) (2000) 256–261.
- [39] A.S. da Silva Sobrinho, M. Latrèche, G. Czeremuskin, J.E. Klemberg-Sapieha, M.R. Wertheimer, Transparent barrier coatings on polyethylene terephthalate by single- and dual-frequency plasma-enhanced chemical vapor deposition, *J. of Vacuum Science & Technology A: Vacuum, Surfaces, and Films* 16 (6) (1998) 3190–3198.
- [40] M. Creatore, F. Palumbo, R. D'Agostino, Deposition of SiO_x films from hexamethyldisiloxane/oxygen radiofrequency glow discharges: process optimization by plasma diagnostics, *Plasmas and Polymers* 7 (3) (2002) 291–310.
- [41] C. Lasorsa, P.J. Morando, A. Rodrigo, Effects of the plasma oxygen concentration on the formation of SiO_xC_y films by low temperature PECVD, *Surface and Coatings Technology* 194 (1, 20) (2005) 42–47.
- [42] N. Selamoglu, J. Mucha, D. Ibbotson, D. Flamm, Silicon oxide deposition from tetraethoxysilane in a radio frequency downstream reactor: mechanisms and step coverage, *J. of Vacuum Science & Technology B: Microelectronics and Nanometer Structures* 7 (6) (1989) 1345–1351.
- [43] H. Chatham, Oxygen diffusion barrier properties of transparent oxide coatings on polymeric substrates, *Surface and Coatings Technology* 78 (1996) 1–9.
- [44] A. Da Silva Sobrinho, M. Latrèche, G. Czeremuskin, G. Denler, M.R. Wertheimer, A study of defects in ultra-thin transparent coatings on polymers, *Surface and Coatings Technology* 116–119 (1999) 1204–1210.
- [45] A.S. da Silva Sobrinho, G. Czeremuskin, M. Latrèche, M.R. Wertheimer, Defect-permeation correlation for ultrathin transparent barrier coatings on polymers, *Journal of Vacuum Science & Technology A: Vacuum, Surfaces, and Films* 18 (1) (2000) 149–157.
- [46] J.D. Affinito, G.L. Graff, M.E. Gross, M.G. Hall, E.S. Mast, and M.K. Shi, Environmental barrier material for organic light emitting device and method of making, US Patent 6,522,067 (2003).
- [47] J.D. Affinito, M.E. Gross, C.A. Coronado, G.L. Graff, E.N. Greenwell, P.M. Martin, A new method for fabricating transparent barrier layers, *Thin Solid Films* 2 (290–291) (1996) 63–67.
- [48] G. Cicala, A. Milella, F. Palumbo, P. Rossini, P. Favia, R. D'Agostino, Morphological and structural study of plasma deposited fluorocarbon films at different thicknesses, *Diamond and Related Materials* 12 (10–11) (2003) 2020–2025.
- [49] H.J. Griesser, C.R. Chatelier, T.R. Gengenbach, G. Johnson, J.G. Steele, Growth of human cells on plasma polymers: Putative role of amine and amide groups, *Journal of Biomaterials Science, Polymer Edition* 5 (6) (1994) 531–554.

Micro-/Nano-Fibers by Electrospinning Technology: Processing, Properties and Applications

Ioannis S. Chronakis

INTRODUCTION

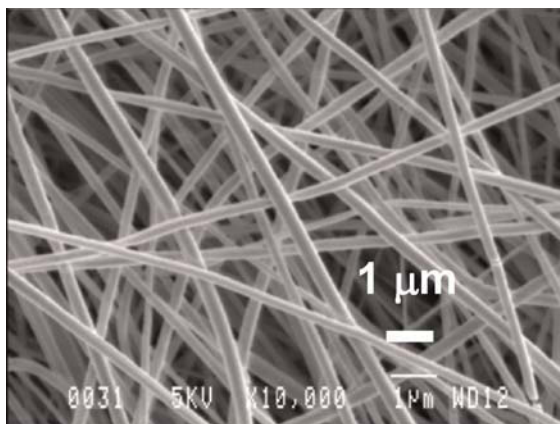
Human beings have used fibers for centuries. In 5000 BC, our ancestors used natural fibers such as wool, cotton silk and animal fur for clothing. Mass production of fibers dates back to the early stages of the industrial revolution. The first man-made fiber – viscose – was presented in 1889 at the World Exhibition in Paris. Developments in the polymer and chemical industries – as well as in electronics and mechanics – have led to the introduction of new types of man-made fibers, especially the first synthetic fibers, such as nylon, polypropylene and polyester. The needs and further progress allowed the production of high functionality fibers (antistatic, flame resistant, etc.) and high performance fibers (carbon fibers in 1960 from viscose and aramid fibers in 1965) that showed high strength, a high modulus and great heat resistance. These fibers are used not only in clothing but also in hygienic products, in medical and automotive applications, in geo-textiles and in other applications.

Traditional methods for polymer fiber production include melt spinning, dry spinning, wet spinning and gel-state spinning. These methods rely on mechanical forces to produce fibers by extrud-

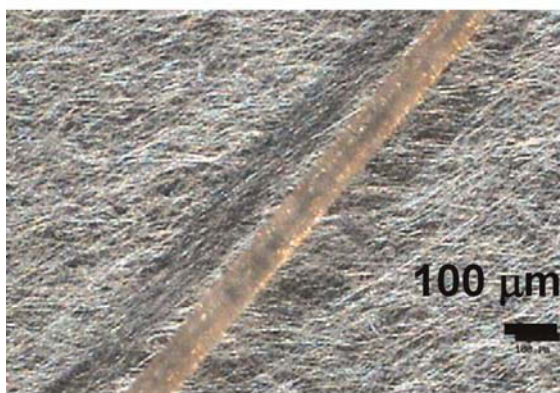
ing a polymer melt or solution through a spinneret and subsequently drawing the resulting filaments as they solidify or coagulate. These methods allow the production of fiber diameters typically in the range of 5 to 500 microns. At variance, *electrospinning technology* allows the production of fibers of much smaller dimensions. The fibers are produced by using an electrostatic field [1].

Electrospinning is a fiber-spinning technology used to produce long, three-dimensional, ultra-fine fibers with diameters in the range of a few nanometers to a few microns (more typically 100 nm to 1 micron) and lengths up to kilometers (Fig. 16-1). When used in products, the unique properties of nano-fibers are utilized, such as extraordinarily high surface area per unit mass, very high porosity, tunable pore size, tunable surface properties, layer thinness, high permeability, low basic weight, ability to retain electrostatic charges and cost effectiveness, among others [2].

While electrospinning technology was developed and patented by Formhals [3] in the 1930s, it was only about fifteen years ago that actual developments were triggered by Reneker and co-workers [4].



(a)



(b)

FIGURE 16-1 (a) SEM image of poly(ethylene terephthalate) (PET) nano-fiber web. The nano-fibers were electrospun from a PET solution in THF:DMF. The diameter of the fibers is about 200 nm. (b) PET nano-fiber web – comparison with human hair [1].

Interest today is greater than ever and this cost-effective technique has made its way into several scientific areas, such as biomedicine, filtration, electronics, sensors, catalysis and composites [5,6]. Electrospinning is a continuous technique and is hence suitable for high volume production of nano-fibers. The ability to customize micro-/nano-fibers to meet the requirements of specific applications gives electrospinning an advantage over other, larger-scale, micro-/nano-production methods. Carbon and ceramic nano-fibers made of polymeric precursors further expand the list of possible uses of electrospun nano-fibers [7].

WORKING PRINCIPLE AND CONFIGURATION OF ELECTROSPINNING PROCESSING

Electrospinning is increasingly being used to produce ultra-thin fibers from a wide range of polymer materials. This non-mechanical, electrostatic technique involves the use of a high voltage electrostatic field to charge the surface of a polymer-solution droplet, thereby inducing the ejection of a liquid jet through a spinneret (Fig. 16-2). In a typical process, an electrical potential is applied between a droplet of a polymer solution held at the end of a capillary tube and a grounded target. When the electric field that is applied overcomes the surface tension of the droplet, a charged jet of polymer solution is ejected. On the way to the collector, the jet will be subjected to forces that allow it to stretch immensely. Simultaneously, the jet will partially or fully solidify through solvent evaporation or cooling, and an electrically charged fiber will remain, which can be directed or accelerated by electrical forces and then collected in sheets or other useful shapes.

A characteristic feature of the electrospinning process is the extremely rapid formation of the nano-fiber structure, which occurs on a millisecond scale. Other notable features of electrospinning are a huge material elongation rate of the order of 1000 s^{-1} and a reduction of the cross-sectional area of the order of 10^5 to 10^6 , which have been shown to affect the orientation of the structural elements in the fiber.

The Electrospinning Mechanism

In spite of the simple set-up for electrospinning, the actual spinning mechanism is quite complex. Although extensive studies have been conducted to explore the mechanism, some aspects and phenomena are not yet fully understood.

Formation of the Taylor Cone and Subsequent Fluid Jet. When the high voltage field is applied, the droplet of polymer solution at the tip of the needle will become highly electrified and the charges induced will be evenly distributed over the polymer solution surface. The droplet will

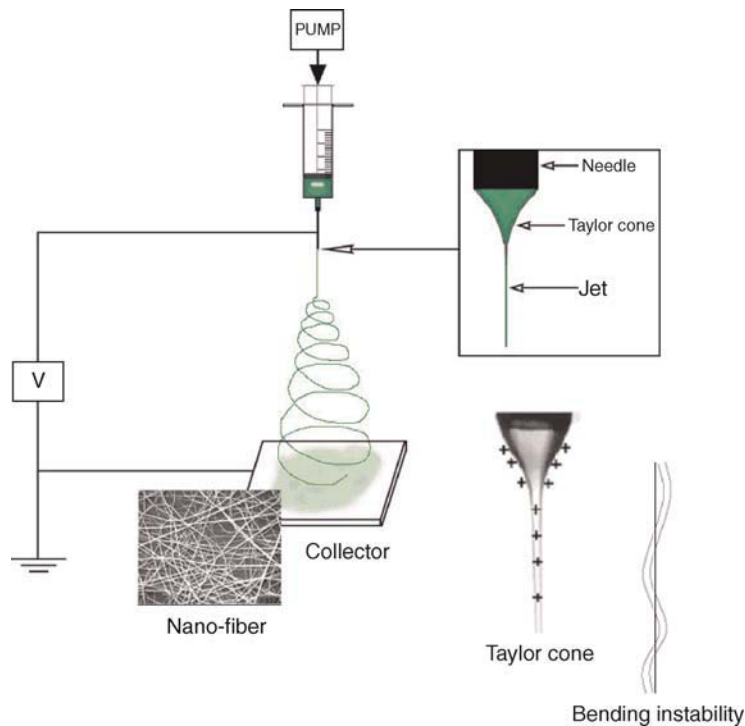


FIGURE 16-2 Schematic illustration of the conventional set-up for electrospinning. The insets show a drawing of the electrified Taylor cone, bending instability and a typical SEM image of the non-woven mat of PET nano-fibers deposited on the collector. The bending instability is a transversal vibration of the electrospinning jet. It is enhanced by electrostatic repulsion and suppressed by surface tension.

experience two types of electrostatic forces: electrostatic repulsion between the charges on the surface and Coulombic forces in the external field. Under the influence of these two forces, the droplet will be elongated and finally distorted into a so-called Taylor cone. As the voltage increases, the electrostatic forces will become stronger and eventually overcome the surface tension, and a charged jet of fluid will be ejected.

Both electrostatic and fluid dynamic instabilities can contribute to the basic operation of the process.

Reznik et al. [8] experimentally and numerically studied the shape evolution of small droplets attached to a conducting surface that was subjected to relatively strong electric fields. Three different scenarios of droplet shape evolution are distinguished, based on numerical solution of the Stokes equations for perfectly conducting droplets:

1. In sufficiently weak (subcritical) electric fields, the droplets are stretched by the electric Maxwell stresses and acquire steady-state shapes where equilibrium is achieved by means of surface tension.
2. In stronger (supercritical) electric fields the Maxwell stresses overcome the surface tension, and jetting is initiated from the droplet tip if the static (initial) contact angle of the droplet with the conducting electrode is $\alpha_s < 0.8\pi$; in this case, the jet base acquires a quasi-steady, nearly conical, shape with a vertical semi-angle of $\beta \leq 30^\circ$, which is significantly smaller than that of the Taylor cone ($\beta_T = 49.3^\circ$).
3. In supercritical electric fields acting on droplets with a contact angle in the range $0.8\pi < \alpha_s < \pi$, there is no jetting and almost the whole droplet jumps off: this is similar to gravity or drop-on-demand dripping.

The droplet-jet transitional region and the jet region proper are studied in detail for the second case using quasi-one-dimensional equations, taking into account the inertial effects and additional features such as the dielectric properties of the liquid (leaky dielectrics). The flow in the transitional and jet region is matched to that in the droplet. This is used to predict the current–voltage characteristic, $I = I(U)$, and the volumetric flow rate, Q , in electrospun viscous jets, given the potential difference applied. The predicted dependence, $I = I(U)$, is nonlinear due to the convective mechanism of the charge redistribution superimposed on the conductive (ohmic) mechanism. Realistic current values $I = O(10^2 \text{ nA})$ have been predicted for $U = O(10 \text{ kV})$ and fluid conductivity $\sigma = 10^{-4} \text{ Sm}^{-1}$.

Thinning of the Fluid Jet. Beyond the conical base, immediately at the end of the capillary tip, the jet continues to become thinner. This jetting mode is known as the electrohydrodynamic cone jet. The jet will initially travel in a straight line towards the collector but will eventually become unstable. To the naked eye, it looks like the jet splits into multiple jets and it was thought before 1999 that this was the main reason for the small diameter of the electrospun fibers. However, when the jet is examined with a high speed camera, it can clearly be seen that the splaying is actually one single fiber rapidly bending or whipping, causing the fiber to make lateral excursions that grow into spiraling loops.

Jet splitting does occur, but it is not as common as previously thought and it is not the dominant process that occurs during spinning. Bending or whipping is caused by a phenomenon called *bending instability* and can occur in electrified fluid jets. Every loop then grows larger in diameter and the jet becomes thinner. New bending instabilities arise when the jet is thin enough and enough stress relaxation of the viscoelastic stress has taken place. This is called the second instability region and is very similar to the first instability region but acts on a much smaller scale. A tertiary-bending instability has also been documented. Each cycle of

bending instability can be described in three steps:

1. A smooth, straight or slightly curved segment starts to bend.
2. The segment of the jet in each bend elongates and a spiral of growing loops develops.
3. As the perimeter of the loops increases, the diameter of the jet decreases. When the perimeter of the loop is large enough and the diameter of the jet is small enough, the conditions of the first step of the cycle are fulfilled. The next cycle of bending instability then begins.

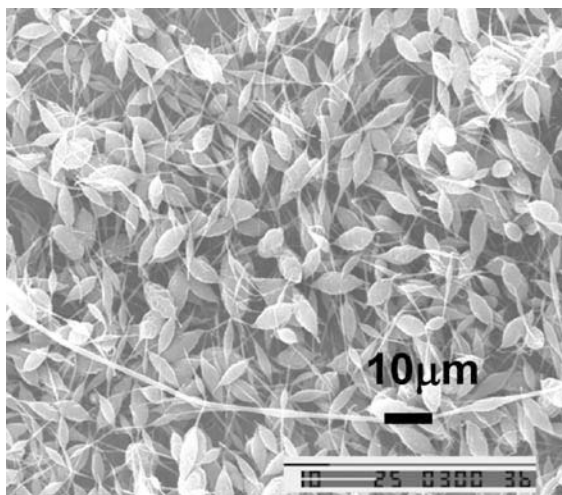
Several research groups have attempted to explain the bending instability by mathematical models.

ELECTROSPINNING PROCESSING PARAMETERS – CONTROL OF THE MICRO-NANO-FIBER MORPHOLOGY

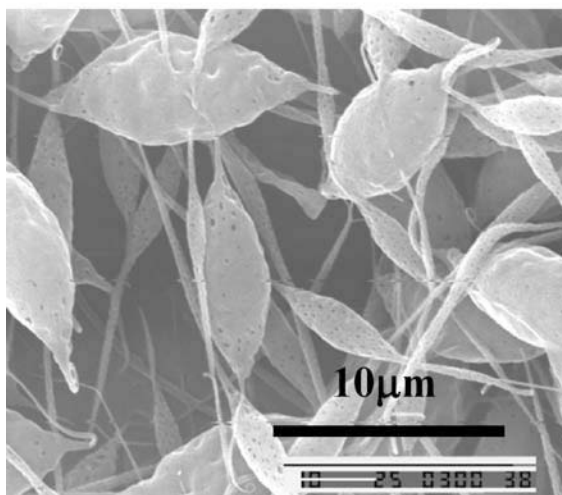
The fiber morphology has been shown to be dependent on process parameters, namely solution properties (system parameters), process conditions (operational parameters) and ambient conditions [1,2].

Solution Properties

Solution properties are those such as molecular weight, molecular weight distribution and architecture of the polymer, and properties such as viscosity, conductivity, dielectric constant and surface tension. The polymer solution must have a concentration high enough to cause polymer entanglements, yet not so high that the viscosity prevents polymer motion induced by the electric field. The resulting fibers' diameters usually increase with the concentration of the solution according to a power law relationship. Decreasing the polymer concentration in the solution produces thinner fibers. Decreasing the concentration below a threshold value causes the uniform fiber morphology to change into beads [9]. The main factors affecting the formation of beads (Fig. 16-3) during electrospinning have been shown to be solution viscosity, surface tension



(a)



(b)

FIGURE 16-3 Example of bead formation during electrospinning: SEM micrographs of poly(propyl carbonate) (PPC) beads prepared by electrospinning a PPC solution in dichloromethane [9].

and the net charge density carried by the electrospinning jet. Higher surface tension results in a greater number of bead structures, in contrast to the parameters of viscosity and net charge density, for which higher values favor fibers with fewer beads. This reduction in thickness is due to the solution conductivity, which reflects the charge density of the jet and thus the elongation level. The surface tension also controls the distribution

and the width of the fibers, which can be decreased by adding a surfactant to the solution. Adding a surfactant or a salt to the solution is a way of increasing the net charge density and thus reducing the formation of beads. Finally, the choice of solvent(s) directly affects all of the properties mentioned and is of major importance to the fiber morphology.

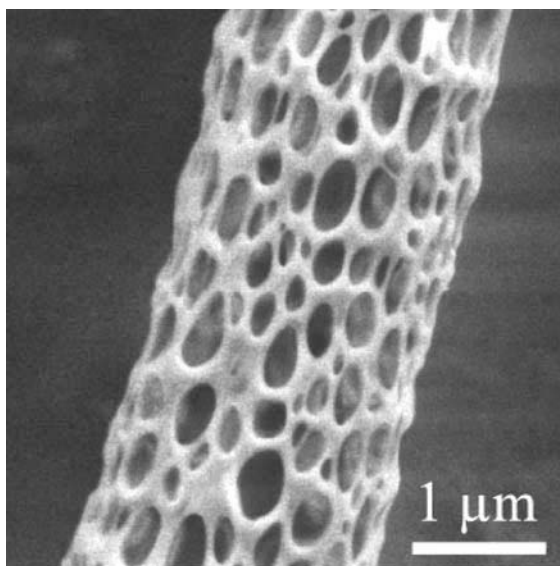
Process Conditions

The parameters in the process are spinning voltage, distance between the tip of the capillary and the collector, solution flow rate (feed rate), needle diameter and, finally, the motion of the target screen. Voltage and feed rate show different tendencies and are less effective in controlling fiber morphology as compared to the solution properties. Too high a voltage might result in splaying and irregularities in the fibers. A bead structure is evident when the voltage is either too low or too high. However, a higher voltage also leads to a higher evaporation rate of the solvent, which in turn might lead to solidification at the tip and instability in the jet. Morphological changes in the nanofibers can also occur upon changing the distance between the syringe needle and the substrate. Increasing the distance or decreasing the electrical field decreases the bead density, regardless of the concentration of the polymer in the solution.

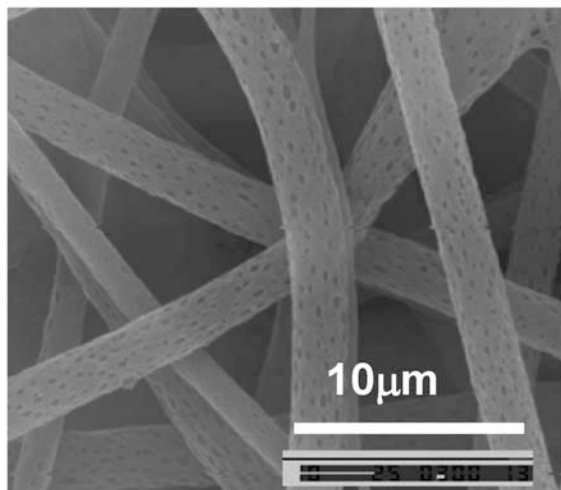
Ambient Conditions

Ambient conditions include factors such as humidity and temperature, air velocity in the spinning chamber and atmospheric pressure. Humidity primarily controls the formation of pores on the surface of the fibers. Above a certain threshold level of humidity, pores begin to appear and, as the level increases, so does the number and size of the pores.

The precise mechanism behind the formation of pores and texturing on the surface is complex and is thought to be dependent on a combination of breath figure formation and phase separation. Breath figures are imprints formed due to the evaporative cooling during evaporation of the



(a)



(b)

FIGURE 16-4 SEM images of (a) porous poly(L-lactide) (PLA) nano-fibers prepared by electrospinning a solution of PLA in dichloromethane [5]. (b) Poly(propyl carbonate) (PPC) nano-fibers with a porous surface electrospun from a PPC solution in dichloromethane [9].

solvent, which results in condensed solvent drops on the surface and, later, pores. Surface porosity (Fig. 16-4) can also be achieved by selective removal of one of the components in the polymer blend after spinning. The pores formed on the fiber surface can be used, for example,

to capture nano-particles, act as a cradle for enzymes or increase the surface area for filtration applications.

Baumgarten studied the spinning velocities in addition to the effect of the flow rate, voltage, gap and the surrounding atmosphere [10]. He was able to determine the spinning velocity using the power balance:

$$IV = \frac{\dot{m}_s \dot{V}_s^2}{2} \quad (1)$$

where V is the potential, I is the current and \dot{m}_s and \dot{V}_s are the mass flow rate and the spinning velocities, respectively. The calculation showed velocities close to the velocity of sound in air. Other researchers calculated velocities of the fibers reaching the collector to be 140 to 160 m/s. Obviously, these speeds must depend on the process parameters and solution used.

Increasing the solution temperature is also a method for speeding up the process, but it might cause morphological imperfections, such as the formation of beads. Furthermore, the regulation of scale and bifurcation-like instability in electrospinning are intriguing problems that remain to be solved. Regulatory mechanisms for controlling the radius of electrospun fibers at the different states are clearly illustrated in the work by He et al. [11].

ELECTROSPINNING SET-UPS AND TOOLS

Novel Set-ups

The traditional set-up for electrospinning has been modified in a number of ways during the last few years in order to be able to control the electrospinning process and tailor the structure of micro-nano-fibers.

Yarin and Zussman achieved upward electrospinning of fibers from multiple jets without the use of nozzles; instead using the spiking effect of a magnetic liquid [12]. The concept (Fig. 16-5) consists of a bath filled with a layer of magnetic liquid (a). This liquid is covered by the solution to be spun (b). An electrode is submerged into the

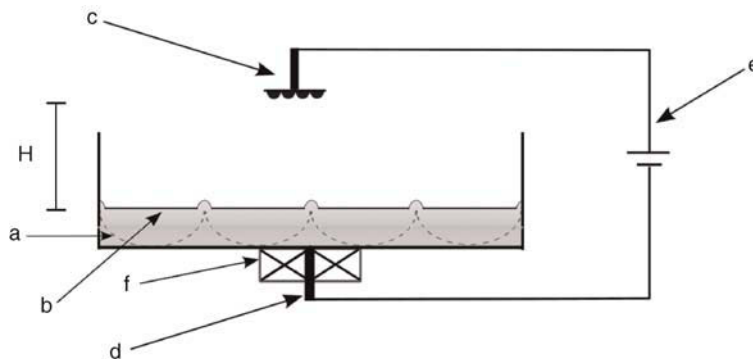


FIGURE 16-5 Schematic representation of the upward electrospinning set-up [12].

magnetic fluid (d). A counter-electrode (c) as a collector is placed a certain distance above this bath. A strong permanent magnet or electromagnet (f) is placed under the bath around the electrode. When a magnetic field is applied, the spiking effect causes some of the polymer solution to protrude into the electrical field applied between the electrodes (c and d). The protrusion is sufficient to initiate multiple jets of polymeric fibers traveling towards the collector. The production rate was reported to be about 12 times that of a conventional set-up. This approach also avoids clogging problems.

Using supercritical CO_2 -assisted electrospinning, polymer fibers of high molecular weight polydimethylsiloxane (PDMS) and poly(D,L-lactic acid) (PLA) were produced by means of only electrostatic forces and without the use of a liquid solvent. The fibers were formed between two electrodes in a high pressure view cell. This supported the idea that the supercritical CO_2 reduces the polymer viscosity sufficiently to allow fibers to be pulled electrostatically from an undissolved bulk polymer sample.

Electrospinning in a vacuum is also a novel set-up. Compared to electrospinning in air, a vacuum allows higher electric field strength over large distances and higher temperatures compared to what can be achieved in air, which influences both the spinning process and the morphology of the fibers that are produced. Other attempts have been made to incorporate vibration technology in polymer electrospinning. The idea is to produce finer

nano-fibers under lower applied voltage by vibration technology. Other electrospinning set-ups are discussed in a recent review by Teo and Ramakrishna [6].

Set-ups Involving Dual Syringes

A set-up was developed for electrospinning involving a dual syringe spinneret (Fig. 16-6). The development enables spinning highly functional nano-fibers such as hollow nano-fibers, nano-tubes and fibers with a core-shell structure [13]. A recent study describes the formation of hollow nano-tubular fibers in a single step using electrospinning and sol-gel chemistry. The method exploits electrohydrodynamic forces that form coaxial jets of liquids with microscopic dimensions. A high voltage is applied to a pair of concentric needles used to inject two immiscible liquids that lead to the formation of a two-component liquid cone that elongates into coaxial liquid jets and forms hollow nano-fibers.

Set-ups Controlling the Orientation and Alignment of Micro-nano-fibers

A number of set-ups that allow control over the orientation of fibers have been developed. The orientation is crucial for different applications of nano-fibers and opens new opportunities for manufacturing yarn, micro-nano-wire devices, etc. Most of the set-ups are based on rotating collection devices.

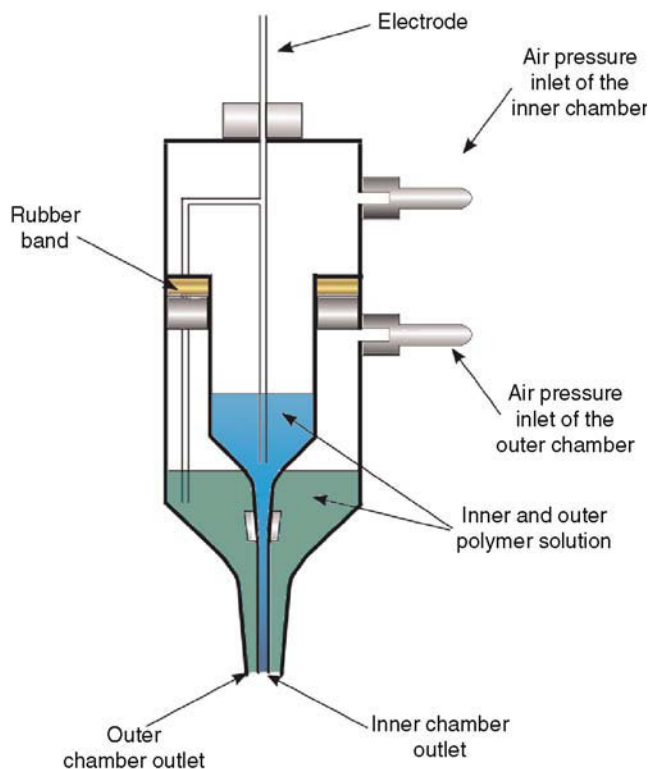


FIGURE 16-6 Schematic illustration of the set-up used to co-electrospin compound core-shell nano-fibers [13]. It involves the use of a spinneret consisting of two coaxial capillaries through which two polymer solutions can simultaneously be ejected to form a compound jet.

A technique called *dry rotary electrospinning* involves the organization and alignment of electrospun nano-fibers into planar assemblies [14]. The technique (Fig. 16-7) involves a rotating disc as a grounded collector that stretches the coils into aligned rings. The dry fibers in a ring shape can be collected into linear strands to form a nano-fibrous yarn.

Another method for controlled deposition of oriented nano-fibers uses a micro-fabricated scanned tip as an electrospinning source [15]. The tip is dipped in a polymer solution to gather a droplet as a source material. A voltage applied to the tip causes the formation of a Taylor cone and, at sufficiently high voltages, a polymer jet is extracted from the droplet. By moving the source relative to a surface, thus acting as a counter-electrode, oriented nano-fibers can be deposited

and integrated with micro-fabricated surface structures. This electrospinning technique is called a *scanned electrospinning nano-fiber deposition system*. In addition to achieving uniform fiber deposition, the scanning tip electrospinning source can produce self-assembled composite fibers of micro- and nano-particles aligned in a polymeric fiber.

Using a frame as a counter electrode also allows an oriented deposition of fibers [16]. The same effect can be accomplished by placing two electrodes parallel to each other that are separated by a void [17]. A modified method for electrospinning that generates uniaxially aligned arrays of nano-fibers over large areas has also been reported. A collector composed of two conductive strips separated by an insulating gap of variable width was used. Directed by electrostatic

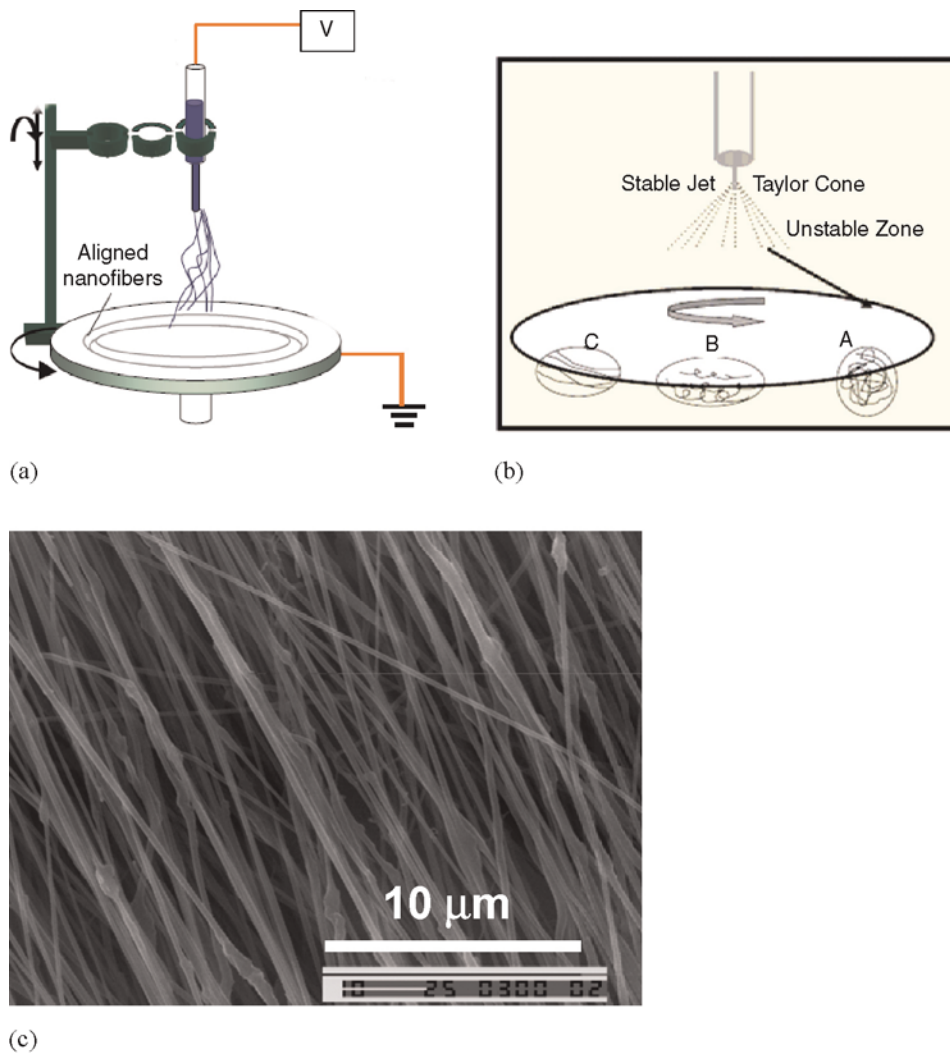


FIGURE 16-7 The rotary electrospinning apparatus: (a) schematic illustration of the set-up used for electrospinning nano-fibers as uniaxially aligned arrays. (b) Schematic illustration of the effect of the rotating speed on the formation of fibers [14]. (c) Aligned poly(vinylidene–Fluoride) (PVDF) nano-fibers (Chronakis et al., unpublished results).

interactions, the charged nano-fibers are stretched to span across the gap and become uniaxially aligned arrays. Two types of gaps were demonstrated: void gaps and gaps made of a highly insulating material. When a void gap was used, the nano-fibers could readily be transferred onto the surfaces of other substrates for various applications. When an insulating substrate was involved, the electrodes could be patterned into various designs on the solid insulator. In both cases, the

nano-fibers could be conveniently stacked into multi-layered architectures with controllable hierarchical structures.

Zussman et al. reported an approach to a hierarchical assembly of nano-fibers into cross-bar nano-structures [18]. The polymer nano-fibers are created through an electrospinning process with diameters in the range of 10–80 nm and lengths up to centimeters. When the electrostatic field and the polymer rheology of

the nano-fibers are controlled, they can be assembled into parallel periodic arrays. These authors also observed failure of nano-fibers owing to a multiple necking mechanism, sometimes followed by the development of a fibrillar structure, during electrospinning using a rotating tapered accumulating wheel (electrostatic lens). This phenomenon was attributed to a strong stretching of solidified nano-fibers by the wheel, if its rotation speed became too high. Necking has not been observed in the nano-fibers collected on a grounded plate.

Various other set-ups have been reported in the production of oriented, continuous nano-fibers such as using copper wires spaced evenly in the form of a circular drum as a collector and the use of a rotating wheel. In particular, the work by Theron and co-workers described an electrostatic field-assisted assembly technique that was combined with an electrospinning process used to position and align individual nano-fibers on a tapered and grounded wheel-like bobbin [19]. The bobbin is able to wind a continuous as-spun nano-fiber at its tip-like edge. The alignment approach resulted in nano-fibers with diameters ranging from 100–300 nm and lengths of up to hundreds of microns.

CHARACTERISTICS AND DESIGN CONSIDERATIONS OF ELECTROSPUN MICRO-NANO-FIBERS

Molecular Orientation

In traditional fiber spinning, the molecular orientation obtained by stretching the fibers after their formation is critical for their strength. The molecular orientation of electrospun fibers has also been a subject of various studies.

Dersch and co-workers studied the intrinsic structure of polyamide (nylon 6) and PLA electrospun fibers [16]. They found that the fibers do not differ a great deal from as-spun thicker fibers obtained by melt spinning and showed rather disordered crystals and different degrees of crystal orientations. The orientation seems to be almost

absent in the PLA fibers and to be locally strong, yet inhomogeneous, in the polyamide fibers. However, stretching the PLA fibers did lead to an increased orientation of the crystals along the fibers' axis. On the other hand, the electrospinning of polyethylene oxide (PEO), for example, causes some molecular orientation but a poorly developed crystalline micro-structure.

Collecting electrospun fibers onto a high speed rotating drum can enhance the molecular orientation up to an optimal speed, after which the orientation can decrease slightly [20]. In the report of a study using a high speed winder, it was suggested that a critical winding speed exists that just matches the 'natural' velocity of the fiber (due to electrohydrodynamic forces) and that additional drawing of the fiber should occur for higher winding speeds. This work concluded that the degree of molecular orientation, which develops only due to electrohydrodynamic forces and, hence, would be expected in non-woven electrospun fabrics, is quite low.

Shapes and Sizes

In addition to circular fibers, a variety of cross-sectional shapes and sizes can be obtained from different polymers during electrospinning. Koombhongse and co-workers actually obtained branched fibers, flat ribbons, ribbons of other shapes and fibers that were split longitudinally from larger fibers in electrospinning a polymer solution [21]. Studies of the properties of fibers with these cross-sectional shapes from a number of different kinds of polymers and solvents indicate that effects of the fluid mechanics, the electrical charge carried with the jet and evaporation of the solvent all contributed to the formation of the fibers.

Sung and Gibson used polycarbonate in another study [22]. Electrospun fibers created in this process showed a wrinkled structure that was found to depend on the rate of evaporation of the solvent from the surface related to the rate of evaporation from the core. Indeed, as the solvent on the surface evaporated and a 'skin' formed, the solvent entrapped in the core diffused into the

ambient atmosphere and caused what they called a 'raisin-like structure'. A rapid evaporation of solvent from the jet that creates a skin, as mentioned above, can in fact give rise to hollow fibers that can collapse into a ribbon.

Alterations of Secondary Structure and Functionality

The electrospinning process is highly versatile and allows not only the processing of many different polymers into polymeric nano-fibers but also the co-processing of polymer mixtures and mixtures of polymers and low molecular weight non-volatile materials. This is done simply by using ternary solutions of the components for electrospinning to form a combination of nano-fiber functionalities. Polymer blends, core-shell structures and side-by-side bicomponent electrospinning are growing research areas that are connected with the electrospinning of multi-component systems. The targets are either to create nano-fibers of an 'unspinnable' material or to adjust the fiber morphology and characteristics.

The option of spinning a polymer blend renders possible the creation of core-shell nano-fibers through phase separation as the solvent evaporates. Another method for creating a structure of this kind is to co-electrospin two different polymer solutions through a spinneret consisting of two coaxial capillaries (see Fig. 16-6). Nano-fibers with hollow interiors are used in several applications, such as nano-fluidics and hydrogen storage. Electrospun tubular fibers can also be used as sacrificial templates.

The electrospinning technique also provides the capacity to lace together a variety of types of nanoparticles or nano-fillers to be encapsulated into an electrospun nano-fiber matrix (Fig. 16-8) [23]. Several functional components (e.g. nanometer-sized particles, nano-fillers, carbon nano-tubes, drugs, enzymes and DNA) can be dispersed in the initial polymer solutions, which are then electrospun to form composites in the form of continuous nano-fibers and nano-fibrous assemblies.

Another interesting aspect of nano-fiber processing is that it is feasible to modify not only their

morphology and their (internal bulk) content but also their surface structure in order to carry various chemically reactive functionalities. Thus, nano-fibers can be easily post-synthetically functionalized, for example by using plasma modification, physical or chemical vapor deposition (PVD, CVD) and chemical modifications such as cross-linking or grafting. By varying the processing parameters, it is also possible to produce fibers with unique surface features and secondary structures such as micro-textured/nano-porous fibers and micro-nano-webs.

APPLICATIONS OF ELECTROSPUN FUNCTIONAL MICRO-NANO-FIBERS

Electrospun micro-nano-structures are a class of novel materials that is exciting because of several of the unique characteristics discussed above. Significant progress has been made in this field in the last few years, and the resulting micro-nano-structures may serve as a highly versatile platform for a broad range of important technological applications in areas such as biomedicine, pharmacy, sensors, catalysis, filter, composites, ceramics, electronics and photonics. Some of the most recent developments in their processing and the relevant applications that are considered are presented below.

Biomedical Applications

Tissue Engineering. Electrospun 3D nano-fibrous structures meet the essential design criteria of an ideal tissue engineered scaffold based upon their unique action in supporting and guiding cell growth [24]. Most studies confirm that the electrospun nano-fibrous structure is capable of supporting cell attachment and proliferation (Fig. 16-9) [25]. The structure features a morphological similarity to the extracellular matrix of natural tissue, which is characterized by a wide range of pore diameter distribution, high porosity and effective mechanical properties.

Nano-fibers have been studied for engineering *cardiovascular tissues* such as heart tissue constructs and blood vessels. Ramakrishna's group

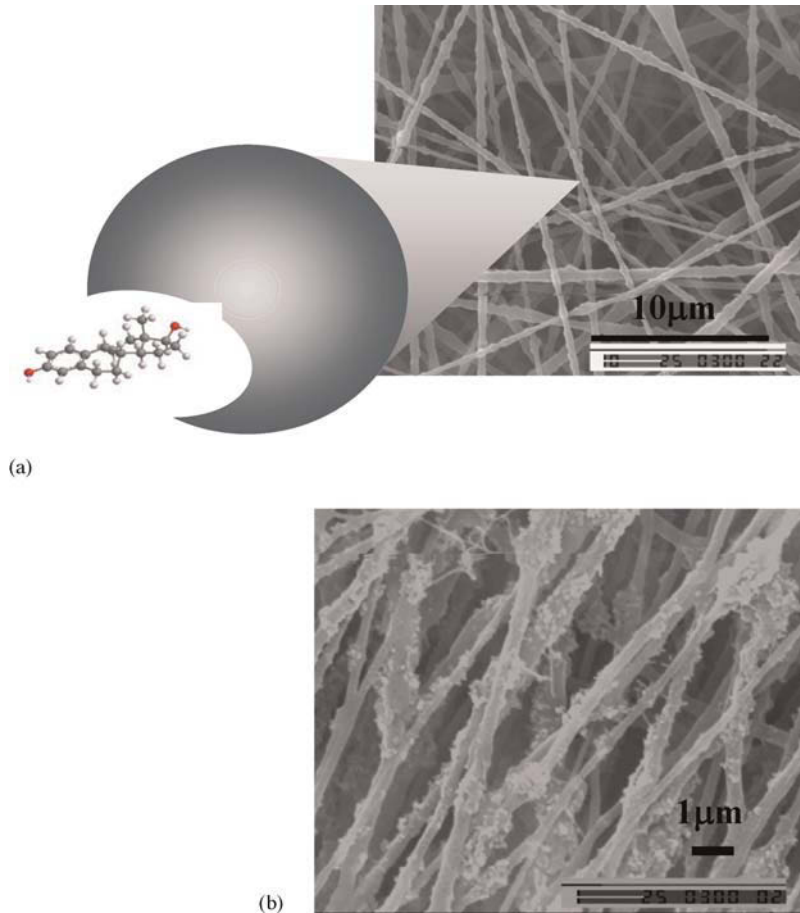


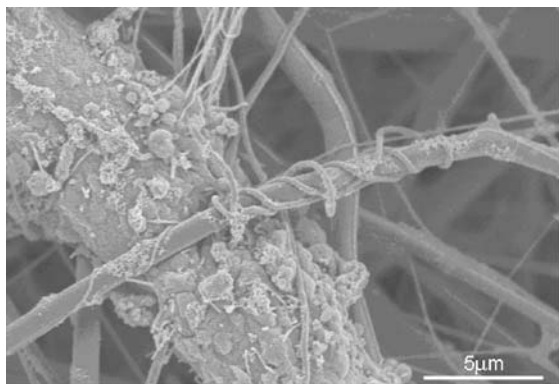
FIGURE 16-8 SEM images of (a) electrospun poly(ethylene terephthalate) (PET) nanofibers containing encapsulated molecular imprinted 17β -estradiol nano-particles (50% of the nano-fibers content) [23]. (b) Electrospun polyurethane (PU) nano-fibers coated with SiC ceramic nano-particles (Chronakis et al., unpublished results).

published several articles on the use of nano-fibers as a scaffold for blood vessels and looked at the influence of fiber diameter, orientation and other parameters on cell proliferation [26]. Nano-fibers made of poly(L-lactid-co- ϵ -caprolactone) P(LLA-CL) or poly(ethylene terephthalate) (PET) were primarily used.

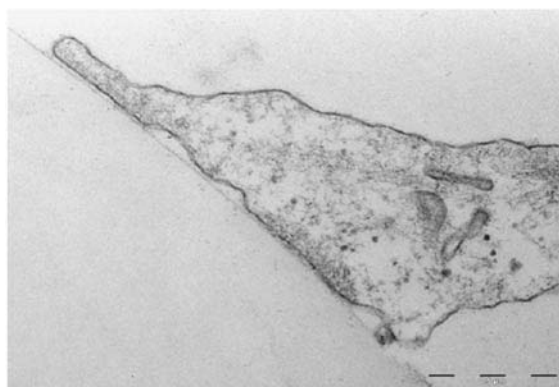
Biomimeticism towards human ligament has been considered, and the effects of fiber alignment and direction of mechanical stimuli on the extracellular matrix (ECM) generation of human ligament fibroblast (HLF) was studied [27]. An elastic biodegradable material in a tubular form was produced by combining polylactide with cross-linked

elastin [28]. The tubular material obtained showed excellent mechanical properties equal to those of blood vessel and peripheral nerve tissue.

Nano-fibers are potential structures for *bone tissue engineering*. Yoshimoto et al. used poly(ϵ -caprolactone) (PCL) scaffolds to grow mesenchymal stem cells (MSCs) derived from bone marrow [29]. Polylactide combined with cross-linked elastin shows a potential for *neural applications* [28]. The regeneration of peripheral nerve axons was observed in transplantation using a rat model with sciatic trauma. Silk-like polymers with fibronectin functionality (extracellular matrix proteins) have been electrospun to make biocompatible films



(a)



(b)

FIGURE 16-9 (a) SEM image showing fibroblast (human MRC-5) extension wrapping around the electrospun nano-fiber. (b) TEM image showing a fibroblast extension in close contact with electrospun Artelon® nano-fiber [25].

for use in prosthetic devices intended for implantation in the central nervous system [30].

Wound Dressings and Healing. Electrospun nano-fibrous membranes can be used in the production of novel wound dressings. These membranes are particularly important because of their favorable properties, such as high specific surface area, combined with antibacterial and drug release functionality. Recent studies support that nano-fibrous dressings promote hemostasis, have better absorptivity, semi-permeability and conformability and allow scar-free healing [31]. The nano-fibrous membrane also shows controlled evaporative water loss, excellent oxygen permeability and promoted fluid drainage ability, but it can still inhibit exogenous microorganism inva-

sion because its pores are ultra-fine. Histological examinations also indicate that the rate of epithelialization is increased and that the dermis becomes well organized when wounds are covered with electrospun nano-fibrous membrane.

A nano-fiber mat made of fibrinogen, a soluble protein that is present in blood, has been produced by electrospinning [32]. The mat could be placed and left on a wound, thereby minimizing blood loss and encouraging the natural healing process. Fibrinogen increases the 'stickiness' of clotting cells, thickens the blood and promotes the formation of fibrin (the stringy protein that forms the basis of blood clots). Electrospinning can also be used to create biocompatible, thin films with a useful coating design and a surface structure that can be deposited on implantable devices in order to facilitate the integration of these devices in the body.

Drug Carrier and Delivery Systems. Electrospun fiber mats have also been explored as drug delivery vehicles, with promising results. The application of electrostatic spinning in pharmaceutical applications resulted in dosage forms with useful and controllable dissolution properties. For instance, hydroxy propoxy methylcellulose (HPMC), a cellulose derivative commonly used in pharmaceutical preparations, together with the drug has also been tested [33]. Poly-(L-lactic acid) (PLLA) and poly(D,L-lactide-coglycolide) (DLPLGA) nano-fibers are other polymers that have been electrospun with an encapsulated drug and have shown promising drug release properties. Incorporation of an antibiotic in fibers developed for scaffold applications has also been reported. The combination of mechanical barriers based on non-woven nano-fibrous biodegradable scaffolds and their capability for local delivery of antibiotics makes them desirable for applications in the prevention of post-surgical adhesions and infections.

Micro-nano-fibers as Support for Enzymes and Catalysts

Electrospun micro-nano-fibers are an attractive class of supports for enzymes and catalysts due to their ultra-thin sizes and large surface areas.

Reneker and co-workers demonstrated the possibility of using nano-fibers for the immobilization of enzymes, showing catalytic efficiency for biotransformations [34]. Enzyme-modified nano-fibers of PVA and PEO achieved by loading the enzymes, i.e. casein and lipase, into the polymer solutions have also been reported. The membranes with encapsulated enzymes were six times more reactive than cast films from the same solutions.

Investigations have been made of the catalytic activity of nano-fibers obtained by incorporating catalysts. For instance, the incorporation of palladium (Pd) nano-particles has been studied in detail using carbonized and metal oxide nano-fibers [35].

Generation of Micro-nanomechanical and Micro-nano-fluidic Devices through Electrospinning

As mentioned earlier, electrospun micro-nano-fibers can serve as sacrificial templates for the generation of micro-nano-structures with hollow interiors. Czaplewski and co-workers prepared nano-fluidic channels [36]. The channels obtained were elliptical and presented no sharp corners, as in conventional lithographic techniques, which promotes a smoother fluid flow through them. Furthermore, the spin-on glass is optically transparent and compatible with chemical analysis, thereby opening applications in biomolecular separation and single molecule analysis. They also demonstrated the use of these templates for the fabrication of micro-electromechanical devices, such as nano-scale mechanical oscillators.

Deposits of oriented poly(methyl methacrylate) nano-fibers, combined with contact photolithography, created silicon nitride nano-mechanical oscillators with dimensions in the order of 100 nm. The fibers were used as etch masks to pattern nano-structures in the surface of a silicon wafer. The oriented polymeric nano-fiber deposition method that was used in this experiment offers an approach for rapidly forming arrays of nano-mechanical devices, connected to micro-mechanical structures, that would be difficult to form using a completely self-assembled

or completely lithographic approach. This approach may provide a useful method for realizing nano-scale device architectures in a variety of active materials.

Furthermore, magnetite nano-particles were incorporated as a colloidal stable suspension into polyethylene oxide or polyvinyl alcohol solutions [37]. After electrospinning, the nano-particles were aligned along the fibers' axis. These nano-fibers exhibited superparamagnetic behavior and deflected when subjected to a magnetic field at room temperature. A micro-aerodynamic decelerator based on permeable surfaces of nano-fiber mats was reported by Zussman and Yarin [38]. The mats were positioned on light, pyramid-shaped frames. These platforms fell freely through the air, apex down, at a constant velocity. The drag of this kind of passive airborne platform is of significant interest in a number of modern aerodynamics applications including, for example, dispersion of 'smart dust' carrying various chemical and thermal sensors, dispersion of seeds, and movement of small organisms with bristle appendages.

Micro-nano-fibers in Sensors

Recent advances in micro-nano-technology and the electrospinning technique offer great potential for the construction of cost-effective, next-generation chemical and biosensor devices. The high surface area per volume unit makes electrospun micro-nano-structures great candidates for a variety of sensing applications as they can offer high sensitivity and response time. These sensors can find applications in medical diagnosis and environmental and bioindustrial analysis, among others [1,23].

Conducting electroactive polymers have remarkable sensing applications because of their ability to be reversibly oxidized or reduced by applying electrical potentials. For biosensing applications, conducting electroactive polymers combine the role of a matrix immobilization template and the generation of analytical signals. The most common conducting electroactive polymers include polypyrrole, polyaniline and polythiophene and are characterized by an

electronic conductivity of up to $10^4 \Omega^{-1}$. Resistive-type sensors made from undoped or doped polyaniline nano-fibers outperform conventional polyaniline on exposure to acid or base vapors, respectively [39].

Electrospinning of lead zirconate titanate, $\text{Pb}(\text{Zr}_x\text{Ti}_{1-x})\text{O}_3$ (PZT) fibers should be mentioned because of its technological importance in the field of sensors, electronics and non-volatile ferroelectric memory devices. PZT is one example of one-dimensional nano-structures, the smallest dimension structures for efficient transport of electrons and optical excitation, that can be used as building blocks in a bottom-up assembly in diverse applications in nano-electronics and photonics [40]. Wang et al. showed that ultra-fine PZT fibers could be synthesized from metallo-organic compounds simply by using metallo-organic decomposition (MOD) and vacuum heat treatment electrospinning techniques [40].

Other developments are electrospun nano-fibers of polyvinylpyrrolidone (PVP) containing the urease enzyme that show a potential as a urea biosensor and nano-fibers coated with metal oxides (TiO_2 , MoO_3) for the detection of toxic gases. Molecular imprinted nano-fibers with selective molecular recognition ability and a chemosensor material with a high surface area obtained by electrospinning a fluorescent conjugated polymer have also been developed [23,41].

Micro-nano-fibers in Electric and Electronic Applications

Electrospun nano-fibers with electrical and electro-optical activities have received a great deal of interest in recent years because of their potential application in nano-scale electronic and optoelectronic devices, such as nano-wires, LEDs, photocells, etc. Lead zirconate titanate (PZT) and carbon nano-fibers are two typical and challenging examples of one-dimensional nano-structures that can be used as building blocks in bottom-up assembly in diverse applications in nano-electronics and photonics [40].

Studies support that electrospinning can be a simple method for fabricating a one-dimensional

polymer field-effect transistor (FET), which forms the basic building block of logic circuits and switches for displays [42, 43]. In addition, the excellent adherence of the nano-fibers to SiO_2 and to gold electrodes may be useful in the design of future devices. By means of electrospinning processing, extremely low dimensional conducting nano-wires have been made from, e.g., polyaniline or polypyrrole for use in nano-electronics (Fig. 16-10) [44].

Other studies report the development of carbon nano-fiber webs from the oxidation and steam activation of a polyacrylonitrile (PAN) nano-fiber web for use as an electrode in a supercapacitor [43], poly(vinylidene fluoride) (PVDF) nano-fibers for applications as a separator or as an electrolyte in batteries [45] and fabrication of a lithium secondary battery comprising a fibrous film made by electrospinning [46].

Electrospinning mixtures of ceramic particles with polymers and subsequent pyrolysis of the polymer to form pure ceramic nano-fibers is an area of intense research [7]. Because of their large surface-to-volume ratios and narrow-band optical emission, these nano-fibers can be used as selective emitters for thermophotovoltaic applications and as emitting devices in nano-scale optoelectronic applications.

Micro-nano-fibers in Filters

The efficiency of nano-fibers in filtration has been studied by several groups. Generally, the electrospun webs have been found to be much more effective than other commercial high-efficiency air filter media. In most cases, the nano-fiber webs are applied on a substrate chosen to provide mechanical properties, while the nano-fiber dominates the filtration performance. Electrospinning can also be used to produce charged fibers for use in filtration media. Obviously, the charge induction and charge retention characteristics are related to the polymer material used for electrospinning.

Controlling the parameters of electrospinning allows the generation of micro-nano-fiber webs with different filtration characteristics. A study

done by Schreuder-Gibson and Gibson showed that it is possible to tailor pore size, air permeability and aerosol filtration of elastic non-woven media by applying very light-weight layers of electrospun elastic fibers to the coarser webs [47]. It has been found that a significant deformation of the elastic webs increases air flow, and it might be possible to design controlled flow filters or air bags that are modulated by a pressure drop across elastic webs with correspondingly variable porosities. Many filtering applications of electrospun micro-nano-fibers are related to air filtration, but liquid filtration can also occur [48].

Moreover, ion exchange materials (such as resins, membranes, etc.) have been widely used in various industries for water deionization or softening, metal recovery, biological process, food and beverages, pharmaceuticals and fuel cell applications. Polymer nano-fiber ion exchangers are new, promising materials as they have a much higher surface area than common ion exchangers.

Micro-nano-fibers in Textiles

Electrospun micro-nano-membranes composed of elastomeric fibers are of particular interest in the development of several protective clothing applications. The excellent ability to capture aerosols and the possibilities to incorporate any kind of active substances make electrospun nano-fiber materials potential candidates for use in protective clothing and smart cloths responding to changes in the surrounding environment. Much work is being done with the aim to develop garments that reduce soldiers' risks for chemical exposure [49]. The idea is to lace several types of polymers and fibers to make protective ultrathin layers that would enhance, for example, chemical reactivity and environmental resistance. Such mats have been found to have a higher convective resistance to air flow while the transport of water vapor is much higher than in normal clothing materials. These products exhibit remarkable 'breathing' properties, which are now required in clothing applications.

In some other uses of protective clothing, thermal and flammability properties are essential

[50]. Electrospun poly(methyl methacrylate-co-methacrylic acid) (P(MMA-co-MAA)) and its layered silicate nano-composites have shown good thermal stability, reduced flammability and increased self-extinguishing properties. The possibility of using sub-micron and nano-scale fibers and fibrous assemblies based on conductive PEDOT for wearable electronics has also been explored [14]. Finally, the development of electrospinning apparatuses for fiber orientation that allow the fabrication of yarns is of considerable interest [51] (Figs. 16-9 and 16-10).

Micro-nano-fibers as Composite Reinforcement

The strength of a composite material is effectively enhanced by fiber-based reinforcement. Thus, the high surface-to-volume ratio of nano-fibers significantly improves the stiffness and mechanical strength of the composites compared to conventional fibers due to the increased interaction between the fibers and the matrix [52]. Another positive aspect is that the composites are able to maintain their optical transparency related to the small cross-section of the nano-fibers.

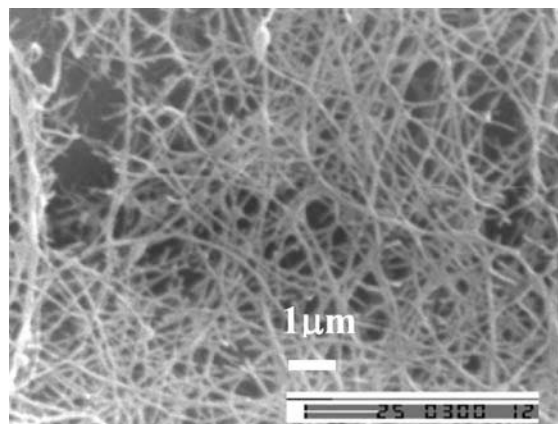


FIGURE 16-10 SEM micrograph of conductive polypyrrole nano-fibers. The nano-fibers were electrospun from a solution of $((\text{PPy3})^+(\text{DEHS})^-)_x$ in DMF [44].

Attempts to Increase the Production Rate of Electrospun Micro-nano-fibers

Electrospinning using Multiple Nozzles. The most obvious way to increase the rate of production of micro-nano-fibers is to increase the number of nozzles used in the spinning process. In a patent, Chu et al. described an electrospinning apparatus with multiple nozzles, as shown in Fig. 16-11 [53]. The essential invention in this patent was not the use of multiple nozzles but the possibility to better control the jet formation, jet acceleration and fiber collection for individual jets. This was achieved using several additional electrodes to homogenize the electric field that accelerates the jets from the nozzles to the collector. The possibility of controlling both the flow of the conducting fluid (polymer solution or melt) and the properties of the electric field for each jet was described as essential for producing nano-fibers using multiple nozzles. A later patent by the same group focused on controlling multiple fiber jets as opposed to individual jets or adding the possibility of blowing a temperate gas in the fiber spinning direction. The gas flow gives a higher production rate than traditional electrospinning, as well as lower energy consumption.

Electrospinning without Nozzles. Perhaps the most successful way to increase the electrospinning production rate that can be recognized thus far is the Nanospider™ technology, patented by O. Jirsak et al. [54]. This technology is now owned by ElMarco (Czech Republic). Instead of using capillaries as a spinneret for introducing the polymer solution into the electric field, a rotating charged electrode is used that is partly immersed into the polymer solution. This set-up allows the creation of many Taylor cones and hence many jets that travel upwards to a conveyor belt that can be covered with a material to be coated.

A great advantage of this method is the possibility to create multiple jets of nano-fibers without the risk of the nozzles clogging. Another advantage of the technique is that the spinning direction is upwards, which minimizes the risk of solution droplets forming in the product. The process is schematically shown in Fig. 16-12.

The polymer solution (2) is applied to the charged cylindrical electrode (3) as it rotates partly immersed in the solution. Multiple fiber jets are formed from the surface of the electrode towards the oppositely charged electrode (40). The fibers are drawn to the electrode (40), not

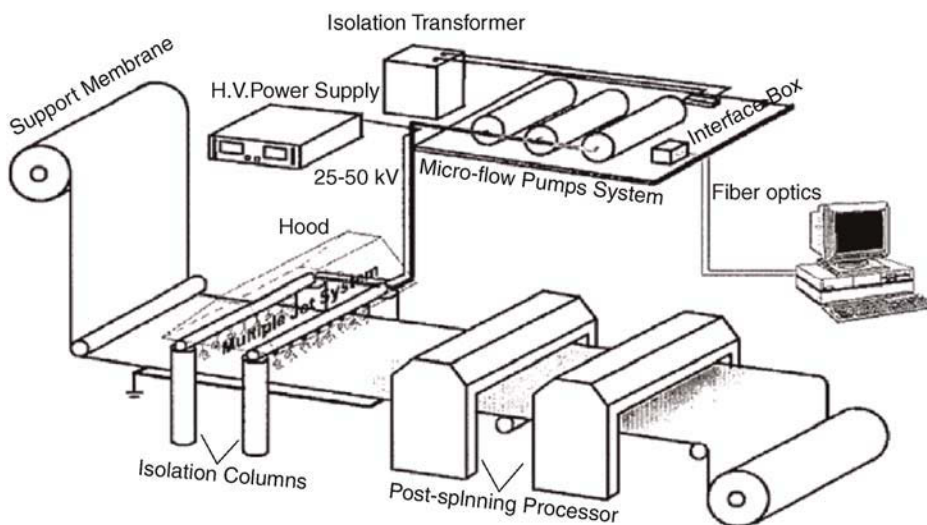


FIGURE 16-11 Schematic drawing of an apparatus for large-scale electrospinning of nano-fibers [53].

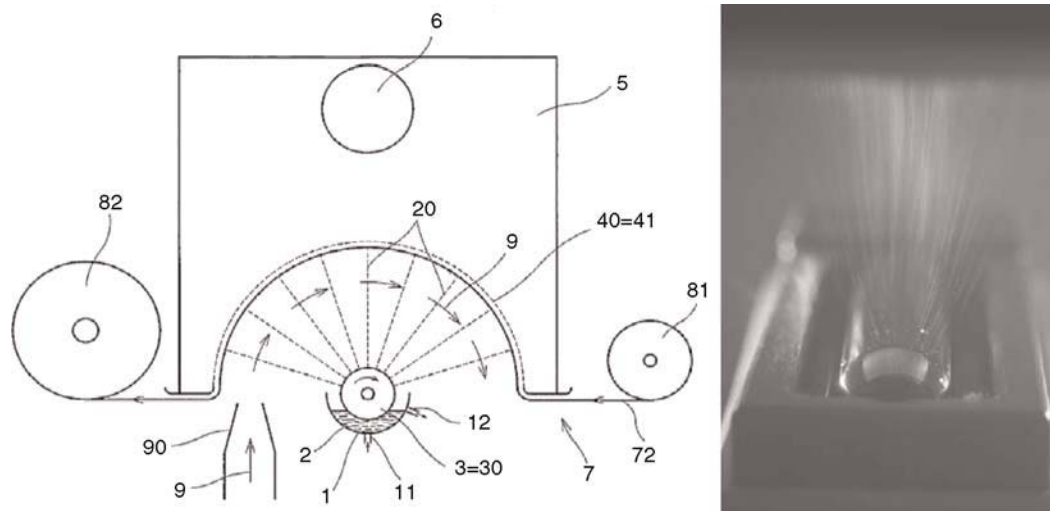


FIGURE 16-12 (a) Schematic drawing of the Nanospider™ technology [54]. (b) Picture of the Nanospider™ technology in action (from www.nanospider.cz).

only by the electric force but also due to the action of a vacuum chamber (5). The patent also covers rotating cylindrical electrodes with different patterned surfaces. Using this technology, ElMarco claims that they will have a production capacity of 3000 m²/day (1 m in width) (2006).

Another approach to spinning nano-fibers without nozzles is to use a porous tube of polyethylene (Fig. 16-13), as reported by Reneker et al. [55]. By applying air pressure to a polymer solution inside a cylindrical porous tube, these authors were able to form multiple jets of polymer solution in the electric field. With this porous tube, the production rate could be increased to about 250 times that of the corresponding production rate for a single needle.

Recently, a new technology with the use of centrifugal forces has been developed and patented from Swerea IVF [56]. The process is schematically shown in Fig. 16-14.

Commercial Products

It should be noted that some companies already have commercial products based on electrospun nano-fibers. One of the first companies to start an

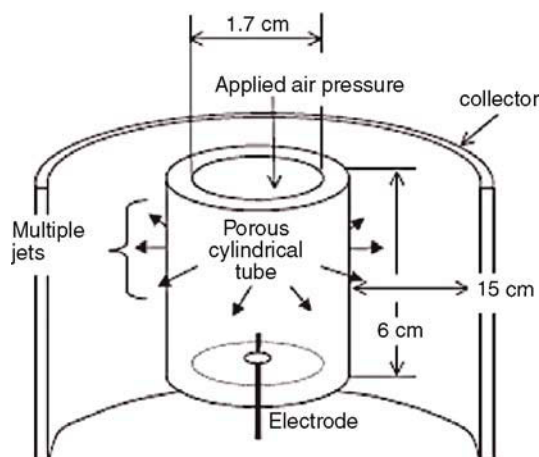


FIGURE 16-13 Schematic illustration of the electrospinning set-up using a porous polyethylene tube [55].

industrial production line of nano-fiber web is NanoTechnics Co., Ltd, in Korea. The company offers nano-fiber webs of PA6 and PA66 for application in filters and PAN for electrodes in batteries. Other companies that claim to be able to electrospin webs for use in filters are Hollingsworth & Vose, Germany, and eSpin Technologies, USA. Donaldson Company Inc., USA, is also an

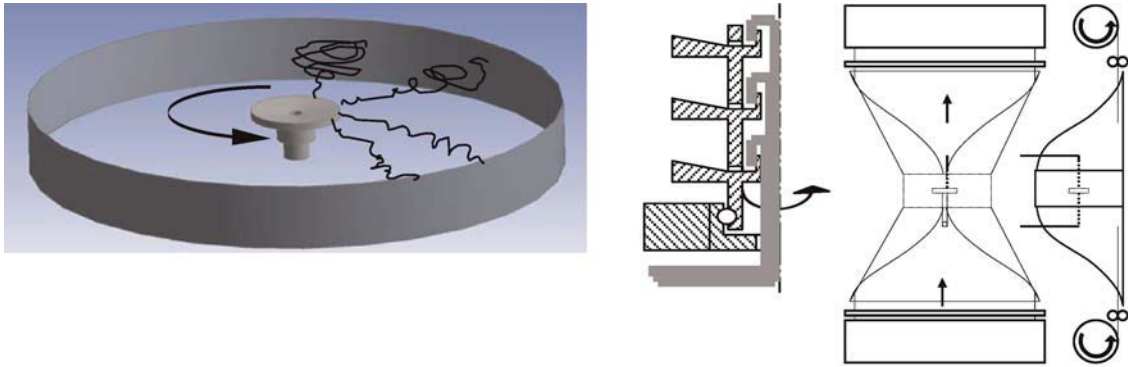


FIGURE 16-14 Schematic illustration of the micro-nano-fiber formation from rotating disc [56].

important actor in the field of nano-fiber-based filters. Donaldson has several US and international patents that cover nano-fiber innovations, configurations and uses.

TECHNOLOGICAL COMPETITIVENESS AND OPERATION ECONOMICS

Electrospinning is a very simple and versatile method for creating polymer-based, high functional and high performance micro-nano-fibers that can revolutionize the world of structural materials. The process is versatile in that there is a wide range of materials that can be spun (Table 16.1). At the same time, electrospun micro-nano-fibers possess unique and interesting features. The ability to customize micro-nano-fibers to meet the requirements of specific applications gives electrospinning an advantage over other larger-scale micro-nano-production methods. Combining well-established technologies of today with the emerging field of electrospun micro-nano-fibers can potentially lead to the development of new technologies and new micro-nano-structured smart assemblies and stimulate opportunities for an enormous number of applications. Thus, electrospinning technology can provide a connection between the worlds of the nano-scale and the macro-scale.

Another advantage of this top-down micro-nano-manufacturing process is its relatively low cost compared to that of most bottom-up methods. The electrospinning method itself is environmentally friendly because it consumes only a small amount of electrical energy. In spite of the high potential difference (10,000–40,000 V) that is applied, only a small electrical current flows through the nano-fibers (in the order of nano-amperes). In addition, the electrospinning method provides nano-fiber structures that imply a large reduction in material consumption. For instance, the formation of a true nano-coating (monolayer-like) will result in a thickness of only a few nanometers, while current coatings have a thickness of a few micrometers. This means that the consumption of materials is also about 1000 times less for nano-coatings while it results in the same surface properties as are obtained with micro-coatings. Moreover the resulting micro-nano-fiber samples are often uniform and continuous and do not require expensive purification (unlike submicrometer-diameter whiskers, inorganic nano-rods and carbon nanotubes). Overall, despite the existence of some commercial products, it is evident that an upscaling of the electrospinning process and productivity improvements are essential features and merit more effort to ensure full success in socio-economic terms.

TABLE 16.1 Examples of Some Polymer-Biopolymer Materials that have been Electrospun and Solvents Used (in Alphabetical Order)

Materials	Solvents
ABS	N,N-Dimethyl formamide (DMF) or tetrahydrofuran (THF)
Cellulose	Ethylene diamine
Cellulose acetate	Dimethylacetamide (DMAc)/Acetone or acetic acid
Ethyl-cyanoethyl cellulose ((E-CE)C)	THF
Chitosan and chitin	1,1,1,3,3,3-hexafluoro-2-propanol (HFIP)
Dextran	Water, DMSO/water, DMSO/DMF
Gelatin	2,2,2-Trifluoroethanol
Nylon	Formic acid
Poly(2-acrylamido-2-methyl-1-propane sulfonic acid) (PMAAPS)	Ethanol/Water
Polyacrylonitrile (PAN)	DMF
Polyalkyl methacrylate (PMMA)	Toluene/DMF
Polycarbonate	THF/DMF
Poly(ethylene oxide) (PEO)	Water, ethanol, DMF
Polyethylene terephthalate (PET)	Trifluoroacetic acid (TFA)/dichloromethane (DCM)
Poly(lactic-based polymers)	Chloroform, HFIP, DCM
Poly(ϵ -caprolactone)-based polymers	Acetone, acetone/THF, chloroform/DMF, DCM/methanol, chloroform/methanol, THF/acetone
Poly(3-hydroxybutyrate-co-3-hydroxyvalerate) (PHBV)	2,2,2-Trifluoroethanol
Polyphosphazenes	Chloroform
Polystyrene	1,2-Dichloroethane, DMF, ethylacetate, methylethylketone (MEK), THF
Bisphenol-A polysulfone	DMAc/Acetone
Polyurethane (PU)	THF/DMF
Polyvinyl alcohol (PVA)	Water
Polyvinyl chloride (PVC)	DMF, DMF/THF
Poly(vinylidene fluoride) (PVDF)	DMF/THF
Poly(vinyl pyrrolidone)	Ethanol, DCM, DMF
Silk	Hexafluoroacetone (HFA), hexafluoro-2-propanol, formic acid

REFERENCES

- [1] A. Frenot, I.S. Chronakis, Polymer nanofibers assembled by electrospinning, *Current Opinion in Colloid and Interface Science* 8 (2003) 64–75.
- [2] D. Li, Y. Xia, Electrospinning of nanofibers: reinventing the wheel? *Advanced Materials* 16 (2004) 1151–1170.
- [3] Formhals, Process and apparatus for preparing artificial threads. US Patent, 1-975-504 (1934).
- [4] D.H. Reneker, I. Chun, Nanometre diameter fibres of polymer produced by electrospinning, *Nanotechnology* 7 (1996) 216–223.
- [5] R. Dersch, M. Steinhart, U. Boudriot, A. Greiner, J.H. Wendorff, Nanoprocessing of *polymers*: applications in medicine, sensors, catalysis, photonics, *Polymers for Advanced Technologies* 16 (2005) 276–282.
- [6] W.E. Teo, S. Ramakrishna, A review on electrospinning design and nanofibre assemblies, *Nanotechnology* 17 (2006) R89–R106.
- [7] I.S. Chronakis, Novel nanocomposites and nanoceramics based on polymer nanofibers using electrospinning process – a review, *J. of Materials Processing Technology* 167 (2005) 283–293.
- [8] S.N. Reznik, A.L. Yarin, A. Theron, E. Zussman, Transient and steady shapes of droplets attached to a surface in a strong electric field, *J. of Fluid Mechanics* 516 (2004) 349–377.
- [9] A. Welle, M. Kröger, M. Döring, K. Niederer, E. Pindel, I.S. Chronakis, Electrospun aliphatic poly(carbonate)s nanofibers as tailored tissue scaffold materials, *Biomaterials* 28 (2007) 2211–2219.
- [10] P.K. Baumgarten, Electrostatic spinning of acrylic microfibrils, *J. of Colloid and Interface Science* 36 (1971) 71–79.
- [11] J.H. He, Y.Q. Wan, M.Y. Yu, Allometric scaling and instability in electrospinning, *Int. J. of Nonlinear Sciences and Numerical Simulation* 5 (2004) 243–252.
- [12] A.L. Yarin, E. Zussman, Upward electrospinning of multiple nanofibers without needles/nozzles, *Polymer* 45 (2004) 2977–2980.
- [13] Z. Sun, E. Zussman, A.L. Yarin, J.H. Wendorff, A. Greiner, Compound core-shell polymer nanofibers by co-electrospinning, *Advanced Materials* 15 (2003) 1929–1932.
- [14] A.K. El-Aufy, Nanofibers and nanocomposites poly(3,4-ethylene dioxythiophene)/poly(styrene sulfonate) by electrospinning, PhD thesis, Drexel University (2004).
- [15] D. Czuplewski, J. Kameoka, H.G. Craighead, Non-lithographic approach to nanostructure fabrication using a scanned electrospinning source, *J. of Vacuum Science & Technology B (Microelectronics and Nanometer Structures)* 21 (2003) 2994–2997.
- [16] R. Dersch, T. Liu, A.K. Schaper, A. Greiner, J.H. Wendorff, Electrospun nanofibers: internal structure and intrinsic orientation, *J. of Polymer Science Part A: Polymer Chemistry* 41 (2003) 545–553.
- [17] D. Li, Y. Xia, Direct fabrication of composite and ceramic hollow nanofibers by electrospinning, *Nano Letters* 4 (2004) 933–938 and D. Li, Y. Wang and Y. Xia, Electrospinning nanofibers as uniaxially aligned arrays and layer-by-layer stacked films, *Advanced Materials* 16 (2004) 361–366.
- [18] E. Zussman, A. Theron, A.L. Yarin, Electrostatic field-assisted building 3-D nano-structures from electrospun nanofibers, *Applied Physics Letters* 82 (2003) 973–975.
- [19] A. Theron, E. Zussman, A.L. Yarin, Electrostatic fields-assisted alignment of electrospun nanofibres, *Nanotechnology* 12 (2001) 384–390.
- [20] S.F. Fennessey, R.J. Farris, Fabrication of aligned and molecularly oriented electrospun polyacrylonitrile nanofibers and the mechanical behavior of their twisted yarns, *Polymer* 45 (2004) 4217–4225.
- [21] S. Koombhongse, W. Liu, D.H. Reneker, Flat ribbons and other shapes by electrospinning, *J. of Polymer Science, Polymer Physics Ed* 39 (2001) 2598–2606.
- [22] C. Sung, H. Gibson, N.K. Ravi Varma, Electrospinning of polycarbonates and their surface characteristics, *The Fibre Society Spring Conference Raleigh NC, J. of Textile and Apparel, Technology and Management* 1(special issue) (2001).
- [23] I.S. Chronakis, A. Jakob, B. Hagström, L. Ye, Encapsulation and selective recognition of molecularly imprinted theophylline and 17beta-estradiol nanoparticles within electrospun polymer nanofibers, *Langmuir* 22 (2006) 8960–8965 and V. Romeo, G. Gorrasi, V. Vittoria and I.S. Chronakis, Encapsulation and exfoliation of inorganic lamellar fillers into polycaprolactone by electrospinning, *Biomacromolecules* 8 (2007) 3147–3152.
- [24] Q.P. Pham, U. Sharma, A.G. Mikos, Electrospinning of polymeric nanofibers for tissue engineering applications: a review, *Tissue Engineering* 12 (2006) 1197–1211.
- [25] E. Borg, A. Frenot, P. Walkenström, K. Gisselält, P. Gatenholm, Electrospinning of degradable elastomeric nanofibers with various morphology and their interaction with human fibroblasts, *J. of Applied Polymer Science* 108 (2008) 491–497.
- [26] Z. Ma, M. Kotaki, T. Yong, W. He, S. Ramakrishna, Surface engineering of electrospun polyethylene terephthalate (PET) nanofibers towards development of a new material for blood vessel engineering, *Biomaterials* 26 (2005) 2527–2536.
- [27] C.H. Lee, H.J. Shin, I.H. Cho, Y.-M. Kang, I.A. Kim, K.-D. Park, J.-W. Shin, Nanofiber alignment and direction of mechanical strain affect the ECM

- production of human ACL fibroblast, *Biomaterials* 26 (2005) 1261–1270.
- [28] E. Kitazono, H. Kaneko, T. Miyoshi, K. Miyamoto, Tissue engineering using nanofiber, *Yuki Gosei Kagaku Kyokaiishi, J. of Synthetic Organic Chemistry Japan* 62 (2004) 514–519.
- [29] H. Yoshimoto, Y.M. Shin, H. Terai, J.P. Vacanti, A biodegradable nanofiber scaffold by electrospinning and its potential for bone tissue engineering, *Biomaterials* 24 (2003) 2077–2082.
- [30] C.J. Buchko, L.C. Chen, Y. Shen, D.C. Martin, Processing and microstructural characterization of porous biocompatible protein polymer thin films, *Polymer* 40 (1999) 7397–7407.
- [31] Y. Zhang, C.T. Lim, S. Ramakrishna, Z.-M. Huang, Recent development of polymer nanofibers for biomedical and biotechnological applications, *J. of Materials Science: Materials in Medicine* 16 (2005) 933–946 and D.S. Katti, K.W. Robinson, F.K. Ko and C.T. Laurencin, Bioresorbable nanofiber-based systems for wound healing and drug delivery: optimization of fabrication parameters, *J. of Biomedical Materials Research* 70B (2004) 286–296.
- [32] G. Bowlin, Natural bandages from fibrinogen, *Medical Textiles* 13 (2003) 4.
- [33] G. Verreck, I. Chun, J. Peeters, J. Rosenblatt, M.E. Brewster, Preparation and characterization of nanofibers containing amorphous drug dispersions generated by electrostatic spinning, *Pharmaceutical Research* 20 (2003) 810–817.
- [34] H. Jia, G. Zhu, B. Vugrinovich, W. Kataphinan, D.H. Reneker, P. Wang, Enzyme-carrying polymeric nanofibers prepared via electrospinning for use as unique biocatalysts, *Biotechnology Progress* 18 (2002) 1027–1032.
- [35] M.M. Demir, M.A. Gulgun, Y.Z. Menciloglu, B. Erman, S.S. Abramchuk, E.E. Makhaeva, A.R. Khokhlov, V.G. Matveeva, M.G. Sulman, Palladium nanoparticles by electrospinning from poly (acrylonitrile-co-acrylic acid)-PdCl₂ solutions. Relations between preparation conditions, particle size, and catalytic activity, *Macromolecules* 37 (2004) 1787–1792.
- [36] D.A. Czaplewski, J. Kameoka, R. Mathers, G.W. Coates, H.G. Craighead, Nanofluidic channels with elliptical cross sections formed using a nonlithographic process, *Applied Physics Letters* 83 (2003) 4836–4838.
- [37] A. Wang, H. Singh, T.A. Hatton, G.C. Rutledge, Field-responsive superparamagnetic composite nanofibers by electrospinning, *Polymer* 45 (2004) 5505–5514.
- [38] E. Zussman, A.L. Yarin, D. Weihs, A micro-aerodynamic decelerator based on permeable surfaces of nanofiber mats, *Experiments in Fluids* 33 (2002) 315–320.
- [39] J. Huang, S. Virji, B.H. Weiller, R.B. Kaner, Nanostructured polyaniline sensors, *Chemistry – A European Journal* 10 (2004) 1314–1319.
- [40] Y. Wang, R. Furlan, I. Ramos, J.J. Santiago-Aviles, Synthesis and characterization of micro/nanosopic Pb(Zr_{0.52}Ti_{0.48})O₃ fibers by electrospinning, *Applied Physics A* 78 (2004) 1043–1047.
- [41] P.I. Gouma, Nanostructured polymorphic oxides for advanced chemosensors, *Reviews on Advanced Materials Science* 5 (2003) 147–154.
- [42] N.J. Pinto, A.T. Johnson, A.G. MacDiarmid, C.H. Mueller, N. Theofylaktos, D.C. Robinson, F.A. Miranda, Electrospun polyaniline/polyethylene oxide nanofiber field-effect transistor, *Applied Physics Letters* 83 (2003) 4244–4246.
- [43] C. Kim, K.S. Yang, Electrochemical properties of carbon nanofiber web as an electrode for supercapacitor prepared by electrospinning, *Applied Physics Letters* 83 (2003) 1216–1218.
- [44] I.S. Chronakis, S. Grapenson, A. Jakob, Conductive polypyrrole nanofibers via electrospinning: electrical and morphological properties, *Polymer* 47 (2006) 1597–1603.
- [45] S.-S. Choi, Y.S. Lee, C.W. Joo, S.G. Lee, J.K. Park, K.-S. Han, Electrospun PVDF nanofiber web as polymer electrolyte or separator, *Electrochimica Acta* 50 (2004) 339–343.
- [46] W.B. Cho, S.W. Choi, J.S. Mu, H.S. Kim, U.S. Kim and W.I. Cho, A lithium secondary battery comprising a super fine fibrous polymer separator film and its fabrication method, Patent WO0189022 and WO0189023 (2001).
- [47] P. Gibson, H. Schreuder-Gibson, D. Rivin, Transport properties of porous membranes based on electrospun nanofibers, *Colloid and Surfaces A – Physicochemical and Engineering Aspects* 187 (2001) 469–481.
- [48] K. Yoshimatsu, L. Ye, J. Lindberg, I.S. Chronakis, Selective molecular adsorption using electrospun nanofiber membranes, *Biosensors and Bioelectronics* 23 (2008) 1208–1215.
- [49] H. Schreuder-Gibson, P. Gibson, K. Senecal, M. Sennett, J. Walker, W. Yeomans, D. Ziegler, P.P. Tsai, Protective textile materials based on electrospun nanofibers, *J. of Advanced Materials* 34 (2002) 44–55.
- [50] M. Wang, A.J. Hsieh, G.C. Rutledge, Electrospinning of (MMA-co-MMA) copolymers and their layered silicate nanocomposites for improved thermal properties, *Polymer* 46 (2005) 3407–3418.
- [51] F. Ko, Y. Gogotsi, A. Ali, N. Naguib, H. Ye, G. Yang, C. Li, Electrospinning of continuous carbon nanotube-filled nanofiber yarns, *Advanced Materials* 15 (2003) 1161–1165.
- [52] M.M. Bergshoeff, G.J. Vancso, Transparent nanocomposites with ultrathin electrospun nylon-4,6

- fiber reinforcement, *Advanced Materials* 11 (1999) 1362–1365.
- [53] B. Chu, B.S. Hsiao and D. Fang, Apparatus and methods for electrospinning polymeric fibers and membranes, US2002175449.
- [54] O. Jirsak, F. Sanetnik, D. Lukas and V. Kotek, A method of nanofibres production from a polymer solution using electrostatic spinning and a device for carrying out the method, WO2005/024101A1.
- [55] O.O. Dosunmu, G.G. Chase, W. Kataphinan, D.H. Reneker, Electrospinning of polymer nanofibers from multiple jets on a porous tubular surface, *Nanotechnology* 17 (2006) 1123–1127.
- [56] B. Hagström, Method and device for manufacturing nanofibers, Swedish Patent SE530751C2 (2007).

Tooling Process Chains and Concepts

*Hans Nørgaard Hansen, Mogens Arentoft, Peter T. Tang,
Giuliano Bissacco and Guido Tosello*

INTRODUCTION

Miniaturization has been one of the driving forces of technology during the last 20 years. As predicted by Taniguchi in 1983, by now the technology has moved into the nano-processing era and even for precision machining processes sub-micrometer precision is achievable [1]. This development has been made very clear in the semiconductor industry during the last 30 years, where the number of components on a chip has been approximately doubled each 18 months. This phenomenon is usually referred to as Moore's law. In recent years the need for micro-mechanical systems has increased, for example in connection with medical devices such as hearing aids, drug delivery systems, lab-on-chip systems, etc. The consequence is that traditional engineering materials such as metals and polymers are seen increasingly more often in micro-products. This requires the development of industrially viable manufacturing methods to support the demand for components and products.

Replication methods such as injection molding and cold forging belong to the preferred choice of macro-scale manufacturing methods when the focus is on mass production and high productivity and yield. The same processes are found in micro-scale manufacturing, now typically referred to as micro-injection molding and micro-cold forging [2]. Special focus on size effects, process charac-

teristics and optimization, etc. has been reported in, e.g. [3–5]. However, a basic prerequisite for process realization is the availability of the tools to be used in the process. For example, the tolerances and dimensions of the tools cannot be scaled down directly, since no methods would then exist for fabrication, i.e. to meet the requirements. Consequently, the choice of processes and their integration into coherent process chains becomes one of the major decisive issues in micro-manufacturing.

Definition of Tooling

A tool is a component that can be used (preferably more than once) to make other components. Normally the tool will be a durable component with a well-defined geometry, but tools that are only used once can be envisaged, for example in casting. In most cases, the tool will be used to fabricate a large number of identical components before it is destroyed due to wear, corrosion and mechanical failure. Tools are essential in replication processes such as hot embossing, injection molding, casting, hot and cold forging, cold forming (punching, stamping, etc.) and so on.

As product features are scaled down, the available technologies for tooling are changed, since traditional tooling technologies such as high precision milling, die-sinking EDM, wire EDM,

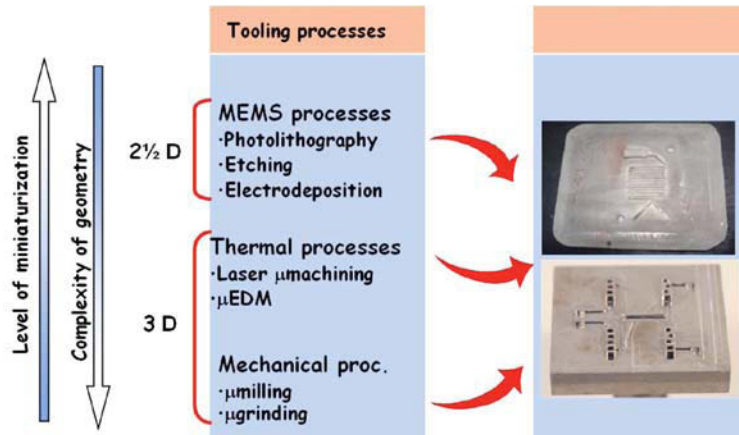


FIGURE 17-1 Example of mold-making technologies in micro-manufacturing.

etc. have lower limits as to the obtainable dimensions and geometries. New precision tooling technologies for potential micro-forming application have emerged as stand-alone technologies (e.g. micro-EDM milling, laser ablation, etc.) but equally interesting are the possibilities that emerge when processes are combined into new process chains. Figure 17-1 illustrates possible technology combinations in mold making for micro-manufacturing. Focus is usually given to the production of the part of the mold actually shaping the micro-part, and this is also the case for Fig. 17-1. However, the integration of such inserts into larger tools actually placed into processing equipment (injection molding machines, presses, etc.) is also of great importance.

Hot embossing and injection molding is usually applied for polymeric materials, while casting,

forging and cold forming are applied to metallic materials. In special cases it is possible to produce ceramic components by replication processes, e.g. the hot embossing of glass components is possible at temperatures of from around 550°C and above.

Definition of 'Process Chain'

In the broadest definition a process chain consists of all of the process steps necessary to produce the part or product in question. This means that a full process chain starts with design, selection of materials and processes, programming or other preparations of the production equipment, actual machining, quality assessment, cleaning, finishing and packaging. If the product consists of more than one component, assembly processes are also included in the process chain (Fig. 17-2).

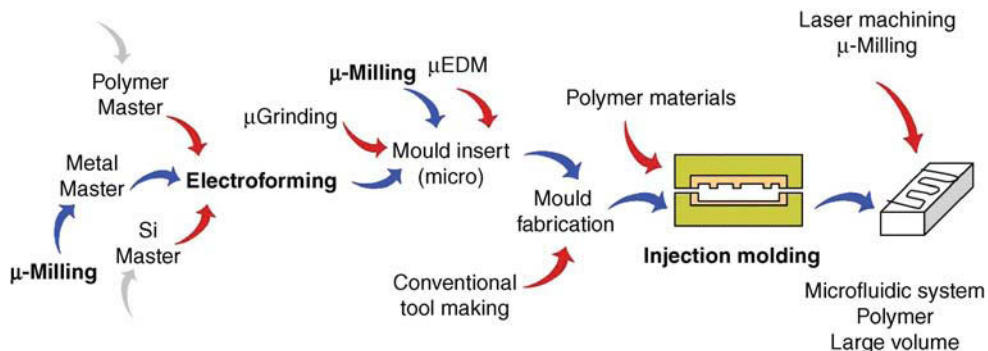


FIGURE 17-2 Possible process chains for the production of a polymer micro-component.

TOOLING CONCEPTS

Utilizing a strictly systematic approach, the possible tooling concepts can be divided into four groups or schemes. The first division is made by identifying the most important shaping process, i.e. the process that creates the shape of the finished tool. This process can either place material on a substrate (additive process) or remove material from a substrate (subtractive process). The substrate is normally a homogeneous material, typically metallic or ceramic (silicon), but it could also be a hybrid material (multi-layered, containing particles or fibers, etc.). The shape of the substrate is typically that of a flat disc or plate, but other simple shapes (rods, spheres, etc.) are also possible.

The second division is made with regards to the way the final tool is obtained. If the tool is fabricated *directly* it is understood that the substrate – after additive or subtractive machining – will become the tool. In the case where the substrate is removed during one of the subsequent steps in the process chain, the tooling concept will be considered an *indirect* one.

Additive processes used in micro-fabrication include:

- electroforming;
- laser sintering;
- physical and chemical vapor deposition;
- printing.

Subtractive processes used in micro-fabrication are:

- milling, turning or other machining processes;
- electrodischarge machining (EDM);
- chemical etching;
- electrochemical machining (ECM);
- laser machining/ablation (alternatively, other beam-processing technologies).

Some of the processes mentioned above require photolithography or other masking methods to define the areas that will be affected (and thus also the areas that will remain unchanged). To a certain extent, lithography can also be considered as belonging to the group of subtractive processes.

The various processes can be combined in almost infinite combinations, but in order to obtain the best and most accurate tooling concepts it is of the utmost importance to consider the various process properties such as tolerances and material compatibility (see also selection criteria for tooling process chains).

Material Compatibility

For almost every micro-machining process imaginable, perhaps with the exception of water-jet erosion, the substrate or workpiece material plays an immensely important role regarding the feature sizes, aspect ratios, surface roughness and virtually any other property that can be obtained using the process. Table 17-1 lists some well-known material-process combinations, and some of the typical results that have been obtained in micro-machining.

TABLE 17-1 Typical Results Obtained using Selected Subtractive Micro-machining Processes and Materials

Material	Process	Hole Diameter (μm)	Aspect Ratio	Roughness (R_a) (nm)
German silver	Diamond turning	–	–	5
Silicon	Reactive ion etching	10	10	500
Steel	EDM	60	20	500
Aluminum	Milling	50	10	1000
PMMA	CO ₂ laser	100	20	2000
PEEK	Eximer laser	20	20	500

TABLE 17-2 Typical Results Obtained using Selected Additive Micro-machining Processes and Materials

Process	Material	Hardness (HV)	Aspect Ratio	Deposition Rate ($\mu\text{m}/\text{hour}$)
Magnetron sputtering	Copper	90	2	2
Electroforming	Nickel	440	2	70
PVD	TiN	1200	0.5	1
Pulse plating	NiCo alloy	580	3	20

Although the subtractive processes are by far the most widely used, the additive processes can in a similar manner also provide very different material properties and results. For some of the additive processes, such as printing and laser sintering, the main geometrical limitations are inherently in the processes themselves. Other additive processes, mainly electroplating (or electroforming) and physical deposition (PVD, CVD, magnetron sputtering, etc.) rely on other (subtractive) processes for the definition of the minimum obtainable feature size and other machining properties (Table 17-2).

For laser-based additive processes the minimum feature size is strongly related to the spot size of the laser beam, which again is interacting with the thermal and optical properties of the material that is being formed (particles sintered together or polymerization of monomers).

Using the physical deposition processes, which are all based on the condensation of materials within a chamber with extreme control of gas flows and pressure, a number of pure metals, alloys, ceramics and semiconductor materials can be deposited. Even with the best magnetron sputtering techniques, the deposition rate is relatively low. The processes are useful for building entire tools or tool inserts. However, the physical-deposition processes are essential for the deposition of hard-wearing resistant coatings, for applying electrically conducting layers on top of insulators and for many other surface-treatment or enhancement steps.

Electrochemical deposition can be divided into two major sub-groups, namely electroplating and

electroless or chemical plating. The first group uses an external power supply to generate the electrons needed for the deposition of metal, while the second group utilizes a chemical reducing agent to supply the necessary electrons.

Typical deposition rates for electroplating are from 10 to 400 $\mu\text{m}/\text{h}$. The greatest deposition rates are obtained using highly concentrated sulfamate nickel baths for the deposition of nickel stampers for the manufacturing of optical storage discs (CD, DVD, HD-DVD, Blue-ray discs, etc.). Electroless deposition processes, which can be used for the metallization of non-conductors such as polymers or ceramics, are typically at least ten times slower.

Since electrochemical deposition takes place at relatively low temperature (always below 90°C, and sometimes even at room temperature), the mechanical properties of the deposited materials can be quite different as compared to the values found for forged or molded parts. This is mainly because the grain size of the deposited materials is smaller, due to the low deposition temperature. Materials with small grain sizes (electroless nickel is considered to be amorphous [6]) result in high hardness values and the possibility to reduce the surface roughness of parts machined by diamond turning or micro-milling (Fig. 17-3).

Direct versus Indirect Tooling

Figure 17-4 is a simplified illustration of the four basic process chains for micro-tooling. The result

1																	2																		
H 0,07 - 1,008																	He 0,13 - 4,003																		
3		4																		10															
Li 0,53 - 6,941	Be 1,85 12 9,012																	B 2,34 - 10,81	C 2,22 - 12,01	N 0,81 - 14,01	O 1,14 - 16,00	F 1,51 - 19,00	Ne 1,20 - 20,18												
11		12																		18															
Na 0,97 70 22,99	Mg 1,74 25 24,31																	Al 2,70 25 26,98	Si 2,33 3 28,09	P 1,82 - 30,97	S 2,07 - 32,06	Cl 1,56 - 35,45	Ar 1,40 - 39,95												
19		20		21		22		23		24		25		26		27		28		29		30		31		32		33		34		35		36	
K 0,86 83 39,10	Ca 1,54 - 40,08	Sc 3,00 - 44,96	Ti 4,51 8,5 47,90	V 6,11 8 50,94	Cr 7,20 6 52,00	Mn 7,44 22 54,94	Fe 7,86 12 55,85	Co 8,86 12 58,93	Ni 8,90 13 58,71	Cu 8,92 16,6 63,55	Zn 7,13 35 65,37	Ga 5,91 - 69,72	Ge 5,32 - 72,60	As 5,73 - 74,92	Se 4,79 37 78,96	Br 3,12 - 79,90	Kr 2,60 - 83,80																		
37		38		39		40		41		42		43		44		45		46		47		48		49		50		51		52		53		54	
Rb 1,53 - 85,47	Sr 2,60 - 87,62	Y 4,48 - 88,91	Zr 6,49 - 91,22	Nb 8,55 7 92,91	Mo 10,20 5 95,94	Tc 11,50 - 99,0	Ru 12,40 - 101,1	Rh 12,40 8 102,9	Pd 12,00 - 106,4	Ag 10,50 19 107,9	Cd 8,65 30 112,4	In 7,31 - 114,9	Sn 7,30 20 118,7	Sb 6,70 9 121,8	Te 6,25 - 127,6	I 4,94 - 126,9	Xe 3,06 - 131,3																		
55		56		57		72		73		74		75		76		77		78		79		80		81		82		83		84		85		86	
Cs 1,87 - 132,9	Ba 3,50 - 137,3	La 6,17 - 138,9	Hf 13,10 6,5 178,5	Ta 16,60 6,5 180,9	W 19,30 4,5 183,9	Re 21,00 - 186,2	Os 22,70 5 190,2	Ir 22,60 6 192,2	Pt 21,50 9 195,1	Au 19,30 14,2 197,0	Hg 13,53 - 200,6	Tl 11,85 - 204,4	Pb 11,30 29 207,2	Bi 9,80 13 209,0	Po 9,40 - 210,0	At - - 210,0	Rn 4,40 - 222,0																		
87		88		89																															
Fr - - 223	Ra 5,00 - 226	Ac - - 227																																	

FIGURE 17-3 Portion of the periodic table showing the elements that can be deposited electrochemically from an aqueous solution [6].

of all four chains is a metallic tool insert, illustrating a simple tool for the replication of a micro-fluidic pattern.

For the indirect process chains, one particular process is common, and has some special demands on the choice of materials. Indirect tooling, additive or subtractive, always requires – at some point – the separation of the substrate and the almost-finished tool. A complex tool, with micrometer-sized features and high accuracy, is not easy to separate from a substrate using mechanical methods or brute force. Consequently, the gentlest way to effect the separation is to chemically dissolve the substrate. In this case the substrate material should be one that can be dissolved easily and cleanly, without damaging the surface or structure of the tool. There are other ways to effect the separation, such as: melting the substrate, providing a poor but well-controlled adhesion between the substrate and the tool, rapid cooling to enable the differences in thermal

expansion to force the two materials apart, and many others.

One of the safest separation processes is to use a simple solution of sodium or potassium hydroxide to secure the dissolution of substrates such as aluminum, zinc or silicon. This can be done cleanly and effectively without damaging tool surfaces of metals such as nickel or stainless steel, which form a passive layer that protects them from dissolution. In the case where aluminum or zinc alloys are used (typically on account of their easier machinability), the various alloying elements (Cu, Mn, Si, Fe, etc.) may create a layer on the tool surface which can be difficult to remove [7] (Table 17-3).

SELECTION CRITERIA FOR TOOLING PROCESS CHAINS

The focus of this section is on tooling for the mass replication of micro-components in polymers,

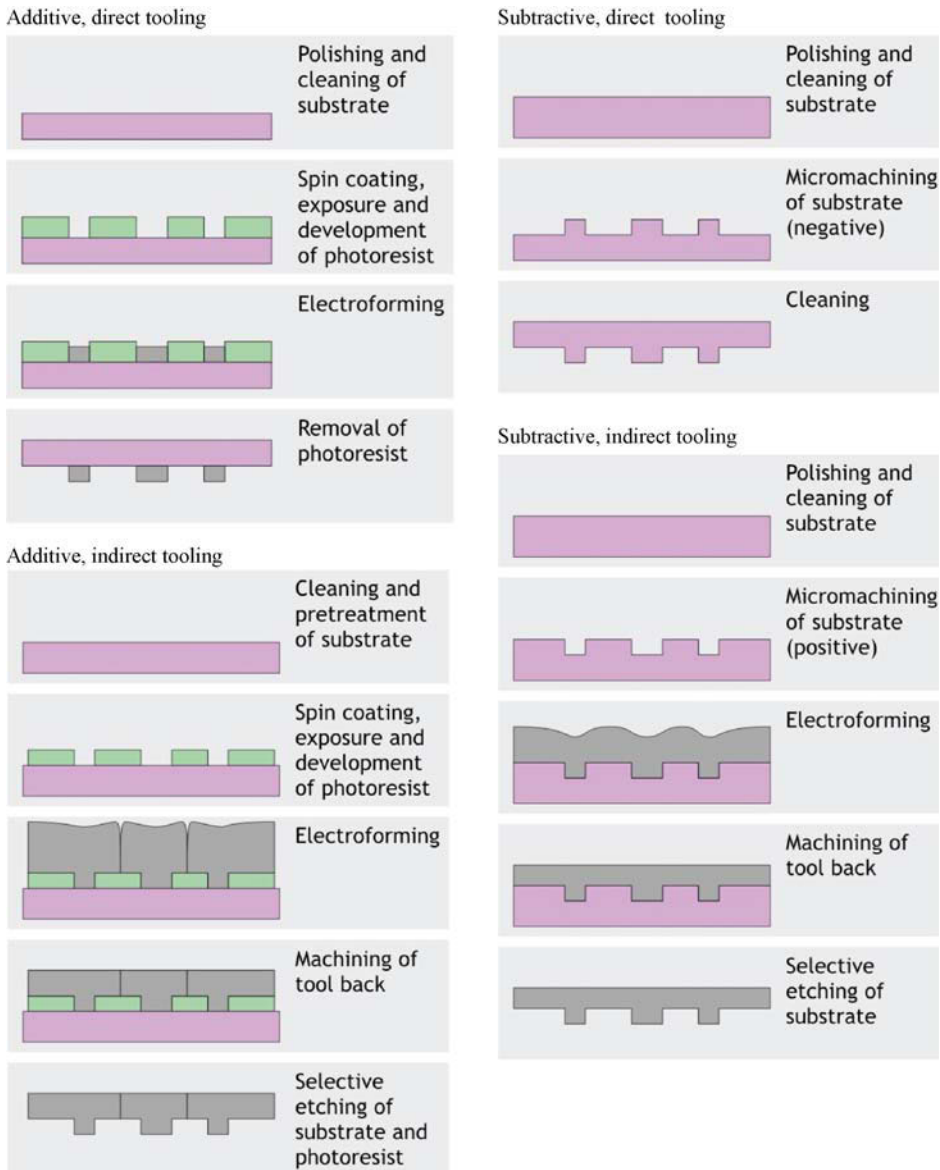


FIGURE 17-4 Schematic presentation of the four basic process chains for micro-tooling.

metals and ceramics. The tools considered are therefore essentially mold inserts, dies, punches, etc. carrying the negative geometry of the part to be produced. Normally micro-replication processes are used for the mass production of micro-components, with production volumes ranging from several thousands to millions of

units. However, it is not uncommon in applications where replication processes are used for prototyping in the product-development phase, particularly if the performance of the replication process has a critical influence on the design of the product. Thus the tool requirements will differ substantially, depending on the application.

TABLE 17-3 Chemical Solutions used in Indirect Process Chains for the Selective Etching of Substrates

Name (formula)	Conc. g/l	Temp. °C	pH	Etch Rate ($\mu\text{m}/\text{hour}$)										
				Ni	Cu	Au	Zn	Pt	Al	Pd	Cr	Ti	Si	
KOH	60	80	>14	0		0	X		X					X
HCl + HNO ₃		38	<0	X	X	X	X	X	X			X		
K ₂ S ₂ O ₈	25	25		▽	20	0	X	0	X	0	0	0	0	0
	25	40		▽	30	0								
(NH ₄) ₂ S ₂ O ₈	25	25		▽	25	0	X		X	0	0	0	0	0
	25	40		▽	35	0								
HNO ₃	200	25	0.2	5	X	0		0	X	▽	0	0	0	0
HCl	500	25	<0			0	X	0						
NaCN + NaOH	50 + 30	60	12.0	0	X	X	X							X

Circles mean that the material is not damaged by the etching solution, a triangle means that the substrate is stained or mildly etched and a cross means that it is heavily etched (and eventually completely dissolved). In some cases the etching rate is listed in $\mu\text{m}/\text{hour}$ [6].

The main issues influencing the tool requirements are:

- the chosen replication process;
- the production volume and thus the acceptable tooling cost;
- the material of the replicated part;
- the smallest feature size and the complexity (3D surfaces, through-holes, etc.).

For large series production, micro-mold inserts and dies must generally be characterized by high wear and corrosion resistance as well as by fatigue resistance. Except for these general requirements, the characteristics of the tool must match the demands set by the replication process. Hence, while mold inserts intended for polymer replication require a surface hardness of 300–550 HV, dies for micro-forging will require a hardness of above 1000 HV as a consequence of the greater stresses necessary for the plastic flow of the material.

When a mold is produced for prototyping purposes, the surface hardness of the tool falls to a lower level of priority, while the functional performance of the tool and/or process is the main concern. In this case mold inserts can be made in soft metals or alloys, such as aluminum or brass, simplifying tremendously the manufac-

ture of the tool. The complexity of the mold also influences the tool requirements. Tools with simple geometries and large tolerances are relatively inexpensive. In such cases, in the set-up phase of a mass production process, it can be acceptable to change the tool design based on the initial evaluation of the performance of the tool and the process using prototype tools. If, on the other hand, the tool is very complex and the cost associated with producing the geometry is high, redesign iterations must be avoided and the tool will be produced to last for as long as possible, selecting harder materials and setting higher demands on the tool-manufacturing processes.

Once the tool requirements have been defined, a coherent process chain that enables the production of the tool can be selected/defined. It is very important to note that at this point the tool design must not be considered to be rigidly defined. Indeed, based on the capabilities and limitations of the selected/available manufacturing processes, changes in the tool design are allowed in order to ease or improve manufacturing. The redesign (redesign for manufacturing) must of course ensure that the functionality of the tool and of the final part is not compromised.

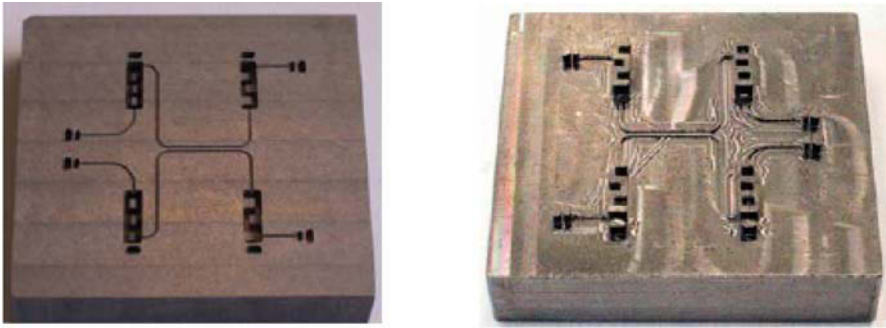


FIGURE 17-5 Micro-fluidic tooling. Aluminum master geometry for subsequent electroforming (left); hardened tool steel insert (right).

In many cases one single process will be able to generate the complete geometry of the part according to the requirements. However, in some cases more complex process chains might be chosen, either because they enable relevant improvements in terms of tool performance or simply because the tool cannot be produced otherwise. An important issue in drafting a process chain is the minimization of repositioning of the mold insert in proceeding from one process step to the next. Each time the insert is moved, alignment errors are introduced, reducing the tolerance window available for the individual manufacturing processes.

On the basis of the defined tool requirements a range of materials can be selected for the tool (mold insert, die, punch, etc.). The material must match the requirements in terms of surface hardness and at the same time allow the manufacture of all features within the prescribed tolerances by means of the available processes. In this respect, it is important to consider that the tool may not need to be machined directly from material having all of the required properties. Indeed, indirect tooling is often a more suitable solution for all those applications where a high surface hardness is not mandatory. Mold inserts for polymer replication show, in general, lower demands in terms of wear resistance and can therefore take advantage of the indirect tooling approach.

Another important point when selecting a tooling process chain is the type of features to be

realized and their relationship with the rest of the insert. As many micro-structuring processes are based on material removal (e.g. subtractive processes such as micro-milling, micro-EDM, etc.), the lesser the total amount of material to be removed, the faster will the tool production be completed. Thus when the tool is characterized by small cavities on a relatively large substrate, direct machining of the tool can be an advantage. By contrast, when the tool is characterized by small protrusions that are relatively isolated on a large substrate, indirect tooling is often the best approach, as in this case the machined master (having the opposite geometry to that of the tool) would consist of small isolated cavities on a large substrate (see Fig. 17-5). The two cases considered here represent two extreme configurations, where the convenience of one approach or the other is apparent. There are many intermediate configurations between those two cases, such that the choice of the most convenient approach might not be so evident and other considerations might become determinant. In those cases when additive processes are used for the micro-structuring of the mold or master, the convenience of either the direct or indirect approach with respect to features type is obviously reversed.

Tool requirements and thereby the final tool material, the type of geometry and the type of processes (additive or subtractive) available for the generation of the basic 3D geometry concur in determining the chosen tooling approach (direct or indirect). At this point the most critical

choice regards the combination of the specific 3D structuring processes used to generate the insert geometry and their sequence. In selecting the tooling approach an idea of the structuring processes available is of course necessary, as this could be a major limitation and enforce the employment of many of the choices discussed above. The process-sequence selection must be compatible with the limitations of the individual processes with respect to machinable materials, machinable geometries, achievable accuracy, minimum feature size, surface and sub-surface characteristics. The capabilities and limitations of a number of micro-structuring processes with respect to tooling applications will be discussed later. The sequential order of the micro-structuring processes concurring in the generation of the tool must be defined with focus on productivity, minimization of alignment errors and compatibility of the succeeding process steps. In fact, subsequent process steps influence each other in complex ways, originating forward coupling (one process step influences the outcome of the following process steps) and backward coupling (one process step influences the features generated by the previous process steps).

APPLICATIONS

Application 1: Polymer Micro-fluidics

Injection molding or hot embossing of polymer micro-fluidic components is a promising area, but also one of the relatively few areas that can already demonstrate real production capability and commercial applications.

Mainly depending on the required production capabilities, the first thing to decide upon is the replication process. Generally, injection molding is preferred for mass-production applications, while hot embossing is adequate for smaller series and prototyping. In some cases, unusual requirements such as channels widths of below 100 μm , combinations of wide and narrow channels, through-holes, embedded optics, 3D channeling, etc., can change this general perception, since the two replication processes have their own unique

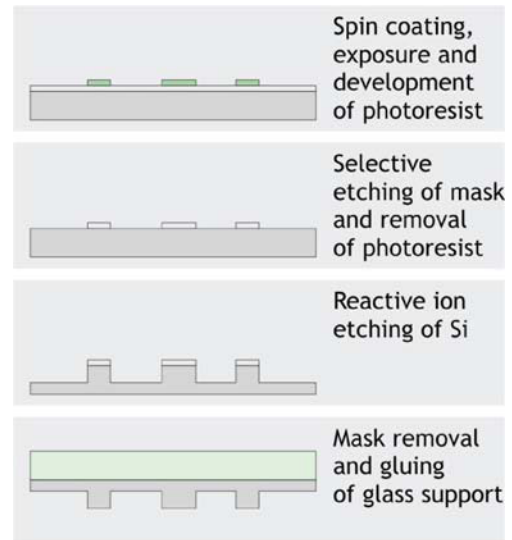


FIGURE 17-6 Process chain for the fabrication of a silicon embossing tool for the manufacturing of a small series of polymer micro-fluidic components.

features that might be exploitable for a special requirement (Fig. 17-6).

A more durable tool, compared to the silicon/glass hybrid illustrated above, is necessary for injection molding. In order to be able to produce a metallic tool, and still be able to have channel widths and other features in the 20–40 μm range, an indirect tooling concept based on EDM and electroforming was reported recently [8]

Application 2: Die/Mold Fabrication for Micro-bulk Forming

Different tooling approaches were applied and compared on the basis of a cold-forged industrial micro-component as shown in Fig. 17-7. The component consists of seven diameters and a non-symmetrical geometry at the top. The largest diameter is 3 mm, the smallest outer diameter is 0.6 mm and the length is 3 mm. This component is currently fabricated using cutting. Micro-cold forging is highly attractive, since the productivity can be increased up to 100 times using cold forging compared to cutting. The component must be produced using a two-step cold forging procedure [1].

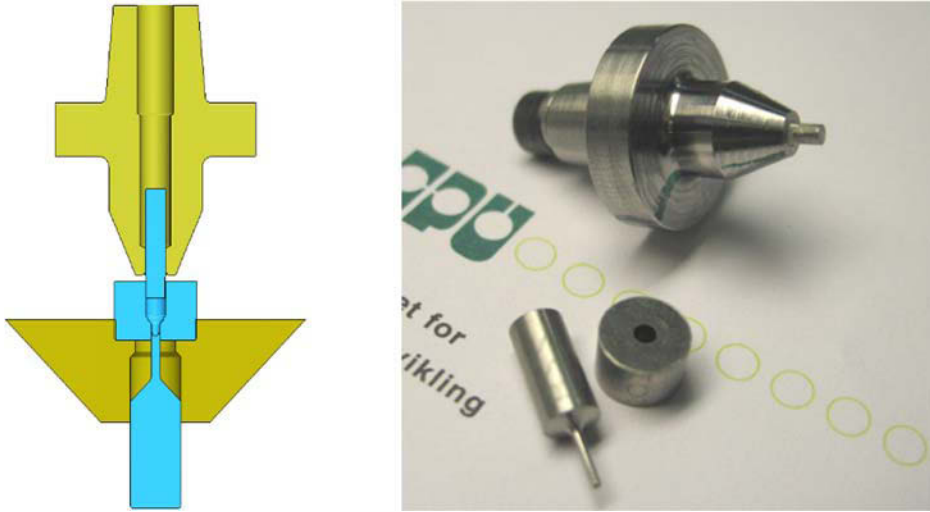


FIGURE 17-7 Direct Die Manufacturing by Micro-EDM Milling.

Two different approaches were followed in order to manufacture the die. The direct tooling approach includes micro-EDM milling. The chosen tool material is a slice of an 8 mm ISO 8020 form B cutting punch made of Vanadis 23 hardened to HRC62-64. By using micro-EDM milling with a 0.3 mm electrode, the die was machined in less than one day. Figure 17.7 illustrates one of the dies.

In the indirect tooling approach, a cathode of aluminum was machined to an outer geometry

similar to the inner geometry of the die. A hard nickel alloy is deposited on the aluminum. Subsequently, the aluminum can be etched away, leaving a die with the required inner geometry (Fig. 17-8). The method has been tested with three different nickel alloys. At present, a die with a hardness of 440 HV25g has been tested in the forging of a lead billet. A die with a hardness of more than 800 HV25g is currently being produced. A qualitative and quantitative comparison of the two molds obtained using the two

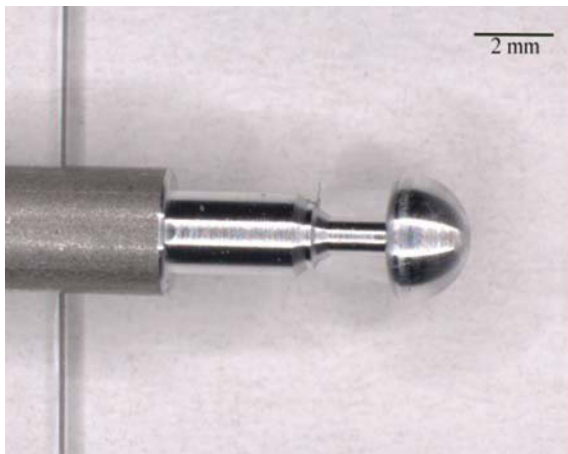


FIGURE 17-8 Indirect Approach for Dies for Micro-metal Forming. Turned Geometry (left) and Cross-section of Electroformed Die (right).

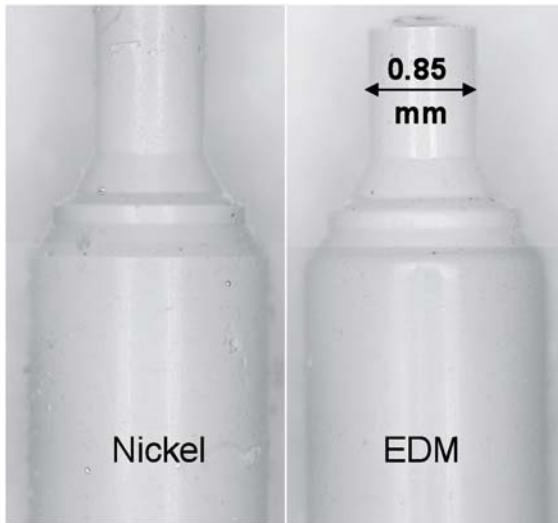


FIGURE 17-9 Replicas of Dies for Micro-metal Forming.

different methods was performed. A silicone replica of the inner geometry of both molds was taken and analyzed by optical methods (Fig. 17-9). It is seen that the EDM approach yields non-sharp corners, whereas these can be obtained in the indirect approach. Furthermore, the dimensions are comparable and within specification for both methods.

CONCLUSIONS

This chapter has introduced the concept of tooling process chains for micro-manufacturing. Two main approaches have been described: indirect tooling and direct tooling. The building blocks

of tooling process chains can be combined in numerous ways and obtainable dimensions and geometries are dependent on specific choices of these building blocks. Selection criteria for tooling process chains were discussed and application examples presented.

REFERENCES

- [1] N. Taniguchi, Current status in, and future trends of, ultraprecision machining and ultrafine materials processing, *Annals of CIRP* 32 (2) (2003) 573–582.
- [2] L. Alting, F. Kimura, H.N. Hansen, G. Bissacco, Micro engineering, *Annals of CIRP* 52 (2) (2003) 635–658.
- [3] M. Geiger, et al. Microforming, *Annals of CIRP* 50 (2) (2003) 445–462.
- [4] U.R.A. Theilade, Surface micro topography replication in injection moulding, PhD thesis, Department of Manufacturing Engineering and Management, Technical University of Denmark (2005).
- [5] U.A. Theilade, H.N. Hansen, Surface microstructure replication in injection molding, *The Int. J. of Advanced Manufacturing Technology* 33 (2007) 157–166.
- [6] P.T. Tang, Fabrication of micro components by electrochemical deposition, PhD thesis, Department of Manufacturing Engineering, The Technical University of Denmark (1998).
- [7] P.T. Tang, A method of manufacturing a mould part, WO (PCT) 2006/026989 A1.
- [8] G. Tosello, G. Bissacco, P.T. Tang, H.N. Hansen, P.C. Nielsen, Micro tools manufacturing for polymer replication with high aspect ratio structures using μ EDM of silicon, selective etching and electroforming, *Microsystem Technology* (2008) 10.1007/s00542-008-0564-9.
- [9] H.N. Hansen, M. Arentoft, Precision tooling technologies for micro forming, Proc. of the 2nd International Conference on New Forming Technology, Bremen (2007) 157–165.

Handling for Micro-Manufacturing

Antonio J. Sánchez

INTRODUCTION

Presently, a large number of industrial developments are being made for compact products. The trend toward miniaturizing products such as electronic, optical and mechanical devices is motivating fundamental innovation in production processes. These compact products are composed of micro-components which are fabricated using different kinds of micro-manufacturing machines. Therefore a micro-manufacturing plant must be composed of different kinds of manufacturing machines and several inspection, assembling and packaging stations.

At a micro-manufacturing facility, the handling process includes transporting components from one location to another, orientation control and sorting. It is essential that the components are presented in a specific position, are facing the right direction and are at a suitable rate at all workstations. These points are the main objectives of a handling system. The aim of this chapter is to emphasize the importance of the handling process in micro-manufacturing, compared to conventional manufacturing at a meso-scale.

Several definitions can be found in the literature to characterize meso-handling and micro-handling domains. In this chapter the following definitions have been adopted. Micro-handling is basically the manipulation of small parts with high accuracy. Typical part dimensions are in the range of micrometers up to a few millimeters.

The typical location accuracy is in the range of 0.1 to 10 microns. Meso-handling is concerned with the transport and location of parts greater than a few millimeters (as a reference, the meso-domain is defined as products fitting in a box of $200 \times 200 \times 200 \text{ mm}^3$).

Automated positioning at the meso-scale is easily solved using conventional closed-loop control and a variety of sensors. In meso-handling, the main challenge concerns the picking of objects and the subsequent development of tools that are stiff enough to resist the effects of gravity and inertial forces. However, automated positioning at a micro-scale becomes a difficult problem. When the size of the components decreases, handling becomes the bottleneck in the fabrication process and the most expensive task, owing to automation difficulties. This is especially true for very small components that require very restricted positioning tolerances. The main handling challenges at an automated micro-manufacturing plant are: (1) how to transport the micro-components between the different stations (inter-machine transport problem) and (2) how to handle the micro-components at an intra-machine station (intra-machine micro-handling problem).

One key feature that characterizes micro-manufacturing facilities is the need to manipulate a large number of different micro-components. This chapter is focused on the serial pick-and-place approach. However, given that

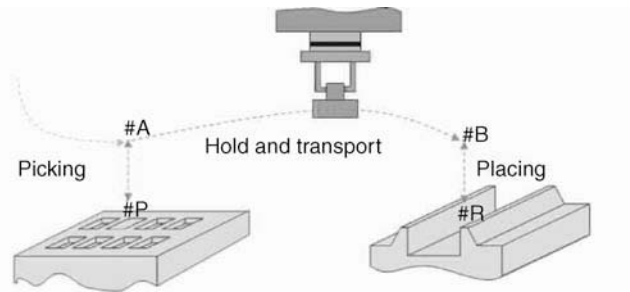


FIGURE 18-1 Pick-and-place task.

micro-fabrication processes can yield thousands of micro-parts, it is interesting to consider whether a large number of micro-parts can be handled simultaneously. This class of micro-handling is called the parallel approach [1].

SERIAL PICK-AND-PLACE TASK

The handling task of picking a part from #P location and placing it at #R location is called a 'pick-and-place' task (see Fig. 18-1). Serial micro-handling is a concept used in conjunction with a manipulator and a gripper, which must perform pick-and-place cycles for each object. A serial pick-and-place task is composed of the following sub-tasks:

1. Picking sub-task
2. Hold and transport sub-task
3. Placing sub-task.

Each sub-task is composed of a sequence of actions. Consider the following list of possible actions for the pick-and-place task:

1. Grasp actions (close the gripper, set vacuum, etc.)
2. Move actions (approach, depart, transport, etc.)
3. Release actions (open the gripper, reset vacuum, vibrate, etc.).

The 'move' actions will be performed by a manipulator and the 'grasp' and 'release' actions will be performed by a gripper which will be based on different types of grasping principles (stick, friction, suction, magnetic, etc.).

The complete sequence of actions in a pick-and-place task is described in Table 18-1. The picking sub-task includes the actions for grasping

the part from #P location. The hold and transport sub-task includes the actions to transport the part from #A to #B location. Finally, the placing sub-task includes the actions to place the part at #R location.

This chapter provides an overview of the fundamentals of the micro-handling process, with particular reference to the serial pick-and-place task. After a brief description of inter-machine transport systems, the principal requirements, methods and components of intra-machine micro-handling systems are presented. The chapter ends with a short discussion of different handling applications.

INTER-MACHINE TRANSPORT SYSTEMS

The evolution of new types of micro-components has contributed to an inefficient proliferation of separate and sometimes even unique special-purpose machines. For example, the use of specialized stand-alone equipment for assembling, inspection, packaging, etc., inherently requires multiple queuing steps for each machine as well as returning the components to an interim packaging mode between stations.

A flexible and automated transport system must be integrated in a fully automated micro-manufacturing facility. In any multi-task automation system, the need to simultaneously perform operations with different time cycles presents a difficult challenge. It is also important to build flexibility into multi-function stations to accommodate variations in overall production requirements. Some automation

TABLE 18-1 Sequence of Actions in a Pick-and-Place Task

Sub-task	Action	Velocity	Trajectory
Picking	0. Move to #A	100%	Joint space
	1. Approach to #P	30%	Cartesian space
	2. Grasp	0%	Cartesian space
	3. Depart to #A	70%	Cartesian space
Hold and transport	4. Transport to #B	100%	Joint space
Placing	5. Approach to #R	30%	Cartesian space
	6. Release	0%	Cartesian space
	7. Depart to #B	70%	Cartesian space

approaches include rotary-turret architectures and linear pick-and-place architectures based on carriers.

Rotary-dial indexers are well established in the industry for their efficiency, flexibility and ability to deliver high speed performance. These systems generally use central, high accuracy, direct-drive indexing to synchronize a number of operations nested around the circumference of the dial. Rotary-turret system designs offer a simple, rugged-core mechanism that can be used for integrating a variety of assembling, inspection and other processing operations on individual stations around the periphery of the rotary-indexer platform. Some of the primary advantages of rotary-indexed architectures are simplicity, precision, reliability, durability, and high throughput within a relatively small footprint.

Although rotary-turret architectures generally provide the most efficient approach for the high speed integration of most applications, linear pick-and-place architectures can also be the best choice for certain applications. For example, systems that process parts from carrier-to-carrier or carrier-to-tape often can benefit from using a linear pick-and-place strategy instead of rotary-turret architecture. The use of carriers throughout the stations makes it most efficient and appropriate to feed the machines directly from carriers (see Fig. 18-2). By combining advanced carrier-scan techniques with multi-head pick-and-place systems, linear architecture can deliver a balanced

combination of flexibility and speed that fits smoothly into carrier-oriented production-floor operations.

Standard Carriers

A key problem area limiting the emergence of automated micro-handling technology is the lack of standardization, which causes equipment makers to spend an excessive amount of time and resources on custom-automation solutions [2].

A carrier or tray is a flat magazine that can take up pieces for storage, transport and handling in an orderly manner and is adaptable to automatic piece-feeding to the production equipment.

A cassette or cartridge is a container for carriers, which can be plugged into production equipment for the purpose of automatic feeding.

There are some standards defined for micro-handling issues. However, many standardized systems are available in the semiconductor industry, where some examples are:

1. **Trays:** standardized plastic carriers (2 or 4 inches) (50.8 or 101.6 millimeters) with depressions for the individual placement of components. The parts move freely within the limits of these depressions. Manufacturers offer standard-sized depressions in a range of variations. To protect the components, the trays are closed with a lid with accompanying retaining clips.
2. **Gel packs:** components are held by adhesion to glass or plastic carrying materials with gel

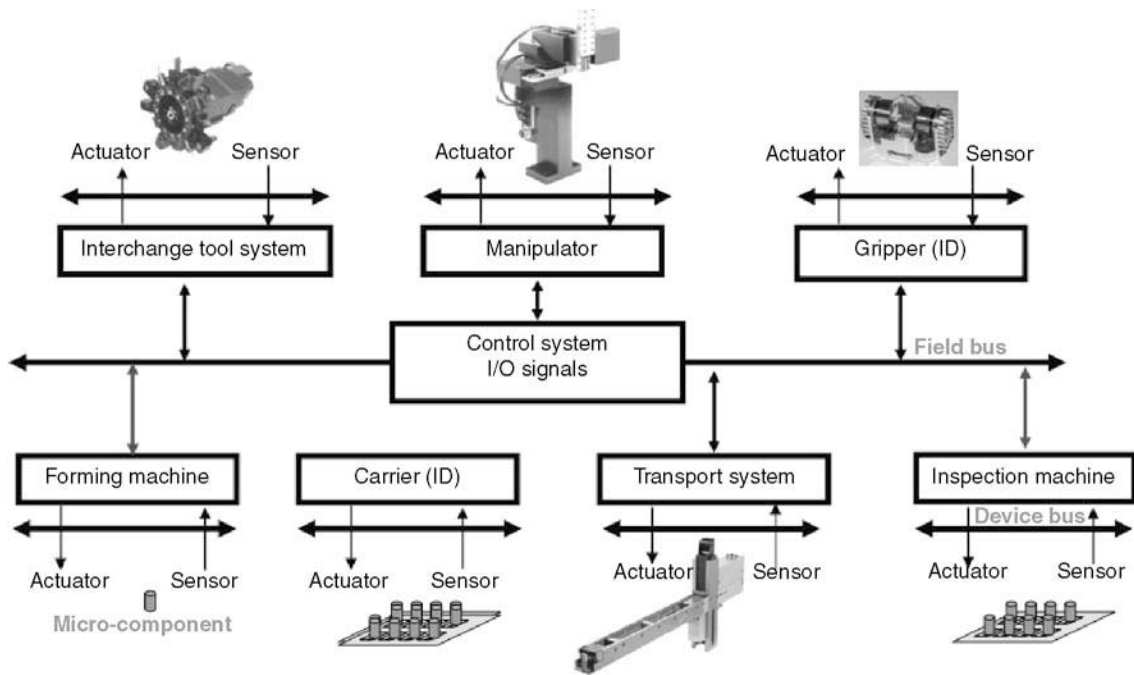


FIGURE 18-2 Linear pick-and-place concept based on carriers.

coatings. Gels with different levels of adhesive strength are available depending on the sizes of the components.

3. **Belt magazines:** a belt magazine has a band made with depressions into which the component is locked by a covering layer of foil. For small pieces, plated and embossed belts are available to enclose the components.
4. **Tube magazines:** in the case of tube magazines, the components are either stacked or lined up. The lengths of the tubes, which are made of plastic, are shaped like the components themselves, thus preventing the components from becoming distorted.

In general, a dimensionally specific carrier is well suited for large volume production where changes of micro-component types are not frequent.

Conventional Transport Equipment

Conventional transport equipment such as stockers, vehicles, conveyors, manipulators, indexers and lifters are used for transporting materials,

components and tools between the different stations in a linear pick-and-place plant based on carriers.

Conveyors usually consist of a looped belt or chain moving along a predetermined path. Instead of conveyors, vehicles could be more flexible and easier to adapt to changes in the environment. Both conveyors and vehicles are used to transport the carriers and cassettes between the different stations. Some examples of transport equipment are: a person-guided vehicle (PGV); an overhead-hoist transport (OHT); a rail-guided vehicle (RGV); and an autonomous-guided vehicle (AGV).

1. An OHT is a conveyor suspended from the ceiling that loads/unloads carriers or cassettes.
2. An AGV is a trackless mobile robot typically with a single gripper, a single manipulator and two buffers. A buffer refers to a place on the vehicle where one or two carriers can be placed. Loading/unloading of carriers and transfer between two carriers can be performed.

3. An RGV is a rail-guided mobile robot of which there are several types with various numbers of grippers, manipulators and buffers.
4. Finally, a PGV is a person-guided vehicle. There are several types of vehicle, as with the RGV.

Other components such as optical character recognition (OCR), ionization units, carrier ID or light curtains are occasionally added, based on system requirements.

INTRA-MACHINE MICRO-HANDLING SYSTEMS

A key problem area limiting the emergence of automated micro-handling technology is the non-availability of flexible and highly precise micro-handling machinery [2].

The most significant difference between meso- and micro-handling is the required positional accuracy of automatic handling systems. Micro-handling often requires sub-micron precision. This degree of precision is beyond the calibration range of the normal open-loop precision-handling devices used in industry. Closed-loop strategies, such as real-time vision feedback, are required to compensate for poor kinematic models and thermal effects. Additionally, in micro-handling the structural vibration due to link flexibility must be controlled at a sub-micron level.

Another major difference between handling in the meso- and micro-domains is the mechanics of object interactions. People usually think in meso-scale terms, but when talking about handling methods at the micro-scale, gravity and inertial forces cannot be considered the main forces being applied to the part. In the micro-world, surface forces dominate due to scaling effects, and the mechanics of manipulation can be unpredictable. For example, when a gripper opens, the part may not drop downwards.

Finally, it is necessary to emphasize that micro-handling requires greater care in manipulation and in cleanliness because the micro-parts are very fragile. Usually it is mandatory to control the

grasping forces and to work under clean-room conditions.

Since micro-scale positioning becomes a difficult problem, manual micro-handling is the most commonly used method. In this case micro-handling tasks are carried out by operators, who position and align objects manually in a specific station. The application of tele-operating micro-handling, which transforms the human operator's hand motion by means of a joystick into the finer 3D motion of the system's manipulator systems, is normally tailored to specific complex tasks. Finally, an automated serial pick-and-place task is only applied to micro-parts which can be handled and released using a well-suited gripper.

A micro-handling system is composed of the following sub-systems:

1. Micro-part feeder sub-systems;
2. Fixture and gripper sub-systems;
3. Sensor and control sub-systems.

Significant Forces at the Micro-scale

In micro-handling, surface forces such as friction or adhesion are immensely more significant than in meso-handling. Therefore at the micro-scale (masses $< 10^{-6}$ kg), gravity forces are not significant compared to surface forces, and releasing an object becomes a real challenge due to adhesion between the micro-part and the tool (see Fig. 18-3).

Formally, a force is defined to be short-range if it decreases with distance quicker than d^{-n} where n is the dimensionality of the system (usually 3). Short-range interactions are commonly dealt with by imposing a cut-off to the potential $V(d)$, d_c , beyond which $V(d)$ is set to zero. On the other hand, long-range forces have a range of infinity.

Inter-molecular and surface-force interactions are classified into several categories. The first category includes long-range attractive interactions that bring particles to surfaces and establish adhesive contact. These forces include van der Waals, electrostatic, and magnetic forces. The second category of forces is focused on adhesion, including diffusion, condensation, diffusive mixing, mutual dissolution, liquid and solid bridges

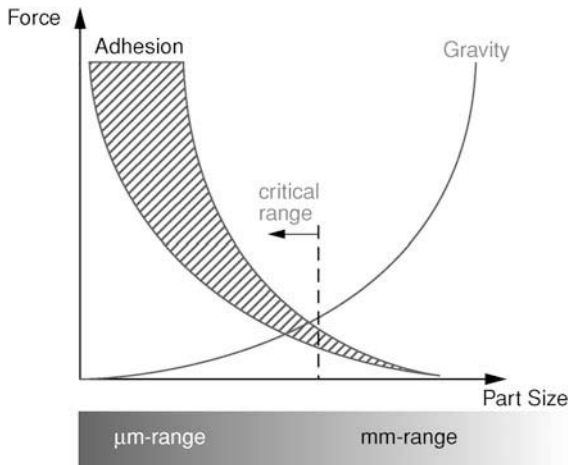


FIGURE 18-3 Significant forces depending on part size.

between particles and surfaces, and capillary forces. The third category includes very short-range interactions, which can contribute to adhesion only after an adhesive contact area has been established. These forces include chemical bonds, intermediate bonds and hydrogen bonds.

Balancing these forces depends on environment conditions, such as humidity and temperature, the surface condition, material properties, geometry, and relative motion. Micro-handling is quite different from meso-object manipulation. To manipulate micro-objects, one must consider micro-physics and pay attention to environmental conditions.

There are three main adhesive forces that are important for handling micro-parts: van der Waals, capillary and electrostatic forces [3]. Van der Waals forces come from inter-molecular potentials and are always present. Capillary- or surface-tension forces depend on the humidity of the environment and electrostatic forces are due to the tribo-electrical phenomenon. Much work has been done by several authors, who have presented the principles of van der Waals forces, surface-tension forces and electrostatic forces [4–5]. Some authors have described numerical methods to compute the van der Waals force between a smooth sphere and a smooth rectangular block [6] or to compare capillary effects with surface-tension forces [7]. However, micro-parts have

different shapes with considerable surface roughness and often show large deformation in the contact region. As a consequence, theoretical predictions are rarely applicable in practice.

In order to improve micro-part manipulation, different strategies have been set up to deal with these surface forces [6,8]. First, the effects of surface forces, F_{adhesion} , can be reduced by choosing an adapted set of manipulation parameters. This can, for example, be done by changing the coating. Surface-tension effects can be reduced with hydrophobic coatings, electrostatic forces by using conductive materials, and van der Waals forces by increasing the roughness profile.

Micro-part Feeders

A micro-part feeder always uses a certain number of functions to ensure the perfect treatment of a micro-part at the workstation. These functions are to: index; extract (isolate, disentangle, separate); sort; turn over; locate; guide; move; load/unload; release/seize; and recognize a micro-component. Micro-part feeders, which singularize and orientate parts prior to the station processes, are a significant bottleneck in successful automation.

The basic kinds of part-feeding, which are designed to feed and to orient the micro-parts, may be classified as follows:

1. Mechanical feeders;
2. Manipulator-based part-feeders.

Mechanical Feeders. Commonly used mechanical feeders for micro-handling are vibratory-bowl feeders and tape-and-reel systems.

The most common approach to automated feeding is the vibratory-bowl feeder, which consists of a bowl filled with parts guided by a mechanical track. The bowl and track are made to vibrate, causing parts to move on the track, where they encounter a sequence of mechanical devices such as grooves, gaps, balconies, etc. Most of these devices are filters that reject parts in all orientations except for the desired one. Thus a stream of oriented parts emerges at the end after successfully running the full track.

Another particular form of mechanical feeder is known as tape-and-reel for feeding parts of

relatively small sizes, which can be placed on tapes of standard width. Tape-and-reel is a method of housing parts in separate cavities in a long continuous strip. The cavities are covered with a plastic sheet to facilitate winding the strip around a reel for component presentation or feeding to automated placement equipment. These particular mechanical feeders are based on standard belt or tube magazines.

For large-volume manufacturing, the employment of a dedicated mechanical part-feeding apparatus may be justified. However, mechanical feeders often fail due to jamming, and, most significantly, generally require retooling when a micro-component is changed.

Manipulator-based Part-feeders. Another common feeding concept is the use of a specially designed carrier for each micro-part family to maintain sufficient accuracy for a completely preprogrammed manipulator. In this case, the manipulator will perform a serial pick-and-place task using a specific gripper mounted on the manipulator.

Conventional manipulators do not meet the repeatability and accuracy requirements needed in the micro-world because joint backlash, temperature drift and structural vibration must be controlled at the sub-micron level.

The state-of-the-art of precision industrial manipulators is summarized in Table 18-2. This table shows the most important parameters of the workspace, the accuracy, the velocity and the load capacity of different manipulators. The most common configurations are SCARA (RRP) and Cartesian (PPP) manipulators, but other configurations are also available. There are important differences in degrees-of-freedom (DOF), accuracy, workspace and load. The most accurate manipulators have reduced speeds. Cartesian manipulators are usually slower than SCARA-type robots, but have greater precision.

Micro-handling flexibility would denote that different products with similar scales and complexity levels are handled at the same station without any hardware modifications, but with software changes. Although there are technological and economic limitations to reach in such a goal,

shorter product life and constant product changes demand greater flexibility in the handling process. The most common principle for achieving flexibility is vision-based flexible part-feeding, which is a concept used in conjunction with a manipulator, whereby the manipulator uses a vision system to locate micro-parts that can be randomly scattered on a conveyor belt. Randomly oriented parts have to be positively identified and accurately located everywhere within the camera's field of view.

The cost and performance of a micro-handling system can be significantly improved by carefully considering issues at multiple scales: precision, compliance, modeling, gripping, fixturing, tolerance, and control. One of the basic challenges in precision handling is the need for very high accuracy over a large range of motion. This fact involves the design of handling tools and processes at multiple scales, and their integration into coherent system architectures. One possible approach to micro-handling systems is to improve the performance of standard manipulator systems. A conventional robot for coarse motion with low accuracy but long traveling distance is used and there is a fine-positioning device between the end effector and the robot with high accuracy and a very small traveling distance.

Existing solutions have the common feature of being expensive and bulky. Due to their dimensions, they are sensitive to environmental perturbations such as vibrations or temperature drifts. A general trend is to reduce manipulator size. The aim is to improve the system's immunity to environmental perturbations such as vibrations and thermal drifts. The development of such robots is now being made possible by new technologies, in particular by zero-backlash micro-gears and highly dynamic micro-motors with integrated incremental encoders, which allow manipulator structures to be miniaturized.

Fixtures and Grippers

Fixtures are used to hold micro-components during machining, inspection and assembly processes. The use of precision fixtures can mitigate

TABLE 18-2 Some State-of-the-Art Industrial Micro-manipulators

Model	By	Type	DOFS	Rep. Acc. (um)	WS (mm)	Load (kg)	Speed (mm/s)
E2C	Epson	Scara	4	8	R250 Z100	5	P&P 0.39 s
RP-1AH	Mitsubishi	Scara	4	±5	150 × 105 × 25	1	400 P&P 0.28 s
YK-120X YK-150X	Yamaha	Scara	4	5–10	R110 Z30	0.5	700–2000 P&P < 300
Tusboscara SR4-Plus	Bosch	Scara	4	±50	R400 Z200	2	1600
Autoplace400	Sysmelec	Cart	4	±2.5	150 × 150 × 150 85 × 85 × 75	4	
MP63-25DC	Feinmess	Cart	3	5	25 × 25 × 25	2	5
MP84	Feinmess	Cart	3	3	25 × 25 × 25 100 × 100 × 100	1.5	250
1940	Kopf	Cart	3	1	128 × 128 × 128		
MM3A	Kleindiek	RRR (antr)	3	1	100 cm ³ z:12 x,y:180°		10
Klocke	Nanomanip	RRP (spher)	3	0.001	5 × 5 × 19		5
MRSI							
Exfo	PCS-4100	RPPPR	5	0.4	25 × 25 × 25		2
Semprex	Univ. pipette manipulator	PPRPP	6		75 × 33 × 25 95° 75,200		
Somapatch	MW3R/L	CART	3	0.25	5 × 5 × 5		
MRSI	Newport	PPPR	4	±10	415 × 415		9000

the need for high positional accuracy. V-groove structures, datum points or other minimum energy surfaces should be used as much as possible to guide the micro-parts into their desired positions and orientations.

Micro-grippers are used to grasp, hold and release micro-components during the handling process. Compliance analysis of micro-handling, including both the gripper and the micro-part, is critical for reducing the necessary positional accuracy of the system, and therefore the cost. The handling system need not require the same precision as the tolerance of the locations if proper use is made of compliance, gripping and fixturing.

Grasping Principles. A grasping principle is the physical principle which produces the necessary force to get and maintain a part in a position with respect to the gripper. Some grasping principles are well known in the meso-domain: friction-based gripping [9]; form-closed gripping [10]; suction-based gripping [11–12]); and magnetic gripping.

Other principles, based on adhesive forces, are particularly applicable in the micro-domain [13]. One example is the use of electrostatics, or the charge difference between the gripper and the part [14–16]. For small, low weight parts, the capillary force and the surface tension of a liquid between the gripper and the part can be sufficient to hold the part [17–18]. Van der Waals force is another grasping principle [19]. Cryogenic gripping means that a small amount of liquid is frozen between the gripper and the part, so that the adhesive property of ice produces the required force. To release the part, the frozen material is broken, and/or molten and evaporated [20]. Ultrasonic pressure waves can also be used to lift a part. Since these forces are small, only extremely light parts can be handled in this way [21]. A focused light source, for example a laser source, can produce a pressure which is sufficient to lift small parts. To compensate for the mass of the part, the operation may take place in a liquid [22,23]. The Bernoulli effect has also been demonstrated to be applicable for raising small parts; an airflow between gripper and part causing a force which brings the gripper and the part close together.

Grasping Requirements. Some grasping principles can only be applied when the environment in which the operation takes place meets certain demands, or, the other way around, the environment puts constraints on the selection of the grasping principle. In some cases conditioned environments are applied. Micro-handling may for instance take place in clean environments, in dry environments, or in a vacuum. The substrate is important because adhesive forces occur between both the part and the gripper and also between the part and the substrate. One possible attractive alternative is to manipulate parts while they are immersed in a fluid, which eliminates electrostatic and surface-tension effects. Fluidic transport provides a powerful means for handling components in many micro-systems and is increasingly being employed in a number of such applications.

Some grasping principles put constraints on the type of material that can be gripped. Where appropriate, the material type of the top layer, a coating for example, must be considered. Adding coatings to parts is a possibility that enables the application of a grasping principle which could not have been applied otherwise. Some examples of the relation between the grasping principle and the material type are: (1) the hydrophilic properties of the material are important for the application of adhesive gripping; (2) gripping using magnetism demands ferromagnetic materials.

The interaction between the gripper and the part takes place via the part's force-interaction surface. This surface must be available for force operation throughout the entire pick-and-place cycle, for example from picking up a part at a feeding position through to releasing the part in the final position. Technical executions of grasping principles demand a certain configuration and shape of the force-interaction surface. Friction-based gripping will demand at least two locations on the side of the part for finger placement. Several other principles only demand one accessible part surface. In developing a grasping solution, it should be noted that geometric constraints may impose limitations on the availability of part surfaces.

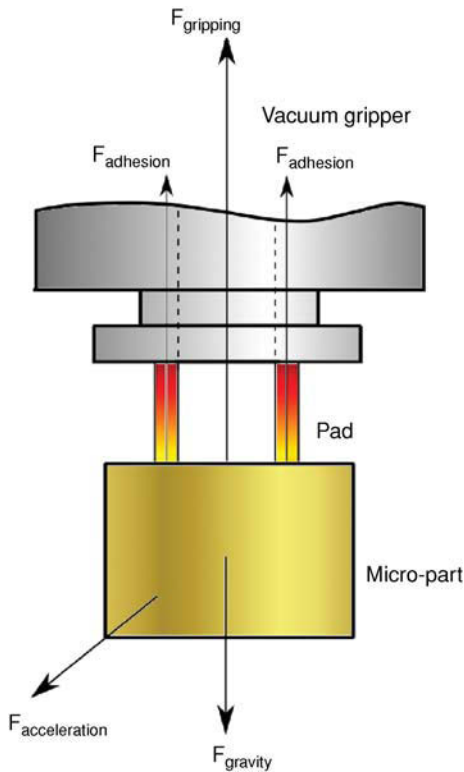


FIGURE 18-4 Force vectors in a contact-handling principle.

In the case of a contact-grasping principle, one possible situation that may occur during the release procedure is that the part may stick to the gripper and not remain static during the release action. In this case $F_{adhesion}$ is greater than $F_{gravity}$ (see Fig. 18-4). This situation would require a device that would hold the part in place during the gripper-release procedure. Such devices do not have to be complicated to design; one common method to overcome this problem is to use sticky paper with an adhesive force slightly greater than that of the adhesive force acting on the part and gripper.

Grippers. Suction grippers, such as vacuum grippers, consist mainly of a thin tube or pipette connected to a vacuum pump. This makes this kind of gripper cheap and easy to replace. This is important since micro-tools are fragile and have to be replaced frequently. The disadvantage is that the

vacuum gripper can obviously not be employed in a vacuum.

Tong grippers grasp a part employing friction between the part and the gripper, usually implemented using a pair of fingers. Gripping parts based on friction certainly provide sufficient force in many cases. Another advantage of this kind of gripper is the ability to center the part between the gripping jaws and to align it parallel to the jaws. This allows more precise handling of micro-parts by putting them in a defined location after being gripped. This is an important attribute in a handling system with a high degree of accuracy and speed. The more reference points that can be applied to the location of the micro-part, the fewer sensors that will be needed to determine the same information. However, with decreasing part size, the parameters of the gripper-finger dimensions need to be small also. Here a technical problem may occur, with this method having to be eliminated due to technical or cost perspectives.

Adhesive grippers utilize the surface forces discussed earlier. The easiest force to control is the electrostatic force, but it is not suitable for the manipulation of charge-sensitive devices. Surface-tension forces due to air humidity can be controlled by incorporating a micro-heater in the gripper. In cold conditions, an object can be picked up simply by touching it. To release the object, the heater evaporates the water in the contact. Common manipulation methods with surface forces include vibration of the gripper, sliding and inclining tools or using dual manipulators.

The disadvantage of contact strategies is that friction between the tool and the part may generate micro-dust from the object. Contactless grippers have several advantages compared to conventional contact grippers. A homogeneously distributed force enables the sensitive gripping of fragile parts. Disadvantages include low flexibility for different part shapes and the need for additional equipment, such as ultrasonic sources and pressure supplies. Contactless grippers include air-cushion grippers and ultra-sound levitation.

The principle of an air-cushion gripper is based on a vacuum prestressed air bearing. The gripper includes several arrays of pressure and vacuum

nozzles. These create an air cushion, separating the gripper and the micro-part, which is levitated about 10 microns underneath the gripper. The weight of the part has to be in equilibrium with the pushing and pulling forces exerted by the air cushion.

Another contactless gripping method is ultrasound levitation, which is based on a squeeze film or acoustic standing waves. Parts can be picked from above by the combination of ultrasonic waves and vacuum. The vacuum forces the parts to the gripper surface. The air cushion generated by the high frequency oscillation of the ultrasound sonotrode produces a repulsive force on the part. Finally, there is balancing of these two forces and the weight of the handled part. A further phenomenon that can be used for handling parts without contact is levitation based on acoustic standing waves. The arrangement consists of a reflector and a vibrating sonotrode, the assembly being called a resonator. The distance between the two elements is an integer multiple of half the wavelength. In the resonator, small parts are levitated in the pressure nodes of the standing wave.

Sensors and Control Systems

Obtaining accurate sensor information is difficult at a micro-scale as sensors can be too large to be placed in a tiny environment. The main sensors used at a micro-scale are displacement, vision and force sensors because motion control, visual servoing and force-control strategies are often required at micro-domains. These sensors have to be extremely sensitive as the forces and displacements involved are very small. Thus, to enable micro-manipulation, miniature sensitive sensors are needed.

Vision Sensors. Vision systems are often used for the recognition and positioning processes to locate the individual micro-components. The camera resolution must be compatible with the size of the manipulated objects. Optical microscopes and scanning-electron microscopes are therefore used. Applications in confined spaces require compact camera systems such as fiber-scopes or micro-cameras.

In a meso-domain, visually servoing has been shown to effectively compensate for uncertainty in the calibration of camera–lens systems, manipulators, and workspaces. However, manufacturing engineers usually prefer strongly calibrated parts-handling systems due to cost and reliability issues. In micro-domains precise calibration is highly dependent on precisely modeled kinematics, which is subject to thermal-growth errors. Two common techniques for compensating for thermal errors include the use of expensive cooling systems, or waiting several hours for the thermal equilibrium of the device to stabilize. These types of factors greatly affect the cost and reliability of handling systems, therefore real-time visual feedback can be used effectively and economically in a micro-domain. However, there are problems with visual control or image processing in controlling these systems. Some of the main problems are low processing speeds, high costs, programming difficulties and being error prone due to glare, reflection and other unwanted contaminants. Moreover, the manipulation tools may obstruct the view. Additionally, it is important to emphasize the problems in setting up image-processing equipment and the long down-times that are involved if an error occurs. Even processes that may seem straightforward such as focusing and aligning the camera properly become complicated and extremely difficult to carry out at these micro-scales.

In micro-handling, structural vibrations due to link flexibility must be controlled at the sub-micron level. Control of machine vibration becomes very important as designers attempt to advance the state-of-the-art with faster and lighter machines. Many researchers have examined different controller configurations in order to control machines without exciting resonances. Even with a sophisticated controller it is difficult to rapidly move flexible machines without deflections and vibrations. A more achievable goal is to eliminate residual vibration once the machine has achieved a desired set-point. Input shaping is a command-generation technique that reduces residual vibration when a machine is moved from one set-point to another. Input shaping works like

a notch filter that is designed to eliminate decaying sinusoidal responses.

Micro-force Sensors. A typical micro-force sensor structure is fabricated by micro-machining technology on a silicon wafer. A diode sensor has a cold-field emission cathode, which is a sharp silicon tip, and a movable diaphragm anode. When a positive potential difference is applied between the tip and the anode, an electric field is generated which allows electrons to tunnel from inside the cathode to the vacuum. The field strength at the tip and the quantity of electrons emitted (emission current) are controlled by the anode potential. When an external force is applied, the anode deflects and changes the field and the emission current.

Impedance control is a strategy adequate for both free- and constrained-motion control. It consists of an imposition of behavior on the system rather than tracking a reference value. Mechanical impedance is the dynamic relation between a force acting on a body and its motion:

$$Z(s) = F(s)/v(s) = M(s) + B(K/s)$$

where Z is the impedance, F the force, v the velocity, M the mass, B the damping and K the stiffness of the system.

Opposition of the body to the force consists of its stiffness, viscous damping and mass. The function of the impedance control is to impose the desired values for these three parameters instead of the real values.

APPLICATIONS

The serial pick-and-place task has been used extensively in the micro-manufacturing industry.

There are specific pick-and-place machines used for placing micro-components. The aim of this section is to show a few examples of handling applications which may refer to different kinds of processes, for example in micro-fabrication, inspection and assembly.

Micro-fabrication

The main intra-machine micro-handling task in a micro-fabrication station is the packaging of the fabricated micro-parts into a standard carrier.

Intra-machine Handling System in a Micro-forming Application

This example consists of the design of a micro-handling system, which arranges the micro-parts produced by a bulk-forming machine into a standard carrier.

The forming machine is set in a specific location and will leave the micro-pieces in an output buffer. This buffer guides the micro-parts along a mechanical track, like a vibratory bowl feeder system. A vision control strategy for actuating on the vibration will allow the individual micro-parts to flow in order to synchronize the buffer release process with the load process into the carrier cells.

The carrier has been defined following the DIN-32561 standard. This carrier is a small tray able to store hundreds of small pieces on it (see Fig. 18-5). The shape of the cells for locating the pieces depends on the piece shape. An empty carrier will be attached to a 2 DOF manipulator, which will move the carrier under the vibration sub-system, so that the empty cells in it are exactly below the buffer output, permitting the pieces to

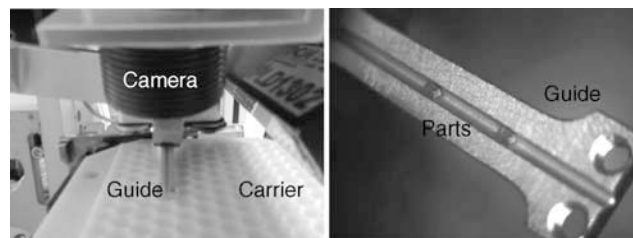


FIGURE 18-5 Vibration sub-system details.

fall into them. The vision system indicates to the manipulator when a micro-part is into the cell to proceed to locate the next empty cell.

When the carrier is full, the 2 DOF manipulator will move it to a specific location where the unload sub-system will take the carrier and put it into a cassette. The load sub-system will take another empty carrier and load it on the manipulator.

Inspection

Usually component inspection requires different points of view. A micro-handling system can be used to obtain all the views required for a complete inspection. For example, a rotational movement can be used for inspecting cylindrical surfaces.

Stent Inspection System. A cardiovascular stent is a small, expandable, slotted, metal tube that acts like a mechanical scaffold in an artery. Cardiovascular stents have hundreds of critical features with tight tolerances. These stents require 100% inspection over all surfaces.

Stent inspection has been traditionally accomplished by manually operated stereo-microscopy. The typical drawbacks of inspecting cylindrical surfaces with this method are non-referenced fields of view and the focal depths of stereo-microscopes, which increase operator fatigue and error. Often parts are rotated under the microscope while the operator is looking from checkpoint to checkpoint.

Nowadays the quality control of stents is made by an automatic visual-inspection system but the handling process is usually manual. In the sampling plant, the stent is inside a plastic tube, which protects it throughout the process. This tube is also useful for identifying one stent from the others. An operator manually extracts the stent from the plastic tube and inserts it into a needle. The operator fixes the needle on a rotary-gripping system in front of a vision system, and then the system rotates the needle while the vision system scans the stent surface. Once the automated inspection has been done, the operator removes the needle and extracts the

stent from it, puts the stent into the tube again and screws its top on.

The aim of this example is to describe a stent quality control application without human intervention. In this application all the manipulation is done by a 6-degrees-of-freedom manipulator. The whole handling system is composed of different sub-systems (carriers, unscrewing/screwing gripper, manipulator, funnel system, rotating disk, insertion pin).

The inter-machine transport system consists of a linear pick-and-place architecture based on carriers. The tube arrives in a carrier that is able to transport nine tubes (Fig. 18-6). This carrier approaches the inspection station on a powered belt conveyor. The manipulation process is divided into the following parts:

1. **Picking:** the manipulator picks the plastic tube from the carrier.
2. **Unscrewing:** the manipulator carries the tube to the unscrewing/screwing gripper and removes the screwed cap.
3. **Extraction:** the manipulator transports the uncapped tube to the funnel zone and empties its content (the stent).
4. **Gripping:** the funnel guides the stent to a vertical pin on the rotating disk, where it is inserted by gravity and vibration principles. A piezoelectric system mounted on the pin holds the stent.
5. **Inspection:** the pin is rotated to the horizontal inspection zone. There is a horizontal position to perform the machine vision quality control.
6. **Collection:** the pin carrying the analyzed stent is transported to the collection position, where the stent is released and put into the tube.
7. **Screwing:** the tube with the stent is taken to the unscrewing/screwing gripper where its cap is located and then screwed on.
8. **Placing:** the tube is placed in a new carrier.

The first task must be the opening of the tube. This must be done by a rotating four-fingered gripper. The fingers of the gripper are developed in order to accurately grip the top of the transporting tube.

A 6-degrees-of-freedom manipulator is needed, in order to be able to move the tube around the

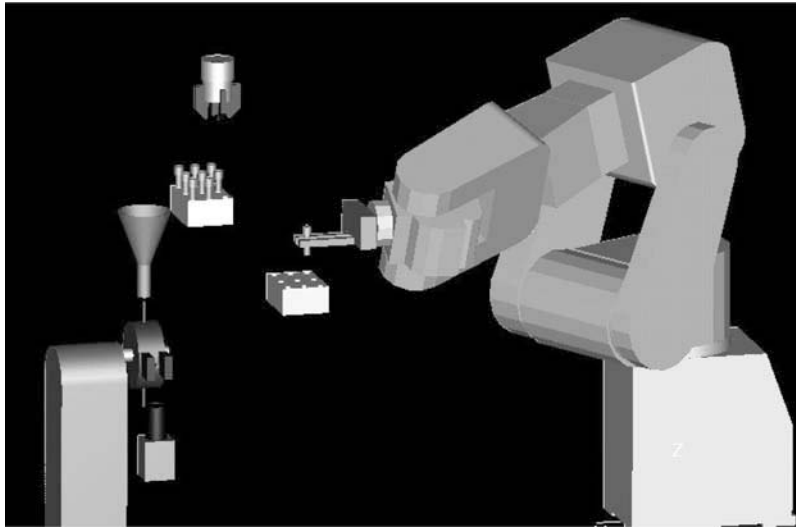


FIGURE 18-6 Stent inspection concept.

working area. A FANUC manipulator (LR Mate 200iB model), which is a six-axis, modular construction, AC electric servo-driven robot, is used. It is optimized for operations in sensitive, contamination-controlled environments and occupies minimal floor space. It provides high throughput, industry-leading reliability and sophisticated motion control for part handling. It can move along three-dimensional curved paths and approach any position from virtually any direction.

The stent is very fragile, but is heavy enough to be subject to the effects of gravity. If the stent is allowed to fall into the pin vertically, it is possible to feed the pin without problems. In any case, this process must be done with extreme accuracy, because subjecting the stent to a little stress renders it useless. Therefore a rotating disc can be used to locate a pin in the vertical position to load the stent, after which the disc rotates the pin to an horizontal location to perform the inspection of the stent surface and finally the disc rotates the pin to the unload vertical position to release the stent.

Assembly

Micro-handling and micro-assembly are closely linked topics because several positioning move-

ments are always involved in micro-assembly processes.

Optical-fiber communication systems are increasing because of the demand for large-capacity and high speed data transmission on local area networks. With the growth in optical-fiber communications, fiber alignment has become a key production process because its efficiency greatly influences the overall production rates for the opto-electric products used in optical-fiber communications. Fiber alignment is necessary when two optical fibers are connected, when an optical fiber is connected to a photo-diode (PD) or a light-emission diode (LED), and when an optical-fiber array is connected to an optical waveguide (Fig. 18-7). Connecting optical fibers is difficult because the connecting edges should be aligned with sub-micrometer resolution. Therefore, it is time consuming even for human experts.

Active Optical-fibre Alignment. The technique for aligning the optical fiber to maximize optical coupling efficiency while monitoring the signals, in respect of the amount of light coupled to the input fiber, is known as active alignment. This widely adopted method consists of rough and fine searches. In the rough search a coordinate where the coupled light is maximized is found approximately. In the fine search, a peak coordinate is

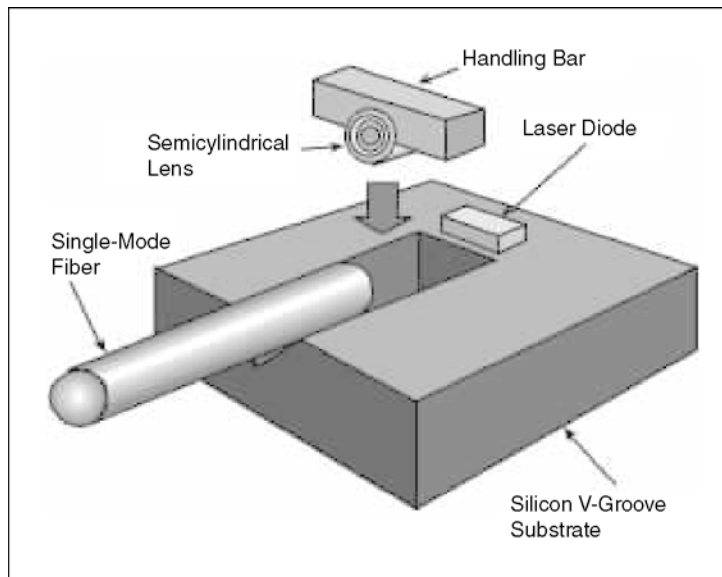


FIGURE 18-7 Optical-fiber alignment.

strictly identified to the order of sub-microns. More specifically, in the rough search a scan is made in a zig-zag or spiral manner. In the fine search, a cross-scan is repeated around the (coarse search) coordinate showing a maximum amount of coupled light, to seek a new coordinate showing a maximum amount of coupled light. The fiber alignment ends when the distance between the newly found coordinate showing a maximum amount of coupled light and the previous coordinate showing a maximum amount of light converge to less than a given value.

In this application a precision manipulator is needed in order to move the optical fibers while monitoring the signals during the automated alignment process.

CONCLUSIONS

A review of existing systems for handling of micro-parts was carried out in this chapter. A key problem area limiting the emergence of micro-handling technology is the non-availability of flexible, highly precise, micro-handling machinery.

Due to the increasing number of topics related to MEMS, some standards for automated gripping and handling of micro-parts have arisen. Irrespectively, the standardization of these micro-systems is quite new, so there are few standards defined at this moment. For example, to deal with different part sizes an automated interchange tool system can be used (DIN 32565). This norm is the result of the work committee 'NAFuO'. It specifies requirements of a mechanical interface between an end effector and a handling device for micro-systems.

The combination of different grip principles in the same gripper is recommended to increase flexibility. Additionally sensors mounted on smart grippers can help to compensate for inaccuracies in part gripper relations. Machine vision is a widespread technology for high precision handling of parts in industrial environments. In micro-scale, machine vision can be used to 'see' exactly what it is going in the working place and to 'actuate' in consequence. With dedicated algorithms, the features of an object in the image can be extracted for robot localization and control. For the latter, a real-time processing of images is a crucial issue.

Compliance analysis of micro-handling, including both gripper and part is critical for reducing the necessary positional accuracy of the system, and therefore the cost. The handling system need not require the same precision as the tolerance of the locations if a proper use of positioning, sensing, modeling, and control tools is made. The use of precision fixtures can mitigate the need for high positional accuracy. V-groove structures, datum points, or other minimum energy surfaces should be used as much as possible to guide the micro-parts into desired positions and orientations.

The following are key areas of the research in micro-handling systems:

- ‘Contactless’ and smart micro-grippers;
- Modeling of micro-assembly processes using molecular dynamics simulation (MDS);
- High resolution micro-feeding techniques;
- Plug and produce micro-assembly modules (control and hardware integration);
- Integration of automated assembly processes applicable to ‘super-clean room’.

ACKNOWLEDGMENT

This work was financially supported by the European Community FEDER funds and European Community research funds (MASMICRO, Project number 500095-2). The authors also would like to thank the R&D&I Linguistic Assistance Office at the ‘Universidad Politecnica de Valencia’.

REFERENCES

- [1] K.F. Böhringer, R.S. Fearing, K.Y. Goldberg, Micro-assembly, *The Handbook of Industrial Robotics*, 2nd ed., in: Shimon Nof (Ed.), John Wiley & Sons (February 1999) 1045–1066.
- [2] A.J. Sanchez, R. Lopez, R. Gunman, C. Ricolfe, Recent development in micro-handling systems for micro-manufacturing, *J. of Materials Processing Technology* 167 (22) (2005) 499–507.
- [3] J. Israelachvili, *Intermolecular & Surface Forces*, 2nd Ed., Academic Press Ltd (1992).
- [4] R.A. Bowling, A theoretical review of particle adhesion, in: K.L. Mittal (ed.), *Particles on Surfaces I: Detection, Adhesion, and Removal*. Plenum, New York (1988) 129–155.
- [5] R.S. Fearing, Survey of sticking effects for micro parts handling, *Proc. IEEE-RSJ Intelligent Robots and Systems*, Pittsburgh, PA (August 3-5, 1995).
- [6] J.T. Feddema, P. Xavier, R. Brown, Micro-assembly planning with Van Der Waals force, *Proceedings of the 1999 IEEE International Symposium on Assembly and Task Planning*, Porto, Portugal (July 1999) 32–38.
- [7] A. de Lazzer, M. Dreyer, H.J. Rath, Particle-surface capillary forces, *Langmuir* 15 (1999) 4551–4559.
- [8] F. Arai, D. Ando, T. Fukuda, Y. Nonoda, T. Oota, Micro manipulation based on micro physics – strategy based on attractive force reduction and stress measurement, in *Proc. IEEE/RSJ 2* (1995) 236–241.
- [9] M. Kohl, B. Krevet, E. Just, SMA microgripper system, *Sensors and Actuators A* 97-98 (2002) 646–652.
- [10] J. Ok, M. Chu, C.-J. Kim, Pneumatically driven microcage for micro-objects in biological liquid, *IEEE MEMS* (1999) 459–463.
- [11] W. Zesch, M. Brunner, A. Weber, Vacuum tool for handling micro-objects with a NanoRobot, *IEEE Int. Conf. on Robotics and Automation*, 2 (April 20-25 1997) 1761–1766.
- [12] D. Petrovic, G. Popovic, E. Chatzitheodoridis, O. Del Medico, A. Almansa, F. Sümeçz, W. Brenner, H. Detter, Gripping tools for handling and assembly of microcomponents, *Proc. 23rd International Conference on Microelectronics 1* (May 2002) 247–250.
- [13] Y. Rollot, S. Régnier, Micromanipulation par adhésion, *Nano et micro technologies* 1 (2) (2000) 213–241.
- [14] K. Tsuchiya, A. Murakami, G. Fortmann, M. Nakao, Y. Hatamura, Micro assembly and micro bonding in nano manufacturing world, *SPIE* 3834 (1999) 132–140.
- [15] E.T. Enikov, K.V. Lazarov, Optically transparent gripper for microassembly, *SPIE* 4568 (2001) 40–49.
- [16] J. Hesselbach, S. Büttgenbach, J. Wrege, S. Bütefisch, C. Graf, Centering electrostatic microgripper and magazines for microassembly tasks, *Proc. of SPIE Microrobotics and Micromanipulation* 4568 (2001) 270–277.
- [17] C. Bark, T. Binnenböse, G. Vögele, T. Weisener, M. Widmann, Gripping with low viscosity fluids, *IEEE Micro Electro Mechanical Systems Workshop*, Heidelberg, Germany (Feb. 1998) 301–305.
- [18] H. Grutzeck, L. Kiesewetter, Downscaling of grippers for micro assembly, *Microsystem Technologies* 8 (2002) 27–31.
- [19] F. Arai, T. Fukuda, A new pick up and release method by heating for micromanipulation, *IEEE Micro Electro Mechanical Systems Workshop*, Nagoya, Japan (Jan. 1997) 383–388.

- [20] A. Kochan, European project develops ice gripper for micro-sized components, *Assembly Automation* 17 (2) (1997) 114–115.
- [21] G. Reinhart, J. Hoepfner, Non-contact handling using high-intensity ultrasonic, *Annals of the CIRP* 49 (1) (2000) 5–8.
- [22] P.A. Bancel, V.B. Cajipe, F. Rodier, J. Witz, Laser seeding for biomolecular crystallization, *J. of Crystal Growth* 191 (1998) 537–544.
- [23] C.L. Ramin, R.O. Warrington, Micro-assembly with a focused laser beam, *IEEE MEMS* (1994) 285–290.

Robotics in Micro-Manufacturing and Micro-Robotics

Rafa López Tarazón

INTRODUCTION

This chapter is focused on robotics in micro-manufacturing and micro-robotics. First, an introduction to robotics is made, so as to provide a clear differentiation between three different type-scales of robots: macro-robots, micro-robots and nano-robots. MEMS are also commented upon, as they are closely related to micro-robots. Next, the chapter goes in depth into two main micro-robotics applications: micro-assembly and micro-handling. Sensors and actuators in micro-robotics are explained later, and finally, several current examples of micro-robots are presented.

ROBOT DEFINITIONS

A robot can be seen as an electromechanical system programmable in three or more axes and with some degree of intelligence and ability to make choices based on its environment. Based on its size (and scale), robots may be classified as:

1. Macro-robots (macro-scale)
2. Micro-robots (micro-scale)
3. Nano-robots (nano-scale).

In 1954 the first modern macro-robot was invented, called the Unimate. This robot was installed to automatically remove hot metal from a

die-casting machine. From that time up to the present, millions of robots have been developed and manufactured. Numerous companies are currently selling robots, two examples are shown in Fig. 19-1.

Nowadays macro-robots are used for many applications: car production, packaging, palletizing, PCB manufacturing, goods transportation, vacuum cleaning, lawn mowing, care assistance for the elderly, and even for military applications or laparoscopic surgeries. Although new applications are arising, this kind of robot is used mainly in industrial environments.

On the other hand, a micro-robot is basically a small robot usually capable of operating at the microscopic scale. Micro-robotics is used widely for biologic applications, mainly biotechnology (cells localization, particles separation, chromosome cutting or even genetic manipulation) but also for a large number of micro-manufacturing applications.

An example of an industrial micro-robot suitable for micro-manufacturing is the RP-1AH robot from Mitsubishi Electric [1], which is a miniature-format robot designed specifically for high precision micro-handling applications. Its footprint is no larger than that of a DIN A5 sheet of paper. The RP-1AH is designed for small, cramped work areas and applications such as



FIGURE 19-1 Two different commercially available robots from Robotnik Automation Company.

the placement of components on SMD circuit boards and micro-mechanics.

Finally, a nano-robot can be defined as a robot at or close to the scale of nanometers. Another definition sometimes used is a robot which allows precise interactions with nano-scale objects, or can manipulate with nano-scale accuracy. In general, nano-robots are still under development, but some initial results and tests have been made. An example is the first single-molecule car with buckyballs for wheels (by Rice University) (Fig. 19-2).

Possible applications for nano-robots are: nano-surgery, nano-manufacturing, weaponry and cleaning.

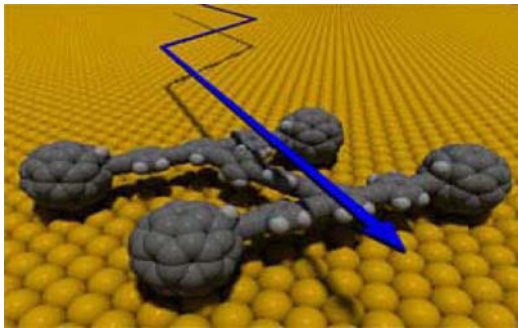


FIGURE 19-2 The Nanocar.
(Source: courtesy of Rice University.)

Table 19-1 summarizes the main features of the different robot technologies.

Very closely related to micro-robotics are MEMS (micro-electromechanical systems), which can be defined as the technology of small things. MEMS are usually used to make sensors by incorporating silicon-based mechanical and electrical components. Sensing devices are generally two dimensional in shape and use the electrical and mechanical properties of bulk silicon and deposited thin film.

Nowadays, there are numerous applications in which MEMS take part, such as in pressure measurement, material straining, fluid flowing and chemical compounding.

MICRO-ROBOTICS APPLICATIONS

Something about the actual applications of micro-robotics in micro-manufacturing is now explained. Many of these have arisen with the growth of the MEMS market. One of the first applications is in micro-assembly, which can be defined as the assembly of micro-products, where the main goal is the construction of a micro-structure by means of several micro-components under microscopic tolerances. Micro-assembly may combine many different techniques from many different disciplines, such as robotics, chemistry

TABLE 19-1 Robot Technologies

Type	Size	Interaction with Environment	Main Application
Macro-robot	Centimeters to meters	Mechanical	Industrial
Micro-robot	Micrometers to centimeters	Mechanical, chemical and electromagnetic	Micro-assembly
Nano-robot	Nanometers to micrometers	Chemical	Surgery (future)

and pneumatics or computer vision. The second main application is in micro-handling, where not only is the accuracy of the movement important, but also that of the physical gripper that holds the micro-part.

Micro-assembly

In general, assembly applications are very well known in the robotic macro-world, as they are spread over numerous industrial applications, but these applications are completely different and relatively unknown when referring to the micro-scale.

As explained in [1], there are two main differences between micro- and macro-assembly:

1. **The final accuracy needed:** as an example, a typical assembly SCARA robot has an accuracy of 0.01 mm, while the precision needed by a micro-assembly application is below the sub-micron level. This problem is further increased by the accuracy needed by the sensors placed on the micro-robot, as the displacements and movements involved are very small and slow.
2. **Manipulation strategies:** the interaction between objects is completely different for the micro-world and the macro-world. In the former, gravity is not the main force, and other forces appear, as surface-related forces (electrostatic, van der Waals) and surface-tension forces, that are dominant over gravitational force. This means that in the macro-world mechanical interaction between objects will not perform as one might think it should. As an example, if a gripper is opened in the macro-world, the object being gripped will be released and will fall to the floor. If the same experiment is made in the micro-world, the object will not fall, as it will probably remain in place, adhering to the micro-gripper due to surface-related forces.

A review of many different types of micro-assembly systems is made next:

1. Tele-operated micro-assembly systems [2]
2. Master slave micro-assembly systems [3]
3. Automatic micro-assembly machines [4]

4. Serial or parallel micro-assembly [5,6]
5. Environment-controlled micro-assembly systems [7]
6. Hybrid micro-assembly systems [8]
7. Micro-assembly by micro-robots [9,10].

A good example of a micro-assembly system can be found in [11], where 3D MEMS micro-structures are created by assembling multiple surface, micro-machined micro-components together. In this case, the micro-assembly process consists of the following sub-processes: grasping a micro-component with a micro-gripper, removing the micro-component from a chip substrate, reorienting the micro-component to a new location, and joining the micro-component to another micro-component.

Another good example of micro-assembly of MEMS is found in [12]. In this case, the assembly process is done using adhesive films, and the example case is a micro-part being assembled on a printed circuit board.

The last example presented of micro-assembly systems is the Pocket Delta robot, developed at CSEM (the Swiss Center for Electronics and Microtechnology). Based on parallel kinematics, this micro-assembly robot has a repeatability of 2.5 μm and a pressing force of up to 2 N (Fig. 19-3).

Micro-handling

The second main application for micro-robotics is in micro-manipulation or micro-handling.



FIGURE 19-3 The Pocket Delta robot.
(Source: courtesy of CSEM, SA Switzerland.)

Micro-manipulation consists basically in moving a micro-component from one location to another. To achieve this task, the end-effector plays an important role as it has the task of physically picking up and releasing the micro-part.

There are many different end-effectors used for micro-handling operations. The most commonly used are the micro-grippers, which have been designed in many types. They usually use flexure or rotatory joints and also piezoelectric actuators.

An example of a micro-gripper is found in [13], where a flexible micro-gripper is designed for the high precision handling of very small components. This micro-gripper uses flexure hinges, an inchworm piezoelectric actuator and exchangeable gripping jaws.

Finally, another example is shown in [14], where a new micro-gripper which can realize a parallel movement of the gripping arms is developed. The piezoelectric actuation principle is used to move the micro-gripper mechanism. The micro-gripper was fabricated by means of a UV-lithographic process and chemical wet-etching technology from micro-structurable photosensitive glass.

SENSORS AND ACTUATORS IN MICRO-ROBOTICS

Sensors

In robotics, sensors play important roles as they are responsible for collecting information about the environment. In robotics, sensors are used for a large number of tasks, such as finding locations, measuring parameters (internal or external), avoiding collisions, etc.

On the other hand, example applications where sensors are used are:

- Displacement measurement
- Temperature measurement
- Velocity measurement
- Obstacle avoidance
- Distance measurement
- Beacon detection
- Collision detection.

When considering micro-world applications, sensors are even more important, as they must be more precise and accurate than those for normal macro-world applications.

Basically, a sensor makes a conversion of energy from one form to another. To achieve this conversion, the sensor makes use of a transducer and an electronic circuit. A transducer is a device that converts a quantity of energy to a signal able to be measured electrically. Some examples are:

- **Thermistor:** temperature-to-resistance
- **Electrochemical:** chemistry-to-voltage
- **Photocurrent:** light intensity-to-current.

After the transducer, the electronic circuit conditions the obtained signal into an electrical signal that can be processed further.

Combining signals from several sensors to form a world model is known as sensor fusion.

In robotics, sensors are basically classified into two groups: internal and external. Internal sensors (also called proprioceptive) are used to measure robot parameters relative to the reference frame of the robot, such as a joint angle, a linkage deflection and a gripping force. External sensors (also called exteroceptive) are used to measure the environment and the position of the robot relative to that environment.

Sensors can be also classified as active, if they transmit energy into the environment, or passive, if they receive energy from the environment.

Finally, the sensors that are most commonly used in robotics can be summarized:

- Resistive sensors (i.e. potentiometer)
- Tactile sensors (i.e. bumpers)
- Infrared sensors (i.e. proximity sensors)
- Ultrasonic distance sensors
- Inertial sensors (i.e. accelerometers)
- Orientation sensors (i.e. compasses)
- Laser range sensors
- Vision sensors.

Almost every sensor has its micro-sensor, so it is possible to find micro-sensors for a large number of micro-robotics applications. A review of micro-sensors (strain, pressure, acceleration, force and angular-rate sensing) is presented in [15]. As an example, [16] shows a ceramic



FIGURE 19-4 A Piezo-actuator.
(Source: courtesy of CEDRAT Group.)

capacitive sealed-gage pressure micro-sensor which is able to work under high temperature applications.

Actuators

An actuator is a device (usually mechanical) responsible for generating a movement in a mechanism or system. While sensors make conversions between different forms of energy, actuators make a conversion from one form of energy to a mechanical movement. From another point of view, an actuator is the provider of the motion to the robot. Current actuators for macro-robots are electrical, pneumatic or hydraulic.

Obviously, micro-robots need micro-actuators to generate their movement. There are many different micro-actuators that can be used in micro-robotics, such as piezoelectric actuators, micro-motors, micro-pneumatic actuators, shape-memory-alloy composite micro-actuators (based on materials that deform at low temperature and regain their original shape when they are heated), electrostatic actuators or even ferro-fluid actuators. Next, the most important are explained: piezo-actuators and micro-motors.

Piezoelectric Actuators. This type of actuator generates motion in the sub-nanometer range. These actuators make use of piezoelectric materials and the movement is based on the frequencies derived from solid-state crystalline effects. There are no moving parts in contact, so there are no friction forces generated.

Piezo-actuators usually have a very short response time (below 1 ms) and a very long life time (i.e. require no maintenance). Figure 19-4 shows an example of a piezoelectric actuator from the CEDRAT Group.

Micro-motors. There are two main types of micro-motors: electromagnetic and piezoelectric. A good review of electromagnetic micro-motors is reported in [17], where their main types are illustrated (variable-reluctance, induction and permanent-magnet micro-motors), the permanent-magnet micro-motor being confirmed to be the best in terms of developed power. These electromagnetic micro-motors operate the same as the bigger ones in the macro-world, but with their parts reduced to the minimum possible size. Numerous companies are selling electromagnetic micro-motors, among which the Faulhaber Group and Maxon Motor stand out.

On the other hand, piezoelectric micro-motors are based on the change in shape of a piezoelectric material. The motion is produced from the ultrasonic vibrations of the material when applying an electrical field. There are both linear- and rotary-motion micro-motors (Fig. 19-5).

MICRO-ROBOT EXAMPLES

Next, some state-of-the-art micro-robots are presented. Their applications are countless, although the Hexapod M-850 micro-robot is especially designed for micro-manufacturing tasks. Some

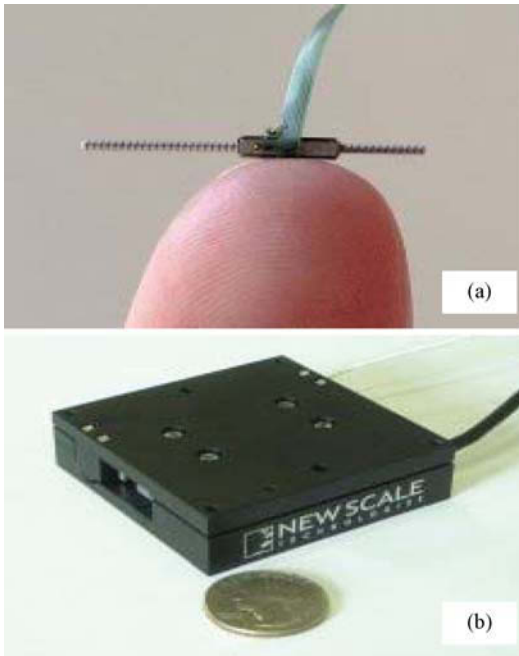


FIGURE 19-5 Piezoelectric rotary micro-motor and linear nano-positioning stage.
(Source: courtesy of CEDRAT Group.)

of them are still in the development stage, but they show real examples of their importance in this field.

Micro-air-vehicle

The first example of a micro-robot can be found in [18], where a micro-air-vehicle (MAV) is designed and prototyped. This 10 cm, 2 g MAV is capable of autonomous flight, target sensing and obstacle avoidance, and makes use of articulated and rigid composite micro-structures, high performance micro-actuators and low power biomimetic sensors. Figure 19-6 shows this MAV.

The electronics and control are located on a PCB at the center of the fuselage. The power is placed on the front part and consists of a 20 mAh lithium polymer battery. There are also two bimorph piezoelectric actuators and an optical flow sensor for obstacle avoidance.

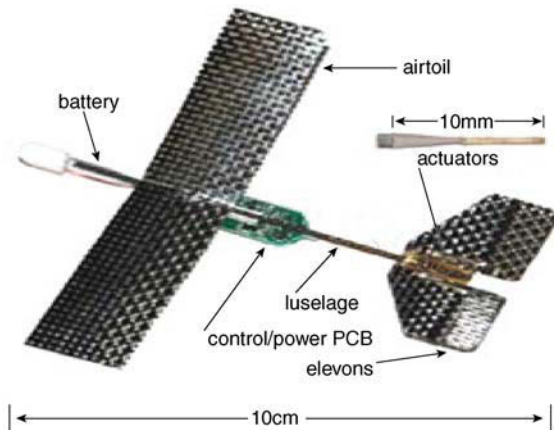


FIGURE 19-6 A micro-glider.
(Source: courtesy of UC Berkeley.)

Hexapod M-850 Micro-robot

Produced by Physik Instrumente (PI) GmbH & Co. KG, the M-850 Hexapod is a micro-positioning system for all complex positioning tasks that require high load capacity and accuracy in six independent axes (Fig. 19-7). Its main features are:

- 6 degrees of freedom
- Repeatability to $\pm 1 \mu\text{m}$
- Actuator resolution to $0.005 \mu\text{m}$

Current applications for this micro-robot are:

- Surgical robots
- Micro-machining
- Micro-manipulation (life sciences)
- Semiconductor handling systems.

Open-source Micro-robotic Project

This Open-source micro-robotic project aims to develop a cheap, reliable and swarm-capable micro-robot. Currently there are two developed robot versions: ‘Jasmine II’ and ‘Jasmine III’ (Fig. 19-8). The robots (hardware, software and simulations) are available under the GNU General Public License.

Waalbot [19]

This robot (developed at Nano-Robotics Laboratory, Carnegie Mellon University) is a new approach to wall-climbing robots (Fig. 19-9).



FIGURE 19-7 The Hexapod M-850.
(Source: courtesy of Physik Instrumente (PI) GmbH & Co. KG.)

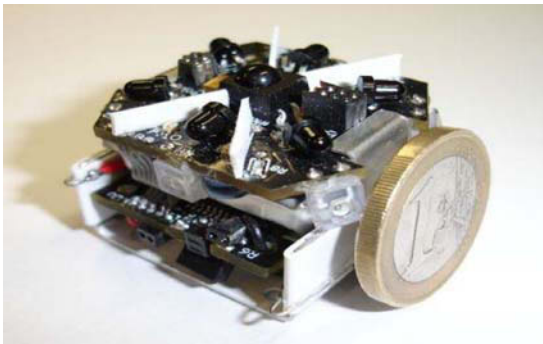


FIGURE 19-8 The Jasmine III Robot.
(Source: courtesy of Open-source micro-robotics project.)

Using two actuated legs with rotary motion and two passive revolute joints at each foot, this robot can climb and steer in any orientation. The main applications for this robot are inspection and surveillance, and space missions.

Strider Micro-robot [20]

This micro-robot (also developed at Nano-Robotics Laboratory, Carnegie Mellon University) was inspired by water-strider insects (Fig. 19-10). The robot (as with the insects) uses surface-tension force to balance its weight on water by using hydrophobic Teflon-coated wire legs. The maximum forward speed has been measured to be 3 cm/s and its rotational speed is 0.5 rads/s.



FIGURE 19-9 The Waalbot Robot.
(Source: courtesy of Metin Sitti, Nano-Robotics Laboratory, Carnegie Mellon University.)



FIGURE 19-10 The Strider Micro-robot.
(Source: courtesy of Metin Sitti, Nano-Robotics Laboratory, Carnegie Mellon University.)

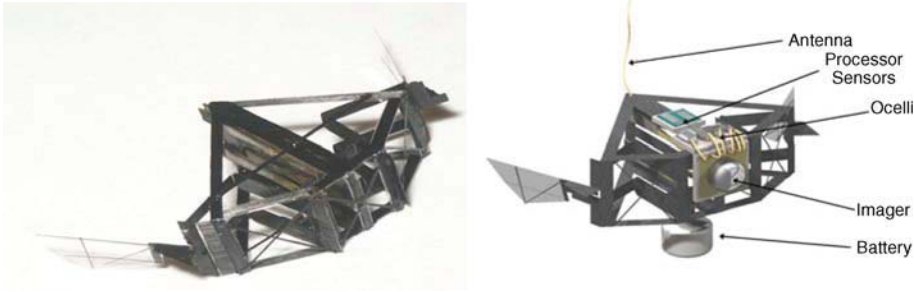


FIGURE 19-11 The MFI Project at UC Berkeley.

MFI Project

Closely related to the strider micro-robot (inspired by insects) and the micro-air-vehicle (autonomous flying micro-robot) is the Micro-mechanical Flying Object (MFI) developed at the Biomimetic Millisystem Lab. at UC Berkeley (Fig. 19-11).

The goal of the project is to develop a very small device capable of sustained autonomous flight, based on the flight performance of flies and by means of piezoelectric actuators and flexible thorax structures.

CONCLUSIONS

As has been seen throughout this chapter, micro-robotics is a relatively new field with a large amount of research still to be done. Numerous laboratories and investigation centers are concentrating their efforts towards obtaining increasingly more sophisticated and smaller robotic devices.

Future applications of micro-robots are numerous and extend from searching for survivors during rescue missions to extremely precise surgical operations (even autonomously by a micro-robot inside the patient's body) all the way up to top-secret espionage missions.

REFERENCES

- [1] M.B. Cohn, K.F. Böhringer, J.M. Novorolski, A. Singh, C.G. Keller, K. Goldberg, R.T. Howe, Micro-assembly technologies for MEMS, Proc. SPIE Micro-machining and Microfabrication, Conference on Micromachining and Microfabrication Process Technology IV, Santa Clara, CA (Sept. 21–22, 1998) 2–16.
- [2] G. Reinhart, O. Anton, M. Ehrenstrasser, C. Patron, B. Petzold, Framework for teleoperated microassembly systems, Proc. SPIE 4570, pp. 86–96, Telemanipulator and Telepresence Technologies VIII, Matthew R. Stein (ed.) (2002).
- [3] K. Kaneko, H. Tokashiki, K. Tanie, K. Komoriya, Impedance shaping based on force feedback bilateral control in macro-microteleoperation system, Proc. ICRA (1997) 710–717.
- [4] K. Shimamura, Y. Sasaki, M. Fujii, Low cost micro-assembly machine, FUJITSU Sci. Tech. J 43 (1) (Jan. 2007) 59–66.
- [5] G. Danuser, I. Pappas, B. Vögeli, W. Zesch, J. Dual, Manipulation of microscopic objects with nanometer precision: potentials and limitations in nano-robot design, Int. J. of Robotics Research (1997) 1–47.
- [6] M.B. Cohn, Y.C. Liang, R.T. Howe, A.P. Pisano, Wafer-to-wafer transfer of microstructures for vacuum packaging, 1996 Solid-State Sensor and Actuator Workshop, Hilton Head Island, SC, USA (June 26, 1996).
- [7] Q. Zhou, A. Aurelian, B. Chang, C. del Corral, H.N. Koivo, Microassembly system with controlled environment, J. of Micromechatronics 2 (3) (2004) 227–248.
- [8] B. Kim, H. Kang, D.H. Kim, J.O. Park, A flexible microassembly system based on hybrid manipulation scheme for manufacturing photonics components, The Int. J. of Advanced Manufacturing Technology (Springer London) 28 (3–4) (2005) 379–386.
- [9] T. Zhu, D. Tan, Research on microrobot-based microassembly system, Intelligent Control and Automation 2 (2002) 1236–1240.
- [10] S. Fatikow, J. Seyfried, S. Fahlbusch, A. Buerkle, F. Schmoedel, A flexible microrobot based micro-assembly station, J. of Intelligent and Robotic Systems 27 (1–2) (Jan. 2000) 135–169.

- [11] N. Dechev, W.L. Cleghorn, J.K. Mills, Construction of 3D MEMS microstructures using robotic micro-assembly, International Conference on Robots and Intelligent Systems (IEEE/RSJ IROS 2003), Las Vegas, Nevada, USA (Oct. 27–31, 2003).
- [12] I. Karjalainen, T. Sandelin, J. Uusitalo, R. Tuokko, Robotic assembly and joining of miniature and MEMS components using adhesive films – test environments and experiences, *J. Assembly Automation* 24 (1) (2004) 58–62.
- [13] S. Henein, M. Thurner, A. Steinecker, Flexible microgripper for micro-factory robots, Created by SHE/Rev (July 2003).
- [14] R. Keoschkerjan, H. Wurmus, A novel microgripper with parallel movement of gripping arm, Proceedings of the Eighth International Conference on New Actuators, Bremen, Germany (June 10–12, 2002) 321–324.
- [15] M. Goldfarb, A. Strauss, E.J. Barth, Overview of mechatronics. Chapter 5: An introduction to micro and nanotechnology, CRC Press LLC (2002).
- [16] C.B. Sippola, C.H. Ahn, A thick film screen-printed ceramic capacitive pressure microsensor for high temperature applications, *J. of Micromechanics and Microengineering* 16 (5) (2006) 1086–1091.
- [17] E. Dereine, B. Dehez, D. Grenier, B. Raucant, A survey of electromagnetic micromotors, Proceedings of the 1st International Precision Assembly Meeting (IPAS 2003), Bad Hofgastein, Austria (March 17–19, 2003) 85–94.
- [18] R.J. Wood, S. Avadhanula, E. Steltz, M. Seeman, J. Entwistle, A. Bachrach, G. Barrows, S. Sanders, R.S. Fearing, An autonomous palm-sized gliding micro air vehicle, *IEEE Robotics & Automation Magazine* (2007) 82–91.
- [19] M.P. Murphy, Waalbot: an agile small-scale wall-climbing robot utilizing dry elastomer adhesives, *IEEE/ASME Transaction on Mechatronics* 12 (3) (2007) 330–338.
- [20] Y.S. Song, M. Sitti, Surface tension driven biologically inspired water strider robots: theory and experiments, *IEEE Trans. on Robotics* 23 (3) (June 2007) 578–589.

FURTHER READINGS

- [1] P.J. McKerrow, Introduction to Robotics, Ed. Addison Wesley (1990).
- [2] A.J. Sanchez, R. Lopez, R. Guzman, C. Ricolfe, Recent development in micro-handling systems for micro-manufacturing, *J. of Materials Processing Technology* 167 (22) (2005) 499–507.
- [3] G. Lin, R.A. Lawton, 3D MEMS in standard processes: fabrication, quality assurance and novel measurement microstructures, NASA Technical Report (2000).
- [4] J. Bell, Automated packaging of MEMS devices, *J. of SMT* 16 (2) (2003) 22–26.

Optical Coherence Tomography for the Characterization of Micro-Parts and -Structures

David Stifter

INTRODUCTION

Optical coherence tomography (OCT) was presented in 1991 for the first time as a powerful technique for applications in the field of medical diagnostics [1]. It was demonstrated that with OCT high resolution cross-sectional images of biological tissue can be obtained in a contactless and non-invasive way. The investigation of retinal diseases, such as glaucoma, belonged to the first applications, with a main consequence being that commercial retinal OCT scanners are already available and used in eye clinics and hospitals. The OCT method has been further refined in the meantime and a multitude of new developments and extensions for this technique have been introduced, as also summarized in several books and reviews (e.g. [2–3]). The main applications and driving forces for these developments in the field of OCT research can still be found in the area of biomedical diagnostics, ranging from the investigation of the eye (e.g. also cornea), skin (e.g. melanoma), teeth (caries) or of interior organs and vessels (e.g. by OCT endoscopy) to life science applications providing image details down to the sub-cellular level.

Although the main route of OCT developments is for biomedical purposes, the potential

of OCT for contactless and non-destructive evaluation of non-biological materials and components has been recognized due to the fact that depth-resolved structural information can be obtained with high accuracy in a fast and easy way from the interior of materials, even for those of a highly scattering nature. Consequently, a variety of technical applications for OCT have now emerged, as compiled in a recent comprehensive review [4], anticipating a future increase in their number with respect to their biomedical counterparts.

In this chapter, initially, an introduction is provided to the underlying measurement principle of OCT and a short overview of different alternative and advanced OCT measurement concepts. A selection of proven applications of classical and advanced OCT techniques for the evaluation of micro-structures is then presented. It is worth noting that due to the novelty of the herein-introduced OCT techniques and results, routine testing and evaluation of micro-structures by OCT is not yet standard but it is expected to fully emerge in the next few years, as OCT measurement technology further develops and matures.

MEASUREMENT PRINCIPLES OF STANDARD AND SELECTED ADVANCED OCT TECHNIQUES

The basic physical principle of OCT is low coherence interferometry (LCI): an interferometer, mostly built in Michelson geometry, is illuminated with spectrally broad light, as depicted in Figure 20-1(a). The sample is placed in one arm of the interferometer, the reference arm itself is equipped with a movable mirror. Since low coherence light is used, interference is only observed if the length of the optical path between the beamsplitter and a backscattering feature within the sample, such as a buried interface, equals the optical path length of the reference arm. In this way, the absolute positions of back-scattering and -reflecting features can be determined. In the example of Figure 20-1(a), two interference peaks are observed when moving the reference mirror (from surface and interface). Usually, the envelope of the interference signal is taken and it represents a reflectivity depth profile of the sample at a fixed lateral position (so-called A-scan). By measuring several depth profiles at adjacent positions, e.g. by scanning the focused light beam over the sample, cross-sectional images (B-scans) and 3D volume data can be acquired.

The width of the peaks in a depth profile, determining the axial resolution of the system, is given by the coherence length of the used light source: the broader the spectrum, the higher the axial resolution [5]. Standard OCT systems exhibit axial resolutions in the 5–15 μm range, ultra-high resolution OCTs (UHR-OCT [6]) have been reported showing even sub-micron resolution with very broadband light sources, like thermal or super continuum sources. The light sources are spectrally situated mostly in the near-infrared region (800 nm–1500 nm) with an average power in the mW range, ensuring damage-free (non-invasive) investigation of living tissue. Consequently, no special safety precautions have to be taken when handling OCT apparatus, as is mandatory for, e.g., X-ray computed tomography.

For OCT the axial resolution is decoupled from the lateral one, which is determined by the spot-size of the focused light beam on the sample. Due to the decoupling, a high axial resolution can be maintained even for long working distances, in contrast to confocal microscopy where high numerical aperture (NA) optics have to be used for high depth discrimination [7]. The axial resolution in OCT should not be mistaken for the accuracy with which the position of the envelope peaks can be determined: on smooth surfaces

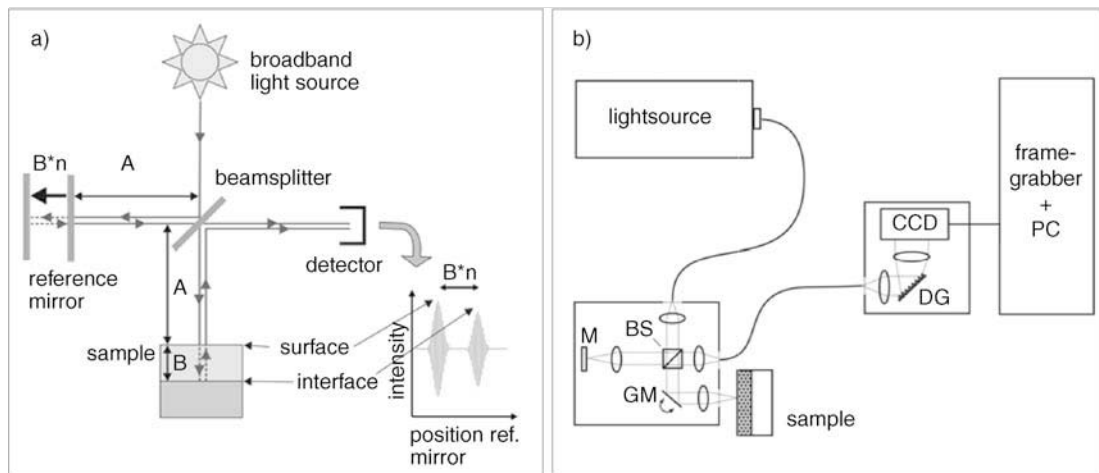


FIGURE 20-1 (a) Schematic sketch of a standard (time-domain) OCT set-up with a broadband light source illuminating a Michelson interferometer. A, B: path lengths, n: refractive index of sample layer; (b) layout of a spectral-domain OCT set-up. Abbreviations: beamsplitter (BS), reference mirror (M), galvano-scanner mirror for lateral scanning (GM), diffraction grating (DG), line camera (CCD).

and interfaces, precision in the nanometer range is feasible. In this context, scanning white-light interferometry (SWLI) and coherence probe microscopy (CPM) shall be mentioned, since these methods share the same principle (LCI) and a similar set-up as OCT [8]: in contrast to conventional OCT, mostly whole surface areas are illuminated at once and area cameras are used to register the interference signal when moving a reference mirror. Such systems were optimized for the measurement of surface topographies with sub-nanometer accuracy and are now widely employed in the semiconductor industry for the inspection of integrated circuits [9] or for the characterization of micro-electromechanical structures (MEMS) [10]. Although transparent layers can also be measured with these systems (e.g. thickness), only OCT is also capable of determining the internal structure of scattering and turbid media with reasonable penetration depth (in the millimeter range). However, the border between the different techniques start to blur, as a combination of the CPM technique and OCT leads, e.g. to full-field OCT using high NA optics, area illumination and area cameras [11].

The concept of obtaining depth information by moving the reference mirror (Figure 20-1(a)) is referred to as time-domain (TD) OCT configuration. A new trend is to build OCT devices preferably in the Fourier-domain (FD) configuration. In FD-OCT the reference mirror is fixed and the wavelength of a narrow-band light source is rapidly tuned (swept-source OCT) or the spectrum of a broadband light source is acquired by a spectrum analyzer as depicted in Figure 20-1(b) (spectral-domain OCT (SD-OCT)). The obtained spectral data is Fourier transformed to obtain at once the desired depth information in the form of a whole A-scan. The main advantages of FD-OCT over TD-OCT can be found in the fact that no movable parts are needed for depth scanning, in the increased system sensitivity and in the high measurement speed with A-scan rates of more than 100 kHz (e.g. [12,13]).

Besides measuring the intensity of the back reflected light to gain structural information, further sample properties and enhanced con-

trast can be obtained by taking additional physical phenomena into account with advanced OCT extensions: a determination of the frequency shift of the reflected light from moving particles leads to optical Doppler tomography (ODT) for the depth-resolved measurement of flow velocities [14]. Finally, polarization-sensitive OCT (PS-OCT) shall be mentioned: the evaluation of the polarization state of the light gives insight into the birefringence properties of a material [15].

APPLICATIONS OF OCT FOR THE EVALUATION OF STRUCTURES ON THE MICRON SCALE

In the following, a short selection of instructive examples for OCT recently applied by the author to measurement tasks in micro- and miniature manufacturing are given, especially with the intention to familiarize the reader with the potential of the novel OCT techniques for these kinds of applications and to promote OCT for future routine tasks in the characterization and testing of micro- and miniature structures.

At first, an OCT study on photoresist molds for the production of miniature gear wheels with the LIGA molding technology (LIGA, German acronym for lithography-electroplating-molding) is presented, with the results depicted in Fig. 20-2. High aspect ratio trenches exhibiting widths down to 30 μm were etched in thick photoresist layers deposited on gold-coated silicon wafers. Residual particles in the trenches as well as the defects of the resist/wafer interface are of primary concern since they affect the quality of the molds, crucial for the subsequent electroplating step. As can be seen from the OCT cross-sectional image in Fig. 20-2(a), the thickness of the photoresist layer can easily be determined. However, since the optical path length within the material is different to the path length in the (air-filled) trenches, a virtual step is observed at the wafer surface. From the height of this virtual step the refractive index of the material can be determined and therefore also the geometrical (and not only the optical) thickness of the resist layer can be obtained.

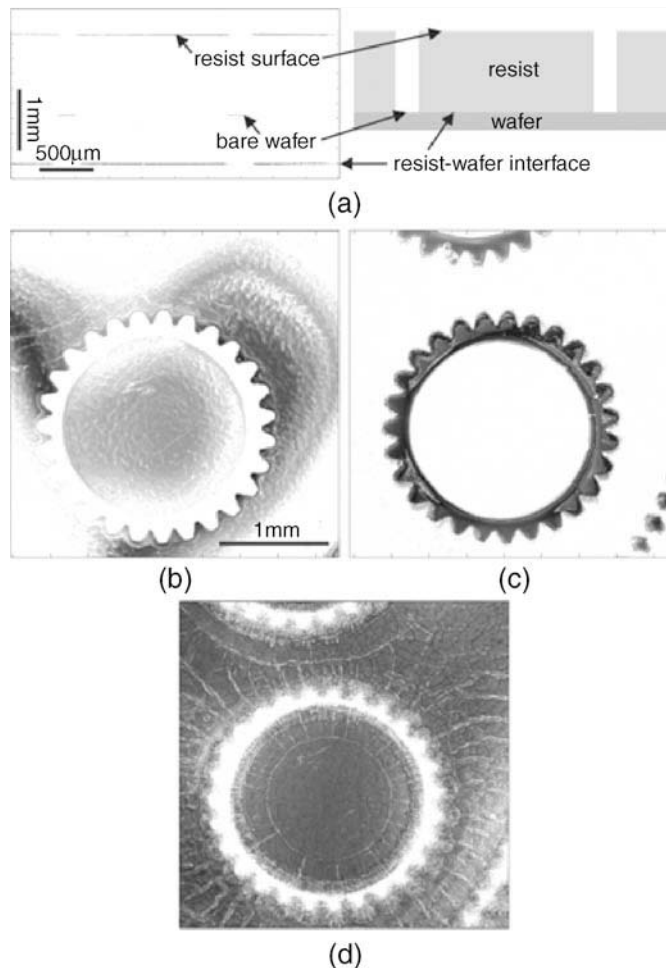


FIGURE 20-2 (a) Cross-sectional scan and schematic drawing of a mold for a miniature wheel in a 1.3 mm thick photoresist layer on a gold coated wafer; (b)–(d) $3 \times 3 \text{ mm}^2$ *en-face* scans of the structure. In (a), only the surfaces of the bare resist and the wafer, and the resist/wafer interface can be distinguished. In (b)–(d), the full geometric information of the structure at these levels is obtained. In (b) the resist surface is imaged, (c) and (d) were recorded at depth positions of the optical path length corresponding to the bare wafer surface and the resist/wafer interface (as shown in (a)), respectively.

From [16], © Optical Society of America 2005.

Furthermore, it should be noted that the rather low NA optics of OCT is of significant advantage in order to access the bottom of the high aspect ratio trenches.

By using so-called *en-face* scanning OCT [16], single planes parallel to the sample surface can be at once imaged at defined depth locations, as shown in Fig. 20-2(b)–(d). In addition to the geometrical form of the wheel, surface corrugations with a maximum height of less than

100 nm (Fig. 20.2(b)), residual particles in the trenches (white spots in the black wheel structure, Fig. 20-2(c)) and a network of ridges (most probably caused by undercutting, Fig. 20-2(d)), could be observed and evaluated.

A second example is presented in Fig. 20-3, where a drug-eluting medical stent has been investigated. The stent structure is essentially a thin metallic network in the shape of a tube (see also the schematic sketch in the inset of Fig. 20-3(a))

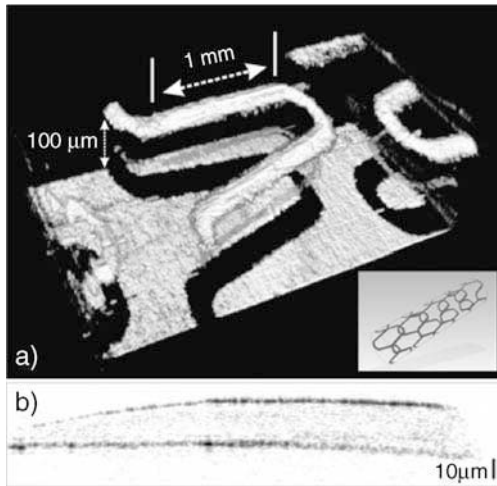


FIGURE 20-3 OCT inspection of a coated (drug-eluting) medical stent: (a) topography of one stent segment with schematic structure of the whole stent in the inset; (b) cross-section of the polymer coating on the metal surface of the stent (scan taken along the straight part of the segment as indicated in (a)); measurements performed in cooperation with K. Wiesauer, UAR GmbH.

which is inserted, e.g. in blood vessels, and dilated to counteract a disease-induced decrease of vessel and duct diameter and helps in this way to maintain the flow. Of interest is the topography and roughness of the individual metallic meanders (Fig. 20-3(a)). The stent structure is also coated with a thin ($\sim 5\text{--}20\ \mu\text{m}$) drug-containing polymer layer. Its homogeneity and thickness are crucial

for a determined delivery of a drug – enclosed in the polymer layer – to the surrounding tissue in order to hinder the formation of thick tissue at the interior of the dilated vessel, which could again obstruct the blood flow. As can be seen in the cross-section of Fig. 20-3(b), taken along one of the linear segments of the meander structure, the polymer layer can easily be resolved with OCT on the rough metal surface and exhibits inhomogeneous regions with thickness variations of more than 100%.

The extension of OCT towards PS-OCT leads to additional contrast and information, exemplified in Fig. 20-2. *En-face* PS-OCT has been performed on resist molds, similar to those depicted in Fig. 20-4: PS-OCT is capable of detecting the birefringence caused by residual stress in the photoresist layer allowing in this way high resolution strain/stress mapping within the wheel mold structures. In addition to the standard intensity image, a retardation image (middle image in Fig. 20-4) is obtained. This image is grayscale coded and gives the phase lag of the reflected light of one polarization direction with respect to the other, orthogonal one. Highly strained areas show strong birefringence leading to higher optical retardation and are depicted in light gray and white in the image. By calibration procedures, i.e. determining the stress–optical coefficient of the material under investigation, even a quantitative evaluation of the strain distribution is possible

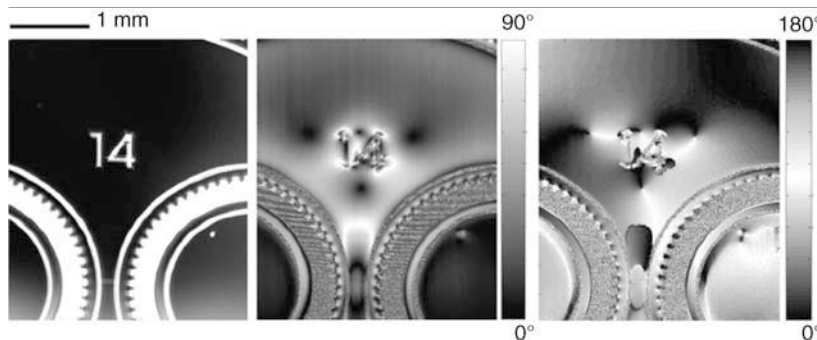


FIGURE 20-4 *En-face* images of photoresist molds for miniature gearwheels. Left: OCT intensity image; middle: optical retardation image (phase lag grayscale coded from 0° to 90°); right: orientation of optical axis indicating the direction of the internal stress (orientation grayscale coded from 0° to 180°).

From [18], © Oldenbourg Verlag 2007.

[17]. Furthermore, the orientation of the optical axis, which is related to the orientation of the internal stress within the sample, can also be measured, as shown in the right image of Fig. 20-4. With the help of PS-OCT valuable insight for the optimization of the production process with its individual photolithographic steps can consequently be gained, especially focusing on the minimization of internal stress, which can cause distortions of the wheel geometries and may lead to detrimental cracks at the wafer/resist interface and between trenches.

This section is concluded on selected measurement applications for micro-structures by recalling the evaluation of micro-fluidic devices with OCT: the knowledge of the flow characteristics in micro-fluidic networks and devices, such as micro-mixers and lab-on-a-chip systems, helps to assess the predicted performance and verify the functionality of novel fluidic chip designs. In this view, the flow behavior of micro-mixers was studied by conventional OCT imaging: two liquids with a different concentration of scatterers were used to visualize flow patterns in the OCT images, giving in this way information on the status of intermixing and the spatial distribution of vortices in the fluidic structure [19]. Besides the retrieval of geometrical information of the flow structure, ODT can now be applied to measure even the flow velocity profiles in the micro-channels in a spatially resolved way, as recently reported in, e.g. ref. [20].

CONCLUSIONS AND OUTLOOK

Classical OCT and advanced OCT techniques, providing high resolution and taking advantage of different contrast mechanisms such as birefringence or flow velocity, have been introduced for the evaluation of micro-structures and -parts. The fact that depth resolved information can be obtained – even from the interior of scattering materials – in a contactless way by OCT using harmless infrared light renders this method especially promising for future routine applications in the metrology of micro-structures. From the technological point of view the advantage of FD-OCT

with respect to robustness, speed and achievable sensitivity will promote its breakthrough. Currently, the potential is recognized by companies which offered up to now only commercial biomedical OCT systems but are preparing their products for the industrial metrology market, such as, e.g. automated inspection of thin multilayer systems. Routine applications for advanced OCT techniques such as PS-OCT or for phase-resolved OCT microscopy providing sub-nanometer accuracy [21] are yet to come. Finally, it shall be considered that hybrid techniques based on SWLI, CPM and OCT will allow tailoring the characteristics of measurement systems to the exact requirements imposed by the specific micro-structure evaluation tasks.

ACKNOWLEDGMENTS

Financial support by the Austrian Science Fund FWF (projects: L126-N08 and P19751-N20) is acknowledged.

REFERENCES

- [1] D. Huang, E.A. Swanson, C.P. Lin, J.S. Schuman, W.G. Stinson, W. Chang, M.R. Hee, T. Flotte, K. Gregory, C.A. Puliafito, J.G. Fujimoto, Optical coherence tomography, *Science* 254 (1991) 1178–1181.
- [2] B.E. Bouma, G.J. Tearney, (eds), *Handbook of Optical Coherence Tomography*, Marcel Dekker Inc, New York (2002).
- [3] A.F. Fercher, C.K. Hitzenberger, Optical coherence tomography, *Progr. Opt* 44 (2002) 215–301.
- [4] D. Stifter, Beyond biomedicine: a review of alternative applications and developments for optical coherence tomography, *Appl. Phys. B* 88 (2007) 337–357.
- [5] E.A. Swanson, D. Huang, M.R. Hee, J.G. Fujimoto, C.P. Lin, C.A. Puliafito, High-speed optical coherence domain reflectometry, *Opt. Lett* 17 (1992) 151–153.
- [6] W. Drexler, U. Morgner, F.X. Kartner, C. Pitris, S.A. Boppart, X.D. Li, E.P. Ippen, J.G. Fujimoto, In vivo ultrahigh-resolution optical coherence tomography, *Opt. Lett* 24 (1999) 1221–1223.
- [7] C.J.R. Sheppard, *Confocal Laser Scanning Microscopy* (1997) Springer, New York.
- [8] C.J.R. Sheppard, M. Roy, M.D. Sharma, Image formation in low-coherence and confocal interference microscopes, *Appl. Opt* 43 (2004) 1493–1502.

- [9] M. Davidson, K. Kaufman, I. Mazor, F. Cohen, An application of interference microscopy to integrated circuit inspection and metrology, *Proc. SPIE* 775 (1987) 233–247.
- [10] C. O'Mahoni, M. Hill, M. Brunet, R. Duane, A. Mathewson, Characterization of micromechanical structures using white-light interferometry, *Meas. Sci. Technol* 14 (2003) 1807–1814.
- [11] A. Dubois, A.C. Boccara, M. Lebec, Real-time reflectivity and topography of depth-resolved microscopic surfaces, *Opt. Lett* 24 (1999) 309–311.
- [12] M.W. Jenkins, D.C. Adler, M. Gargasha, R. Huber, F. Rothenberg, J. Belding, M. Watanabe, D.L. Wilson, J.G. Fujimoto, A.M. Rollins, Ultrahigh-speed optical coherence tomography imaging and visualization of the embryonic avian heart using a buffered Fourier Domain Mode Locked laser, *Opt. Express* 15 (2007) 6251–6267.
- [13] B. Potsaid, I. Gorczynska, V.J. Srinivasan, Y. Chen, J. Jiang, A. Cable, J.G. Fujimoto, Ultrahigh speed spectral/Fourier domain OCT ophthalmic imaging at 70,000 to 312,500 axial scans per second, *Opt. Express* 16 (2008) 15149–15169.
- [14] Z. Chen, T.E. Miller, S. Srinivas, X.J. Wang, A. Malakafzali, M.J.C. van Gemert, J.S. Nelson, Noninvasive imaging of in vivo blood flow velocity using optical Doppler tomography, *Opt. Lett* 22 (1997) 1119–1121.
- [15] C.K. Hitzenberger, E. Götzinger, M. Sticker, M. Pircher, A.F. Fercher, Measurement and imaging of birefringence and optic axis orientation by phase resolved polarization sensitive optical coherence tomography, *Opt. Express* 9 (2001) 780–790.
- [16] K. Wiesauer, M. Pircher, E. Götzinger, S. Bauer, R. Engelke, G. Ahrens, G. Grützner, C.K. Hitzenberger, D. Stifter, En-face scanning optical coherence tomography with ultra-high resolution for material investigation, *Opt. Express* 13 (2005) 1015–1024.
- [17] K. Wiesauer, A.D. Sanchis Dufau, E. Götzinger, M. Pircher, C.K. Hitzenberger, D. Stifter, Non-destructive quantification of internal stress in polymer materials by polarisation sensitive optical coherence tomography, *Acta Materialia* 53 (2005) 2785–2791.
- [18] D. Stifter, K. Wiesauer, M. Pircher, E. Götzinger, R. Engelke, G. Ahrens, G. Grützner, C.K. Hitzenberger, Optische Kohärenztomografie als neues Werkzeug für die zerstörungsfreie Werkstoffprüfung, *TM* 74 (2007) 51–56.
- [19] C. Xi, D.L. Marks, D.S. Parikh, L. Raskin, S.A. Boppart, Structural and functional imaging of 3D microfluidic mixers using optical coherence tomography, *Proc. Nat. Acad. Sci* 101 (2004) 7516–7521.
- [20] Y.C. Ahn, W. Jung, J. Zhan, Z. Chen, Investigation of laminar dispersion with optical coherence tomography and optical Doppler tomography, *Opt. Express* 13 (2005) 8164–8171.
- [21] C. Joo, T. Akkin, B. Cense, B.H. Park, J.F. de Boer, Spectral-domain optical coherence phase microscopy for quantitative phase-contrast imaging, *Opt. Lett* 30 (2005) 2131–2133.

In-situ Testing of Mechanical Properties of Materials*

*Fredrik Östlund, Karolina Rzepiejewska-Malyska, Laetitia Philippe,
Patrick Schwaller and Johann Michler*

INTRODUCTION

The mechanical properties of small structures, typically with dimensions within the range of a few hundred microns down to several microns or below, cannot simply be extrapolated from the properties of bulk samples. This is due to two effects. First, samples used for bulk mechanical testing usually have dimensions which are much larger than the micro-structural features, such as grains or particles. Second, mechanical behavior is controlled by certain fundamental length scales. For example, plasticity in metals involves the motion of dislocations, which are hindered when they try to pass between obstacles more closely spaced than about 100 nm, and fracture in brittle materials is initiated at flaws with a critical size of several tens of micrometers [1]. The mechanical properties of a material will fundamentally change as the sample dimensions become smaller than these fundamental length scales. It is therefore necessary to measure the mechanical properties at a length scale comparable to the feature sizes used in miniature or micro-electromechanical devices. An example is the flow stress dependence on pillar size in micro-compression experiments shown by Uchic et al. [2], who performed

compression tests on Ni pillars having different diameters ranging from 40 μm down to 5 μm and found that for the smallest samples the flow stress is almost three times greater than for bulk Ni.

Accurate prediction of a material's response also requires an understanding of the fundamental mechanisms of material deformation and fracture in the micro- and nano-scale. It is therefore essential that small specimens, for instance for tensile or compression testing, can be manufactured for which appropriate handling and manipulation techniques and equipment with appropriate load and displacement resolution are available. Also it has to be possible to observe the material under load in-situ to study plastic-deformation and crack-propagation mechanisms. The scanning electron microscope (SEM) is an ideal platform for in-situ mechanical testing, as it covers a magnification range from 10 to 10^6 times, exhibits a relatively large specimen chamber that can accommodate mechanical testing equipment and has analytical capabilities for determining local chemical composition and crystal structure.

In the following sections the reader will be introduced to the peculiarities of integrating materials testing within an SEM. The most popular techniques will be explored, i.e. miniaturized tensile tests, compression tests and nano-indentation tests. Then the subject of image analysis will be touched upon and finally a case study

*Figures 1, 2, 3 and Table 1, plus similarities in this Chapter are re-produced with permission of MRS Journal of Materials Research.

combining the use of compressive- and tensile-testing methods will be presented.

INTEGRATING A MECHANICAL TESTING SET-UP IN AN SEM

At the time of writing there are no fully commercialized products for in-situ materials testing on the micrometer scale established on the market. Integrating a mechanical testing set-up within an SEM raises some difficulties. In the following some important details about this process will be described.

It is of course necessary to use actuators and load sensors that can deliver the required displacements and measure the low loads encountered at these scales. Additionally, a major limit is the space available in an SEM chamber. This requires that the actuators and sensors have small dimensions. In particular, to achieve an optimal performance of the SEM, the distance between the objective lens of the SEM and the sample has to be kept to a minimum. Typically, the optimal working distance is between 2 and 5 mm.

The vacuum in the chamber also has to be taken into account when designing a mechanical-testing device. All elements of the device have to be vacuum compatible, meaning that they do not emit gas in vacuum. Special care should be taken to avoid, for example, plastics and oil.

Note that some materials which normally do not emit gas in vacuum can do so when exposed to an electron beam. Teflon, for example, releases fluorine when exposed to high energy electrons. To facilitate the evacuation of the chamber, parts that contain threads should have extra channels to allow air to exit the components.

Magnetic materials should be avoided, since their magnetic fields can affect the electron beam of the SEM, resulting in a distorted image with bad resolution. Similarly, electrical components must have sufficient electrical shielding. All parts close to the electron beam should also be conductive and grounded in order to avoid electrical charging. In particular, this applies to the tip used in compression and indentation tests. Usually these tips are made of diamond because of the high hardness

requirements. Pure diamond, however, is a very poor electrical conductor. Therefore, boron-doped diamond is a preferred choice. Even if these rules are followed, the maximum resolution of the SEM will generally not be achieved.

Note that not all experiments have to be performed in-situ: cost and time have to be weighted against gain of information. In addition, not all materials can be tested in-situ. The electron beam might affect the sample by, for example, breaking chemical bonds or the sample might become too highly charged to be imaged. Charging problems can often be solved by depositing a thin metal layer on the samples before the testing. However, this can potentially change the mechanical properties of the material.

TENSILE TESTS

Tensile testing is probably the most commonly used standardized [3] method to determine the mechanical properties of materials [4]. In a typical tensile test a specimen having a small, uniform cross-section is strained until failure. The deformation (increase in length) and applied load are continuously measured during the whole experiment. The applied engineering stress σ is defined by the load F divided by the initial cross-sectional area A_0 of the sample. The engineering strain ε is defined by the measured length change Δl divided by the initial length L_0 :

$$\sigma = \frac{F}{A_0} \quad \varepsilon = \frac{\Delta l}{l_0} \quad (1)/(2)$$

A schematic representation of an engineering stress/strain curve obtained this way is shown in Figure 21-1.

From such a curve the following properties can be inferred. The linear increase at low strain is an elastic deformation that is described by Young's modulus E (the slope of the stress/strain curve). The transition between elastic and plastic deformation is defined by the 0.2% offset yield stress $R_{p0.2}$ commonly used in materials technology. In Figure 21-1 a straight line shifted by a strain of 0.002 is drawn parallel to the linear elastic part.

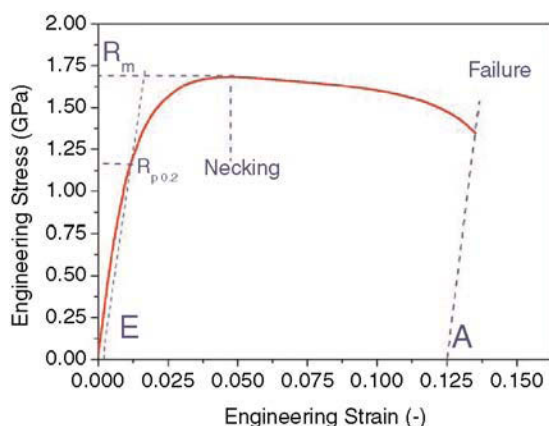


FIGURE 21-1 Engineering stress/strain curve for an NiCo sample indicating the relevant quantities that can be extracted from the curve (see text for the details).

The intersection of this line with the stress/strain curve is taken as the yield stress.

The tensile strength R_m indicates the deformation where a necking of the sample starts. Finally, the elongation at rupture A indicates the strain at failure of the sample. The uniaxial deformation is usually applied using a constant strain rate, i.e. using a displacement control, in contrast to a load control. This is because as a sample yields there can be a decrease in the load. If that occurs with load control the feedback system will try to re-establish the load by increasing the strain. This causes the sample to be rapidly deformed until failure in an uncontrolled manner.

It is also worthwhile mentioning the difference between engineering and true stress and strain values. Engineering stress and strain are defined by Eqns (1) and (2) as shown above. Both quantities refer to the initial cross-section and initial length. True stress σ_{true} and true strain ϵ_{true} values take small changes of the deformation into account starting from an instantaneous elastic or plastic deformation. σ_{true} and ϵ_{true} can be calculated as follows:

$$\sigma_{\text{true}} = \sigma(1 + \epsilon) \quad \epsilon_{\text{true}} = \ln(1 + \epsilon) \quad (3)/(4)$$

For samples in the millimeter range tensile tests can be performed under an optical micro-

scope. If the samples are smaller, the higher resolution of an SEM allows imaging. This is especially important if the images are used to extract the strain.

From the image sequence, it is sometimes interesting to observe the propagation of cracks induced by the tensile strain and to correlate the crack path or the crack type with other material properties that can be inferred from SEM images. Instead of imaging the sample using secondary electrons, chemical mapping can be done using energy-dispersive X-ray spectroscopy (EDX) and the orientation of grains of the sample can be recorded using electron backscatter diffraction (EBSD).

Due to the limited overall size of the test stage, the sample dimensions also have to be small (typically only several millimeters length and of a few 100 micrometers thickness). This means that surface properties gain importance and rough surface regions or a slightly different composition in the surface region may influence the measured stress/strain curves. The most critical issue, however, is the correct fixing of the tensile test specimen. Mechanical clamping may be unsuitable because a deformation could already have been induced prior to the actual test. A suitable solution is to use sample holders having the 'negative' shape of the specimen and to fit the specimen inside these holding forms: an example of this is shown in Figure 21-2.

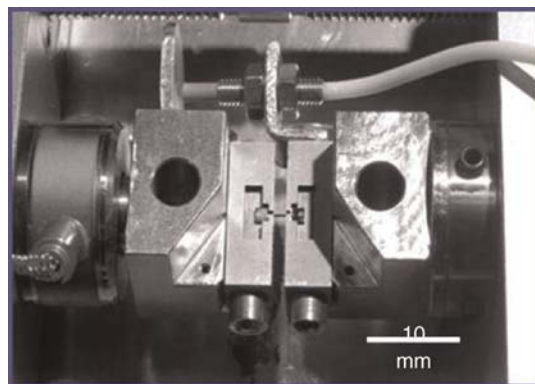


FIGURE 21-2 A specimen for tensile testing positioned in the sample holder of a tensile testing set-up.

Due to the small dimensions of the tensile test specimens, extensometers or conventional strain gauges cannot be clamped onto the samples. However, the SEM images can be used to calculate strain values. The quantitative evaluation of the strain values from SEM images recorded during the tensile tests, however, is difficult. The total elongation until fracture in the images is often only a few pixels and specialized image analysis routines allowing sub-pixel resolution have to be used to obtain reliable strain data: this will be further discussed below. In contrast to the displacement measurements, the load measurements can be performed using conventional load cells.

COMPRESSION TESTS

As an alternative and complement to tensile testing, materials can be tested by compression tests. This is also a method with very old roots and has the advantage that the specimen does not have to be attached at the ends of the testing set-up. Compression tests are analogous to tensile tests: a cylindrical sample with uniform diameter is compressed by applying an increasing force on the ends until it fractures; typically starting with a purely elastic region followed by plastic deformation with strain hardening and finally fracture. Throughout the compression the load on the sample and the deformation are recorded. Typically, these numbers are then converted to engineering stress and strain and these are

plotted against each other, providing characterization of the material as described above for tensile tests.

As for tensile tests, it is an advantage if the actuators can be run with displacement control. Although there is no necking phenomenon as for tensile tests, crystalline samples can exhibit a load drop at the onset of plasticity which can cause an uncontrolled compression if load control is used. In addition, the mechanical behavior of a material is often dependent on the rate of compression, making constant displacement more logical than load control.

New load cells and piezo-actuators have made it possible to perform compression tests in the sub-micrometer scale [5]. Also vital for this type of testing is the possibility to manufacture rods or pillars using, for example, lithography or focused ion beams (for an excellent example of compression tests on FIB-machined metal pillars, cf. [2]).

Figure 21-3 shows an image series from a compression test on a gallium arsenide pillar of 4.2 μm diameter. This pillar was manufactured by photolithography and reactive-ion etching. The crystallographic direction of the surface is (001). (a) and (d) show the pillar before and after compression, respectively. (c) shows plastic deformation along three different (111) slip planes and (d) reveals cracking along 110 planes.

The stress/strain curve recorded during this experiment is shown in Figure 21-4. The letters

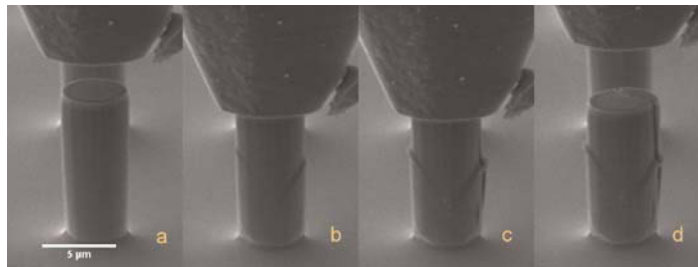


FIGURE 21-3 Image sequence from the video captured during the compression of a gallium arsenide pillar. The total time of the compression experiment was about 90 s and the frame rate of the video 0.58 frames/s. In (b) plastic deformation along three different slip planes can be seen. (c) reveals some cracking of the pillar. (d) shows the pillar after compression. The stress/strain curve for this particular experiment is shown in Figure 21-4.

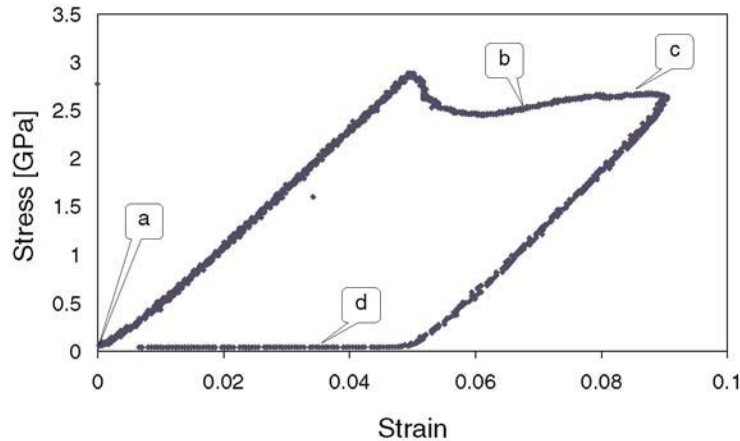


FIGURE 21-4 Stress/strain curve for a compression experiment of a gallium arsenide pillar. The letters refer to the images in **Figure 21-3**. Note that after the initial elastic part of the curve there is a drop in the measured force. This is common for crystalline samples and is caused by the introduction and subsequent multiplication of dislocations within the material [6].

a–d correspond to the images in Figure 21-3. From this curve it is not possible to see the cracking of the pillar. If the experiment had not been performed in an SEM it would not have been possible to deduce whether the cracks or the slip occurred first. This is an example of the strength of in-situ testing. In this particular study, the transition from brittle to ductile behavior of gallium arsenide as a function of the dimensions was investigated [7].

Micrometer-sized compression experiments do not necessarily have to be performed within an SEM, but doing so offers some advantages. First, being able to see the sample and tip (compression punch) facilitates the positioning of the sample under the tip. A further benefit of this is that there will not be any doubt as to whether the tip only partially contacts the sample, which could be possible with an experiment without direct observation. Also, contaminants on the sample, which potentially can affect the experiment, can be detected immediately.

If the pillar and the tip are badly aligned the pillar might buckle or bend, thus producing an entirely different load/displacement curve. Such effects are easily detected in an in-situ experiment so that experiments showing these effects

can be discarded. By analyzing the video with image-analysis software (see below) it is possible to extract more information than just load and displacement. For example, the lateral expansion can be measured and from this the value of Poisson's ratio can be calculated. Also, during a typical compression experiment the pillar sinks into the substrate. This effect, called sink-in, can easily be measured. In fact, because it is possible to measure the top and bottom of the pillar, the strain extracted from a video will be entirely free of instrumental compliance.

In principle, the image from an SEM only gives two-dimensional information. This complicates the approach of the tip to the sample. In order to make the alignment of the tip over the pillar possible it is necessary that the set-up be tilted to the electron beam so that the sample substrate can be seen (as seen in Figure 21-3). The focus of the SEM can be used to give an estimation of the height difference between the sample and the tip. When the tip is very close to the substrate a 'shadow' of the tip can be seen. This shadow arises from the constrained geometry, preventing a fraction of the secondary electrons from reaching the detector of the SEM. Most configurations

allow for physically touching the substrate with the tip at a position close to the pillar before the experiment. After this the distance between the sample and the tip is known and positioning becomes easier.

INSTRUMENTED INDENTATION/ NANO-INDENTATION

Instrumented indentation or nano-indentation is an excellent tool for the determination of the hardness and Young's modulus of thin coatings or small objects. In a typical experiment a diamond indentation body is pressed into the specimen. The term nano-indentation is commonly used for indentation depths ranging from a few nanometers to 100 nm. The load P and the displacement into the surface h are continuously measured during loading and unloading: for an overview, cf. [8]. An example of such a load/displacement curve is shown in Fig. 21-5. Young's modulus E_{Indent} can be calculated from the unloading part of the curve, as the unloading is a purely elastic recovery process. However, the procedure is not as straightforward as for tensile and compression tests, therefore a method to determine E_{Indent} in more detail is described. The full procedure is presented by Oliver and Pharr in [9].

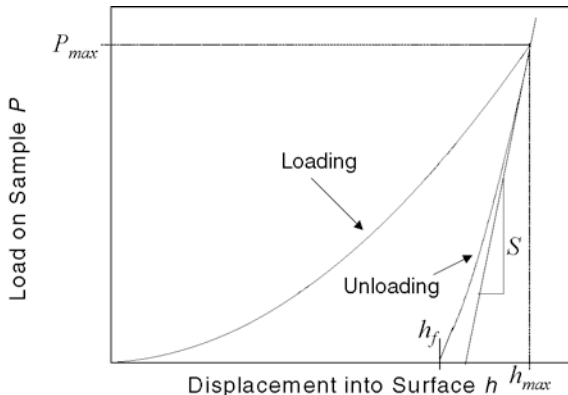


FIGURE 21-5 A typical load/displacement curve from an indentation experiment.

The first step of the Oliver–Pharr data analysis procedure consists of fitting the unloading part of the load/displacement data to a power/law relation derived from contact mechanics theory:

$$P = B(h - h_f)^m \quad (5)$$

where P denotes the applied load, h the penetration into the surface, h_f the final displacement after complete unloading (cf. Fig. 21-5) and B and m are empirically determined fitting parameters. From this equation, the unloading stiffness $S = dP/dh$ can be calculated by differentiating the equation and evaluating it for $h = h_{\text{max}}$:

$$S = Bm(h_{\text{max}} - h_f)^{m-1} \quad (6)$$

Using S , the so-called contact depth h_c can be calculated according to:

$$h_c = h - \varepsilon P/S \quad (7)$$

where ε is a constant depending on the indenter geometry. For three-sided pyramidal indenters (Berkovich tips), $\varepsilon = 0.75$. Note that the correction for h_c has to be used with some caution because it is not valid in the case of material pile-up around an indentation. Using h_c , the projected contact area as a function of the penetration, $A(h_c)$ can be calculated. With S and A , the so-called reduced Young's modulus E_r can be determined:

$$E_r = \frac{(\sqrt{\pi} S)}{2\beta \dot{s} A} \quad (8)$$

β depends on the indenter geometry and is equal to 1.034 for Berkovich pyramids. The reduced Young's modulus does not take the finite stiffness of the tip into account. The Young's modulus of the sample – E_{Indent} – can be extracted from the relation:

$$\frac{1}{E_r} = \frac{(1 - \nu^2)}{E_{\text{Indent}}} + \frac{(1 - \nu_i^2)}{E_i} \quad (9)$$

Here, ν is the Poisson's ratio of the test material and E_i (1141 GPa) and ν_i (0.07) are the

Young's modulus and the Poisson's ratio, respectively, of the diamond indenter. It may seem counter-intuitive that the Poisson's ratio of the investigated material has to be known. However, ν is about 0.3 for most metals and even an uncertainty of ± 0.1 produces an error for E_{Indent} of only about $\pm 5\%$. The scattering of E_{Indent} values from measurements on the same material with fixed measurement parameters is within $\pm 10\%$.

The hardness of the material is defined by:

$$H = \frac{P}{A(h_c)} \quad (10)$$

The largest error source for the calculation of hardness and Young's modulus is the expression used to calculate the area as a function of the displacement. Only for an ideal (i.e. infinitely sharp) Berkovich indenter is the relation $A = 24.5\dot{s}h_c^2$ valid. In reality each tip will be blunted and may have other defects. This can be corrected to some extent by using an area function of the form:

$$A(h_c) = a_0\dot{s}h_c^2 + \sum_{i=1}^n a_i\dot{s}h_c^{1/2^i}. \quad (11)$$

The parameters a_i can be obtained by performing nano-indentation experiments on materials with a known value of Young's modulus.

INDENTATION INSIDE THE SEM

Nano-indentation enables the measurement of hardness and Young's modulus of small samples or thin coatings. However, it is not possible to have an insight of the deformed zone of the sample during the indentation process. As a consequence, no information about possible crack formation or pile-up (cf. Fig. 21-6) can be obtained. In Fig. 21-6, an SiO_2 surface was indented by a cube-corner tip. The information about cracking can be used to evaluate the fracture toughness of the material. Information about pile-up and sink-in can be used in models of the flow, providing more accurate

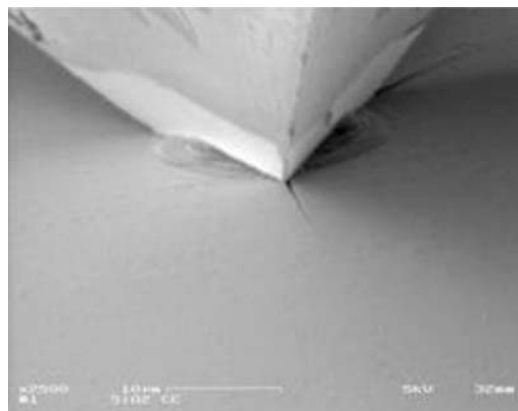


FIGURE 21-6 In-situ indentation showing cracking and pile-up.

data about the material. Another advantage of in-situ indentations is the possibility to precisely position the tip with respect to the sample surface. This makes indentation experiments on small structures or at specific locations possible. Finally, there is no need to locate the indent after a test for measuring the area of the residual imprint. For ex-situ indentations this can be a very time consuming task since the size of the imprints is only in the order of nanometers. In the next paragraph issues that have to be addressed for in-situ SEM devices will be briefly described.

As for all in-situ mechanical tests, the SEM environment induces several 'design boundaries' that do not have to be considered in a standard indentation device working in air. It has to be ensured that the set-up allows an unhindered view of the indentation region. The indentation tip axis normal to the sample surface has therefore to be inclined with respect to the beam axis of the SEM. In addition the indentation tip geometries which are normally used in indentation experiments (the four-sided Vickers pyramid or the three-sided Berkovich pyramid [10]) cannot be used because they have too large an opening angle (140.6 degrees). For measurements inside the SEM, sharper indenters such as the cube-corner (opening angle 84.6 degrees) have to be used.

Figure 21-7 shows a custom-made instrumented indentation device working inside the SEM

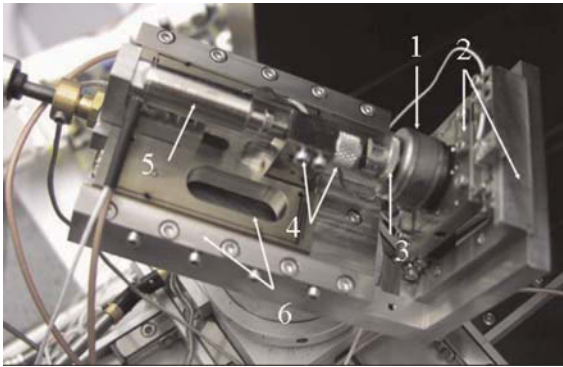


FIGURE 21-7 The SEM-micro-indenter: 1 load cell; 2 XY-positioning table; 3 sample holder; 4 tip holder and adapter; 5 piezo-actuator, displacement sensor; 6 sample coarse positioning.

[11]. The indentation head (4) is composed of a parallel mechanism (flexure hinges) that holds the diamond tip. The head is driven by a stack piezo (5) with 20 μm range and a built-in displacement sensor (strain gauge). The indentation head and its actuator are assembled on a coarse positioning stage (6) (also a flexure mechanism) and driven by

a fine-pitch precision screw, remotely controlled with a cable connected to a knob installed on the SEM chamber's door. The stage is fixed on the main body by a dovetail sliding bearing. An XY slip-stick piezo stage (2) holds the load cell (1) and the sample (3).

As an application example, Fig. 21-8 shows the result of an indentation experiment of a thin nano-composite coating. Whereas the load/displacement curve does not show any irregularities, the SEM images recorded simultaneously show the formation of pile-up and the formation of a crack upon unloading. Interestingly, the crack almost closes completely after full unloading and it would therefore be very difficult to detect it by inspection of the residual impression only. This demonstrates nicely the added value that can be gained by in-situ SEM indentation experiments.

IMAGE ANALYSIS

Most modern SEMs allow the recording of a video, which can be later used to extract the

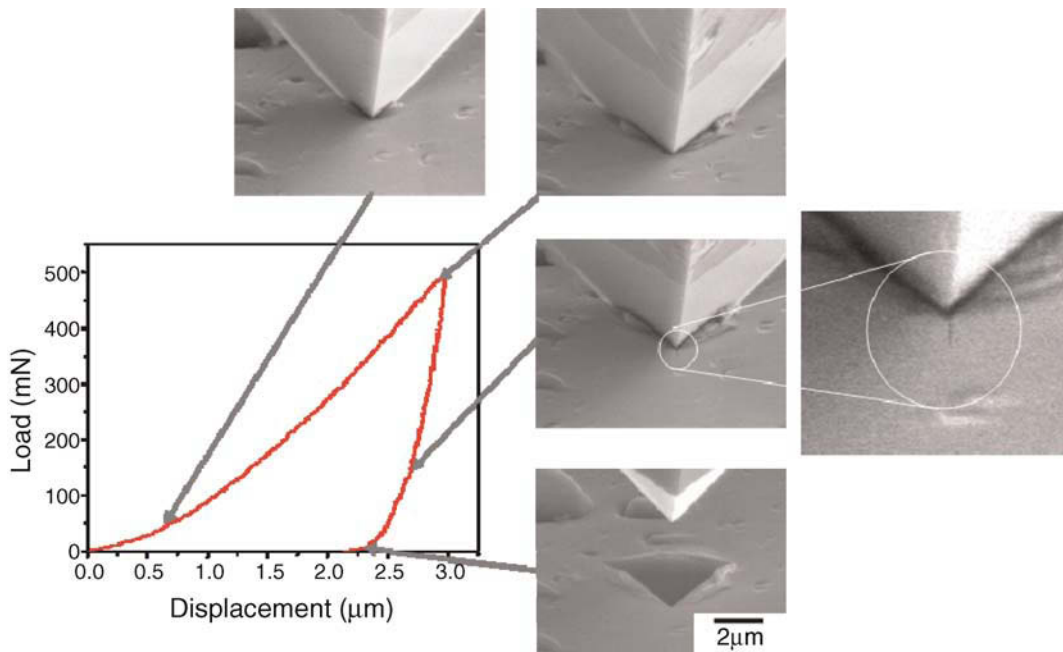


FIGURE 21-8 In-situ SEM indentation of a thin nano-composite coating.

displacement of different features of the sample. Rough measurements can be done simply by directly measuring distances with some imaging software. However, image-analysis tools can do this with a far greater resolution. Also, through image-analysis algorithms it is possible to track features throughout a whole video automatically in order to construct, for example, a time vs strain relationship.

There are several algorithms available for tracking motion in an image sequence. Here, it will be assumed that an algorithm called cross-correlation is employed. For a description of this algorithm, cf. [12]. This algorithm takes a small image and a large image as inputs. The output will be a map showing how similar the small image is to each position in the larger one. By taking the peak value the position of the smaller image in the larger image is found. This algorithm works even if there is no exact copy of the small image within the larger. By selecting a small feature in the first frame of the video and trying to find this part in the following frames gives the displacement of this particular feature. For the case of compressive or tensile tests, if two features that are close to the ends of the sample are tracked the strain can be calculated. This strain will be entirely independent of instrument compliance. As mentioned above, strain is not the only property that can be measured from the images. For example, by tracking several parts on the samples, buckling and lateral expansion of the samples can be measured.

The cross-correlation algorithm can be improved, making it possible to track changes with a sub-pixel resolution, provided that the image is well focused and that the level of noise is low. This is important, because the total size of an image is often about 500 pixels in width. In this case one single pixel corresponds to 0.2% strain assuming that the sample covers the whole image. This low resolution would normally be considered insufficient.

When working close to the resolution limit of an SEM, the signal is usually very weak, requiring a very long integration time for each image. In this case, the acquisition time for a single frame can be

several seconds. It must therefore be taken into account also that different parts of the image are scanned at different times, usually starting from the top and ending at the bottom.

CASE STUDY: A COMPARISON OF IN-SITU MICRO-TENSION AND MICRO-COMPRESSION FOR STUDYING THE PLASTIC PROPERTIES OF NANO-CRYSTALLINE ELECTRODEPOSITED NICKEL AT DIFFERENT LENGTH SCALES

In order to evaluate the effects of grain size or geometrical constraints on measured mechanical properties, there is a need to understand the influence of the measurement technique, load distribution, strain rate, etc., on the measurement values and to correlate the measurements with deformation mechanisms. Uniaxial in-situ methods are interesting tools for this purpose. In the following case study a comparison of in-situ and ex-situ micro-compression with in-situ micro-tensile tests is shown; all the tests being used to study the mechanical properties of electrodeposited nano-crystalline (nc) nickel. As the material is nano-crystalline, it would be expected that the size of the probed volume does not influence the mechanical properties as long as it is at least of the order of a cubic micrometer. Micro-tensile tests that probe a volume of more than $2.10^6 \mu\text{m}^3$ show reasonable agreement with results from micro-compression tests that probe much smaller volumes of down to a few μm^3 . In-situ uniaxial solicitation in compression mode reveals several advantages for studying stress/strain properties.

In the same way as for tensile measurements, a quantitative evaluation of the deformation during compression through video frame records [13] was found possible.

The material investigated was electrodeposited nano-crystalline (nc) nickel. Figure 21-9 shows an HRSEM picture of the nc Ni surface. The sizes of the grains vary between 30 and 200 nm with an average of 50 nm. The inset in Fig. 21-9 displays a TEM cross-section of the film. The grains have a

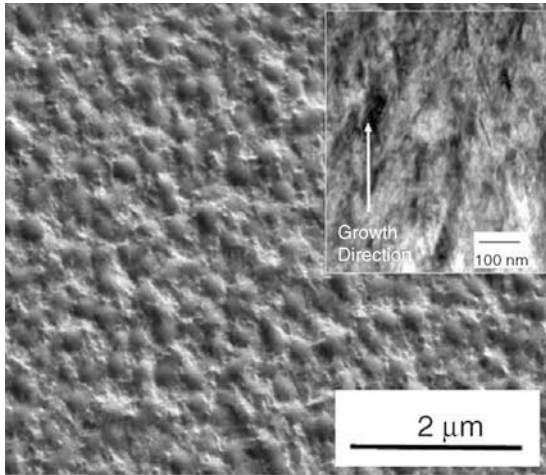


FIGURE 21-9 HRSEM image of the nc Ni surface; roughness and grain size are easily identified on this picture. The inset of the right of the picture shows a TEM bright-field image of the specimen indicating the growth direction of the electrodeposition.

predominantly columnar structure parallel to the deposition direction.

The samples for tensile testing were manufactured by a LIGA process. The 10 μm pillars for in-situ compression were also manufactured by LIGA, whereas the 2 μm pillars for

ex-situ compression were produced by FIB machining.

The in-situ tensile tests were carried out at a constant strain rate of $0.2 \cdot 10^{-3} \text{ s}^{-1}$. Figure 21-10 shows the average true stress/strain (σ/ϵ) curve (i.e. measurements made prior to necking) obtained from micro-tensile measurements. The curve indicates weak strain hardening leading to an increase of the required stress for further deformation of the tested specimen. Figure 21-10(a) shows an SEM image of the dog-bone central section extracted from the video frames recorded at the beginning of a measurement and Fig. 21.10(b) represents SEM video frame of the micro-tensile bars just before fracture, revealing necking in the central part. An inset on the left part of the graph shows an optical picture of the typical dog-bone used.

The in-situ compressive tests were carried out using a flat diamond punch of 15 μm diameter. The strain rate was $0.2 \cdot 10^{-3} \text{ s}^{-1}$. Figure 21-11 displays true σ/ϵ curves obtained on 10 micrometer diameter pillars (aspect ratio 3:1) with in-situ compressive tests. Figure 21-11(a) and (b) for the 10 micrometer diameter pillar tested represent the video frames extracted at the beginning and at the end of a typical in-situ compressive test,

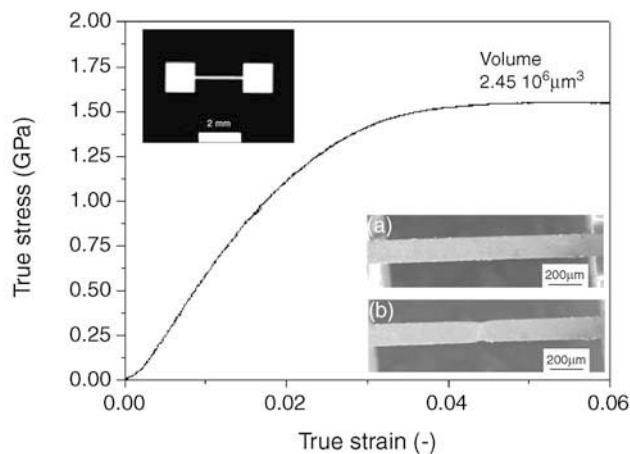


FIGURE 21-10 Average tensile stress/strain curves obtained from four samples. The inset of the left part of the graph shows an optical picture of the typical dog-bone specimen tested.

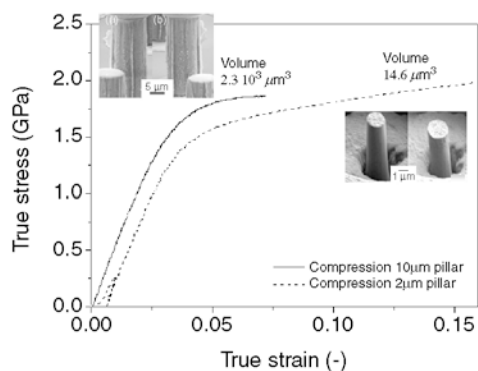


FIGURE 21-11 Average micro-compressive stress/strain obtained from five measurements for in-situ compressive tests (10 μm pillars) and for ex-situ compressive tests (2 μm pillars). On the ex-situ curves, a reloading procedure at the beginning of the compressive test in order to rectify the misalignment of the pillar with the tip is visible.

respectively. Buckling or crack formation was found only rarely in the video recording and those were not used.

Finally, for comparison, ex-situ compressive tests were performed in a commercial MTS NanoXP nano-indentation with a truncated diamond tip of 8 μm diameter.

Table 21-1 lists the respective material properties inferred from σ/ϵ curves obtained with the different testing methods. The yield stress values listed are equal to the 0.2% offset yield stress as described by Figure 21-1. The complete stress/strain curves determined in four different ways reveal that there is reasonable agreement between the two compressive tests and the single tensile test despite the fact that the probed volume differs by 5 orders of magnitude.

Measurement errors that are intrinsic to each technique are prone to give differences in σ/ϵ curves. For tensile tests, the major source of uncertainty in the stress calculation is the measurement of the specimen cross-section, an average value for the cross-section of 20 tensile bars being calculated. As all tensile bars tested were fabricated from the same plating batch, it is assumed that an average value of their cross-sections gives sufficient accuracy. For compression measurements, the cross-section was measured at ten different positions over the entire length of the pillar. For 2 μm pillars, ten measurements of the cross-section were made directly on the pillar SEM image over its entire length, for obtaining an average value of the pillar volume, i.e. the pillar shape is a source of error as the diameter is not constant over its length. In both cases, for micro-compressive and micro-tensile tests, the pillar sizes (length L and surface area A) and the tensile bar sizes (length L , and cross-section A) can be measured to within an error of 5% for L and L_0 (displacement), and to within an error of 15% for A . These induce statistical errors, with a scatter of 25% in the Young's modulus estimation and 15% for σ_y . Such experimental errors in the measurements might explain the discrepancies found between tensile and compressive tests.

A comparison between ex-situ and in-situ micro-compressive tests reveals the advantage of the in-situ method. First, for the ex-situ compressive tests the measured displacement values had to be corrected by accounting for the sink-in of the pillar into the substrate, whereas this correction is not necessary when strain values are determined from SEM images recorded during compression.

TABLE 21-1 Young's Modulus E and Yield Stress σ_y for Nano-crystalline Ni as Determined from Micro-tensile and -compression Testing. Also Shown is a Comparison of the Strain-rate Values used for Each Method.

Method	E (GPa)	σ_y (GPa)	Strain Rates (s^{-1})
Tensile	63 ± 16	1.2 ± 0.1	$0.2 \cdot 10^{-3}$
Compression (2 μm pillar)	51 ± 13	1.3 ± 0.2	$0.9 \cdot 10^{-3}$
Compression (10 μm pillar)	54 ± 14	1.4 ± 0.2	$1.5 \cdot 10^{-3}$

Also, this correction has to take into account the complex geometry of the post-base connection to ensure the avoidance of an overestimation of Young's modulus with a simple elastic contact model [14]. Finally, without continuous video control, a misalignment of the tip to the pillar can lead to a decrease of the measured elastic modulus or, in excessive cases, to the buckling of the pillars.

In nc Ni, the difference of probed volume in the different tests, i.e. external size effects, should not have a significant influence on the σ/ϵ curves. The Young's moduli and the yield stresses are somewhat lower than already reported for fully densified nc electrodeposited nickel [15], suggesting that the influence of textures, pre-existing voids, columnar grain structure and hydrogen on the mechanical response cannot be neglected [16, 17]. In this case, it is expected that pores and flaws within the matrix tested are prone to play a bigger role on the mechanical response in the tensile mode.

Cheng et al. proposed a deformation-mechanism map for FCC metals [18]. The model predicts not only the strength as a function of grain size, but also the observed tensile/micro-compressive asymmetry of the yield strength. It is predicted that a greater yield stress will be found in compression than in tension for FCC metals with grain sizes ranging from 2 nm up to 100 nm. The tension/compression asymmetry which is explained by a pressure dependence of the dislocation self-energy during bow-out may be responsible for the difference in the yield/stress values plotted in Table 21-1 for the tested FCC nc nickel.

To summarize, the potential of in-situ micro-compression and micro-tensile methods to characterize nano-crystalline nickel has been assessed and potential measurement errors have been discussed. Due to the small size of the micro-structure, size effects could be neglected, which allowed the revelation on the one hand of the importance of the load cases particular to each method, and on the other hand the influence of the probed volume and of the micro-structure. Whether surface effects, stress state or strain rate is the most important could not be distinguished.

It was found that in-situ uniaxial tensile and compression testing is able to provide accurate data and similar mechanical insights of the tested materials ranging over five orders-of-magnitude of probed volume. Comparing the aforementioned advantages and drawbacks of the different approaches, it may be concluded that uniaxial in-situ methods are appropriate to study the mechanical properties of isotropic nc metals.

CONCLUSION AND OUTLOOK

Discussed above are instrumented micro-indentation, micro-compression and micro-tensile testing methods for use inside an SEM and the application potential of the techniques is presented in a case study on UV-LIGA materials. Coupled with advanced image-analysis techniques, these in-situ SEM micro-mechanical testing methods are used to study scale-dependent material properties and to observe deformation and fracture mechanisms in-situ. Also, the SEM enables for accurate sample positioning and visual control of the experiment. Current leading-edge research in instrumentation is focused on micro-electromechanical systems for the tensile testing of nano-wires and carbon nanotubes, and on nano-bending experiments on nano-wires; using (1) atomic-force microscopy techniques and (2) vibrational analysis of different types of nano-structures inside the SEM. Both of these techniques require, however, high resolution SEMs or alternatively transmission electron microscopes.

REFERENCES

- [1] E. Arzt, Size effects in materials due to microstructural and dimensional constraints: a comparative review, *Acta Mater* 46(16) (1998) 5611–5626.
- [2] M.D. Uchic, D.M. Dimiduk, J.N. Florando, W.D. Nix, Sample dimensions influence strength and crystal plasticity, *Science* 305 (2004) 986.
- [3] Current standards for metals: EN 10002-1 and -5, ISO 6892, ASTM E 8, ASTM E 21, DIN 488, DIN 501.
- [4] J. Mencik, *Mechanics of Components with Treated or Coated Surfaces*, Dordrecht (Netherlands): Kluwer Academic Publishers (1996) .

- [5] L. Philippe, P. Schwaller, G. Bürki, J. Michler, A comparison of microtensile and microcompression methods for studying plastic properties of nanocrystalline electrodeposited nickel at different length scales, *J. of Materials Research* 23(5) (2008) 1383–1388.
- [6] D. Hull, D.J. Bacon, *Introduction to Dislocations*, (4th ed.): Butterworth-Heinemann, Oxford (2001).
- [7] J. Michler, K. Wasmer, S. Meier, F. Östlund, K. Leifer, Plastic deformation of gallium arsenide micropillars under uniaxial compression at room temperature, *Appl. Phys. Lett* 90 (2007) 043123.
- [8] B. Bhushan, *Handbook of Micro/Nano Tribology*, New York: CRC Press (1999) 433.
- [9] W.C. Oliver, G.M. Pharr, Measurement of hardness and elastic modulus by instrumented indentation: advances in understanding and refinements to methodology, *JMR* 19 (2004) 3–20.
- [10] A.C. Fischer-Cripps, *Nanoindentation*, Springer, New York (2002).
- [11] R. Rabe, J.M. Breguet, P. Schwaller, S. Stauss, F.J. Haug, J. Patscheider, J. Michler, Observation of fracture and plastic deformation during indentation and scratching inside the scanning electron microscope, *Thin Solid Films* 469–470 (2004) 206–213.
- [12] W.G. Kropatsch, H. Bischof, *Digital image analysis: selected techniques and applications*, Springer, New York (2001).
- [13] B. Moser, K. Wasmer, L. Barbieri, J. Michler, Strength and fracture of Si micropillars: a new scanning electron microscopy-based micro-compression test, *J. of Materials Research* 22(4) (2007) 1004–1011.
- [14] H. Zhang, B.E. Schuster, Q. Wie, K.T. Ramesh, The design of accurate micro-compression experiments, *Scripta Materialia* 54 (2006) 181–186.
- [15] W.D. Nix, J.R. Greer, F. Feng, E.T. Lilleodden, Deformation at the nanometer and micrometer length scales: effects of strain gradients and dislocation starvation, *Thin Film Solids* 515(6) (2007) 3152–3157.
- [16] K.S. Kumar, H. Van Swygenhoven, S. Suresh, Mechanical behavior of nanocrystalline metals and alloys, *Acta Materialia* 51 (2003) 5743–5774.
- [17] R.J. Asaro, S. Suresh, Mechanistic models for the activation volume and rate sensitivity in metals with nanocrystalline grains and nano-scale twins, *Acta Materialia* 53 (2005) 3369–3382.
- [18] S. Cheng, J.A. Spencer, W.W. Milligan, Strength and tension/compression asymmetry in nanostructured and ultrafine-grain metals, *Acta Materialia* 51 (2003) 4505–4518.

Testing and Diagnosis for Micro-Manufacturing Systems

Pietro Larizza

INTRODUCTION

Testing and diagnosis are terms often associated with the same topic, nevertheless their true sense is commonly related to a different meaning. A main difference is that testing does not deal with fault repairing but focuses only on fault detection, while diagnosis consists of determining the nature of a detected fault, of locating it and hopefully repairing it. There is another difference between the two topics: this is related to the work conditions and functional states which permit the execution of testing or diagnostic procedures. Testing is often considered as an *offline* procedure conducted by proper, prefixed excitation signals using suitable testing models; however, it is ever more frequent to implement testing procedures as *online* conditions thanks to automated test-bench and computer-based measurement equipment. Diagnosis procedures can also be executed under normal working conditions, permitting real-time response and fast fault identification and compensation. A common application area for testing and diagnosis procedures is measurement, which can be performed following both classical and modern approaches. The classical approach generally provides a number of sensors that is equal to the number of signals to be acquired, while the modern, or model-based, approach provides a number of sensors (observations) that are less than the

number of signals (variables) to be acquired. In such a type of approach more information is provided by the knowledge model of the system.

Testing or diagnostic procedures applied to micro-manufacturing systems, or miniaturized systems for processing and machining, could be assisted by the use of measurement techniques based on the modern approach, principally due to the minimum space available and difficulties associated with the location of the sensors. In order to achieve a further reduction of the problem related to the allocation of the sensors, especially with reference to micro-systems, testing and diagnostic procedures often require non-contact sensors or special transducers in order to avoid external influences, under normal working conditions, of the reduced size of parts and devices to be tested. Other important aspects are the precision and accuracy of the measurement system, which for the specific micro-manufacturing area have to be related to the local and global concepts.

Precision is defined as the degree to which further measurements, or calculations, show the same or comparable results, so the concept of precision is linked to that of repeatability. The accuracy is the degree of conformity of a measured or calculated quantity to its actual or true value (Fig. 22-1). Often the two concepts have to be related to the local and global meaning because

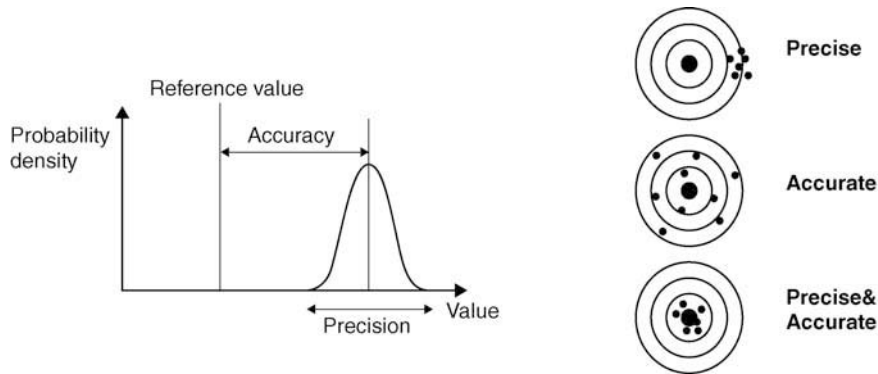


FIGURE 22-1 Definition of precision and accuracy.

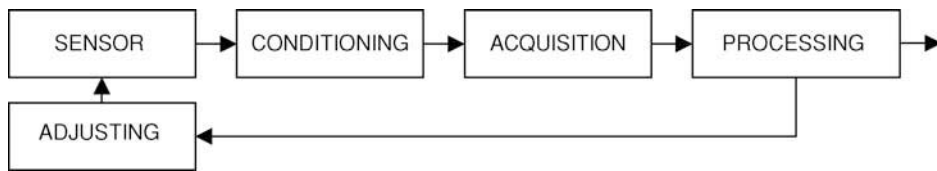


FIGURE 22-2 A typical measurement system suitable for micro-nano-applications.

local measurement space and global measurement space could be several orders of magnitude apart. This imposes strong requirements in terms of accuracy and stability of the measurement system which can be overcome by proper local reference points and (auto) calibration procedures.

Typically, a measurement system consists of sensors, conditioning, acquisition and processing systems. Depending on the nature of the measurement, the sensor system could be considered as a complex transducer system or could even be reduced to a simple sensing element. For example, dimensional measurements could require, as sensing element, a simple linear encoder or a complex charge coupled device (CCD) camera joined with a laser beam. If the dimensional measurement of micro-parts is considered, performed with the aid of a microscope, a precise positioning of the sensing element (optics, lenses, camera) is required. Often this task is accomplished by a servo actuator connected in a closed-loop configuration. Precise positioning is also required for the focusing of the camera's optical system, in order to accomplish inspection of micro-parts both in static and dynamic mode (dependent on shape and dimensions of the part).

Precise positioning devices are largely used in modern measurement systems either as single-stage devices (1D) or multi-stage devices (2D–3D or even more). Characterized by a precision of a few nanometers, up to micrometers, the linear movements are implemented either with piezo devices or electromagnetic devices (moving coil, brushless linear motor). These devices are either coupled directly with the end-moving part, without a mechanical joint, or, depending on the final application, using several very precise kinematic configurations (serial-Cartesian, or parallel-Tripode or Exapode). Many measurement systems suitable for micro- or nano-technology areas are based on the laser interferometer principle. A laser interferometer, together with a CCD or position sensing detector (PSD) and galvanometer motor, are used to realize precise 1D to 6D measurements (orders of nanometer or below) by exploiting laser tracking techniques. Very fast sampling times are also possible (up to 100 kHz) rendering this kind of measurement suitable for the ultra-precise real-time measurement of vibrating parts.

Within micro-manufacturing processes, both testing and diagnostic procedures are of great



FIGURE 22-3 Six d.o.f. Exapode system.

importance for quality assurance (QA). The main *scenario* of QA involves statistical process control (SPC) as a set of tools capable of controlling the quality of the products by statistical analysis methodologies [1]. The SPC techniques use data and measurements coming from testing and diagnostic equipment in order to take decisions on quality levels of the production, and ensure eventual cor-



FIGURE 22-4 1D laser-based displacement measurement system.



FIGURE 22-5 A motorized, vision-based measurement system (X,Y,Z resolution: 50 nm).

rections of the production process. There are several tools which permit the control of the incoming data from a process. When the measurement data are collected, they are analyzed by extracting *means* and *ranges* that are plotted on *charts*. More complex analyses can be accomplished by calculating the *indices of capability*, which become tools suitable for the evaluation of how much the process or sub-processes meet the initial requirements. While the precision of a process is related to the spread of the collected data around a mean value, the capability relates the precision to the range of the permitted values fixed by the specifications (or specification tolerance). Generally, if the precision is characterized by the *standard deviation* σ , the capability index relates the specification tolerance to the value of 6σ .

From a more general point of view the testing and diagnostic decision-making processes can be viewed as a series of transformations, or mappings, on process measurements. Figure 22-7 shows the various transformations that process

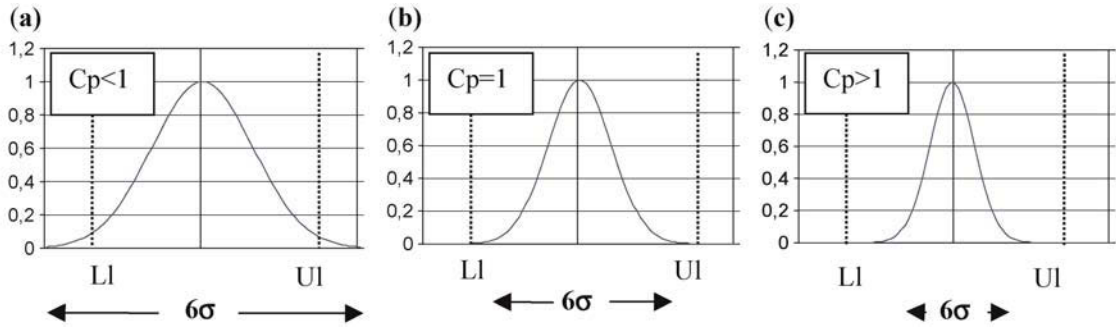


FIGURE 22-6 Capability index for a low capability (a), medium capability (b), high capability (c) system (process). (Cp: capability index, LI: tolerance lower limit, UI: tolerance upper limit, σ : standard deviation).

data go through during diagnosis [2]. The measurement space defines a set of measurements incoming from sensors and transducers. These are the input to the diagnostic system. The feature space is a space of points that are obtained as a function of the measurements by utilizing *a priori* knowledge. Here, the measurements are analyzed and combined with the aid of *a priori* process knowledge, in order to extract useful features about the process behavior to aid diagnosis. The mapping from the feature space to decision space is usually designated to meet some objective function (such as minimizing of misclassification). Typically, this transformation is achieved by using either threshold functions or template matching. In the class space, the features are separated by suitable classifiers. The class space is thus the final interpretation of the diagnostic system delivered to the user.

In the following sections a deeper analysis of some aspects of the diagnosis and testing for micro-manufacturing systems will be detailed. In the first section the main non-contact measurement techniques used in the micro-applications area are recalled. The second section focuses on testing and diagnostic methods, in particular, related to quantitative techniques such as Kalman filters. The third section reports an application where model-based testing is used to detect the

failures and performance of a piezoelectric micro-positioning device.

PRECISION MEASUREMENT SYSTEMS

Starting from the measurement space, it results that primary importance is usually given to how signals and data are collected in order to proceed through a testing or diagnostic process. The main elements involved in the capturing of signal are the sensors.

The production of *meso*-, *micro*- and *nano*-devices requires a high level of precision due the millimeter or sub-millimeter dimensions of the devices to be assembled, handled or tested. Within the sub-millimeter range of dimensions, many phenomena are no longer negligible with respect to the macro-world (adhesion, deformation, thermal variation), so the external influences of probes or tools for handling purposes are to be avoided in order to achieve the required precise measurements. For example, even some well-defined procedures, in the vibration detection and analysis area, can no longer be applied by adopting standard sensing elements (contact accelerometers).

Nowadays non-contact sensors are largely used in order to avoid external influences on the



FIGURE 22-7 Transformations in a testing/diagnostic system.

measurement system, thus enabling ultra-high precision measurements (i.e. up to the 10^{-9} range of the whole dimensions of the part to be measured). Due to the property of coherence in the emitted radiation, the laser is the main technique applied within high precision applications, not only within the realm of dimensional control, but also within a wide range of applications where the physical characteristics of materials have to be measured in a direct or indirect manner.

Laser applications on measurement systems go from dimensional analysis to vibration measurement. Some applications in material characterization even use the laser as a power source in order to produce mechanical waves. This is achieved by impacting the laser beam onto targets and then measuring the ultrasound reflections (LUS: laser ultrasound inspection).

The laser is also used within optical applications in order to inspect transparent or semi-opaque materials using a coherence light source (OCT – optical coherence tomography). However, even high resolution image analysis is increasing its influence within the high precision measurement domain, especially when in-line inspection and testing of micro-parts are required. Laser interferometers, LUS, OCT and image processing can easily ensure resolutions of below $1\ \mu\text{m}$ with very simple equipment and, in some cases, at a very competitive cost.

Recalling these applications, one may also recognize the wide use of precise positioning systems suitable to move the probe or the sensor, as shown in Fig. 22-2. Precision movements are often achieved with mechatronic systems based on piezo-actuators, sub-micrometric brushless motors, galvo motors, moving coil motors, etc. Note also that high precision mechanical devices have to ensure optimal isolation from vibration and other external disturbances.

Of particular importance, dimensional measurement sensors are especially valuable because by dimensional measurement it is possible to retrieve a large amount of information about the observed system, and not only from a purely dimensional point of view. For example, laser displacement sensors can report information about

dimensional, dynamical, thermal, and vibrational behavior. Therefore, it may be useful to briefly detail a number of such sensors, especially of the non-contact type, which are particularly suited for micro-testing applications.

Mono- and Multi-dimensional Measurement

Precise non-contact dimensional measurement systems are largely based on the laser interferometer technique (i.e. the Michelson interferometer). Comprising just the interferometer, i.e. being a system capable of detecting only differences on beam paths, it is suitable for incremental, or displacement, measurements. Typically, the time response is very fast (typ. $<100\ \mu\text{s}$) and the measuring accuracy, by the use of interpolator devices, easily reaches values below $10^{-8}\ \text{m}$. The laser interferometer system is very suitable for coordinate measuring machine (CMM) applications. Very accurate measurements on micro-parts are possible by placing the part on a positioning system (one stage: X or multistage: X-Y or X-Y-Z table) provided with reflectors.

Other dimensional measurement techniques are based on different principles, such as laser beam triangulation, which use a laser source and a detector (CCD or PSD as represented by Fig. 22-4). In this case the system performances depend on the surface characteristics of the target material. Both the precision and the distance range are affected by material typology and surface texture.

Thickness Measurement

There are several techniques which are suitable for the precise and ultra-precise measurement of thickness. Inductive measurement, based on differential measurement techniques, is a methodology often adopted for low cost applications. This method is affected by the type of material being measured. Higher levels of stability and precision are achieved by laser techniques which consist of a laser beam shaped by the target. A sensor, in these systems, consists of emitter and receiver elements, with the field of measurement situated between

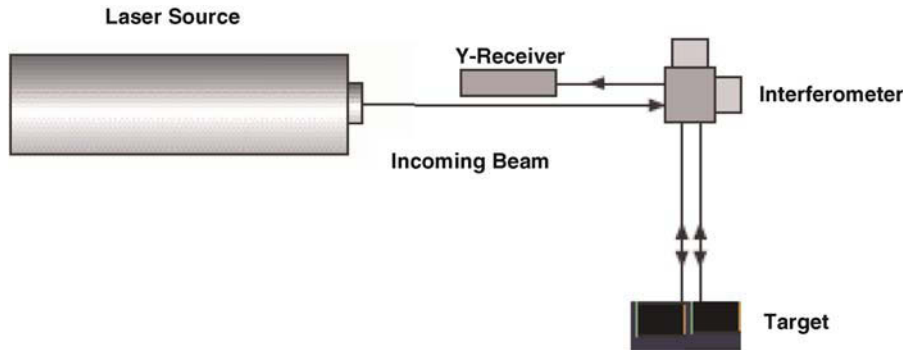


FIGURE 22-8 One-dimensional displacement measurement by laser interferometer.

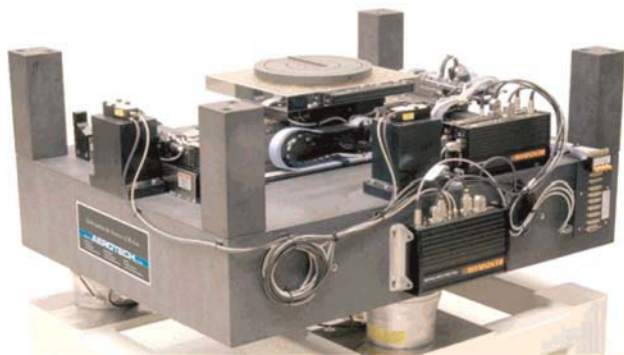


FIGURE 22-9 High precision X-Y feedback system (Aerotech Inc.) using two laser interferometers (Renishaw) with total precision up to 10 nm. The system is suitable also for testing 2D tables and precise linear motors.

them. The width of the ‘shading’ (e.g. behind an object) or the light (e.g. through a gap) can thus be measured (Fig. 22-10). Alternative techniques are possible, mainly by using two displacement sensors as represented in Fig. 22-11. This kind of technique requires, however, highly accurate calibrations (usually accomplished with the use of a calibrated target).

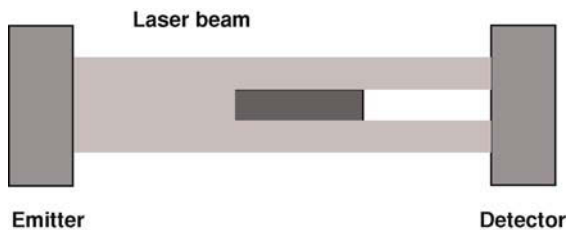


FIGURE 22-10 Thickness measurement using a laser beam.

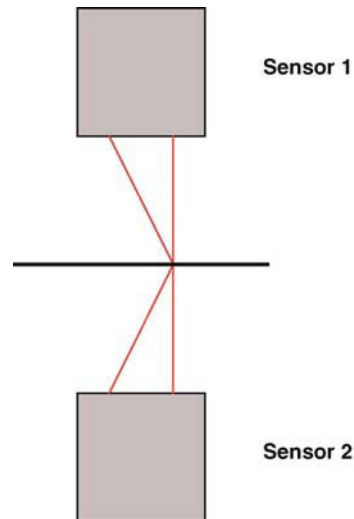


FIGURE 22-11 Thickness measurement using two displacement-sensors.

Model	Micro-Epsilon ILD 2200-2
Measuring range	2 mm
Start of measuring range SMR	24 mm
Midrange MMR	25 mm
End of measuring range EMR	26 mm
Linearity	1 μm $\pm 0.05\%$ FSO
Resolution(at 10 kHz without averaging)	0.03 μm
Measuring rate	10kHz
Permitted ambient light	30,000 lx
Spot diameter	SMR 80 μm MMR 35 μm EMR 80 μm
Light source	semiconductor laser <1 mW, 670 nm
Temperature stability	0.01 % FSO/ $^{\circ}\text{C}$



FIGURE 22-12 Thickness measurement systems.

In this domain, great importance is given to the laser ultrasound system (LUS), which is capable of reaching high levels of precision by using a hybrid technique. The technique is based on a very narrow pulsed laser beam, which is launched towards the target with the reflected ultrasound wave being received by an acoustic sensor. The variations of the acoustic impedance of the material are analyzed subsequently by a processing unit in order to deliver a map of the discontinuity of the material. The accuracy of this measurement, depending on the type of material, sound velocity and time resolution of the signal processing unit, can reach a few micrometers.

2D Profile and Shape Measurement

Profile and shape measurement are often accomplished by a combined use of laser and image analysis techniques.

A very thin laser beam is projected onto the part to be measured. The projection is analyzed by a CCD linear-array camera. A precise 1D linear movement may be imposed onto the measurement system or onto the part to be measured. Depending on the laser beam thickness, linear array CCD, optics and positioning system resolution, sub-micrometric accuracy can easily be achieved.

Suitable calibration procedures, using master profiles, are used to calibrate the analyzed image, thus permitting compensation for optical field deformations.

This kind of equipment is particularly suitable in continuous-control processes when the parts to be measured are brought by a linear-transportation system or by tape. In such cases, high efficiency image-analysis algorithms and high speed computational systems are required.

Shape and profile analyses are also accomplished by suitable image-analysis techniques

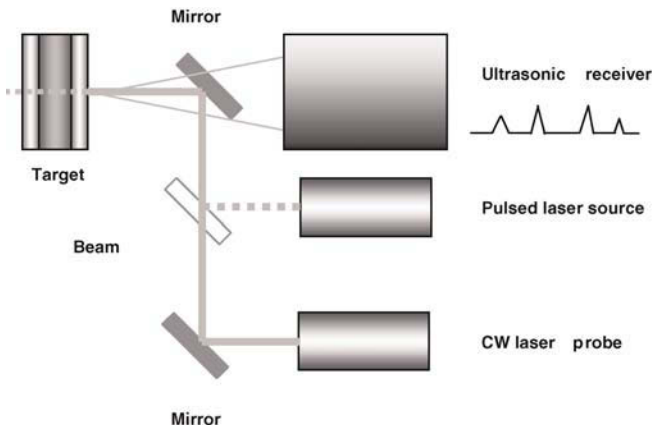


FIGURE 22-13 LUS principle and a system by TECNAR working on the B scan and C scan mode.

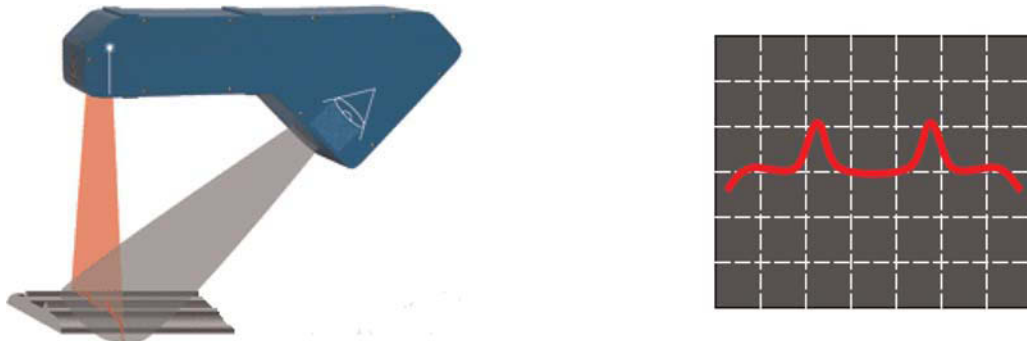


FIGURE 22-14 A profile measurement system using laser and CCD devices.

(sub-pixeling) that adopt high resolution CCD linear or matrix sensor arrays. High resolution (below $1\ \mu\text{m}$) bi-dimensional and stereoscopic image analysis can be carried out by 2D arrays of sizes greater than 20 megapixels or by linear arrays of sizes greater than $300\ \text{pixels} \times \text{mm}$. As with laser beam profilers, a continuous and very accurate movement of the analyzed part, or the linear array, has to be considered.

Vibration Measurement and Analysis

Vibration analysis is a very wide and complex domain which exploits several aspects of the testing and diagnosis disciplines, from condition monitoring to defect detection. Improvements in sensor technology now permit the use of vibration analysis methodology within the micro-/meso-world also. Non-contact high speed (wide bandwidth) laser sensors (typically displacement sensors) can overcome the traditional limits exhibited by accelerometers, so highly accurate and localized analyses can be performed.

Vibration analysis methodology could be subdivided into four principal domains:

- Time domain
- Frequency domain
- Joint domain (time/frequency domain)
- Modal analysis.

Each domain provides specific information on the working conditions and features of the vibrating part.

Typically, time-domain analysis is devoted to detecting the integral performance of the tested

part: peak, average, root-mean-square (rms), envelope values of vibration amplitude. These values are compared with threshold values in order to detect abnormal performance or latent defects.

Frequency domain is able to provide more information as the measured signal is decomposed into a sequence of frequency components (spectrum) by a Fourier transform calculation (or fast Fourier transform – FFT). Local analysis of the different frequency components permits the association of a signature with the processed signal, such that the tested part can be identified precisely by its own signature (signature analysis). Due to the time-varying property of the signal, calculating many spectrums on the time observation window can be found to be useful. To do so, a joint time/frequency technique (Gabor–Wigner–Wavelet) can be used very efficiently. In a particular case of time/frequency analysis, the spectrums are related to the rotational speed of the tested devices (order analysis), such that the analysis of the single order which is represented by a frequency component varying with the speed is rendered possible.

Modal analysis permits the study of the dynamic properties of structures under vibration excitation. This technique uses FFT in order to carry out a transfer function which shows one or more resonances, by means of which it is possible to estimate the characteristic mass, damping, stiffness and other properties of the tested part. Using a laser interferometer, and suitable software tools, it is possible to apply non-contact vibration analysis for the test and measurement of MEMS

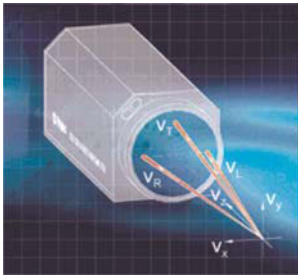


FIGURE 22-15 3D laser vibrometer by Polytec. The system is capable of detecting speed components with a resolution of $0.2 \mu\text{m/s}$ using a laser spot of $65 \mu\text{m}$.

(micro electro mechanical system) and MOEMS (micro optical electro mechanical system) dynamics and topography.

Mixed Qualitative—Quantitative Analysis Systems

Surface-texture Analysis. This is a typical application of image analysis techniques whereby properties, or features, of analyzed surfaces are compared with known properties belonging to a sample image. Due to its mainly qualitative aspect, surface-texture analysis could be considered more properly as an inspection methodology; however, its output may provide information on both processes and good working conditions of machines (typically in machining or assembly areas) and may provide quantitative evaluations through proper morphological analyses on shapes and forms.

Principally, the features extraction is performed by a joint domain (spatial-frequency) transformation (Gabor, Wavelet) [3] and the features comparison is performed by a suitable statistical classifier: for example, the Mahalanobis distance, which is scale invariant with respect to the Euclidean distance (minimum distance classifiers), or maximum likelihood classifiers of which the Mahalanobis distance is a particular case. A more complex classifier tool is represented by the neural network.

A neural network (typically of the back-propagation type) is able to activate particular output ports when a set of input signals determines the



FIGURE 22-16 The Polytec MSA-400 Micro System Analyzer: by scanning laser-doppler vibrometry it is capable of performing the precise 3D dynamic characterization of MEMS and MOEMS micro-structures.

satisfaction of conditions for which the network was previously trained. Independently of the classifier used and the analysis methodology, image acquisition is the more critical aspect that involves both the optical system and the illumination technique. In the testing of micro-parts, the additional use of a microscope and coherent light paths is a primary requirement. Quantitative aspects and morphological analyses are performed mainly in the spatial domain.

SEM, AFM and STM. Scanning electron microscopy (SEM), atomic force microscopy (AFM) and scanning tunneling microscopy (STM) are all widely used surface analysis techniques capable of very high accuracies (in the range from 10^{-9} to 10^{-7} m [4]).

In SEM, the primary electrons hit a surface with an energy of $0.5\text{--}30$ keV, and generate many low energy secondary electrons. The intensity of these secondary electrons is affected by the surface topography of the target. An image of the target surface can then be constructed by measuring the secondary electron intensity as a function of the position of the scanning primary electron beam.

AFM systems detect the z -displacement of a cantilever by the reflection of a laser beam focused onto the top surface of the cantilever. The feedback from this sensor maintains the probe at a constant force. STM systems measure the quantum tunneling current between a wire or a metal-coated silicon tip and the object surface. An

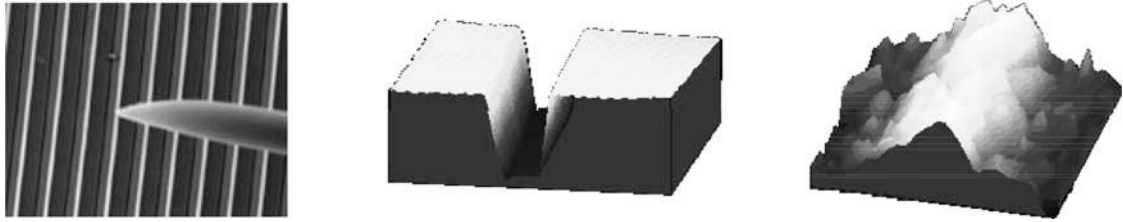


FIGURE 22-17 SEM image of a Nanonics® AFM Probe in contact with sample. 10 × 10 micron AFM image of a 10 micron deep/2 micron wide trench and a 1 × 1 micron AFM image of the bottom of the deep trench.

electronic feedback system maintains a constant current by positioning the tip to just make contact with the surface.

SEM is often used to survey surface-analysis problems before proceeding to techniques that are more surface sensitive and more specialized, such as AFM or STM. High resolution images of surface topography, with excellent depth of field, are produced using a highly focused SEM. These kinds of SEM are also able to provide high spatial resolution, except when the target consists of very narrow and deep wells. This is the case, for example, of a trench in a semiconductor wafer in which an SEM cannot view the bottom or the sidewall of the trench structure. In these cases the combination of SEM and AFM (or STM) analysis has to be considered.

TESTING AND DIAGNOSIS METHODS

As mentioned earlier in the introduction, testing and diagnosis for micro-manufacturing products/machines may now take advantage of new approaches in measurement and control system methodologies. Contactless sensors systems and model-based measurement systems are two examples of such approaches. Both methodologies aim to minimize interaction between the measurement system and the tested workpiece, in order to:

- save space for sensor allocation;
- retrieve more information from the observed system.

Another advantage is that, in the model-based measurement systems, the number of sensors is

TABLE 22-1 Performance of Measurement Systems

Measurement	Measurement Technique	Size of Parts (mm)	Accuracy (μm)	Measurement Time (μs)	Online Analysis
Dimensional measurement	1D, 2D, 3D Laser interferometer	>0.01	0.01	>1	Yes
	1D Laser triangulation	>0.1	0.1	>10	Yes
Thickness measurement	Laser barrier	>0.001	0.1	>10	Yes
Profile and shape measurement	Laser-Optics	>0.01	0.1	>10	Yes
Vibration measurement	Laser interferometer	>0.1	0.1	>10	Yes
Surface texture and profile measurement	Optics/Laser	>0.1	1	>100	Yes
	SEM, AFM, STM	>0.01	0.001	>100	No

minimized. This characteristic is an important requirement because the sensors are fault sensitive, and critically increase the production costs of the systems.

Basic foundations of testing and diagnosis rest upon fault detection and isolation techniques (FDI) and can be based on qualitative, quantitative or history-based information/data with the use of modeling techniques. These methods permit process adjustment and tuning in order to achieve optimal performance and to ensure product quality assurance approaches [5]. The term 'fault' is generally defined as 'a departure from an acceptable range of an observed variable or a calculated parameter associated with a process'. This defines a fault as a process abnormality or symptom, such as a high vibration level in a machine or a high positional error in a controlled

device. The underlying cause of this abnormality, such as a failed ball bearing, or a defective controller, is called the *basic event* or the *root cause*.

Note that there are several main characteristics that a testing/diagnostic system has to satisfy and that these will not usually be met by any single diagnostic method. Therefore, it may be useful to benchmark various methods in terms of the *a priori* information that needs to be provided, the reliability of the solution, and the generality and efficiency in computation. Table 22-2 summarizes the main requirements of a generalized diagnostic system.

Diagnostic systems can be classified according to the *a priori* knowledge used (Fig. 22-18). The basic *a priori* knowledge that is needed for fault diagnosis is the set of failures and the relationship between the observations (symptoms) and the

TABLE 22-2 Main Characteristics of a Testing/Diagnostic System

Quick detection and diagnosis	The diagnostic system should respond quickly in detecting and diagnosing process malfunctions. These characteristics are related to the bandwidth of the diagnostic system.
Isolability	It is the ability of the diagnostic system to distinguish between different failures.
Robustness	Rejection to various noise and uncertainties.
Novelty identifiability	The diagnostic system is able to decide, given current process conditions, whether the process is functioning normally or abnormally, and, if abnormal, whether the cause is a known malfunction or an unknown, novel, malfunction.
Classification error estimate	An important practical requirement for a diagnostic system is in building the user's confidence on its reliability. This could be greatly facilitated if the diagnostic system could provide <i>a priori</i> estimates of classification errors that can occur.
Adaptability	Processes in general change and evolve due to changes in external inputs or structural changes due to retrofitting and so on. Process operating conditions can change not only due to disturbances but also due to changing environmental conditions. Thus the diagnostic system should be adaptable to changes.
Explanation facility	Besides the ability to identify the source of malfunction, a diagnostic system should also provide explanations of how the fault originated and propagated to the current situation.
Modeling requirements	Modeling is any <i>a priori</i> knowledge about the system to be observed. For fast and easy deployment of a real-time diagnostic system, the modeling effort should be minimal.
Storage and computational requirements	Usually, quick real-time solutions would require algorithms and implementations which are computationally less complex, but might entail high storage requirements. One would prefer a diagnostic system that is able to achieve a reasonable balance of these two competing requirements.
Multiple fault identifiability	The ability to identify multiple faults. In a general non-linear system, the interactions would usually be synergistic and, hence, a diagnostic system may not be able to use the individual fault patterns to model the combined effect of the faults.

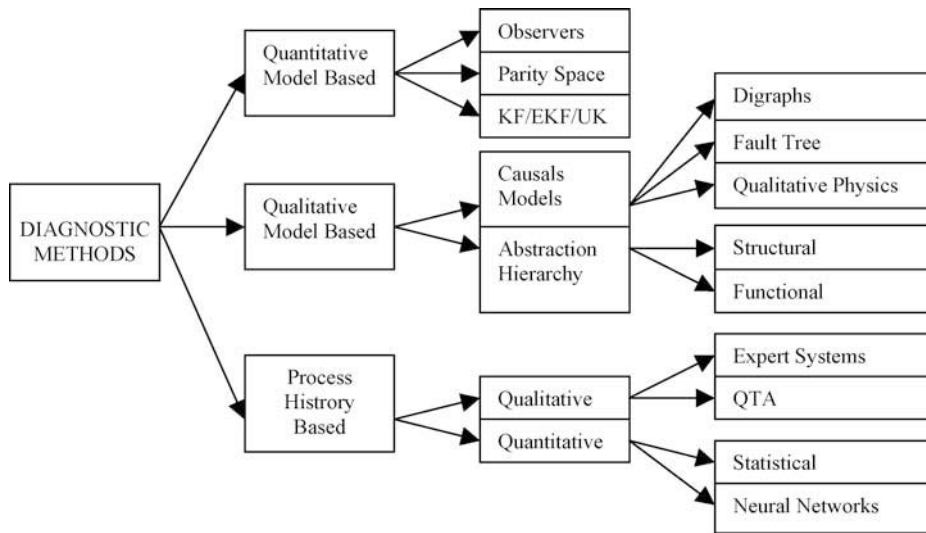


FIGURE 22-18 Classification of diagnostic techniques.

failures. The relationship between observations and failures could be explicit (as in a look-up table), or it may be inferred from some source of knowledge. In particular such knowledge is referred to as causal or model-based knowledge. On the other hand, it may be gleaned from past experience with the process. This knowledge is referred to as process history-based knowledge. The model-based knowledge can be broadly classified as qualitative or quantitative. The model is usually developed based upon some fundamental understanding of the physics of the process. In quantitative models this understanding is expressed in terms of mathematical functional relationships between the inputs and outputs of the system. In contrast, in qualitative model equations these relationships are expressed in terms of qualitative functions centered around different units in a process.

Process history-based methods differ from the model-based approaches, where *a priori* knowledge about the model of the process is assumed (either quantitative or qualitative), in that only the availability of large amounts of historical process data is assumed.

The remainder of this chapter will focus on diagnostic methods based on a quantitative approach.

Quantitative Model-based Testing

In model-based methodology the feature space is characterized by the use of suitable analytical techniques which permit the achievement of features starting from measurements (observed signals), mathematical or experimental models of the observed system, some statistical information about model uncertainties and signal noise. Some of the most suitable techniques are:

- Adaptive observers;
- Parity relations;
- Kalman filters (KF); and
- Parameters estimation algorithms.

The performances of various methods are summarized in Table 22-3, with reference to feature extraction capability, non-linear systems handling, noise rejection and the possibility to estimate not only state, but also parameter deviations. In particular, extended (EKF) and unscented (UKF) formulations are very efficient and can be implemented with a low/medium level of computation complexity. These will be described in the following paragraph as *state estimators*.

A state estimator permits the extraction of a greater number of features than the observed signals, for example: by measuring the position of a slide, driven by a linear motor, and the currents in

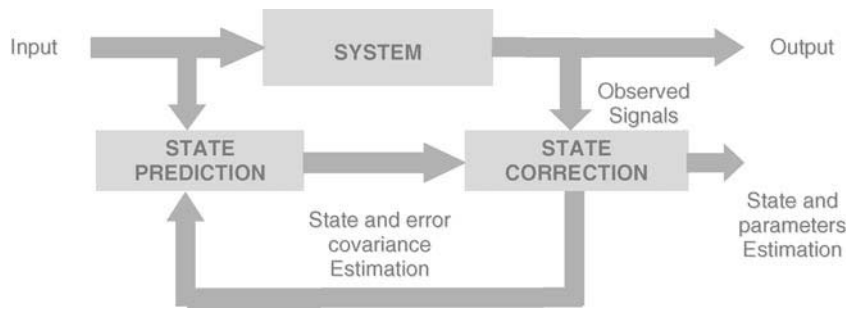


FIGURE 22-19 Standard Kalman state-estimator representation.

the motor coils, it is possible to estimate velocity, force, friction, stiffness and other system parameters. Of course it is necessary to exploit a model of the system to be observed and this task can be carried out by the use of suitable simulation software. The advantages of using state estimators for testing application in the micro-manufacturing area are clear; in fact, in order to enhance both the fault detection and classification sensibility it is possible to minimize the number of sensors by increasing the estimated features.

Figure 22-19 illustrates a typical Kalman state-estimator representation.

This approach, thanks to knowledge of the model, allows both the observed signals (as part of the output system) and input to be used to produce a prediction of the current state of the observed system. The prediction is then used to correct the current state in order to produce an estimation of the next system state by a recursive cycle. If the system model, which represents the knowledge, includes both variables and parameters of interest (features), then these will be

used as failure detectors when the deviation (residual) referred to the nominal value is greater than a pre-fixed threshold.

The generation of residuals is a recursive and online procedure capable of controlling the behaviors of the system and can even provide a forecast of possible faults (detection) and their classification.

Differently from diagnostic procedures, those of testing can involve test-pattern generation for the inputs to the system to be tested. Therefore, achieving optimal performance of the testing system will require both a suitable choice for the system model (the estimation of the most suitable variables and parameters) and the best selection of test-pattern input for target faults.

The major advantage of using the quantitative model-based approach is that full control over the behavior of the system will be attained. The mathematical relationships give an analytical redundancy that is useful for relating the internal state variation to the measurements. As the states can be associated to the particular physical

TABLE 22-3 Performance Comparison of the Main Quantitative Model-based Estimators

	Features Greater than Measurements	Non-linear System	Disturbance Rejection	Parameters Estimation
Parity space	NO	YES	POOR	NO
Observers	YES	YES	GOOD	YES
Kalman filters:				
LKF (linear)	YES	NO	HIGH	NO
EKF (extended)	YES	YES(CRITICAL)	HIGH	YES
UKF (unscented)	YES	YES	HIGH	YES

characteristics of components inside the system, a fault can be detected rapidly by the abnormal change of states and incorrect component identified.

The main problems associated with the model-based diagnosis methods refer to the complexity of the system, high dimensionality and process non-linearity. Such problems often result in difficulties in developing accurate mathematical models of the system. Another problem in these approaches is the simplistic approximation of the disturbances that include modeling errors. In most cases, the disturbance includes only additive uncertainty. However, in practice, it may be advisable to proceed as follows, where appropriate:

1. Begin with a simple model, stating the assumptions in order to focus on particular aspects of the phenomenon.
2. Identify important variables and constants and determine how they relate to each other.
3. Develop the equations that express the relationships between the variables and constants.

Mathematical models typically contain three distinct types of quantities: *input variables*, *dynamic state output variables*, and *parameters*. Output variables give the model solution. When parameters depend on environment interaction then the choice of what to specify as input variables and what to specify as parameters is somewhat arbitrary and, often, model dependent. Input variables may raise severe modeling uncertainties in the form of multiplicative uncertainties. Another disadvantage with these methods is that, if a fault is not specifically modeled (novelty identifiability), there is no certainty that the residuals will be able to detect it.

When a large-scale process is considered, the size of the bank of filters may seriously increase the computational complexity, although, with the recent increase in computational power and the essential linear nature of these problems, this may no longer be a serious bottleneck.

The core of a quantitative model-based testing procedure is the state estimator. The important issue in the estimators is the knowledge of the system model. Building a mathematical model

for a system can be a difficult, yet interesting, task: it is essential to know all the features of the process and, therefore, a thorough understanding of the underlying scientific concepts is necessary. Although problems may require very different methods of solution, the following steps outline a general approach to the mathematical modeling process [6]:

1. Identify the problem, define the terms, and draw diagrams which characterize a single physical problem while the parameters determine the context or setting of the physical problem. Dynamic systems are also characterized by a set of variables called states that represent the memory of the system. A typical representation in state variables is:

$$\frac{dx(t)}{dt} = f(t, x(t), u(t), \theta(t)) \quad (1)$$

$$y(t) = h(t, x(t), \theta(t)) \quad (2)$$

where x are the states, u the inputs, y the outputs and θ the parameters.

2. The simplest case is when the system is time invariant and is modeled with linear differential equations:

$$\frac{dx(t)}{dt} = Fx(t) + Gu(t) \quad y(t) = Hx(t) + Lu(t) \quad (3)$$

3. The equations are typically continuous, but for computer processing purposes they are expressed in discrete time:

$$\begin{aligned} x_{k+1} &= Ax_k + Bu_k \\ y_k &= Cx_k + Du_k \end{aligned} \quad (4)$$

The problem of a state estimator is to measure the output y and, by knowledge of input u and the matrices of the model A , B , C , D , to extract the state x .

During the design and analysis of technical systems that encompass several physical domains, the use of adequate models is of great importance. Using suitable techniques of modeling and simulation, these models are easy to create and can be

updated rapidly when this is required. Generally, an important aspect of systems is their dynamic behavior. This is especially true for systems that exhibit fast changes or systems that should behave accurately: in such cases it is useful to choose the most appropriate model that meets the achievement of performance and then simulate to update the best parameter values.

In micro-engineering, the characterization of materials, micro-structures and properties is frequently carried out through simulations. This is often done to better understand and reproduce mechanical behavior. During the development of a new micro-device, mathematical equations governing the physics of the process are known. Due to this feature, model-based techniques for fault diagnosis or testing can be applied in this field. In fact, a reduced number of sensors are often required for systems having reduced dimensions. The state-estimator method can easily reduce the number of sensors because there is an analytical redundancy introduced by the mathematical relationship. In this manner some sensors can be omit-

ted because the measurements are estimated. Some techniques, such as the Kalman filters, are also useful because they produce reliable estimates from noisy measurements. This permits the reduction of the scale of the application without serious problems.

Together, the state and parameter estimations are useful to follow the performance alterations of internal components of a complex system. If the characteristics of a component vary slowly, and the maximum allowed displacement is known, then the time at which a substitution will be necessary may be calculated. This is the core of predictive diagnosis. With parameter estimation, the changes in some machine parameter (for example, the friction) may be estimated, such that the coefficients of a software controller may be rapidly reconfigured. This is an auto-compensation technique which leads to auto-repairing strategies.

All these features of the model-based diagnosis methods meet the most important requirements of a micro-application system, as evidenced in Table 22-4.

TABLE 22-4 How Model-based Diagnosis meets the Requirements of a Micro-application

	Sensors Reduction	Predictive Diagnosis	Disturbance Rejection	Auto Repairing
Space saving	X			
High efficiency	X	X	X	X
High reliability	X	X	X	X
Low cost	X	X		

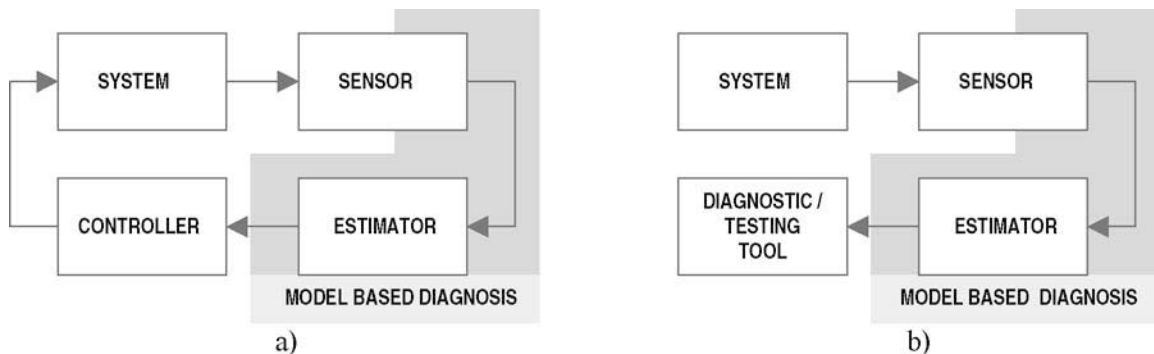


FIGURE 22-20 Architectures of model-based diagnosis: (a) controlled systems; (b) diagnostic systems.

The Kalman Estimator

The Kalman estimator, or Kalman filter (KF), is a mathematical algorithm that provides efficient computational and recursive methods to estimate the state of a process by minimizing the variance of the estimate error. The filter is very powerful in several aspects: it supports estimations of past, present, and even future states, and it can do so even when the precise nature of the modeled system is unknown [7,8].

The basic framework for the discrete KF involves the estimation of the state of the dynamic system: this can be a discrete time-linear or a non-linear system represented in state variables. The dynamic system behavior is assumed as a well-known model with Eqns (4) modified in order to take into account model inaccuracy w_k and measurement noise η_k :

$$\begin{aligned}x_{k+1} &= Ax_k + Bu_k + w_k \\y_{k+1} &= Cx_{k+1} + \eta_k\end{aligned}\quad (5)$$

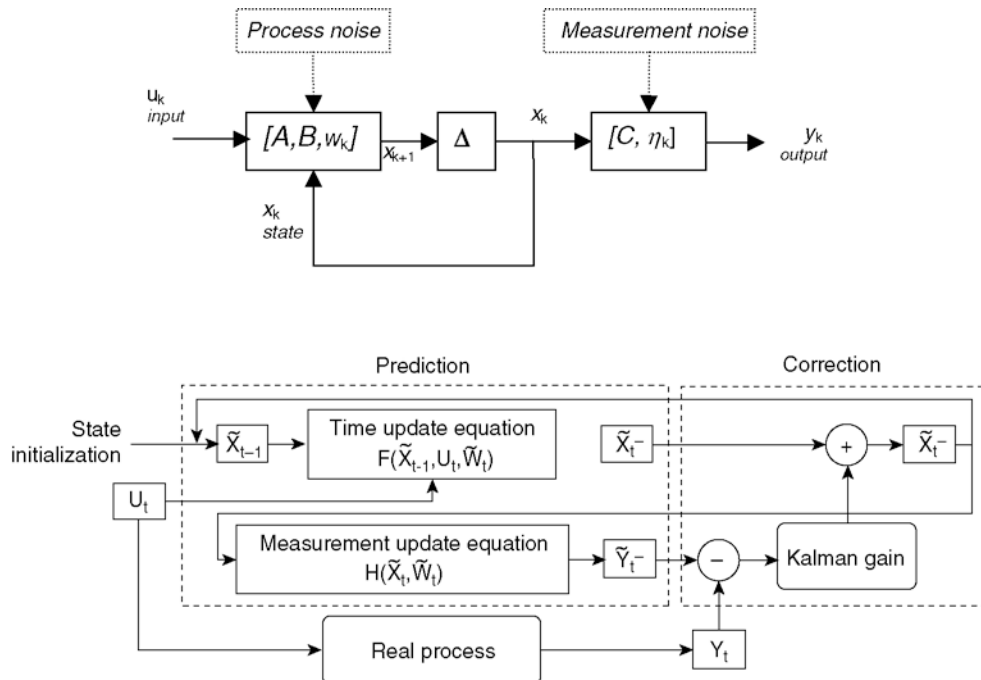


FIGURE 22-21 General ‘prediction-correction’ structure of the Kalman filter. Model parameters are assumed to be known.

The KF estimates a process by using a feedback concept: the filter estimates the *state* at a given time and then obtains feedback in the form of innovations or residuals.

The equations for the KF fall into two groups: time update equations and measurement update equations. In order to obtain the *a priori* estimates for the next time step, the time update equations are responsible for projecting forward (in time) the current state and error covariance estimates. The measurement update equations are responsible for the feedback; i.e. for incorporating a new measurement into the *a priori* estimate to obtain an improved *a posteriori* estimate.

The time update equations can also be thought of as predictor equations, while the measurement-update equations can be thought of as corrector equations: the time update projects the current-state estimate forward in time. The measurement update adjusts the projected estimate by an actual measurement at that time. The final estimation algorithm resembles that of a predictor-corrector algorithm for solving numerical problems [9].

The Kalman filter, also called the LKF (linear Kalman filter), is only used for linear systems; unfortunately, many real-world systems, especially mechanical systems, are non-linear in nature. Since even the measurement relationships to the process are often non-linear, the KF cannot be used to estimate the states. The extended Kalman filter (EKF) was developed to account for these non-linearities: in order to estimate the state, even if the system is non-linear, this evolution of the Kalman filter obtains a linearization around the current mean and covariance. This filter is based upon the principle of linearizing the measurements and evolution models using Taylor series expansions (truncated at the first-order term, with the assumption that the error incurred by neglecting the higher-order terms is small in comparison to the first-order terms). The series approximations in the EKF algorithm can, however, lead to poor representations of the non-linear functions and probability distributions of interest.

It is important to note that a fundamental flaw of the EKF is that the distributions (or densities in the continuous case) of the various random variables are no longer normal after undergoing their respective non-linear transformations. When the system has strong non-linear transformations, the EKF may be an inadequate state estimator, because the system loses its features, especially for estimation of convergence time.

For heavily non-linear systems, the UKF (unscented Kalman filter) solves the approximation issues of the EKF. The state distribution is represented by a Gaussian random variable (GRV), using a minimal set of carefully chosen sample points (called sigma points). These sample points completely capture the true mean and covariance of the GRV, and, when propagated through the true non-linear system, capture the posterior mean and covariance accurately to the third order (Taylor series expansion) for any non-linearity. The unscented Kalman filter is based on the unscented transform (UT) and does not require linearization to handle non-linear equations [10].

The UKF leads to more accurate results than the EKF and, in particular, it generates much better estimates of the covariance of the states (the

EKF seems to underestimate this quantity). The UKF has, however, the limitation that it does not apply to general non-Gaussian distributions.

The SRUKF (square-root unscented Kalman filter) is a filter based on UKF and it reduces the algorithm complexity by the adequate use of the Cholesky and QR decompositions.

APPLICATION ON MICRO-DEVICES AND MACHINES

As an example of how model-based testing can be applied to the testing of devices particularly suited for micro-positioning application, the case of piezoelectric inchworm motors may be considered. These devices take advantage of piezo-ceramic characteristics to produce displacements with nanometer resolution, while large travel is assured by an inchworm technique. The inchworm technique is based on the simple concept of the incremental sum of the relatively small displacements produced by piezo-ceramic elements in order to generate a large displacement.

As shown in Fig. 22-22, a typical inchworm-type linear motor has three major components: two clamping mechanisms (referred to as brakes B1 and B2) and an extending mechanism (referred as mover M). During the greater part of a typical inchworm cycle, only one clamping device is to be activated at any given time, thus allowing the extender to extend and retract freely. The clamping mechanisms are normally designed to create a frictional force that can withstand the static forces produced by a constant load and dynamic forces produced by the extending mechanism. The purpose of the extending mechanism is to generate the small displacements which the inchworm technique sums to produce a large displacement.

The typical cycle of an inchworm technique linear motor reveals that the velocity of the motor is directly dependent on the step size of the motor and on the rate at which the cycle is repeated. To determine a model for a designed motor, the important parameters to be considered all relate to the behavior of the model [11]. The chosen parameters are the stiffness and damping of the extending mechanism, the mass of the clamping

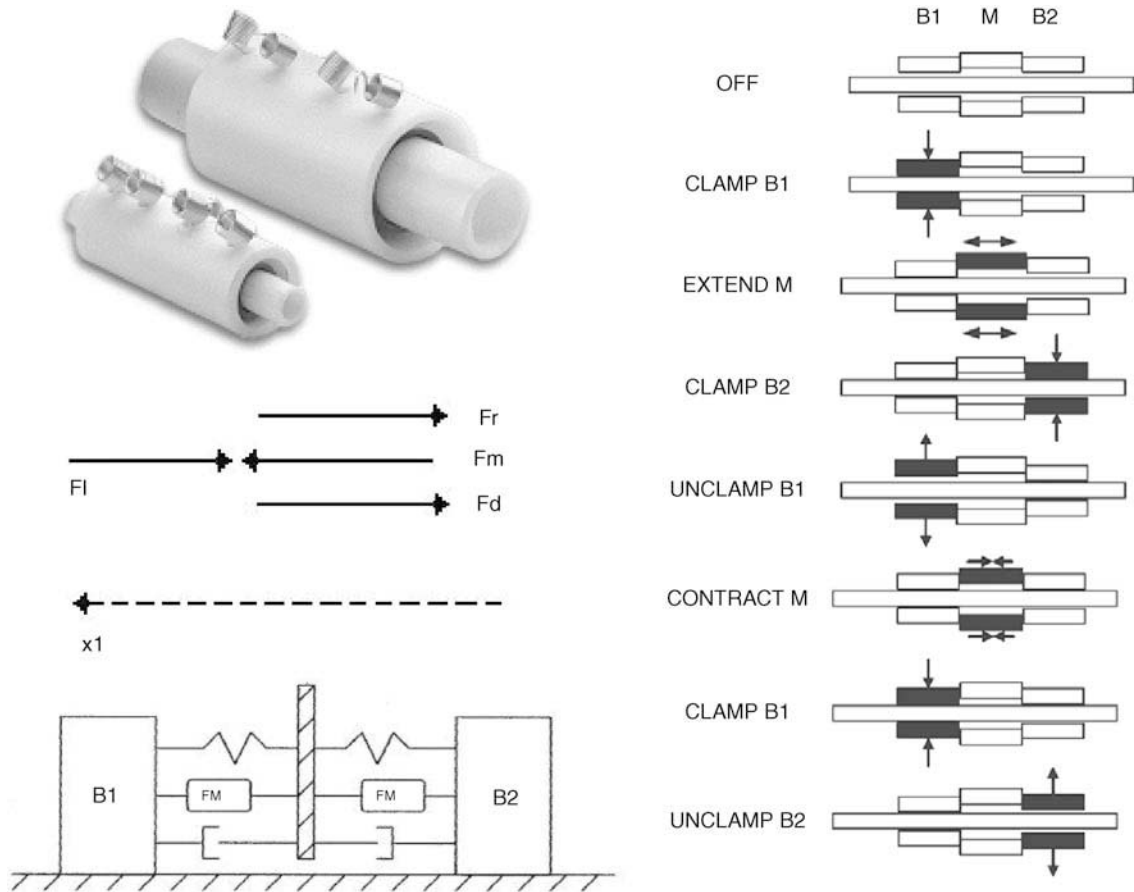


FIGURE 22-22 Modeling of an inchworm piezo-motor and cycle.

mechanisms, the forces applied to the motor, and the forces generated by the motor. Using these parameters, a second-order (mass–spring–damper) system is used to model the behavior of the model.

Figure 22-22 also shows a diagram of the chosen model, supposing that the central point of the extender is fixed in space. The symbols are:

- x_1 : displacement of brake 1
- Fr : stiffness force of the extending actuator
- Fm : force generated by the extending actuator
- Fd : damping force of the extending actuator
- Fl : force of the applied load
- V : voltage supply

By summing the forces shown in the diagram, the equations of motion are derived according to Newton’s second law:

$$\begin{aligned}
 M \frac{d^2 x_1}{dt^2} &= Fm - Fr - Fd - Fl \\
 &= Kv * V - Kr * x_1 - Kd * \frac{dx_1}{dt} - Fl
 \end{aligned}
 \tag{6}$$

The parameters in this equation are:

- M : mass of brake
- Kv : voltage constant of the piezoelectric effect
- Kr : stiffness coefficient
- Kd : damping coefficient

Assuming $\frac{dx_1}{dt} = v_1$ and writing Eqn (6) in a state-space form, provides:

$$\begin{bmatrix} \frac{dx_1}{dt} \\ \frac{dv_1}{dt} \end{bmatrix} = \begin{bmatrix} 0 & 1 \\ -\frac{Kr}{M} & -\frac{Kd}{M} \end{bmatrix} \begin{bmatrix} x_1 \\ v_1 \end{bmatrix} + \begin{bmatrix} 0 & 0 \\ \frac{Kv}{M} & -\frac{1}{M} \end{bmatrix} \begin{bmatrix} V \\ Fl \end{bmatrix} \quad (7)$$

which represents the first of Eqns (5).

The second equation depends on the outputs chosen to observe the system. In order to estimate, for example, position, velocity, load force, the stiffness and the voltage constant parameter, all that is needed is the voltage supply V , an input to the system, and the measurement of mover position x_1 , an observation represented by the following equation:

$$[yx] = [1 \quad 0] \begin{bmatrix} x_1 \\ v_1 \end{bmatrix} \quad (8)$$

TABLE 22-5 Number of Measurements (=2) vs Number of Estimated Features (=5)

Estimated State Variables		Estimated Parameters		Measurement (sensors)	
Position	x (m)	Stiffness	K_R (N/m)	Voltage	V
Velocity	dx/dt (m/s)	Piezo voltage	K_v (N/V)	Transducer	X_1
Drag force	Fl (N)	coeff.		Linear encoder	

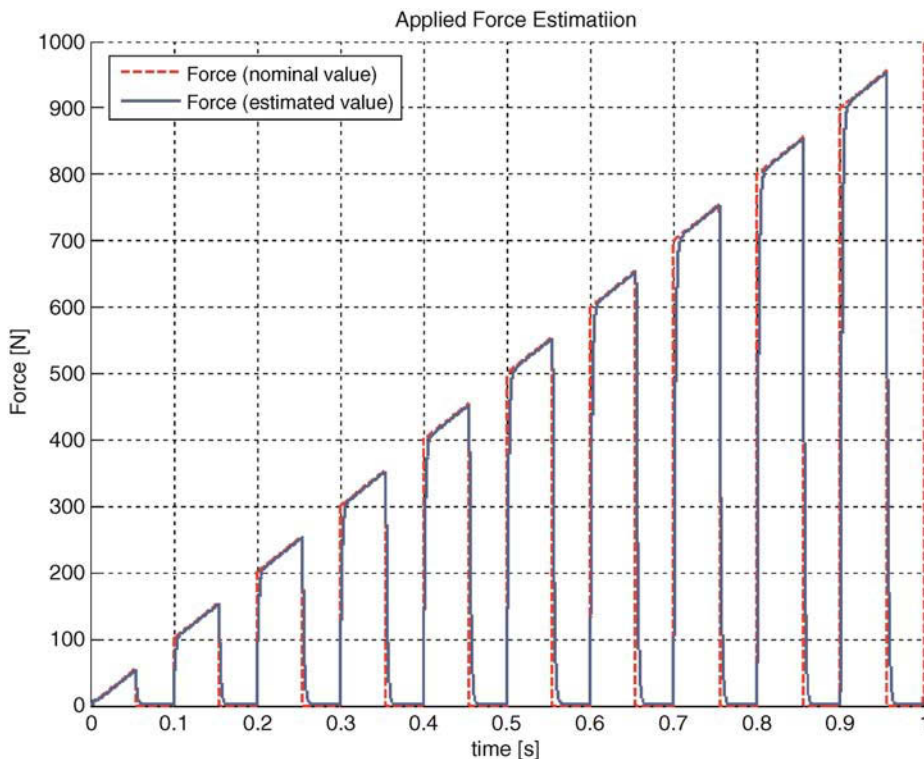


FIGURE 22-23 Force of a load applied to the inchworm.

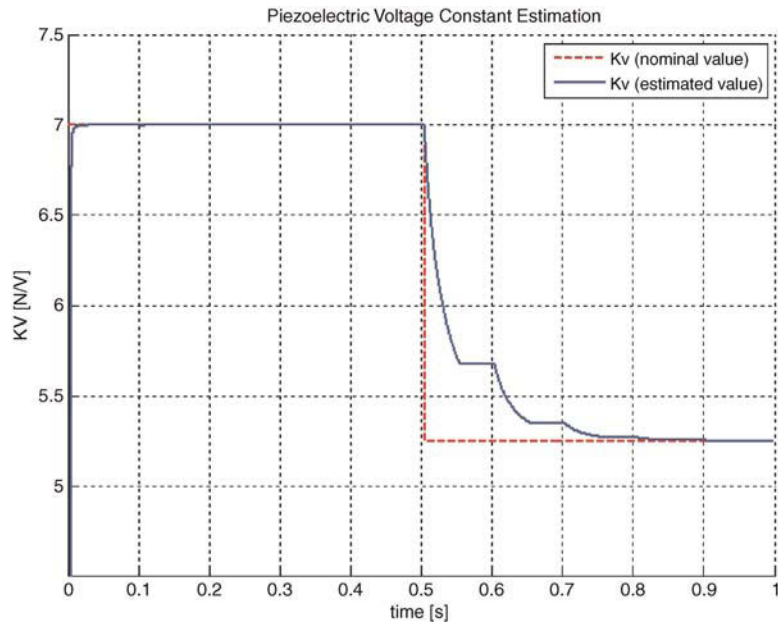


FIGURE 22-24 Piezoelectric parameter variation.

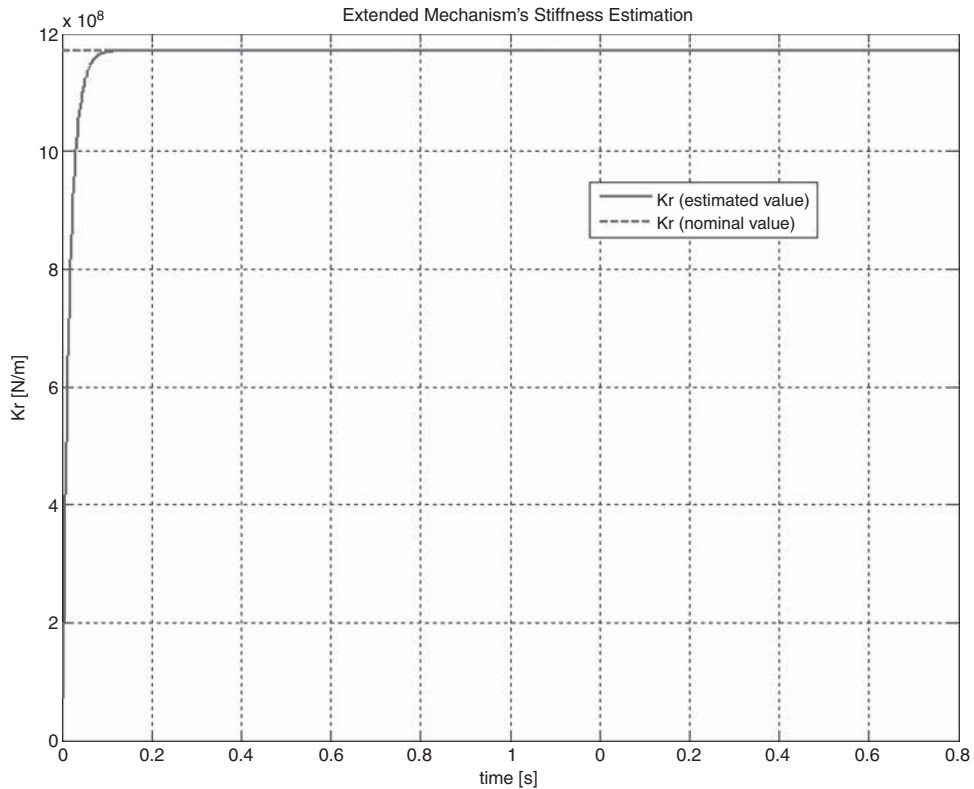


FIGURE 22-25 Stiffness estimation.

Figure 22-23 shows the applied load force (dashed line) and its estimate (solid line). The signal is modulated by the control signal on the piezo-element. Figure 22-24 shows the estimation of the piezoelectric coefficient (solid line) and its true value (dashed line). The variation corresponds to a fault which changes the coefficient from 7 N/V to 5.25 N/V. As shown in the figure, the convergence time to the second value is 0.3 s because the mover is controlled by an ON/OFF signal and the estimated curve tends to reach the right value only when the control is ON. This means that the system needs to be in an excited state in order to enable possible fault detection.

Figure 22-25 shows the estimation of the stiffness coefficient. The very low convergence time (below 0.1 s) shows the high dynamic capability of the Kalman estimator.

CONCLUSIONS

Testing for micro-manufacturing processes is characterized by requirements on:

- precision;
- non-invasiveness;
- being contactless;
- minimization of the number of sensors;
- low complexity.

Non-contact measurement techniques based on laser sensors and precise movement systems represent the best choice in order to achieve a complete testing system based on direct measurement. When a great number of signals have to be acquired in order to improve the monitoring of the normal working conditions of devices or complex machines, model-based testing can be used to reduce the number of direct measurements (without a reduction of the number of interested signals).

Model-based testing and diagnosis for micro-manufacturing may exploit advantages from the application of estimations techniques in order to extract features from modeled systems. The reduction of the number of sensors is possible by increasing the information flow from the tested system. This information could be well represented by a proper system model. Estimation tech-

niques, such as the Kalman filters, can aid the extraction of variables and parameters which cannot be measured in a direct way, allowing a number of available features greater than the number of signals measured.

The application of model-based testing and diagnostic procedures to the micro-/meso-devices world represents a very efficient and powerful way to increase quality and reliability, while at the same time reducing system complexity.

ACKNOWLEDGMENTS

Special thanks to Professor Biagio Turchiano, Full Professor of Automatic Control and Head of Department, Dipartimento di Elettrotecnica ed Elettronica, Politecnico di Bari, Italy, and to Professor Mauro Onori, Associate Professor, Evolvable Production Systems Group, KTH, Stockholm, Sweden. Thanks also to colleague Eng. Orlando Petrone, Mechatronic Group leader of MASMEC Research and Development Department. Many issues included in this work are related to results achieved by MASMEC Srl, Bari, Italy, for the European Research Project MASMICRO.

REFERENCES

- [1] J.S. Oakland, *Statistical Process Control*, Butterworth-Heinemann (1996).
- [2] R. Isermann, *Model-Based Fault Detection and Diagnosis – Status and Applications*, IFAC (2004).
- [3] Chen, C.H., Pau, L.F., Wang, P.S.P., (eds.), *The Handbook of Pattern Recognition and Computer Vision* (2nd Ed.), World Scientific Publishing Co (1998) 207–248.
- [4] D. Sarid, *Scanning Force Microscopy*, Oxford Series in Optical and Imaging Sciences, Oxford University Press, New York (1991).
- [5] V. Venkatasubramanian, R. Rengaswamy, K. Yin, S.N. Kavuri, A review of process fault detection and diagnosis, Part I: Quantitative model-based methods, *Computers and Chemical Engineering* 27 (2003) 293–311.
- [6] L. Ljung, *System Identification, Theory for the User*, (2nd ed.), Thomas, Kailath, (Ed.) Prentice Hall PTR (1999).
- [7] G. Bishop, G. Welch, An introduction to the Kalman Filter, Technical report, Department of Computer Science, University of North Carolina at Chapel Hill, Chapel Hill, NC 27599-3175 (May 2003).

- [8] Haykin, S., (ed.), Kalman Filtering and Neural Networks John Wiley & Sons, Inc (2001).
- [9] P. Dewallef and O. Léonard, On-line measurement validation and performance monitoring using robust Kalman filtering techniques, Turbomachinery Group – University of Liège, Belgium.
- [10] LaViola Jr., A comparison of unscented and extended Kalman filtering for estimating quaternion motion, Joseph J. Brown University Technology Center for Advanced Scientific Computing and Visualization, PO Box 1910, Providence, RI, 02912, USA.
- [11] N. Hagood, W. Chung, A. von Flotow, Modelling of piezoelectric actuator dynamics for active structural control, *J. Intell. Mat., Syst., and Struct* 1 (July 1990) 327–354.

Micro-Mechanics Modeling for Micro-Forming Processes

W. Zhuang, J. Cao, S. Wang and Jianguo Lin

INTRODUCTION

In recent decades, the development towards miniaturization of products and devices in industries such as electronics, optics, communications, etc. has increased the demand for metallic parts manufactured at micro-scale. Such parts encompass a wide variety of geometries, materials, functionalities and production processes. Examples of micro-parts include screws, fasteners, connector pins, springs, micro-gears and micro-shafts. These are manufactured by employing a variety of manufacturing processes such as machining, folding, bending, stamping, drawing, molding, lithography and forward/backward extrusion [1]. Some examples of extruded micro-parts are shown in Fig. 23-1 [2]. Forming is a particularly appropriate manufacturing technique for these parts, as often they have a complicated shape and machining would be time consuming and produce low yield. Process modeling plays an ever-increasing role in these areas, for product design and for reducing lead time and manufacturing costs.

To enable process design to be undertaken on a scientific basis, knowledge of the underlying theory of micro-mechanics is essential. Plastic deformation can be observed at various length scales, which can be from the atomic scale where the atomic arrangement and individual defect properties of a material are of crucial importance, up to the macroscopic scale where the actual material micro-structure is not resolved

and plasticity is described on phenomenological grounds. A schematic diagram of the length scales at which plasticity may be addressed – the nanometer scale (atomistic), the mesoscopic scale (tens of microns) and the macroscopic scale – is given in Fig. 23-2.

In conventional metal-forming processes the size of the workpiece is usually large compared with the grain size of the metal from which it is constituted. Standard continuum-plasticity models are local in the sense that the stress at a material point is assumed to be a function of a strain at that point only. Local theories do not make reference to the characteristic length scale for dislocations and, therefore, are not able to resolve dislocation structures. As a consequence, such models also exhibit no size dependence. The crystals and their inherent directions of preferred slip (slip-plane) are usually oriented randomly. Thus, although a workpiece may be deformed by an external force (or stress) in a clearly defined direction, internally the crystal deformations are multi-directional. It is the resolution of the multi-directions along a common axis that gives rise to the macro-deformation, resulting in the change in shape of the workpiece. Because of the large number of crystals and the randomness of crystal orientation, at the macro-scale a material appears homogeneous and different samples of the same material in the same thermo-mechanically treated condition exhibit the same properties.



FIGURE 23-1 Examples of micro-pins (Shinko, NME) [2].

At the micro-level, the grain size can be similar to that of the part being formed. Thus a cross-section of a workpiece may contain a single-digit number of grains, compared with the tens or hundreds at the macro-level. Thus the metal is not homogeneous and the deformation characteristics are likely to be different, as the resolved crystal deformation exhibited as the workpiece shape will be the result of slip on relatively few slip-planes and a common outcome between different workpieces is unlikely. Due to this influence of the

micro-structure on the forming process, the workpiece for a micro-part can no longer be regarded as a homogeneous continuum for process-simulation purposes. Thus in the process simulation of forming micro-parts, it is important to choose appropriate FE simulation theories, so that the length scale of material deformation can be considered. In most of the cases in the forming of micro-parts, continuum-mechanics theories break down and crystal plasticity finite-element (CPFE) methods have to be used. Thus, in this chapter, numerical procedures for CPFE are introduced.

MICRO-MATERIAL MODELS

Physical Basis for Single-crystal Deformation

Crystal plasticity is a physically based plasticity theory that represents the deformation of a metal at the micro-scale. The flow of dislocations in a metallic crystal along slip systems is represented in a continuum framework. Plastic strain is assumed to be due solely to crystallographic dislocation slip. Slip is the dominant mechanism for deformation, which occurs due to dislocation motion. A crystalline material is constructed of a

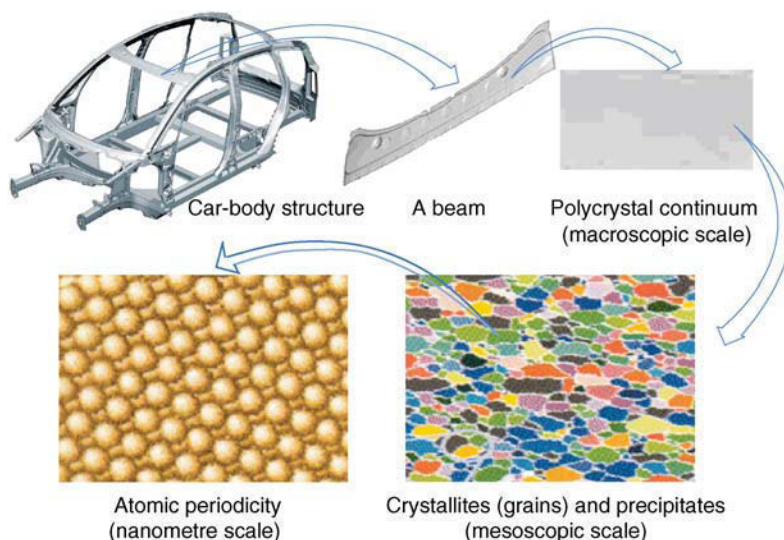


FIGURE 23-2 Plasticity in metals at various length scales.

periodic packing of atoms. A crystal structure refers to a group of atoms that is situated in repeating or periodic arrays or a unit cell. For metals, there are three simple crystal structures, namely FCC (face-centered cubic), BCC (body-centered cubic) and HCP (hexagonal close-packed) structures. Figure 23-3(a) shows the pure crystal structures for FCC metals.

Observation of single crystals shows that slip tends to take place most readily in specific directions (i.e. slip-directions) on certain crystallographic planes (i.e. slip-planes). A slip-plane refers to the plane of greatest atomic density and the slip-direction is the closest packed direction within the slip-plane. A combination of preferred slip-planes and slip-directions is called a slip-system. For FCC crystals, the most densely packed planes are the diagonal planes of the unit cell, see Fig. 23-3(b). The full family of slip systems in an FCC crystal may be written as $\langle 110 \rangle \{111\}$. There are 12 such systems in an FCC crystal (four planes each with three directions).

Considered a single crystal of zinc, this is a few millimeters in width and has been loaded beyond its yield in tension. The planes that can be seen are those on which slip has occurred resulting from many hundreds of dislocations running through the crystal and emerging at the edge. Each

dislocation contributes just one Burger's vector of relative displacement, but with many such dislocations, the displacements become large (Fig. 23.3(c)).

Crystal Kinematics

The general kinematics of the elastic–plastic deformation of a crystal at finite strains were given by Taylor (1938) [3], Hill (1966) [4], Rice (1971) [5], Hill and Rice (1972) [6], Asaro and Rice (1977) [7] and Asaro (1983) [8]. The total deformation gradient of finite strain from the reference frame to the current frame, F_{ij} , is defined by:

$$F_{ij} = \frac{\partial x_i}{\partial X_j} \quad (1)$$

where X_j and x_i denote the reference- and current-particle positions, respectively. Here, tensor conventions for subscripts are adopted. All indices i, j, k and l are running from 1 to 3 throughout this chapter.

In crystal plasticity theory, a crystalline material is embedded on its lattice, which undergoes elastic deformation and rotation. The inelastic deformation of a single crystal is assumed here to arise solely from crystalline slip. The material

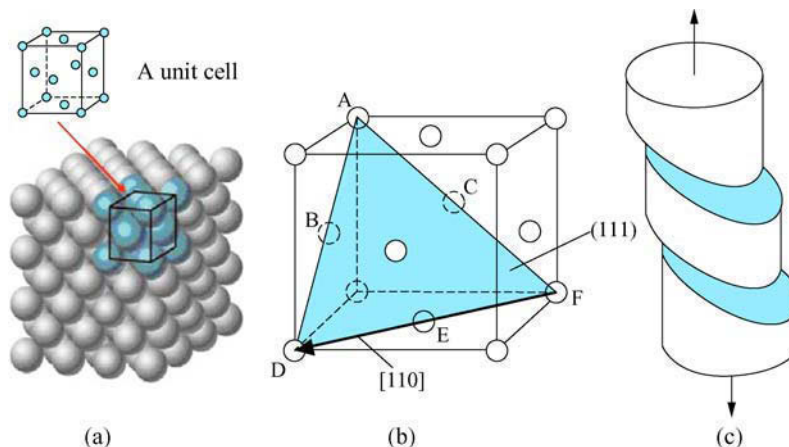


FIGURE 23-3 (a) FCC-structures in a crystalline material; (b) a particular slip-system $(111)[\bar{1}10]$ in an FCC lattice; and (c) a schematic diagram representing single-slip.

flows through the crystal lattice via dislocation motion. The total deformation gradient F_{ij} is given by:

$$F_{ij} = F_{ik}^* F_{kj}^P \quad (2)$$

where F_{kj}^P denotes plastic shear of the material to an intermediate reference configuration in which the lattice orientation and spacing are the same as in the original reference configuration, and where F_{ik}^* denotes stretching and rotation of the lattice. These are shown in Fig. 23-4. The rate of change of F_{ij}^P is related to the slipping rate $\dot{\gamma}^\alpha$ of the α th slip system by:

$$\dot{F}_{ik}^P F_{kj}^{P-1} = \sum_{\alpha} \dot{\gamma}^\alpha s_i^\alpha m_j^\alpha \quad (3)$$

where the sum ranges over all activated slip systems and unit vectors s_i^α and m_j^α are the slip-direction and the normal to the slip-plane in the reference configuration, respectively. The number of slip-systems and their orientations depend on the crystal lattice, e.g. an FCC crystal contains four slip-planes and each slip-plane

has three slip-directions, which results in $\alpha = 1, 2, \dots, 12$.

It is convenient to define the vector $s_i^{*\alpha}$, lying along the slip-direction of the system α in the deformed configuration, by:

$$s_i^{*\alpha} = F_{ik}^* s_k^\alpha \quad (4)$$

A normal to the slip-plane which is the reciprocal base vector to all such vectors in the slip-plane is:

$$m_i^{*\alpha} = m_k^\alpha F_{ki}^{*-1} \quad (5)$$

The velocity gradient in the current state is:

$$L_{ij} = \dot{F}_{ik} F_{kj}^{-1} = D_{ij} + \Omega_{ij} \quad (6)$$

where the symmetric rate of stretching D_{ij} and the anti-symmetric spin tensor Ω_{ij} may be decomposed into lattice parts (superscript *) and plastic parts (superscript P) as follows:

$$D_{ij} = D_{ij}^* + D_{ij}^P, \quad \Omega_{ij} = \Omega_{ij}^* + \Omega_{ij}^P \quad (7)$$

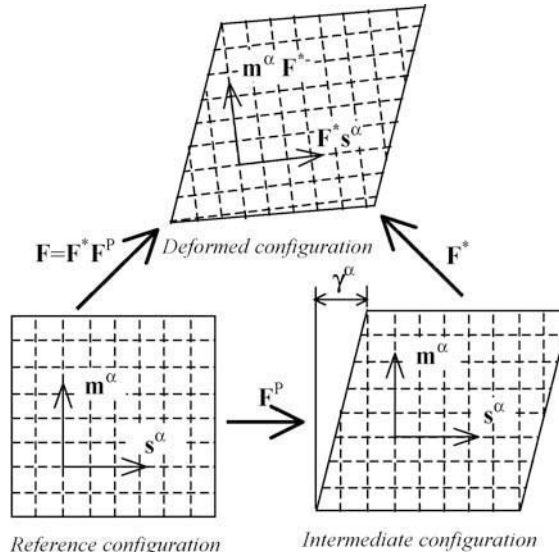


FIGURE 23-4 Schematic diagram of single crystal kinematics.

Satisfying:

$$D_{ij}^* + \Omega_{ij}^* = \dot{F}_{ik}^* F_{kj}^{*-1}, D_{ij}^p + \Omega_{ij}^p = \sum_{\alpha} \dot{\gamma}^{\alpha} s_i^{\alpha} m_j^{\alpha} \quad (8)$$

Finally, it is noted that the plastic parts of the rate of stretching and the rate of spin are given by the symmetric and skew part of Eqn (8). If it is defined that:

$$P_{ij}^{\alpha} = \frac{1}{2} (s_i^{\alpha} m_j^{\alpha} + s_j^{\alpha} m_i^{\alpha}), W_{ij}^{\alpha} = \frac{1}{2} (s_i^{\alpha} m_j^{\alpha} - s_j^{\alpha} m_i^{\alpha}) \quad (*.9)$$

then:

$$D_{ij}^p = \sum_{\alpha} P_{ij}^{\alpha} \dot{\gamma}^{\alpha}, \Omega_{ij}^p = \sum_{\alpha} W_{ij}^{\alpha} \dot{\gamma}^{\alpha}, \quad (*.10)$$

It is worth noting that the plastic part of the rate of stretching, D_{ij}^p , is that part of the rate of stretching arising from slip in the current lattice direction s_i^{α} , in a plane where the current normal is m_i^{α} , while the plastic part of the rate of spin, Ω_{ij}^p , is that part of the rate of plastic spin resulting from the summation of rotation on each slip-system.

Crystal Plasticity Constitutive Equations

The main feature of the crystal plasticity constitutive theory will be briefly introduced here. For each grain, linear elasticity constitutive relations are given by the generalized Hooke's law:

$$\tau_{ij}^{\nabla*} = L_{ijkl} D_{kl}^* \quad (11)$$

where L_{ijkl} the fourth-order stiffness tensor and D_{ij}^* the second-order symmetric rate of stretching of the lattice. $\tau_{ij}^{\nabla*}$ represent the Jaumann rates of Kirchhoff stress formed on axes that spin with the lattice:

$$\tau_{ij}^{\nabla*} = \dot{\tau}_{ij} - \Omega_{ik}^* \tau_{kj} + \tau_{ik} \Omega_{kj}^* \quad (12)$$

where $\dot{\tau}_{ij}$ is the material rate of Kirchhoff stress. The Kirchhoff stress τ_{ij} is defined as $(\rho_0/\rho)\sigma_{ij}$, where σ_{ij} is the Cauchy stress and ρ_0 and ρ are the material density in the reference and current states. On the other hand, τ_{ij}^{∇} is the Jaumann rate

of Kirchhoff stress formed on axes that rotate with the material:

$$\tau_{ij}^{\nabla} = \dot{\tau}_{ij} - \Omega_{ik} \tau_{kj} + \tau_{ik} \Omega_{kj} \quad (13)$$

The difference between these two rates is:

$$\tau_{ij}^{\nabla*} - \tau_{ij}^{\nabla} = \sum_{\alpha} (W_{ik}^{\alpha} \tau_{kj} - \tau_{ik} W_{kj}^{\alpha}) \dot{\gamma}^{\alpha} \quad (14)$$

When Eqns (9–11) and Eqn (14) are combined, the resulting constitutive law becomes:

$$\tau_{ij}^{\nabla} = L_{ijkl} D_{kl} - \sum_{\alpha} (L_{ijkl} P_{kl}^{\alpha} + W_{ik}^{\alpha} \tau_{kj} - \tau_{ik} W_{kj}^{\alpha}) \dot{\gamma}^{\alpha} \quad (15)$$

In crystal plasticity, plastic deformation is assumed to be caused solely by crystalline slip and crystalline slip to be driven by Schmid stress (or resolved shear stress), τ^{α} [3], which is defined by:

$$\tau^{\alpha} = m_i^{\alpha} \tau_{ij} s_j^{\alpha} \quad (16)$$

where m_i^{α} and s_j^{α} are slip-plane normals and directions for the α th slip-system, respectively. The rate changes of this Schmid stress is given by [9]:

$$\dot{\tau}^{\alpha} = m_i^{\alpha} (\tau_{ij}^{\nabla*} - D_{ik}^* \tau_{kj} + \tau_{ik} D_{kj}^*) s_j^{\alpha} \quad (17)$$

The slipping strain rate $\dot{\gamma}^{\alpha}$ is assumed to be governed by the resolved shear-stress τ^{α} given by a constitutive equation shown below:

$$\dot{\gamma}^{\alpha} = \dot{a} \left(\frac{\tau^{\alpha}}{g^{\alpha}} \right) \left(\left| \frac{\tau^{\alpha}}{g^{\alpha}} \right| \right)^{n-1} \quad (18)$$

where \dot{a} is the reference strain rate, n is the stress-sensitivity parameter and g^{α} is the current strain-hardened state of the crystal. In the limit as n approaches infinity, this power law approaches that of a rate-independent material. The current hardened state g^{α} is defined by:

$$\dot{g}^{\alpha} = \sum_{\beta} h_{\alpha\beta} \dot{\gamma}^{\beta}, \beta = 1, 2, \dots, 12 \text{ for FCC crystals} \quad (19)$$

where $h_{\alpha\beta}$ is the slip-hardening moduli. Self- ($h_{\alpha\alpha}$) and latent- ($h_{\alpha\beta}$) hardening moduli are defined as:

$$h_{\alpha\beta} = \begin{cases} h_0 \operatorname{sech}^2 \left| \frac{h_0 \gamma}{\tau_s - \tau_0} \right| & \alpha = \beta \\ qh(\gamma) & \alpha \neq \beta \end{cases} \quad (20)$$

$$\gamma = \sum_{\alpha=1}^{12} |\gamma^\alpha| \quad (21)$$

where h_0 is the initial hardening modulus, τ_0 is the initial shear strength of the material; at $t = 0$, all g^α are equal to τ_0 ; τ_s is the breakthrough stress when plastic flow initiates; γ is the cumulative slip strain and q is a hardening factor. The material constants within the crystal plasticity constitutive equations are determined from experimental data. As an example, a set of the constants is listed in Table 23-1 for a single-crystal copper [9]. The high value of n is used here to reduce the viscoplastic behavior of the material, as it is used in room-temperature forming processes.

INTEGRATED CPFEE ANALYSIS FOR THE FORMING OF MICRO-PARTS

CPFEE Implementation

CPFEE calculations can be carried out using commercial FE software. While detailed implementations can be found either in the form of implicit [10] or explicit [11] format, a brief introduction of the explicit implementation will be given in this section and a sample simulation on the forming of micro-pins with an integrated micro-mechanics analysis system will be given in the following section.

TABLE 23-1		Material Parameters for the Crystal-plasticity Model		
n	$\dot{a}(\text{s}^{-1})$	h_0 (MPa)	τ_s (MPa)	τ_0 (MPa)
10.0	0.001	541.5	109.5	60.8

In crystal plasticity, the constitutive equations are expressed in an intermediate configuration, shown in Fig. 23-4, obtained by unloading the deformed crystal from the current configuration. Because the total deformation applied to the crystal is provided by the FE solution, only single crystal response is needed. A set of crystal constitutive equations can be implemented into ABAQUS/Explicit via a user-defined sub-routine VUMAT. In explicit finite element calculation procedures, the task can be split up easily and solved by a number of processors. Hence, VUMAT can be constructed with a vectorized interface. This means that when a simulation is carried out using multiple processors, the analysis data can be split up into blocks and solved independently. Thus, vectorization can be preserved in the writing of the sub-routine in order that optimal processor parallelization can be achieved.

The time integration of the set of constitutive equations can be carried out by discretizing the deformation history in time and integrating the equations numerically over each time increment. For this purpose, the configuration of the body is considered at t_n and t_{n+1} , with $t_{n+1} = t_n + \Delta$. The integration scheme developed assumes that: (1) a given crystal deformation represented by F_{ij} (or L_{ij}) is given at each time increment, Δt ; (2) the variables (τ^α , g^α , γ^α) in each crystal are known at time t_n ; and (3) the slip-systems ($m^{*\alpha}$, $s^{*\alpha}$) are known. The purpose of the integration scheme is to determine the updated values (τ^α , g^α , γ^α), which are then used to calculate the stress/strain response of the crystal at time t_{n+1} .

An explicit integration method is employed in ABAQUS/Explicit. In this approach, the accelerations and velocities at a particular point in time are assumed to be constant during a time increment and are used to solve for the next point in time. To reduce the dynamic effects, a value of the ratio of the duration of the load and the fundamental natural period of the model of greater than five is recommended [12]. It has been found that by keeping the ratio of kinetic energy to the total internal strain energy at $<5\%$, dynamic effects in the model are negligible [13,14].

The overall numerical-calculation procedure for the CPFEE implementation into the commercial FE code ABAQUS via the user defined sub-routine VUMAT is summarized in Fig. 23-5.

Development of the CPFEE Model

In crystal plasticity modeling, a workpiece contains a number of grains which are in random shapes that also possess random grain orientation [15–18]. The finite element mesh, which takes account of different orientations of grains, requires that different mechanical properties be assigned to individual grains.

The grain structures and grain boundaries are described in terms of vector graphics by means of differentiation between points of different colors in the micrograph. The scale of the specimen is defined and the axes of a coordinate are assigned. The grain objects must be assigned with mechanical properties according to the data from an EBSD (electron backscatter diffraction) micrograph. An EBSD micrograph of a low carbon steel has been used for preparation of a sample mesh according to the above principle. The original micrograph is shown in Fig. 23-6(a). The extracted grains with orientations have been created (see Fig. 23-6(b)) from the EBSD micrograph. The selected grains

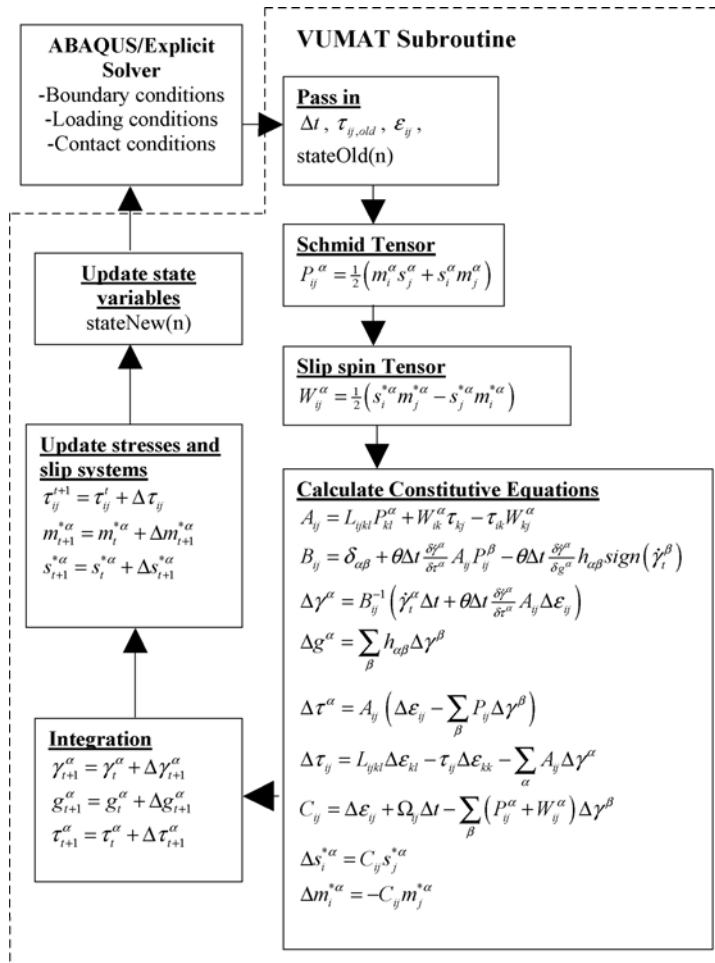


FIGURE 23-5 The implementation procedure for CPFEE analysis using ABAQUS (after [11]).

can be further discretized and the final mesh for CPFE analysis is shown in Fig. 23-6(c).

The above process for creating an FE mesh is complicated and time consuming. Thus Voronoi tessellation, like the stochastic method, was introduced recently to generate grain structures based on probability theories [19–22]. The concept of the Voronoi polygon has been used extensively in material science, especially for modeling random micro-structures such as aggregates of grains in polycrystals. If the micro-structure of a material is known, some physical parameters, such as average, minimum and maximum grain sizes, should be given. If a micro-film is cold rolled, the average aspect ratio of grains can be obtained fairly easily. Significant studies have confirmed that the one-parameter gamma distribution can be used to represent the distribution probability of grain structures [23–25].

The Integrated Numerical Process

A virtual grain structure is generated according to the physical parameters of a material, such as the dimensions of the workpiece and the grain

size information [26]. The orientation of grains is assigned according to a probability distribution, either in the random form or with a designed distribution. The generated grain structure, together with its orientation, can be transferred to commercially available FE codes, where further preprocessing, such as meshing, boundary conditions and loading assignment, can be carried out. In this research, the generated virtual grains with their orientation information are transferred into ABAQUS/CAE for further preprocessing.

Figure 23-7 shows the overall scheme of the integrated numerical procedure for CPFE modeling using ABAQUS. In the preprocessing, virtual grain structures with their orientation information are generated and input into ABAQUS/CAE, which is employed for further preprocessing. A complete CPFE model with meshing, contact interaction, boundary and loading conditions is created using ABAQUS/CAE. The crystal plasticity material model is implemented in ABAQUS via the user-defined sub-routine VUMAT. This enables explicit micro-mechanics analyses to be carried out.

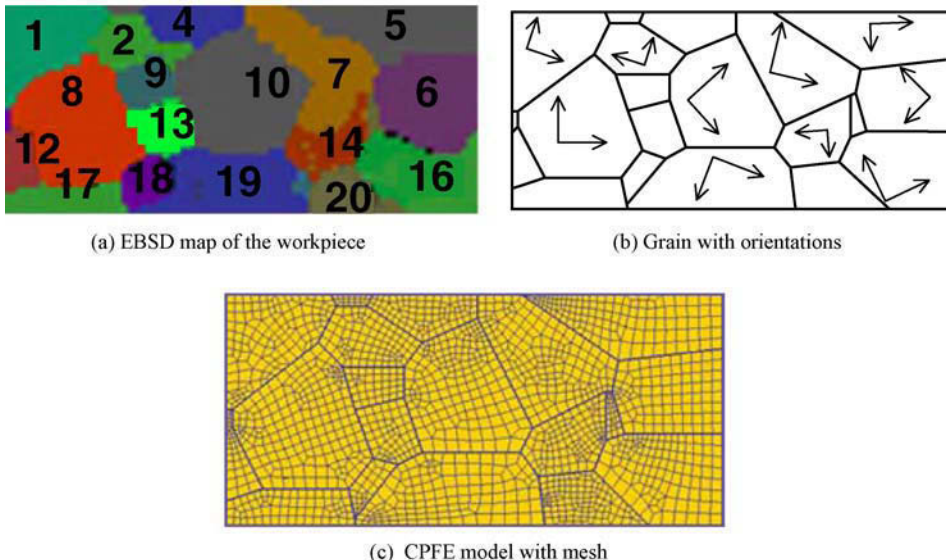


FIGURE 23-6 An approach to create an FE mesh from the physical micro-structure of a material.

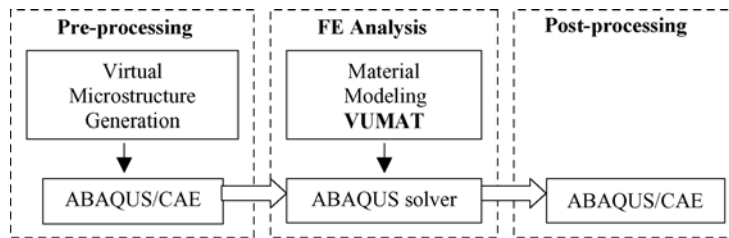


FIGURE 23-7 An integrated numerical procedure for micro-mechanics modeling.

PROCESS SIMULATION FOR THE FORMING OF MICRO-PINS

Extruded micro-pins are now used widely in electronics devices. It is estimated that 24 billion micro-pins are used annually for IC carriers [27]; they have diameters of the order of 100 μm to 2 mm. The quality of the formed micro-pins is affected by the grains size, grain orientation and grain distributions of the material and the geometrical defects cannot be captured using conventional continuum-based FE forming simulation techniques.

Figure 23-8(a) shows micro-pins of 0.57 mm diameter extruded using the same material, but which was heat treated to produce different grain sizes [28]. It was reported that for material with a grain size of 32 μm , or about 16~18 grains across the extruded diameter, and the deformation ratio is about 1.3, fairly straight micro-pins can be extruded and continuum FE analysis can be used for this prediction. However, for material with a grain size of 211 μm , i.e. about 2~3 grains across the diameter of the extruded micro-pins, uncontrollable bending and curvature of the extruded micro-pins is observed experimentally for the same extrusion ratio [28].

Numerical investigations have been carried out using the developed integrated CPFE simulation system. Randomly distributed grains with an average grain size of 211 μm were generated using the Voronoi tessellation method (Fig. 23-8(b)). The dimensions of the workpiece and the die are also shown in Fig. 23-8(b) and the FE mesh was created using ABAQUS/CAE with quad-dominated elements (CPE4R). The sub-routine VUMAT was used for the crystal plastic model implementation. A displacement of 2280 μm is applied on the extrusion punch. The friction

coefficients are zero at the interfaces between the punch and the workpiece and 0.1 between the die and the workpiece: the latter value is commonly used for cold-extrusion processes. In Fig. 23.8(b), the grain orientation is assigned randomly. It should be noted that the CPFE model described above is based on a plane-strain description, which is a simplified model and different from that for the extrusion of circular micro-pins. However, similar features of the geometric variations of those of the extruded and simulated micropins can be observed.

Figure 23-8(c) shows the virtually ‘formed’ micro-pins and the contours of cumulative shear strain distribution for the results of two CPFE analyses. Both use the same FE model and grain structure and the only difference is that the grain orientations are assigned to the grains using the same probability theories twice: thus the grain orientations are different from the two CPFE models. It can be seen clearly that the geometric errors for the extruded micro-pins are different. This could confirm the results obtained experimentally, that if the ratio of the diameter of the micro-pins and the grain size of the material is small, uncontrollable bending and curvature of the extruded micro-pins are the major geometrical defects. This CPFE analysis result demonstrates the validity of the developed CPFE tools in capturing the grain size effects in the process of the forming of micro-pins. It can be observed also from the figure that the maximum cumulative shear strains occur locally along grain boundaries, which effect is induced by strong mismatches of the orientations among the grains. The uncontrollable curvature feature (Fig. 23-8(a) and (c)) cannot be modeled, if continuum FE analysis is used.

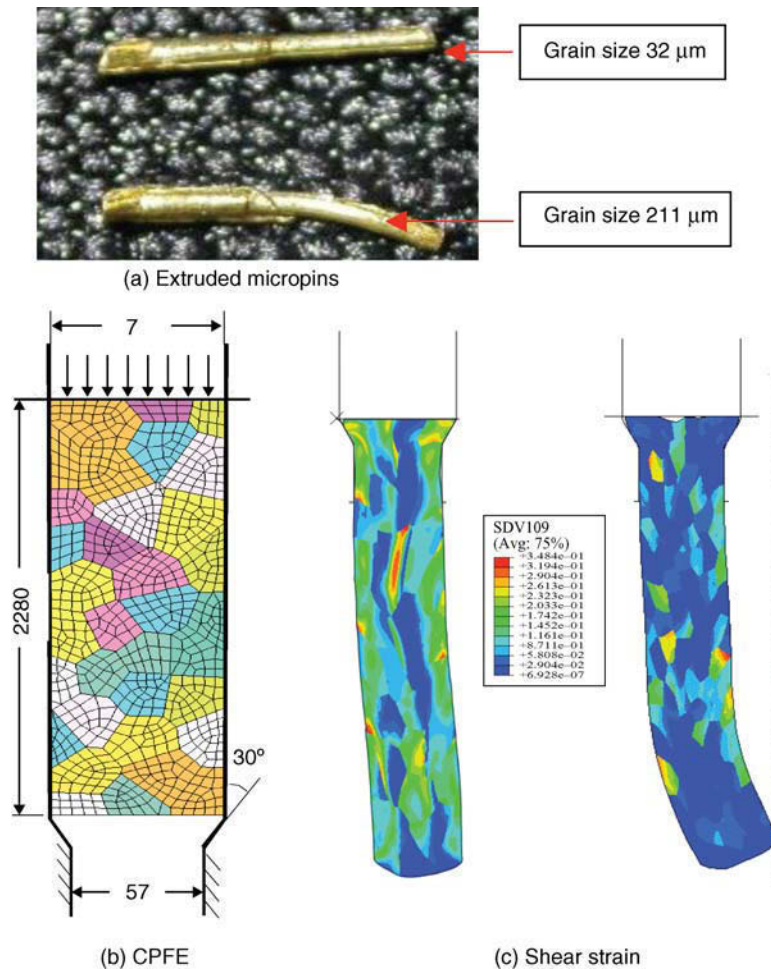


FIGURE 23-8 Extrusion of micro-pins.

This shows clearly the grain size effect during the micro-forming process and that CPFE needs to be employed to predict such features.

CONCLUSIONS

In traditional metal forming processes, continuum mechanics-based FE techniques can be used for process simulation. However, in micro-forming processes, if the ratio of the minimum dimension of a micro-part and the grain size of the

material is small, CPFE analysis has to be used, otherwise the important features of the forming of micro-parts cannot be captured. CPFE analysis can be carried out using existing commercial FE codes, such as ABAQUS: there is no need to generate special FE codes for this purpose. The main difficulties in the simulation of micro-forming processes using CPFE are: (1) the creation of the CPFE model, which includes the generation of the micro-structures of materials, material orientations and the creation of an FE mesh within grains

and (2) crystal plasticity material models, which include the development and determination of micro-mechanics material models and the implementation of the models in commercial FE codes. Thus significant efforts should be made on these two aspects of research for micro-forming applications.

REFERENCES

- [1] M. Geiger, M. Kleiner, R. Eckstein, N. Tiesler, U. Engel, *Microforming*, CIRP Ann. 50 (2) (2001) 445–462.
- [2] U. Engel, R. Eckstein, *Micro-forming – from basic research to its realization*, J. Mater. Process. Technol. 125–126 (2002) 35–44.
- [3] G.I. Taylor, *Plastic strain in metals*, J. Inst. Met. 62 307–325.
- [4] R. Hill, *Generalized constitutive relations for incremental deformation of metal crystals by multislip*, J. Mech. Phys. Solids 14 (2) (1966) 95–102.
- [5] J.R. Rice, *Inelastic constitutive relations for solids: an internal-variable theory and its application to metal plasticity*, J. Mech. Phys. Solids 19 (6) (1971) 433–455.
- [6] R. Hill, J.R. Rice, *Constitutive analysis of elastic-plastic crystals at arbitrary strain*, J. Mech. Phys. Solids 20(6) (1972) 401–413.
- [7] R.J. Asaro, J.R. Rice, *Strain localization in ductile single crystals*, J. Mech. Phys. Solids 25 (1977) 309–338.
- [8] R.J. Asaro, *Micromechanics of crystals and polycrystals*, Adv. Appl. Mech 23 (1983) 1–115.
- [9] D. Peirce, R.J. Asaro, A. Needleman, *An analysis of nonuniform and localized deformation in ductile single crystals*, Acta Metall 30 (1982) 1087–1119.
- [10] Y. Huang, *A user-material subroutine incorporating single crystal plasticity in the ABAQUS finite element program*, Harvard University Report, MECH 178 (1991).
- [11] F.J. Harewood, P.E. McHugh, *Comparison of the implicit and explicit finite element methods using crystal plasticity*, Comput. Mater. Sci 39 (2007) 481–494.
- [12] L.M. Kutt, A.B. Pifko, J.A. Nardiello, J.M. Papazian, *Slow-dynamic finite element simulation of manufacturing processes*, Comput. Struct 66 (1) (1998) 1–17.
- [13] W.J. Chung, J.W. Cho, T. Belytschko, *On the dynamic effects of explicit FEM in sheet metal forming analysis*, Eng. Computations 15 (6) (1998) 750–776.
- [14] H.-H. Choi, S.-M. Hwang, Y.H. Kang, J. Kim, B.S. Kang, *Comparison of implicit and explicit finite element methods for the hydroforming process of an automobile lower arm*, Int. J. Adv. Manuf. Technol 20(6) (2002) 407–413.
- [15] H. Riesch-Oppermann, *VorTess Generation of 2-D random Poisson-Voronoi mosaics as framework for the micro-mechanical modelling of polycrystalline materials*, Report FZKA 6325, Forschungszentrum Karlsruhe, Karlsruhe, Germany (1999).
- [16] K. Kobayashi, K. Sugihara, *Crystal Voronoi diagram and its applications*, Future Gener. Comp. Sy 18 (5) (2002) 681–692.
- [17] U.F. Kocks, C.N. Tomé, H.-R. Wenk, *Texture and Anisotropy*, Cambridge University Press, Cambridge, UK (1998).
- [18] K.S. Zhang, M.S. Wu, R. Feng, *Simulation of micro-plasticity-induced deformation in uniaxially strained ceramics by 3-D Voronoi polycrystal modelling*, Int. J. Plast. 21 (4) (2005) 801–834.
- [19] J. Cao, W. Zhuang, S. Wang, K. Ho, N. Zhang, J. Lin, T.A. Dean, *An integrated crystal plasticity FE system for micro-forming simulation*, To appear in Int. J. of Multiscale Modelling (2008).
- [20] H.X. Zhu, S.M. Thorpe, A.H. Windle, *The geometrical properties of irregular two-dimensional Voronoi tessellations*, Philos. Mag. A 81 (12) (2001) 2765–2783.
- [21] A. Okabe, B. Boots, K. Sugihara, *Spatial Tessellations: Concepts and Applications of Voronoi Diagrams*, Wiley, New York (1992).
- [22] D. Stoyan, W.S. Kendall, J. Mecke, *Stochastic Geometry and its Application*, Wiley, New York (1987).
- [23] M. Fatima Vaz, M.A. Fortes, *Grain size distribution: the lognormal and the gamma distribution functions*, Scripta Metallurgica 22 (1988) 35–40.
- [24] B. Zhu, R.J. Asaro, P. Krysl, K. Zhang, J.R. Weertman, *Effects of grain size distribution on the mechanical response of nanocrystalline metals: Part II*, Acta Mater. 54 (2006) 3307–3320.
- [25] C. Wang, G. Liu, G. Wang, W. Xue, *On the quasi-stationary grain size distribution from two Gamma size distributions in three-dimensional grain growth*, Mater. Lett 61 (2007) 4262–4266.
- [26] K.C. Ho, N. Zhang, J. Lin, T.A. Dean, *An integrated approach for virtual microstructure generation and micromechanics modelling for micro-forming simulation*, Proceedings of ASME, MNC2007, MicroNanoChina07, Sanya, Hainan, China, (Jan. 10–13, 2007) 1–9.
- [27] J. Cao, N. Krishnan, Z. Wang, H. Lu, K. Wing, A. Swanson, *Micro-forming: experimental investigation of the extrusion process for micropins and its numerical simulation using RKEM*, Trans. ASME 126 (2004) 642–652.
- [28] K. Krishnan, J. Cao, K. Dohda, *Study of the size effect on friction conditions in micro-extrusion: Part 1: Micro-extrusion experiments and analysis*, J. Manuf. Sci. E. -ASME 129 (2007) 669–676.

Manufacturing Execution Systems for Micro-Manufacturing

Matthias Meier

INTRODUCTION

Looking at manufacturing from a bird's-eye perspective reveals two important generic processes that characterize these enterprises – the *product lifecycle process* on the one hand and the *customer order process* on the other. Fig. 24-1 shows a sketch of these processes and their interrelation. The product lifecycle process that is shown on the X-axis describes the activities that are executed to develop new products, i.e. to generate innovations and to bring them to the market. The customer-order process on the Y-axis shows the activities performed to produce these products based on market needs and to deliver them to customers. Over the last few years the integration of activities within both of these processes has been recognized as a major capability for optimization. Furthermore, the time required for the execution of these processes on the one hand and the efficiency and effectiveness of the execution of activities within these processes on the other are considered as generic optimization goals. Adjusting these potentials requires a significant amount of *information technology* (IT) support, as complex control loops have to be built up – some of them even bridging multiple process activities; with large amounts of data needing to be collected and to be processed in order to change the process

variables in the right way. The production activity is the linchpin where both processes overlap and is therefore definitely an activity to be considered when designing the overall IT architecture of an enterprise.

While the foregoing remark is already true for today's state-of-the-art factories, there are a number of reasons that even argue for an increasing need of IT support for the manufacturing of micro-products in future, such as:

1. Operating new manufacturing processes at the edge of technical feasibility in series production often requires sophisticated IT support for monitoring and controlling these processes.
2. There is increasing pressure in terms of quality control, which arises from the automotive industry, for example. While extremely high quality requirements have been known for a long time in aerospace, in defense and in the medical industry, the quality requirements *original equipment manufacturers* (OEM) request from their suppliers in the automotive industry have significantly risen over the last few years. The goal of the OEMs is to reduce the number of quality issues as experienced with several car series in recent years – which were often caused by defective electronic components. The IT environment is one building

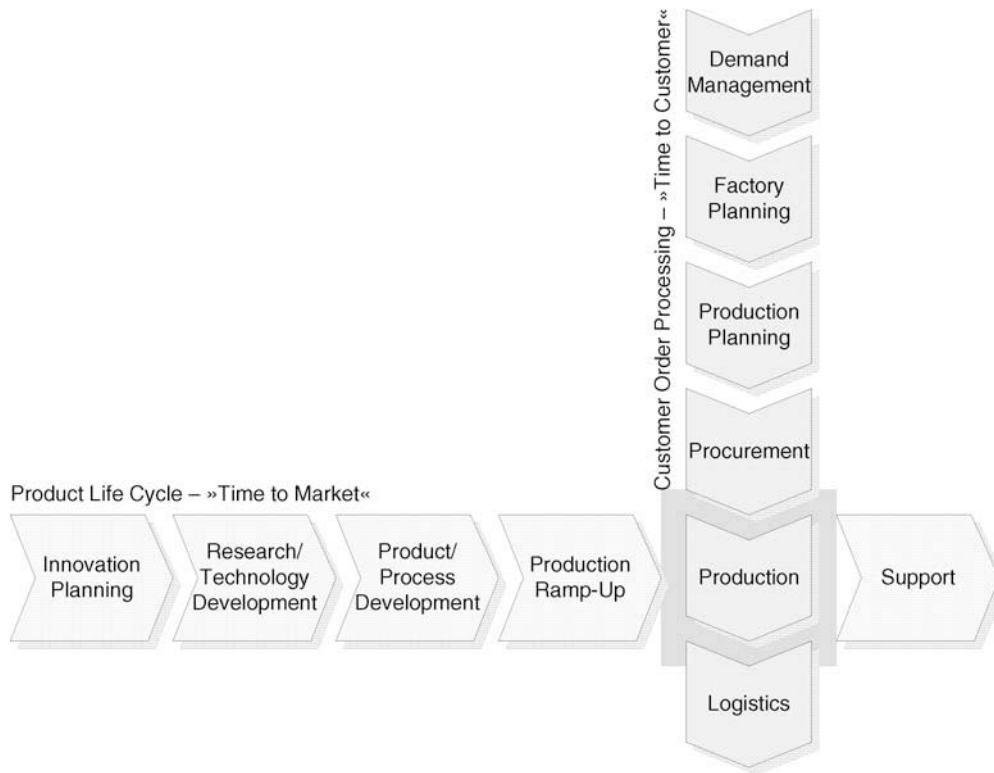


FIGURE 24-1 Product lifecycle and customer-order process.

block for implementing zero-defect strategies as requested by the OEMs.

3. Increasing low cost production capacities in several parts of the world put additional cost pressure on numerous industries. Adjusting optimization potentials throughout the process chains is another goal to be supported by IT systems.

Further discussions within this chapter are focused on the ‘Production’ activity and the IT environment supporting it. This chapter aims to deliver insights into concepts, standards and technologies used to implement the production-related IT environment for micro-/nano-manufacturing. The first section provides a general overview of the production IT landscape. It explains important terms, architecture layers, and corresponding systems and their scope. In the second section the scope is narrowed to the manufacturing-execution systems, which are investigated in more detail. The third section

briefly reviews approaches to implement the concepts discussed earlier. The last section closes the chapter with some considerations on relevant standardization work.

PRODUCTION IT OVERVIEW

For the following considerations, the scope is narrowed to discrete manufacturing. Investigating a micro-manufacturing enterprise from a production IT point of view requires some initial discussion of the organizational structure of the physical assets of such an enterprise. The hierarchical structure shown in Fig. 24-2, which is based on reference [1], is commonly used for this purpose. As the root of the hierarchy, the *enterprise* defines the products to be manufactured and how and where these products are to be manufactured. Each enterprise comprises one or multiple *sites*. A site is mainly characterized by its physical or geographical location and its major

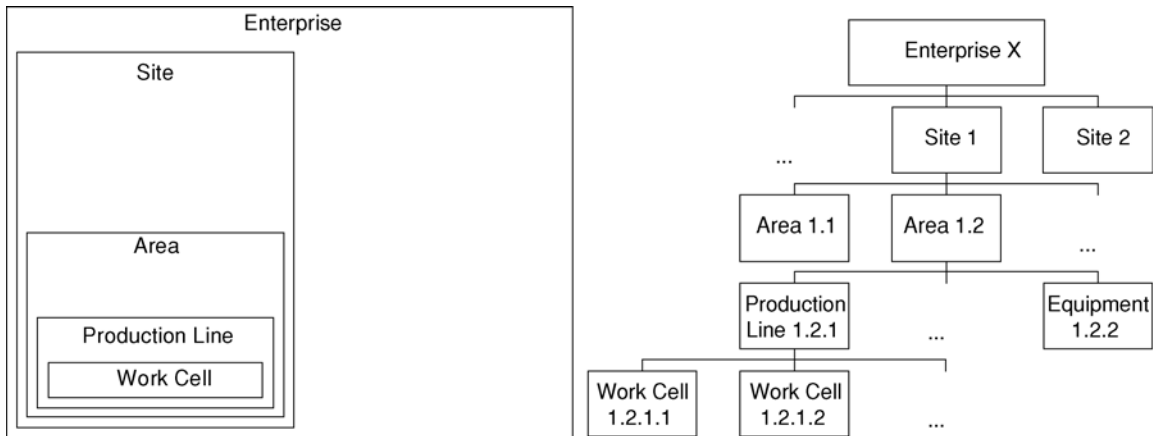


FIGURE 24-2 Hierarchical model of physical assets – conceptual model (left) and example (right).

manufacturing capabilities and serves as a grouping element for the enterprise. Each site contains one or multiple *areas*. Similar to a site, an area is usually characterized by its physical or geographical location within the site and its major manufacturing capabilities. The actual production capabilities are provided by lower-level entities that are grouped within the area, such as *production lines* and *work cells*. Both production lines and work cells are again characterized by their physical location within the area. Additionally, they have well-defined manufacturing capabilities and capacities. A modular precision assembly line for hard disks would be an example for a production line that is made up of several modules (work cells), each providing specific capabilities required to execute the overall assembly process. For some of the concepts described later the detailed distinction between production lines and work cells is no longer required. In this case the generic term *equipment* is used to represent both levels in the hierarchy.

Besides physical enterprises, the concept of *virtual enterprises* (VE) is becoming increasingly more popular – both in research and industry. Virtual enterprises are temporary organizations bridging the classical system boundaries described above. Therefore, their structure will look different compared to that discussed earlier. Although the specific requirements of virtual enterprises in terms of production IT are not considered here,

many of the generic concepts discussed in the following can be adjusted to support VEs. However, additional concepts need to be established from an IT point of view to implement VE organizations.

Figure 24-3 shows a simplified operational scenario within such an enterprise. Based on demand information a site receives from the enterprise level, the site generates and schedules *work orders* for a given quantity of products or components to be manufactured at the site using the capabilities available within one or multiple areas of the site. The goal of the schedule is to deliver the requested product or component at the right point in time while optimizing the utilization of any *resources* required. Resources in this context comprise employees, equipment, *durables*, *consumables* and *material*. Durables are auxiliary materials required in addition to equipment in order to process material, such as tools, tensioning media, carriers, cassettes, etc. In contrast to durables that can be reused many times, consumables are a class of auxiliary materials that are consumed while being used, such as coolant, for example. The work orders are executed according to corresponding *routes*, which define the sequence of *steps* required to manufacture a product or component of the requested type starting from raw material. Each step in the route contains information on the resources required to perform the step. The route is complemented by a corresponding *bill of material*

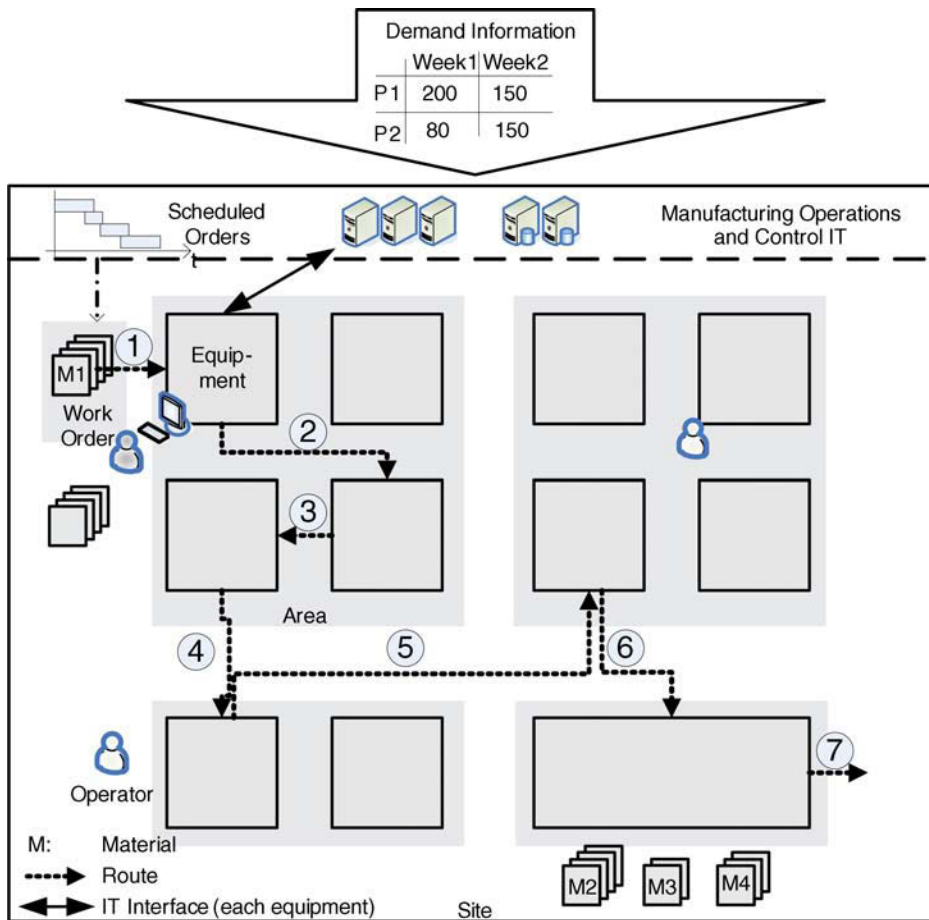


FIGURE 24-3 Operational scenario (example)

that describes in a structured way the parts and components required to manufacture the product or component. In order to monitor the progress of work orders over time, sufficient feedback needs to be provided from the equipment level to higher levels while the route is being executed. Besides the information on progress and process results in terms of quantities, feedback on quality needs to be collected to detect possible issues early and to ensure the required level of quality upon completion of the job.

The term 'Production IT' refers to the IT landscape that is dedicated to support the specific subprocess and activities within the 'Production' activity shown in Fig. 24-1, i.e. it provides tools to efficiently and effectively operate production.

Furthermore, the production IT landscape serves as a building block for process integration within both of the generic processes described earlier – the product lifecycle process and the customer-order process:

1. It supplies both processes with accurate information from production in a timely manner, such as information on the processing status of customer orders, available capacities – both are essential for the customer-order process – and process and quality data from production, which complement product lifecycle-related data that have been generated in other phases. Access to data from production is required as a first prerequisite to control and optimize the overall processes.

2. It provides other activities of the generic processes with suitable interfaces to influence production, which is the second prerequisite to establish overall control loops, including production.

Although the specific requirements to be fulfilled by the production IT environment differ from industry to industry on the one hand and from company to company on the other, there exists a set of generic concepts that many industries have in common: these concepts will be discussed in the following. The common approach to define both the scope and responsibility of the production IT landscape is derived from the *scheduling and control hierarchy*, which is based on the organizational structure of the enterprise, as described earlier. Each level within the hierarchy has corresponding spheres

of responsibility and planning horizons and is mapped to corresponding levels or layers of the IT architecture shown in Fig. 24-4 (tasks based on [2]). On the top-most level, the enterprise management level, the whole enterprise needs to be considered. Thus, planning and control activities on this level cover all sites, have a response time of the order of magnitude of days, span multiple weeks or months, and incorporate the complete list of available orders (strategic level). The sphere of responsibility of the manufacturing operations and control level is limited to single sites. Therefore, the scope of planning and control activities is limited to this site, spanning only one or several shifts while providing a response time in the order of magnitude of a few seconds to a single shift. At the same time, the number of orders to be

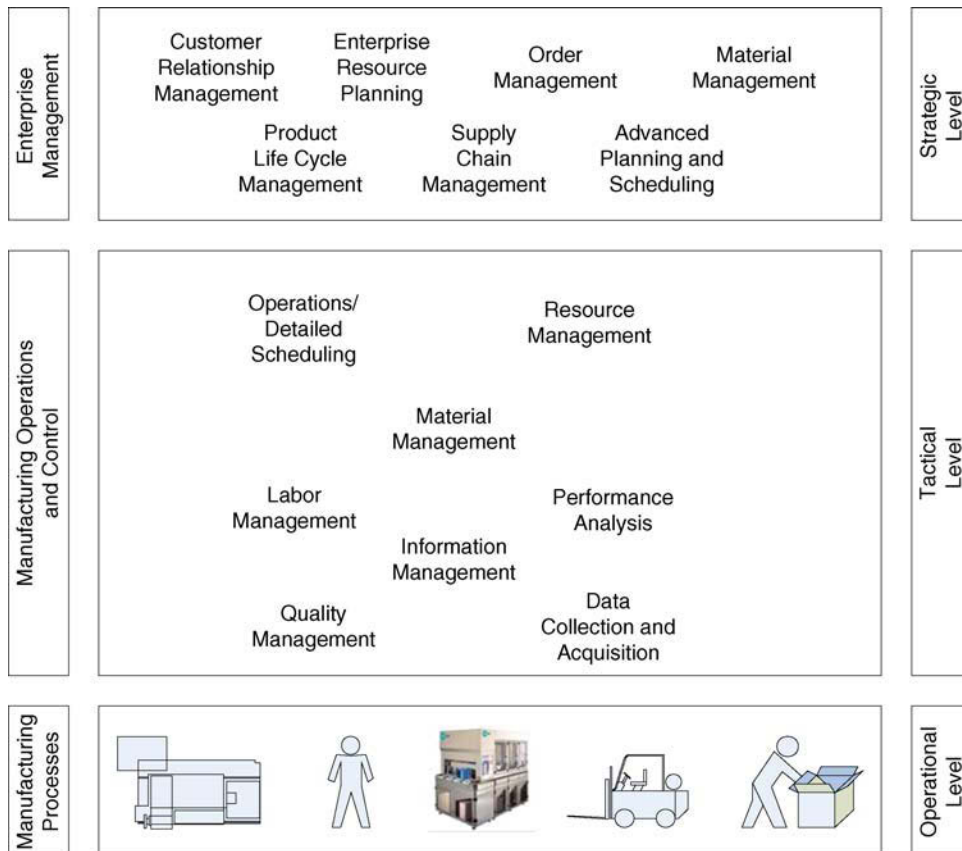


FIGURE 24-4 Production IT landscape – an overview.

considered is rather limited (tactical level). The bottom-most level, which reflects the actual manufacturing processes, is finally concerned with the execution of single process steps. Thus, the planning horizon is further limited to the order of magnitude of seconds or minutes. At the same time a response time of the order of magnitude of milliseconds to seconds has to be provided. In addition to its specific tasks, each level has to present a sufficient amount of transparency, i.e. to supply the upper layer with accurate and meaningful information with a defined maximum delay and with suitable interfaces to propagate information.

Although the specific shape and the boundaries of these levels differ slightly from industry to industry and from solution to solution, the basic concept – including the levels discussed above – is widely spread throughout many industries.

EXPLORING THE MANUFACTURING OPERATIONS AND CONTROL LEVEL

Based on the overall picture of the production IT landscape described above, the following sections will discuss the role of the manufacturing operations and control layer in more detail – especially the class of *manufacturing execution systems* (MES), which plays a major role in this context. MES systems bridge the gap between manufacturing processes – including their control systems – and the enterprise management systems as shown above. They control and monitor operations in production, are targeted to adjust optimization potentials within production, and facilitate the level of transparency between enterprise management and production that is required to implement complex process-integration scenarios, as described above. The task-oriented view defined by [2] has been selected as the basic structure for this discussion, as it gives good insight into the MES world from a user's perspective. The description of the MES tasks is complemented by a discussion of major concepts and terms to be considered in the MES environment.

Operations/Detailed Scheduling

Operations/detailed scheduling optimizes the execution of available work orders – which have usually been generated by higher level systems – based on a set of predefined optimization goals, while considering the constraints of the production under consideration. Generic optimization goals are:

1. The generation of a schedule that is actually executable while considering the availability of resources and material.
2. The reduction of set-up times, cycle time and work in progress.
3. An increase of throughput, resource utilization and on-time delivery.

A major characteristic of this task at the MES level is its real-time behavior, i.e. the schedule is continuously adjusted based on events and disturbances that occur on the shop floor. These changes are immediately enforced in production. Thus, the MES is able to handle unforeseen events, such as resource breakdowns, missing material, issues with production processes and quality issues. Generally, there are two approaches to be distinguished, based on the planning horizon: the *scheduling* approach and the *dispatching* approach. The scheduling approach attempts to generate a plan for assigning a set of *jobs* (task in the context of the architecture level considered) to a set of resources based on given constraints and optimization criteria within the range of a *scheduling horizon*. The dispatching approach is aimed at the optimization of resources in real-time by evaluating context information based on a given set of rules. Two typical questions answered by the dispatching sub-system in the case of job-shop production are:

1. **What is next for a given resource?** – i.e. which of the jobs within the job queue of this resource should be executed first based on the current context information and the set of dispatching rules? Examples for context information are: resource states, job priorities, time constraints, delivery dates, etc.
2. **Where is next for a given material?** – i.e. what is the best-suited next location for some material

after completing a process job on a given resource? In this case the context to be considered could be the next step based on the route assigned to this work order, the state of resources of the type that is required next, etc.

Due to the ad-hoc nature of decisions in the case of dispatching, this approach is mainly followed in highly dynamic environments as known from semiconductor manufacturing, for example, as the large number of disturbances within the production environment would require very frequent rescheduling. As the schedule generation is rather resource consuming (in terms of computational resources) and time consuming, it is difficult to implement the scheduling approach in this environment.

To deal with scheduling conflicts that arise due to disturbances as described above or due to competing optimization goals caused by committed delivery dates and varying job priorities, for example, is an important aspect of the operations/detailed scheduling task. The system needs to provide the capability to handle these conflicts automatically, if possible, or to supply responsible people with sufficient information to be able to take the right decision manually.

Resource Management

Resource management is mainly concerned with the task of ensuring the availability of the resources required for executing work orders. In this context, the term ‘resource’ comprises machines, equipment, durables and non-material durables. The former terms were explained earlier – the latter notion of non-material durables refers to auxiliary resources such as *numerical control* (NC) programs or *process programs* (PP) in general. In several industries process programs are also referred to as *recipes*. Recipes are programs that are executed by the equipment control system in order to control a specific process. The behavior of the control system can be adjusted by selecting different recipes or by adjusting parameters within given recipes.

The first aspect of the resource-management task comprises the management of resource-

related master data. For each resource a record of generic information needs to be maintained, including properties such as the *identifier* (ID), the location, and capacities and maintenance-related data. Furthermore, resources have to be modeled in sufficient detail in order to support the selected operations/detailed scheduling approach and other MES functionalities. Usually, resources are modeled in the form of a hierarchical structure that describes relevant components and their relationship. A simple example would be some cluster equipment, i.e. a class of items of equipment which have several process chambers that can be operated in parallel. Each process chamber offers specific process capabilities. An internal logistics system is responsible for the material transport within the equipment. The mainframe could be modeled as the root of a tree that contains a set of load ports and a set of process chambers. If single chambers are being considered within the process of detailed scheduling, equipment has to be modeled down to the chamber level. Each object within the tree has a specific state model assigned, including states such as ‘idle’, ‘processing’, or ‘locked’ that reflect the current state of the component at run-time. This state model is used to specify rules for operating the resource at run-time. A rule of that type could define that a resource in state ‘locked’ may not be used for processing, for example. Furthermore, resources have a set of *capabilities* assigned that define the type of jobs that can be executed. At the same time, resources are often integrated into an overall resource hierarchy, such as equipment groups, areas and facilities, and are linked with related resources. Machine/tool relations would be an example of this type of link. In addition to the equipment model-related master data, resource management has to cover the sub-tasks of recipe and parameter management.

The second aspect of resource management is related to the run-time behavior of resources. The resource tracking task performs book-keeping on any relevant dynamic data related to resources, including information on jobs and recipes executed on the resource, state changes based on the resource model and maintenance-related

information. The tracking task makes use of events that are gathered online from resources or manually logged at user terminals. If the physical resource starts processing, for example, a corresponding event is either automatically or manually logged for the resource, together with a time stamp. Upon receipt of this event, resource management will update the corresponding resource-state model, i.e. transition it from 'idle' to 'processing', and store the event in the *history* to allow for further analysis. The updated state information is visible for other MES tasks. Up-to-date resource information is an important requirement for realizing complex automation scenarios with the MES, as other MES tasks, especially the detailed scheduling functionality, rely on this data. Furthermore, resource management plays an important role in the process of resource allocation, especially for the appropriate *set-up* of resources before some production job is executed on the resource. The set-up comprises anything that is required in addition to the pure resource in order to process the job, such as the appropriate tools, tensioning media, recipes and parameters. In the case of fully automated scenarios the set-up is performed automatically, e.g. the durables are requested from connected logistics systems and recipes and parameters are downloaded to the resource. As soon as the set-up is complete and material is loaded, remote-controlled resources can even be automatically started via resource management.

The third aspect of resource management is also related to the run-time behavior of resources and is mainly concerned with the availability of resources. Resource properties reflecting the *qualification* state are continuously monitored, such as the operating hours, the number of production jobs executed, or even specific resource- or process-related properties. If limits defined within the master data model are exceeded, requalification of the resource is triggered to ensure the resource does actually provide the expected process capability. Similarly, the maintenance state of resources is monitored. Based on data collected from the resource and corresponding rules maintained in the form of resource master data, *pre-*

ventive or *predictive maintenance* strategies can be implemented in order to control the availability of resources to the maximum extent.

With a preventive maintenance strategy, maintenance activities would be triggered as soon as predefined threshold values of given resource properties are exceeded. Exchanging the coolant after a given number of operational hours would be an example for a preventive maintenance strategy. If required, the resource is locked for productive use until the maintenance job has been executed. In the case of a predictive maintenance strategy, resource parameters are monitored, correlated and evaluated against a set of rules. Maintenance tasks are triggered based on the evaluation results at the best-suited point in time before the resource breaks. The idea of this approach is to reduce the amount of waste that is potentially generated by implementing a purely periodic maintenance strategy, while securing a well-known level of availability for the set of resources. For the coolant example, this would mean changing the coolant only after required material properties have changed, which are continuously monitored. In the event of a resource breakdown, which causes an unscheduled downtime in contrast to the scheduled downtime triggered by preventive or predictive maintenance activities, a maintenance request needs to be generated based on the corresponding resource-state change. Additional data acquired from the resource can be linked to the maintenance request in order to speed up the error-detection-and-repair process.

Material Management

Material management involves all tasks related to material logistics in production. Special focus is put on the *work in progress* (WiP) management. WiP comprises material that is not residing in managed inventories, i.e. raw material, partially completed material and final products. Similar to resources, material has a set of properties that are monitored while it is transferred from the raw state towards the final product. The major properties of a material are its identifier, its location, its quality and its quantity. The material ID allows

the unique identification of an entity of material, based on a serial number, for example. Due to the amount of data that needs to be handled if single entities of material are individually tracked and due to the fact that many processes treat multiple entities of material at the same time, the concept of *lots (batches)* is frequently used to group materials for tracking. Multiple entities of material are grouped to a lot, which has an ID assigned. In addition, lots can have similar properties as single entities of material, such as quality, quantity and state. Managing lots is part of the material management domain, which includes the tasks to *create*, to *split*, to *merge* or to *terminate* them. *Create* supports the process of building lots from single entities. *Split* divides a given parent lot into multiple children. *Merge* combines multiple lots into a single lot. *Terminate* removes the lot from the system.

Maintaining the history of lots or single material entities is a major task within the material management domain, which is also referred to as *material tracking* or *WiP tracking*. These terms describe the process of documenting the complete history (*genealogy*) of lots or single entities of material within production. The history contains information such as links to raw material data, information on the equipment the material has been processed on, process data that has been collected while processing the material on the equipment, information on quality and quantity after each process step and material-related measurement and inspection data. These data are recorded with time stamps and thus lay the foundation for a comprehensive material-related audit trail, which is an important building block for implementing a traceability strategy.

Like the resource states, the material state, which is continuously updated while generating history information, is an important input parameter for the detailed scheduling functionality, as it contains relevant data from an operations perspective. Some examples for material state-related information that needs to be considered for operations are:

1. Material might be locked for further processing (on *hold*). The hold status is set if quality pro-

blems are detected that need further investigation, for example.

2. Time constraints caused by specific process properties might require the next process step to occur within a given time window or after a minimum waiting time. If such constraints are violated this might result in scrap.

Furthermore, information on available material quantities and material locations needs to be evaluated for planning and operations. However, material management does not only monitor material movements, it also triggers material movements by internal or external logistic systems.

Labor Management

The task of labour management is closely related to resource management. It takes the specific properties of ‘human resources’ into account and supports the task of allocating sufficient personnel with the right level of qualification on schedule for the production. Similar to the resource-management domain, the run-time functionality is based on a set of master data for single employees, groups of employees and the organizational structure. Typical attributes of a single employee are the personnel ID, name, qualification or certification, etc. Furthermore, the availability of personnel is maintained in the context of the deployment scheduling.

Based on the master data described above, personnel-related status information needs to be maintained. Time recording allows for gathering information on the actual availability of staff and the jobs or tasks executed within this timeframe. This information is required as a basis to implement complex work-schedule and wage models, including flexible working hours, piecework models, etc. Tracking the association of staff information with production jobs constitutes another building block for implementing traceability strategies, as it documents who did what and whether the person who performed a given job or task had the right level of qualification or not. Functionality supporting the resource deployment gives an overview on the available staff capacities, provides support to manage these

capacities and helps to assign jobs and tasks to personnel in an efficient and effective way.

Data Collection and Acquisition

The availability of data of sufficient quality with little delay from production is an important prerequisite for all of the MES tasks discussed earlier (and those to be described later). Data collection and acquisition realizes the connectivity to the manufacturing processes with a suitable maximum delay. Thereby, it lays the foundation for an up-to-date, correct and consistent process image of the situation in production within the MES. This image is used to *monitor and control* processes in production in real-time – as described in other MES tasks. The meaning of ‘suitable delay’ and ‘real-time’ depends on the actual monitoring and control problem to be solved. Usually, the minimum response time on the MES level is of the order of magnitude of a few seconds.

Generally, three approaches to data collection and acquisition can be distinguished: manual, semi-automated and automated data collection. In the case of manual data collection, an operator manually enters data records using some kind of input device. Manual data collection is frequently performed using electronic forms that the operator has to complete at a user terminal. Semi-automated data collection needs manual interaction by a user – however, part of the data is acquired automatically. Data collection using bar-code guns or RFID readers are examples of semi-automated applications. Automated data collection requires the implementation of suitable IT interfaces for data acquisition. The collection is either triggered by events that occur within the data source or by cyclically polling the data source. Sophisticated mechanisms have been designed to specify both the amount of data to be collected and the frequency, based on the current need. The concept of *data collection plans* (DCP) allows users to dynamically determine the data to be collected for a given process. The user specifies the collection plan by selecting process variables to be monitored from a set of available variables and the desired collection frequency. As soon as

the plan is activated on the corresponding resource, the selected data is available through the IT interface.

Whenever raw data is collected, it needs to be checked for plausibility and consistency before being further processed. These checks are required independently of the approach used for data collection. As correct and consistent data is an important prerequisite for successfully operating an MES, these checks are considered to be part of the data collection and acquisition task in order to prevent the further processing of incorrect data. After performing the plausibility and consistency checks, most of the data records collected have to be preprocessed and consolidated to simplify the downstream tasks. Converting dimensions or evaluating counters to physical values are two examples of consolidation and preprocessing steps.

Performance Analysis

Performance analysis targets the evaluation of the performance on the shop floor, both short term and long term. Thus, it provides support for establishing control loops to influence operations on the one hand and to optimize processes in the long run on the other. Data that have been collected by the MES are consolidated to suitable *key performance indicators* (KPIs) that lay the foundation for further analysis. These KPIs can be compared against organizational and technical targets: suitable corrective actions are derived from the results, if necessary. The following list provides a set of examples of key performance indicators that are used throughout many industries:

1. **Equipment utilization.** This is the fraction of time the equipment is performing its intended function during a specified time period [3]. Measurement of the remaining capacity of equipment or workplaces provides the ability to detect bottlenecks.
2. **Overall equipment efficiency (OEE).** This is the fraction of the total time that equipment is producing effective units at theoretically efficient rates [4]. This is used widely to measure process efficiency.

3. **Cycle time.** This is the analysis for all components of the cycle time for jobs, including non-productive time, and the sum of these components.

There are numerous ways to make use of performance analysis results and to trigger corresponding actions. In the simplest case the results are incorporated into management reports and lay the foundation for further decisions. This is especially true for the long-term case. For the short-term case the results of the performance analysis could automatically trigger actions within the system or could be fed into the dashboards of control centers or information systems on the shop floor to trigger immediate action by operational personnel.

Quality Management

The quality management task supports organizations in reaching the required level of product and process quality as far as the shop floor is concerned. It comprises the aspects of *quality planning*, *management of test equipment* and *quality inspection*. Quality planning requires a variety of input data from previous process stages in the product lifecycle on the one hand and overall quality targets on the other that define the requirements for quality inspection. Test plans need to be transformed into suitable system configurations to ensure that routes and data-collection plans are appropriately set up and that the data acquired from the shop floor are evaluated as needed. The *sampling* functionality is responsible for selecting lots or single products for quality inspection based on *sampling plans* that need to be configured according to the test plan. A simple sampling plan could define every 50th lot to be inspected, for example. *Dynamic sampling* is an extension that allows for dynamic adjustments of sampling plans at run-time. The sampling rate could be automatically increased, if issues are detected in production that might affect quality, for example. Quality assurance processes and measures need to be modeled within the MES system in order to enforce and to document their execution. Access-control based on the current

certification level of operators, the ability to issue directives to operators that need to be confirmed after reading, and quality gates are examples of measures to be supported by the MES environment. Managing test equipment is closely related to resource management. However, some specific characteristics of test equipment have to be taken into consideration. Especially, the support for calibration traceability needs to be taken into account.

Another aspect of the quality-management task is related to documentation, reporting and control. Depending on the quality-management system, corresponding documentation has to be generated which confirms that the defined quality-assurance measures have been properly executed. The quality information collected lays the foundation for reporting the level of quality reached and thus allows for implementing counter-measures early, if issues are detected. Sample data collected can be evaluated using the methodology of *statistical process control* (SPC). SPC provides the means to monitor processes and thus to detect possible quality issues and to correct them in the early stages of the overall production process for a product. The methodology of *fault detection and classification* (FDC) is used to analyze quality-related data, to detect and recognize possible issues and to derive suitable actions from these issues. Example actions that could be triggered automatically are:

1. Put lots on hold;
2. Stop process equipment.

Information Management

Information management is a cross-sectional task that is built on top of the tasks that have been described earlier. It makes use of data and context information available in the system, provides suitable views of the data – both for users as well as for other MES tasks – and complements this information by suitable reports and evaluation results. Furthermore, the task of information management has an active component – it responds to events reported from production in real-time. Both aspects lay the foundation for establishing

complex control loops for production that take a variety of parameters into account.

Suitable views providing information in the appropriate context are not only relevant for management reporting, production management and control or quality assurance, they also provide the tools required to implement *paperless* production concepts or at least strategies that require a minimum amount of paper in production. Replacing paper-based *lot travelers* by electronic lot travelers is one element of paperless strategies. A lot traveler contains basic properties of the lot, such as: its identifier and priority information; information on the route to be used, i.e. the process steps to be performed; and additional information to be considered by the operator. Furthermore, it is often used to collect feedback from production, such as the signatures of operators confirming that certain instructions have been executed, quality inspection results, process data, etc. An electronic lot traveler provides users with the type of information required in a given context using IT systems. In this case, 'context' could mean a given job at a given equipment instance. Other views could provide operators with specific information on quality trends achieved at a particular work station which would help to achieve a constant level of quality. The capability to access relevant documents in a given context, such as drawings, manuals and work instructions, helps operators to work efficiently and effectively.

The ability to design, execute and monitor workflows for the shop-floor environment that allow the guidance of operational sequences on the shop floor is a major task to be supported by the MES. These workflows describe sequences of actions, roles and responsibilities and drive all operational sequences in a defined way. Implementing this task might require the MES to support additional classes of master data, if this data cannot be supplied by other tasks or external systems. *Exception management* is an additional sub-task of information management. It targets the automatic resolution of exceptions that occur in production, if possible, or at least the support of users for resolving exceptions. Semi-automated

exception resolution would provide responsible users with information on possible corrective actions and generate exception notifications for these users by e-mail or short-message service, for example. More sophisticated approaches to influence production based on collected information are covered by the methodologies of *advanced process control* (APC). This term covers a variety of process-control methods and tools, such as SPC and FDC as described above, *run to run* (R2R) control and others.

MES IMPLEMENTATION AND INTEGRATION INTO THE PRODUCTION IT

There exists a variety of approaches to implement MES solutions supporting the tasks described above. In most cases these tasks will not be supported by a single system, but rather by a collection of cooperating systems. Furthermore, the set of implemented tasks heavily depends on the requirements of the industry or group of industries that a given solution targets and – most importantly – the specific requirements of the organization to be supported. The same holds true for the complexity of the IT landscape and the enterprise architecture of the production IT environment. Figure 24-5 shows a simplified example of a production IT environment that contains some typical concepts used. It is based upon the hierarchical structure shown in Fig. 24-4.

1. The bottom-most layer is the equipment layer. Equipment provides one or multiple manufacturing-process capabilities that are monitored and controlled by internal process-control systems, such as *programmable logic controllers* (PLC), *computer numeric controllers* (CNC), *embedded PCs* or *industry PCs* (IPC). Typically, these control systems are connected to *sensors* and *actuators* using standardized *field bus* systems, such as PROFIBUS and CANOpen. Depending on the complexity of the equipment, it might again use a hierarchical IT infrastructure internally. Examples of complex equipment would be cluster equipment,

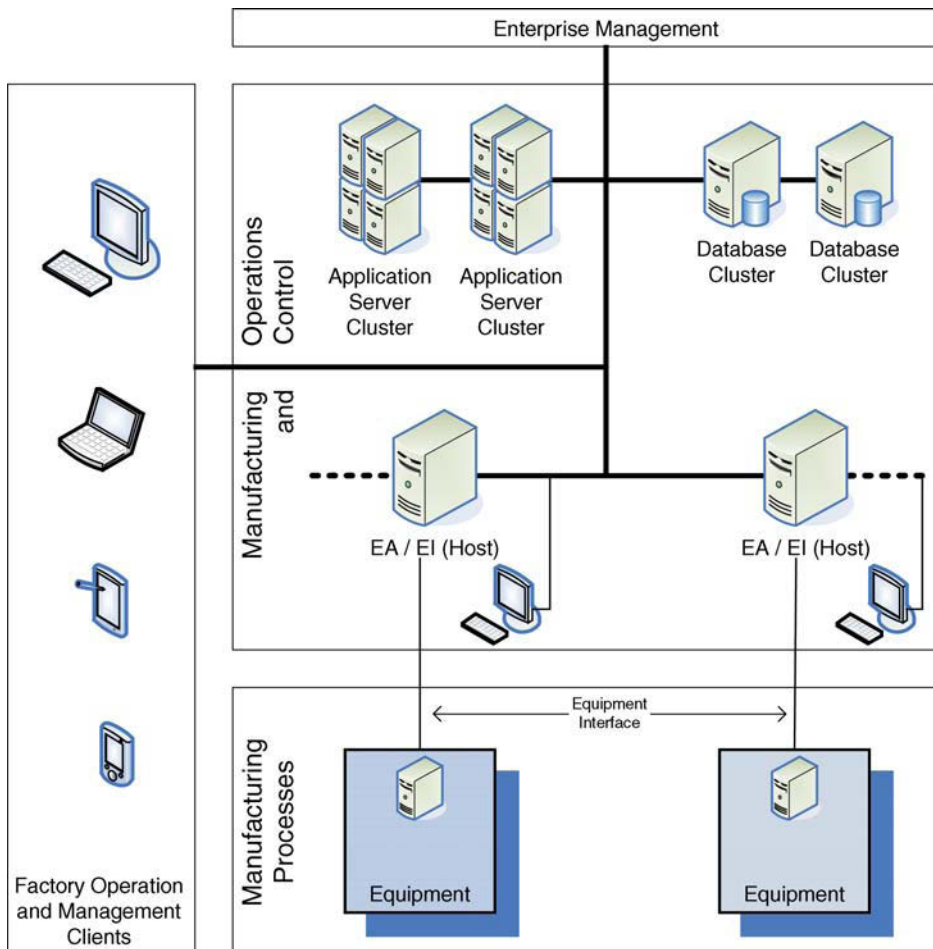


FIGURE 24-5 IT Infrastructure (example).

automated lines or transport systems. Equipment is able to autonomously control at least their basic process capabilities using these internal control systems. IT interfaces (in Fig. 24-5 marked as ‘Equipment Interface’) expose selected properties of the internal control system of the equipment to the outside world. In the simplest cases the interfaces provides access to data available within the internal control system, such as process variables that contain sensor results. Furthermore, such interfaces can provide notification of events or alarms that occur within the equipment, configurable data collection based on collection plans, remote control and other capabilities.

Sufficient equipment interface capabilities are an important prerequisite for supporting the tasks described above on the MES layer. For this reason, they provide a broad field for standardization, which will be described in more detail in the following section.

2. The *equipment automation (EA)/equipment integration (EI)* layer connects equipment to IT systems on higher layers by using the equipment interfaces discussed earlier. The main goal of the equipment integration is to provide a common view of all types of production equipment to be monitored and controlled within the factory and to connect equipment to the factory communication system (usually

Ethernet based). Thus, it implements part of the resource management tasks. At the same time, several of the data-collection and acquisition-related tasks described earlier are implemented on the EI layer, such as unit conversion and data verification. Equipment automation refers to the implementation of equipment (type)-specific operational scenarios, i.e. it provides the IT support required to execute process steps of equipment in a defined way at a given instance. These scenarios comprise equipment-related material logistics, material verification, set-up instructions, remote-control commands and data collection, for example. User-interface clients are attached to single items of equipment or to groups of equipment, if operational scenarios require user interaction or supervision. These user-interface clients support the information-management tasks in the context of a given item of equipment or equipment group. In many installations, the EA/EI components and the user clients are either deployed on dedicated PCs or IPCs for single items of equipment or equipment groups or deployed on larger server systems within the factory's computational center.

3. The majority of tasks described above are implemented on top of the EA/EI layer. Older implementations of MES solutions followed a rather database-centered approach and were usually based on mainframe technologies. This turned out to be a limitation during recent years, especially in terms of agility. One of the non-functional requirements to be taken into account for implementing MES solutions is the ability to change, i.e. to support new requirements. Reasons for change and new requirements are the introduction of new technologies, new equipment, new products and process improvements, for example. Furthermore, there is a need for horizontal integration within the manufacturing and control level. Due to the variety of tasks to be supported, there is usually the need to integrate multiple applications – in many cases even from different suppliers – in order to realize the required level of IT support for

production. However, all applications require a correct and consistent view of the current situation in production. Both issues were not sufficiently supported by the old mainframe solutions. Fortunately, current state-of-the-art architectures promise to do better. To use the paradigms of a *service oriented architecture* (SOA) looks particularly promising: the MES tasks described above are implemented by a collection of independent *services*. Each service covers a well-defined functional scope (such as recipe management) and exposes its capabilities through public-service interfaces. In order to implement a given business process in production, a corresponding set of services needs to be *orchestrated*, i.e. to be combined, in the right way. This approach does not only improve agility, as services can be rewired or complemented by additional services to support changing requirements, it also greatly simplifies both horizontal as well as vertical integration within the production IT landscape.

PRODUCTION IT STANDARDIZATION

As shown in the preceding sections, establishing a pervasive shop-floor IT environment requires a variety of software systems to cooperate – starting from the enterprise layer down to the equipment layer. For each type of software system, there exists a variety of products and suppliers in the market. Therefore, accepted and implemented industry standards turn out to be an important enabler for realizing production IT environments. Among others, standards are created to serve the following goals:

1. They provide common definitions of important terms and concepts and thus facilitate a common understanding, which is especially important for the specification phase of MES solutions.
2. They define system classes and their scope and thus create transparency regarding the capabilities of a given system class.

3. They provide unified interface definitions and enable or simplify the task of integrating different systems, even if they are provided by different suppliers.

Standardization activities are performed throughout all layers of the shop-floor IT – usually based on specific needs. There exists a variety of organizations that provide platforms for standardization that have to be considered in the shop-floor IT environment – some of them targeting on specific industries (e.g. Semiconductor Equipment and Materials International – SEMI [5]), some of them approaching cross-industry topics (e.g. Manufacturing Enterprise Solutions Association – MESA international [6]), others focusing on specific technologies (e.g. Internet Society – ISOC [7]). The following sections give a rough overview of selected organizations and standard collections in the shop-floor IT area – both on the factory-automation layer and on the equipment-automation layer.

General Production IT Standards

Several organizations have made a number of attempts over the last few years to create extensive standard frameworks or reference models describing approaches to realize a pervasive production IT landscape that integrates well with the overall IT landscape within the enterprise and thus supports the goal of process optimization described at the beginning of this chapter. One approach that shaped the discussion for several years, especially in the early 1990s, was the ‘Reference Model for Computer Integrated Manufacturing (CIM)’ [8]. This describes a hierarchical IT architecture that is built up from six levels based on the scheduling and control hierarchy and has been designed as a guideline for establishing a vertically integrated production-IT landscape. Although the concept has not yet been implemented to its full extent, it served as a basis for many successors. In 1997 MESA [6] presented a definition for MES, which is still considered to be valid, and its potential scope by describing a set of 11 functional groups. The scope of a concrete MES solution was defined to be a subset of the potential scope based on the

user’s priorities and requirements. A few years later, in 2000, ISA-95 Part I was published. This is based on the concepts of CIM (especially the scheduling and control hierarchy) and focuses on the specification of interface between business systems and manufacturing operations and control systems. Furthermore, ISA-95 integrates the functional groups defined by MESA to describe the functionalities of the manufacturing operations and control, i.e. the MES, level. ISA-95 Part II [9] and Part III [10] followed later and complement Part I with the detailed specification of the data model on the one hand and the activity model and dataflow specification for the manufacturing operations and control level on the other. VDI 5600 [2] is currently the latest standard in this series. It comes from a task-oriented view of the MES that rather reflects the user’s perspective than the system perspective and updates and extends the MESA MES model.

Equipment Interface Standards

An important prerequisite for implementing several requirements described in the preceding sections is the ability to communicate with process equipment in order both to remotely control the equipment and to acquire a variety of data from the equipment, such as operational data, machine data and process data. As a factory usually houses equipment from a variety of suppliers, the effort to connect them to the production IT environment of a given factory is comparably high, as a specific connector has to be implemented for each equipment type. This is where the idea of the definition of a standard IT interface for equipment, as shown in Fig. 24-5, comes into play.

One of the standard frameworks that is frequently used to integrate equipment with higher levels of the production IT landscape is the OPC [11] framework. However, an industry-specific framework from the semiconductor industry has been selected for further discussion, as it provides a more comprehensive approach, which can serve as a generic example. Figure 24-6 (based on [12]) gives a compressed overview of the standards framework that is widely used in the

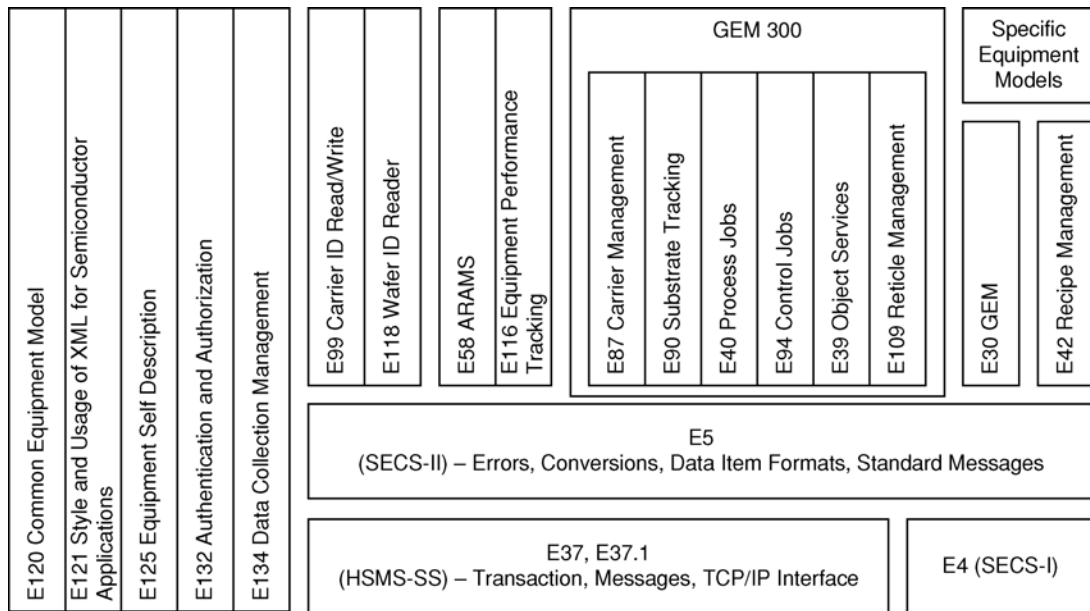


FIGURE 24-6 Equipment interface standard framework – as defined by SEMI

semiconductor industry. The communication protocol defined by E5 lays the foundation of the standard framework. Today, it is usually bound to a TCP/IP-based message transport layer according to E37 (HSMS-SS), which enables communication with equipment using a unified message format. While this protocol basically allows for the communication of a host system with an equipment instance, it leaves the supplier with a high degree of freedom regarding the actual implementation of the interface. For this reason, the effort for integrating equipment into the shop-floor IT still turned out to be rather high. Furthermore, different interface implementations provided largely varying capabilities that needed to be taken into account. To overcome these limitations, additional standards have been added on top of E5. The ‘Generic Model for Communications and Control of Manufacturing Equipment’ (GEM) defines the semantics of the interface, i.e. the behavior of the equipment from the IT interface perspective. This step led to a significant reduction of the effort required for the integration of equipment and allowed for the introduction of standard compliance tests. E30 is complemented by a standard for *recipe* management and stan-

dards for specific equipment models. While E30 contains specifications that have to be considered for all types of semiconductor equipment, specific equipment models comprise equipment characteristics and behavior definitions that have to be implemented in addition to GEM for specific equipment types only, for example transport systems: these take the specific needs based on the equipment type into account.

The standard framework is completed by the family of GEM300 and a couple of auxiliary standards. As the transition from 200 mm to 300 mm wafer processing was accompanied by the demand for a higher level of automation, the requirements for additional automation capabilities on top of E5 arose and led to the definition of these standards, such as the capabilities to manage carriers or to track substrates. Additionally, there was an increasing need to acquire data from process equipment. The family of Equipment Data Acquisition (EDA) standards has been created to meet these requirements. The EDA stack is implemented in parallel with the GEM/SECS interface, is limited to data acquisition and allows an arbitrary number of clients to acquire data from equipment based on web technologies.

CONCLUSIONS

Today, it is virtually unthinkable to operate state-of-the-art manufacturing facilities without a variety of IT systems supporting production. Several classes of IT systems can be found over the different layers of these facilities – from enterprise resource planning systems as an example on the enterprise management layer down to programmable logic controller-based applications on the manufacturing processes layer. The term MES usually refers to a collection of integrated software applications that is located between those two layers – on the manufacturing operations and control layer. On the one hand the MES ensures the right level of information transfer between upper and lower layers and thereby supports the integration of processes on the shop floor into the overall business process framework. On the other hand the MES provides a rich set of functionalities to optimize operations on the shop floor in different dimensions, such as product quality, resource utilization and the adherence to delivery dates. A variety of standards have been created in different industries to enable and simplify the set-up of the MES environment. Looking at the potential provided by an MES, the relevance of this topic in the area of micro-manufacturing will continue to grow in the future.

REFERENCES

- [1] Enterprise-control system integration, Part I: Models and terminology. ANSI/ISA-S95.00.01-2000. Instrument Society of America, Research Triangle Park, NC, USA (2000).
- [2] Manufacturing execution systems – production management systems. VDI 5600 Blatt 12006-08. Verein Deutscher Ingenieure. Published by: Beuth Verlag GmbH, 10772 Berlin, Germany (2006).
- [3] Specification for definition and measurement of equipment reliability, availability and maintainability (RAM). SEMI E10. Semiconductor Equipment and Materials International, 3081 Zanker Road, San Jose, CA, USA (2004).
- [4] Specification for definition and measurement of equipment productivity. SEMI E79. Semiconductor Equipment and Materials International, 3081 Zanker Road, San Jose, CA, USA (2006).
- [5] Semiconductor Equipment and Materials International – SEMI [Last access: 30.10.2007]; <http://www.semi.org>.
- [6] Manufacturing Enterprise Solutions Association – MESA International [Last access: 30.10.2007]; <http://www.mesa.org>.
- [7] Internet Society – ISOC [Last access: 30.10.2007]; <http://www.isoc.org/>.
- [8] Williams, T. J., (ed.), A reference model for computer integrated manufacturing (CIM), a description from the viewpoint of industrial automation, Instrument Society of America, Research Triangle Park, NC, USA (1989).
- [9] Anonymous, Enterprise-control system integration, Part II: Object model attributes. ANSI/ISA-S95.00.02-2001. Instrument Society of America, Research Triangle Park, NC, USA (2001).
- [10] Anonymous, Enterprise-control system integration, Part III: Activity models of manufacturing operations management. ANSI/ISA-S95.00.03-2005. Instrument Society of America, Research Triangle Park, NC, USA (2005).
- [11] The OPC Foundation [Last access: 30.10.2007]; <http://www.opcfoundation.org/>.
- [12] M. Meier, P. Dreiss and J. Seidelmann, Potentials and limitations of standardization of shop floor IT based on examples from semiconductor industry, PPS Management 12 (2007) 4, Gito Verlag mbH, Klixstr. 1 A, 13403 Berlin, Germany (2007).

Sustainability of Micro-Manufacturing Technologies

Arnaud De Grave, Stig Irving Olsen, Hans Nørgaard Hansen and Mogens Arentoft

INTRODUCTION

The common view in the field of the environmental impact of micro-products is that small-size products involve the use of less material, require less production energy and produce less waste material, and hence are more environmentally friendly. This view is not fully valid and there are many benefits in applying tools for sustainability in micro-product development.

When looking at any technology, at least three different levels are of interest to consider in the complete product development scheme:

1. **The final product** is defined as the product that is closest to the requirements of the end-user. It is fairly easy to define it in the case of, e.g., hearing-aid equipment, but less evident in the case of an MEMS RF switch used in a mobile phone antenna. The size of the production chain of such a product can involve many sub-contractors and in terms of environmental aspects all the steps have to be taken into account.
2. Some parts are not included in the final product, e.g. the waste from manufacturing. These parts are called ‘**intermediate parts**’. Examples of such parts can be the excess material from an injection molding runner system for feeding of the molds, parts especially designed for ease of handling and assembly, or even the sections of a silicon wafer that are ground before packaging, this excess thickness being

required for mechanical stability during production.

3. **The production system** is mainly considered as the manufacturing process chain, but the system also includes the necessary material production chain and the recycling and disposal chain.

This categorization is especially pertinent in the case of micro-products, where the intermediate parts can represent up to 98% of the product component, as, for example, is the case of micro-injection-molded components.

In the following, first the technical aspect of environmental assessment over the lifecycle is described, then the aspect of how to use the knowledge so obtained in product development is presented.

LIFECYCLE ASSESSMENT

Theory

Lifecycle assessment (LCA) is a valuable tool for the environmental assessment of products. The principles of LCA form the backbone of DFE, EcoDesign, etc., in product development [1]. LCA has been developed to analyze and assess the environmental impact attributable to a product through the whole lifecycle of that product, i.e. the extraction of resources, conversion into materials, production, use and disposal, as well

as transport and infrastructure. LCA therefore covers not only the production, but also all supportive functions during the life of the product. The inclusion of the supportive functions demanded by a product in the assessment extends to include all types of impact that a company (or a product) is responsible for – not only within the manufacturing chain, but also in all stages in the life of the product. In a quest for sustainability these are important aspects to include in product development, since this is the stage at which decisions can be taken concerning the environmental impact of the product.

The importance of LCA as a tool to assess the environmental sustainability of products and manufacturing is increasing in the European Union. Examples are the use of LCA in the EcoDesign of Energy using Products Directive (2005/32/EC) and the requirements for LCAs in some of the recently published calls for the European Seventh Framework program for research and technological development.

LCAs involve the following steps:

1. Choice of product and identification of service (the functional unit);
2. Establishing boundaries for the system;
3. Collection of data;
4. Environmental assessment;
5. Interpretation.

The initial step in all LCAs is to define the goal and scope of the study [2] – what is the aim

of the study? What is the object of investigation, the so-called functional unit? What are the system boundaries for the investigated system, e.g. should the production of the manufacturing equipment be included? The chain of processes in the system will be defined thus, also identifying the processes for which data need to be collected. LCA is made in an iterative way, initially starting with the most easily available data and making a screening analysis with focus on the materials, energy and chemicals used. The next steps imply the use of more detailed data on the inputs and outputs for each process. Figure 25-1 provides a schematic overview of the lifecycle of a product and the data needed for carrying out the analysis.

One important issue is the type of data needed to be gathered in order to have a pertinent way of evaluating the process chain. This data falls mainly into two categories: process data and material-use data. Many problems arise from the difficulty of gathering the necessary data.

Process Data. The easiest parameter to collect is the energy – electrical or thermal – consumed in the production of a specified amount of product, usually 1 kg of product or, e.g., 1000 pieces. This may be measured directly at the manufacturing equipment or averaged from the energy consumption at the facility. It is important to know the type of energy and whether, e.g., it is produced

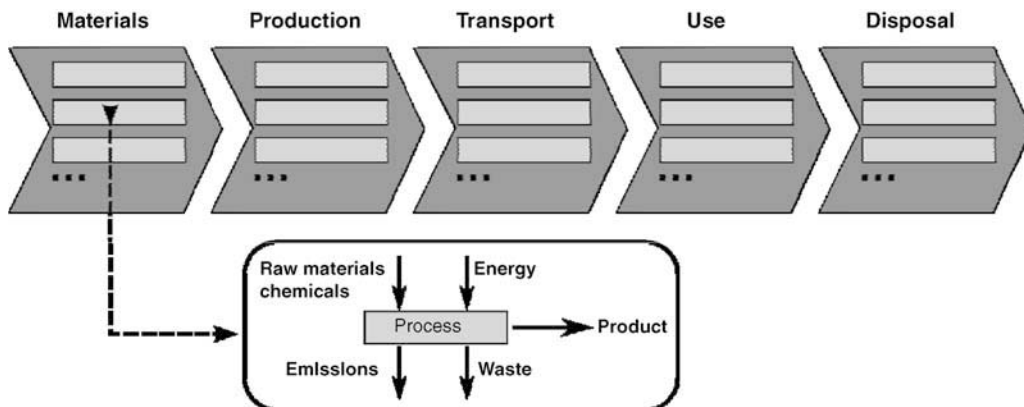


FIGURE 25-1 An LCA flow.

internally as waste energy from other processes. Energy is consumed both in the manufacturing process as well as during handling and assembly.

Outputs (emissions, waste and products) from the processes should be inventoried. Of course the product is an important output serving as a reference for all other data, but also all types of waste (solid, liquid or gaseous) from the processes should be measured. This is, e.g. waste material (the difference between what is in the product and what is consumed as raw material). There will probably also be some emissions from the process, e.g. welding fumes. In the initial steps of the LCA, data of the latter type may be hard to acquire. If more than one product is produced by the same process this is important also, since the environmental impact from the process should be allocated between the products.

Material-use Data. Data on the use of materials is important, not only because of the environmental impact associated with the extraction of materials, but also to keep track of the losses during manufacturing processes.

The total amount of raw materials consumed in the process should be registered (i.e. what goes in through the factory gate), and including also the amount of internal recycling. The type and quality of raw material is important, since different materials cause different impacts during extraction and differ significantly in scarcity. Chemicals (for etching, cleaning, metal working fluids, etc.) should be registered both in terms of the consumption as well as the losses as emissions or waste. Chemicals may cause toxic impact on humans and the environment.

In the lifecycle impact assessment the inventory is translated into environmental impact such as climate change, acidification and toxicity. The environmental impact of different options, e.g. choice of materials, disassembly options, etc. can be compared or environmental-improvement options can be identified, or it can be identified whether a choice to reduce environmental impact in one part of the lifecycle creates a greater environmental impact in other parts of the lifecycle, see also Fig. 25-1. A more

detailed explanation of LCA methodologies can be found in [1].

A range of software tools is available for making the more detailed LCAs, e.g. GaBi, SimaPro, LCAiT, TEAM, etc. Demo versions are often available on the internet.

Application of LCA in Micro-manufacturing

Micro-components are often assumed to be more environmentally friendly than their macro-counterparts, although this may be challenged, and in some cases even contradicted, as proposed in [3,4] (Fig. 25-2).

In micro-manufacturing, LCA has been used predominantly in the MEMS sector. The rapid development of technologies and limited availability of data in the MEMS industry make complete LCAs difficult to produce and they are quite quickly outdated. One example is the manufacture of a PC, for which the energy requirement in the late 1980s was approximately 2150 kWh, whereas in the late 1990s efficiency was improved and only 535 kWh were necessary [5]: the use of old data could result in erroneous results. Looking at the overall environmental impact, this four-fold increase in efficiency has been overcompensated for by an increase in the number of computers sold, from approximately 21 million to more than 150 million [5]. The latter provides an example of a rebound effect, showing that economic and social aspects may have a huge implication for the overall environmental impact.

A major trend is that shrinking product dimensions increase the requirements of the production environment to prevent pollution of the product. This involves energy-intensive heating, and ventilation and air-conditioning systems. A clean room of class 10,000, for example, requires approximately 2280 kWh/m² per year, whereas a class 100 requires 8440 kWh/m² per year. The same increase in requirements is relevant for supply materials such as chemicals and gases. The demand for greater purity levels implies more technical effort for chemical purification, e.g. additional energy consumption and

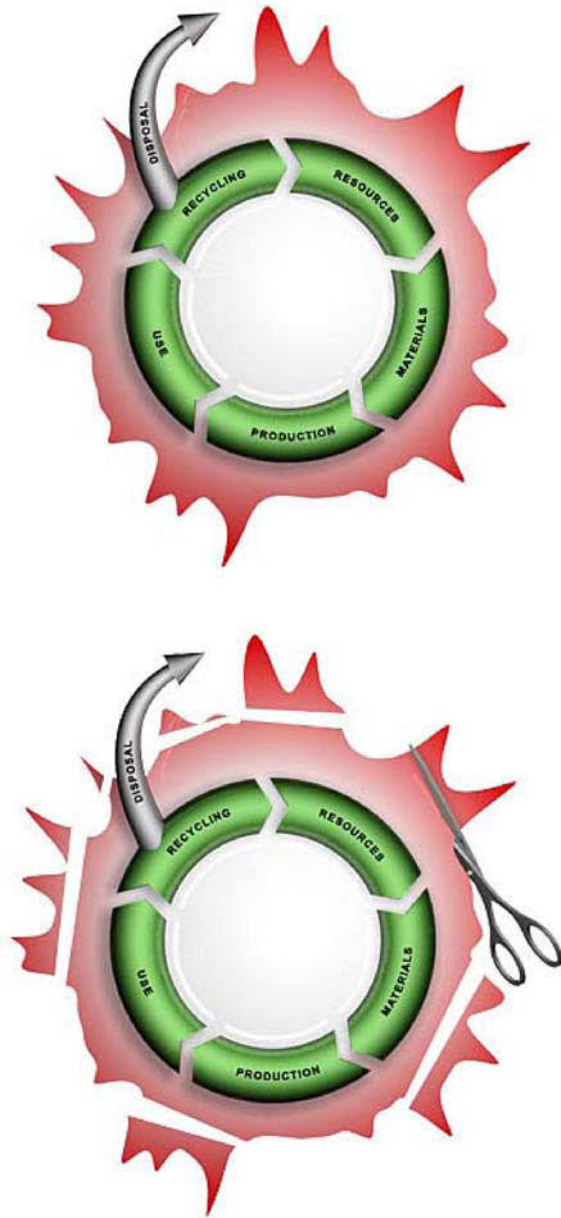


FIGURE 25-2 Illustrating that LCA identifies environmental hot-spots in the lifecycle and how this information can be used in, e.g., DFE to make environmental improvements. The scissors show where the reduction in impact is greater, therefore where effort should be targeted [1].

possibly more waste. Most purification technologies are highly energy intensive, e.g. all of the distillation processes, which are used often in wet chemical purification, account in total for

about 7% of the energy consumption of the chemical industry of the USA [6]. Chemicals used in large volumes in the semiconductors industry are hydrofluoric acid (HF), hydrogen peroxide (H_2O_2) and ammonium hydroxide (NH_4OH). These materials are used in final cleaning processes and require XLSI grades (0.1 ppb). Sulfuric acid is also used in large amounts, but it is a less critical chemical and mainly requires an SLSI level purity [6]. LCA studies of electronics show that by far the greatest energy consumption and waste are generated in the production of the smallest components (microchips and integrated circuits) [7].

Micro-manufacturing of other types of products also puts higher requirements onto the quality and purity of the materials. Exploitation and loss of scarce resources is a concern, since the consideration of economics is a primary obstacle in the use of precious or rare materials in everyday products. When products become smaller and the components that include the rare materials reach the micro- or nano-scale, economy is not the most urgent issue, since it will not significantly affect the price of the product. Therefore, developers will be more prone to use materials that have the exact properties that they are searching for. While an increased usage of such materials may be foreseen due to the expected widespread use of micro- and nano-technological products, the recycling will be more difficult. An issue apart from the loss of resources is that the extraction of the rarest materials uses more energy and generates more waste than are associated with more abundant materials. Table 25-1 illustrates the energy intensity of a range of materials, i.e. how much energy has been used for the production of 1 kg.

ECODESIGN/DFENVIRONMENT

Framework (from Reuse to Recycle)

First of all, it has to be stated that EcoDesign and Design For Environment (DFE) are synonymous.

These frameworks take into account recycling, remanufacturing, reuse and lifecycle assessment

TABLE 25-1 Energy Intensity of the Selected Materials (modified from [7])

Material	Energy Intensity of Materials (MJ/kg)
Glass	15
Lead	54
Ferrite	59
Steel	59
Plastics	84
Copper	94
Epoxy resin	140
Aluminum	214
Tin	230
Nickel	340
Silver	1570
Gold	84,000

(LCA) during the design phases of the product, as shown in Fig. 25-2. It is widely acknowledged that the more is known about a product the less it can be changed. This classical remark is also valid in the case of DFE and has been pointed out in [8].

One of the key ideas in sustainability and Eco-Design is to reduce the use of materials. This can be done through process optimization, reuse of the product or part of it, or when this is not possible, through considering the recycling of material. Reused parts can be in the same field (broken parts being replaced by remanufactured parts, upgrade of systems. . .) or in some other unrelated fields (a common example is the protection of boats in docks of harbors by the use of old car/truck tires). DFE can be seen as a cradle to favor the use of many DfX components such as Design for Recycling (DFR), Design for Remanufacture (DFRm), Design for Assembly and for De-assembly (DFA and DFD), Design for Manufacturing (DFM) and the combination DFMA. Figure 25-3 shows the framework of DFE.

DFE also involves other objectives. For example, the manufacturing chain should aim at causing the least possible environmental impact, an

issue which is more specifically addressed by the concept of Environment Benign Manufacturing (EBM) [9] and LCA of manufacturing processes. From [10], DFE relies on eight axioms:

1. Manufacture without producing hazardous waste;
2. Use clean technologies (not in the ‘clean room’ meaning, but by taking care of minimizing the impact in terms of pollution, etc. and also using clean energy, such as windmill power, whenever possible);
3. Reduce product chemical emissions;
4. Reduce product energy consumption;
5. Use non-hazardous recyclable materials;
6. Use recyclable material and reuse components;
7. Design for ease of disassembly;
8. Product reuse or recycle at end of life.

Although originating from DFE of electronic devices, it is quite clear that these axioms are of a level of abstraction sufficiently high so as not to be technology dependent and are well adaptable to micro-scale mechanically based technologies. They can be applied in the case of such micro-systems as MEMS, and manufactured using VLSI technologies. MEMS are just a portion of the diversity of micro-products: they attract a lot of media attention and are often seen as examples. In this case, assembly and disassembly are related to packaging and are dealing with the issue of recycling chips. MEMS can also be applied in any kind of non-silicon product development and have to be seen as guidelines and checklists.

Many tools within the DFE family have been developed through the years, from either academia or industry. A thorough overview of them is given in [1]. Standardization work has resulted in some EcoDesign guidelines, as in [11]. These tools

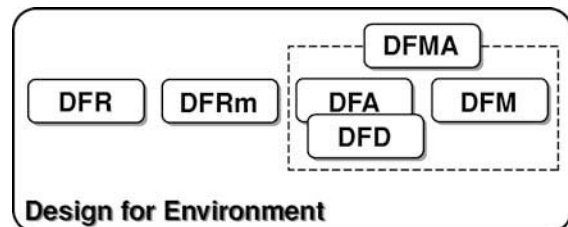


FIGURE 25-3 The Design for Environment (DFE) framework.

are sometimes generic, and sometimes created by one industry specifically for its needs and range of products. They are not specific to particular technologies, although the electronic and mechanical industries have been known for developing different set of tools. In the case of micro-products, often lying at the crossing between the miniaturization of mechanical manufacturing and the non-standardized use of micro-electronic manufacturing processes, tools coming from both fields can be used, albeit not optimally.

The new ISO TR 14062 tries to integrate environmental aspects into the complete scheme of product design and development. Even if it does not specifically target micro-technologies, its management perspective brings valuable knowledge to improve product design. [12] presents some examples of cases to demonstrate what is possible and provides details of some tools.

How to Apply to Micro-manufacturing Technologies

To be capable of targeting the specifics of micro-products, several issues have to be overcome. One of the difficulties of micro-products development is a lack of knowledge, on manufacturing processes, solution principles and development methods. This lack of knowledge applies to an even greater extent in the field of reliability and end-of-life behavior. There are no known databases for LCA in micro-technologies and therefore it is very difficult to secure all the necessary information to be able to take reliable design decisions concerning the environment.

Most DFE components make a tremendous use of handling and assembly. Unfortunately, handling and assembly is a large issue that still, to a high extent, remains to be solved at the micro-scale, as seen in earlier parts of the present chapter and as reported in [13], for example. The maturity of the knowledge in the field of handling and assembly for micro-components is still far from being suitable for industrial applications. In the case of an MEMS device, the concept of disassembly does not really apply. Indeed, these devices are often monolithic or embedded, thus making it

difficult to separate the parts and materials. Moreover, the trend in micro-technologies is greatly oriented towards the integration of functions and components. For instance, in two-component injection molding, there is a strong bond between the two polymers, or between the metal insert and the polymer. Indeed, it is the goal of such a technology to create such a strong bond, hence going against DFD principles.

Remanufacturing poses even more problems than reassembly, due to the relative repositioning accuracy and the skimming/trimming inherent in the process. The amount of material may even not be sufficient to allow a remanufacturing operation.

Micro-components and DF Intermediate Parts

On the one hand it is perhaps impossible to apply remanufacturing concepts to micro-components, but on the other these concepts can possibly be applied to the intermediate parts.

For a typical micro-injection-molded part, the runner system and other wasted parts can amount to 95 to 98% of the total mass, due to the minimum volume of a shot possible on available hardware that was not specifically made for micro-injection molding. Such parts can be seen in Fig. 25-4. The effects of recycling of polymer, both with and without fiber reinforcement, have been studied in [14]. Even if the mechanical characteristics of a part decrease with the number of injection cycles, it is possible to design a piece with a mechanical limit that allows a number of recycling cycles. Stress/strain curves in relation to the number of successive injections or recycled polymer are available in the literature.

After a certain amount of injections, it is shown that there is a loss in mechanical properties (mainly due to fiber degradation), but these characteristics may still be in the range of use for some other design. Moreover, by starting with mechanical properties greater than necessary it is possible to stay within expected limits after a number of injections. Of course, a careful choice of material is needed in order not to select a very

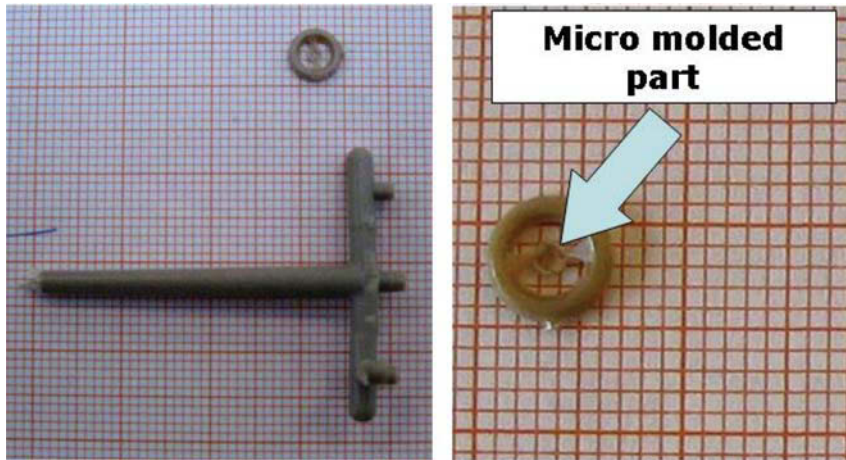


FIGURE 25-4 Relative size of micro-injection-molding components.

unenvironmentally friendly material, hence losing on the one hand what is won on the other.

A DFE way of solving this problem could be the use of carbon nano-tube reinforced polymers. Indeed, nano-tube polymer composites not only behave differently in use, but also in manufacturing processing [15]. Of course, such composites will also require LCA and health-hazard studies. The recycling of carbon nano-tubes is usually targeted at recycling them without alteration or cost-related issues. Environmentally-benign ways of recycling polymer-based composites with nano-tubes are investigated in [16,17]

Micro-factories

Likewise, it may be assumed that environmental impact can be reduced by reducing the size of the factory. However, few studies have as yet been established to assess the actual environmental impact of micro-factories and thus sustain this assumption. Presupposing that the aim is to develop environmentally-sustainable manufacturing methods, the need to examine the environmental aspects of micro-factories is therefore evident, as is the application of LCA as a tool.

The concept of the micro-factory is to create small-sized production centers for small-sized products in a 'diverse-types-and-small-quantity production'. It is based on the idea that the manufacturing and manipulation processes are

often much bulkier than the parts that they produce and this is even more true for micro-components. The manufacturing of micro-components is very demanding. Indeed, it often requires a special working environment not only for the handling and assembly of the parts, but also for their production. The maintenance of this working environment (white- or clean-rooms with controlled atmosphere and pressure for instance) is very expensive, both in economic terms and in respect of environmental impact.

One of the benefits of the micro-factory approach is, of course, that the footprint is smaller, hence inducing a lower cost in land occupation and, more importantly, atmosphere control, if need be. It is also assumed that there is a substantially lesser use of energy.

The example of the DTU (Technical University of Denmark) micro-factory [18] can be used. This system is targeting at hearing-aid and medical devices needing micro-components both in polymer and in metal. The manufacturing processes chain can be seen in Fig. 25-5. It includes: micro-injection molding, metal micro-forming, die making, handling operations, and assembly operations.

Unfortunately, there are often some difficulties in data gathering, some of which to a certain degree can be overcome by collecting data continuously: using power meters, registering the use of chemicals and raw materials, and

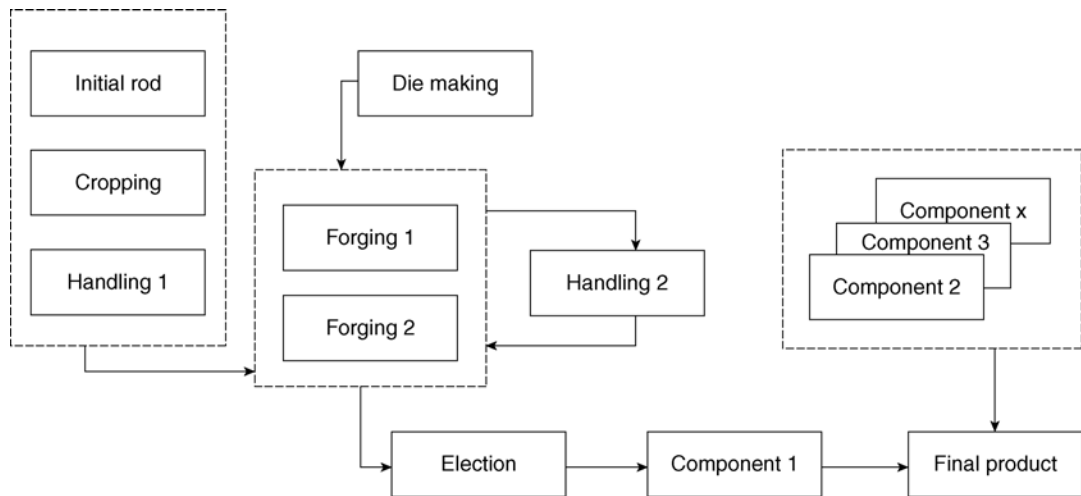


FIGURE 25-5 The DTU micro-factory process chain.

registering the output of useful product and waste. To perform a complete LCA would require not only energy data but also data for raw materials, and the end-of-life has to be estimated. One issue that needs to be better investigated is scenarios of product end-of-life and waste management, especially since disassembly and recycling may be troublesome.

Another example can be seen in [19] where a Japanese micro-factory targeting miniature ball-bearings is described. The small factory includes: milling and turning, sheet metal micro-forming, handling and assembly. It is stated that each of the processes of the chain is achievable, but acknowledged bottlenecks are precision in fixturing and time consumption during handling and assembly, which are done manually. The portable version of the micro-factory weighs 34 kg and fits into a 625 mm × 490 mm × 380 mm box. It requires a 100 V AC power supply, although no data about power consumption is given. In this example, the making of the die for the sheet-metal forming operation is not studied.

Scientists at DuPont have taken the concept of the micro-factory to the VLSI industry and crafted a complete chemical plant using just three silicon wafers taken from a modern IC process [20]. This micro-factory is capable of synthesizing 18,000 kg/yr of the toxic industrial chemical methylisocyanate. Reports of the concept of

micro-factories can be found in the MEMS industry [21] and also in the mechatronics industry [22].

Using LCA is as relevant in micro-factories as it is in other types of manufacturing facilities. There are some issues that need to be taken into account, e.g. the flexibility of micro-factories making them less comparable with production lines, or the potential need for clean-room facilities and the assessment of the added value of miniaturization, which could affect their applications. Nevertheless, there is a clear advantage in the possibilities of identifying environmental-improvement potentials in the process chain.

ETHICAL ISSUES AND TOXICOLOGY – ADDITIONAL ISSUES CONCERNING NANO-TECHNOLOGIES

There is a trend to integrate micro-manufacturing and nano-manufacturing with a view to bridging the gaps between two length-scale manufacturing, and hence, to deliver more engineering-significance products. As far as the LCA is concerned, there is a need to mention ethical issues and toxicology relevant to nano-manufacturing – nano-technology in general. While nano-technology broadly describes the field of working at the nano-scale, emphasis has been put on the environmental and health risks of nano-particles. Two

factors are mainly responsible for the hazard potential of nano-particles: their high surface-to-volume ratio (which is due to their small size) and their composition.

First, potential risks of nano-particles are related to their use in applications where they can be taken up by humans through inhalation, ingestion or via the skin. This could be from: free particles in the air, for example in the work environment; nano-particles in liquid suspension, for example in skin lotion; or nano-particles in surface treatment that can be released during use or disposal. As indicated, the risks may occur during production, use or disposal. Moreover, also because of their small size, nano-particles may have toxicological properties that are different from those of their macro-counterparts.

Second, the geometry and surface chemistry of many nano-particles increases their uptake into the human body, especially through the lungs after inhalation, and through ingestion, but also potentially through the skin. Additionally, the human immune system may have problems dealing with the particles and the increased surface

area of the particles compared to that of larger particles can make them more reactive in the human organism. A recently published review of the potential risks of nano-particles shows that they can be deposited in the lungs after inhalation and cause oxidative stress and inflammation. They may also be taken up into the body and translocated into other tissues: translocation to the brain has been seen. Uptake via the intestine after oral intake has been encountered and some evidence shows that oxidative stress and inflammation may also occur in the body after oral uptake. Uptake through the skin is, however, not sufficiently documented. Only a few specific nano-particles have as yet been investigated and the toxicity of many new engineered nano-particles is largely unknown [23].

Figure 25-6 shows a comparison of size between asbestos and carbon nano-tubes. There is a drastic difference between the diameter and length of a nano-tube and a fiber of asbestos, but the history of the material could be considered: use of material for a specific property without proper examination of the potential health

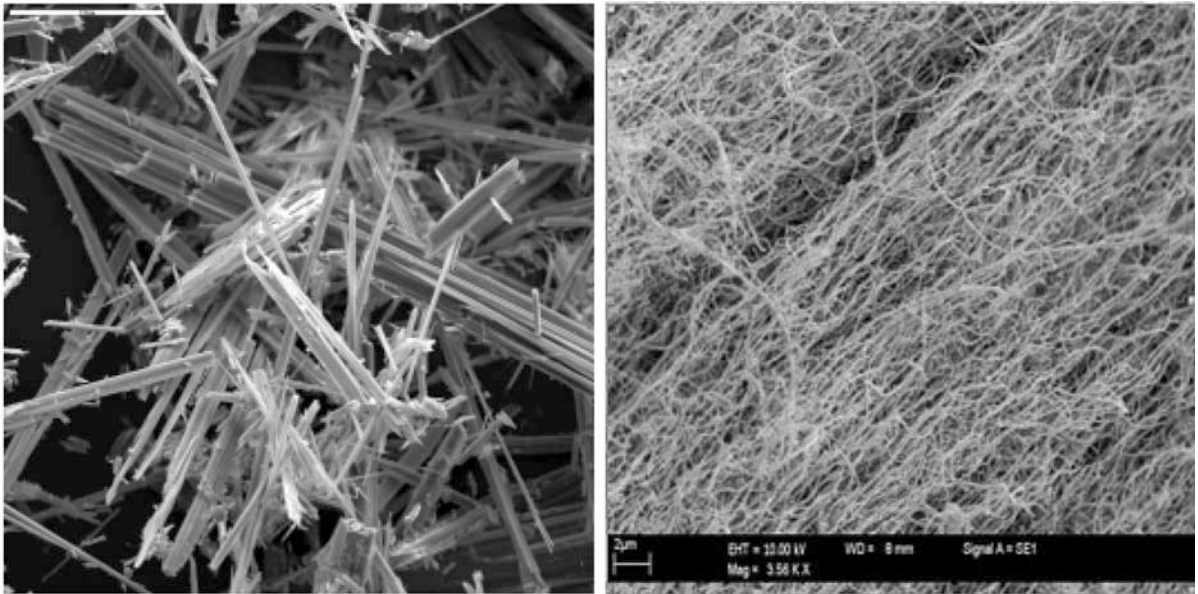


FIGURE 25-6 SEM pictures of anthophyllite asbestos and carbon nano-tubes. The scale bar is 50 μm in the case of asbestos (on the left, picture taken from Wikipedia) and 2 μm in the case of carbon nano-tubes (on the right, picture taken from [24]).

hazard. Mainly, scientists affirm that the lesson of asbestos is to be learned and that a principle of precaution is to be adopted.

Moreover, as said in the editorial of *Nature* [25]: ‘Nano-technology is set to be the next campaign focus for environmental groups’, which enhances that research has not only to be performed in the field of nano-toxicology, but also that scientists have to communicate about it in order to make it acceptable for a massive use in society. For example, the European Union funded the NANOSAFE project to assess the technology’s environmental and health risks in 2003, and at the same time the US Environmental Protection Agency invited proposals to study the environmental and health impact of nano-technology. Similarly, the Royal Society and the Royal Academy of Engineering began some UK studies in 2004. In Denmark, the Ministry of Science, Technology and Innovation issued an action plan including attention to health hazards, environmental and ethical considerations regarding nano-science and nano-technology, in 2004. In the USA, a study about the military environmental-health considerations has been reported in [24]. In this study the potential use and impact are listed and research priorities are highlighted. Again, the mechanisms of the absorption of nanoparticles into the body and the reaction from the immune system are considered as critical areas to prevent or reduce risks, together with pollution-related issues (e.g. the disposal and recycling of carbon nano-tubes).

REFERENCES

- [1] M. Hauschild, J. Jeswiet, L. Alting, From life cycle assessment to sustainable production: status and perspectives, *Annals of CIRP* 54 (2) (2005) 535–555.
- [2] ISO 14040: <http://www.iso-14001.org.uk/iso-14040.htm>. (1999).
- [3] A. De Grave, S.I. Olsen, Challenging the sustainability of micro products development, *Proceedings of the 2nd International Conference on Multi-material Micro Manufacturing (4M 2006)*, Grenoble, France (September 2006) 285–288.
- [4] A. De Grave, H.N. Hansen, S.I. Olsen, Sustainability of products based on micro and nano technologies, *Proceedings of the 4th International Symposium on Nanomanufacturing (ISNM 2006)*, MIT, Cambridge, MA USA (November 2006) 40–45.
- [5] K. Schischke, H. Griese, Is small green? *Life Cycle Aspects of Technology Trends in Microelectronics and Microsystems (2004)*. http://www.lcacenter.org/InLCA2004/papers/Schischke_K_paper.pdf.
- [6] A. Plepys, The environmental impacts of electronics. Going beyond the walls of semiconductor fabs, *IEEE International Symposium on Electronics and the Environment (2004) Conference Record*.
- [7] R. Kuehr, E. Williams (eds.). *Computers and the Environment: Understanding and Managing their Impacts*, Kluwer Academic Publications, Dordrecht (2003).
- [8] M. Hauschild, H. Wenzel, L. Alting, Life cycle design – a route to the sustainable industrial culture? *Annals of CIRP* 48 (1) (1997) 393–396.
- [9] T. Gutowski, C. Murphy, D. Allen, D. Bauer, B. Bras, T. Piwonka, P. Sheng, J. Sutherland, D. Thurston, E. Wolff, Environmentally benign manufacturing: observations from Japan, Europe and the United States, *J. of Cleaner Production* 13 (2005) 1–17.
- [10] B. Hill, Industry’s integration of environmental product design, *IEEE International Symposium on Electronics and the Environment (1993)*.
- [11] ISO/TR 14062, Environmental management – integrating environmental aspects into product design and development, *International Organisation for Standardisation, Geneva, Switzerland (2002)*.
- [12] F. Quella and W.-P. Schmidt, Integrating environmental aspects into product design and development – the new ISO TR 14602 – Part 2 Contents and practical solutions, gate to EHS: life cycle management – design for environment (Mar. 17, 2003) 1–7.
- [13] H. Van Brussel, J. Peirs, D. Reynaerts, A. Delchambre, G. Reinhart, N. Roth, M. Weck, E. Zussman, *Assembly of Microsystems, Annals of CIRP* 49 (2) (2000) 451–472.
- [14] J.R. Sarusua, J. Pouyet, Recycling effects on microstructure and mechanical behaviour of PEEK short carbon-fibre composites, *J. of Material Science* 32 (2) 533–536.
- [15] O. Breuer, U. Sundararaj, Big returns from small fibers: a review of polymer/carbon nanotube composite, *Polymer Composites* 25 (6) (2004) 630–645.
- [16] E.V. Barrera, L.P.F. Chibante, B. Collins, F. Rodriguez-Marcias, M. Shofner, J.D. Kim, F.D.S. Marquis, Recycling nanotubes from polymer nanocomposite (2001) 267–282. In: *Powder Materials: Current Research and Industrial Practices*.
- [17] B. Muruyama, K. Alam, *SAMPE J* 38 (3) (May/June 2002) 59.
- [18] H.N. Hansen, T.E. Eriksson, M. Arentoft, N. Paldan, Design rules for microfactory solutions, *Proceedings*

- of the 5th International Workshop on Microfactory, Besançon, France (October 2006).
- [19] N. Mishima, Evaluation of manufacturing efficiencies of microfactories considering environmental impact, Proceedings of the 5th International Workshop on Microfactory, Besançon, France (October 2006).
- [20] R. Service, Miniaturization puts chemical plants where you want them, *Science* 282 (1998) 400.
- [21] I. Verettas, Microfactory: desktop cleanrooms for the production of microsystems, Proceedings of the IEEE International Symposium on Assembly and Task Planning (2003) 18–23.
- [22] Y. Ishikawa, T. Kitahara, Present and future of micromechatronics, Proceedings of the 1997 International Symposium on Micro Mechatronics and Human Science (1997) 13–20.
- [23] P.J.A. Borm, D. Robbins, S. Haubold, T. Kuhlbusch, H. Fissan, K. Donaldson, R.P.F. Schins, V. Stone, W. Kreyling, J. Lademann, J. Krutmann, D. Warheit, E. Oberdorster, The potential risks of nanomaterials: a review carried out for ECETOC, *Particle and Fibre Toxicology* 3 (11) (Aug. 14, 2006).
- [24] J.C. Glenn, Nanotechnology: future military environmental health considerations 73 (2) (2006) 128–137. In: *Technological Forecasting & Social Change*.
- [25] Don't believe the hype, *Nature* 424 (July 17, 2003) 217.

D

- Deep X-ray Lithography, 202–20
 - Commercial applications, 216–17
 - Micro gears, 217
 - Micro-spectrometer-mold, 217
 - Polymer compound refractive x-ray lenses, 216
- Design rule, 213–14
- Features of the LIGA process, 215
- Introduction, 202–03
- LIGA manufacturing steps, 203–11
 - Irradiation technology, 205–11
 - Resist deposition, 205
 - Resist technology, 203–05
 - PMMA degradation, 208–09
 - PMMA development, 209–10
 - Special computer programs for X-ray, 210–11
 - Synchrotron source, 205–08
- LIGA process and its strengths, 203
- Market, 215–16
- Mask-technology, 213–14
- Metrology, 214–15
- Micro-electroplating technology, 211–13
 - Micro gears - direct metal parts, 217
 - Micro-spectrometer-Mold, 217
 - Polymer compound refractive x-ray lenses, 216

H

- Handling for Micro-Manufacturing, 298–314
 - Case study, 309–11
 - Assembly, 311
 - Inspection, 310

- Micro-fabrication, 309
- Fundamentals, 298–99
 - General considerations for handling, 298
 - Grasping principles, 306
 - Serial pick-and-place task, 299
 - Significant forces at micro-scale, 302
- Handling systems, 299–308
 - Inter-machine transport systems, 299–301
 - Conventional transport equipment, 301
 - Standard carriers, 300
 - Intra-machine micro-handling systems, 302–09
 - Force sensors, 309
 - Grasping principles, 306
 - Grasping requirements, 306
 - Grippers, 307
 - Industrial manipulators, 305
 - Mechanical feeders, 303
 - Manipulator-based part-feeders, 304
 - Sensors and control systems, 308
 - Significant forces at micro-scale, 302
 - Vision sensors, 308
- Hot Embossing, 68–89
 - Applications, 85–87
 - Micro-fluidic devices, 86
 - Micro-needles, 87
 - Micro-optical devices, 85
 - Introduction, 68–69
 - Fresnel lenses, 69
 - LIGA, 69
 - Micro reaction injection molding, 69
 - Nanoimprint Lithography, 70
 - Replication processes, 68
 - RIM, 69
 - Tensile testing machine, 69
- Hot embossing process, 70–71
 - Adhesion, 70
 - Characteristics of hot embossing, 71
 - Cooling, 71
 - Demolding, 71
 - Double-sided embossing, 71
 - Force controlled molding, 70
 - Glass transition temperature, 71
 - Holding time, 70
 - Packing pressure, 70
 - Packing time, 70, 71
 - Residual layer, 70
 - Single sided hot embossing, 70
 - Substrate plate, 70
 - Thickness polymer foil, 70
 - Vacuum, 70
 - Velocity controlled molding, 70
- Process Variations, 71–77
 - Double-sided Molding, 72
 - Adjustment mold halves, 72
 - Misalignment, 72
 - Through holes, 72
 - Hot Punching, 74
 - Cutting holes, 75
 - Embossing alignment, 75
 - Embossing, two step, 74
 - Glass transition temperature, 75
 - Matrix, 75
 - Release agent, 75
 - Shearing process, 75
 - Multi-Layer Molding, 72
 - Polymer stack, 72
 - Separation by peeling, 72
 - Roller embossing, 76
 - Cylinder mold method, 76
 - Flat mold method, 77
 - Role-to-role embossing, 76
 - Roller nanoimprint-lithography, 76
 - Roller speed, 77

- Roller temperature, 77
- Thermoforming by hot embossing, 75
 - Demolding by peeling, 76
 - Film thickness, 75
 - LCP, 75
 - Material combinations, 75
 - Molding temperatures, 75
 - PEEK, 75
- Through-holes, 73
 - Residual layer, 73
 - Squeeze flow, 73
 - Substrate, flexible, 73
- Materials, 77–78
 - Aggregate states of polymers, 77, 78
 - Amorphous polymer, 77
 - Glass transition range, 77
 - Melting range, 77
 - Molding window, 77
 - Semicrystalline polymer, 77
 - Shear modulus, 78
 - Thermal behavior, 77
 - Thermoplastic polymers, 77
 - Transitions ranges, 78
- Outlook, 88
 - Automation, 88
 - Cost effectiveness, 88
 - Standardization, 88
- Techniques, 77–79
 - Commercial machines, 79
 - EVG, 79
 - Jenoptik Mikrotechnik, 79
 - Wickert Press, 79
 - Components, 77–78
 - Alignment system, 78
 - Controlling system, 78
 - Heating system, 77
 - Hot embossing machine, 77
 - Hot embossing tool, 77
 - Mold insert, 78
 - Vacuum chamber, 77
- Tools, 79–85
 - Basic tool for hot embossing, 81
 - Air gap, 81
 - Clamping system, 82
 - Cooling block, 81
 - Heating, electrical, 81
 - Prestressed spring, 81
 - Temperature distribution, 82
 - Thermal mass, 81
 - Micro-structured mold inserts, 83
 - Conductivity, 84
 - Demolding angles, 84
 - E-beam lithography, 84
 - EDM, 84
 - LIGA, 85
 - Mechanical machining, 84
 - PDMS, 84
 - Requirements for molding, 83, 84
 - Surface roughness, 84
 - Undercuts, 84
 - UV-lithography, 84
 - X-Ray-lithography, 85
 - Yield stress, 84
 - Mold insert integration, 79
 - Tool tasks, 80
- I**
 - In-situ Testing of Materials, 331–43
 - Case-study, 340–42
 - Comparison, 341–42
 - Length scale, 340, 342
 - LIGA, 331
 - Micro-compression, 340–42
 - Micro-tension, 340–42
 - Nickel, 340–42
 - Plastic properties, 341
 - Size-effect, 342
 - Compression tests, 334–335
 - Buckle, 335
 - Loadcell, 334
 - Piezo-actuator, 334
 - Pillar, 334
 - Stress/strain curve, 335
 - Tip, 334–35
 - Image analysis, 338–39
 - Algorithms, 339
 - Tracking motion, 339
 - Materials, 332
 - Mechanical properties, 331–43
 - Micro and nano scale, 331–43
 - Nano-indentation, 335–38
 - Contact depth, 337
 - Displacement, 336–37
 - Hardness, 337–38
 - Indenter, 337–38
 - Load, 336
 - SEM-micro-indenter, 338
 - Young's modulus, 337
 - SEM, 331–43
 - SEM image, 333–40
 - Tensile testing, 332–34
 - Mechanical clamping, 333
 - Propagation of cracks, 333
 - Sample dimension, 333
 - Stress/strain curve, 332–33
 - Testing in SEM, 332
 - Integration, 332
 - SEM chamber, 332
 - Setup, 332
 - Vacuum, 332
- L**
 - Laser-Assisted Micro-Forming, 162–73
 - Introduction, 162
 - Processes, 164–73
 - Burr, 165
 - Cold forming, 165
 - Compressive strength, 164
 - De-Embossing, 167
 - Elastic deformation, 164
 - Embossing, 167
 - Female die, 164
 - Fracture zone, 164
 - glass-transition temperature, 167
 - Gliding planes, 166
 - Hot forming, 165
 - Hybrid Component, 171
 - LIFTEC, 169
 - Mold-in technique, 169
 - Plastic deformation, 164
 - Post-molding technology, 170
 - Punch, 164
 - Recrystallization temperature, 165
 - Roll-over, 164

- Shearing zone, 164
 - Stamping, 164
 - Strain hardening, 166
 - Tamman rule, 165
 - Warm forming, 165
 - System Technology, 162–64
 - Axicon, 163
 - Conductive heating, 162
 - Convective heating, 162
 - Inductive heating, 162
 - Laser heating, 162
 - Optical path, 163
 - Pyrometer, 163
 - Sapphire, 164
 - Thermocouple, 163
 - Laser Beam Micro-Joining, 185–201
 - Laser beam soldering, 185–92
 - Au Sn solder alloy, 192
 - Brazing, 185
 - Electrical contacting of solar cells, 191
 - Electro-optical efficiency, 188
 - Fiber lasers, 188
 - Flux, 185
 - Galvanometric scanner, 189
 - Heating cycle, 186
 - High power diodes, 187
 - Laser processing optics, 189
 - Laser soldered joint, 191
 - Production cell, 189
 - Pyrometer, 190
 - Pyrometric sensor, integrated, 190
 - Pyrometric signal, 190
 - Sapphire, metallized, 192
 - Selective soldering techniques, 187
 - Solder alloy, 185
 - Solder joint configuration, 190
 - Soldering, 185
 - TLP bonding, 185
 - Transient liquid phase bonding, 185
 - Laser beam welding, 193–201
 - Alternative joining methods, 193
 - Beam delivery, 194
 - Butt joint configuration, 200
 - Classification, 195
 - Conduction welding, 195
 - Contamination, 198
 - Continuous welding, 196
 - Difficult-to-weld materials, 198
 - Energy input, 197
 - Fiber delivery, 194
 - Fiber laser, 194
 - Fine mechanics, 198
 - Footprint, 200
 - Galvanometric scanner, 194
 - Gaps, 200
 - Joint geometries for micro welding, 193
 - Keyhole, 200
 - Nd:YAG, flashlamp pumped, 193
 - Positioning of the laser beam, 195
 - Process speed, 197
 - Pulse forming, 196
 - SHADOW, 197
 - Spaced spot welding, 196
 - Splatters, 198
 - Spot weld, 193
 - Spot welding, 195
 - Thermosonic ribbon bonding, 201
 - Laser Micro-Structuring, 59–67
 - Case studies laser micro machining, 65–67
 - Functional surfaces, 65
 - Injection moulding tool, 65
 - Lotus effect, 65
 - Micro fluidics, 66
 - Laser ablation basics, 60–62
 - Absorption Effects, 60–61
 - Absorption coefficient, 60
 - Gaussian radiation, 61
 - Laser ablation depth, 60
 - Photon-matter-interaction, 60
 - Threshold intensity, 61
 - Thermal effects, 61–62
 - Nanosecond laser pulses, 61
 - Pikosecond laser pulses, 61
 - Pulse duration, 61
 - Thermal penetration depth, 62
 - Threshold fluence, 62
 - Ultrashort laser processing, 61
 - Laser machining principles, 62–64
 - Mask techniques
 - Focal length, 63
 - Imaging, 63
 - Resolution, 63
 - Scribing techniques
 - Galvanometer mirrors, 64
 - Numerical aperture, 64
 - Processing diameter, 64
 - Scanning, 64
 - Wavelength, 64
- ## M
- Manufacturing Execution System (MES), 377–93
 - IT-enabled business processes, 377–78
 - Customer order process, 377
 - Product lifecycle process, 377
 - MES implementation and integration, 388–390
 - Equipment automation/integration, 389
 - Equipment layer, 388
 - MES services, 390
 - MES tasks, 382–388
 - Data collection and acquisition, 386
 - Automated data collection, 386
 - Manual data collection, 386
 - Semi-automated data collection, 386
 - Information management, 387
 - Advanced Process Control (APC), 388
 - Paperless production, 388
 - Reporting, 388
 - Workflow management, 388
 - Labor management, 385
 - Material management, 384
 - Lot/Batch, 385
 - Work in Progress (WiP), 384

- WiP tracking, 385
- Operations/detailed scheduling, 382
 - Dispatching, 382
 - Scheduling, 382
- Performance analysis, 386
 - Cycle time, 387
 - Equipment utilization, 386
 - Key performance indicators, 386
 - Overall equipment efficiency (OEE), 386
- Quality management, 387
 - Fault detection and classification (FDC), 387
 - Sampling, 387
 - Statistical process control (SPC), 387
- Resource management, 383
 - Maintenance management, 384
 - Master data, 383
 - Resource tracking, 382
- Production IT overview, 378–82
 - Hierarchical enterprise model, 378
 - Operational scenarios, 380
 - Production IT enterprise architecture, 380
 - Generic tasks, 380
 - Layered architecture, 381
 - Standards regarding the production IT, 390–92
 - Equipment interface standards, 391
 - General production IT standards, 391
 - SEMI equipment interface standards framework, 392
- Micro-Bulk-Forming, 114–29
 - Die design, 119–25
 - also see Machine design
 - Forming processes, 114–15
 - Bulk-forming, 114
 - Forming steps, 114–15
 - Process chain, 114
 - Machine design, 119–25
 - Alignment of tooling, 120
 - Billet preparation, 119
 - Die system, 120–22
 - Ejection, 123–24
 - Flexibility of tools, 121
 - Handling, 123–24
 - Press system, 120
 - Process supervision, 125
 - Transfer system, 124
 - Warm forging, 122–23
- Micro-tribology, 125–27
 - Amortons' Law of friction, 125
 - Friction, 125–26
 - Friction coefficient, 126
 - Lubricant, 127
 - Micro-size 125–27
 - Size-effect, 125–26
- Process analysis, 127–29
 - Double-can extrusion, 128
 - FEM, 127
 - FE simulation, 128
- Size-effect, 115–16
 - Density effect, 115
 - Scale, 115
 - Scaling effect, 116
 - Shape effect, 115
 - Size, 115
 - Tolerances, 116
- Tool materials, 118–19
 - Ceramics, 119
 - Hardness, 118
 - Powder metallurgical steel, 118–19
 - Machining, 119
 - Tungsten carbide, 119
- Workpiece materials, 116–18
 - Amorphous metals, 117–18
 - BMG, 117
 - Metallic glass, 117
 - Properties, 116
 - Selection of materials, 117
- Micro Electrical Discharge Machining (EDM), 39–58
 - Applications, 54
 - Design considerations, 52–54
 - Material Selection, 53
 - μ -EDM Optimized Design, 52–53
 - Tool electrodes for μ -EDM, 53–54
- Economical considerations, 54–56
- Introduction, 39
- Machine and tools, 49–52
 - Generator types, 51–52
 - Adaptive feed control, 52
 - Relaxation generators, 51–52
 - Static pulse generators, 51
- Machine design, 49–51
 - Die-sinking EDM machine, 50
 - Wire EDM machine, 50–51
- Outlooks, 56
- Processes, 42–49
 - Micro die-sinking EDM, 45–47
 - Dielectric fluid and flushing, 46
 - Dimensions and applications, 46–47
 - Micro-die sinking Electrodes, 46
 - Micro Electrical Discharge Contouring, 48–49
 - Dielectric fluid and flushing, 49
 - Dimensions and applications, 49
 - Electrodes, 48–49
 - Micro Electrical Discharge Drilling, 47–48
 - Dielectric Fluid and flushing, 47–48
 - Dimensions and applications, 48
 - Micro-drilling electrodes, 47
 - Micro Wire EDM, 43–45
 - Dielectric Fluid and flushing, 44–45
 - Dimensions and applications, 45
 - Micro-wire Electrodes, 44
 - Micro-wire Electrical Discharge grinding, 45
 - Multiple cutting strategies, 44

- Single discharge, 42–43
- References, 56–58
- Technological competitiveness, 54–56
- Working principles, 39–42
 - Dielectric fluid, 41
 - General flushing strategies, 42
 - Machining principle of EDM, 39
 - Process variants, 39–41
- Micro-Hydroforming, 146–61
 - Conclusion, 159
 - Design considerations, 155
 - Corner radii, 155
 - Cross-sections, 155
 - Expansion, 155
 - Ratio of wall thickness to outer diameter, 155
 - Tolerances for inner dimensions, 155
 - Hydroforming process design, 152–55
 - Failures, 152
 - Buckling, 152, 154
 - Bursting, 152, 154
 - Necking, 154
 - Wrinkling, 152, 154
 - Forming loads, 152–54
 - Axial force, 152
 - Axial stress, 152
 - Bursting pressure, 154
 - Calibration pressure, 153
 - Circumferential stress, 152
 - Effective stress, 153
 - Friction force, 153
 - Internal pressure, 152
 - Minimum axial force, 153
 - Sealing force, 153
 - Material parameters, 152–53
 - Ultimate tensile strength, 153
 - Yield stress, 152
 - Membrane theory, 152
 - Process control, 154–55
 - Rotationally symmetrical workpiece, 152–53
 - Shell theory, 152
 - Size effects, 152
 - T-piece components, 152, 154
- Theory of plasticity, 152
- Micro-hydroforming machines, 155–59
 - Control system, 158
 - Forming loads, 157
 - Axial force, 157
 - Closing force, 157
 - Internal pressure, 157
 - Machine concepts, 158
 - Part handling, 157
 - Part insertion, 157
 - Part removal, 157
 - Press frame, 157
 - Pressure intensifier, 158
 - Pressurizing media, 158
 - Sensors, 158
 - Spindle-driven pressure intensifier, 159
 - Stroke, 157
- Micro-hydroforming tools, 155–57
 - Design of micro-hydroforming tools, 156
 - Adjusting plates, 156
 - Conical punch, 156
 - Die cavity, 155–56
 - Ejectors, 156
 - Part handling, 156
 - Sealing punches, 156
 - Tool inserts, 155–56
 - Loads, 155
- Applications, 155
 - Medical engineering, 155
 - Micro-fluidic, 155
 - Micro-mechatronics, 155
- Principle of hydroforming, 147
 - Forming dies, 147
 - Forming loads, 147
- Process chain, 150–52
 - Bending, 151
 - Cutting, 152
 - Hydroforming, 152
 - Notching, 152
 - Preforming, 151
 - Beveled dies, 151
 - Cross slides, 152
 - Methods for preforming, 151
- Wrinkles, 152
- Trimming, 152
- Process variants, 147–78
 - Assembly, 148
 - Classification, 148
 - Piercing, 147
 - T-piece hydroforming, 147
 - Counter-force, 148
 - Counter-punch, 147
 - T-shaped component, 147
- Semifinished products, 148–50
 - Aluminium alloys, 148
 - Copper alloys, 148
 - Extruded profiles, 149
 - Hydroformed micro-part, 149
 - Magnesium alloys, 149
 - Material testing methods, 149
 - Bulge test, 150
 - Formability, 150
 - Mechanical expansion testing, 150
 - Strain analysis, 149
 - Yield curve, 150
 - Sheet materials, 148
 - Steel alloys, 148
 - Tubular materials, 148
 - Annealing, 148
 - Micro-tubes, 148
 - Ratio of wall thickness to outer diameter, 148
 - Weld seam quality, 149
- Micro-Injection-Molding, 90–113
 - Micro-injection-molding products, 90
 - Dimensions, 91
 - Micro part weight, 91
 - Tolerances, 91
 - Micro-injection-molding technology, 91
 - Conventional machine, 92
 - Cooling, 92
 - Ejection, 92
 - Injection, 92
 - Packing phase, 92
 - Plastification, 92
 - Runner system, 93
 - Injection moulding, 92

- Clamping force, 91
- Minimum shot weight, 92
- Micro injection moulding machine, 94
 - Injection plunger, 94
 - Injection speed, 95
 - Metering plunger, 94
 - Shut-off valve, 95
- Process control, 95
 - Filling analysis, 96
 - Flow markers, 100–103
 - Flow visualization, 97
 - Length flow test, 99–100
 - Short shots, 96–98
- Process analysis, 101
 - Cavity injection time, 105
 - Cavity pressure, 104
 - Injection pressure, 101
 - Micro flashes, 104
- Process simulation, 109
 - Heat transfer coefficient, 110
 - Implementation strategies, 112
 - Meshing, 110
 - Polymer rheology, 110
 - Short shots, 111
 - Software validation, 110
- Weld lines, 106
- Micro-Manufacturing Overview, 1–23
 - Assembly & packaging, 13
 - Design considerations, 3
 - Development & utilisation strategies, 18–21
 - Business, 18
 - Driving other industries, 20
 - Integration with other activities, 19
 - Life cycle assessment (LCA), 18, 394–404
 - Manufacturing & supply chain, 19
 - Market gateway analysis, 18
 - Other issues, 21
 - Technological performance & maturity level, 20
- Dimensions, 3
- Examples of micro-parts, 4
- Local Features, 3
- Manufacturing equipment, 14
 - See, also Manufacturing system
- Manufacturing methods, 7–9
 - Considerations, 7
 - List of typical methods & processes, 9
- Manufacturing processes, 8–14
 - Deposition methods, 12, 287–97
 - ECM/EDM, 14, 39–58
 - EDM & Laser assembly, 14, 39–58
 - Efab, 12
 - Hybrid processes, 13, 287–97
 - Laser heating, 11, 162–73
 - Laser technology, 11, 59–67, 162–73, 185–201
 - LIGA, 12, 202–20
 - Mechanical machining, 8, 24–38
 - Micro-casting, 12, 202–20
 - Micro-EDM, 9, 39–58
 - Micro-electrochemical machining, 10
 - Micro-embossing, 12, 68–89
 - Micro-forming, 10, 114–29, 130–45, 146–161, 162–73
 - Micro-injection moulding, 12, 90–113
 - Rapid prototyping & micro-machining, 14
 - Replication techniques, 11, 68–89, 90–113, 202–20, 241–63
 - Shape deposition manufacturing, 12
 - UPSAMS, 14
- Manufacturing System, 14–16
 - Bench-top machines, 15, 24–38, 68–89, 114–29, 130–45, 146–61
 - CNC machine, 16, 24–38
 - Forming of micro-bulk products, 15, 114–29
 - Micro-factories, 15
 - Micro-hydroforming, 16, 146–61
 - Micro-machining, 16, 24–38
 - Micro-sheet-forming, 15, 130–45
- Miniature systems, 15, 24–38, 114–29, 130–45, 146–61
- Multiple-axis machine tool, 16
- Multiple-process equipment, 16
- Material capability, 5
- Material factors, 6
- Material properties after processing, 6
- MEMS, 2
- Non-MEMS, 2
- Process chains, 13, 287–97
- Shape capability, 3
- Supporting technologies & devices, 17
 - 3D measurement, 17
 - Handling, 17, 174–83, 298–314, 315–23
 - Quality assurance, 17
 - Sensor system, 17
- Tolerance and Surface Quality, 5
- Volume production, 6
- Micro-Mechanical-Assembly, 174–83
 - Application example, 180–83
 - Assembly, 181–82
 - Gripper, 182
 - Handling, 181–82
 - Robot, 182–83
 - Push button parts, 180–181
 - Screwdriver, 182–83
 - Classification of assembly, 176–179
 - Micro-injection-molding, 179
 - Micro-joinery, 178
 - Micro-rievting, Folding and Clinching, 179–80
 - Micro-screwing, 176–77
 - Micro-snap fits, 176
 - Micro-Velcro, 177
 - Handling, 180–81 *also see* Systematic approach
 - Introduction, 174–75
 - Asembly functions, 174
 - Challenges in assembly, 175
 - Handling, 175, 180–81
 - Micro-products, 175
 - Systematic approach, 180–81
- Micro-Mechanics Modelling, 366–76

- Integrated CPFE, 371–74
 - CPFE Model, 372–75
 - Gamma distribution, 373
 - Integrated numerical procedure, 373–74
 - Polycrystals, 367–73
 - Probability, 373–74
 - Voronoi tessellation, 373–74
 - Implementation, 371–72
 - ABAQUS, 371–73, 374
 - dynamic effect, 371
 - VUMAT, 371–74
 - Integrated numerical process, 373–74
 - ABAQUS/CAE, 373–74
 - Grain size, 373–75
 - Orientation, 366, 369, 372–75
 - Pre-processing, 373–74
 - Virtual grain structure, 373
 - Introduction, 366–67
 - Crystal, 366–76
 - Crystal orientation, 366, 369, 372–75
 - Crystal Plasticity Finite Element (CPFE), 367, 371–75
 - Dislocation, 366–69
 - Length-scale, 366, 367
 - Micro-forming, 366, 367, 371, 374
 - Micro-parts, 366, 367, 371, 375
 - Microstructures, 366, 367, 373, 375
 - Miniaturization, 366
 - Micro-materials models, 367–371
 - Constitutive Equations, 370–71
 - Hardened state, 370
 - Hooke's law, 370
 - Jaumann rates, 370
 - Latent hardening, 371
 - Resolved shear stress, 370
 - Rotate, 370
 - Schmid stress, 370
 - Self hardening, 371
 - Spin, 370
 - Strain rate, 370
 - Crystal kinematics, 368
 - Deformation gradient, 368–69
 - Rotation, 368–70
 - Slip direction, 368–69
 - Slip plane normal, 370
 - Stretching, 369–70
 - Physical basis, 367
 - BCC (Body Centred Cubic), 368
 - FCC (Face Centred Cubic), 368–69
 - HCP (Hexagonal Close Packed), 368
 - Slip systems, 367–69, 371–72
 - Process simulation, 374–75
 - ABAQUS/CAE, 374
 - CPFE analysis, 374–75
 - Micropins, 374–75
 - Micro-/Nano-Fibers by Electrospinning Technology, 264–86
 - Applications, 274–82
 - Biomedical applications, 274–76
 - Drug carrier and delivery, 276
 - Tissue engineering, 274
 - Wound dressings and healing, 276
 - Composite reinforcement, 279
 - Commercial products, 281
 - Electric and electronic, 278
 - Enzymes and catalysts, 276
 - Filters, 278
 - Micro-nano-fluidic devices, 276–77
 - Micro-nanomechanical devices, 276–77
 - Sensors, 277
 - Textile, 278
 - Production rate, 280
 - Centrifugal forces, 281
 - Multiple Nozzles, 280
 - Without Nozzles, 280
 - Characteristics of micro-nano-fibers, 273–74
 - Alterations of functionality, 274
 - Alterations of structure, 274
 - Molecular orientation, 273
 - Shapes and sizes, 273
 - Configuration, 265–69
 - Electrospinning mechanism, 265–67
 - Bending instability, 267
 - Fluid jet, 265–66
 - Taylor cone, 265–66
 - Thinning of the fluid jet, 267
 - Control of morphology, 267–69
 - Design considerations, 273–74
 - Operational economics, 282
 - Processing parameters, 267–69
 - Ambient conditions, 268
 - Process conditions, 268
 - Solution properties, 267
 - Set-ups of electrospinning, 269–73
 - Control of the alignment, 270
 - Control of the orientation, 270
 - Dry rotary electrospinning, 271
 - Scanned deposition, 271
 - Dual syringes set-ups, 270
 - Novel set-ups, 269
 - Technological competitiveness, 282
 - Tools of electrospinning, 269–73
 - Working principle, 265–67
- Micro & Nano Machining, 24–38
 - Applications, 35–37
 - Competitive technologies, 37
 - Economic considerations, 37
 - Fundamentals, 24–27
 - Chip formation, 25–26
 - Cutting force, 24–25
 - Ductile mode cutting, 26–27
 - Micro-structure, 27
 - Minimum chip thickness, 25–26
 - Specific energy, 24–25
 - Introduction, 24
 - Micro-tooling, 34–35
 - CVD diamond cutting tools, 34
 - Diamond cutting tools, 34
 - Modelling, 27–30
 - FE modelling, 28–29
 - MD modelling, 29

- Multi-scale modelling, 29–30
 - Precision machines, 30–34
 - Micro and meso machines, 33–34
 - Ultra-precision machine tools, 30–33
 - Control system, 32
 - Drive system, 31–32
 - Feedbacksystem, 32
 - In-process condition monitoring, 32
 - Inspection system, 32
 - Mechanical structure, 31
 - Position measurement, 32
 - Spindle, 31–32
 - Micro-Sheet-Forming, 130–45
 - Case study, 142–43
 - Forming machine, 143
 - Micro-spring, 142
 - Progressive die, 143
 - Samples, 143
 - Design considerations, 141–42
 - Forming tools, 138–40
 - Considerations for tool design, 138
 - Handling, 139
 - Micro-tooling, 139
 - Pilot pins, 139
 - Punch/die clearance, 138
 - Size-effect, 138
 - Tool dynamics, 138
 - Fundamentals, 131–37
 - Also see Manufacturing processes, 131
 - General considerations for manufacturing, 137–38
 - Manufacturing processes, 131–37
 - Bending, 134–35
 - Bending operation, 134
 - Bending radius, 134
 - Bening allowance, 134
 - Distortion, 134
 - Forming error compensated, 135
 - Forming errors, 134–35
 - Process parameters, 134
 - Springback, 134–35
 - Blanking & punching, 131–33
 - Burr, 133
 - Burr-free punching, 133
 - Grain, 132
 - Laser heating, 133
 - Micro-structure, 132
 - Punch-die clearance, 132
 - Shearing action, 131
 - Size effect, 132
 - Deep drawing, 135–37
 - Drawing ratio, 135–36
 - Fracturing, 136
 - Part failure forms, 136
 - Wrinkles, 136
 - Other micro-sheet-metal-forming processes, 137
 - Operational economics, 144–45
 - Presses and machines, 140–41
 - Bench-top, 140
 - Large scale, 140
 - Linear-motor driving, 140
 - Micro-machines, 141
 - Sheet metal components, 130
 - Technological competitiveness, 144–45
- O**
- Optical Coherence Tomography (OCT), 324–30
 - Evaluation of microstructures, 326–29
 - Birefringence, 328
 - Optical axis, 329
 - Residual/internal stress, 328–29
 - Retardation, 328
 - Stress-optical coefficient, 328
 - Drug-eluting medical stent, 327–28
 - en-face scanning OCT, 327
 - Microfluidic devices, 329
 - Photoresist molds, 326–28
 - Future developments, 329
 - Introduction, 324
 - Biomedical diagnostics, 324
 - Technical applications, 324
 - Measurement principles, 325–26
 - Coherence probe microscopy, 326
 - Fourier-domain OCT, 326
 - Spectral-domain OCT, 326
 - Swept-source OCT, 326
 - Low coherence interferometry, 325
 - Optical Doppler tomography, 326
 - Polarization-sensitive OCT, 326
 - Scanning white-light interferometry, 326
 - Time-domain OCT, 326
 - Ultra-high resolution OCT, 325
- P**
- Polymer Thin Film, 241–63
 - Conclusion, 261
 - Extrusion coating, 242
 - Adhesion properties, 243
 - Frozen time, 243
 - Principle of extrusion coating, 242
 - Process parameters, 243
 - Sealing properties, 244
 - Introduction, 241
 - Organic coating deposited in solution, 245
 - Barrier properties, 251
 - Dwell time, 249
 - Optical properties optimisation, 250
 - Polymer used in roll coating, 246
 - Principle of organic coating deposition, 247
 - Process parameters, 249
 - Roll coating, 246
 - Sealing properties, 252
 - Surface preparation, 247
 - Various roll coating approaches, 248
 - Viscosity, 250
 - Vacuum deposition, 253
 - Barrier properties, 257, 258
 - Chemical vapor deposition, 253, 254
 - Major precursor families, 255, 256

- Oxygen barrier, 257, 258
 - Permeability, 259
 - Physical vapor deposition, 253, 254
 - Polymerization, 254
 - Principle of vacuum deposition, 253
 - Process parameters, 256, 257
 - Surface properties, 260
- R**
- Robotics, 315–23
 - Micro-robot examples, 319–22
 - Hexapod M-850 Micro-robot, 320
 - MFI Project, 322
 - Micro-air-vehicle, 320
 - Open-source Micro-robotic Project, 320
 - Strider Micro-robot, 321
 - Waalbot, 320
 - Micro-robotics applications, 316–18
 - Micro-assembly, 317
 - Micro-handling, 317–18
 - Robot definitions, 315–16
 - Sensors and Actuators in micro-robotics, 318–19
 - Actuators, 319
 - Micro-motors, 319
 - Piezoelectric actuators, 319
 - Sensors, 318–19
- S**
- Surface Engineering, 221–40
 - Applications in Micro-Manufacturing, 230
 - Cutting tools, 230–33
 - Micro-forming, 221, 232–36
 - Tool fabrication, 237
 - Focussed ion beam (FIB), 237
 - Electroforming, 235
 - Photolithography, 235
 - Chemical vapor deposition (CVD), 225
 - Diamond like carbon (DLC), 226, 230, 233–37
 - Plasma Assisted CVD, 225–26
 - Thermal CVD, 225–26
 - Electrodeposition, 225, 236
 - Electroless Ni, 225
 - Electroplating, 225
 - Hard Chromium, 225
 - Ion implantation, 224
 - Physical vapor Deposition (PVD), 226
 - Cathodic arc evaporation, 227
 - Chromium based coatings, 229–30
 - CrN, 230, 234
 - CrCN, 230
 - Duplex, 230
 - Electron beam, 227
 - Magnetron sputtering, 227
 - Ion beam assisted deposition, 227
 - Closed field unbalanced magnetron sputtering, 231
 - HIPIMS, 227
 - Titanium based coatings, 228–30, 232, 234
 - TiN, 228–31
 - TiAlN, 228–31, 234
 - (Al,Si)TiN, 228, 230, 232
 - Plasma nitriding, 222–23, 230
 - Tribology, 221, 222
 - Built up edge (BUE), 231
 - Coefficient of friction, 221, 225, 226, 230, 233, 237
 - Corrosion, 221, 222, 225
 - DLC, 226, 227, 230, 234, 235
 - Galling, 230, 234
 - Losses due to wear, 221
 - Low friction coatings, 226, 227, 230, 234, 235
 - Me:C, 226, 227, 230, 234, 235
 - MoS₂, 226, 227, 230, 234, 235
 - Sticking, 230, 234
 - Wear, 221, 222, 224, 228
 - Sustainability of Micro-manufacturing, 394–404
 - Application of DFE, 399–400
 - Carbon nanotubes reinforced polymer, 399
 - DFIP, 399
 - Fibres characteristics in recycled polymer, 399
 - Handling and assembly use, 399
 - Integration of functions, 399
 - Material selection, 399–400
 - Micro factories, 400
 - Design for Environment (DEF), 397–98
 - DFD - design for de-assembly, 398
 - DFMA - design for manufacturing and assembly, 398
 - DFR - design for recycling, 398
 - DFRm - design for remanufacturing, 398
 - EBM - environment benign manufacturing, 398
 - ReUse, 397
 - EcoDesign, 397
 - Ethical Issues, 401
 - LCA for micro components, 396
 - Clean room classes, 396
 - Types of micro components, 396
 - Life Cycle Assessment, 394–96
 - DFE, 394
 - EcoDesign rules, 394
 - Environmental impact, 394
 - Functional unit, 395
 - Goal and scope, 395
 - LCA theory, 394
 - Material-use data, 396
 - Process data, 395
 - Product directives, 395
 - System boundaries, 395
- T**
- Testing and Diagnosis for Micro-manufacturing Systems, 344–65
 - Micro-devices and machines, 360–64
 - Precision measurement systems, 347–53
 - Mixed qualitative-quantitative analysis systems, 352
 - SEM, AFM and STM, 352

- Surface-texture analysis, 352
- Mono- and multi-dimensional measurement, 348
- Thickness measurement, 348
- Vibration measurement and analysis, 351
- 2D profile and shape measurement, 350
- Testing and diagnosis methods, 353–60
 - Quantitative model-based testing, 355
 - The Kalman Estimator, 359
- Tooling and Process Chains, 287–97
 - Applications, 295–297
 - Die/mold fabrication, 295–96
 - Aluminum, 296
 - Etching, 296
 - Micro-bulk-forming, 114–29, 295–96
 - Micro-EDM, 39–58, 296
 - Nickel, 296
 - Silicone replica, 297
 - Polymer micro-fluidics, 295
- Process chain, 288, 291–95
 - Definition, 288
 - Selection criteria, 291
 - Basic process chains, 292
 - Features, 294
 - Inserts, 293–94
 - Material selection, 294
 - Micro-structuring processes, 294–95
 - Tool requirements, 293
- Tooling, 287–88
 - Definition, 287–88
 - Injection moulding, 90–113, 288
 - Laser ablation, 59–67, 288
 - Micro-EDM, 39–58, 288
 - Precision milling, 24–38, 287
 - Tooling concepts, 288
 - Additive processes, 289
 - CVD, 221–40, 290
 - Deposition, 290
 - Electrochemical deposition, 290–91also see
 - Eletroforming
 - Electroforming, 235, 290–91
 - Material capability, 289–90
 - PVD, 221–40, 290
 - Tooling technologies, 287–88